



T.C.  
ÇANAKKALE ONSEKİZ MART ÜNİVERSİTESİ  
LİSANSÜSTÜ EĞİTİM ENSTİTÜSÜ

***CANAKKALE ONSEKİZ MART UNIVERSITY  
JOURNAL OF ADVANCED  
RESEARCH IN NATURAL AND  
APPLIED SCIENCES***





**Journal of Advanced Research in Natural  
and Applied Sciences**

**e-ISSN: 2757-5195**

**Volume 9 / Issue 4**

**Sayı 9 / Cilt 4**

**2023-Aralık/December**

**Yayıncı / Publisher:** Çanakkale Onsekiz Mart Üniversitesi

**Rektör / Rector:** Prof. Dr. R. Cüneyt ERENOĞLU

**Dergi Editör Kurulu / Editorial Board**

Doç. Dr. Filiz UĞUR NİGİZ (Editor-in-Chief)

Doç. Dr. Ayça AYDOĞDU

Doç. Dr. Tuğba GÜNGÖR

Doç. Dr. Deniz ŞANLIYÜKSEL YÜCEL

Doç. Dr. Mehmet Ali YÜCEL

Doç. Dr. Özgür Turay KAYMAKÇI

Doç. Dr. Alper SAĞLIK

Dr. Öğretim Üyesi Gülçin ÖZCAN ATEŞ

Dr. Öğretim Üyesi Şebnem ÖNDER

Dr. Öğretim Üyesi Doğukan TAŞER

Dr. Öğr. Üyesi İsmail Onur TUNÇ

**Dil Editörü**

Doç. Dr. Sercan Hamza BAĞLAMA

Öğr. Gör. Oksana YESHYORKİNA BAYLAN

**Mizanpaj Editörü**

Arş. Gör. Gökhan KELEŞ

**Önsöz:**

Journal of Advanced Research in Natural and Applied Sciences Dergisi Fen, Mühendislik, Doğa ve Temel bilimler alanlarında daha önce yayımlanmamış orijinal araştırma makalesi, derleme yazılar, teknik not türünde araştırmaları yayınlayan ulusal ve uluslararası indekslerde taranan, hakemli ve bilimsel bir dergidir. Journal of Advanced Research in Natural and Applied Sciences Dergisi Mart, Haziran, Eylül, Aralık olmak üzere yılda dört sayı yayınlanacaktır. Tr-Dizin’de taranan Journal of Advanced Research in Natural and Applied Sciences Dergisi’nin 9.cilt 4.sayısında 20 adet araştırma makalesi yayına kabul edilmiştir.

	TÜBİTAK TR DİZİN tarafından taranmaktadır. Indexed by TR-DİZİN Database.
	TÜBİTAK-ULAKBİM DergiPark Akademik tarafından yayımlanmaktadır. Published by TÜBİTAK-ULAKBİM Turkish Journal Park Academic Database.
	CROSSREF® veri tabanı tarafından taranmakta ve makaleler DOI numarası ile yayımlanmaktadır. Indexed by CROSSREF® Database and articles are published with DOI number.
	Google Scholar'da ve SOBIAD'da taranmaktadır. Indexed by Google Scholar and SOBIAD Database.

### İletişim Adresi / Publisher Address

Çanakkale Onsekiz Mart Üniversitesi Lisansüstü Eğitim Enstitüsü  
Terzioğlu Yerleşkesi Çanakkale (Sağlık Hizmetleri Meslek Yüksekokulu Binası)

**Tel:** 0286 218 05 23

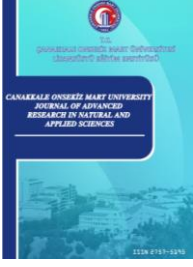
**Belgegeçer / Fax:** 0286 218 05 24

**E-posta / E-mail:** [jarnas.journal@gmail.com](mailto:jarnas.journal@gmail.com)

**Dergi Web Sayfası / Journal Home Page:**

<http://jarna.dergi.comu.edu.tr/>

<https://dergipark.org.tr/tr/pub/jarnas>



**CONTENTS / İÇİNDEKİLER**  
**(2023, 9:4)**

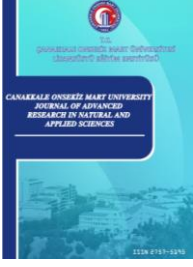
No	Articles & Authors / Makaleler & Yazarlar	Pages / Sayfa No
1	Gemideki Buhar Sıkıştırılmalı Soğutma Ünitesinde Deniz Suyu Sıcaklığının Soğutma Performansına Etkisinin Eksergoekonomi Metoduyla Analizi Cihan Nacak*, Betül Saraç, Teoman Ayhan Research/Araştırma	775-787
2	Development of Small Hydroelectric Power Plant Maintenance Costs using Chaos Embedded Adaptive Particle Swarm Optimization Soner Çelikdemir*, Mahmut Temel Özdemir Research/Araştırma	788-803
3	Volatile Organic Compounds, Total Phenolic Content, Color, and Heating Uniformity of Lemon Peel as Affected by Rotational Speed of Turntable During Microwave Drying Işıl Barutçu Mazı*, Sevilay San Research/Araştırma	804-821
4	Kepler Light Curve Modeling of KIC 9788457 Fahri Aliçavuş* Research/Araştırma	822-830
5	Prioritization of Negative Carbon Strategies in the Cargo Industry with the SWARA/WASPAS Method Emel Yontar*, Onur Derse Research/Araştırma	831-843
6	Kidney Segmentation with LinkNetB7 Cihan Akyel* Research/Araştırma	844-853



Çanakkale Onsekiz Mart University Journal of Advanced Research in Natural and Applied Sciences

Aralık (December) 2023 / Cilt (Volume) 9 / Sayı (Issue) 4 / e-ISSN 2757-5195

7	Investigation of Some Real Estate Valuation Problems in Turkey Varol Koç* Research/Araştırma	854-870
8	Seasonal changes in the fatty acid profile of <i>Cystoseira crinita</i> Duby, 1830, distributed on the Sinop Peninsula Coast of the Black Sea Ali Karaçuha*, Gökhan Yıldız, Melek Ersoy Karaçuha Research/Araştırma	871-880
9	Detection and Validation of A2 Milk Suitable for Consumers Having Milk Intolerance by ELISA Method Mediha Esra Altuntop Yayla* Research/Araştırma	881-892
10	Kent Parklarının Değerlendirilmesinde Biyofilik Tasarım Yaklaşımı: Ordu Örneği Bağlan Özel Karaağaç, Ömer Atabeyoğlu* Research/Araştırma	893-911
11	Determination of Protein Amount in Nanosized Synthetic Liposomes by Surface Enhanced Raman Spectroscopy (SERS) Şeyma Parlatan* Research/Araştırma	912-922
12	Investigation of Chlorophyll Mutations in Gamma Irradiated Naked Barley Genotypes Namuk Ergün*, Güray Akdoğan, Saime Ünver İkincikarakaya Research/Araştırma	923-930
13	Analysis of Acoustic Signals of Footsteps from the Piezoelectric Sensor Bilge Çiğdem Çiftçi, Gamze Kaya*, Mustafa Kurt Research/Araştırma	931-937



Çanakkale Onsekiz Mart University Journal of Advanced Research in Natural and Applied Sciences

Aralık (December) 2023 / Cilt (Volume) 9 / Sayı (Issue) 4 / e-ISSN 2757-5195

14	Anti-aging effect of TMQ on EPDM for Various Cure Systems Şehriban Öncel*, Gürcan Gül, Mahir Burak Efe, Hakan Erdoğan, Bağdagül Karaağaç Research/Araştırma	938-951
15	Gıda Sektöründe Çalışanların Salgın Hastalık Farkındalıkları: Çanakkale İli Örneği Orkun Dalyan*, Mehmet Pişkin, Erdal Canpolat, Ömer Faruk Öztürk Research/Araştırma	952-963
16	Çanakkale Kent Merkezi Kamusal Açık Alanlarının Kadın Kullanımı Açısından İrdelenmesi Füsun Erduran Nemetli*, Sena Aksoy, Nurana Nurullayeva, Zeynep Pelin Morgül Research/Araştırma	964-980
17	Atık Karbon Keçenin Pirol ile Polimerizasyonu ve Katot Olarak Kullanılabilirliği Mesut Sezer*, Melike İşgören, Sevil Veli, Anatoli Dimoglo Research/Araştırma	981-989
18	The Effect of the Increasing Doses of Vermicompost Applications to Soil on Some Nutrient Concentrations in Olive (Olea europaea L.) Leaves Ayşe Nur Coşkun, Ali Sümer* Research/Araştırma	990-1004
19	Position Control Using Trajectory Tracking and State Estimation of a Quad-rotor Muharrem Mercimek*, Onur Sarıpınar Research/Araştırma	1005-1019
20	Yapı Bilgi Modellemesi ve Coğrafi Bilgi Sistemleri Entegrasyonu için IFC'den CityGML ve CityJSON Veri Formatlarına Dönüşümün İncelenmesi Özlem Korkmaz*, Melih Başaraner Research/Araştırma	1020-1038



## Gemideki Buhar Sıkıştırma Soğutma Ünitesinde Deniz Suyu Sıcaklığının Soğutma Performansına Etkisinin Eksergoekonomi Metoduyla Analizi

Cihan Nacak<sup>1\*</sup>, Betül Saraç<sup>2</sup>, Teoman Ayhan<sup>3</sup>

<sup>1</sup>Motorlu Araçlar ve Ulaştırma Teknolojileri Bölümü, Fatsa Meslek Yüksekokulu, Ordu Üniversitesi, Ordu, Türkiye

<sup>2</sup>Gemi İnşaatı ve Gemi Makineleri Mühendisliği Bölümü, Karadeniz Teknik Üniversitesi, Trabzon, Türkiye

<sup>3</sup>Soğanlı Sokak No 18/12 61080 Ortahisar, Trabzon, Türkiye

### Makale Tarihi

Gönderim: 10.02.2023

Kabul: 10.07.2023

Yayın: 20.12.2023

### Araştırma Makalesi

**Öz** – Bu çalışmada, deniz suyunun kondensere giriş sıcaklığı araştırma parametresi olarak alınan buhar sıkıştırma bir gemi soğutma sisteminin performansı eksergoekonomik analiz yöntemiyle belirlenerek soğutma sistem süreçlerinin ekserji maliyetleri hesaplanmıştır. Deniz suyunun kondensere giriş sıcaklıkları 20.5 °C, 24.5 °C ve 29.5 °C olarak ölçülmüş ve soğutucu akışkan olarak R22 kullanılmıştır. Buhar sıkıştırma soğutma sisteminin her bir elemanında oluşan ekserji tahribatlarının maliyeti eksergoekonomik analiz metodu ile hesaplanmıştır. Eksergoekonomik analiz sonuçları, kondenserdeki R22 soğutucu akışkanın yoğunlaşma sürecinde ekserji tahribatı maliyetinin en yüksek seviyede olduğunu göstermiştir. Çalışmanın yapıldığı gemiye ait soğutma sisteminde bulunan kondenserin ekonomiklik kriterinin kondensere giren deniz suyu sıcaklığı arttıkça iyileştiği gözlemlenmiştir. Parasal giderler açısından sistem bileşenleri değerlendirildiğinde, en yüksek maliyetli bileşenin kompresör olduğu bulunmuştur. Ekserji tahribatı maliyetleri açısından sistem bileşenleri değerlendirildiğinde, kondenser, kompresör, LT evaporatörü ve MT evaporatöründe sırasıyla 0.2552 (\$/saat), 0.2519 (\$/saat), 0.0527 (\$/saat), 0.0288 (\$/saat) olarak hesaplanmıştır. Bu sonuca göre, sistem performansının iyileştirilmesi için, kondenser işletim performansının iyileştirilmesi veya kondenserin yenilenmesi gerektiği bulunmuştur. Bileşenler arasında kondenser 0.2552 \$/saat değeri nedeniyle en yüksek ekserji tahribat maliyetine sahip olduğu hesaplanmıştır.

**Anahtar Kelimeler** – Buhar sıkıştırma soğutma, eksergoekonomik analiz, enerji, ekserji, yük gemisi

## Exergoeconomic Analysis of The Performance of a Ship Cooling System Whose Condensing Unit is Cooled by Seawater

<sup>1</sup>Motor Vehicles and Transport Technologies Department, Fatsa Vocational School, Ordu University, Ordu, Türkiye

<sup>2</sup>Department of Naval Architecture and Marine Engineering, Karadeniz Technical University, Trabzon, Türkiye

<sup>3</sup>Soğanlı Street No 18/12 Ortahisar, Trabzon, Türkiye

### Article History

Received: 10.02.2023

Accepted: 10.07.2023

Published: 20.12.2023

### Research Article

**Abstract** –In this study, the exergy costs of the cooling system processes were calculated by determining the performance of a vapour compression cooling system, whose seawater inlet temperature to the condenser was taken as the research parameter, using exergoeconomic analysis method. Seawater temperatures were measured as 20.5 °C, 24.5 °C and 29.5 °C and R22 was used as the refrigerant in the cooling system. The cost of exergy destruction in each element of the vapor compression refrigeration system was calculated by the exergoeconomic analysis method. The exergoeconomic analysis results showed that the exergy destruction cost of the R22 refrigerant in the condenser is at the highest level in the condensation process. It has been observed that the economic criteria of the condenser in the cooling system of the ship where the study was carried out improves as the sea water temperature entering the condenser increases. When system components are evaluated in terms of monetary costs, it has been found that the compressor is the costliest component. When the system components were evaluated in terms of exergy destruction costs, it was calculated respectively as 0.2552 (\$/hour), 0.2519 (\$/hour), 0.0527 (\$/hour), 0.0288 (\$/hour) for the condenser, compressor, LT evaporator and MT evaporator. According to this result, it was found that the condenser operating performance should be improved, or the condenser should be renewed in order to improve the system performance. It was calculated that among the components, the condenser had the highest exergy destruction cost due to its value of 0.2552 \$/hour per.

**Keywords** – Vapour compression refrigeration, exergoeconomic analysis, energy, exergy, vessel

<sup>1</sup> cihanacak@odu.edu.tr

<sup>2</sup> bsarac@ktu.edu.tr

<sup>3</sup> profayhan@gmail.com

\*Sorumlu Yazar

## 1. Giriş

Gemilerde kullanılan soğutma sistemleri personelin konfor şartlarını sağlamasının yanında, gemilerdeki yiyeceklerin ve taşınan kargo türüne göre kargonun belirli şartlarda soğutulup uzun sürelerde sağlıklı bir şekilde muhafaza edilmesi ve depolanması amacını taşımaktadır. Kargo gemileri seferlerinin sonuna kadar kargolarının kalitesini muhafaza ederek taşımaları birincil görevleri arasında yer almaktadır. Buhar sıkıştırımlı soğutma sistemleri, yüksek verimliliği ve performans katsayısı nedeniyle gemilerde yaygın olarak kullanılmaktadır.

Gemi enerji verimliliğini arttırmak için farklı uygulamalar ele alınmaktadır. Bu uygulamalar ile yaklaşık %25'ten %75'e kadar gemide kullanılacak yakıttan tasarruf edilebilmektedir (IMO, 2009). Günümüzde gemilerde enerji verimliliğini artırmak için gemi işletim sistemlerinde bulunan ünitelerin enerji verimliliğinin ve sistem verimliliğinin enerji tasarrufuna etkilerinin araştırılması enerji politikaları açısından en önemli konular arasında yer almaktadır. Bu bağlamda, geminin soğutma sisteminde kullanılacak enerjinin optimizasyonu gemi enerji verimliliğinin artmasını sağlayacaktır.

Enerjinin optimizasyonunda, sistemin soğutma tesir katsayısını olumsuz etkileyen bileşenlerdeki ekserji tahribatlarının belirlenmesi ve maliyeti açısından değerlendirilmesi önem kazanmaktadır. Termodinamiğin birinci kanunu (enerji analizi) yöntemiyle gemide kullanılan soğutma sistemine ait her bir eleman için enerji dönüşümüne ait enerji çeşitleri belirlenmektedir. Termodinamiğin ikinci kanunu (ekserji analizi) yöntemiyle de soğutma sistemindeki her bir elemanda meydana gelen tersinmezliklerin büyüklüğü (ekserji tahribatı) ve kaynağı tespit edilerek soğutmaya harcanan enerjinin kullanılabilir kısmı belirlenmektedir. Termodinamiğin ikinci kanununa dayalı sistemin enerji verimliliği analizleri ekserji tanımından yararlanılarak tanımlanabilmektedir. Sistemdeki ekserji tahribatının parasal değerlendirilmesi eksergoekonomi metodu ile yapılabilmektedir. Eksergoekonomi metodunda sistemi oluşturan her bir bileşenin entropi üretim terimi ve buna bağlı olarak ekserji tahribatı hesabının yanında sistemde tüketilen yakıtın ekonomik maliyetiyle beraber sistemin kurulum ve işletim maliyetleri göz önüne alınarak bileşenler ve sistem için gereken para miktarı parasal maliyet olarak tanımlanmaktadır. (Valero vd., 2006), (Tsatsaronis, 1993), ekserji analizini, eksergoekonominin tarihçesini ve eksergoekonomik optimizasyon tekniklerinin uygulamalarını özetlemiş ve ayrıca bu yöntemleri bir enerji prosesine uygulayarak, eksergoekonomik analiz ile tesisinin optimum tasarımını ve performansını belirlemiştir. (Lozana & Valero, 1993), eksergoekonomi alanında temel bir yaklaşım olan ekserjetik maliyet teorisinin teorik temelini ve çeşitli uygulamalarını sunmuşlardır. Termodinamiğin ikinci kanunu ile ele aldıklarını çevrime uygulayarak tersinmezlikleri üreten bileşenleri ve eksergoekonomi ile ekserji tahribatı maliyetlerini belirlemiştirler. Maliyet oluşturma sürecinin tanımlanmasına ve enerji sistemlerinde verimliliğin değerlendirilmesine dayalı temeller ve kriterler oluşturmuşlardır. Uyguladıkları yöntemin, enerji sistemlerinin analizinde güçlü bir araç olduğunu belirtmişlerdir. Bu yöntem ile enerji tasarrufu elde edebilmek için alternatiflerin değerlendirilmesi, maliyet tahsisi, operasyon optimizasyonu, alt sistemlerin yerel optimizasyonu, enerji denetimleri ve yakıt ile ilgili arızaların değerlendirilmesindeki konuları içeren uygulamaları sunmuşlardır. Eksergoekonomik analiz üzerine yapılan bir diğer çalışma (Kotas, 1995), tarafından ele alınarak, ekserji kavramının bağıntılarının temelleri, termal proseslerin analizleri, farklı sistemlerin ekserji analizleri üzerinde ayrıntılı bilgiler sunmuştur. Ayrıca eksergoekonomik analiz uygulamalarının geliştirilmiş yöntemlerini değişik mühendislik problemlerine uygulayarak tanıtmıştır. (Tsatsaronis, 2006), ekserji analizinde ve ekserji maliyet yönteminde kullanılan terimlerin tanımlarını açıklayarak, ekserji ve eksergoekonomik değişkenler için kullanılacak sembollerin seçeneklerini tartışmakta ve kalan terimler için terminolojiyi tanıtarak bu konuda ayrıntılı bilgiler vermiştir. (Rami & Dinçer, 2013), organik Rankine çevrimli yeni bir tip jeotermal rejeneratif üzerine eksergoekonomik analiz metodunu uygulayarak ısı eşanjörlerinin toplam yüzey alanı parametresine dayalı olarak bir optimizasyon yapmışlardır. Çalışma parametrelerinin etkilerini parametrik olarak araştırmışlar, bu parametrelerle sistemin enerji, ekserji verimliliği ve eksergoekonomik analizlerini incelemiştirler. (Silva vd., 2014), Brezilya'da üretilen petrolden türetilen yakıtların yenilenebilir ve yenilenemeyen ekserji ve CO<sub>2</sub> maliyetlerini, ekserji maliyetlerini ve birden fazla ürün içeren süreçlerde salınan CO<sub>2</sub>'yi rasyonel bir şekilde dağıtmak amacıyla eksergoekonomik analiz metoduyla değerlendirmişlerdir. (Ortiz vd., 2020), Hollanda'da elektriğin performansını belirlemek için ekserji ve çevre analizleri geliştirmişlerdir. Fosil ve yenilenebilir enerji kaynaklarının tüketimi dahil olmak üzere çeşitli teknolojik yolların karşılaştırmalı bir

değerlendirmesinin, ekserji maliyetleri ve spesifik CO<sub>2</sub> emisyonları cinsinden yapılabilir olduğunu belirtmişlerdir. (Siahaya, 2009), Jakarta’da kurulan bir gaz türbin santrali için ekserji, eksergoekonomi ve optimizasyonunu yapmıştır. Maliyeti en aza indirmek için bileşenlerin ekserji tahribatlarını hesaplayarak ekserji tahribatı maliyetini değerlendirmiştir. Kompresörlerdeki ve yanma odalarındaki ekserji tahribat maliyetinin düşük olmasıyla üretilen elektrik maliyetinin düşük olacağını belirtmiştir. (Soltani vd., 2013), dışarıdan ateşlenen biyokütle ve biyokütle-doğal gazın birlikte ateşlenmesiyle oluşan kombine çevrimden elektrik üretimi için gazlaştırma uygulamasını enerji, ekserji ve eksergoekonomi açısından incelemiştir. Her iki sistemi eksergoekonomi kriteri açısından karşılaştırdıklarında biyokütle-doğalgazlı kombine çevrimin diğerine göre %2 ile %4 arasında daha ekonomik olduğunu bulmuşlardır. (Rosen ve Dinçer, 2003), fosil kökenli yakıtlar ile nükleer yakıtlı elektrik üretim tesislerinde kullanılan sistem bileşenlerindeki ekserji tahribatlarını hesaplayarak, bileşenler için ekserji maliyetlerinin hesaplanması için bağıntılar vermişlerdir. (Mert, 2010), çalışmada Erdemir Ereğli Demir ve Çelik Fabrikası’nda gaz türbinlerinin egzoz gazlarının değerlendirildiği kojenerasyon ve konvansiyonel elektrik üretim tesisinin her bir birimin ve tüm sistemin enerji, ekserji ve eksergoekonomi analizlerini yapmış ve tesisin enerji görünümü ortaya koymuştur. Santralde, ekserji tahribatının en fazla meydana geldiği bileşenin buhar kazanlarının olduğunu belirtmiştir. Buhar kazanlarındaki döner hava ısıtıcılarının buhar kazanlarında oluşan ekserji kaybını artırdığını bildirmiştir. (Doseva ve Chakyrova, 2019), Bulgaristan’ın Varna şehrindeki, biyogaz motoru ile gaz türbininden oluşan kojenerasyonlu elektrik üretim sistemiyle tahrik edilen atık su üretim sisteminin eksergoekonomik analizini incelemiştir. (Cavalcanti ve Motta, 2015), güneş enerjisi ve fosil kökenli yakıt ile çalışan 57 kW elektrik gücü üreten Rankine çevrimini eksergoekonomik açıdan değerlendirmişlerdir. Güneş ışınım değerleri yüksek iken kollektör veriminin daha yüksek olduğunu hesaplamışlardır. (Luo vd., 2019), soğutucu akışkan olarak CO<sub>2</sub> kullanan bir soğutma tesisinde, kompresörün CO<sub>2</sub>’nin kritik basınç bölgesindeki basınç değerlerinin sistem performansı için termodinamik ve eksergoekonomik analizini ele almışlardır. (Saraç, 2015) çay üretim tesisinde değişik atmosfer havası şartlarının çay soldurma işlemi üzerindeki etkilerini ekserji analizi metodu ile incelemiş ve atmosfer havası sıcaklığının artmasıyla ekserji veriminin azaldığını belirtmiştir. (Başhan ve Parlak, 2016), farklılık gösteren deniz suyu sıcaklıklarında çalışan, R134A soğutucu akışkanlı buhar sıkıştırımlı bir gemi soğutma sistemine ekserji analizini uygulayarak deniz suyu sıcaklığı azaldıkça soğutma tesir katsayısı ve II. Kanun verimi artarken ekserji tahribatlarının azaldığını bildirmişlerdir.

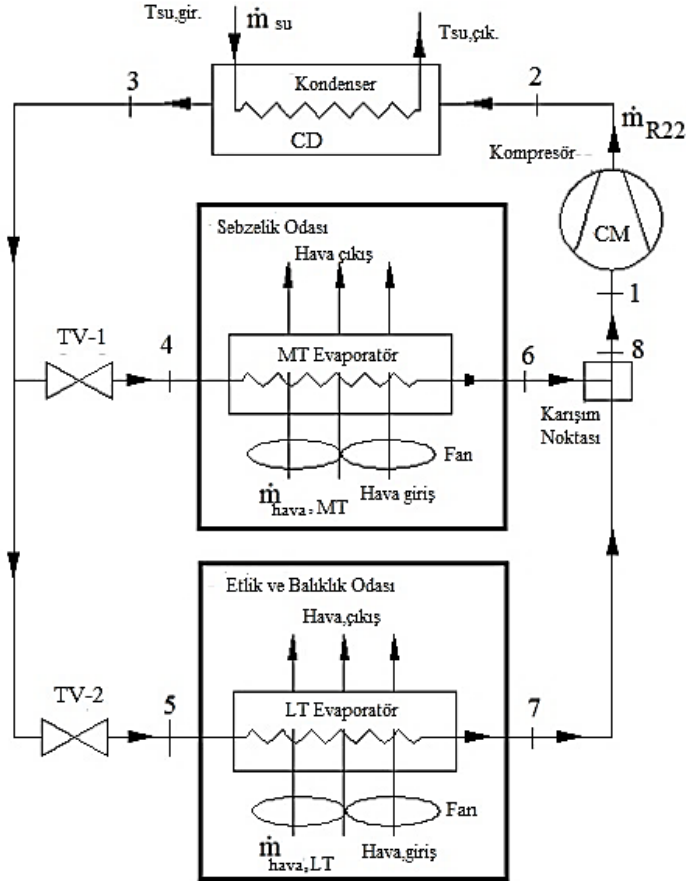
Bu çalışmada bir kargo gemisindeki R22 soğutucu akışkanlı buhar sıkıştırımlı soğutma sisteminde, kondenser ünitesine giren deniz suyu giriş sıcaklığının sistem performansına etkileri eksergoekonomi analizi metoduyla araştırılmıştır. Soğutucu sistemin gerçek çevriminin her bir elemanında oluşan ekserji tahribatları ile toplam sistemin ekserji tahribatı farklı deniz suyu sıcaklıklarına göre hesaplanarak ekserji tahribatı maliyeti hesaplanmıştır. Gerçek çevrime dayalı hesaplamalarda elde edilen tersinmezlik kaynaklarının ve büyüklüklerinin belirlenmesiyle eksergoekonomik analize dayalı maliyet bilançosu elde edilmiştir. Bu çalışmanın amacı, bir kargo gemisinin soğutma sisteminin kondenser ünitesindeki farklı sıcaklıklardaki deniz suyunun soğutma sisteminin performansına etkilerini ve sebep olduğu tersinmezliklerinin belirlenerek maliyeti açısından değerlendirilmesidir.

## 2. Materyal ve Yöntem

Bu çalışmada Boybeyi Denizcilik firmasına ait 9282338 IMO numaralı, Panama bayraklı, M/V Saros B isimli kuru yük gemisine ait buhar sıkıştırımlı soğutma ünitesinden elde edilen veriler kullanılmıştır. Gemi 110,67 metre tam boya, 19,20 metre genişliğe, 9,214 metre drafta, 7442 gros tona ve 3957 net tona sahip olup, ana makinesi MAKITA-MITSUI-MAN B&W/6L35MC marka iki zamanlı bir dizel motordur. Ana makinenin gücü 3900 kW’dır. Gemi personeli 18 kişidir. (Nacak, 2020; Nacak & Saraç, 2020).

### 2.1. Materyal

Çalışmada ele alınan M/V Saros B gemisinin soğutma sistemi; iki evaporatör, bir kondenser, iki genişleme valfi ve bir kompresörden oluşmaktadır. Soğutma sisteminde soğutucu akışkan R22 içermektedir. Buhar sıkıştırımlı soğutma sisteminin şematik resmi Şekil 1’ de verilmiştir. Gemide sebzelik ve etlik odası olmak üzere iki adet buzluk odası bulunmaktadır.



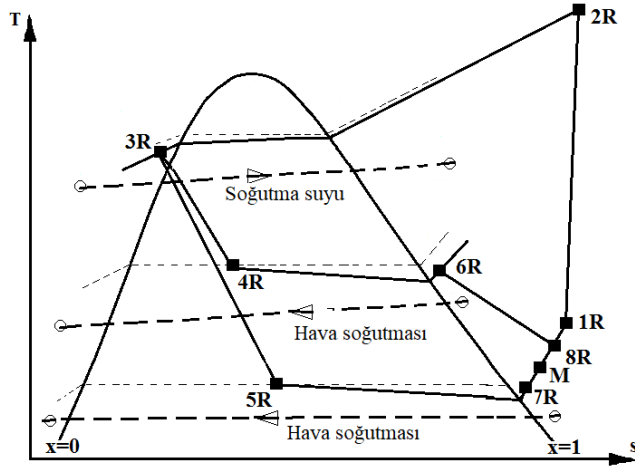
Şekil 1. Gemideki soğutma sisteminin şeması (Nacak, 2020; Nacak & Saraç, 2020)

Termodinamik hesaplamada aşağıdaki kabuller ele alınmıştır.

1. Sistem zamandan bağımsız ve sürekli akışlı olarak ele alınmıştır.
2. Sistemin ısı, kinetik ve potansiyel enerji kayıpları diğer kayıplara göre küçük mertebede olduğu için hesaplamalarda ihmal edilmiştir.
3. Hem kondanser hem de evaporatörde, teorik çevrimdeki maksimum basınç ile gerçek çevrimdeki basınç farkı yaklaşık %10 olarak hesaplanmıştır. Bu nedenle sistemi oluşturan elemanlardaki ve boru bağlantılarındaki basınç kayıpları %10 alınmıştır.
4. Kompresörün izantropik verimi 0,75 olarak alınmıştır.
5. Bu çalışma için ölü hal  $T_0=15\text{ }^{\circ}\text{C}$  ve  $P_0=100\text{ kPa}$  olarak seçilmiştir.
6. Evaporatörlerde hava ideal gaz olarak kabul edilmiştir.

## 2.2. Metot

Çalışmada ele alınan soğutma ünitesinin gerçek işletim parametrelerine ve tasarlanan termodinamik verilerine göre çevrimin T-s diyagramı Şekil 2’de gösterilmiştir. Gerçek çevrimin çalışma koşulları Tablo 1’de verilmiştir. Soğutucu akışkan R22’nin yoğuşma sıcaklığı ile kondanserdeki deniz suyu giriş sıcaklığı arasındaki sıcaklık farkı ( $\Delta T_R$ ) 8 °C, 13 °C, ve 18 °C dir. Termodinamiğin enerji ve ekserji kanunları ile soğutma sisteminin elemanlarında oluşan enerji ve ekserji tahribatı miktarları hesaplanarak, eksergoekonomik analiz metodu soğutma sistemine uygulanmıştır.



Şekil 2. Gemideki soğutma sisteminin şeması (Nacak, 2020; Nacak &amp; Saraç, 2020)

Tablo 1

Gerçek çevrim çalışma koşulları ( $T_{su,g} = 24.5 \text{ } ^\circ\text{C}$  ve  $\Delta T_R = 13 \text{ } ^\circ\text{C}$ ) (Nacak, 2020; Nacak & Saraç, 2020)

Parametreler	
Basınç düşüşü, $\Delta P$	$\Delta P^*0,02\%$ [kPa]
Farklı minimum sıcaklık farkları $\Delta T$	13 $^\circ\text{C}$
MT evaporatöründe farklı minimum sıcaklık farkları, $\Delta T_{MT}$	3 $^\circ\text{C}$
LT evaporatöründe farklı minimum sıcaklık farkları, $\Delta T_{LT}$	7 $^\circ\text{C}$
Kompresörün izantropik verimliliği, $\eta_{kompresör}$	%75
TV-1 kısılma süreci 3-4	Tersinmez
TV-2 kısılma süreci 4-5	Tersinmez
Kondenserden aşırı soğutma tahliye hattı	12 $^\circ\text{C}$
Kompresörden önce emiş hattının aşırı ısıtma sıcaklığı	15 $^\circ\text{C}$
Soğutma suyu	
Suyun giriş sıcaklığı	$T_{su,g} = 24,5 \text{ } ^\circ\text{C}$
Suyun giriş basıncı	$P_{su,g} = 400 \text{ kPa}$
Suyun çıkış sıcaklığı	$T_{su,\phi} = 30 \text{ } ^\circ\text{C}$
Suyun çıkış basıncı	$P_{su,\phi} = 101,325 \text{ Pa}$
MT evaporatöründeki hava soğutması	
Hava giriş sıcaklığı	$T_{hava,g} = 6 \text{ } ^\circ\text{C}$
Hava giriş basıncı	$P_{hava,g} = 101,325 \text{ kPa}$
Hava çıkış sıcaklığı	$T_{hava,\phi} = 3,5 \text{ } ^\circ\text{C}$
Hava çıkış basıncı	$P_{su,\phi} = 101,325 \text{ Pa}$
LT evaporatöründeki hava soğutması	
Hava giriş sıcaklığı	$T_{hava,g} = -10 \text{ } ^\circ\text{C}$
Hava giriş basıncı	$P_{hava,g} = 101,325 \text{ kPa}$
Hava çıkış sıcaklığı	$T_{hava,\phi} = -18 \text{ } ^\circ\text{C}$
Hava çıkış basıncı	$P_{hava,\phi} = 101,325 \text{ kPa}$

### 2.2.1. Enerji ve Ekserji Analizleri

Kütle ve enerjinin korunumu ilkelerinin yanında sistemin her bir elemanı için ekserji dengesi yazılarak sistemin performansı belirlenmektedir. Bir termal sistemde tersinmezlikler içeren üniteleri ve tersinmezliklerin büyüklüğünü belirlemek ekserji analizi metodu ile analiz edilerek belirlenmektedir. Ekserji analizi tersinmezlik kaynağının belirlenmesinin yanı sıra sürecin tersinmezliği hakkında da bilgi sağlar. Sistemdeki her bir bileşende oluşan ekserji tahribatı ve ekserji tahribatının büyüklüğünün belirlenmesi, ekserji eşitliğinin sistemdeki her bir üniteye ayrı ayrı uygulanmasıyla bulunur. Buharlaştırma soğutma sisteminin termodinamik modelinde sistemi meydana getiren her bir bileşenin akışkan giriş ve çıkış ekserjileri (Denklem 2.1), ekserji akışı (Denklem 2.2) ve her bir elemanda oluşan ekserji tahribatı da (Denklem 2.3) ile hesaplanmıştır. Denklemlerdeki “h” entalpi, “s” entropi ve “e” ekserji akışını belirtmekte olup, bileşenlerin giriş ve çıkış noktalarındaki şartlara göre değerler almaktadır. “0” indisi ise ekserji analizi değerlendirilmesinde ölü hal şartlarına karşılık gelen değerleri simgelemektedir.

$$e = h - h_0 - T_0(s - s_0) \quad (2.1)$$

$$\dot{E} = \dot{m} e \quad (2.2)$$

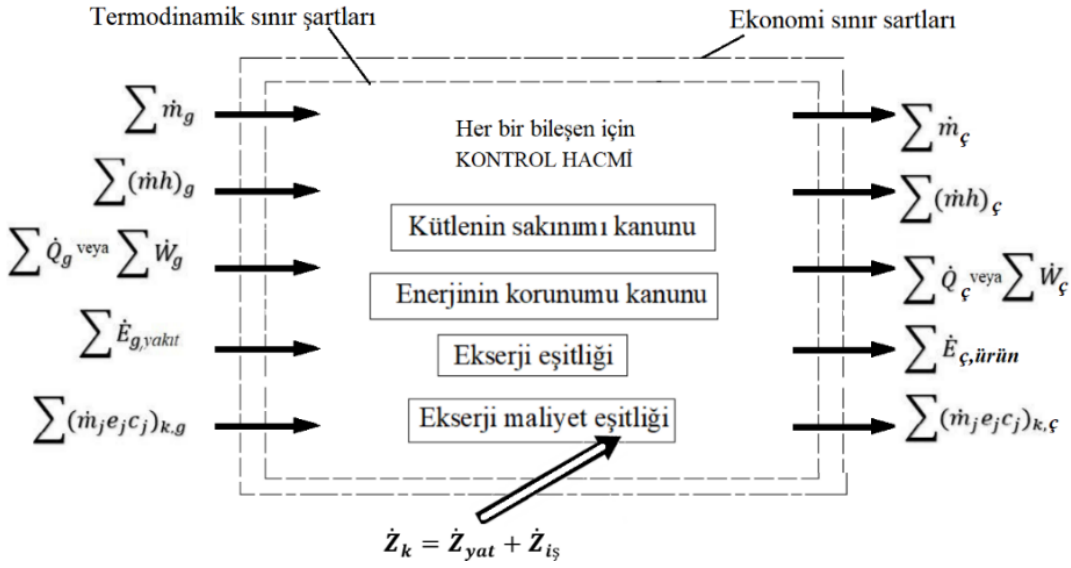
$$\dot{E}_D = \sum_k \left(1 - \frac{T_0}{T_k}\right) \dot{Q}_k - \dot{W} + \sum_k \dot{E}_{k,g} - \sum_k \dot{E}_{k,\phi} \quad (2.3)$$

### 2.2.2. Eksergoekonomik Analiz

Eksergoekonomi metodu termik sistemlerin enerji verimliliğinin ve maliyetinin değerlendirilmesi açısından uygulanan yeni bir yöntem olup, tasarım mühendislerine ve işletim mühendislerine mali açıdan en ekonomik bir tasarımı ve işletme koşullarının belirlenmesini sağlar. Bu yöntem literatüre (Bejan vd., 1996) tarafından tanıtılmıştır. Eksergoekonomik analiz, ekserji analizi, ekonomik analiz, ekserji maliyeti ve eksergoekonomi aşamalarını içermekte ve genellikle sistem elemanları seviyesinde uygulanan bir analiz yöntemidir. Eksergoekonomik analizin amacı, sistem süreçlerinin maliyetini, sistemin maliyet akışını ve şeklini anlamak, sistem elemanlarının spesifik değişkenlerini belirlemek ve bu değişkenleri optimize etmek ve sistemi bütün olarak ele alıp optimizasyonunu yapmaktır.

#### 2.2.2.1. Ekserji Maliyet Tanımları

Ekserji analizinde sistemdeki kütle ve enerji akımları ile ilgili maliyetler hesaplanarak her bir elemanda meydana gelen ekserji kaybı belirlenir. Bir sistemin ekserji üretebilmesi için harcaması gereken ekserji miktarına ekserji maliyeti adı verilir. Eksergoekonomik analizin amacı, sistem süreçlerinin maliyetini ve sistemin ürün akışlarının birim başına ekserji maliyetini ortaya çıkarmaktır. İşletimden elde edilen ürünlerin birim ekserji maliyeti çevrimin ekonomik optimizasyonu için kullanılmaktadır. Her bir ekserji ürünün birim maliyetini hesaplamak için bir maliyet denge denklemi ve yardımcı denklemler, çevrimin her bileşenine uygulanmaktadır. Sistemdeki her bir eleman için ilk yatırım, bakım ve onarım maliyet toplamının hesabında termodinamik sınır şartlarına ve ekonomi sınır şartlarına dayalı eşitlikler şematik olarak Şekil 3’te gösterilmiştir. Termodinamik süreçlerde her bir ekserji akımı için ekserji maliyeti yapılır. Termodinamik ve ekonomik sınır şartlarını göz önüne alınan bir kontrol hacmine, giren ve çıkan madde akımının taşıdığı ekserji  $\dot{E}_g$  ve  $\dot{E}_\phi$ , güç  $\dot{W}$  ve ısı transferiyle yapılan ekserji transferi  $\dot{E}_q$  ile simgelenmiştir.



Şekil 3. Termodinamik ve ekonomik eşitliklerin kontrol hacminde şematik gösterimi (Nacak, 2020)

Ekserji maliyet değerlendirilmesinde, her bileşen ekserji akımı maliyeti ile ilişkilendirilir. Sistemdeki madde ve enerji aktarımı ile ekserji transferi gerçekleşirken tersinmezlik sebebiyle ekserjinin bir bölümü yok olmaktadır. Ekserji maliyeti (Denklem 2.4) veya (Denklem 2.5) ile belirlenmektedir.  $\dot{C}_j$  dönem maliyeti fiyatını,  $c_j$  ekserjinin birim fiyat birimini (\$/gün) ve  $e_j$  ise bileşendeki her bir iş akışkanının özgül ekserjisini simgelemektedir.  $E$  ekserji akışı olarak ifade edilir.

$$\sum (\dot{C}_j)_g + \dot{Z}_k = \sum (\dot{C}_j)_\zeta \quad (2.4)$$

$$\sum (\dot{m}_j e_j c_j)_g + \dot{Z}_k = \sum (\dot{m}_j e_j c_j)_\zeta \quad (2.5)$$

Kontrol hacmine giren iş akışkanının ekserji maliyeti;

$$\dot{C}_g = c_g \dot{E}_g = c_g (\dot{m}_g e_g) \quad (2.6)$$

Kontrol hacminden çıkan iş akışkanının ekserji maliyeti;

$$\dot{C}_\zeta = c_\zeta \dot{E}_\zeta = c_\zeta (\dot{m}_\zeta e_\zeta) \quad (2.7)$$

Kontrol hacmindeki gücün ekserji maliyeti;

$$\dot{C}_w = c_w \dot{W} \quad (2.8)$$

$\dot{Q}$  ısı transferinin,  $\dot{E}_q$  ekserjisinin maliyeti olan  $\dot{C}_q$  ise (Denklem 2.9) ile belirlenmiştir.

$$\dot{C}_q = c_q \dot{E}_q \quad (2.9)$$

$\dot{E}_F$  ekserji yakıtı ve  $\dot{E}_P$  ekserji ürünü ifadeleri için ekserji maliyetleri (Denklem 2.4)'te yerine yazılırsa,  $\dot{C}_{P,top}$  ekserji ürün maliyeti ve  $\dot{C}_{F,top}$  ekserji-yakıt maliyeti (Denklem 2.10) ile belirlenir.  $\dot{Z}_{top}^{yat}$  ilk toplam yatırım maliyetini ve  $\dot{Z}_{top}^{i\dot{s}}$  toplam işletme ve bakım maliyetini tanımlamaktadır.

$$\dot{C}_{P,top} = \dot{C}_{F,top} + \dot{Z}_{top}^{yat} + \dot{Z}_{top}^{i\check{s}} \quad (2.10)$$

Bir sistemin termal performansının ekonomik olarak uygulanabilirliđi ekserji maliyetine gre deđerlendirildiđinde, ele alınan kontrol hacminde oluřan ekserji tahribatı, ekserji-yakıtı ve ekserji-rn, evre řartlarına ve sistemde ortaya ıkan tersinmezlik reten kaynaklara gre deđerlendirilmektedir. K indisi sistemi oluřturan her bir bileřeni ifade etmektedir. Her bir bileřene ait zel ilave ekonomiklik denklemler yazılarak ortalama ekserji maliyeti (Denklem 2.11) ile hesaplanılır (Luo vd., 2019). Her bir bileřene ait zel ekonomiklik denklemleri Tablo 3'te verilmiřtir.

$$\sum_{\check{c}}(c_{\check{c}}\dot{E}_{\check{c}})_{\check{c}} + c_w W_k = c_{q,k}\dot{E}_q + \sum_g(c_g\dot{E}_g)_g + \dot{Z}_k \quad (2.11)$$

### 2.2.2.2. Ekserji Maliyet Eřitliđinin Sistem Bileřenlerine Uygulanması ve Deđerlendirme

Maliyet deđerlendirilmesinde ekonomik kriterlerden ana para geri kazanım oranı, bir deđere indirgenmiř dzeltme faktr ve eskalasyon dzeltme faktr kriterleri sistemdeki her bir bileřene uygulanarak, ana para geri kazanım oranı CRF (Denklem 2.12) ile bir deđere getirilmiř dzeltme faktr K (Denklem 2.13) ile eskalasyon dzeltme faktr CELF (Denklem 2.14) ile bir deđere getirilme faktr M (Denklem 2.15) ile belirlenir.

$$CRF = \frac{i_{f,t}(1+i_{f,t})^n}{(1+i_{f,t})^n - 1} \quad (2.12)$$

(Denklem 2.13) 'te  $r_n$  eskalasyon oranı;

$$K = \frac{1+r_n}{1+i_{f,t}} \quad (2.13)$$

(Denklem 2.14) 'te n sisteminin mrn,  $i_{f,t}$  geri deme oranını ifade etmektedir.

$$CELF = \frac{k(1-k^n)}{1-k} CRF \quad (2.14)$$

$$M = \frac{CELF}{1+r_i} \quad (2.15)$$

### 2.2.2.3. Maliyet Tahminleri

Sisteme ait toplam maliyet fiyatı (Denklem 2.16) ile belirlenmektedir (Bejan vd., 1996). Her bir bileřenin toplam maliyet fiyatı  $Z_k$ , sisteme ait her bir bileřenin ilk yatırım maliyet fiyatı  $Z_{yat}$  ile, iřletme ve bakım maliyet fiyatı  $Z_{i\check{s}}$  toplamı olarak tanımlanmaktadır.

$$Z_k = Z_{yat} + Z_{i\check{s}} \quad (2.16)$$

$Z_{yat}$  Yatırım maliyeti ile iřletme ve bakım maliyeti  $Z_{i\check{s}}$  (Denklem 2.17) ve (Denklem 2.18) 'te verilmiřtir.

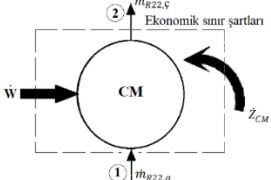
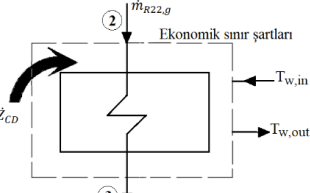
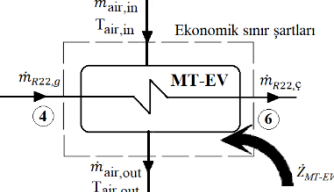
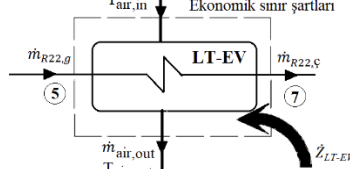
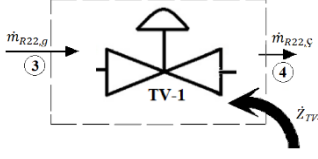
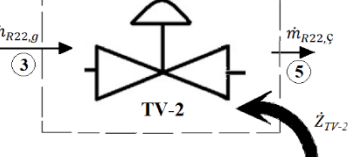
$$Z_{yat} = Z_{komp} + Z_{nakil} + Z_{i\check{s}ci} + Z_{tesis} \text{ [\$]} \quad (2.17)$$

$$Z_{i\check{s}} = Z_{servis} + Z_{bakim} + Z_{vergi} + Z_{elektrik} \text{ [\$]} \quad (2.18)$$

Deniz suyu ile sođutulan gemi sođutma sistemi kompresr, kondenser, MT evaporatr, LT evaporatr ve iki adet termostatik genleřme valfi olmak zere altı bileřenden oluřmaktadır. (Denklem 2.17) ve (Denklem 2.18) 'e ait birimler dzenlenerek sođutma sisteminin her bir elemanı iin bir yıla indirgenmiř toplam ekserji maliyetleri, sođutma sisteminin mr  $n=20$  yıl, gnlk alıřma saati  $\Delta\tau$  16 saat/gn, eskalasyon oranı  $r_n$  % 4, faiz oranı  $r_i$  % 3 ve geri deme oranı  $i_{f,t}$  % 6 olarak seilerek Tablo 2' de verilen eřitliklerle hesaplanmıřtır.

Tablo 2.

Soğutma sistem elemanlarına ait ekserji maliyeti

<p style="text-align: center;"><b>Kompresör</b></p> 	$\dot{Z}_{CM} = (Z_{yat} + Z_{i\dot{s}}).M$ $\dot{Z}_{CM} = \left( Z_{yat}/(n.24.365) + Z_{i\dot{s}}/(\Delta T.365) \right).M \quad [$/saat]$ $c_2 \dot{E}_2 = c_1 \dot{E}_1 + \dot{Z}_{CM} + c_{elektrik} \dot{W}_{CM}$ $\dot{C}_2 = \dot{C}_1, \quad \dot{C}_{tahribat_{CM}} = c_1 \dot{E}_{tahribat_{CM}} \quad [$/saat]$
<p style="text-align: center;"><b>Kondenser</b></p> 	$Z_{yat} = Z_{komp} + Z_{nakil} + Z_{i\dot{s}\dot{c}i} + Z_{tesis} \quad [\$]$ $Z_{i\dot{s}} = Z_{servis} + Z_{bakim} + Z_{vergi}$ $\dot{Z}_{CD} = \left( Z_{yat}/(n.24.365) + Z_{i\dot{s}}/(\Delta T.365) \right).M \quad [$/saat]$ $c_{su,\dot{c}} \dot{E}_{su,\dot{c}} + c_3 \dot{E}_3 = c_{su,g} \dot{E}_{su,g} + c_2 \dot{E}_2 + \dot{Z}_{CD}$ $\dot{C}_3 = \dot{C}_2, \quad c_{su,g} = 0,0, \quad \dot{C}_{tahribat_{CD}} = c_2 \dot{E}_{tahribat_{CM}} \quad [$/saat]$
<p style="text-align: center;"><b>MT evaporatörü</b></p> 	$Z_{yat} = Z_{MT-EV} + Z_{nakil} + Z_{i\dot{s}\dot{c}i} + Z_{tesis} \quad [\$]$ $Z_{i\dot{s}} = Z_{servis} + Z_{bakim} + Z_{vergi}$ $\dot{Z}_{MT-EV} = \left( Z_{yat}/(n.24.365) + Z_{i\dot{s}}/(\Delta T.365) \right).M \quad [$/saat]$ $c_{hava,\dot{c}} \dot{E}_{hava,\dot{c}} + c_6 \dot{E}_6 = c_{hava,g} \dot{E}_{hava,g} + c_4 \dot{E}_4 + \dot{Z}_{MT-EV}$ $\dot{C}_6 = \dot{C}_4, \quad c_{hava,g} = 0,0, \quad \dot{C}_{tahribat_{MT-EV}} = c_4 \dot{E}_{tahribat_{MT-EV}} \quad [$/saat]$
<p style="text-align: center;"><b>LT evaporatörü</b></p> 	$Z_{yat} = Z_{LT-EV} + Z_{nakil} + Z_{i\dot{s}\dot{c}i} + Z_{tesis} \quad [\$]$ $Z_{i\dot{s}} = Z_{servis} + Z_{bakim} + Z_{vergi}$ $\dot{Z}_{LT-EV} = \left( Z_{yat}/(n.24.365) + Z_{i\dot{s}}/(\Delta T.365) \right).M \quad [$/saat]$ $c_{hava,\dot{c}} \dot{E}_{hava,out} + c_7 \dot{E}_7 = c_{hava,g} \dot{E}_{hava,g} + c_5 \dot{E}_5 + \dot{Z}_{LT-EV}$ $\dot{C}_7 = \dot{C}_5, \quad c_{hava,g} = 0,0, \quad \dot{C}_{tahribat_{LT-EV}} = c_5 \dot{E}_{tahribat_{LT-EV}} \quad [$/saat]$
<p style="text-align: center;"><b>TV-1</b></p> 	$Z_{yat} = Z_{M-TV} + Z_{nakil} + Z_{i\dot{s}\dot{c}i} + Z_{tesis} \quad [\$]$ $Z_{i\dot{s}} = Z_{servis} + Z_{bakim} + Z_{vergi}$ $\dot{Z}_{TV-1} = \left( Z_{yat}/(n.24.365) + Z_{i\dot{s}}/(\Delta T.365) \right).M \quad [$/saat]$ $c_4 \dot{E}_4 = c_3 \dot{E}_3 + \dot{Z}_{TV-1}$ $\dot{C}_4 = \dot{C}_3, \quad \dot{C}_{tahribat_{TV-1}} = c_3 \dot{E}_{tahribat_{TV-1}} \quad [$/saat]$
<p style="text-align: center;"><b>TV-2</b></p> 	$Z_{yat} = Z_{M-TV} + Z_{nakil} + Z_{i\dot{s}\dot{c}i} + Z_{tesis} \quad [\$]$ $Z_{i\dot{s}} = Z_{servis} + Z_{bakim} + Z_{vergi}$ $\dot{Z}_{TV-2} = \left( Z_{yat}/(n.24.365) + Z_{i\dot{s}}/(\Delta T.365) \right).M \quad [$/saat]$ $c_5 \dot{E}_4 = c_3 \dot{E}_3 + \dot{Z}_{TV-2}, \quad \dot{C}_5 = \dot{C}_3, \quad \dot{C}_{tahribat_{TV-2}} = c_3 \dot{E}_{tahribat_{TV-2}} \quad [$/saat]$

- **Termoekonomik Faktöre Göre Değerlendirme**

Termoekonomik faktör ( $f$ ) tanımı (Bejan vd., 1996) tarafından tanımlanmış ve (Denklem 2.19)'da verilmiştir. Termoekonomik faktör, sistemin tersinmezlik maliyeti azaldığında sistemin ideal çalışma şartlarındaki maliyet koşullarına ulaşıldığını ve ekserji tahribatı ile maliyetin azaldığını gösteren bir kriterdir. Termoekonomiklik kriterinin 1 değerine ulaşması o bileşenin ekonomik çalıştığını göstergesidir.

$$f_k = \frac{\dot{Z}_k}{\dot{Z}_k + \dot{C}_{\text{tahribat}_k}} \quad (2.19)$$

Karsan-Soğutma Ltd. Şti. firmasının sunduğu maliyet değerlerine göre, sisteme ait yatırım maliyetleri Tablo 3'de, işletim maliyetleri Tablo 4'de verilmiştir.

Tablo 3.

Sistem bileşenlerinin yatırım maliyetleri tablosu

Bileşen	Bileşen Maliyeti [\$]	Nakil Maliyeti [\$]	İşçilik Maliyeti [\$]	Tesisat Maliyeti [\$]
CM	1350	150	750	500
CD	900	150	350	350
MT-EV	770	150	600	300
LT-EV	950	150	700	350

Tablo 4.

Sistem bileşenlerinin işletim maliyetleri tablosu

Bileşen	Servis Maliyeti [\$]	Bakım Maliyeti [\$]	Yasal Vergi Maliyeti [%]	Elektrik Maliyeti [\$]
CM	850	1250	18	0
CD	700	400	18	0
MT-EV	600	200	18	0
LT-EV	700	350	18	0

### 3. Bulgular ve Tartışma

Gemi soğutma sistemin gerçek çevrimine ait noktalarının termodinamik analiz sonuçları, soğutma suyunun kondensere giriş noktasındaki 24.5 °C sıcaklık değeri için Tablo 5 'te verilmiştir.

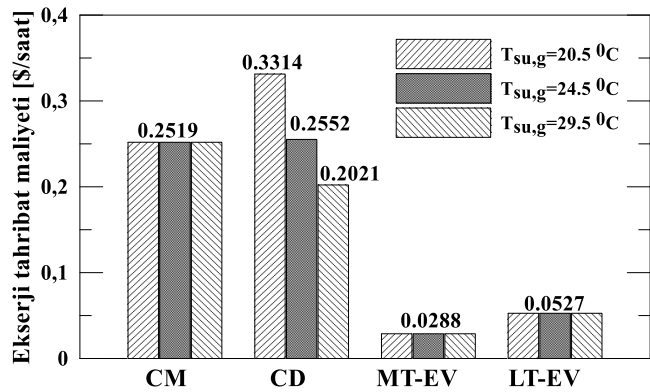
Tablo 5.

Gerçek çevrim için termodinamik parametreler ( $T_{su,g} = 24.5 \text{ }^\circ\text{C}$  ve  $\Delta T_R = 13 \text{ }^\circ\text{C}$ ) (Nacak ve Saraç, 2020)

S.Point	Akışkan	Termodinamik Parametreler					
		$\dot{m}$ [kg/s]	T [ $^\circ\text{C}$ ]	P [kPa]	h [kJ/kg]	s [kJ/kgK]	e [kJ/kgK]
1	R22	0.01806	3.893	193.4	413.9	1.868	17.64
2	R22	0.01806	136.1	1149	498.1	1.921	86.53
3	R22	0.01806	31	1633	238	1.128	54.81
4 [x4=0.184]	R22	0.0088	0	488.2	238	1.139	51.75
5 [x5=0.298]	R22	0.00917	-25	193.4	238	1.160	45.87
6	R22	0.0088	3	201.5	406.7	1.758	41.99
7	R22	0.00917	-15	193.4	401.5	1.822	18.59
8	R22	0.0088	-7.093	193.4	406.7	1.841	18.08
M	R22	0.01806	-11.11	193.4	404.1	1.831	18.32
$T_{su,g}$	Su	0.2067	24.5	405.3	103	0.359	0.9451
$T_{su,\phi}$	Su	0.2067	30	101.3	125.8	0.436	1.579
$T_{hava,g,MT}$	Hava	0.3316	6	101.3	16.93	5.671	0.1938
$T_{hava,\phi,MT}$	Hava	0.3316	3	101.3	12.41	5.654	0.3445
$T_{hava,g,LT}$	Hava	0.1687	-10	101.3	-8.077	5.578	1.676
$T_{hava,\phi,LT}$	Hava	0.1687	-18	101.3	-16.97	6.703	2.68

Eksergoekonomik analizde termostatik genleşme valflerinin yatırım ve işletim maliyeti diğer bileşenlere göre çok küçük maliyette olmasından dolayı hesaplamalarda göz önüne alınmamıştır.

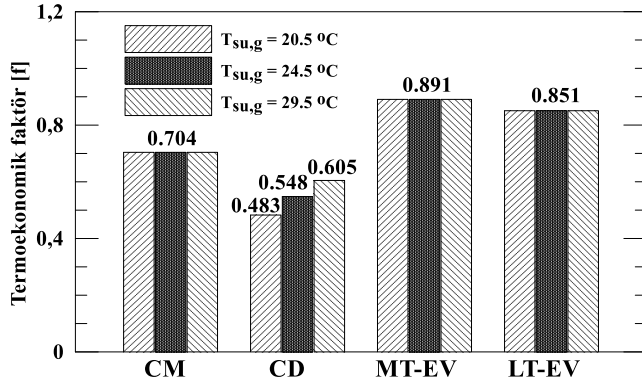
Şekil 4' de kondenser girişinde deniz suyu sıcaklık değişimi ile ekserji tahribat maliyetine olan etkileri ve bileşenlerde oluşan ekserji tahribatı maliyeti değerleri verilmiştir. Kondensere giren deniz suyu sıcaklığı azaldıkça kondenserde oluşan ekserji tahribatı maliyetinin yükseldiği Şekil 4 'te görülmektedir. Kondensere giren deniz suyu sıcaklığının ekserji tahribatı maliyetine olan etkileri CM, MT-EV ve LT-EV 'de görülmemektedir.



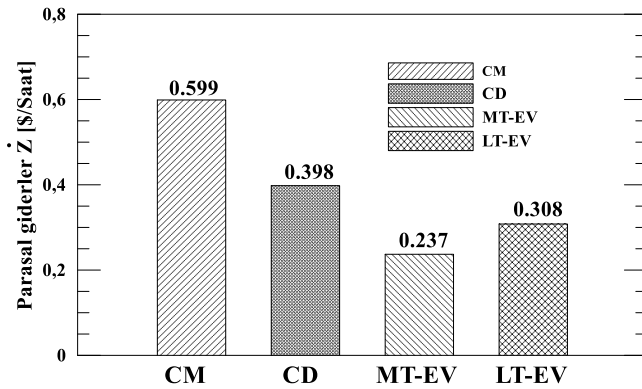
Şekil 4. Ekserji tahribatı maliyetinin bileşenlerdeki değerleri

Soğutma sisteminin bileşenlerine ait termoeconomik faktör değerleri Şekil 5'te verilmiştir. MT evaporatörü, LT evaporatörü ve kompresörün termoeconomiklik kriterlerinin limitlerde olduğu görülmektedir. Şekil 5 incelendiğinde, kondensere ait 0.483, 0.548 ve 0.605 termoeconomik faktör değerlerinden kondenserin ekonomiklik kriterinin en düşük değer aldığı görülmektedir. Mevcut kondenserin ekonomiklik kriterinin kondensere giren deniz suyu sıcaklığı arttıkça iyileştiği görülmektedir.

Yatırım ve işletim maliyetleri en yüksek değerleri kapsadığından, MT ve LT evaporatörlerinin ekonomiklik kriterleri yüksek olarak hesaplanmıştır. Kompresörün izantropik verimi küçük seçildiğinden kompresörün termoeconomiklik kriteri MT ve LT evaporatörlerinin termoeconomik kriterlerinden küçük çıkmıştır. Parasal giderler açısından sistem bileşenleri değerlendirildiğinde, Şekil 6'da görüldüğü gibi, en yüksek maliyetli bileşenin kompresör olduğu bulunmuştur. Çünkü Tablo 3'ten de görüldüğü gibi kompresörün yatırım maliyeti diğer bileşenlerden daha fazladır.



Şekil 5. Sistem bileşenlerinin termoeconomik kriter değerleri



Şekil 6. Sistem bileşenlerinin parasal giderleri

#### 4. Sonuçlar

Bu çalışmada, M/V Saros B kargo gemisinde bulunan ve kondenser ünitesi deniz suyu ile soğutulan bir buhar sıkıştırımlı soğutma sistemine eksergoekonomik analiz uygulanmıştır. Çalışmada kondenserde soğutucu akışkan R22'nin yoğuşma sıcaklığı ile deniz suyu sıcaklık farkı araştırmanın etkin değişken parametresidir. Ekserji tahribatı maliyetleri açısından sistem bileşenleri değerlendirildiğinde kondenser, kompresör, LT evaporatörü ve MT evaporatöründe sırasıyla 0.2552 (\$/saat), 0.2519 (\$/saat), 0.0527 (\$/saat), 0.0288 (\$/saat) olarak hesaplanmıştır. Sistem bileşenleri işletme ve yatırım maliyetleri açısından değerlendirildiğinde, parasal giderler sırasıyla kompresör, kondenser, MT evaporatörü ve LT evaporatöründe, 0.599 (\$/saat), 0.398 (\$/saat), 0.308 (\$/saat) ve 0.237 (\$/saat) olarak bulunmuştur.

#### Yazar Katkıları

Cihan Nacak: Verilerin toplanması, analizi ve makale yazımı konularında katkıda bulunmuştur.

Betül Saraç: Çalışmanın tasarlanması, verilerin analizi ve yorumlanması konularında katkıda bulunmuştur.

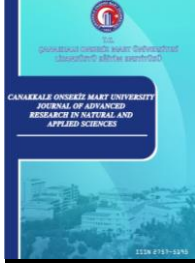
Teoman Ayhan: Verilerin analizi ve yorumlanması konularında katkıda bulunmuştur.

#### Çıkar Çatışması

Yazarlar çıkar çatışması bildirmemişlerdir.

**Kaynaklar**

- Başhan, V., & Parlak, A. (2016). Değişken deniz suyu sıcaklıklarında çalışan bir gemiye ait soğutma sisteminin ekserji analizi. *Journal of Eta Maritime Science*, 4(2), 149-155. <https://doi.org/10.5505/jems.2016.55264>
- Bejan, A., Tsatsaronis, G., & Moran, M. J. (1995). *Thermal design and optimization*. John Wiley & Sons. Erişim adresi: <https://124.im/k5YyT6>
- Cavalcanti, E. J., & Motta, H. P. (2015). Exergoeconomic analysis of a solar-powered/fuel assisted Rankine cycle for power generation. *Energy*, 88, 555-562. <https://doi.org/10.1016/j.energy.2015.05.081>
- Chakyrova, D. (2019). Thermoeconomic analysis of biogas engines powered cogeneration system. *Journal of Thermal Engineering*, 5(2), 93-107. <https://doi.org/10.18186/thermal.532210>
- El-Emam, R. S., & Dincer, I. (2013). Exergy and exergoeconomic analyses and optimization of geothermal organic Rankine cycle. *Applied Thermal Engineering*, 59(1-2), 435-444. <https://doi.org/10.1016/j.applthermaleng.2013.06.005>
- International Maritime Organization (IMO). (2009). Second IMO Greenhouse Gas Study. Erişim adresi: <https://www.imo.org/en/OurWork/Environment/Pages/Second-IMO-GHG-Study-2009.aspx>
- Lozano, M. A., & Valero, A. (1993). Theory of the exergetic cost. *Energy*, 18(9), 939-960. [https://doi.org/10.1016/0360-5442\(93\)90006-Y](https://doi.org/10.1016/0360-5442(93)90006-Y)
- Luo, J., Morosuk, T., Tsatsaronis, G., & Tashtoush, B. (2019). Exergetic and economic evaluation of a transcritical heat-driven compression refrigeration system with CO<sub>2</sub> as the working fluid under hot climatic conditions. *Entropy*, 21(12), 1164. <https://doi.org/10.3390/e21121164>
- Mert, M. S. (2010). *Bir güç santralının ekserjik ve termoekonomik analizi* (Doktora Tezi). Erişim adresi: <http://www.dspace.yildiz.edu.tr/xmlui/bitstream/handle/1/1705/0047328.pdf?sequence=1&isAllowed=y>
- Nacak C. (2020). *Gemi rotasına bağlı olarak gemideki soğutma sisteminin performansının enerji, ekserji, ileri ekserji ve eksergoekonomi yöntemleri kullanarak belirlenmesi*, (Yüksek Lisans Tezi). Erişim adresi: <https://tez.yok.gov.tr/UlusalTezMerkezi/tezDetay.jsp?id=pa87sJKqeKrYeoIRVYHCKg&no=Z-0SA-fAdaqvxxveYaxnnew>
- Nacak, C., & Saraç, B. (2021). The performance assessment of a refrigeration system which exists on a cargo vessel influenced by seawater-intake temperature. *Journal of Thermal Analysis and Calorimetry*, 146, 1229-1243. <https://doi.org/10.1007/s10973-020-10060-y>
- Ortiz, P. S., Flórez-Orrego, D., de Oliveira Junior, S., Maciel Filho, R., Osseweijer, P., & Posada, J. (2020). Unit exergy cost and specific CO<sub>2</sub> emissions of the electricity generation in the Netherlands. *Energy*, 208, 118279. <https://doi.org/10.1016/j.energy.2020.118279>
- Rosen, M. A., & Dincer, I. (2003). Exergoeconomic analysis of power plants operating on various fuels. *Applied thermal engineering*, 23(6), 643-658. [https://doi.org/10.1016/S1359-4311\(02\)00244-2](https://doi.org/10.1016/S1359-4311(02)00244-2)
- Sarac, B. A. (2015). Exergy analysis in the withering process for Turkish black tea production. *International Journal of Exergy*, 18(3), 323-339. <https://doi.org/10.1504/IJEX.2015.072894>
- Siahaya, Y. (2009). Thermoeconomic analysis and optimization of gas turbine power plant. *Parameters*, 86, 86. Erişim adresi: <https://124.im/TSC5>
- Silva, J. A., Flórez-Orrego, D., & Oliveira Jr, S. (2014). An exergy based approach to determine production cost and CO<sub>2</sub> allocation for petroleum derived fuels. *Energy*, 67, 490-495. <https://doi.org/10.1016/j.energy.2014.02.022>
- Soltani, S., Mahmoudi, S. M. S., Yari, M., Morosuk, T., Rosen, M. A., & Zare, V. (2013). A comparative exergoeconomic analysis of two biomass and co-firing combined power plants. *Energy Conversion and Management*, 76, 83-91. <https://doi.org/10.1016/j.enconman.2013.07.030>
- Tsatsaronis, G. (2007). Definitions and nomenclature in exergy analysis and exergoeconomics. *Energy*, 32(4), 249-253. <https://doi.org/10.1016/j.energy.2006.07.002>
- Tsatsaronis, G. (1993). Thermoeconomic analysis and optimization of energy systems. *Progress in energy and combustion science*, 19(3), 227-257. [https://doi.org/10.1016/0360-1285\(93\)90016-8](https://doi.org/10.1016/0360-1285(93)90016-8)
- Valero, A., Serra, L., & Uche, J. (2006). Fundamentals of exergy cost accounting and thermoeconomics. Part I: Theory. <https://doi.org/10.1115/1.2134732>



## Development of Small Hydroelectric Power Plant Maintenance Costs using Chaos Embedded Adaptive Particle Swarm Optimization

Soner Çelikdemir<sup>1\*</sup>, Mahmut Temel Özdemir<sup>2</sup>

<sup>1</sup>Bitlis Eren University, Adilcevaz Vocational High School, Electric and Energy, Bitlis, 13000, Türkiye

<sup>2</sup>Firat University, Engineering Faculty, Electrical and Electronics Engineering, Elazığ, 23000, Türkiye

### Article History

Received: 01.11.2022

Accepted: 17.07.2023

Published: 20.12.2023

### Research Article

**Abstract** – In this study, a new equation model is proposed to improve the maintenance costs of Small Scale Hydroelectric Power Plants (SHPP). The proposed equation model consists of 4 terms and 7 parameters using the Chaos Embedded Adaptive Particle Swarm Optimization (CEAPSO). The MATLAB program was used to calculate the parameters in the proposed equation model. In this study, the main error value for 14 maintenance items required for a SHPP is calculated as 17.4819%. The maintenance cost of a SHPP to be installed in this way can be predicted with high accuracy using the proposed equation model. In the study, the sensitivity analysis of the proposed equation model is also performed, and maintenance cost changes are expressed in different parameter values. In the study, corrected data from 8 SHPP in India are used. These data cover the maintenance costs of all components for the years 2015-2016. In the study, unlike the literature, the flow parameter is added to the power and head parameters. In this way, a more sensitive equation model is developed for SHPP data. In addition, realistic results are obtained by applying constraints to the parameters. Considering the 14 different maintenance cost parameters examined in the study, a correlation model is proposed to give better results than the literature for other maintenance costs except the power channel and penstock cost.

**Keywords** – Chaos embedded adaptive particle swarm optimization, Correlation model, Sensitivity analysis, Small hydroelectric power plants, Maintenance cost estimation

## 1. Introduction

The need for energy is increasing rapidly with developing technology and increasing world population. This increasing need for energy is usually provided by fossil resources. Considering the damage caused by this situation to the environment, the importance of renewable energy sources increases (Dincer, 2012; Uzar, 2020; Karmendra K. A. et al., 2022). Renewable energy sources consist of hydroelectric, wind, solar, geothermal and biomass energy sources.

Hydroelectric energy resources have a great potential for the world. It is important to use this potential efficiently as well as to evaluate it. Cost information is important for evaluating the current potential and converting it into investment. Therefore, cost analysis and estimation is a topic addressed by researchers (Ogayar and Vidal 2009; Aggidis et al. 2010; Cavazzini et al. 2016; Celikdemir, Yildirim, and Ozdemir 2017; Filho, Santos, and Barros 2017;). After the investment decision is taken for a new power plant installation, techno-economic cost information is analyzed. This analysis information influences cost planning. The parameters for installation cost of Small Scale Hydroelectric Power Plant (SHPP) projects are analyzed in three main sections. These are respectively; civil works, hydromechanical and electromechanical equipment. In the studies, cost correlations based on the installed power and head parameters of electromechanical equipment

<sup>1</sup>  scelikdemir@beu.edu.tr

<sup>2</sup>  mto@firat.edu.tr

\*Corresponding Author

have been developed (Mishra et al., 2011). In addition to these parameters, the flow parameter has been added to the equation model as a new approach for cost estimation (Cavazzini et al., 2016; Çelikdemir and Özdemir, 2022). In such a way, the smallest mean error values with the best performance were obtained. In later studies, better results were obtained by developing equation model parameters. Optimization methods were used to determine equation model parameters (Çelikdemir, S. and Ozdemir 2021; Çelikdemir and Özdemir 2022). Further, cost estimates were obtained with less error rate. In the studies examined, head, flow and turbine types parameters were used in the equation models developed by the researchers.

Another issue addressed by researchers is maintenance costs. As result of that, it is seen that increased operating and maintenance costs increase the unit production cost of energy. This increase in the production cost of energy decreased the net profit of the projects. In the studies, different maintenance costs were analyzed and correlations based on power and head parameters were developed (Kumar, Singal, Dwivedi, and Shukla, 2020).

#### Motivation of the Study;

In this study, the maintenance costs of SHPPs, which are not often addressed by researchers, were examined. For this, the previously examined SHPPs in India are addressed. There are two main sources of motivation for this study. First, the flow parameters were also added to the correlation models created by the researchers based on only power and head parameters. In such a way, a more sensitive and comprehensive correlation model was obtained. While developing this correlation model, corrected current data of SHPPs were also used. The second, while the correlation models were being developed, some coefficients were found to be negative because there was no limit on the coefficients of power, head and flow parameters. Such a situation would not reflect reality. Because with increasing flow, power and head parameters, the cost value will decrease. For this, a limitation has been applied to the coefficients of the parameters in the proposed equation model. Thus, these two main issues ignored by the researchers constitute the main motivation of the study.

In this study was carried out in three different stages. First, the error rates of the correlation model developed in the literature were recalculated using the corrected SHPP data. In the second stage, new coefficients were obtained by adding the flow parameter to the correlation equation model. These calculated error values were compared with the error rates in the existing studies. In the last stage, sensitivity analysis was performed. For the sensitivity analysis, the effects of the parameters in the proposed equation model were examined respectively. As a result, the maintenance costs of the equation model proposed in the study were calculated with less errors.

## 2. Materials and methods

In the literature, optimization methods developed in the literature are generally developed for the most appropriate solution to a problem. There are many different optimization algorithms in the literature. Commonly used algorithms; bee algorithm, genetic algorithm, Particle Swarm Algorithm (PSO). The most preferred among these is the PSO. It is an algorithm developed in 1995 (Elbatran et al., 2015). This method imitates the swarming behavior of some living things that live in flocks. These behaviors are both to reach food sources and to be protected from external dangers. This is achieved by communicating with all living things in the swarm. Living things in the swarm consist of  $N$  particles living in an  $n$ -dimensional space. Here  $x_i(t)$  represents the position of particle "i" in iteration "t". This expression is used to evaluate the state of the particle. PSO needs information sharing among the living things in the swarm to solve problems. Each individual updates its position towards the best position in the swarm to avoid danger and forage. He also uses his previous experiences for this. Particles in the swarm set their best position to the personal best position ( $X_{pbest}$ ) and the best position in the whole swarm ( $X_{gbest}$ ). The following equation is used for the next velocity and position of each particle (Alatas et al., 2009; Özdemir, 2021a);

$$v_i(t + 1) = wv_{i,j}(t) + c_1r_1(t) (X_{pbest} - x_{i,j}(t)) + c_2r_2(t) (X_{gbest} - x_{i,j}(t)) \tag{2.1}$$

$$x_i(t + 1) = x_i(t) + v_i(t + 1) \tag{2.2}$$

Where  $c_1$  and  $c_2$   $X_{gbest}$  are velocity factors,  $v_i$  is the velocity of the particles,  $x_i$  is the position of the particle and  $w$  is the inertia coefficient. The flow diagram of the developed CEAPSO algorithm is given in Figure 1 (Alatas et al., 2009). The velocity expression for CEAPSO is given in Equation (2.3).

$$v_i(t + 1) = CM1v_{i,j}(t) + c_1CM2(t) (X_{pbest} - x_{i,j}(t)) + c_2CM3(t) (X_{gbest} - x_{i,j}(t)) \tag{2.3}$$

Where, CM1, CM2, and CM3 are the results of the determined chaotic maps with values between 0-1. There are many CMs used in the literature (Alatas et al., 2009). However, in this study, Chebyshev CM is preferred as the velocity function. In this situation (Özdemir, 2021);

$$CM_{1,2,3} = CM_{t+1} = \cos(n * \arccos(CM_t)) \tag{2.4}$$

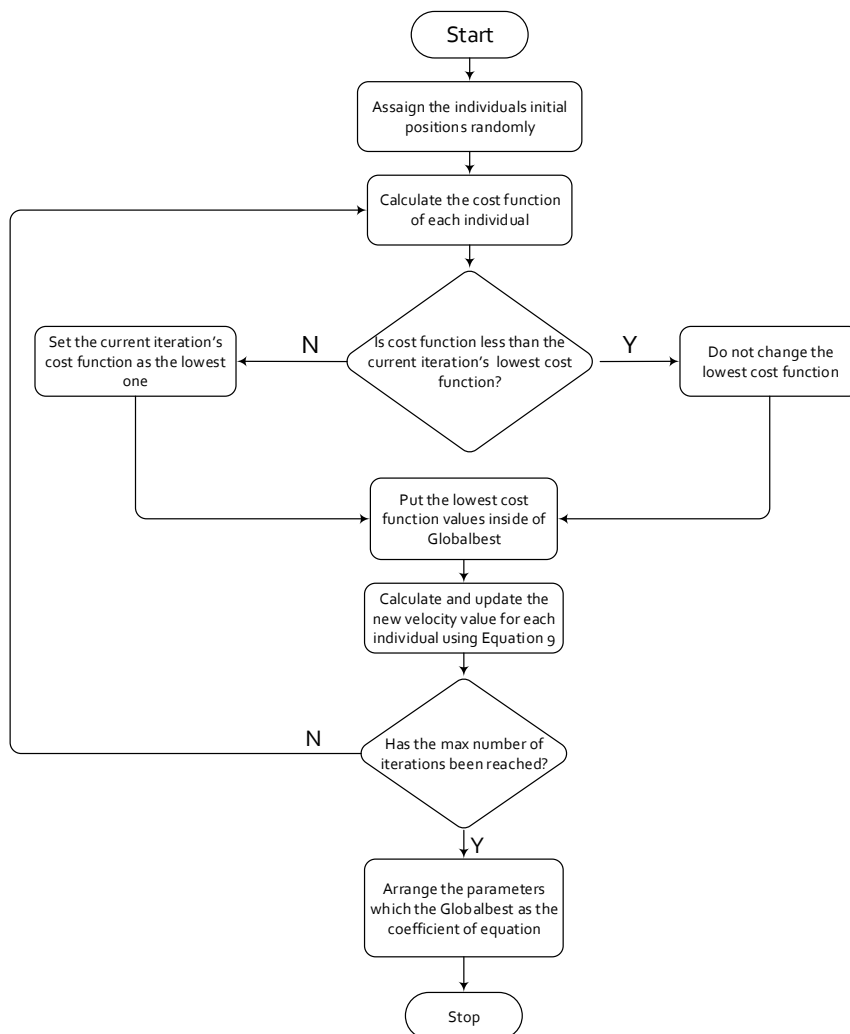


Figure 1. CEAPSO flowchart

The work of CEAPSO, on the other hand, first begins with the determination of the initial positions of the individuals. Then, cost values are calculated for each individual using the cost function. As a result of the calculations, the cycle continues until the lowest cost is calculated. The lowest cost value is assigned as globalbest. The new velocity value is calculated using the velocity equation and the calculations are updated. This process continues until the maximum number of iterations is reached. At the end of the process, the coefficients in globalbest are given as a result. The position and speed values of individuals are determined from the chaotic map. For this, the studies of Alataş et al. were taken as reference. Where, the initial value of CMs was determined as 0.6. In addition, as the other parameter in the CEAPSO algorithm, the number of iterations is 1200, the inertia coefficient is 0.8,  $c_1=0.12$ ,  $c_2=1.2$  and the herd size is 150. It is seen that the best mean error values for the data applied to the heuristic swarm algorithms are CEAPSO. Therefore, CEAPSO was preferred in subsequent studies.

**2.1. Classification of hydropower plant**

SHPPs are classified according to different criteria. These criteria differ from country to country. The differences in the economic and hydraulic potentials of the countries cause this situation. In many countries, the classification of SHPPs is made according to the installed power of the plant. The classification determined by the United Nations Industrial Development Organization (UNIDO) for different countries is given in Table 1.

Table 1  
Worldwide HPP classification

Country	UK	UNIDO	Sweden	Colombia	Australia	India	China	Philippines	New Zealand
Capacity	< 5	< 10	< 15	< 20	< 20	< 25	< 25	< 50	< 50

In addition, different classifications are made according to the head, flow rate, turbine type and structures of SHPPs. SHPPs according to their structures; It is classified as river structure, water storage, channel structure and pump structure.

**2.2. Small hydropower plant and components**

Energy production in river type SHPP’s, which is one of the types of hydroelectric power plants, is proportional to the flow of water. Although the unit costs of small SHPPs are high, they have a long life. In addition, the negative effects on humans and the environment are negligible. A river type SHPP consists of main inlet valve, penstock, power channel, gates, desilting tank. In addition, it consists of turbines, generators, transformer, switchyard, governor, thrust bearing, oil pressure unit, control panel and station auxiliary.

A SHPP consists of construction, electromechanical and hydromechanical equipment and their subcomponents. These components are given in detail in Figure 2 (Kumar et al., 2020).

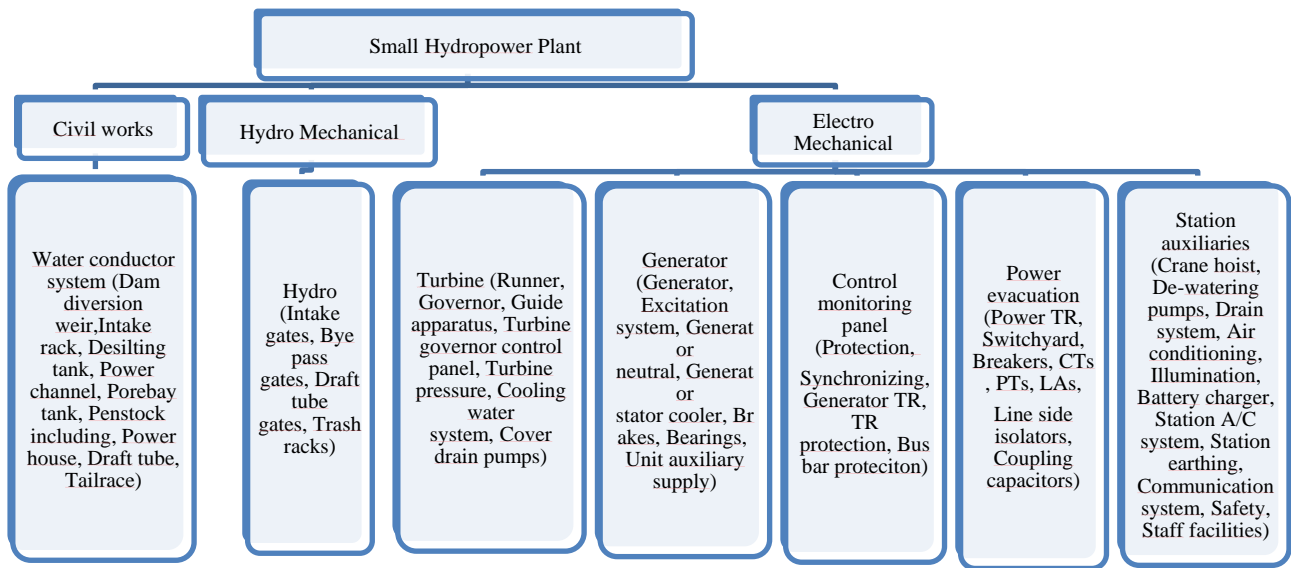


Figure 2. Detail of SHPP components

Repair and maintenance at SHPP directly affect the operating life of the system. Therefore, maintenance work includes regular and systematic work. Effective operation and maintenance is one of the most cost-effective approaches to achieving high energy efficiency. Insufficient maintenance of power plants causes an increase in unit energy costs.

**2.3. Data collection**

In this study, data from 8 SHPP in India were used. These data cover the maintenance costs of all components for the years 2015-2016. The power plant data for SHPP are given in Figure 3 (United Nations Framework Convention on Climate Change, n.d.).

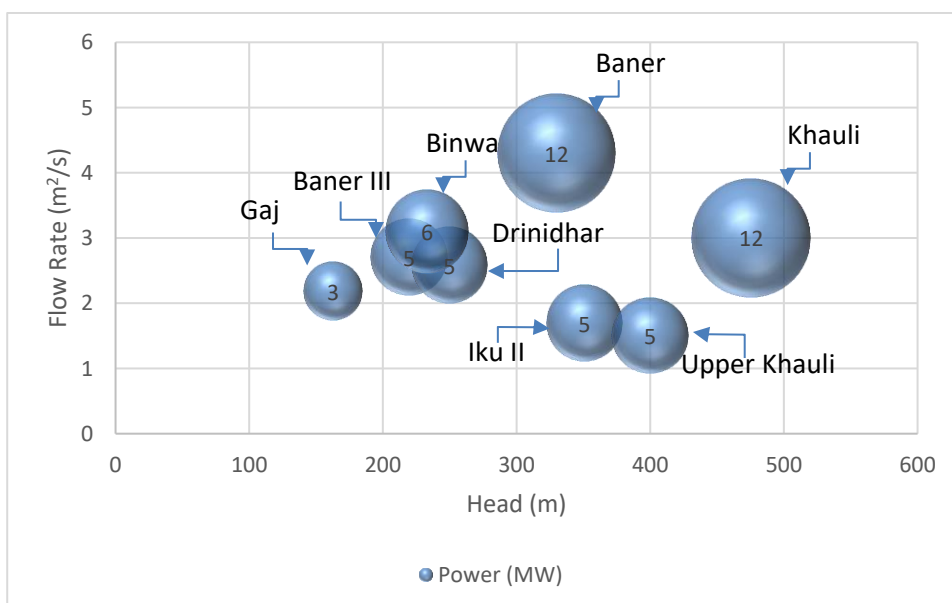


Figure 3. SHPP data diagram

Where, data for 8 SHPPs in India referenced in the study are given. Horizontal axis in Figure 3, the head (m) information of the SHPPs, the vertical axis, the flow rate (m<sup>3</sup>/s) information of the SHPPs and the sizes of the figures on the graph give the installed power (MW) values of the SHPPs.

Table 2  
SHPP data

Plant Name	Power (MW)	Head (m)	Flow (m <sup>3</sup> /s)	Turbine	Date
Baner III	5	219.8	2.7	Pelton	2009
Iku II	5	351	1.69	Pelton	2009
Drinidhar	5	250	2.58	Pelton	2010
Upper Khauli	5	400	1.5	Pelton	2010
Binwa	6	233.2	3.1	Pelton	1984
Baner	12	330.1	4.3	-	1996
Gaj	3	163	2.18	Pelton	1996
Khauli	12	475.7	3	-	2007

In addition, the adjusted data of 8 hydroelectric power plants used in the study are given in Table 3.

#### 2.4. Developed equation model

The power expression of SHPPs is generally expressed as the conversion of potential energy of water into kinetic energy. Flow and head parameters are used in the calculation of power. The expression of the work performed in SHPPs is given in Equation (2.5).

$$dW = \rho g dV H \quad (2.5)$$

Where  $\rho$  is the water density (kg/m<sup>3</sup>),  $dW$  is the work,  $g$  is the gravity constant (m/s<sup>2</sup>),  $dV$  is the volume of the water and  $H$  is the head (m). Equation (2.6) is used for volume information of water (Celikdemir et al., 2017).

$$dq = \frac{dV}{dt} \quad (2.6)$$

Where  $t$  is time (s) and  $q$  is flow rate (m<sup>3</sup>/s). The definition of power is given Equation (2.7);

$$dP = \frac{dW}{dt} \quad (2.7)$$

The arranged form of the equations is given in Equation (2.8) and Equation (2.9).

$$dP = \frac{\rho g dq dt H}{dt} \quad (2.8)$$

$$P = \rho g q h \eta \quad (2.9)$$

Where  $P$  is the power (Watt) converted from the turbine shaft and  $\eta$  the turbine efficiency (%).

In the literature, three basic models are mostly used in proposing cost equations. These models are Sigma, Linest and Logest equation models. Linest equation model is preferred as the most preferred equation model, which is accepted to give correct results by researchers. As this preference factor, Linest equation model was preferred in this study. Many equation models have been proposed in the literature for electromechanical equipment cost estimation of SHPPs. These proposed equation models are given in Equation (2.10).

$$Cost [\text{\$}] = a.P^b + c.H^d + e.Q^f + g \quad (2.10)$$

In Equation (3.10), “a and b” are the expression of power  $P$  (kW), “c and d” are the expression of head  $H$  (m), and “e and f” are the expression of flow  $Q$  (m<sup>3</sup>/s). Where the coefficients are constrained to be positive for them. In this situation, more realistic results are obtained.

In the study, the maintenance costs of SHPPs, which are not often addressed by researchers, were examined. For this, few data available in the literature with the SHPPs in India belonging to the study were examined.

One of the motivation sources of the study was to propose an equation model with less mean. While doing this, it is aimed to obtain a more general expression and realistic results. The calculated results were compared with the literature results. (Kumar et al., 2020).

### 3. Result and discussion

The cost data used in the calculations were calculated in dollars over the exchange rate of the maintenance year using the Central Bank data. The coefficients in Equation 2.10 have been developed for the estimation of electromechanical equipment cost calculation of SHPPs. CEAPSO was used to calculate these values. MATLAB program was used to calculate the parameters of the proposed equation model. The calculated coefficients are given in Table 2 (Wang et al., 2022). The corrected data of 8 hydropower plants used in the study are given in Table 3. Corrected data are from Clean Development Mechanism (CDM).

Table 3

Calculated coefficient parameters

Component	a	b	c	d	e	f	g
Turbine	0.698557	4.294794	32.72562	0.562217	2081.046	1.714907	144.5411
Main inlet valve (MIV)	851.2471	0.791228	7.01079	0.791732	3.874605	4.081728	-264.658
Generator	1047.519	1.107083	10.67688	0.132195	74.67233	2.901739	96.94424
Thrust bearing	0.393331	3.707275	8.8809	0.816154	0.190436	5.783192	6.051182
Governor	678.0206	1.023596	0.464932	0.452947	124.7796	2.193964	-25.8276
Oil pressure unit (OPU)	107.4133	1.462108	12.2603	0.462201	196.0348	1.633853	794.357
Control panel	27.75594	2.568188	2.860927	0.718667	4112.165	0.762245	-5344.14
Transformer	3.517244	2.530749	0.742108	1.258029	0.555896	4.256665	897.8485
Switchyard	1.857732	2.49357	10.71817	0.915983	4.046528	4.305202	4758.941
Desilting tank	0.997891	2.811734	359.8555	0.429108	0.487902	4.863487	-1.93133
Power channel	0.001008	0.286092	11139.34	1.07E-06	14.14716	9.72E-06	-653.26
Penstock	1.68E-05	0.079193	419.7806	0.386657	39.57226	0.00281	-8.27214
Gates	11.21851	2.729121	0.006329	0.361564	2818.363	0.683863	-3780.71
Station auxiliaries	46.02745	0.562321	2.91556	1.229814	515.1306	1.538834	1297.404

In this section, 14 different maintenance cost data for 8 hydroelectric power plants are analyzed. The cost and error rates calculated as a result of the analysis are given in Table 4. For this, the 4 term 7 parameter equation model in the proposed Equation 3.10 was used.

Table 4  
Costs and error rates of hydroelectric power plants

Component	Plant Name	Actual Maintenance	(Kumar et al., 2020) Cost	(Kumar et al., 2020) Error	(Kumar et al., 2020) Cost (Corrected)	(Kumar et al., 2020) Error (Corrected)	Analysed Maintenance	Analysed Error
Turbine	Baner III	3311.26	3564.35	-7.64	4888.34	-47.63	4289.54	-29.54
	Iku II	2317.88	2554.27	-10.20	2849.53	-22.94	2267.20	2.19
	Drinidhar	4966.89	4341.34	12.59	4419.04	11.03	4022.55	19.01
	Upper Khauli	1490.07	1458.72	2.10	2088.08	-40.13	1976.03	-32.61
	Binwa	6622.52	6796.33	-2.62	6796.33	-2.62	5584.94	15.67
	Baner	17935.98	17987.88	-0.29	17987.88	-0.29	18715.07	-4.34
	Gaj	16556.29	16634.80	-0.47	1538.55	90.71	2886.08	82.57
	Khauli	15866.45	15725.30	0.89	15725.30	0.89	14907.12	6.05
Main inlet valve (MIV)	Baner III	1158.94	1189.75	-2.66	1241.92	-7.16	1159.43	-0.04
	Iku II	1192.05	1149.96	3.53	1161.59	2.56	1170.85	1.78
	Drinidhar	1158.94	1220.37	-5.30	1223.43	-5.56	1164.71	-0.50
	Upper Khauli	1192.05	1106.79	7.15	1131.59	5.07	1192.85	-0.07
	Binwa	1379.69	1430.60	-3.69	1430.60	-3.69	1379.70	0.00
	Baner	2649.01	2552.60	3.64	2552.60	3.64	2648.92	0.00
	Gaj	8278.15	2329.02	1.53	882.92	89.33	746.53	90.98
	Khauli	2345.47	2463.45	-5.03	2463.45	-5.03	2345.27	0.01
Generator	Baner III	2317.88	2472.20	-6.66	2821.75	-21.74	2541.24	-9.64
	Iku II	2384.11	2205.53	7.49	2283.48	4.22	2213.62	7.15
	Drinidhar	2483.44	2677.33	-7.81	2697.85	-8.63	2486.81	-0.14
	Upper Khauli	2152.32	1916.29	10.97	2082.45	3.25	2180.60	-1.31
	Binwa	3311.26	3424.39	-3.42	3424.39	-3.42	3219.83	2.76
	Baner	7174.39	6972.54	2.81	6972.54	2.81	7174.33	0.00
	Gaj	23178.81	6466.94	2.35	1739.55	92.50	1446.81	93.76
	Khauli	6070.64	6375.19	-5.02	6375.19	-5.02	6070.61	0.00

Table 4

Costs and error rates of hydroelectric power plants (continued)

<b>Thurst bearing</b>	<b>Baner III</b>	0.00	41.14	0.00	0.00	0.00	0.00	0.00
	<b>Iku II</b>	0.00	-16.78	0.00	0.00	0.00	0.00	0.00
	<b>Drinidhar</b>	0.00	85.69	0.00	0.00	0.00	0.00	0.00
	<b>Upper Khauli</b>	0.00	-79.60	0.00	0.00	0.00	0.00	0.00
	<b>Binwa</b>	397.35	382.67	3.70	382.67	3.70	397.39	-0.01
	<b>Baner</b>	1931.57	1961.62	-1.56	1961.62	-1.56	1931.67	-0.01
	<b>Gaj</b>	6070.64	1649.73	4.89	-387.43	106.38	203.27	96.65
	<b>Khauli</b>	1793.60	1831.88	-2.13	1831.88	-2.13	1793.48	0.01
<b>Governor</b>	<b>Baner III</b>	1324.50	1441.22	-8.81	1623.58	-22.58	1524.42	-15.09
	<b>Iku II</b>	1324.50	1302.09	1.69	1342.76	-1.38	1290.29	2.58
	<b>Drinidhar</b>	1490.07	1548.24	-3.90	1558.94	-4.62	1489.86	0.01
	<b>Upper Khauli</b>	1258.28	1151.19	8.51	1237.88	1.62	1260.34	-0.16
	<b>Binwa</b>	1986.75	19309917.8	2.81	1930.99	2.81	1893.00	4.72
	<b>Baner</b>	3863.14	3.74	3.18	3740.14	3.18	3864.17	-0.03
	<b>Gaj</b>	12130.79	3.49	-0.60	1072.97	91.15	912.61	92.48
	<b>Khauli</b>	3311.26	3.43	-3.54	3428.50	-3.54	3310.95	0.01
<b>Oil pressure unit (OPU)</b>	<b>Baner III</b>	927.15	957.51	-3.27	1056.28	-13.93	1015.19	-9.50
	<b>Iku II</b>	927.15	882.16	4.85	904.19	2.48	851.09	8.20
	<b>Drinidhar</b>	993.38	1015.48	-2.22	1021.27	-2.81	994.65	-0.13
	<b>Upper Khauli</b>	827.81	800.43	3.31	847.38	-2.36	827.80	0.00
	<b>Binwa</b>	1214.13	1237.24	-1.90	1237.24	-1.90	1214.13	0.00
	<b>Baner</b>	2373.07	2303.85	2.92	2303.85	2.92	2371.51	0.07
	<b>Gaj</b>	7505.52	2144.98	-0.03	729.15	90.29	714.97	90.47
	<b>Khauli</b>	2069.54	2135.06	-3.17	2135.06	-3.17	2069.54	0.00
<b>Control panel</b>	<b>Baner III</b>	1324.50	1420.35	-7.24	1891.77	-42.83	1752.60	-32.32
	<b>Iku II</b>	1059.60	1060.70	-0.10	1165.82	-10.02	899.00	15.16
	<b>Drinidhar</b>	1655.63	1697.00	-2.50	1724.67	-4.17	1658.15	-0.15
	<b>Upper Khauli</b>	728.48	670.61	7.94	894.70	-22.82	728.78	-0.04
	<b>Binwa</b>	2759.38	2719.28	1.45	2719.28	1.45	2419.38	12.32
	<b>Baner</b>	7312.36	7593.06	-3.84	7593.06	-3.84	7861.95	-7.52
	<b>Gaj</b>	24834.44	6889.05	2.91	402.74	98.38	888.00	96.42
	<b>Khauli</b>	6898.45	6787.43	1.61	6787.43	1.61	6886.99	0.17

Table 4  
Costs and error rates of hydroelectric power plants (continued)

<b>Transformer</b>	<b>Baner III</b>	596.03	636.99	-6.87	532.63	10.64	595.50	0.09
	<b>Iku II</b>	761.59	716.60	5.91	693.33	8.96	758.75	0.37
	<b>Drinidhar</b>	529.80	575.74	-8.67	569.62	-7.52	631.46	-19.19
	<b>Upper Khauli</b>	827.81	802.95	3.00	753.34	9.00	827.99	-0.02
	<b>Binwa</b>	662.25	649.54	1.92	649.54	1.92	662.50	-0.04
	<b>Baner</b>	1379.69	1371.21	0.62	1371.21	0.62	1378.13	0.11
	<b>Gaj</b>	3863.14	1076.91	2.43	262.07	93.22	470.25	87.83
	<b>Khauli</b>	1517.66	1549.54	-2.10	1549.54	-2.10	1517.78	-0.01
<b>Switchyard</b>	<b>Baner III</b>	2317.88	2313.08	0.21	2283.20	1.50	2202.14	4.99
	<b>Iku II</b>	2384.11	2335.87	2.02	2329.21	2.30	2384.00	0.00
	<b>Drinidhar</b>	2185.43	2295.54	-5.04	2293.79	-4.96	2247.06	-2.82
	<b>Upper Khauli</b>	2483.44	2360.59	4.95	2346.39	5.52	2475.66	0.31
	<b>Binwa</b>	2317.88	2408.00	-3.89	2408.00	-3.89	2327.71	-0.42
	<b>Baner</b>	3311.26	3162.57	4.49	3162.57	4.49	3312.46	-0.04
	<b>Gaj</b>	10485.65	2941.33	1.82	2023.09	80.71	2000.80	80.92
	<b>Khauli</b>	3035.32	3213.63	-5.87	3213.63	-5.87	3035.35	0.00
<b>Desilting tank</b>	<b>Baner III</b>	1456.95	1411.05	3.15	1289.29	11.51	1255.43	13.83
	<b>Iku II</b>	1655.63	1503.95	9.16	1476.79	10.80	1505.38	9.08
	<b>Drinidhar</b>	1192.05	1339.60	-12.38	1332.45	-11.78	1319.88	-10.72
	<b>Upper Khauli</b>	1589.40	1604.70	-0.96	1546.82	2.68	1589.45	0.00
	<b>Binwa</b>	1324.50	1379.57	-4.16	1379.57	-4.16	1326.25	-0.13
	<b>Baner</b>	1986.75	1944.81	2.11	1944.81	2.11	1986.75	0.00
	<b>Gaj</b>	6070.64	1670.62	3.68	1065.86	82.44	1073.97	82.31
	<b>Khauli</b>	2069.54	2152.89	-4.03	2152.89	-4.03	2069.54	0.00
<b>Power channel</b>	<b>Baner III</b>	3642.38	3884.60	-6.65	3424.75	5.98	3476.92	4.54
	<b>Iku II</b>	4304.64	4.24	1.61	4132.88	3.99	3476.92	19.23
	<b>Drinidhar</b>	3476.82	3614.74	-3.97	3587.75	-3.19	3476.92	0.00
	<b>Upper Khauli</b>	4768.21	4615.94	3.19	4397.35	7.78	3476.92	27.08
	<b>Binwa</b>	3311.26	3130.85	5.45	3130.85	5.45	3476.92	-5.00
	<b>Baner</b>	1490.07	1456.50	2.25	1456.50	2.25	3476.92	-133.34
	<b>Gaj</b>	4966.89	1373.27	3.23	3850.63	22.47	3476.92	30.00
	<b>Khauli</b>	2152.32	2242.35	-4.18	2242.35	-4.18	3476.92	-61.54

Table 4  
Costs and error rates of hydroelectric power plants (continued)

<b>Pentstock</b>	<b>Baner III</b>	1324.50	1369.87	-343.00	1119.29	15.49	1128.75	14.78
	<b>Iku II</b>	1655.63	1561.04	5.71	1505.16	9.09	1350.61	18.42
	<b>Drinidhar</b>	1125.83	1222.82	-8.61	1208.11	-7.31	1185.83	-5.33
	<b>Upper Khauli</b>	1821.19	1768.38	2.90	1649.27	9.44	1420.06	22.03
	<b>Binwa</b>	1103.75	1121.62	-1.62	1121.62	-1.62	1154.64	-4.61
	<b>Baner</b>	1241.72	1184.09	4.64	1184.09	4.64	1319.20	-6.24
	<b>Gaj</b>	3311.26	895.03	5.40	1026.41	69.00	1006.66	69.60
	<b>Khauli</b>	1517.66	1612.31	-6.24	1612.31	-6.24	1517.80	-0.01
<b>Gates</b>	<b>Baner III</b>	662.25	697.43	-5.31	1034.57	-56.22	889.09	-34.25
	<b>Iku II</b>	450.33	440.23	2.24	515.41	-14.45	384.47	14.62
	<b>Drinidhar</b>	827.81	895.28	-8.15	915.07	-10.54	832.74	-0.60
	<b>Upper Khauli</b>	165.56	161.27	2.59	321.52	-94.20	279.83	-69.02
	<b>Binwa</b>	1655.63	1548.43	6.47	1548.43	6.47	1265.06	23.59
	<b>Baner</b>	4552.98	4566.33	-0.29	4566.33	-0.29	4553.06	0.00
	<b>Gaj</b>	14569.54	4179.75	-0.41	125.55	99.14	412.79	97.17
	<b>Khauli</b>	4001.10	3990.19	0.27	3990.20	0.27	4000.84	0.01
<b>Station auxilia- ries</b>	<b>Baner III</b>	1986.75	2140.10	-7.72	2104.01	-5.90	1986.58	0.01
	<b>Iku II</b>	2152.32	2167.63	-0.71	2159.58	-0.34	2152.82	-0.02
	<b>Drinidhar</b>	1986.75	2118.92	-6.65	2116.80	-6.55	2059.14	-3.64
	<b>Upper Khauli</b>	2317.88	2197.48	5.19	2180.33	5.93	2315.88	0.09
	<b>Binwa</b>	2483.44	2273.07	8.47	2273.07	8.47	2232.27	10.11
	<b>Baner</b>	3311.26	3294.37	0.51	3294.37	0.51	3309.14	0.06
	<b>Gaj</b>	10485.65	2999.67	-0.13	1753.20	83.28	1531.11	85.40
	<b>Khauli</b>	3311.26	3356.03	-1.35	3356.03	-1.35	3310.01	0.04

In this study, a correlation model was developed by examining the maintenance costs of 8 river type SHPPs in India. For this, realistic maintenance costs and adjusted plant data for the years 2015-2016 were used. Developed and literature correlation model mean error results are given in Table 5.

Table 5  
Error rates of maintenance costs

Parameters	Max. Error (%)		Min. Error (%)		Standart Deviation		Mean Error	
	(Kumar et al., 2020)	Proposed Model	(Kumar et al., 2020)	Proposed Model	(Kumar et al., 2020)	Proposed Model	(Kumar et al., 2020)	Proposed Model
<b>Turbine</b>	11.030	19.013	-47.628	-32.614	19.508	12.203	27.030	23.998
<b>MIV</b>	5.072	1.779	-7.160	-0.498	1.516	0.658	15.256	11.672
<b>Generator</b>	4.221	7.151	-21.738	-9.636	6.782	3.881	17.698	14.345
<b>Thrust B.</b>	3.695	0.006	-2.135	-0.011	1.106	0.003	14.221	12.084
<b>Governor</b>	3.184	4.719	-22.580	-15.094	7.536	5.534	16.361	14.386
<b>OPU</b>	2.917	8.203	-13.928	-9.495	4.299	4.315	14.981	13.546
<b>Control P.</b>	1.609	15.157	-42.829	-32.321	15.370	11.751	23.140	20.513
<b>Tr.</b>	10.637	0.373	-7.516	-19.189	4.127	7.213	16.745	13.457
<b>Switchyard</b>	5.519	4.993	-5.875	-2.820	1.638	1.942	13.654	11.189
<b>D. Tank</b>	11.508	13.832	-11.778	-10.723	4.407	6.135	16.188	14.509
<b>Power C.</b>	7.778	27.081	-4.183	-133.340	1.857	47.844	6.911	35.092
<b>Penstock</b>	15.493	22.026	-7.309	-6.240	4.365	8.195	15.354	17.627
<b>Gates</b>	6.475	23.590	-94.200	-69.016	35.686	25.242	35.199	29.907
<b>Station A.</b>	8.471	10.114	-6.546	-3.644	3.324	3.822	14.042	12.422
<b>Mean Error of Absolute Values</b>							17.62	17.48

Considering the 14 different maintenance cost parameters examined in the study, the correlation model was carried out to give better results than the literature for 12 maintenance costs except the power channel and penstock cost. In addition, the best error values are shown in green in Table 5. The reason why the correlation model developed for these two maintenance costs gave worse results is that there is no limitation to the head, flow and power parameters, which are not discussed in the literature. On the other hand, the developed correlation model gives more realistic results. Although the correlation model developed for the power channel and penstock cost gives worse results, the total mean error still gives better results than the literature. The main error results of the correlation model developed and in the literature are given in Figure 4.

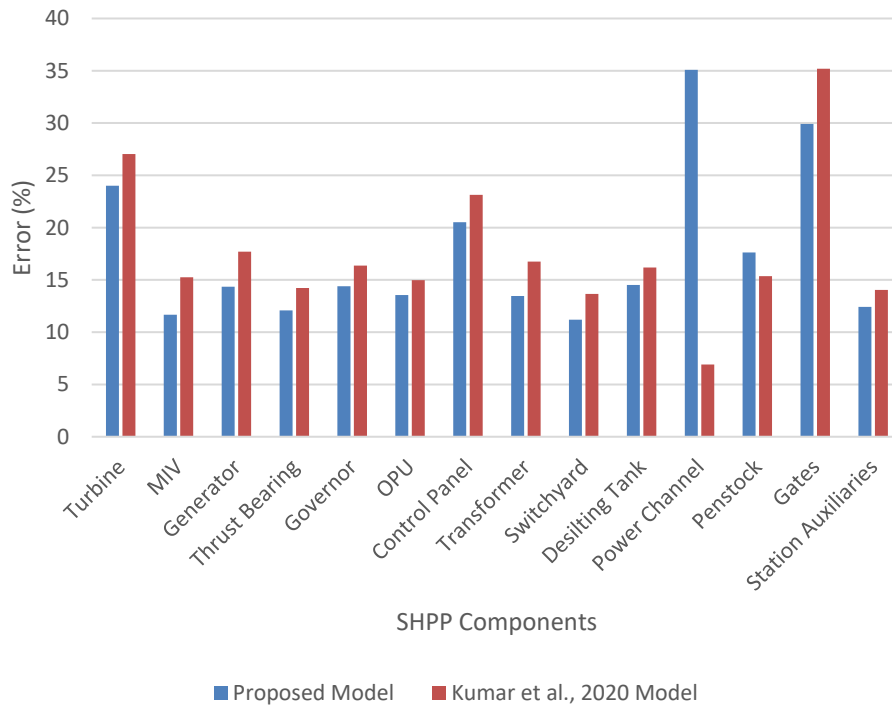


Figure 4. Literature and proposed equation model mean error values

The standard deviation results of the correlation model developed in the literature are given in Figure 5.

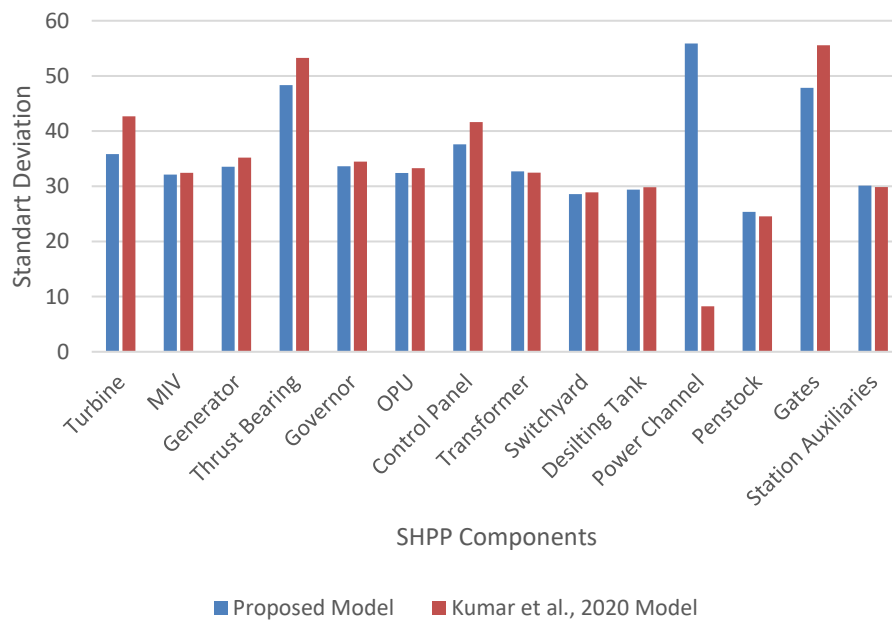


Figure 5. Literature and proposed equation model standard deviation error values

Similarly, when the results of the developed and literature correlation model are examined, the biggest error rate belongs to Gaj SHPP. Since this error rate is not within the acceptable range, it can be assumed that there is an error in the data and maintenance costs of this plant.

In this section, a sensitivity analysis was performed. The effect of the parameters in the equation model proposed for the sensitivity analysis was examined. For this, the changes of the parameters in the proposed

equation model were examined respectively. In this way, the effect of the parameters on the cost can be seen clearly. In the proposed equation model, sensitivity analyses for some maintenance costs were examined using the coefficients in Table 2.

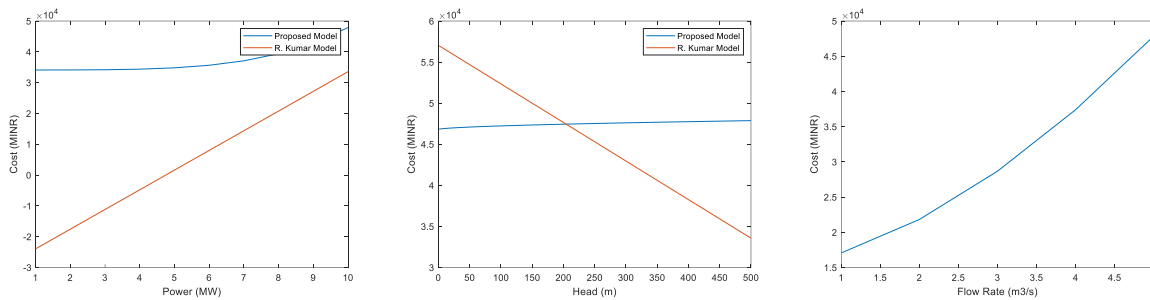


Figure 6. Sensitivity analysis for turbine cost

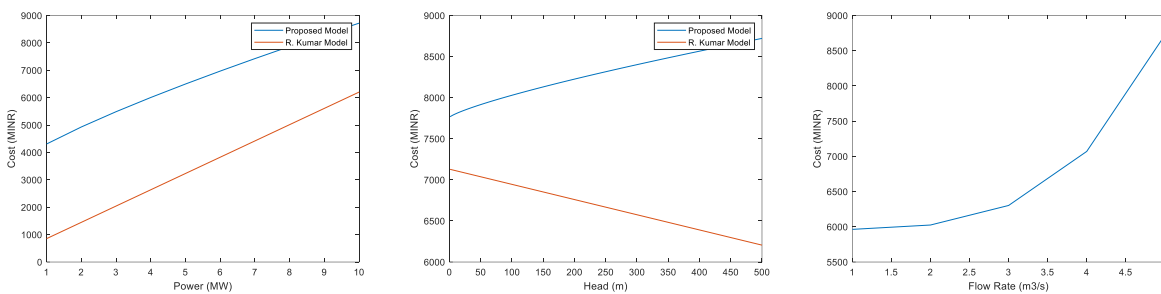


Figure 7. Sensitivity analysis for MIV cost

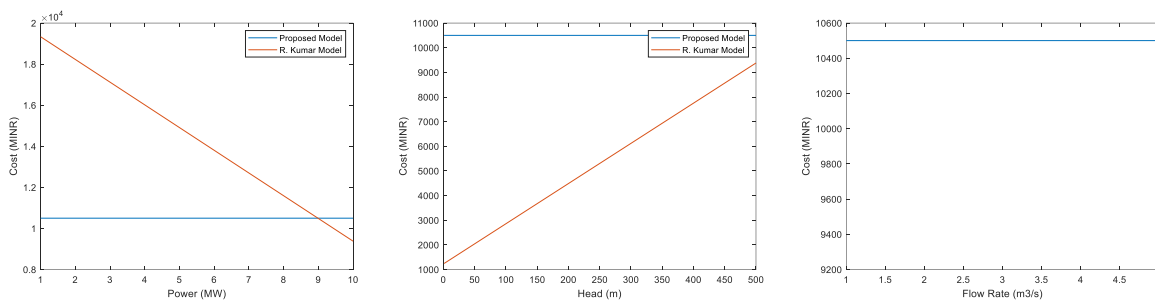


Figure 8. Sensitivity analysis for power channel cost

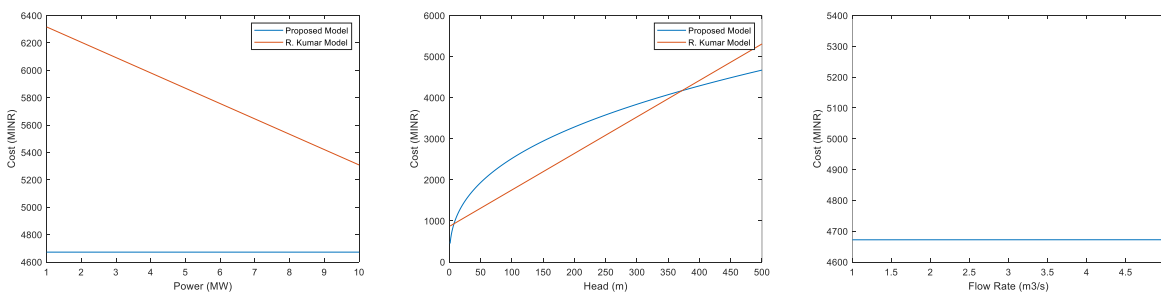


Figure 9. Sensitivity analysis for penstock cost

Sensitivity analysis of turbine maintenance costs is given in Figure 6. According to this; in the literature correlation, it is seen that the maintenance cost decreases with the increasing flow parameter, but the maintenance cost increases in the developed correlation. Similarly, the sensitivity analysis of main inlet valve maintenance costs is given in Figure 7. According to this; In the literature correlation, it is seen that the maintenance cost decreases with the increasing flow parameter, but the maintenance cost increases in the

developed correlation. Sensitivity analysis of power channel maintenance costs is given in Figure 8. According to this; in the literature correlation, it is seen that the maintenance cost decreases with the increasing power parameter, but the maintenance cost increases in the developed correlation. Similarly, the sensitivity analysis of penstock maintenance costs is given in Figure 9. According to this; in the literature correlation, it is seen that the maintenance cost decreases with the increasing power parameter, but the maintenance cost increases in the developed correlation.

#### 4. Conclusions

Maintenance costs of power plants have a direct impact on the unit production cost of energy. Therefore, it is important to carry out regular and periodic maintenance in order to reduce the unit cost of energy and increase the operating life of the power plant. In this study, a realistic correlation model is proposed for investment costs. The correlation model is proposed with 4 terms and 7 parameters. In the study, model parameters were determined by using the CEAPSO, which was developed because it has many advantages.

Considering the 14 different maintenance cost parameters examined in the study, a correlation model was proposed to give better results than the literature for other maintenance costs except the power channel and penstock cost. With this study, the cost of a SHPP to be maintained can be predicted with high accuracy using the proposed equation model. Also, in the future, its accuracy can be further improved by adding new SHPP data to the proposed equation model. The equation model proposed in this study can be improved by adding different parameters.

The literature of this study;

- ✓ Suggesting a more sensitive equation model by adding a new parameter to the correlation model,
- ✓ Obtaining more realistic results by limiting head, flow and power parameters in the correlation model,
- ✓ Suggesting a CEAPSO algorithm to estimate of cost equation parameters

contributions have been made.

#### Acknowledgement

This research did not receive a grant from any funding agency.

#### Author contributions

The authors declared that they contributed equally to the article.

#### Conflicts of interest

The authors declare no conflict of interest.

#### References

- Aggidis, G. A., Luchinskaya, E., Rothschild, R., & Howard, D. C. (2010). The costs of small-scale hydro power production: Impact on the development of existing potential. *Renewable Energy*. <https://doi.org/10.1016/j.renene.2010.04.008>
- Alatas, B., Akin, E., & Ozer, A. B. (2009). Chaos embedded particle swarm optimization algorithms. *Chaos, Solitons & Fractals*, 40(4), 1715–1734. <https://doi.org/10.1016/j.chaos.2007.09.063>
- Cavazzini, G., Santolin, A., Pavesi, G., & Ardizzon, G. (2016). Accurate estimation model for small and micro hydropower plants costs in hybrid energy systems modelling. *Energy*. <https://doi.org/10.1016/j.energy.2016.03.024>
- Çelikdemir, S. and Özdemir, M. T. (2021). A New Methodological Approach for the Techno-Economic Analysis of Hydroelectric Power Plants in Turkey. *TUBA World Conference on Energy Science and Technology (TUBA WCEST-2021)*.

- Çelikdemir, S., & Özdemir, M. T. (2022). A new approach in the cost estimation of a hydroelectric power plants in Türkiye based on geographical features. *International Journal of Energy Research*, 46(14), 20858–20872. <https://doi.org/10.1002/er.8384>
- Celikdemir, S., Yildirim, B., & Ozdemir, M. T. (2017). Cost Analysis of Mini Hydro Power Plant Using Bacterial Swarm Optimization. *International Journal of Energy and Smart Grid*. <https://doi.org/10.23884/IJESG.2017.2.2.05>
- Dincer, I. (2012). Green methods for hydrogen production. *International Journal of Hydrogen Energy*, 37(2), 1954–1971. <https://doi.org/10.1016/j.ijhydene.2011.03.173>
- Elbatran, A. H., Yaakob, O. B., Ahmed, Y. M., & Shabara, H. M. (2015). Operation, performance and economic analysis of low head micro-hydropower turbines for rural and remote areas: A review. In *Renewable and Sustainable Energy Reviews*. <https://doi.org/10.1016/j.rser.2014.11.045>
- Filho, G. L. T., Santos, I. F. S. dos, & Barros, R. M. (2017). Cost estimate of small hydroelectric power plants based on the aspect factor. In *Renewable and Sustainable Energy Reviews*. <https://doi.org/10.1016/j.rser.2017.03.134>
- Karmendra Kumar Agrawal, Shibani Khanra Jha, Ravi Kant Mittal, S. V. (2022). Assessment of floating solar PV (FSPV) potential and water conservation: Case study on Rajghat Dam in Uttar Pradesh, India. *Energy for Sustainable Development*, 66, 287–295. <https://doi.org/https://doi.org/10.1016/j.esd.2021.12.007>
- Kumar, R., Singal, S. K., Dwivedi, G., & Shukla, A. K. (2020). Development of maintenance cost correlation for high head run of river small hydro power plant. *International Journal of Ambient Energy*. <https://doi.org/10.1080/01430750.2020.1804447>
- Mishra, S., Singal, S. K., & Khatod, D. K. (2011). Approach for Cost Determination of Electro-Mechanical Equipment in Ror Shp Projects. *Smart Grid and Renewable Energy*. <https://doi.org/10.4236/sgre.2011.22008>
- Ogayar, B., & Vidal, P. G. (2009). Cost determination of the electro-mechanical equipment of a small hydro-power plant. In *Renewable Energy*. <https://doi.org/10.1016/j.renene.2008.04.039>
- Özdemir, M. T. (2021a). A novel optimum PI controller design based on stability boundary locus supported particle swarm optimization in AVR system. *Turkish Journal of Electrical Engineering & Computer Sciences*, 29(1), 291–309. <https://doi.org/10.3906/elk-1910-81>
- Özdemir, M. T. (2021b). Optimal parameter estimation of polymer electrolyte membrane fuel cells model with chaos embedded particle swarm optimization. *International Journal of Hydrogen Energy*, 46(30), 16465–16480. <https://doi.org/10.1016/j.ijhydene.2020.12.203>
- United Nations Framework Convention on Climate Change*. (n.d.). <http://cdm.unfccc.int/Reference/Documents>
- Uzar, U. (2020). Political economy of renewable energy: Does institutional quality make a difference in renewable energy consumption? *Renewable Energy*. <https://doi.org/10.1016/j.renene.2020.03.172>
- Wang, J., Yang, B., Chen, Y., Zeng, K., Zhang, H., Shu, H., & Chen, Y. (2022). Novel phasianidae inspired peafowl (*Pavo muticus/cristatus*) optimization algorithm: Design, evaluation, and SOFC models parameter estimation. *Sustainable Energy Technologies and Assessments*. <https://doi.org/10.1016/j.seta.2021.101825>



# Volatile Organic Compounds, Total Phenolic Content, Color, and Heating Uniformity of Lemon Peel as Affected by Rotational Speed of Turntable During Microwave Drying

Işıl Barutçu Mazi<sup>1,\*</sup>, Sevilay San<sup>2</sup>

<sup>1,2</sup> Department of Food Engineering, Faculty of Agriculture, Ordu University, Ordu, Türkiye

## Article History

Received: 05.08.2023

Accepted: 14.09.2023

Published: 20.12.2023

## Research Article

**Abstract** – In this study, the effects of rotational speed of microwave turntable (0, 6.5, 9.5, and 12.5 rpm) on surface temperature distribution of lemon peels during drying and, on some quality attributes (color, water activity, total phenolic content (TPC), and volatile organic compounds) of dried lemon peel powders were investigated. The quality analyses were also performed in freeze-dried peels. During microwave drying with rotation, speed of turntable affected the surface temperature values and TPC depending on the power level but did not exert a clear effect on the homogeneity of the surface temperature distribution and the color parameters. The percentage amount of major monoterpene hydrocarbons (limonene,  $\gamma$ -terpinene, myrcene, *p*-cymene, and  $\alpha$ -*p*-dimethylstyrene) detected in fresh lemon peel decreased after microwave and freeze-drying. At 600W, formation of furan compounds (furfural, furfuryl alcohol, tetrahydrofurfuryl alcohol, 2-acetyl furan, 5-methyl furfural, and HMF) were identified. Microwave drying without rotation (0 rpm) caused uneven heating which led to the production of peel powders with unacceptable dark color especially at 450 and 600W. Drying at 600W-0 rpm gave the darkest color, the highest amount of TPC (1730.7 mg GAE/100g d.b.) and furan compounds. Therefore, microwave drying at low power levels with rotation function preserved the quality of lemon peel powder better.

**Keywords** –Lemon peel, microwave drying, turntable speed, uniformity, volatile compound, waste utilization

## 1. Introduction

Citrus peel is the primary by-product of citrus juice processing. Citrus peel is a rich source of valuable phytochemicals, such as phenolic compounds, carotenoids, dietary fibers, ascorbic acid, and essential oils (Singh et al., 2020). Since it contains many valuable substances, it may be utilized as a source of healthy and functional ingredient in food industry. There are various studies in literature where dried powder of citrus by-products has been used in preparation of various foods like bread, sausage, yogurt, ice cream (Han et al., 2021; Yi et al., 2014; Crizel et al., 2014; Tomaschunas et al., 2013). Positive results have been obtained from the incorporation of citrus by-product powders into different food products depending on the dose and properties of powder. The use of this by-product in food formulations provides economic benefits to food industries without sacrificing the environment.

The quality of peel powder is important to obtain the desired food characteristics. It is well known that drying conditions during powder processing greatly influence the physicochemical or nutritional properties of the final product (Karam et al., 2016). So, the application of proper drying treatment is important to obtain high quality product while extending its storage life. Various studies have been performed to investigate the effects of different drying treatments on physicochemical, nutritional, and technological properties of citrus peels. Drying of citrus peels may promote important modifications affecting phenolic compounds (M'Hiri et al.,

<sup>1</sup> [ibarutcu@odu.edu.tr](mailto:ibarutcu@odu.edu.tr)

<sup>2</sup> [sevilaysan1993@gmail.com](mailto:sevilaysan1993@gmail.com)

\*Corresponding Author

2017), induce significant changes in color parameters (Ghanem et al., 2012, 2020) depending on the method of drying and type of citrus. Drying process was shown to have remarkable effect on the compounds identified in essential oils extracted from citrus peels (Tekgül & Baysal, 2018, 2019; Zhang et al., 2018; Farahmandfar et al., 2020; Kamal et al., 2011).

Microwave drying has been used by some researchers for drying of citrus peels (Ozcan et al., 2020; Farahmandfar et al., 2019, 2020; Abou Arab et al., 2017; Mahmoud et al., 2015; Ghanem et al., 2012, 2020; Bejar et al., 2011b; Tekgül & Baysal, 2018; Tuncer et al., 2020; Assefa & Keum, 2017). During microwave drying, volumetric heat generation occurs within the product. This offers opportunity of higher drying rate, especially in the falling rate period compared to traditional drying methods. Microwave power level affects the rate of drying. The effect of microwave power level was studied by Ghanem et al. (2012, 2020) for lemon peel, by Bejar et al. (2011b) for orange peel and by Shu et al. (2020) for tangerine peel. They noted that microwave power level is an important factor influencing dehydration rate and some quality attributes of citrus peels. While the microwave drying method provides many advantages it also brings some disadvantages when used alone. The major drawback of using microwave drying alone is the non-uniform heating (Zhang et al., 2006). The turntable, one of the basic elements of a home type microwave oven, is one of the methods to increase temperature homogeneity (Geedipalli et al., 2007). To our knowledge, no studies have been conducted on the effect of rotational rate of the turntable on quality characteristics of a food material. Thus, the objective of the present study was to investigate the effect of the rotational rate of turntable on uniformity of surface temperature distribution of lemon peels during microwave drying and some quality properties (color, total phenolic content, and volatile organic compounds) of lemon peel powder.

## 2. Materials and Methods

Lemon fruit (*Citrus limon* (L.) var. Meyer) cultivated in Adana was obtained from a local grocery store in Giresun, Türkiye. Lemon fruits were kept in a refrigerator at  $4\pm 0.5^{\circ}\text{C}$ . Before drying experiments, lemon fruits were taken out of the refrigerator and left for 2 hours to reach the ambient temperature. The fruits were washed with tap water and dried with tissue paper. Peels (containing flavedo and albedo) of the fruits were manually separated and cut into 10 mm-sided square slab shapes (~4 mm thickness).

### 2.1 Drying Process

The lemon peel samples were dried using a domestic microwave oven (MC32F604TCT, Samsung, Port Klang, Malaysia). The microwave oven was modified to adjust the speed of the turntable. Lemon peel samples were spread on a petri dish of 11.5 cm diameter as a single layer, with the albedo tissue at the top. Then, the petri dish was placed at the centre of the turntable. Microwave drying was performed at power levels of 180W, 300W, 450W, and 600W and at rotational rates of 0 rpm, 6.5 rpm, 9.5 rpm, and 12.5 rpm. Drying was continued until reducing moisture content of fresh lemon peel (78.4%) to the final moisture content of about 10% (Tekgül & Baysal, 2018). For each drying condition, preliminary experiments were performed to determine the drying time required to attain final moisture content. After drying, lemon peels were ground (SCM-2934, Sinbo, Türkiye) and sieved (40 mesh sieve) to obtain peel powder.

Freeze drying produces the highest-quality dried foods. Therefore, to have a basis of comparison for the quality parameters of peel powders, lemon peels were dried also by freeze drying in a lab-scale freeze dryer (FreeZone 2.5L 7670530, Labconco, Fort Scott, KS, USA, at  $-50^{\circ}\text{C}$  and 0.1 mbar vacuum pressure).

### 2.2 Determination of Moisture Content

The moisture content of lemon peel was determined by drying in an oven at  $105^{\circ}\text{C}$  to constant weight (AOAC, 1995).

### 2.3 Infrared (IR) Thermal Imaging

Infrared (IR) thermal camera (PTi120, Fluke Corp., Everett, WA, USA) was used to obtain the surface temperatures of the samples. During drying, the sample was taken out of the microwave-oven at certain intervals, its thermal image was taken and placed back into the oven. The imaging process was repeated in 3 parallels. The IR images were analyzed using Fluke SmartView 4.4 software program (Everett, WA, USA).

### 2.4 Color

A colorimeter (Minolta CR-400, Minolta Co. Ltd., Osaka, Japan) was used to determine the L\* (lightness-darkness), a\* (redness-greenness), and b\* (yellowness-blueness) color parameters of dried peel powders. For color determination, each drying treatment was replicated nine times and the results were averaged. The color parameters of a sample were obtained by taking the average of L\*, a\*, and b\* readings from five different positions on its surface.

### 2.5 Total Phenolic Content (TPC)

TPC of samples was determined by a modified Folin–Ciocalteu method (Apak et al., 2008). For extraction of phenolic compounds, 0.5 g of peel powder was mixed with 5 ml of 90% ethanol solution. This mixture was thoroughly mixed in a shaker (Rocker-shaker MR-12 Biosan, Vetrotecnica, Padova, Italy) at 50 rpm for 60 min. Then, the extracts were centrifuged (D2012 Plus, ISOLAB Laborgeräte GmbH, Wertheim, Germany) at 15,000 x g for 10 min. The supernatant was taken and diluted with 90% ethanol solution (1:10). 60 µL of diluted extract solution was mixed with 3.48 mL distilled water and 300 µL of Folin–Ciocalteu reagent (2 N). After waiting the mixture for 8 min at dark, 900 µL of 20% Na<sub>2</sub>CO<sub>3</sub> solution was added to it. Then, the mixture was incubated in a water bath (WSB 18L, Daihan Scientific, Korea) at 40 °C for 30 min. The absorbance was determined at 760 nm in a spectrophotometer (UV mini-1240, Shimadzu, Kyoto, Japan). Results were expressed as milligram gallic acid equivalents (mg GAE/100g d.b.).

### 2.6 Headspace - Solid Phase Microextraction (HS-SPME)

One gram of the finely crushed fresh peel or dried peel powder sample was weighed into a 15ml vial closed with a PTFE/Silicone septa cap. The samples were placed on the heating block at 60°C and equilibrated for 15 minutes. After equilibration, a carboxen/polydimethylsiloxane (CAR/PDMS) manual fiber (75 µm Fused Silica, Supelco Ltd., Bellefonte, PA, USA) was inserted into the vial. CAR/PDMS fiber was maintained in the headspace for 60 min at 60°C for solid-phase microextraction (SPME) of volatile organic compounds (VOCs) from the sample (Mazı et al., 2019).

### 2.7 Gas Chromatography – Mass Spectrometry (GC/MS) Analysis

The effect of different drying methods on the VOCs of lemon peel was determined using gas chromatography/mass spectrometry (GC/MS). The desorption and chromatographic separation of VOCs was performed in a gas chromatograph (GC) (GC-2010 plus, Shimadzu, Japan) equipped with a mass spectrometry (MS) detector, and a Restek Rxi-5 MS capillary column (30m x 0.25mm i.d. x 0.25 µm film thickness). The carrier gas was Helium at a flow rate of 1.44 ml/min; the column temperature program of GC was initially set at 40°C for 2 min and gradually increased (4°C/min) to 250°C, then kept there for 3 min. The temperatures of the injector and detector were 250°C. For GC/MS detection, electron ionization (EI) system was used with ionization energy at 70 eV. VOCs from the samples were identified by comparing their mass fragmentation pattern with those stored in the mass spectral libraries (NIST, Wiley and FFNSC) (Mazı et al., 2019).

### 2.8 Statistical Analysis

The data represent mean±standard deviation of triplicate determinations unless otherwise specified. The results were analyzed by analysis of variance (ANOVA) followed by Tukey's multiple comparison test (p < .05) (Minitab, version 17).

### 3. Results and Discussion

#### 3.1 Surface Temperature Distribution

IR thermal image provides information about the surface temperature distribution. IR thermal images of lemon peels obtained during microwave drying at 180, 300, 450 and 600W power levels were presented in Figures 1, 2, 3, and 4, respectively.

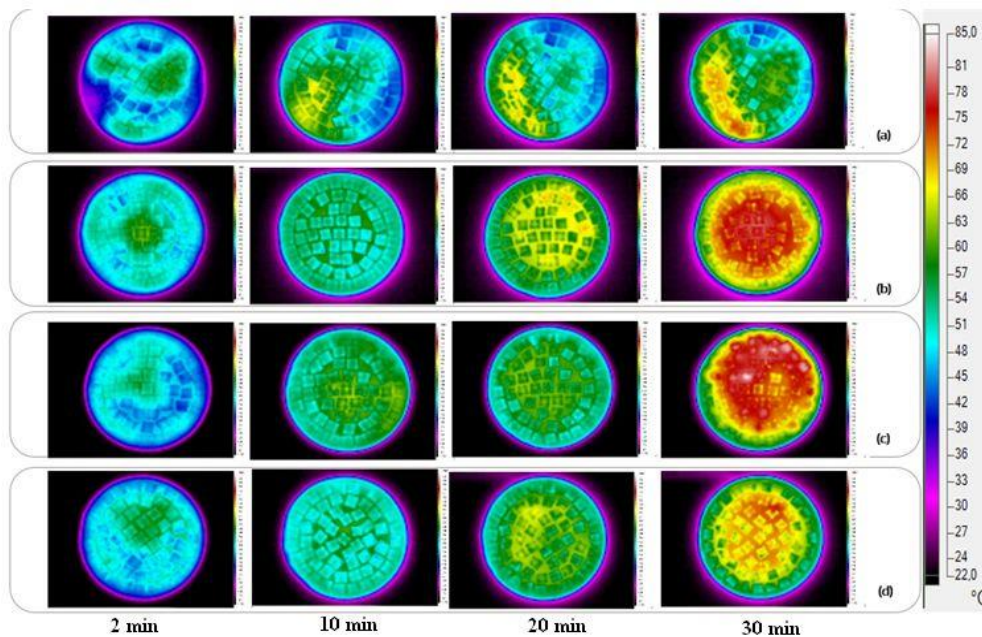


Figure 1. IR thermal images of lemon peels during microwave drying at 180 W and rotational rate of 0 rpm a), 6.5 rpm b), 9.5 rpm c), 12.5 rpm d)

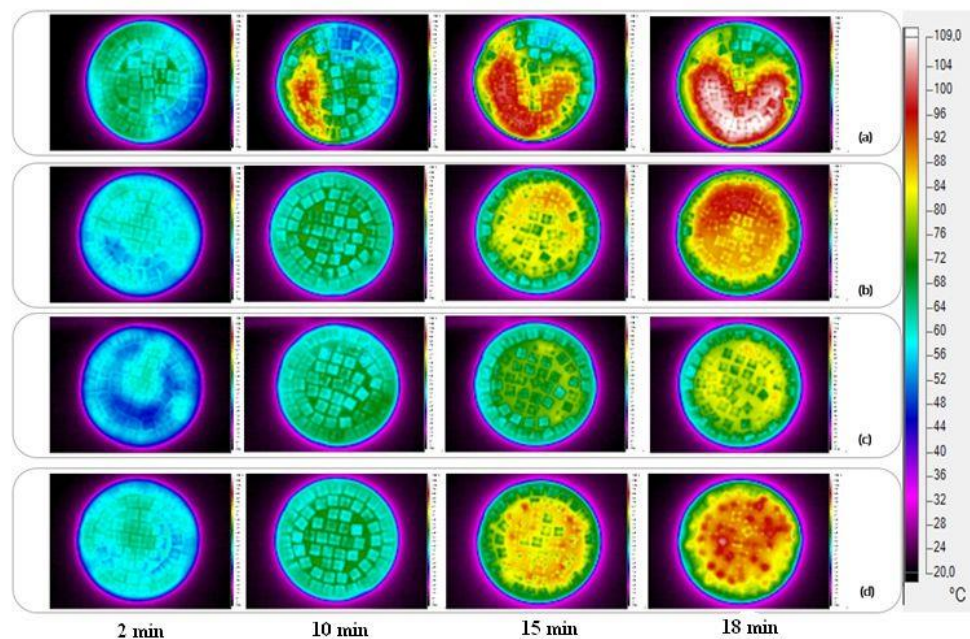


Figure 2. IR thermal images of lemon peels during microwave drying at 300 W and rotational rate of 0 rpm a), 6.5 rpm b), 9.5 rpm c), 12.5 rpm d)

As expected, the homogeneity of the temperature distribution during microwave drying without rotation (0 rpm) was lower compared to the microwave drying with rotation irrespective of the power level. During drying at 0 rpm, surface temperature raised to high levels in a certain region outside the center which caused non uniformity of temperature distribution in the product and, hence, inhomogeneous drying. In the case of microwave drying with rotation at high power levels (450, 600W), the surface temperature of samples located in the intermediate diameter were higher compared to the ones located at other regions. At lower power levels, microwave drying with rotation provided more uniform temperature distribution. During microwave drying, the drying time ranged from 32 to 36 min, 16 to 21 min, 9.0 to 11.3 min, and 7.0 to 8.5 min at power levels of 180, 300, 450, and 600 W, respectively. Longer drying time required at lower power levels may allow transfer of heat by conduction from hot regions to relatively colder regions and consequently formation of more uniform temperature distribution. Change of turntable rotation speed did not yield a noticeable effect on the homogeneity of the surface temperature distribution.

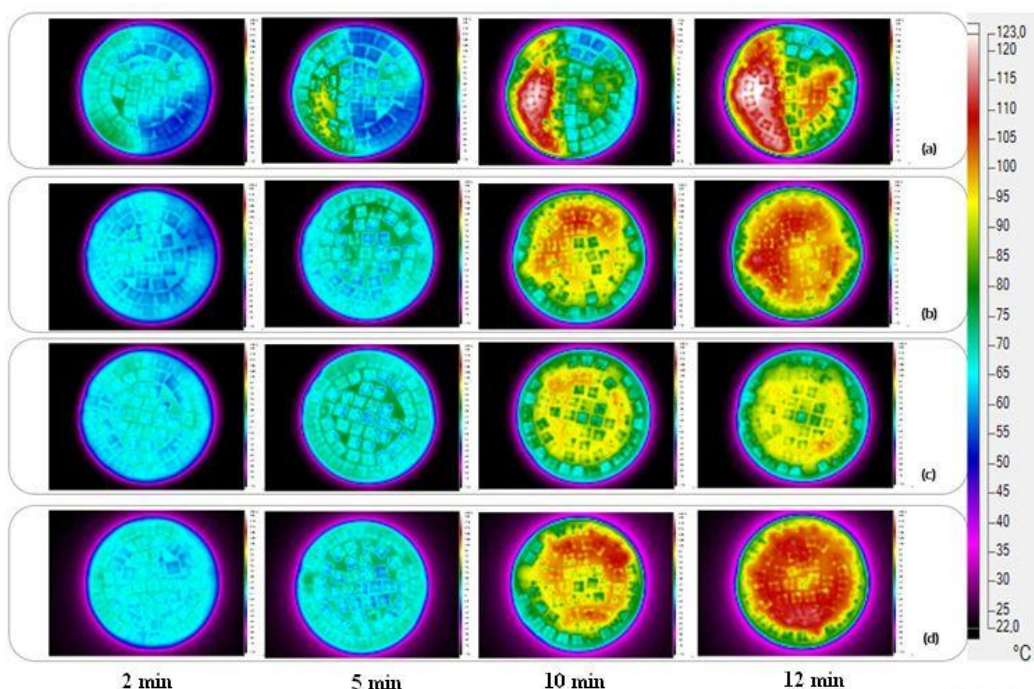


Figure 3. IR thermal images of lemon peels during microwave drying at 450 W and rotational rate of 0 rpm a), 6.5 rpm b), 9.5 rpm c), 12.5 rpm d)

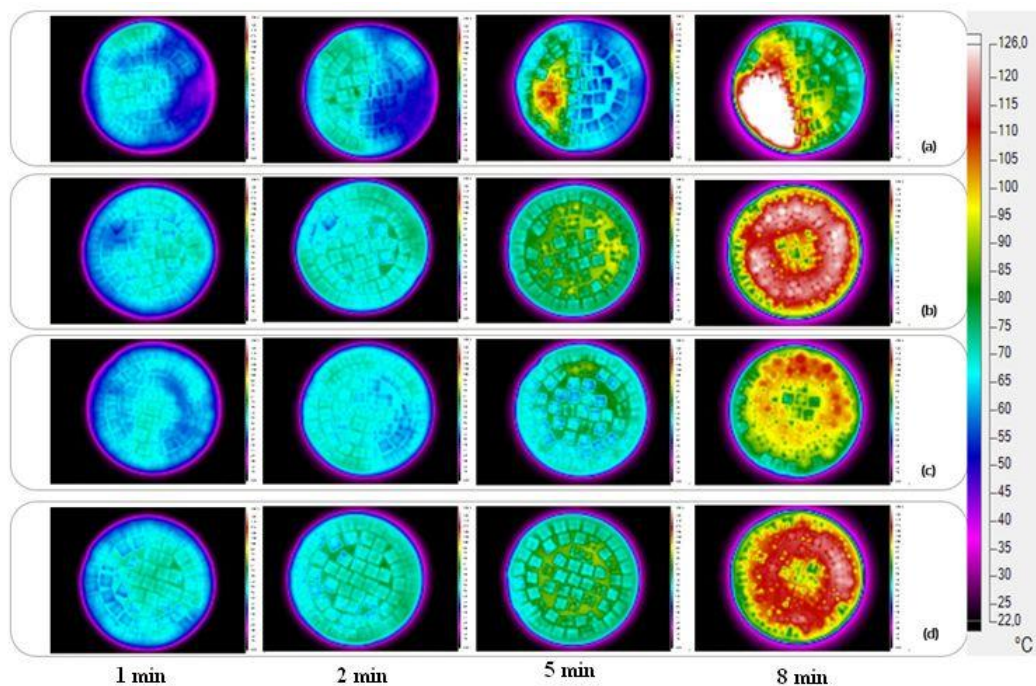


Figure 4. IR thermal images of lemon peels during microwave drying at 600 W and rotational rate of 0 rpm a), 6.5 rpm b), 9.5 rpm c), 12.5 rpm d)

Histograms of the thermal images were obtained using the SmartView (4.4.355.0) program of the Fluke camera (Figures 5-8). During initial period of microwave drying with rotation, a narrow single peak existed in histograms, but the number and width of the peaks increased in the later stages of drying process. This shows that there was a decrease in the homogeneity of the surface temperature distribution during the drying process. At power levels above 180 W, lower surface temperature values were reached at 9.5 rpm compared to 6.5 and 12.5 rpm rotation speeds at the end of the drying process. On the contrary, at 180 W power level, it was seen that the temperature values obtained at 9.5 rpm were higher. Acquisition of thermal images was performed in triplicate for each drying condition. The average of maximum temperature values obtained in samples during drying was calculated. At the end of the microwave drying without rotation, the maximum temperatures recorded were  $71.4 \pm 2.7$  °C,  $109.7 \pm 2.4$  °C,  $127.6 \pm 2.9$  °C and  $153.5 \pm 9.5$  °C at power levels of 180, 300, 450 and 600 W, respectively. The maximum temperatures recorded during microwave drying with rotation ranged between 74.2-82.0 °C, 90.4-103.8 °C, 104.5-116.4 °C, and 114.4-120.1 °C at power levels of 180, 300, 450 and 600 W, respectively. At 180 W power level, the temperature remained below 100 °C during drying. During microwave drying without rotation, the temperature in certain parts of the samples exceeded 100 °C in approximately 15 min at 300 W, within the first 10 min at 450 W and within the first 5 min at 600 W. Occurrence of overheating in these regions caused local burns. Similarly, during microwave drying with rotation, overheating was observed in certain areas at 450 W and 600 W power levels. The degree of local burns was less at 9.5 rpm than at 6.5 and 12.5 rpm.

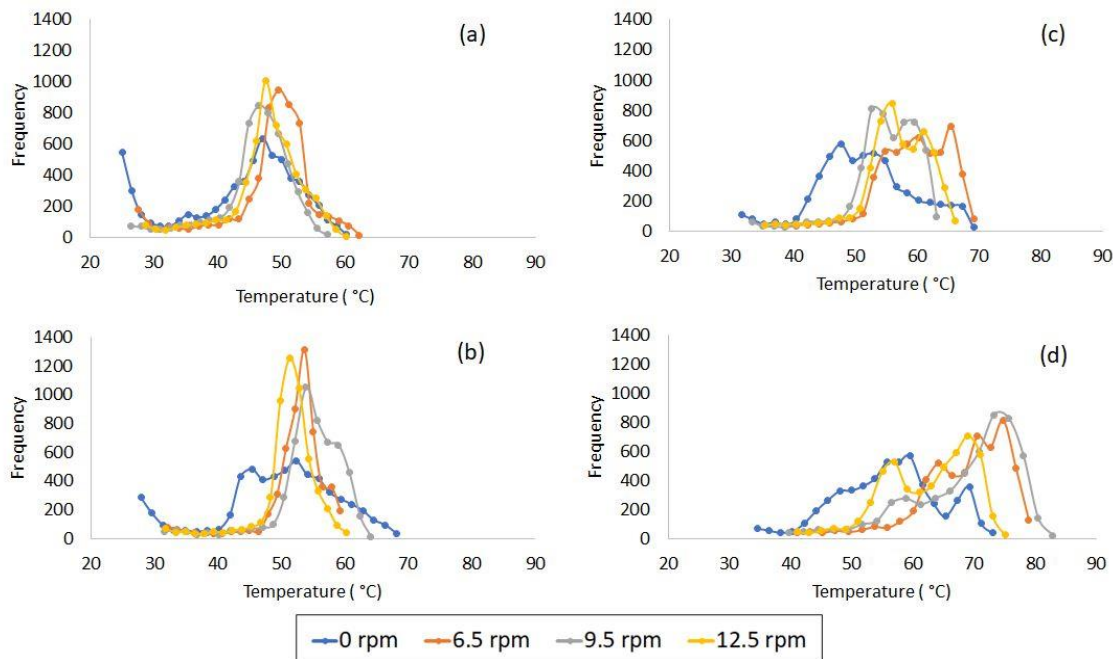


Figure 5. Histograms obtained from thermal images of lemon peels after 2 min a), 10 min b), 20 min c), and 30 min d) of microwave drying at 180 W

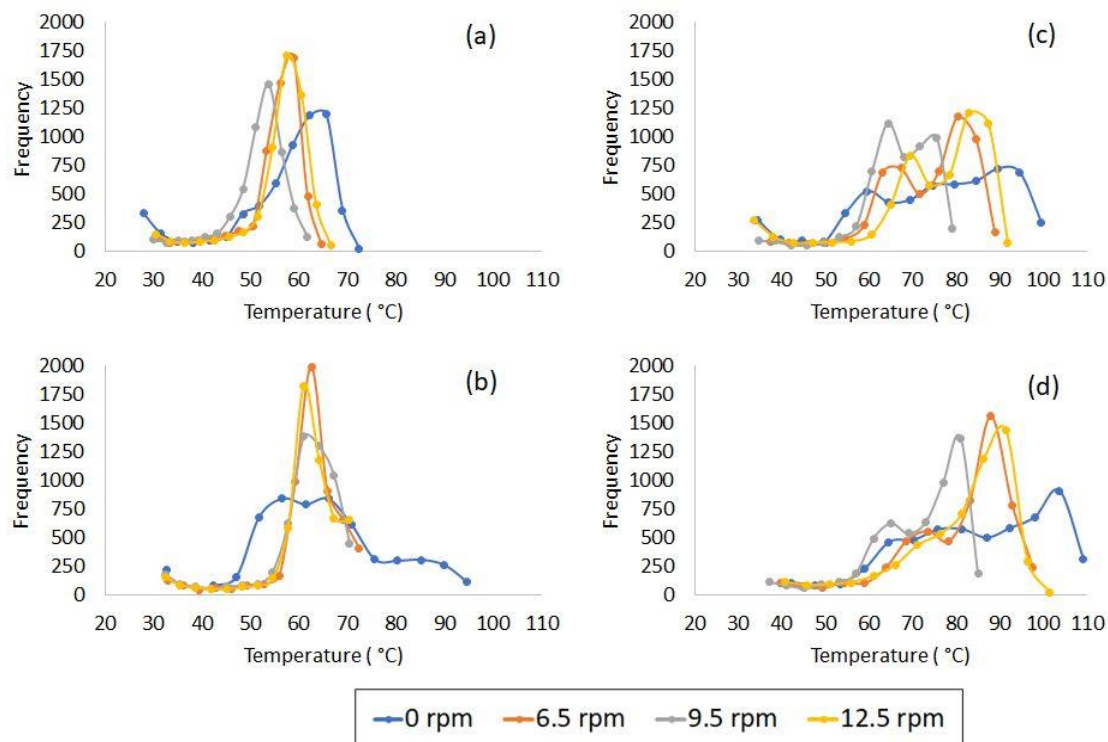


Figure 6. Histograms obtained from thermal images of lemon peels after 2 min a), 10 min b), 15 min c), and 18 min d) of microwave drying at 300 W

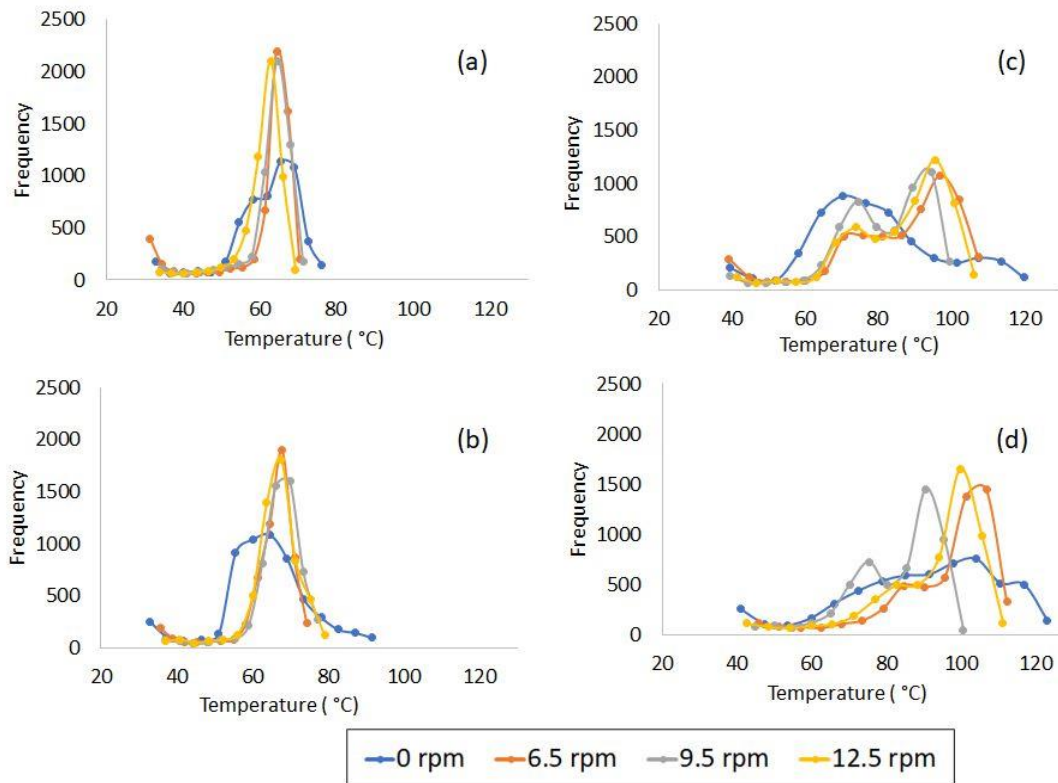


Figure 7. Histograms obtained from thermal images of lemon peels after 2 min a), 5 min b), 10 min c), and 12 min d) of microwave drying at 450 W

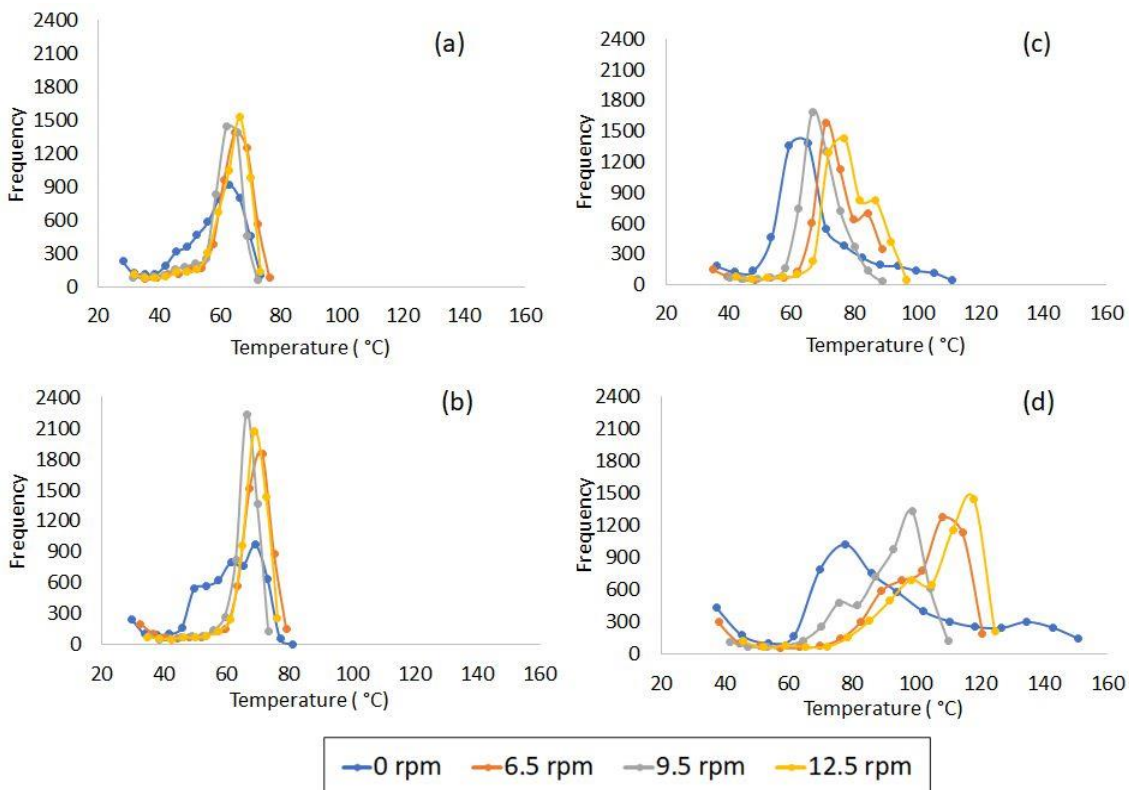


Figure 8. Histograms obtained from thermal images of lemon peels after 1 min a), 2 min b), 5 min c), and 8 min d) of microwave drying at 600 W

### 3.2 Color and Water Activity

The pictures of microwave dried lemon peel powders were given in Figure 9. Lemon peels were dried until reaching moisture content of 10%. Water activity ( $a_w$ ) of dried powders were given in Table 1. Water activity of peel powders ranged between 0.528 and 0.545. All  $a_w$  values were below 0.6 which is the limit for microbial growth (Tapia et al., 2020).

Color is one of the most important quality attributes of dried foods. The  $L^*$ ,  $a^*$ , and  $b^*$  values of peel powders varied between 42.03-83.66, 10.65-17.29, and 26.86-49.35, respectively (Table 1). The highest  $L^*$  and the lowest  $a^*$  value belonged to the freeze-dried sample. The decrease in  $L^*$  is generally attributed to the formation of brown pigments. A lower  $L^*$  value means darker color. During microwave drying, the occurrence of Maillard reactions due to high temperatures may contribute to darkening of sample. Freeze dried lemon peel powder had similar or higher  $b^*$  values compared to microwave dried ones depending on the microwave drying conditions. During drying, apart from the Maillard reactions, color of lemon peel is influenced by many factors such as degradation of carotenes, ascorbic acid oxidation, the removal of water and its replacement with air, the increase in the dry matter and color substance concentration, and the change of the surface and internal structure of the material (Pathare et al., 2013). Carotenoids are the primary pigments responsible for the color of the peel of most mature citrus fruits. The proportion of each carotenoid in peel is the determining factor on the color of peel. During microwave drying, high temperatures may produce higher degree of deterioration of color pigments which gave lower  $b^*$  values. While the temperature is high during microwave drying, the drying time was very short compared to freeze drying. This may, at least in part, limit the color degradation during microwave drying.

In general, an increase in power level yielded a reduction in  $L^*$  and  $b^*$  values. This may be related with the higher temperatures reached in samples at higher power levels. Lower  $b^*$  value indicates lower yellowness. The reduction in yellowness was attributed to the higher degree of deterioration of color pigments. In a study searching the effect of drying on total carotenoid content of kinnow peel, Rafiq et al. (2019) detected a decrease in carotenoid content and yellowness of peel after drying and interpreted that reduction in yellowness of peel is associated with the degradation of carotenoids. During microwave drying with rotation, 450 and 600 W provided similar  $L^*$ ,  $a^*$ , and  $b^*$  color parameters irrespective of the rate of rotation. Changing the rate of rotation between 6.5 and 12.5 rpm did not cause a marked influence on color parameters of lemon peel powders. Microwave drying without rotation created lower  $L^*$  and  $b^*$  values compared to microwave drying with rotation. The effect of rotation function on  $L^*$  and  $b^*$  values was notable at high power levels. At 450 and 600 W power levels, microwave drying without rotation caused local temperature rise in sample. At 0 rpm, the maximum surface temperatures detected at power levels of 450 and 600W was about 128 and 154°C, respectively. This resulted in local burns within samples and consequently formation of unacceptable dark powder. Microwave drying at 600 W -0 rpm gave the darkest sample. At 180 W, all lemon peel powder samples had similar color parameters.



Figure 9. Microwave dried and freeze-dried lemon peel powders

### 3.3 Total Phenolic Content (TPC)

TPC of fresh peel was 896.5 mg GAE/100g d.b. TPC of dried lemon peels were presented in Table 1. Total phenolic content of dried lemon peel samples ranged between 554 and 1731 mg GAE/100 g d.b. TPC of samples dried by freeze-drying and microwave drying at 180 W were found to be lower when compared to fresh sample. For citrus peels, a decrease in TPC after drying has been reported by several authors (Bejar et al., 2011a; Ghanem et al., 2020; Romdhane et al., 2015; Zhang et al., 2018; Li et al., 2020; Assefa & Keum, 2017). In these studies, the reduction level in TPC of citrus peels ranged between 10 and 70%. In our study, freeze-drying caused 36.8% reduction in TPC and microwave drying at 180 W resulted in a reduction ranging between 21.6 and 33.7%.

The reduction in TPC with drying has been attributed to various factors such as activation of oxidative enzymes, thermal degradation of polyphenols, changes in the chemical structures of polyphenols, binding of polyphenols to proteins and lower extraction yields of phenolics (Deng et al., 2019; Li et al., 2020). Except 180 W, lemon peels subjected to microwave drying had similar or higher TPC compared to fresh peel. Although most of the studies reported a decrease in TPC of citrus peels, in some cases, depending on the drying conditions and the type of citrus, an increase in TPC with drying has been detected (Tekgül & Baysal, 2018, 2019). The release of bound phenolics or some cell wall phenolics due to the high pressure and temperature generated within the tissue during microwave drying may be a possible reason for the increase in TPC (Ghanem et al., 2020; Xu et al. 2017). Phenolics are heat sensitive compounds. However, while some phenolic components are inactivated by heat treatment, some phenolic components are released by the degradation of the cell wall and matrix, resulting in an increase in TPC content. Ghanem et al. (2020) detected that, the TPC of lemon peel subjected to microwave drying between power levels of 300 and 600 W degraded following first-order kinetics during initial period but increased after a certain period. It is well known that freeze-drying is an effective method to obtain high quality dried products. However, in this study, freeze-drying did not

provide the best results in terms of TPC of lemon peel powder. At all conditions, TPC of microwave dried peels were higher than that of freeze-dried one. This may be at least in part due to the increase in free fraction of phenolic acids. Hayat et al. (2010) subjected the mandarin peel powders to microwave treatment and observed an increase in the contents of free phenolic acid, flavanol, flavanone, flavonol compounds but a decrease in bound phenolic acid content. This study's finding agrees with those obtained by Chen et al. (2011) who showed that drying of the orange peel over 70 °C provided higher TPC compared to the freeze-drying and by Papoutsis et al. (2017) who found higher TPC in hot air dried (70-110 °C) lemon peels compared to freeze-dried one. They attributed this to the release of some bound phenolics and the decrease of the polyphenol oxidase enzyme by the heating effect.

Table 1

Water activity ( $a_w$ ), color parameters, and total phenolic content (TPC) of lemon peels

Drying treatment		$a_w$	Color			TPC (mg GAE/100g d.b.)
Power	Rate of rotation (rpm)		L*	a*	b*	
Freeze-drying		0.528 ± 0.000 <sup>e*</sup>	83.66 ± 1.38 <sup>a</sup>	10.65 ± 0.80 <sup>f</sup>	46.77 ± 2.91 <sup>abcd</sup>	566.30 ± 29.2 <sup>j</sup>
180W	0	0.538 ± 0.003 <sup>bcd</sup>	76.33 ± 0.95 <sup>bc</sup>	13.64 ± 1.20 <sup>de</sup>	46.52 ± 3.23 <sup>abcdefg</sup>	675.01 ± 16.1 <sup>ij</sup>
	6.5	0.535 ± 0.000 <sup>de</sup>	77.42 ± 0.77 <sup>b</sup>	13.82 ± 0.91 <sup>cde</sup>	48.96 ± 2.10 <sup>a</sup>	703.22 ± 10.4 <sup>i</sup>
	9.5	0.539 ± 0.003 <sup>abcd</sup>	77.70 ± 1.08 <sup>b</sup>	13.88 ± 0.74 <sup>bcde</sup>	49.35 ± 1.74 <sup>a</sup>	594.60 ± 29.8 <sup>ij</sup>
	12.5	0.542 ± 0.002 <sup>abcd</sup>	77.50 ± 0.87 <sup>b</sup>	14.04 ± 1.19 <sup>bcde</sup>	49.01 ± 2.29 <sup>a</sup>	670.29 ± 8.2 <sup>ij</sup>
300W	0	0.535 ± 0.002 <sup>de</sup>	63.35 ± 3.57 <sup>d</sup>	16.35 ± 0.91 <sup>ab</sup>	41.70 ± 4.36 <sup>bcdefg</sup>	1101.07 ± 11.4 <sup>de</sup>
	6.5	0.537 ± 0.001 <sup>cd</sup>	72.25 ± 2.78 <sup>c</sup>	15.57 ± 1.57 <sup>abcd</sup>	47.76 ± 3.86 <sup>abc</sup>	878.00 ± 17.4 <sup>gh</sup>
	9.5	0.538 ± 0.003 <sup>bcd</sup>	72.68 ± 2.94 <sup>c</sup>	15.49 ± 1.64 <sup>abcd</sup>	48.12 ± 4.26 <sup>ab</sup>	841.80 ± 25.7 <sup>h</sup>
	12.5	0.538 ± 0.001 <sup>bcd</sup>	71.61 ± 2.52 <sup>c</sup>	16.11 ± 1.51 <sup>abcd</sup>	46.97 ± 3.83 <sup>bcdefg</sup>	967.30 ± 41.0 <sup>fg</sup>
450W	0	0.540 ± 0.001 <sup>abcd</sup>	48.37 ± 3.69 <sup>e</sup>	15.39 ± 1.77 <sup>abcd</sup>	31.30 ± 2.66 <sup>h</sup>	1105.00 ± 54.4 <sup>de</sup>
	6.5	0.539 ± 0.001 <sup>abcd</sup>	64.02 ± 4.10 <sup>d</sup>	16.32 ± 1.05 <sup>abc</sup>	40.48 ± 4.51 <sup>efg</sup>	1189.80 ± 29.3 <sup>cd</sup>
	9.5	0.543 ± 0.001 <sup>abc</sup>	62.33 ± 2.85 <sup>d</sup>	17.17 ± 0.94 <sup>a</sup>	41.42 ± 4.01 <sup>defg</sup>	1060.30 ± 94.5 <sup>ef</sup>
	12.5	0.537 ± 0.003 <sup>bcd</sup>	61.58 ± 3.70 <sup>d</sup>	17.17 ± 1.05 <sup>a</sup>	41.78 ± 4.91 <sup>bcdefg</sup>	1115.00 ± 60.8 <sup>de</sup>
600W	0	0.541 ± 0.003 <sup>abcd</sup>	42.03 ± 2.76 <sup>f</sup>	12.71 ± 1.43 <sup>e</sup>	26.86 ± 4.21 <sup>h</sup>	1730.71 ± 12.9 <sup>a</sup>
	6.5	0.543 ± 0.000 <sup>abc</sup>	60.29 ± 3.21 <sup>d</sup>	17.05 ± 0.82 <sup>a</sup>	41.06 ± 4.85 <sup>fg</sup>	1402.90 ± 29.9 <sup>b</sup>
	9.5	0.546 ± 0.001 <sup>a</sup>	62.10 ± 2.86 <sup>d</sup>	17.11 ± 0.81 <sup>a</sup>	41.11 ± 4.74 <sup>g</sup>	1152.10 ± 42.9 <sup>de</sup>
	12.5	0.544 ± 0.001 <sup>ab</sup>	61.35 ± 3.45 <sup>d</sup>	17.29 ± 0.64 <sup>a</sup>	41.56 ± 4.10 <sup>cdefg</sup>	1261.40 ± 24.1 <sup>c</sup>

\*Means ± standard deviation within a column followed by different letters is significantly different ( $p < 0.05$ )

TPC of the samples increased with increasing power level. Ghanem et al. (2012) and Bejar et al. (2011b) also observed similar trend during microwave drying of orange peel. This is probably due to the higher temperatures reached in sample during drying at higher power levels (Table 1). The highest TPC (1730.71 ± 12.9 mg GAE/100 g d.b.) belonged to the sample undergoing microwave drying without rotation (0 rpm) at 600 W. It was seen that the maximum surface temperature recorded under this drying condition was quite high (150 °C). Several researchers subjected the citrus peels to elevated drying temperatures and noted similar findings. Papoutsis et al. (2017) detected higher TPC in lemon peels subjected to hot air and vacuum drying treatments at 110 °C compared to the ones dried at 70 °C. In their study, increasing drying temperature provided significant increase in gallic acid content. Chen et al. (2011) dried orange peels in an oven at different temperatures ranging between 50 and 100 °C and obtained the highest flavonoid and phenolic acid contents in the peels dried at 100 °C. For 300 and 600 W, the highest TPC was determined at 0 rpm. The sample dried at 600 W-0rpm conditions was found to have the highest TPC content among all samples. This was attributed to

the respectively higher temperatures reached in this sample under these drying conditions. According to the Tukey's pairwise comparison test, the group average obtained at 0 rpm rotational speed was the highest and that obtained at 9.5 rpm was the lowest. Considering the surface temperatures, it was seen that, at 0 rpm, the temperature rises to relatively higher values due to local overheating and the surface temperature values obtained at 9.5 rpm are lower compared to those obtained at 6.5 and 12.5 rpm.

### 3.4 Volatile Organic Compounds

The list of volatile compounds in lemon peel and their percentages were given in Table 2. A total of 65 volatile compound was detected in fresh lemon peel. The major volatile compounds in fresh peel were limonene (57.91%),  $\gamma$ -terpinene (6.40%), myrcene (5.59%), p-cymene (3.52%), and  $\alpha$ -p-dimethylstyrene (3.45%) which are monoterpene hydrocarbons. Thymol, a monoterpene phenol, was another main compound identified in lemon peel, with percentage of 2.58%. Drying process caused a decrease in percentage amount of these major monoterpene hydrocarbons. The percentage amount of limonene dropped to 34.9 % after freeze drying and to a value ranging between 25.55% and 35.10% after microwave drying. Previous studies showed that, the effect of drying treatment on volatile components varies depending on the method of drying (Farahmandfar et al., 2020) and citrus species (Kamal et al., 2011).

In general, the rate of rotation did not exert a clear effect on the amount of major monoterpene hydrocarbons detected in lemon peel. Depending on the power level and rotation function, microwave drying caused appearance of some derivatives of furan compounds (furfural, furfuryl alcohol, tetrahydrofurfuryl alcohol, 2-acetyl furan, 5-methyl furfural, and hydroxy methyl furfural (HMF)). Of these compounds, furfuryl alcohol is classified as Group 2B (possibly carcinogenic to humans) by International Agency for Research on Cancer (IARC, 2019). In the samples dried at 600W, all these compounds existed. In the samples dried at 180 W power level with rotation, formation of furfural, 2-acetyl furan, and 5-methyl furfural was observed but in a lower level compared to 600 W. Microwave drying at 600 W without rotation (0 rpm) caused also appearance of 3-furfural. Furan and its derivatives were identified in a variety of heat-treated foods through various mechanisms. Akyıldız et al. (2021) detected formation of furfural and HMF in orange juice subjected to thermal treatment (70-90 °C). Lemon peel contains soluble sugars (glucose, sucrose, fructose, raffinose) and ascorbic acid (Aung et al., 1998). Thus, during drying, derivatives of furan compounds in lemon peel may be formed by Maillard reaction or ascorbic acid degradation. In a study, Randhawa et al., (2020) recorded formation of furfuraldehydes (HMF, 2-furfural, 5-methyl furfural) during storage of orange juice at different temperatures (0-40 °C). They noted a significant correlation between vitamin C loss and HMF accumulation in orange juice during storage and stated that the formation of HMF is mainly due to the ascorbic acid degradation. Garcia-Salas et al., (2013) detected formation of HMF and furfural in freeze-dried and vacuum-dried whole lemon powder. In our study, freeze-dried lemon peel powder contained furfural (0.07 %) but not HMF. Total amount of furan derivatives identified in peels dried at 0 rpm, 6.5 rpm, 9.5 rpm, and 12.5 rpm was 7.683%, 5.048%, 4.071%, and 4.714%, respectively at 600 W and 0.745 %, 0.402 %, 0.484 %, and 0.737 %, respectively at 180 W. Caramelization, which requires high temperature and sugar, may also lead the formation of furfural and HMF (Agcam, 2022). This might contribute to the comparatively higher level of furfural obtained at 600 W.

Table 2

Percentage composition (%) of volatile compounds in fresh and dried lemon peels

Peak No	RT(min)	Compound Name	CAS #	Fresh	FD	MD at 180W				MD at 600W			
						0 rpm	6.5 rpm	9.5 rpm	12.5 rpm	0 rpm	6.5 rpm	9.5 rpm	12.5 rpm
1	4.977	Capronaldehyde	66-25-1	0.20	0.13	0.02	0.02	0.02	0.02	-	0.01	0.01	0.01
2	5.788	3-Furfural	498-60-2	-	-	-	-	-	-	0.28	-	-	-
3	5.884	Furfural	98-1-1	-	0.07	0.48	0.27	0.35	0.57	4.71	3.53	2.83	3.56
4	6.497	E-2-Hexenal	6728-26-3	0.85	1.03	-	-	-	-	-	-	-	-
5	6.630	Furfuryl alcohol	98-0-0	-	-	0.07	-	-	-	0.61	0.54	0.45	0.34
6	7.550	Tetrahydrofurfuryl alcohol	97-99-4	-	-	0.01	-	-	-	0.14	0.08	0.08	0.10
7	7.769	Styrene	100-42-5	0.02	0.04	0.06	0.07	0.08	0.09	0.06	0.06	0.08	0.08
8	8.497	2-acetyl Furan	1192-62-7	-	-	0.08	0.04	0.05	0.07	0.17	0.17	0.15	0.17
9	9.095	$\alpha$ - Thujene	2867-5-2	0.32	0.11	0.08	0.07	0.09	0.08	0.09	0.09	0.08	0.10
10	9.323	$\alpha$ - Pinene	80-56-8	1.23	0.32	0.24	0.22	0.25	0.25	0.30	0.26	0.27	0.29
11	10.173	E-Hept-2-enal	18829-55-5	-	-	0.02	0.01	0.01	0.01	0.03	0.09	0.10	0.09
12	10.282	Benzaldehyde	100-52-7	1.04	0.36	0.47	0.54	0.42	0.37	0.21	0.31	0.29	0.32
13	10.431	5-methyl Furfural	620-2-0	-	-	0.10	0.09	0.09	0.09	1.48	0.60	0.47	0.45
14	10.839	Sabinene	3387-41-5	0.20	0.08	0.06	0.05	0.06	0.06	0.08	0.05	0.05	0.07
15	10.933	$\beta$ - Pinene	127-91-3	0.77	0.24	0.23	0.21	0.24	0.24	0.33	0.22	0.25	0.25
<b>16</b>	<b>11.563</b>	<b>Myrcene</b>	<b>123-35-3</b>	<b>5.59</b>	<b>1.35</b>	<b>0.97</b>	<b>0.80</b>	<b>0.84</b>	<b>0.95</b>	<b>1.07</b>	<b>0.95</b>	<b>0.89</b>	<b>1.26</b>
17	12.019	$\alpha$ - Phellandrene	99-83-2	0.25	0.06	0.07	0.06	0.10	0.06	0.05	0.05	0.05	0.05
18	12.507	$\alpha$ - Terpinene	99-86-5	0.40	0.16	0.15	0.14	0.14	0.15	0.14	0.14	0.13	0.15
<b>19</b>	<b>12.817</b>	<b>p- Cymene</b>	<b>99-87-6</b>	<b>3.52</b>	<b>0.96</b>	<b>0.94</b>	<b>0.80</b>	<b>0.84</b>	<b>0.94</b>	<b>1.03</b>	<b>0.92</b>	<b>0.84</b>	<b>0.86</b>
<b>20</b>	<b>13.039</b>	<b>Limonene</b>	<b>138-86-3</b>	<b>57.91</b>	<b>34.90</b>	<b>32.72</b>	<b>25.55</b>	<b>29.88</b>	<b>31.53</b>	<b>34.78</b>	<b>33.55</b>	<b>31.10</b>	<b>35.10</b>
21	13.101	Eucalyptol	470-82-6	1.28	0.27	0.38	0.34	0.27	0.27	0.36	0.28	0.28	0.26
22	13.394	(Z)- $\beta$ - Ocimene	3338-55-4	0.49	0.07	0.12	0.08	0.07	0.08	0.11	0.13	0.09	0.10
23	13.791	(E)- $\beta$ - Ocimene	3779-61-1	0.56	0.14	0.20	0.18	0.20	0.18	0.16	0.18	0.16	0.16
<b>24</b>	<b>14.182</b>	<b><math>\gamma</math>- Terpinene</b>	<b>99-85-4</b>	<b>6.40</b>	<b>4.23</b>	<b>5.23</b>	<b>4.20</b>	<b>4.55</b>	<b>5.04</b>	<b>4.66</b>	<b>5.05</b>	<b>4.60</b>	<b>4.85</b>
<b>25</b>	<b>15.354</b>	<b><math>\alpha</math>- p- Dimethylstyrene</b>	<b>1195-32-0</b>	<b>3.45</b>	<b>1.84</b>	<b>2.76</b>	<b>2.43</b>	<b>2.41</b>	<b>2.63</b>	<b>2.02</b>	<b>2.60</b>	<b>2.29</b>	<b>2.06</b>
26	15.787	Linalool	78-70-6	0.51	0.86	0.91	0.87	0.95	0.85	0.46	0.51	0.56	0.62
27	15.957	Pelargonaldehyde	124-19-6	0.25	0.16	0.21	0.20	0.21	0.20	0.12	0.17	0.17	0.16
28	16.231	Phenethyl alcohol	60-12-8	0.03	0.04	0.05	0.04	0.04	0.05	0.04	0.05	0.04	0.04
29	17.325	trans-3-Caren-2-ol	0-0-0	0.11	0.22	0.44	0.35	0.39	0.41	0.42	0.64	0.56	0.48
30	17.844	Isopulegol	89-79-2	0.56	1.07	1.65	1.22	1.51	1.50	1.15	1.37	1.43	1.30
31	18.757	Terpinen-4-ol	562-74-3	0.15	0.15	0.21	0.20	0.22	0.21	0.14	0.20	0.18	0.18
32	19.271	$\alpha$ - Terpineol	98-55-5	0.26	1.12	0.85	0.86	0.96	0.86	0.46	0.53	0.54	0.63
33	19.476	Dihydrocarveol	38049-26-2	0.05	0.12	0.21	0.18	0.21	0.20	0.11	0.18	0.18	0.15
34	19.601	$\gamma$ - Terpineol	586-81-2	0.34	0.98	1.81	1.47	1.69	1.56	0.86	1.43	1.45	1.27
35	19.825	Capraldehyde	112-31-2	0.16	0.21	0.31	0.29	0.32	0.29	0.23	0.29	0.29	0.26
36	20.192	Linalyl formate	115-99-1	0.09	0.15	0.23	0.24	0.24	0.24	0.31	0.20	0.21	0.15
37	20.279	Nona-2(E).4(E)-dienal	5910-87-2	0.08	0.19	0.20	0.20	0.21	0.20	0.33	0.29	0.26	0.22
38	20.570	Hydroxy methyl furfural	67-47-0	-	-	-	-	-	-	0.30	0.12	0.08	0.08
39	20.676	L- Citronellol	7540-51-4	0.24	0.62	0.45	0.40	0.43	0.43	0.53	0.56	0.52	0.64
40	20.921	Methylthymol	1076-56-8	0.51	0.69	0.98	0.88	0.98	0.91	0.68	0.81	0.85	0.72

Table 2 (Continued)

Peak No	RT(min)	Compound Name	CAS #	Fresh	FD	MD at 180W				MD at 600W			
						0 rpm	6.5 rpm	9.5 rpm	12.5 rpm	0 rpm	6.5 rpm	9.5 rpm	12.5 rpm
41	21.133	Neral	106-26-3	0.13	0.29	0.41	0.35	0.41	0.37	0.25	0.34	0.35	0.35
42	21.238	Carvone	99-49-0	0.04	0.12	0.08	0.07	0.08	0.07	0.07	0.08	0.07	0.08
43	21.634	Geraniol	106-24-1	0.04	0.13	0.06	0.04	0.06	0.05	0.05	0.05	0.05	0.06
44	21.873	(E)-2- Decenal	3913-81-3	0.01	0.03	0.06	0.05	0.05	0.06	0.05	0.07	0.07	0.06
45	22.215	Geranial	141-27-5	0.32	1.04	0.99	0.93	1.01	0.91	0.62	0.74	0.79	0.80
46	22.342	Perillaldehyde	2111-75-3	0.08	0.64	0.27	0.27	0.28	0.24	0.19	0.20	0.22	0.19
<b>47</b>	<b>23.014</b>	<b>Thymol</b>	<b>89-83-8</b>	<b>2.58</b>	<b>8.58</b>	<b>6.61</b>	<b>6.85</b>	<b>6.80</b>	<b>6.33</b>	<b>4.79</b>	<b>5.44</b>	<b>5.10</b>	<b>6.05</b>
48	23.525	Undecanal	112-44-7	0.13	0.35	0.38	0.41	0.42	0.39	0.32	0.36	0.35	0.35
49	23.753	4-vinyl Guaiacol	7786-61-0	-	0.01	0.07	0.04	0.03	0.05	0.59	0.87	0.68	0.56
50	24.658	$\delta$ - Elemene	20307-84-0	0.10	0.44	0.47	0.63	0.55	0.56	0.52	0.52	0.61	0.57
51	25.082	$\alpha$ - Cubebene	17699-14-8	0.07	0.18	0.26	0.31	0.29	0.26	0.37	0.25	0.29	0.25
52	25.136	Citronellyl acetate	150-84-5	0.08	0.35	0.37	0.35	0.38	0.37	0.27	0.32	0.35	0.27
53	25.526	Neryl acetate	141-12-8	0.19	0.83	0.98	1.00	1.04	0.94	0.75	0.79	0.85	0.76
54	26.002	$\alpha$ - Copaene	3856-25-5	0.17	0.49	0.49	0.56	0.55	0.51	0.44	0.44	0.52	0.46
55	26.178	Geranyl acetate	105-87-3	0.03	0.13	0.13	0.13	0.14	0.13	0.11	0.12	0.12	0.10
56	26.559	$\beta$ - Elemene	33380-83-9	1.36	4.78	4.94	6.05	5.37	5.49	6.20	6.05	6.72	6.06
57	27.128	$\beta$ - Caryophyllene	87-44-5	0.04	0.25	0.37	0.43	0.40	0.38	0.31	0.33	0.34	0.28
58	27.313	$\alpha$ - Cedrene	469-61-4	0.07	0.28	0.32	0.39	0.36	0.33	0.27	0.27	0.32	0.27
59	27.496	$\beta$ - Cedrene	546-28-1	0.72	2.06	1.97	2.32	2.23	2.12	1.67	1.75	2.06	1.91
60	28.001	$\alpha$ -trans- Bergamotene	64727-43-1	1.10	3.78	4.27	5.04	4.78	4.44	3.50	3.75	4.22	3.65
61	28.640	(E)- $\beta$ - Farnesene	18794-84-8	0.73	5.50	5.27	6.73	5.97	5.61	4.57	4.87	5.29	4.47
62	28.812	$\beta$ -Santalene	511-59-1	0.08	0.23	0.23	0.36	0.26	0.25	0.21	0.17	0.27	0.19
63	28.922	Cadina-1(6),4-diene	20085-11-4	0.06	0.20	0.22	0.35	0.23	0.24	0.29	0.17	0.29	0.18
64	29.531	Germacrene D	105453-16-5	0.68	3.93	4.71	5.81	5.26	4.84	2.61	4.16	4.85	4.57
65	29.700	$\beta$ - Selinene	17066-67-0	0.38	0.79	0.73	1.13	0.82	0.83	1.04	0.57	0.75	0.51
66	29.989	$\alpha$ - Bulnesene	3691-11-0	0.82	1.41	1.22	2.08	1.45	1.72	2.25	1.04	1.45	0.89
67	30.146	Bicyclogermacrene	24703-35-3	0.16	0.80	0.79	1.13	0.89	0.84	0.71	0.67	0.84	0.67
68	30.358	$\beta$ -Bisabolene	495-61-4	1.55	7.90	7.85	10.38	8.82	8.33	6.12	6.93	7.66	6.39
69	30.573	$\gamma$ - Cadinene	39029-41-9	0.07	0.20	0.23	0.32	0.26	0.26	0.33	0.21	0.24	0.21
70	30.717	$\beta$ - Sesquiphellandrene	20307-83-9	0.04	0.09	0.10	0.15	0.12	0.12	0.12	0.08	0.09	0.08
71	30.845	$\delta$ - Cadinene	483-76-1	0.26	0.88	0.85	1.20	0.96	0.95	1.01	0.81	0.90	0.80
72	31.298	Lilial	80-54-6	0.03	0.05	0.05	0.09	0.06	0.08	0.12	0.07	0.08	0.06
73	31.404	Neryl butyrate	999-40-6	0.02	0.15	0.13	0.22	0.16	0.17	0.13	0.14	0.17	0.13
74	31.941	Germacrene B	15423-57-1	0.04	0.20	0.17	0.26	0.21	0.20	0.13	0.16	0.19	0.18

Abbreviations: -, not detected; RT, Retention time; FD, Freeze drying; MD, microwave drying. Major volatile compounds were shown in bold text

#### 4. Conclusion

During microwave drying, application of rotation function or the change in rotational speed of turntable did not create a clear influence on homogeneity of surface temperature distribution, color and TPC of lemon peels at 180W. However, at 450 and 600 W, microwave drying without rotation (0 rpm) caused localized overheating which led to the production of peel powders with unacceptable dark color. The maximum temperatures recorded on the surface of the peels during microwave drying, except at 180W, was slightly lower at 9.5 rpm compared to 6.5 and 12.5 rpm. At these power levels, variation in rotational speed of turntable significantly

affected the TPC of lemon peel powders. Freeze-dried peel and peels dried by microwave drying at 180 W had lower TPC while those dried at 450 and 600W had higher TPC compared to fresh peel. Drying caused loss of main volatile compounds detected in fresh peel and formation of some furan compounds depending on the drying conditions. Formation of furfuryl alcohol which is possibly carcinogenic to humans was detected in peels dried at 600W irrespective of speed of rotation and at a relatively lower level in the peel dried at 180W without rotation but not in other samples. Lemon peel powder dried at 600W contained higher percentage concentration of total furan compounds compared to ones dried at 180W. Results showed that good quality lemon peel powder may be produced by microwave drying with rotation at low power levels.

### Acknowledgement

This study was funded by Ordu University (B 2127).

### Author Contributions

Sevilay San: Collected data and performed the analysis.

Işıl Barutçu Mazi: Planned the study, performed statistical analysis, and wrote the paper.

### Conflicts of Interest

The authors declare no conflict of interest.

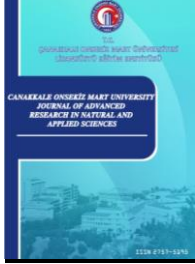
### References

- Abou-Arab, E. A., Mahmoud, M. H., & Abu-Salem, F. M. (2017). Functional properties of citrus peel as affected by drying methods. *American Journal of Food Technology*, 12, 193-200. DOI: <https://doi.org/10.3923/ajft.2017.193.200>
- Agcam, E. (2022). A kinetic approach to explain hydroxymethylfurfural and furfural formations induced by Maillard, caramelization, and ascorbic acid degradation reactions in fruit juice-based mediums. *Food Analytical Methods*, 15, 1286-1299
- Akyıldız, A., Simsek Mertoglu, T., & Ağçam, E. (2021). Kinetic study for ascorbic acid degradation, hydroxymethylfurfural and furfural formations in orange juice. *Journal of Food Composition and Analysis*, 102, 103996. DOI: <https://doi.org/10.1016/j.jfca.2021.103996>
- AOAC (1995). Official methods of analysis. Washington, DC, USA: Association of Official Analytical Chemists
- Apak, R., Güçlü, K., Özyürek, M., & Çelik, S. E. (2008). Mechanism of antioxidant capacity assays and the CUPRAC (cupric ion reducing antioxidant capacity) assay. *Microchimica Acta*, 160, 413-419. DOI: <https://doi.org/10.1007/s00604-007-0777-0>
- Assefa, A. D., & Keum, Y. S. (2017). Effect of extraction solvent and various drying methods on polyphenol content and antioxidant activities of yuzu (*Citrus junos* Sieb ex Tanaka). *Journal of Food Measurement and Characterization*, 11, 576-585. DOI: <https://doi.org/10.1007/s11694-016-9425-x>
- Aung, L. H., Obenland, D. M., & Houck, L. G. (1998). Conditioning and heat treatments influence flavonoid soluble sugars of lemon. *Journal of Horticultural Science & Biotechnology*, 73, 399-440.
- Bejar, A. K., Ghanem, N., Mihoubi, D., Kechaou, N., & Mihoubi, N. B. (2011a). Effect of infrared drying on drying kinetics, color, total phenols and water and oil holding capacities of orange (*Citrus sinensis*) peel and leaves. *International Journal of Food Engineering*, 7, 5. DOI: <https://doi.org/10.2202/1556-3758.2222>
- Bejar, A. K., Kechaou, N., & Mihoubi, N. B. (2011b). Effect of microwave treatment on physical and functional properties of orange (*Citrus sinensis*) peel and leaves. *Journal of Food Processing and Technology*, 2, 109. DOI: <https://doi.org/10.4172/2157-7110.1000109>
- Chen M. L., Yang, D. J., & Liu, S. C. (2011). Effects of drying temperature on the flavonoid, phenolic acid and antioxidative capacities of the methanol extract of citrus fruit (*Citrus sinensis* (L.) Osbeck) peels. *International Journal of Food Science and Technology*, 46, 1179-1185. DOI: <https://doi.org/10.1111/j.1365-2621.2011.02605.x>

- Crizel, T. D. M., Araujo, R. R. D., Rios, A. D. O., Rech, R., & Flôres, S. H. (2014). Orange fiber as a novel fat replacer in lemon ice cream. *Food Science and Technology (Campinas)*, 34, 332-340 DOI: <https://doi.org/10.1590/fst.2014.0057>
- Deng, L. Z., Mujumdar, A. S., Yang, W. X., Zhang, Q., Zheng, Z. A., Wu, M., & Xiao, H. W. (2019). Hot air impingement drying kinetics and quality attributes of orange peel. *Journal of Food Processing and Preservation*, 44, e14294. DOI: <https://doi.org/10.1111/jfpp.14294>
- Farahmandfar, R., Tirgarian, B., Dehghan, B., & Nemati, A. (2019). Comparison of different drying methods on bitter orange (*Citrus aurantium* L.) peel waste: Changes in physical (density and color) and essential oil (yield, composition, antioxidant and antibacterial) properties of powders. *Journal of Food Measurement and Characterization*, 14, 862-75. DOI: <https://doi.org/10.1007/s11694-019-00334-x>
- Farahmandfar, R., Tirgarian, B., Dehghan, B., & Nemati, A. (2020). Changes in chemical composition and biological activity of essential oil from Thomson Navel orange (*Citrus sinensis* L. Osbeck) peel under freezing, convective, vacuum, and microwave drying methods. *Food Science and Nutrition*, 8, 124-138. DOI: <https://doi.org/10.1002/fsn3.1279>
- García-Salas, P., Gómez-Caravaca, A. M., Arráez-Román, D., Segura-Carretero, A., Guerra-Hernández, E., García-Villanova, B., & Fernández-Gutiérrez, A. (2013). Influence of technological processes on phenolic compounds, organic acids, furanic derivatives, and antioxidant activity of whole-lemon powder. *Food Chemistry*, 141, 869–878.
- Geedipalli, S. S. R., Rakesh, V., & Datta, A. K. (2007). Modeling the heating uniformity contributed by a rotating turntable in microwave ovens. *Journal of Food Engineering*, 82, 359-368. DOI: <https://doi.org/10.1016/j.jfoodeng.2007.02.050>
- Ghanem, N., Mihoubi, D., Bonazzi, C., Kechaou, N., & Boudhrioua, N. (2020). Drying characteristics of lemon by-product (*Citrus limon. v. lunari*): Effects of drying modes on quality attributes kinetics. *Waste Biomass Valorization*, 11, 303-22. DOI: <https://doi.org/10.1007/s12649-018-0381-z>
- Ghanem, N., Mihoubi, D., Kechaou, N., & Mihoubi, N. B. (2012). Microwave dehydration of three citrus peel cultivars: Effect on water and oil retention capacities, color, shrinkage, and total phenols content. *Industrial Crops and Products*, 40, 167-77. DOI: <https://doi.org/10.1016/j.indcrop.2012.03.009>
- Han, L., Zhang, J. & Cao, X. (2021). Effects of orange peel powder on rheological properties of wheat dough and bread aging. *Food Science and Nutrition*, 9, 1061–1069. DOI: <https://doi.org/10.1002/fsn3.2080>
- Hayat, K., Zhang, X. M., Chen, H. Q., Xia, S. Q., Jia, C. S., & Zhong, F. (2010). Liberation and separation of phenolic compounds from citrus mandarin peels by microwave heating and its effect on antioxidant activity. *Separation and Purification Technology*, 73, 371-376. DOI: <https://doi.org/10.1016/j.seppur.2010.04.026>
- IARC (2019). IARC working group on the evaluation of carcinogenic risks to humans. Some chemicals that cause tumours of the urinary tract in rodents. Available at: [www.ncbi.nlm.nih.gov/books/NBK546924/](http://www.ncbi.nlm.nih.gov/books/NBK546924/) (accessed 08 March 2023).
- Kamal, G. M., Anwar, F., Hussain, A. I., Sarri, N., & Ashraf, M. Y. (2011). Yield and chemical composition of citrus essential oils as affected by drying pretreatment of peels. *International Food Research Journal*, 18, 1275-1282.
- Karam, M. C., Petit, J., Zimmer, D., Djantou, E. B., & Scher, J. (2016). Effects of drying and grinding in production of fruit and vegetable powders: A review. *Journal of Food Engineering*, 188, 32-49. DOI: <https://doi.org/10.1016/j.jfoodeng.2016.05.001>
- Li, W. F., Li, Y. H., Bi, J., Ji, Q., Zhao, X., Zheng, Q. R., Tan, S., & Gao, X. X. (2020). Effect of hot air drying on the polyphenol profile of Hongjv (*Citrus reticulata* Blanco, cv. Hongjv) peel: A multivariate analysis. *Journal of Food Biochemistry*, 44: e13174. DOI: <https://doi.org/10.1111/jfbc.13174>
- Mahmoud, M. H., Abou-Arab, A. A., & Abu-Salem, F. M. (2015). Effect of some different drying methods on the chemical analysis of citrus by-products. *Research Journal of Pharmaceutical, Biological and Chemical Sciences*, 6, 105-16.
- Mazi, B. G., Koç Güler, S., & Bostan, S. Z. (2019). Post-harvest ripening of kiwifruit: changes in volatile compound profile. In: *Third international conference on agriculture, food, veterinary and pharmacy sciences (ICAFOP)*(pp. 1574-1582). Trabzon, Turkey.

- M'hiri, N., Ioannou, I., Ghoul, M., & Boudhrioua, N. M. (2017). Phytochemical characteristics of citrus peel and effect of conventional and nonconventional processing on phenolic compounds: A review. *Food Reviews International*, 33, 587-619. DOI: <https://doi.org/10.1080/87559129.2016.1196489>
- Ozcan, M. M., Ghafoor, K., Al Juhaimi, F., Uslu, N., Babiker, E. E., Ahmed, I. A. M., & Almusallam, I. A. (2020). Influence of drying techniques on bioactive properties, phenolic compounds and fatty acid compositions of dried lemon and orange peel powders. *Journal of Food Science and Technology*, 58, 147-58. DOI: <https://doi.org/10.1007/s13197-020-04524-0>
- Papoutsis, K., Pristijono, P., Golding, J. B., Stathopoulos, C. E., Bowyer, M. C., Scarlett, C. J., & Vuong, Q. V. (2017). Effect of vacuum-drying, hot air-drying and freeze-drying on polyphenols and antioxidant capacity of lemon (*Citrus limon*) pomace aqueous extracts. *International Journal of Food Science and Technology*, 52, 880-887. DOI: <https://doi.org/10.1111/ijfs.13351>
- Pathare, P. B., Opara, U. L., & Al-Said, F. A. (2013). Colour measurement and analysis in fresh and processed foods. *Food Bioprocess Technology*, 6, 36-60. DOI: <https://doi.org/10.1007/s11947-012-0867-9>
- Rafiq, S., Singh, B., & Gat, Y. (2019). Effect of different drying techniques on chemical composition, color, and antioxidant properties of kinnow (*Citrus reticulata*) peel. *Journal of Food Science and Technology*, 56, 2458-2466. DOI: <https://doi.org/10.1007/s13197-019-03722-9>
- Randhawa, M. A., Javed, M. S., Ahmad, Z., Amjad, A., Khan, A. A., Shah, F. U. H., & Filza, F. (2020). Amassing of hydroxymethylfurfural, 2-furfural and 5-methyl furfural in orange (*Citrus reticulata*) juice during storage. *Food Science and Technology*, 40, 382-386. DOI: <https://doi.org/10.1590/fst.41718>
- Romdhane, N. G., Bonazzi, C., Kechaou, N., & Mihoubi, N. B. (2015). Effect of air-drying temperature on kinetics of quality attributes of lemon (*Citrus limon* cv. lunari) peels. *Drying Technology*, 33, 1581-89. DOI: <https://doi.org/10.1080/07373937.2015.1012266>
- Shu, B., Wu, G. X., Wang, Z. N., Wang, J. N., Huang, F., Dong, L. H., Zhang, R. F., Wang, Y., & Su, D. X. (2020). The effect of microwave vacuum drying process on citrus: drying kinetics, physicochemical composition, and antioxidant activity of dried citrus (*Citrus reticulata* Blanco) peel. *Journal of Food Measurement and Characterization*, 14, 2443-52. DOI: <https://doi.org/10.1007/s11694-020-00492-3>
- Singh, B., Singh, J. P., Kaur, A., & Singh, N. (2020). Phenolic composition, antioxidant potential and health benefits of citrus peel. *Food Research International*, 132, 109114. DOI: <https://doi.org/10.1016/j.foodres.2020.109114>
- Tapia, M. S., Alzamora, S. M., & Chirife, J. (2020). Effects of water activity ( $a_w$ ) on microbial stability as a hurdle in food preservation. In G. V. Barbosa-Cánovas, A. J. Fontana, S. J. Schmidt, & T. P. Labuza (Eds.), *Water Activity in Foods: Fundamentals and Applications* (pp. 323-355). Hoboken, NJ: John Wiley & Sons. DOI: <https://doi.org/10.1002/9781118765982.ch14>
- Tekgül, Y., & Baysal, T. (2018). Comparative evaluation of quality properties and volatile profiles of lemon peels subjected to different drying techniques. *Journal of Food Process Engineering*, 41, e12902. DOI: <https://doi.org/10.1111/jfpe.12902>
- Tekgül, Y., & Baysal, T. (2019). Optimization of process conditions for vacuum microwave drying of lemon peel by response surface methodology: quality characteristics and volatile compounds. *Journal of Food Process Engineering*, 42, e13080. DOI: <https://doi.org/10.1111/jfpe.13080>
- Tomaschunas, M., Zor, R., Fischer, J., Kohn, E., Hinrichs, J., & Busch-Stockfisch, M. (2013). Changes in sensory properties and consumer acceptance of reduced fat pork Lyon-style and liver sausages containing inulin and citrus fiber as fat replacers. *Meat Science*, 95, 629-640. DOI: <https://doi.org/10.1016/j.meatsci.2013.06.002>
- Tuncer, A. D., Güler, H. Ö., & Usta, H. (2020). Modeling of drying characteristics of pomelo (*Citrus maxima*) peel. *El-Cezeri Journal of Science and Engineering*, 7, 198-210. DOI: <https://doi.org/10.31202/ecjse.616497>
- Xu, M. Y., Tian, G. F., Zhao, C. Y., Ahmad, A., Zhang, H. J., Bi, J. F., Xiao, H., & Zheng, J. K. (2017). Infrared drying as a quick preparation method for dried tangerine peel. *International Journal of Analytical Chemistry*, 6254793. DOI: <https://doi.org/10.1155/2017/6254793>
- Yi, T., Huang, X., Pan, S., & Wang, L. (2014). Physicochemical and functional properties of micronized jin Cheng orange by-products (*Citrus sinensis* Osbeck) dietary fiber and its application as a fat replacer

- in yogurt. *International Journal of Food Sciences and Nutrition*, 65, 565-572. DOI: <https://doi.org/10.3109/09637486.2014.898252>
- Zhang, L. L., Lv, S., Xu, J. G., & Zhang, L. F. (2018). Influence of drying methods on chemical compositions, antioxidant, and antibacterial activity of essential oil from lemon peel. *Natural Product Research*, 32, 1184-88. DOI: <https://doi.org/10.1080/14786419.2017.1320791>
- Zhang, M., Tang, J., Mujumdar, A. S., & Wang, S. (2006). Trends in microwave-related drying of fruits and vegetables. *Trends in Food Science & Technology*, 17, 524-534. DOI: <https://doi.org/10.1016/j.tifs.2006.04.011>



## Kepler Light Curve Modeling of KIC 9788457

Fahri Aliçavuş<sup>1,\*</sup>

<sup>1</sup>Çanakkale Onsekiz Mart University, Faculty of Science, Physics Department, Çanakkale, Türkiye

<sup>1</sup>Çanakkale Onsekiz Mart University, Astrophysics Research Center and Ulupınar Observatory, Çanakkale, Türkiye

### Article History

Received: 07.07.2023

Accepted: 10.08.2023

Published: 20.12.2023

### Research Article

**Abstract** – Eclipsing binary systems are significant objects for astrophysical studies since they offer more accurate fundamental stellar parameters (mass, radius). In particular, the determination of the astrophysical parameters of semi-detached binary stars is important in terms of examining the physical processes that occur as a result of interactions between components such as mass transfers and mass losses, since one of their components fills the Roche-lobe. Therefore, in this study, the first binary modeling of KIC 9788457 is presented to estimate the fundamental stellar parameters of the system. The photometric data of the system were taken from Kepler that provides high-quality data. When the light curve was checked it was found that the more luminous massive component has a significant light contribution into total. Therefore, using the spectral energy distribution and also color index (B-V) values effective temperature ( $T_{\text{eff}}$ ) value was estimated for the primary component. Utilizing this  $T_{\text{eff}}$  value, the binary modeling of the system was carried out. As a result, fundamental physical parameters of KIC9788457 were obtained. The radius (R) and mass (M) values of the components are  $M_1=1.89 \pm 0.05 M_{\text{sun}}$  and  $R_1= 2.03 \pm 0.02 R_{\text{sun}}$  for the massive component and  $M_2=0.81 \pm 0.02 M_{\text{sun}}$  and  $R_2= 1.74 \pm 0.03 R_{\text{sun}}$  for the less massive component, respectively. Additionally, the distance of the system was determined to be  $1407 \pm 85$  pc.

**Keywords** – Eclipsing binary, fundamental parameter, photometric analysis

## 1. Introduction

Binary stars are important objects, especially if they are an eclipsing binary star. They are invaluable objects for stellar astrophysics, as their fundamental stellar parameters (mass M, radius R) can be determined with high precision (Torres et. al., 2000; Southworth 2013). Fundamental parameters obtained from the analysis of observational data are essential for checking the accuracy of the evolutionary models and understanding the impact of binarity effects on stellar evolution. Many studies have been carried out in the literature on this subject (e.g. Kahraman Alicavus et al., 2022). Semi-detached binary systems, which are a subclass of the interacting binaries, are valuable for the analysis of the component's interaction in stellar evolution. Therefore, determination of the absolute parameters with the high precision data is essential for discerning the semi-detached binary systems. Hence, in this study, the first binary light curve examination of the Kepler field star, KIC 9788457, is presented by using high-quality Kepler data.

KIC 9788457 (2MASS J19524768+4631476, TIC 273870931, Gaia DR3 2085538610305376128,  $V=12^m.89$ ) was first observed by Kepler. It was classified as an eclipsing binary system with an orbital period of 0.963345 day (Slawson et al., 2011). The binary modeling of the system has not been carried out in the literature yet. Conroy et al. (2014) first examined the Kepler data of the binary system to investigate its orbital-period variation. In their study, they obtained 2938 minima times and found that the system has a third component with a 1000 days orbital period. The Kepler minima times of the system were also analysed by Borkovits et al. (2016). In their study, they showed that the variation on the orbital period caused by a third component

<sup>1</sup>  [fahrialicavus@comu.edu.tr](mailto:fahrialicavus@comu.edu.tr)

\*Corresponding author

which moves around the same centre of mass. Borkovits et al. (2016) also determined that the binary system has an eccentric orbit with a value  $e=0.46$  (1) and it moves around the centre of mass with 1960 days orbital period. They estimated a minimum mass to be  $0.07 M_{\odot}$  for the possible third component.

The out-of-eclipse light variations of the KIC 9788457 were also examined by Gaulme and Guzik (2019). In this study, they found that the system exhibits Delta Scuti type pulsations. The pulsation properties and available third component in the system make it very remarkable to be investigated. Therefore, obtaining the fundamental stellar parameters of the system with a detailed analysis is important. Hence, a high-quality Kepler light curve analysis of KIC 9788457 is presented in the current study.

The paper is organized as follows. In Sect. 2, the observational data and the analysis of spectral energy distribution are introduced. The light curve analysis is presented in Sect. 3. Calculation of the fundamental stellar parameters and conclusions are given in Sect. 4 and Sect. 5, respectively.

## 2. Observational data and Spectral energy distribution

The increasing number of space observations has improved the accuracy of the photometric data and helped us to determine even small amplitude variations. Especially thanks to the Kepler (Borucki et al., 2010) and Transiting Exoplanet Survey Satellite (TESS, Ricker et al. 2010) data, we are now able to reach the high-quality light curves of stellar systems including the eclipsing binaries. Kepler provides two cadences of data: short cadence (SC) and long cadence (LC). KIC 9788457 has LC Kepler data which were observed from quarter 1 to 17 expect for two quarters of 7 and 15. In this study, the quarter 1 and 2 data of the star were used, and these data were taken from the Barbara A. Mikulski Archive for Telescopes (MAST) database. The observational data first were converted to the magnitude, and it was phased by using the values of  $P=0^d.963345$  and  $T_0=2454965.186856$  (Slawson et al., 2011). The observational data were normalized for further analysis.

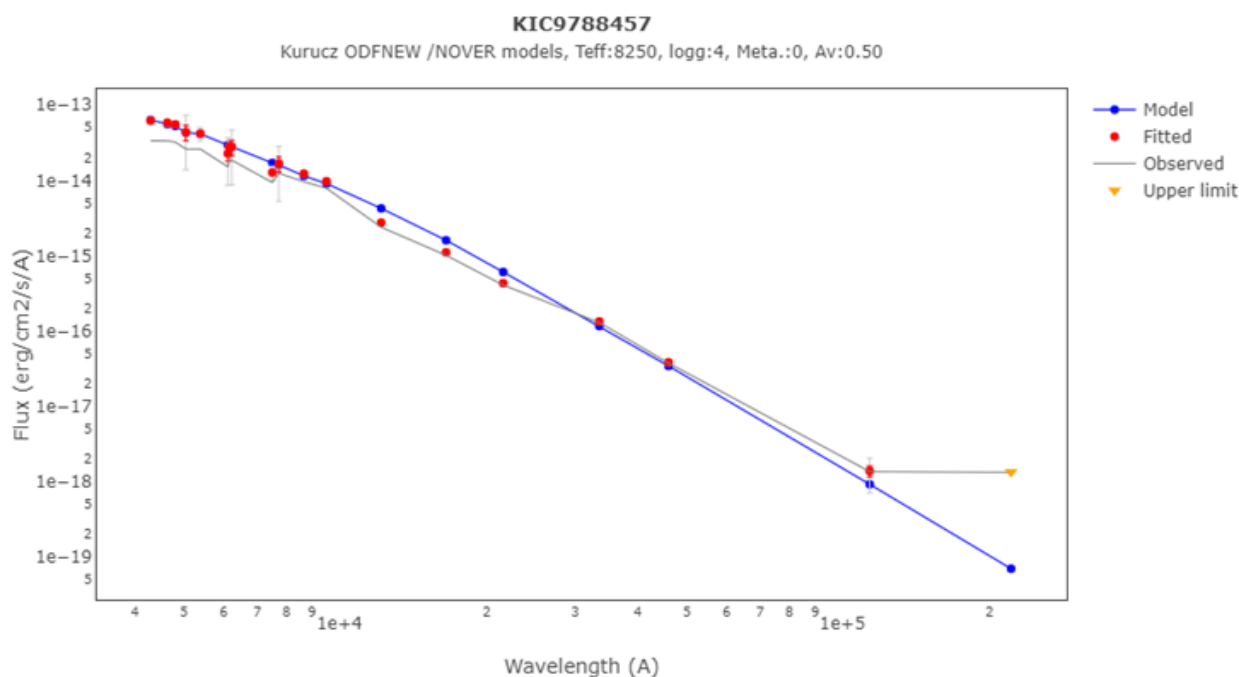


Figure 1. The spectral energy distribution for KIC 9788457.

When the light curve of the system was examined, it was seen that the primary component has a significantly high luminosity contribution in total ( $\sim 93\%$ ). Therefore, the spectral energy distribution analysis of the system will give us a good estimation of the effective temperature ( $T_{\text{eff}}$ ) for the primary component. Hence, the literature magnitudes in different colours were gathered. When the literature magnitudes of KIC 9788457 were searched for, we found that the system has APASS B-V, Sloan SDSS g-r, Pan-STARSS g,r,i,z, y, 2MASS J-H-Ks and also WISE W1, W2,W3 and W4 colors in the literature. The used fluxes in the spectral energy

distribution are given in Table 1. To eliminate the interstellar extinction effect, the extinction coefficient value of the star was calculated by using the Schlafly et al. (2011) and the Gaia DR3 distance (Gaia Collaboration et al., 2021) and the value was obtained to be  $A_v=0^m.516$  (For detail please see Eker et al. 2020). The spectral energy distribution analysis was performed in the Vosa database (Bayo et al., 2008) by using the Kurucz models (Kurucz, 1993) and assuming the surface gravity ( $\log g$ ) and metallicity values (M/H) as 4 and 0. In conclusion, the  $T_{\text{eff}}$  of the primary system was determined to be  $8250 \pm 280$  K. The theoretical spectral energy distribution fit to the observational data is illustrated in Fig. 1.

Table 1

The list of the used fluxes in the generation of spectral energy distribution of KIC 9788457.

Filter	$\lambda_{\text{med}}$	Observed		Dereddened		Model
		Flux	$\Delta\text{Flux}$	Flux	$\Delta\text{Flux}$	Flux
<b>APASS.B</b>	4297.17	3.35E-14	8.64E-16	6.20E-14	1.60E-15	6.34E-14
<b>SDSS.g</b>	4640.42	3.34E-14	4.61E-16	5.84E-14	8.06E-16	5.58E-14
<b>PS1.g</b>	4810.88	3.22E-14	1.02E-16	5.53E-14	1.75E-16	5.27E-14
<b>GAIA.Gbp</b>	5050	2.61E-14	5.94E-15	4.36E-14	9.95E-15	4.30E-14
<b>APASS.V</b>	5394.29	2.61E-14	1.75E-15	4.17E-14	2.80E-15	4.14E-14
<b>SDSS.r</b>	6122.33	1.51E-14	3.14E-15	2.27E-14	4.70E-15	2.94E-14
<b>PS1.r</b>	6156.33	1.89E-14	6.53E-16	2.82E-14	9.76E-16	2.91E-14
<b>GAIA.G</b>	6230	1.86E-14	4.23E-15	2.77E-14	6.31E-15	2.79E-14
<b>PS1.i</b>	7503.66	9.37E-15	6.65E-16	1.27E-14	9.03E-16	1.70E-14
<b>GAIA.Grp</b>	7730	1.24E-14	2.83E-15	1.67E-14	3.81E-15	1.60E-14
<b>PS1.z</b>	8668.53	9.61E-15	1.94E-16	1.23E-14	2.48E-16	1.15E-14
<b>PS1.y</b>	9613.4	7.88E-15	1.53E-16	9.72E-15	1.89E-16	9.07E-15
<b>2MASS.J</b>	12350	2.39E-15	4.40E-17	2.75E-15	5.06E-17	4.25E-15
<b>2MASS.H</b>	16620	1.01E-15	1.96E-17	1.11E-15	2.14E-17	1.61E-15
<b>2MASS.Ks</b>	21590	4.08E-16	7.89E-18	4.32E-16	8.36E-18	6.09E-16
<b>WISE.W1</b>	33526	1.30E-16	2.87E-18	1.34E-16	2.97E-18	1.17E-16
<b>WISE.W2</b>	46028	3.77E-17	7.28E-19	3.85E-17	7.45E-19	3.44E-17
<b>WISE.W3</b>	115608	1.37E-18	2.22E-19	1.39E-18	2.25E-19	9.29E-19
<b>WISE.W4</b>	220883	1.34E-18	3.05E-19	1.35E-18	3.08E-19	7.04E-20

### 3. Light curve analysis

To determine the precise fundamental parameters (M, R) of KIC 9788457, Kepler light curve analysis was performed. The normalized and phased Kepler light curve of the KIC 9788457 was analysed. In the light curve analysis, it is very critical to fix the  $T_{\text{eff}}$  value of the primary component by a good estimation. Armstrong et al. (2014) estimated the  $T_{\text{eff}}$  values of the primary and secondary binary components as  $T_{\text{eff1}}=10107 \pm 1313$  K and  $T_{\text{eff2}}=6148 \pm 1454$  K respectively. Unfortunately, their  $T_{\text{eff}}$  estimations have large error bars. Another  $T_{\text{eff}}$  estimation for the system is given as 7939 K by the investigation of the Kepler data (Prša et. al. 2011; Slawson et. al. 2011; Kirk et. al. 2016). When these  $T_{\text{eff}}$  values were taken into account, the  $T_{\text{eff}}$  value calculated in the current study by a spectral energy distribution was found between the previous  $T_{\text{eff}}$  estimations. Another  $T_{\text{eff}}$  estimation of the system could be done by using the B-V. In the  $T_{\text{eff}}$  calculation with B-V, the E(B-V) value was used by estimating from the calculated  $A_v$ . The  $(B-V)_0$  value was calculated to be  $0^m.164 \pm 0.023$  by using the APASS B ( $13^m.22$ ) and V ( $12^m.89$ ) colours. The  $T_{\text{eff}}$  values from this analysis will give us a good evaluation for the primary components  $T_{\text{eff}}$  when the less flux contribution of the secondary component was considered. By using the  $(B-V)_0$  value and the colour- $T_{\text{eff}}$  relations given by Eker et al. (2020), the  $T_{\text{eff}}$  value for the primary component was obtained to be  $8032 \pm 150$ K. This value was used in the binary light curve analysis as it has

lower uncertainty value. The bolometric albedos and the gravity darkening values of the binary components were fixed during the analysis.

The bolometric albedos were taken as 1 and 0.5 for the radiative and convective atmospheres, respectively (Rucinski, 1969). The gravity darkening values were also fixed as 1 (Von zeipel, 1924) for the primary and 0.32 (Lucy, 1967) for the secondary components. The eccentricity ( $e$ ) value was taken as 0 during the analysis as this value is expected for Algol type binary systems. The synchronize rotation was assumed as well ( $F_{1,2}=1$ ). The  $T_{\text{eff}}$  of the secondary component, the mass ratio ( $q$ ), orbital inclination ( $i$ ), phase shift, third light ( $l_3$ ), the relative luminosities and also dimensionless surface potentials ( $\Omega_{1,2}$ ) of the components were searched for. The light curve analysis was carried out with the Wilson-Devinney (W-D) code (Wilson & Devinney, 1971) simulated with Monte-Carlo (MC) (Zola et al., 2010). In the analysis, no differences between the solutions with third body consideration or without were found. The minimum  $\chi^2$  value was found for the semi-detached configuration mode, mode5. As a result, it was determined that the secondary component fills its Roche lobe, the primary component fills 83% of its first Roche lobe. Also, considering the minimum third body mass found by Borkovits et al. (2016), a significant light contribution could not be obtained as expected. The final parameters of the light curve analysis are given in Table 2. The resulting theoretical fit to the observations and the Roche lobes of the components are demonstrated in Fig. 2.

Table 2

Photometric solution parameters and their errors for KIC 9788457 system. \*fixed parameters.

Parameters	Value	Error
$T_{\text{eff}_1}$ (K)	8032*	150
$T_{\text{eff}_2}$ (K)	4598	180
$i$ (deg)	83.029	0.095
$\Omega_1$	3.296	0.010
$\Omega_2$	2.745	0.029
$q$ ( $=M_2/M_1$ )	0.429	0.001
<i>Phase shift</i>	0.0005	0.0002
$L_1/(L_1+L_2)$	0.923	0.008
$L_2/(L_1+L_2)$	0.077	0.008
$l_3$	0.00	-
<i>Filling factor</i> (%)	83	-
<i>Filling factor</i> (%)	100	-
$r_1$ (mean)	0.3558	0.0001
$r_2$ (mean)	0.3051	0.0001

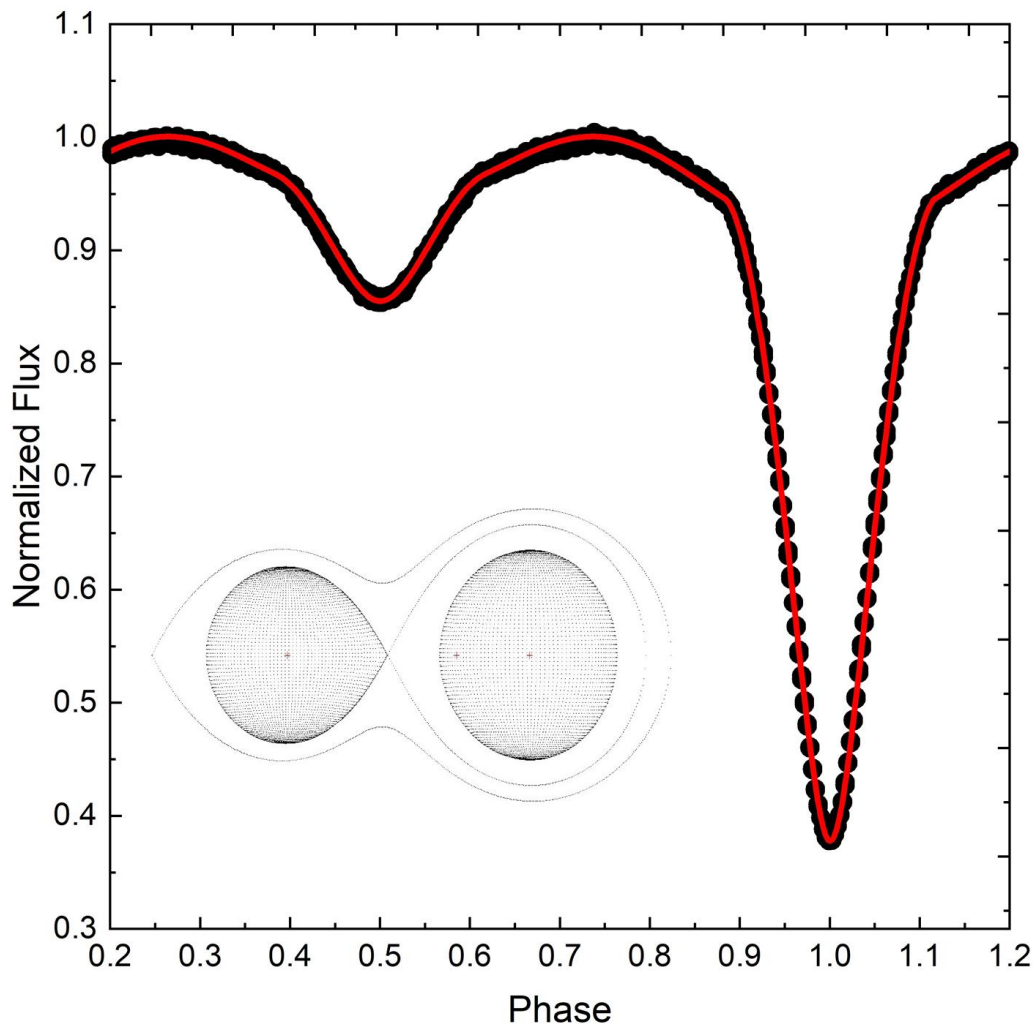


Figure 2. The best fitting theoretical binary modeling of KIC 9788457 and Roche configuration.

#### 4. Fundamental stellar parameters

The fundamental stellar parameters of KIC 9788457 were calculated by using the results of the light curve analysis given in Table 2. This method is commonly used for the binary system not having spectroscopic data (Zola et al., 2010). In the calculations, first  $M$  of the primary component was estimated as  $M_1 = 1.89 \pm 0.05 M_{\text{Sun}}$  by considering it as a main-sequence star and also using the  $T_{\text{eff}} - \text{Spectral type}$  and  $M$  relation given by Eker et al. (2020). Then the  $M$  value of the secondary component was calculated taking into account the  $M_1$  and  $q$  values. The semi-major axes ( $a$ ) was also calculated from the Kepler third law. The  $R$  of the component stars was determined by utilizing the fractional radii obtained in the light curve analysis and  $a$  value. The luminosities ( $L$ ) and the bolometric magnitudes ( $M_{\text{bol}}$ ) of the components were calculated with the help of solar  $T_{\text{eff}} = 5772 \text{ K}$ ,  $M_{\text{bol}} = 4^{\text{m}}.74$  values and bolometric corrections given by Eker et al. (2020). The  $\log g$  values were also determined by using the  $R$  and  $M$  of the components. The distance of the system was estimated using the  $E(B-V)$ , absolute magnitude ( $M_v$ ) values and also flux ratios of the components. For calculation of the distance ( $d$ ) following parameters were used;  $E(B-V) = 0^{\text{m}}.16$ ,  $BC_1 = 0^{\text{m}}.02$ ,  $m_{v1} = 12^{\text{m}}.98$ ,  $M_{v1} = 1^{\text{m}}.74$  and as a result,  $d$  was found to be  $1407 \pm 85 \text{ pc}$ . All calculated astrophysical parameters of KIC 9788457 were given in Table 3. The uncertainties of the parameters given in Table 3 were estimated taking into account the errors revealed by the MC method as a result of the light curve analysis and the observational errors from some basic parameter assumptions. In addition, with the help of the calculated fundamental parameters, the age of KIC9788457 is around 650 million years when the position of the primary component in the H-R diagram is examined considering the single star evolution (MIST models (Dotter 2016; Choi et. al. 2016; Paxton et. al. 2011; Paxton

et. al. 2013; Paxton et. al. 2015; Paxton et. al. 2018) were used and assuming the Asplund et al. 2009 solar abundance as  $Z=0.0142$ ). However, binary star evolution models that take into account mass transfer and loss mechanisms and orbital evolution are very important in order to determine the age of such semi-detached systems more accurately. For such evolution models to give accurate results, spectral data of the components are needed.

Table 3  
Absolute parameters of KIC 9788457.

Parameter	Values	Error
$a$ ( $R_{\text{sun}}$ )	5.72	0.24
$M_1$ ( $M_{\text{sun}}$ )	1.89	0.05
$M_2$ ( $M_{\text{sun}}$ )	0.81	0.02
$R_1$ ( $R_{\text{sun}}$ )	2.03	0.02
$R_2$ ( $R_{\text{sun}}$ )	1.74	0.03
$\log g_1$	4.10	0.02
$\log g_2$	3.86	0.02
$L_1$ ( $L_{\text{sun}}$ )	15.51	1.25
$L_2$ ( $L_{\text{sun}}$ )	1.22	0.18
$M_{\text{bol1}}$ (mag)	1.76	0.09
$M_{\text{bol2}}$ (mag)	4.52	0.16
$d$ (pc)	1407	85

## 5. Conclusion

In this study, the first binary modelling of KIC 9788457 is presented by using the Kepler data. According to the light curve it was estimated that the luminous massive component in the system has significant light contribution. Therefore, the  $T_{\text{eff}}$  parameter for the primary component was determined by using the photometric colours with the spectral energy distribution. In addition,  $T_{\text{eff}}$  value of the primary component was estimated with B-V colour. Since the uncertainty of B-V colour  $T_{\text{eff}}$  is lower, that value was used in the binary modeling. The binary modeling was carried out with the WD program and the binarity parameters were determined. Using the resulting parameters from the binary modelling, some fundamental stellar parameters were estimated. The M parameters for the primary and secondary components were found to be  $1.89 \pm 0.05 M_{\text{sun}}$  and  $0.81 \pm 0.02 M_{\text{sun}}$ , respectively. The R parameters were also estimated as  $2.03 \pm 0.02 R_{\text{sun}}$  and  $1.74 \pm 0.03 R_{\text{sun}}$  for the primary and secondary systems. According to filling factors the secondary component fills its Roche lobe. The distance of the system was calculated as well and found to be  $1407 \pm 85$  pc. When the Gaia distance (1568 pc) was compared with the distance found in this study, there is around 150 pc differences between two distances. This difference may be due to observational measurement errors and inability to calculate interstellar absorption accurately. When the astrophysical parameters found in this study were examined, it is seen that the primary component is in the instability region where delta Scuti type oscillation is dominant, as stated by Gaulme and Guzik (2019). The results obtained because of sensitive satellite observations of such binary systems with pulsating components are very important in terms of contributing to

the studies on the pulsating components. In addition to these, it is very important to make spectral observations of the system in order to control the findings in this study and to conduct evolutionary status studies in detail. In addition, long-term spectral observations are needed to check the existence of a third body.

### Acknowledgement

I would like to thank the reviewers for their constructive and improving comments.

### Author Contributions

Fahri Aliçavuş: All analysis presented in the paper.

### Conflicts of Interest

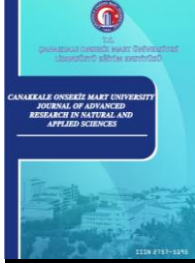
The authors declare no conflict of interest.

### References

- Armstrong, D. J., Gómez Maqueo Chew, Y., Faedi, F., & Pollacco, D. (2014). A catalogue of temperatures for Kepler eclipsing binary stars. *Monthly Notices of the Royal Astronomical Society*, 437(4), 3473-3481. Retrieved from: <https://academic.oup.com/mnras/article/437/4/3473/1006401>
- Asplund, M., Grevesse, N., Sauval, A. J., & Scott, P. (2009). The chemical composition of the Sun. *Annual review of astronomy and astrophysics*, 47, 481-522. Retrieved from: <https://www.annualreviews.org/doi/full/10.1146/annurev.astro.46.060407.145222>
- Bayo, A., Rodrigo, C., y Navascués, D. B., Solano, E., Gutiérrez, R., Morales-Calderón, M., & Allard, F. (2008). VOSA: virtual observatory SED analyzer-An application to the Collinder 69 open cluster. *Astronomy & Astrophysics*, 492(1), 277-287. Retrieved from: <https://www.aanda.org/articles/aa/abs/2008/46/aa10395-08/aa10395-08.html>
- Borkovits, T., Hajdu, T., Sztakovics, J., Rappaport, S., Levine, A., Bíró, I. B., & Klagyivik, P. (2016). A comprehensive study of the Kepler triples via eclipse timing. *Monthly Notices of the Royal Astronomical Society*, 455(4), 4136-4165. Retrieved from: <https://academic.oup.com/mnras/article/455/4/4136/1264839>
- Borucki, W. J., Koch, D., Basri, G., Batalha, N., Brown, T., Caldwell, D., ... & Prsa, A. (2010). Kepler planet-detection mission: introduction and first results. *Science*, 327(5968), 977-980. Retrieved from: <https://www.science.org/doi/10.1126/science.1185402>
- Choi, J., Dotter, A., Conroy, C., Cantiello, M., Paxton, B., & Johnson, B. D. (2016). Mesa isochrones and stellar tracks (MIST). I. Solar-scaled models. *The Astrophysical Journal*, 823(2), 102. Retrieved from: <https://iopscience.iop.org/article/10.3847/0004-637X/823/2/102/meta>
- Conroy, K. E., Prša, A., Stassun, K. G., Orosz, J. A., Fabrycky, D. C., & Welsh, W. F. (2014). Kepler eclipsing binary stars. IV. Precise eclipse times for close binaries and identification of candidate three-body systems. *The Astronomical Journal*, 147(2), 45. Retrieved from: <https://iopscience.iop.org/article/10.1088/0004-6256/147/2/45>
- Dotter, A. (2016). MESA Isochrones and Stellar Tracks (MIST) 0: methods for the construction of stellar isochrones. *The Astrophysical Journal Supplement Series*, 222(1), 8. Retrieved from: <https://iopscience.iop.org/article/10.3847/0067-0049/222/1/8/meta>
- Eker, Z., Soyduğan, F., Bilir, S., Bakış, V., Aliçavuş, Özer, S., ... & Köse, Y. (2020). Empirical bolometric correction coefficients for nearby main-sequence stars in the Gaia era. *Monthly Notices of the Royal Astronomical Society*, 496(3), 3887-3905. Retrieved from: <https://academic.oup.com/mnras/article/496/3/3887/5869829>
- Gaia-Collaboration, Klioner, S. A., Mignard, F., Lindgren, L., Bastian, U., McMillan, P. J., ... & Hodgkin, S. T. (2021). Gaia Early Data Release 3: Acceleration of the Solar System from Gaia astrometry. Retrieved from: [https://www.aanda.org/articles/aa/full\\_html/2021/05/aa39734-20/aa39734-20.html](https://www.aanda.org/articles/aa/full_html/2021/05/aa39734-20/aa39734-20.html)
- Gaulme, P., & Guzik, J. A. (2019). Systematic search for stellar pulsators in the eclipsing binaries observed by Kepler. *Astronomy & Astrophysics*, 630, A106. Retrieved from: [https://www.aanda.org/articles/aa/full\\_html/2019/10/aa35821-19/aa35821-19.html](https://www.aanda.org/articles/aa/full_html/2019/10/aa35821-19/aa35821-19.html)

- Kahraman Aliçavuş, F., Handler, G., Aliçavuş, F., De Cat, P., Bedding, T. R., Lampens, P., ... & Leone, F. (2022). Mass transfer and tidally tilted pulsation in the Algol-type system TZ Dra. *Monthly Notices of the Royal Astronomical Society*, 510(1), 1413-1424. Retrieved from: <https://academic.oup.com/mnras/article-abstract/510/1/1413/6449399?redirectedFrom=fulltext>
- Kirk, B., Conroy, K., Prša, A., Abdul-Masih, M., Kochoska, A., Matijević, G., ... & Borucki, W. (2016). Kepler eclipsing binary stars. VII. The catalog of eclipsing binaries found in the entire Kepler data set. *The Astronomical Journal*, 151(3), 68. Retrieved from: <https://iopscience.iop.org/article/10.3847/0004-6256/151/3/68>
- Kurucz, R. L. (1993). ATLAS9 Stellar Atmosphere Programs and 2 km/s grid. Kurucz CD-Rom. Retrieved from: <https://ui.adsabs.harvard.edu/abs/1993KurCD..13.....K>
- Lucy, L. B. (1967). Gravity-darkening for stars with convective envelopes. *Zeitschrift fur Astrophysik*, 65, 89. Retrieved from: <https://articles.adsabs.harvard.edu/pdf/1967ZA.....65...89L>
- Paxton, B., Bildsten, L., Dotter, A., Herwig, F., Lesaffre, P., & Timmes, F. (2011). Modules for experiments in stellar astrophysics (MESA). *The Astrophysical Journal Supplement Series*, 192(1), 3. Retrieved from: <https://iopscience.iop.org/article/10.1088/0067-0049/192/1/3/meta>
- Paxton, B., Cantiello, M., Arras, P., Bildsten, L., Brown, E. F., Dotter, A., ... & Townsend, R. (2013). Modules for experiments in stellar astrophysics (MESA): planets, oscillations, rotation, and massive stars. *The Astrophysical Journal Supplement Series*, 208(1), 4. Retrieved from: <https://iopscience.iop.org/article/10.1088/0067-0049/208/1/4/meta>
- Paxton, B., Marchant, P., Schwab, J., Bauer, E. B., Bildsten, L., Cantiello, M., ... & Timmes, F. X. (2015). Modules for experiments in stellar astrophysics (MESA): binaries, pulsations, and explosions. *The Astrophysical Journal Supplement Series*, 220(1), 15. Retrieved from: <https://iopscience.iop.org/article/10.1088/0067-0049/220/1/15/meta>
- Paxton, B., Schwab, J., Bauer, E. B., Bildsten, L., Blinnikov, S., Duffell, P., ... & Timmes, F. X. (2018). Modules for Experiments in Stellar Astrophysics (): Convective Boundaries, Element Diffusion, and Massive Star Explosions. *The Astrophysical Journal Supplement Series*, 234(2), 34. Retrieved from: <https://iopscience.iop.org/article/10.3847/1538-4365/aaa5a8/meta>
- Prša, A., Batalha, N., Slawson, R. W., Doyle, L. R., Welsh, W. F., Orosz, J. A., ... & Borucki, W. (2011). Kepler eclipsing binary stars. I. Catalog and principal characterization of 1879 eclipsing binaries in the first data release. *The Astronomical Journal*, 141(3), 83. Retrieved from: <https://iopscience.iop.org/article/10.1088/0004-6256/141/3/83>
- Ricker, G. R., Latham, D. W., Vanderspek, R. K., Ennico, K. A., Bakos, G., Brown, T. M., ... & Worden, S. P. (2010, January). Transiting exoplanet survey satellite (tess). In *American Astronomical Society Meeting Abstracts# 215* (Vol. 215, pp. 450-06). Retrieved from: <https://ui.adsabs.harvard.edu/abs/2010AAS...21545006R/abstract>
- Rucinski, S. M. (1969). The proximity effects in close binary systems. II. The bolometric reflection effect for stars with deep convective envelopes. *Acta Astronomica*, 19, 245. Retrieved from: <https://articles.adsabs.harvard.edu/pdf/1969AcA....19..245R>
- Schlafly, E. F., & Finkbeiner, D. P. (2011). Measuring reddening with Sloan Digital Sky Survey stellar spectra and recalibrating SFD. *The Astrophysical Journal*, 737(2), 103. Retrieved from: <https://iopscience.iop.org/article/10.1088/0004-637X/737/2/103>
- Slawson, R. W., Prša, A., Welsh, W. F., Orosz, J. A., Rucker, M., Batalha, N., ... & Koch, D. (2011). Kepler eclipsing binary stars. II. 2165 eclipsing binaries in the second data release. *The Astronomical Journal*, 142(5), 160. Retrieved from: <https://iopscience.iop.org/article/10.1088/0004-6256/142/5/160>
- Southworth, J. (2013). The solar-type eclipsing binary system LL Aquarii. *Astronomy & Astrophysics*, 557, A119. Retrieved from: [https://www.aanda.org/articles/aa/full\\_html/2013/09/aa22195-13/aa22195-13.html](https://www.aanda.org/articles/aa/full_html/2013/09/aa22195-13/aa22195-13.html)
- Torres, G., Lacy, C. H. S., Claret, A., & Sabby, J. A. (2000). Absolute dimensions of the unevolved B-type eclipsing binary GG Orionis. *The Astronomical Journal*, 120(6), 3226. Retrieved from: <https://iopscience.iop.org/article/10.1086/316855>
- Von Zeipel, H. (1924). The radiative equilibrium of a rotating system of gaseous masses. *Monthly Notices of the Royal Astronomical Society*, 84, 665-683. Retrieved from: <https://academic.oup.com/mnras/article/84/9/665/951714>

- Wilson, R. E., & Devinney, E. J. (1971). Realization of accurate close-binary light curves: application to MR Cygni. *The Astrophysical Journal*, 166, 605. Retrieved from: <https://articles.adsabs.harvard.edu/pdf/1971ApJ...166..605W>
- Zola, S., Gazeas, K., Kreiner, J. M., Ogloza, W., Siwak, M., Koziel-Wierzbowska, D., & Winiarski, M. (2010). Physical parameters of components in close binary systems–VII. *Monthly Notices of the Royal Astronomical Society*, 408(1), 464-474. Retrieved from: <https://academic.oup.com/mnras/article/408/1/464/1058765>



## Prioritization of Negative Carbon Strategies in the Cargo Industry with the SWARA/WASPAS Method

Emel Yontar<sup>1,\*</sup>, Onur Derse<sup>2</sup>

<sup>1,2</sup>Endüstri Mühendisliği Bölümü, Mühendislik Fakültesi, Tarsus Üniversitesi, Mersin, Türkiye

### Article History

Received: 03.05.2023

Accepted: 06.07.2023

Published: 20.12.2023

### Research Article

**Abstract** – The ever-increasing consumption of fossil fuels with the increasing population in the world has brought along the obligation of countries to take some precautions. Determining the measures to be taken to prevent carbon emissions, turning these measures into a strategy and implementing them has become one of the important issues that concern almost every field. Reducing, neutralizing and turning negative carbon emissions significantly reduces the side effects of climate change. In this study, it is aimed to develop strategies within the scope of carbon negative by considering the cargo sector, which is one of the important fields of activity of the transportation sector, where the carbon emission rate is high. SWARA and WASPAS methods, which are among the Multi-Criteria Decision Making methods, are used in the evaluation phase of the strategies determined through the Delphi technique and literature review. Strategies are asked to be prioritized for the implementation of 16 determined strategies within the cargo sector, and “Using electric vehicles” ranked first in both methods. “Use of carbon capture, exploitation and storage technologies”, “Balancing greenhouse gas emissions”, “Existence of carbon tax to reduce carbon emissions” strategies have also been identified as other top priority strategies. It is thought that the strategies listed as a result of the study can help reduce our carbon footprint and help reach negative carbon by reducing CO<sub>2</sub> levels in the atmosphere.

**Keywords** – Cargo industry; delphi technique; negative carbon strategies; SWARA method; WASPAS method

## 1. Introduction

Carbon emission is the main reason of global warming. There are several industrial processes that release significant amounts of CO<sub>2</sub> into the atmosphere (Sinha and Chaturvedi, 2019). Greenhouse gas emissions from human activities have caused significant climate change since the Industrial Revolution (Guo et al., 2022), and climate change and its social, environmental, economic and ethical implications are major interconnected challenges facing human societies. is widely accepted (Huisinigh et al., 2015). However, global awareness of the effects of climate change has led to a more restrictive and demanding society on consumption-related greenhouse gas emissions (Florindo et al., 2018). Furthermore, carbon emissions from processes could be controlled by the technologies in different processes of industries (Sinha and Chaturvedi, 2019). In this context, reducing carbon emissions has been an inevitable tendency and a global concurrence. Therefore, it is an important task for supply chain members to reduce their emissions in a low carbon environment (Ji et al., 2017). So, achieving net zero carbon emissions (Chen et al., 2022) and reducing carbon emissions is an important requirement. In order to meet climate reduction targets and achieve a net reduction in atmospheric carbon, some strategies need to be implemented at a large scale (Sanchez and Kammen, 2016). With negative carbon intensity, efficiency can be achieved both in the conversion of energy and in the conversion of carbon (Budzianowski, 2012). While many countries aim to be carbon neutral by 2050-2070, only 4.5% of countries have achieved carbon neutrality (Chen et al., 2022).

<sup>1</sup> eyontar@tarsus.edu.tr

<sup>2</sup> onurderse@tarsus.edu.tr

\*Corresponding Author

There are various studies in the literature. Such as; related to carbon reduction (Galinato and Yoder, 2010; Li et al., 2021; Siegel et al., 2021; Derse, 2023) and carbon neutral (Kato and Yamagata, 2014; Anderson and Peters, 2016; Van Vuuren et al., 2017; Emmerling et al., 2019) there are many studies on it. Budzianowski (2012) analyzes renewable energy technologies to reach carbon negative. Gallego-Alvarez et al. (2015) analyzes the impact of changes in carbon dioxide emissions on financial and operational performance. Huisingh et al. (2015) focus on researching technical innovations and policy interventions for improved energy efficiency and reduction of carbon emissions for different sectors. Ji et al. (2017) focus on a model that includes a low-carbon preference. The article analyzes a detailed model that includes a low carbon preference. The results show that the introduction of the online channel is profitable for the manufacturer when the low carbon sensitivity degree of consumers meets certain conditions. Florindo et al. (2018) lists in their work, taking into account the criteria in possible improvement actions that allow the reduction of the Carbon Footprint. A SWOT matrix is presented for each evaluated alternative and MCDM methods are applied to measure and rank possible improvement actions. Liu et al. (2019) analyzes the impact of income inequality on carbon emissions in the United States, taking into account the effects of income inequality on carbon emissions and the distribution of emissions. The results provide policymakers with important information on improving the quality of economic development and addressing climate change. In their study, Sinha and Chaturvedi (2019) review the research studies carried out for the execution of energy efficient and low carbon technologies for industries at different stages and classify these studies as process stages. Research studies for the planning of carbon emission limits are also examined. Johansson et al. (2020) produce and compare cost-effective emission routes that meet two different climate targets. Xuan et al. (2020) Based on China's carbon emissions trading experiment, this study adopts a model to explore the impact of carbon emissions trading policies on carbon emission reduction. Zhang et al. (2020) uses an econometric method to evaluate the impact of the emissions trading system on carbon emission reduction in their work. Li et al. (2021) measured the order and differences in the development and use of renewable energy in different regions in terms of carbon emission reduction, which provides an analytical perspective and a renewable energy-based solution for the use and distribution of renewable energy in China. Chen et al. (2022) presents decarbonisation technologies and initiatives, as well as negative emission technologies, and discusses carbon trading and carbon tax. Guo et al. (2022) states that China aims to reach its carbon emission peak before 2030 and carbon neutrality before 2060. The paper reviews and discusses technical strategies to achieve their goals in China's metal mines. Siksnyte-Butkiene et al. (2022) develops a framework by establishing the TOPSIS method to obtain the ideal synthesizing properties, materials and electrochemical measurements of the activated carbons electrode. Rahimirad and Sadabadi (2023) considers the goals of low-carbon energy transition and sustainable carbon-neutral society creation.

In the study, SWARA and WASPAS methods, which are among the Multi-Criteria Decision Making methods, are discussed. It is aimed to rank the negative carbon strategies with the methods discussed. When the literature was evaluated, no study was found in which these methods were sorted. However, there are some studies (Ghorshi Nezhad et al., 2015; Yurdođlu and Kundakç1, 2017; Sremac et al., 2018; Toklu et al., 2018; Ghoushchi et al., 2021; Yücenur and Ipekci, 2021; dealing with SWARA and WASPAS methods.

In this study, which deals with the cargo sector, it is aimed to rank the strategies determined by considering the strategies that can be applied within the scope of reducing and making negative for the carbon arising from the activities occurring in the sector, according to their importance with Multi-Criteria Decision Making methods. Increasing carbon emissions, climate change, the ozone layer, and the negative effects of human health, and increasing awareness and strategies are the motivation of the study. In the first part of the study, information and research on carbon neutrality and carbon reduction are presented. The second part of the study includes Materials and Methods, the third part includes the Findings, the fourth and last part includes Conclusions and Discussions.

## **2. Materials and Methods**

In this part of the study, the determination of the strategies developed for being carbon negative and their evaluation studies are presented (Fig.1). The desired and required strategies for carbon negative were primarily determined through literature review. Then, the opinions of 2 people working in the cargo sector, 4

academicians who are well-versed in carbon emissions, carbon footprint and climate change, and opinions that will affect the cargo sector's reaching negative carbon were received. The Delphi method was used to clarify and decide on the strategies in this context.

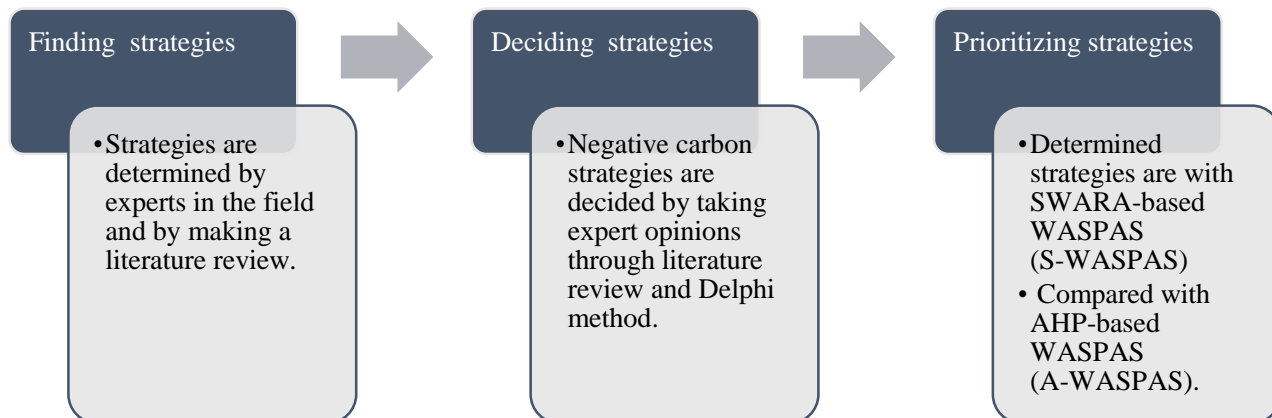


Figure 1. Analysis steps of developed strategies

The Delphi technique is a quantitative method that enables the development, evaluation and synthesis of ideas expressed on a particular subject (Christopher, 1994). According to Dalkey and Helmer (1963), the aim of the Delphi technique is to reach consensus on the opinions of a group of experts on a subject in the most reliable way. The application of the Delphi technique consists of a series of stages to reveal the approaches and perspectives of the experts (Cho and Turoff, 2001) or the representatives of the target audience on the problem situation, to examine and to reach a consensus. In this context, first of all, the development of a strategy for negative carbon includes the general purpose of the problem, in terms of transportation and transportation being a heavy sector in the cargo sector and causing carbon emissions. Within the framework of the defined problem, firstly, possible strategies that will contribute to the literature were discussed with the expert consisting of 6 people and their thoughts were asked. In line with the answers received, the suggested strategies, which were written in items, were presented to the experts' opinions again and they were asked to be scored on the Likert scale. With the repeated answers, one more cycle was achieved and the final criteria table was reached (Table 1). The determined strategies are 16 and are based on the answers of the literature and expert opinions.

Table 1  
Developed negative carbon strategies

Code	Negative carbon strategies	Authors	Description
NC1	Balancing greenhouse gas emissions	*	It refers to the efforts to increase the reduction of greenhouse gas emissions and to prevent their increase.
NC2	Use of carbon capture, exploitation and storage technologies	Chen et al., 2022; Fu et al., 2022; Fawzy et al. 2020	It refers to a series of processes that allow CO <sub>2</sub> to be captured, stored and used directly or indirectly in various products.
NC3	Using electric vehicles	Chen et al., 2022	It refers to the use of alternative vehicles (electric vehicles).
NC4	Ensuring the use of renewable energy sources	Millot and Maïzi 2021; Fawzy et al. 2020	It refers to the use of renewable and sustainable energy as an alternative to fossil fuels.
NC5	Using recyclable packaging in packaging	*	It refers to reducing the carbon footprint and reducing the environmental impact of life cycle assessment.
NC6	Increasing environmental awareness trainings for employees	*	It emphasizes the necessity of organizing periodic trainings on climate change and carbon footprint issues.
NC7	Increasing vehicle efficiency	Chen et al., 2022; Sharifi, 2021	It expresses the quality and number of vehicles used in the cargo sector.
NC8	Existence of carbon tax to reduce carbon emissions	Qiu et al., 2020	In terms of its deterrent feature, it means ensuring the continuity of the carbon tax rate set by the governments.
NC9	Implementation of afforestation/reforestation studies per transport	Terlouw et al., 2021; Schirmer and Bull, 2014	Afforestation refers to afforestation where there is no forest cover recently, while reforestation refers to the re-establishment of deforested forest areas.
NC10	Presence of resistant designs resistant to natural disasters in cargo buildings	Wang et al., 2018	It emphasizes the need to innovate and use resilient designs in cargo buildings as well as in transportation.
NC11	Spreading the circular economy model	*	It refers to the use of resource management with the logic of reduce-recycle-reuse instead of the logic of buy-make-consume.
NC12	Optimization of cargo distribution management	*	It means reducing the transportation time by making a good road analysis of the cargoes for distribution.
NC13	The growth of sharing economies such as parking spaces and crowdsourcing	Chen et al., 2022	It refers to making a less needed tool or service available to other users who need it.
NC14	Existence of recycling incentives for packaging for end users	*	It covers the incentives for the packages in the hands of the customers to be delivered to the cargo companies after the distribution.
NC15	Increasing stakeholder engagement and collaboration	*	It means raising awareness and taking a role of all stakeholders, from the supplier to the customer, for a carbon neutral life.
NC16	Limitation of cargo distribution contrary to what is known	*	It refers to the limitation of the distribution of cargo distributions on certain days and hours (during heavy traffic, etc.).

## 2.1. SWARA method

SWARA (Stepwise Weight Assessment Ratio Analysis) was developed in 2010 by Kersulienė et al. It is a multi-criteria decision-making method developed by and aiming to rank the criteria to be analyzed in order of importance (Kersulienė et al., 2010).

Step 1: The criteria are sorted in descending order of importance in line with expert opinion and the geometric mean is taken.

Step 2: The importance level of the criteria is determined. The value known as  $s_j$  (comparative significance of the mean value),  $j$ . criterion,  $(j+1)$ . by comparison with the criteria  $j$ . your criterion  $(j+1)$ . it is determined as how important it is from the criterion (Ruzgys et al., 2014).

Step 3: The coefficient  $k_j$  for each criterion is determined as in Equ (2.1).

$$k_j = \begin{cases} 1 & |j = 1 \\ s_j + 1 & |j > 1 \end{cases} \quad (2.1)$$

Step 4: The coefficient  $q_j$ , which expresses the weights, is calculated as in Equ (2.2).

$$q_j = \begin{cases} 1 & |j = 1 \\ \frac{q_{j-1}}{k_j} & |j > 1 \end{cases} \quad (2.2)$$

Step 5: With the help of (2.3) in the last step of the method,  $w_j$ ,  $j$ . the relative weight of the criterion is determined.

$$w_j = \frac{q_j}{\sum_{k=1}^n q_k} \quad (2.3)$$

## 2.2. WASPAS Method

WASPAS is a multi-criteria decision-making approach that combines the results of two different models, "Weighted Sum Model" and "Weighted Product Model" (Chakraborty & Zavadskas, 2014). By using these two methods together, it is aimed to increase the reliability of the solution results and to correctly order the decision alternatives.

Step 1: At the stage of creating the decision matrix, the  $x_{ij}$  values are combined into a matrix.

Step 2: In order to normalize the decision matrix, the values are normalized with the help of Equ (2.4) and (2.5) to take values in the range of [0,1].

$$x_{ij} = \frac{x_{ij}}{\max(x_{ij})} \quad i=1,2..m \quad j=1,2..n \quad (2.4)$$

$$x_{ij} = \frac{\min(x_{ij})}{(x_{ij})} \quad i=1,2..m \quad j=1,2..n \quad (2.5)$$

Step 3: Based on the weighted sum method  $i$ . calculation of the total relative importance of the alternative is performed.

$$Q_i^{(1)} = \sum_{j=1}^n x_{ij} \cdot w_j \quad (2.6)$$

Step 4: Based on the weighted multiplication method  $i$ . Calculation of the total relative importance of the alternative is carried out according to equation (2.7) by taking the force.

$$Q_i^{(2)} = \prod_{j=1}^n x_{ij}^{w_j} \quad (2.7)$$

Step 5: The  $(Q_i)$  value is calculated by calculating the weighted common general criterion value for the weighted sum and weighted product models (2.8).

$$Q_i = 0.5Q_i^{(1)} + 0.5Q_i^{(2)} \quad (2.8)$$

## 3. Application of the Study

The next step for the determined negative carbon strategies is to make an evaluation from six experts in the status of expert. At this stage, it was desired to use SWARA and WASPAS techniques. AHP technique was used for comparison. First of all, the criteria determined for the ranking of the strategies were asked from the experts to rank correctly from the most important criterion to the less important criterion with the SWARA technique, and the results obtained in Table 2 are presented.

Table 2  
SWARA expert opinions

Code	Criteria	1	2	3	4	5	6	Rank (Ave)
C1	Strategy implementation cost	1	3	2	1	2	1	1.51
C2	Strategy implementation time	3	2	4	3	3	3	2.94
C3	Contribution to carbon reduction	2	1	1	2	1	1	1.26
C4	Contribution to sustainable development goals	6	5	6	4	6	6	5.44
C5	Social acceptability	4	4	3	5	5	4	4.11
C6	Strategy implementation risk	5	6	5	6	4	5	5.12

SWARA steps were followed for each expert and their importance levels were determined according to the results. Table 3 shows an example order for Expert 3. Accordingly, the most important criteria for Expert 3 were determined as C1 and C3. By applying the same steps with other experts, the importance level of each strategy was averaged and the final ranking was determined (Table 4).

Table 3  
SWARA steps for Expert 3

Code	Negative carbon strategies	Rank	Order of importance	$s_j$	$k_j$	$q_j$	$w_j$
C3	Contribution to carbon reduction	1.26	1.00		1.00	1.00	0.20
C1	Strategy implementation cost	1.51	2.00	0.01	1.01	0.99	0.20
C2	Strategy implementation time	2.94	3.00	0.15	1.15	0.86	0.18
C5	Social acceptability	4.11	4.00	0.15	1.15	0.75	0.15
C6	Strategy implementation risk	5.12	5.00	0.10	1.10	0.68	0.14
C4	Contribution to sustainable development goals	5.44	6.00	0.10	1.10	0.62	0.13

Table 4  
Ranking as a result of averaged values

Code	Negative carbon strategies	$w_j$ Ave	Rank
C1	Strategy implementation cost	0.20	2
C2	Strategy implementation time	0.18	3
C3	Contribution to carbon reduction	0.21	1
C4	Contribution to sustainable development goals	0.12	6
C5	Social acceptability	0.16	4
C6	Strategy implementation risk	0.14	5

When the results obtained according to the SWARA method (Table 3) are interpreted, the “Contribution to carbon reduction” criterion becomes the first priority criterion for negative carbon studies. Then the “Strategy implementation cost” criterion took the second place.

For the WASPAS method, it was first requested to rank the strategies within the framework of certain criteria (C1 (Strategy implementation cost), C2 (Strategy implementation time), C3 (Contribution to carbon reduction), C4 (Contribution to sustainable development goals), C5 (Social acceptability), C6 (Strategy implementation risk)). According to these criteria, a decision matrix was formed by taking the average of the scores between 1-10 obtained from the experts (Table 5).

Table 5  
WASPAS decision matrix

Criteria direction	min	min	max	max	max	min
Code	C1	C2	C3	C4	C5	C6
NC1	1.67	4.67	7.67	6.33	7.67	3.00
NC2	1.33	3.33	7.33	6.00	5.33	2.33
NC3	1.00	3.67	8.33	7.00	8.33	5.33
NC4	2.67	4.33	6.67	7.33	7.00	4.33
NC5	4.33	4.33	5.33	7.00	7.33	4.67
NC6	3.67	4.33	5.00	6.67	7.33	7.33
NC7	5.33	7.33	5.67	6.67	5.67	7.33
NC8	7.00	2.67	7.33	6.00	5.33	4.00
NC9	4.33	5.67	5.33	7.00	5.00	5.33
NC10	4.67	4.00	5.00	5.33	4.67	4.67
NC11	5.67	4.67	4.67	7.33	6.67	5.33
NC12	7.33	6.33	5.33	5.33	5.33	6.00
NC13	6.67	4.67	5.00	5.33	4.67	4.67
NC14	7.00	5.00	4.33	6.00	4.33	6.33
NC15	6.33	4.00	5.33	7.33	4.67	5.00
NC16	7.00	5.67	5.67	5.00	3.67	4.33
<b>Criteria weight</b>	<b>0.20</b>	<b>0.18</b>	<b>0.21</b>	<b>0.12</b>	<b>0.16</b>	<b>0.14</b>

For the normalized decision matrix as a result of the decision matrix, the criterion aspect is taken as minimum for the implementation cost of the strategy, the implementation time of the strategy and the implementation risk criteria of the strategy; maximum direction has been taken for its contribution to carbon reduction, its contribution to sustainable development goals, and social acceptability criteria. Again, in line with the WASPAS steps, the weights of the criteria were determined by the SWARA method with expert opinion (Table 4). As a result of the applications, the ratings based on the weighted sum and weighted multiplication methods in Table 6 and Table 7 were calculated.

Table 6  
Relative importance values based on weighted sum method

	C1	C2	C3	C4	C5	C6	Qi (1)
NC1	0.12	0.1	0.19	0.1	0.15	0.11	0.768097
NC2	0.15	0.14	0.18	0.1	0.1	0.14	0.811492
NC3	0.2	0.13	0.21	0.11	0.16	0.06	0.866688
NC4	0.07	0.11	0.16	0.12	0.13	0.08	0.676897
NC5	0.05	0.11	0.13	0.11	0.14	0.07	0.611165
NC6	0.05	0.11	0.12	0.11	0.14	0.04	0.58014
NC7	0.04	0.06	0.14	0.11	0.11	0.04	0.503139
NC8	0.03	0.18	0.18	0.1	0.1	0.08	0.668735
NC9	0.05	0.08	0.13	0.11	0.1	0.06	0.532059
NC10	0.04	0.12	0.12	0.09	0.09	0.07	0.530694
NC11	0.03	0.1	0.11	0.12	0.13	0.06	0.560166
NC12	0.03	0.07	0.13	0.09	0.1	0.05	0.476877
NC13	0.03	0.1	0.12	0.09	0.09	0.07	0.501077
NC14	0.03	0.09	0.11	0.1	0.08	0.05	0.462485
NC15	0.03	0.12	0.13	0.12	0.09	0.07	0.555812
NC16	0.03	0.08	0.14	0.08	0.07	0.08	0.479009

Table 7  
Relative importance values based on weighted multiplication method

	C1	C2	C3	C4	C5	C6	Qi (2)
NC1	0.9	0.91	0.98	0.98	0.99	0.97	0.753051
NC2	0.94	0.96	0.97	0.98	0.93	1	0.804416
NC3	1	0.94	1	0.99	1	0.89	0.836249
NC4	0.82	0.92	0.96	1	0.97	0.92	0.643782
NC5	0.75	0.92	0.91	0.99	0.98	0.91	0.554095
NC6	0.77	0.92	0.9	0.99	0.98	0.85	0.527121
NC7	0.72	0.84	0.92	0.99	0.94	0.85	0.43906
NC8	0.68	1	0.97	0.98	0.93	0.93	0.559569
NC9	0.75	0.87	0.91	0.99	0.92	0.89	0.487778
NC10	0.74	0.93	0.9	0.96	0.91	0.91	0.492383
NC11	0.71	0.91	0.89	1	0.97	0.89	0.490548
NC12	0.68	0.86	0.91	0.96	0.93	0.88	0.414654
NC13	0.69	0.91	0.9	0.96	0.91	0.91	0.44655
NC14	0.68	0.89	0.87	0.98	0.9	0.87	0.407327
NC15	0.7	0.93	0.91	1	0.91	0.9	0.483385
NC16	0.68	0.87	0.92	0.96	0.88	0.92	0.423011

As a result of the weighted sum method and the weighted multiplication method, the  $\lambda$  value was taken as 0.5 and the final ranking table was created (Table 8).

Table 8  
Strategies sorted by S-WASPAS method

Negative carbon strategies code	Qi	Rank
NC1	0.76	3
NC2	0.81	2
NC3	0.85	1
NC4	0.66	4
NC5	0.58	6
NC6	0.55	7
NC7	0.47	13
NC8	0.61	5
NC9	0.51	11
NC10	0.51	10
NC11	0.53	8
NC12	0.45	15
NC13	0.47	12
NC14	0.43	16
NC15	0.52	9
NC16	0.45	14

As a result of the SWARA-based WASPAS application, the first priority strategy in the ranking was determined as NC3 coded “Using electric vehicles”. In order to compare the results of S-WASPAS, the AHP method was used, and the decision matrix was determined within the framework of the (1-9) scale, which was determined by Saaty's opinion of six experts (Table 9), and the degree of importance was calculated by normalizing it (Table 10).

Table 9  
AHP decision matrix

	<b>C1</b>	<b>C2</b>	<b>C3</b>	<b>C4</b>	<b>C5</b>	<b>C6</b>
<b>C1</b>	1.00	4.33	0.54	4.83	6.00	5.17
<b>C2</b>	0.23	1.00	0.23	3.50	3.50	2.50
<b>C3</b>	2.17	4.50	1.00	5.50	5.33	5.50
<b>C4</b>	0.21	0.29	0.18	1.00	3.50	0.42
<b>C5</b>	0.17	0.31	0.17	0.26	1.00	0.38
<b>C6</b>	0.20	0.42	0.18	2.50	2.83	1.00
<b>Total</b>	<b>3.98</b>	<b>10.85</b>	<b>2.30</b>	<b>17.60</b>	<b>22.17</b>	<b>14.96</b>

Table 10  
AHP normalized matrix

	<b>C1</b>	<b>C2</b>	<b>C3</b>	<b>C4</b>	<b>C5</b>	<b>C6</b>	<b>Importance value</b>
<b>C1</b>	0.251	0.399	0.236	0.275	0.271	0.345	<b>0.30</b>
<b>C2</b>	0.059	0.092	0.098	0.199	0.158	0.167	<b>0.13</b>
<b>C3</b>	0.544	0.415	0.435	0.313	0.241	0.368	<b>0.39</b>
<b>C4</b>	0.053	0.027	0.080	0.057	0.158	0.028	<b>0.07</b>
<b>C5</b>	0.042	0.028	0.072	0.015	0.045	0.025	<b>0.04</b>
<b>C6</b>	0.051	0.038	0.080	0.142	0.128	0.067	<b>0.08</b>

It is desired that the consistency ratio of the importance degrees obtained as a result of the calculation of the normalized matrix should be below 0.1. For this reason, the ratios determined by the experts in the study emerged as CR=0.089 and its consistency was confirmed. Then, the determined weights were applied in the WASPAS method, as in the equation 2.6 and 2.7, and the sequences of operations were applied and the strategies listed as a result of AHP-based WASPAS were determined (Table 11).

Table 11  
Strategies sorted by A-WASPAS method

<b>Negative carbon strategies code</b>	<b>Qi</b>	<b>Rank</b>
<b>NC1</b>	1	3
<b>NC2</b>	1.04	2
<b>NC3</b>	1.2	1
<b>NC4</b>	0.94	4
<b>NC5</b>	0.8	5
<b>NC6</b>	0.77	9
<b>NC7</b>	0.72	11
<b>NC8</b>	0.8	6
<b>NC9</b>	0.77	8
<b>NC10</b>	0.66	12
<b>NC11</b>	0.76	10
<b>NC12</b>	0.61	16
<b>NC13</b>	0.62	14
<b>NC14</b>	0.62	13
<b>NC15</b>	0.78	7
<b>NC16</b>	0.61	15

#### 4. Conclusion and Discussions

According to the results, the “Using electric vehicles” strategy took the first place and gave a similar result with the SWARA technique and AHP technique (Fig.2). “Use of carbon capture, exploitation and storage technologies” took the second place and “Existence of carbon tax to reduce carbon emissions” took the third place.

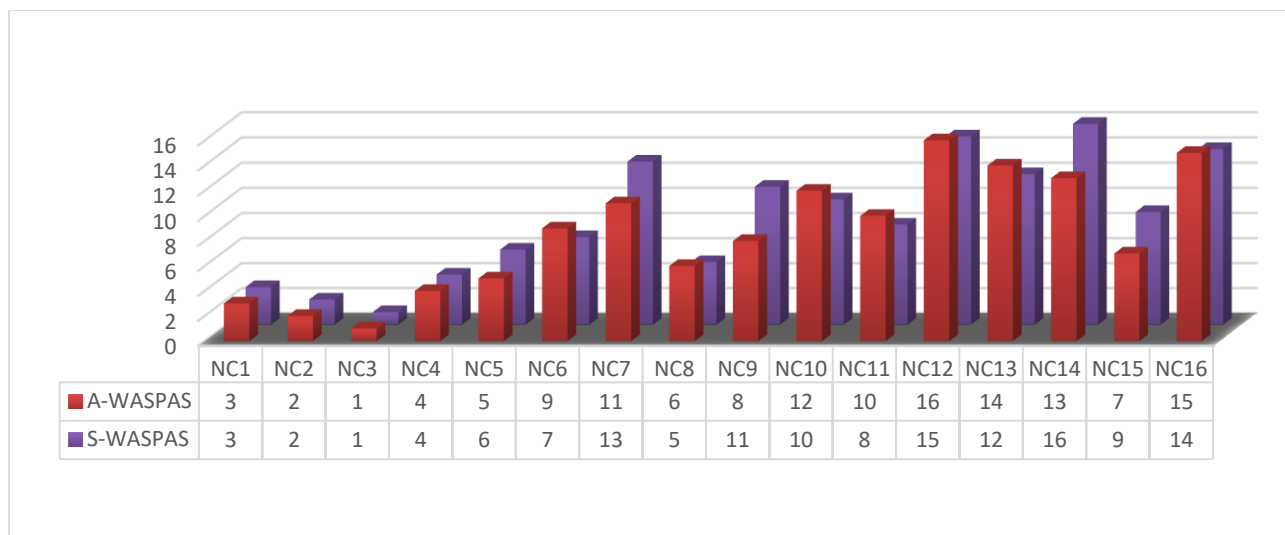


Figure 2. S-WASPAS and A-WASPAS comparison

Considering the strategies that the cargo sector should prioritize in order to reach negative carbon, the top five are; NC3 “Using electric vehicles”, NC2 “Use of carbon capture, exploitation and storage technologies”, NC1 “Balancing greenhouse gas emissions”, NC4 “Ensuring the use of renewable energy sources”, NC5 “Using recyclable packaging in packaging”, NC8 “Existence of carbon tax to reduce carbon emissions” strategies are coming (Fig.2).

The ever-increasing consumption of fossil fuels based on the growing population has caused the greenhouse gas effect with the CO<sub>2</sub> levels in the atmosphere rising rapidly from 280 ppm to 415 ppm by 2021 (Friedlingstein et al., 2020). The increasing greenhouse gas effect, which causes climate change along with global warming, brings along many problems. Therefore, each of the countries, institutions and sectors need to determine and implement strategic targets and policies in order to fulfil their emissions reduction commitments (Fu et al., 2022).

The current study aimed to apply the transportation sector in the cargo sector in order to reduce the greenhouse gas effect as well as to increase the negative carbon applications. Taking into account the activities in the cargo sector, “Balancing greenhouse gas emissions, Use of carbon capture, exploitation and storage Technologies, Using electric vehicles, Ensuring the use of renewable energy sources, Using recyclable packaging in packaging, Increasing environmental awareness trainings for employees, Increasing vehicle efficiency, Existence of carbon tax to reduce carbon emissions, Implementation of afforestation/reforestation studies per transport, Presence of resistant designs resistant to natural disasters in cargo buildings, Spreading the circular economy model, Optimization of cargo distribution management, The growth 16 strategies were determined, of sharing economies such as parking spaces and crowdsourcing, Existence of recycling incentives for packaging for end users, Increasing stakeholder engagement and collaboration, Limitation of cargo distribution contrary to what is known”. Evaluation of the specified strategies in SWARA based WASPAS method and AHP based WASPAS method C1 (Strategy implementation cost), C2 (Strategy implementation time), C3 (Contribution to carbon reduction), C4 (Contribution to Sustainable Development Goals), C5 (Social acceptability), C6 (Strategy implementation risk) ranked in order of importance, taking into account the criteria. When the results of the Multi-Criteria Decision Making methods (S-WASPAS, A-WASPAS) are examined, it is seen that consistent rankings are obtained. “Using electric vehicles” took the first place in both

methods. “Use of carbon capture, exploitation and storage technologies”, “Balancing greenhouse gas emissions”, “Existence of carbon tax to reduce carbon emissions” strategies have also been identified as other top priority strategies.

As a result of increasing environmental concerns, it has become important for the sectors to determine strategies to eliminate this concern, to set relevant targets and to work towards these targets. The cargo sector, which has an important place in the transportation sector, is at the forefront of the companies that want to contribute to sustainability by carrying out these studies. Being carbon negative is an opportunity for the cargo sector by putting the strategies suggested in the current study into practice and putting the prioritized strategies into practice.

As a result of the study, it is thought that the carbon footprint will decrease, the damage to the environment and the greenhouse gas emission levels in the atmosphere will decrease with the implementation of the strategies listed to reach negative and neutral carbon. In future studies, the situation of carbon reduction strategies in different sectors can be examined and the importance of strategies can be examined with different Multi-Criteria Decision Making methods.

### Author Contributions

Emel Yontar: Conceptualization, methodology, analysis and modelling, writing original draft, review and editing.

Onur Derse: Conceptualization, methodology, writing original draft, review and editing.

### Conflicts of Interest

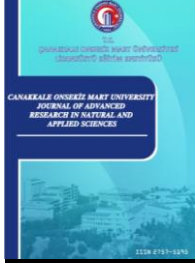
The authors declare no conflict of interest.

### References

- Anderson, K., & Peters, G. (2016). The trouble with negative emissions. *Science*, 354(6309), 182-183. DOI: 10.1126/science.aah4567
- Budzianowski, W. M. (2012). Negative carbon intensity of renewable energy technologies involving biomass or carbon dioxide as inputs. *Renewable and Sustainable Energy Reviews*, 16(9), 6507-6521. <https://doi.org/10.1016/j.rser.2012.08.016>
- Chakraborty, S., & Zavadskas, E. K. (2014). Applications of WASPAS method in manufacturing decision making. *Informatica*, 25(1), 1-20. <https://content.iospress.com/articles/informatica/inf25-1-01>
- Chen, L., Msigwa, G., Yang, M., Osman, A. I., Fawzy, S., Rooney, D. W., & Yap, P. S. (2022). Strategies to achieve a carbon neutral society: a review. *Environmental Chemistry Letters*, 20(4), 2277-2310. <https://doi.org/10.1007/s10311-022-01435-8>
- Chen, Z., Lv, H., Zhang, Q., Wang, H., & Chen, G. (2022). Construction of a cement–rebar nanoarchitecture for a solution-processed and flexible film of a Bi<sub>2</sub>Te<sub>3</sub>/CNT hybrid toward low thermal conductivity and high thermoelectric performance *Carbon Energy*, (1), 115-128. <https://doi.org/10.1002/cey2.161>
- Cho, H. K., & Turoff, M. (2001). Debiasing Group Judgments through Computerized Delphi Systems. [http://aisel.aisnet.org/amcis2001/51?utm\\_source=aisel.aisnet.org%2Famcis2001%2F51&utm\\_medium=PDF&utm\\_campaign=PDFCoverPages](http://aisel.aisnet.org/amcis2001/51?utm_source=aisel.aisnet.org%2Famcis2001%2F51&utm_medium=PDF&utm_campaign=PDFCoverPages)
- Christopher, M. (1994). Developing strategic and operational plans for logistics. *Handbook of Logistics and Distribution Management*. 43-62.
- Dalkey, N., & Helmer, O. (1963). An experimental application of the Delphi method to the use of experts. *Management science*, 9(3), 458-467. <https://doi.org/10.1287/mnsc.9.3.458>
- Derse, O. (2023). CO<sub>2</sub> capture, utilization, and storage (CCUS) storage site selection using DEMATEL-based Grey Relational Analysis and evaluation of carbon emissions with the ARIMA method. *Environmental Science and Pollution Research*, 30(6), 14353-14364. <https://doi.org/10.1007/s11356-022-23108-3>
- Emmerling, J., Drouet, L., van der Wijst, K. I., Van Vuuren, D., Bosetti, V., & Tavoni, M. (2019). The role of the discount rate for emission pathways and negative emissions. *Environmental Research Letters*, 14(10), 104008. <https://doi.org/10.1088/1748-9326/ab3cc9>

- Fawzy, S., Osman, A. I., Doran, J., & Rooney, D. W. (2020). Strategies for mitigation of climate change: a review. *Environmental Chemistry Letters*, 18, 2069-2094. <https://doi.org/10.1007/s10311-020-01059-w>
- Florindo, T. J., Florindo, G. D. M., Talamini, E., da Costa, J. S., de Léis, C. M., Tang, W. Z., ... & Ruviaro, C. F. (2018). Application of the multiple criteria decision-making (MCDM) approach in the identification of Carbon Footprint reduction actions in the Brazilian beef production chain. *Journal of Cleaner Production*, 196, 1379-1389. <https://doi.org/10.1016/j.jclepro.2018.06.116>
- Friedlingstein, P., O'sullivan, M., Jones, M. W., Andrew, R. M., Hauck, J., Olsen, A., ... & Zaehle, S. (2020). Global carbon budget 2020. *Earth System Science Data*, 12(4), 3269-3340. <https://doi.org/10.5194/essd-12-3269-2020>
- Fu, J., Li, P., Lin, Y., Du, H., Liu, H., Zhu, W., & Ren, H. (2022). Fight for Carbon Neutrality with State-of-the-art Negative Carbon Emission Technologies. *Eco-Environment & Health*. <https://doi.org/10.1016/j.eehl.2022.11.005>
- Galinato, G. I., & Yoder, J. K. (2010). An integrated tax-subsidy policy for carbon emission reduction. *Resource and Energy Economics*, 32(3), 310-326. <https://doi.org/10.1016/j.reseneeco.2009.10.001>
- Gallego-Álvarez, I., Segura, L., & Martínez-Ferrero, J. (2015). Carbon emission reduction: The impact on the financial and operational performance of international companies. *Journal of Cleaner Production*, 103, 149-159. <https://doi.org/10.1016/j.jclepro.2014.08.047>
- Ghorshi Nezhad, M. R., Zolfani, S. H., Moztarzadeh, F., Zavadskas, E. K., & Bahrami, M. (2015). Planning the priority of high tech industries based on SWARA-WASPAS methodology: The case of the nanotechnology industry in Iran. *Economic research-Ekonomiska istraživanja*, 28(1), 1111-1137. <https://doi.org/10.1080/1331677X.2015.1102404>
- Ghouschi, S. J., Bonab, S. R., Ghiaci, A. M., Haseli, G., Tomaskova, H., & Hajiaghaei-Keshteli, M. (2021). Landfill site selection for medical waste using an integrated SWARA-WASPAS framework based on spherical fuzzy set. *Sustainability*, 13(24), 13950. <https://doi.org/10.3390/su132413950>
- Guo, Q., Xi, X., Yang, S., & Cai, M. (2022). Technology strategies to achieve carbon peak and carbon neutrality for China's metal mines. *International Journal of Minerals, Metallurgy and Materials*, 29(4), 626-634. <https://doi.org/10.1007/s12613-021-2374-3>
- Huisingh, D., Zhang, Z., Moore, J. C., Qiao, Q., & Li, Q. (2015). Recent advances in carbon emissions reduction: policies, technologies, monitoring, assessment and modeling. *Journal of cleaner production*, 103, 1-12. <https://doi.org/10.1016/j.jclepro.2015.04.098>
- Ji, J., Zhang, Z., & Yang, L. (2017). Carbon emission reduction decisions in the retail-/dual-channel supply chain with consumers' preference. *Journal of cleaner production*, 141, 852-867. <https://doi.org/10.1016/j.jclepro.2016.09.135>
- Johansson, D. J., Azar, C., Lehtveer, M., & Peters, G. P. (2020). The role of negative carbon emissions in reaching the Paris climate targets: the impact of target formulation in integrated assessment models. *Environmental Research Letters*, 15(12), 124024. <https://doi.org/10.1088/1748-9326/abc3f0>
- Kato, E., & Yamagata, Y. (2014). BECCS capability of dedicated bioenergy crops under a future land-use scenario targeting net negative carbon emissions. *Earth's Future*, 2(9), 421-439. <https://doi.org/10.1002/2014EF000249>
- Keršulienė, V., Zavadskas, E. and Turskis, Z. (2010). Selection of rational dispute resolution method by applying new step-wise weight assessment ratio analysis (Swara). *Journal of Business Economics and Management*, 11(2), pp.243-258 <https://doi.org/10.3846/jbem.2010.12>
- Lee, S. R., Lee, J., Lee, T., Tsang, Y. F., Jeong, K. H., Oh, J. I., & Kwon, E. E. (2017). Strategic use of CO<sub>2</sub> for co-pyrolysis of swine manure and coal for energy recovery and waste disposal. *Journal of CO<sub>2</sub> Utilization*, 22, 110-116. <https://doi.org/10.1016/j.jcou.2017.09.018>
- Li, T., Li, A., & Song, Y. (2021). Development and utilization of renewable energy based on carbon emission reduction—evaluation of multiple MCDM methods. *Sustainability*, 13(17), 9822. <https://doi.org/10.3390/su13179822>
- Liu, C., Jiang, Y., & Xie, R. (2019). Does income inequality facilitate carbon emission reduction in the US?. *Journal of Cleaner Production*, 217, 380-387. <https://doi.org/10.1016/j.jclepro.2019.01.242>
- Millot, A., & Maïzi, N. (2021). From open-loop energy revolutions to closed-loop transition: What drives carbon neutrality?. *Technological Forecasting and Social Change*, 172, 121003. <https://doi.org/10.1016/j.techfore.2021.121003>

- Qiu, R., Xu, J., Xie, H., Zeng, Z., & Lv, C. (2020). Carbon tax incentive policy towards air passenger transport carbon emissions reduction. *Transportation Research Part D: Transport and Environment*, 85, 102441. <https://doi.org/10.1016/j.trd.2020.102441>
- Rahimirad, Z., & Sadabadi, A. A. (2023). Green hydrogen technology development and usage policymaking in Iran using SWOT analysis and MCDM methods. *International Journal of Hydrogen Energy*, 48(40), 15179-15194. <https://doi.org/10.1016/j.ijhydene.2023.01.035>
- Sanchez, D. L., & Kammen, D. M. (2016). A commercialization strategy for carbon-negative energy. *Nature Energy*, 1(1), 1-4. <http://dx.doi.org/10.1038/nenergy.2015.2>
- Schirmer, J., & Bull, L. (2014). Assessing the likelihood of widespread landholder adoption of afforestation and reforestation projects. *Global Environmental Change*, 24, 306-320. <https://doi.org/10.1016/j.gloenvcha.2013.11.009>
- Sharifi, A. (2021). Urban sustainability assessment: An overview and bibliometric analysis. *Ecological Indicators*, 121, 107102. <https://doi.org/10.1016/j.ecolind.2020.107102>
- Siegel, D. A., DeVries, T., Doney, S. C., & Bell, T. (2021). Assessing the sequestration time scales of some ocean-based carbon dioxide reduction strategies. *Environmental Research Letters*, 16(10), 104003. <https://doi.org/10.1088/1748-9326/ac0be0>
- Siksnyte-Butkiene, I., Streimikiene, D., & Balezentis, T. (2022). Addressing sustainability issues in transition to carbon-neutral sustainable society with multi-criteria analysis. *Energy*, 254, 124218. <https://doi.org/10.1016/j.energy.2022.124218>
- Sinha, R. K., & Chaturvedi, N. D. (2019). A review on carbon emission reduction in industries and planning emission limits. *Renewable and Sustainable Energy Reviews*, 114, 109304. <https://doi.org/10.1016/j.rser.2019.109304>
- Sremac, S., Stević, Ž., Pamučar, D., Arsić, M., & Matić, B. (2018). Evaluation of a third-party logistics (3PL) provider using a rough SWARA–WASPAS model based on a new rough dombi aggregator. *Symmetry*, 10(8), 305. <https://doi.org/10.3390/sym10080305>
- Terlouw, T., Bauer, C., Rosa, L., & Mazzotti, M. (2021). Life cycle assessment of carbon dioxide removal technologies: a critical review. *Energy & Environmental Science*, 14(4), 1701-1721. <https://doi.org/10.1039/D0EE03757E>
- Toklu, M. C., Çağıl, G., Pazar, E., & Faydalı, R. (2018). SWARA-WASPAS metodolojisine dayalı tedarikçi seçimi: türkiye'de demir-çelik endüstrisi örneği. *Academic Platform-Journal of Engineering and Science*, 6(3), 113-120. <https://doi.org/10.21541/apjes.441362>
- Van Vuuren, D. P., Hof, A. F., Van Sluisveld, M. A., & Riahi, K. (2017). Open discussion of negative emissions is urgently needed. *Nature energy*, 2(12), 902-904. <https://doi.org/10.1038/s41560-017-0055-2>
- Wang, H. F., Tang, C., & Zhang, Q. (2018). A review of precious-metal-free bifunctional oxygen electrocatalysts: rational design and applications in Zn–air batteries. *Advanced Functional Materials*, 28(46), 1803329. <https://doi.org/10.1002/adfm.201803329>
- Xuan, D., Ma, X., & Shang, Y. (2020). Can China's policy of carbon emission trading promote carbon emission reduction?. *Journal of Cleaner Production*, 270, 122383. <https://doi.org/10.1016/j.jclepro.2020.122383>
- Yoon, K., Oh, J. I., Tsang, D. C., Kwon, E. E., & Song, H. (2019). Catalytic thermolysis of oak sawdust using Fe-based catalyst and CO<sub>2</sub>. *Journal of CO<sub>2</sub> Utilization*, 32, 269-275. <https://doi.org/10.1016/j.jcou.2019.04.024>
- Yücenur, G. N., & Ipekçi, A. (2021). SWARA/WASPAS methods for a marine current energy plant location selection problem. *Renewable Energy*, 163, 1287-1298. <https://doi.org/10.1016/j.renene.2020.08.131>
- Yurdoğlu, H., & Kundakçı, N. (2017). SWARA ve WASPAS yöntemleri ile sunucu seçimi. *Balıkesir Üniversitesi Sosyal Bilimler Enstitüsü Dergisi*, 20(38), 253-270. <https://doi.org/10.31795/baunsobed.645105>
- Zhang, Y., Li, S., Luo, T., & Gao, J. (2020). The effect of emission trading policy on carbon emission reduction: Evidence from an integrated study of pilot regions in China. *Journal of Cleaner Production*, 265, 121843. <https://doi.org/10.1016/j.jclepro.2020.121843>



## Kidney Segmentation with LinkNetB7

Cihan Akyel<sup>1,\*</sup>

<sup>1</sup>Ministry of Education, General Directorate of Construction and Real Estate, Ankara, Türkiye

### Article History

Received: 03.01.2023

Accepted: 27.07.2023

Published: 20.12.2023

### Research Article

**Abstract** – Cancer is a deadly disease for which early diagnosis is very important. Cancer can occur in many organs and tissues. Renal cell carcinoma (RCC) is the most common and deadly form of kidney cancer. When diagnosing the disease, segmentation of the corresponding organ on the image can help experts make decisions. With artificial intelligence supported decision support systems, experts will be able to achieve faster and more successful results in the diagnosis of kidney cancer. In this sense, segmentation of kidneys on computed tomography images (CT) will contribute to the diagnosis process. Segmentation can be done manually by experts or by methods such as artificial intelligence and image processing. The main advantages of these methods are that they do not involve human error in the diagnostic process and have almost no cost. In studies of kidney segmentation with artificial intelligence, 3d deep learning models are used in the literature. These methods require more training time than 2d models. There are also studies where 2d models are more successful than 3d models in organs that are easier to segment on the image. In this study, the LinkNetB7 model, which has not been previously used in renal segmentation studies, was modified and used. The study achieved a dice coefficient of 97.20%, precision of 97.30%, sensitivity of 97%, and recall of 97%. As a result of the study, LinknetB7 was found to be applicable in kidney segmentation. Although it is a 2d model, it is more successful than UNet3d and some other 2d models.

**Keywords** – Decision Support System, image processing, image segmentation, kidney cancer, LinkNetB7.

### 1. Introduction

The kidney is a vital organ that filters pollutants from the blood and provides for the excretion of waste through the urine. Although there are several types of kidney cancer, the deadliest and most common form is renal cell carcinoma (RCC). RCC accounts for about 90% of all kidney cancers. Kidney cancer can metastasize to other organs through the bloodstream. For this reason, early diagnosis of kidney cancer is extremely important. It is observed that metastases occur in about 30% of patients when renal cancer is first diagnosed (Demir & Balçık, 2022).

The incidence of kidney cancer may increase due to factors such as smoking and physical inactivity. Early diagnosis of cancer is very important to increase the survival rate of patients and prevent metastasis. Regular screening is important for early detection of kidney cancer. Despite treatment, metastasis can occur in this type of cancer (Kölükçü et al., 2019).

Although the diagnosis can be made by examining CT images, histopathologic examination is required for definitive diagnosis of renal cancer (Devrim, 2019). CT images of the abdominal region are used to detect renal cancer. However, CT images of this region also show other organs such as the liver (Üyetürk et al., 2014). In this case, the differentiation (segmentation) of the kidney on these images becomes important for the diagnostic process.

RCC is the most common urologic cancer with a mortality rate of over 40% (Budak et al., 2013). Diagnosis of RCC can be made by experts by examining ultrasound and/or CT images. Depending on the results, a definitive diagnosis may be made by histopathological examination, if necessary. In the diagnostic process, segmentation

<sup>1</sup>  [cihan.akyel1@gazi.edu.tr](mailto:cihan.akyel1@gazi.edu.tr)

\*Corresponding author

of the kidney in abdominal CT images can be considered as the first step for both classical methods and artificial intelligence-based methods.

To perform kidney segmentation with artificial intelligence algorithms, datasets containing masks suitable for supervised learning are needed. One of these datasets is the dataset named "KiTS19 challenge dataset" in 2019 (KiTS19, 2019). This dataset is preferred in many studies because it is open to the right and allows comparison with other studies.

The biggest challenge for the healthcare industry is to provide quality services at an affordable cost. At this stage, decision support systems (DSS) can help the expert make the right decision. By using artificial intelligence algorithms in decision support systems, greater success can be achieved (Kumar et al. (2011).

There are studies in the literature showing that LinkNet is more successful than UNet in segmenting medical images (Kallam et al. (2020), Akyel and Arıcı (2022)). The success of the models can be increased by hybrid use in medical image segmentation. As an alternative to the 2d and 3d models in the existing literature, the LinkNet-based LinkNetB7 model study was used. LinkNetB7 was preferred due to its flexible structure (encoder-decoder architecture), its great success in medical image segmentation, and the fact that it is not used in this field.

### **1.1. Literature Review**

Deep learning models with a seeker-solver architecture provide successful results in medical image segmentation. In models with this structure, features are extracted from images along coding blocks. Solver blocks attempt to obtain output data corresponding to these features. Hsiao et al. (2022) obtained a dice coefficient of 96.90% using the KiTS2019 dataset. In the study, an algorithm with an encoder-decoder architecture was developed. EfficientNetB5 was chosen as the encoder model. EfficientNet is an algorithm with high success scores that was introduced by Google in 2019. In the study, images were subjected to contrast enhancement before being imported into the system.

The dataset used for kidney segmentation with Deep Learning can directly influence success. In particular, images where the kidney is not included in the dataset can reduce success. As a solution to this situation, some studies do not include images that do not contain the kidney in the training. In the study by Da Cruz et al. (2021), UNet was the preferred model. In the study, CT images that did not contain the kidney were extracted and not included in the segmentation training. In the study, a dice coefficient of 96.33% was obtained with KiTS2019 data.

In image preprocessing, removing the areas outside the kidney that are classified as noise can have a positive impact on success. Zhao et al. (2020) presented a study on kidney segmentation in 2020. In the study, they used a UNet-based algorithm. It was found that the noise on CT can negatively influence the success. From this point of view, it is found that the noise is cleaned in the data to be trained. In this study, a dice coefficient of 96.69% was obtained using the KiTS19 dataset.

The UNet algorithm can be used as a hybrid with different models. Different models can be used for the coding blocks in the UNet model. This increases the success and thus the number of features that can be extracted from images. A review of the literature shows that models such as UNet and Efficient-Net and ResNet can be preferred together. One of the studies that illustrates this type of usage is Li et al. (2022). In the study, residual blocks, which are the basis of ResNet algorithm, are used together with UNet. Using the algorithm called Res-UNet, an accuracy of 96.54% was achieved in the segmentation of kidneys. It was noted that proprietary datasets were used in the study.

Pixel loss in the data being trained is one of the problems encountered in media image segmentation. System constraint can be used to train the images of the dataset by reducing their size. In some studies, the images are divided into slices to solve this situation. In a study by Haghghi et al. (2018), kidney images were segmented. They used a dataset called DCE-MRI, which contains data from 30 patients. One of the most important aspects of the study is the segmentation of each training image. In this study, a dice coefficient of 91.4% was obtained using the UNet model.

LinkNet is a low training time model in the decoder architecture used in image segmentation. There are studies in which it is more successful than the UNet architecture. One of these examples was presented by Akyel and

Arıcı (2022). In their study, about 8% higher detection success was achieved in skin cancer image segmentation than with the standard UNet model. In another study, a modified LinkNet model was used to segment histopathological images. According to this study, LinkNet showed about 2% higher success (Kallam et al. 2020).

3d models are generally preferred for segmentation of organs such as kidney and liver. With this default, it is effective that CT images can be trained in slices. However, there are also examples in the literature of 2d models being effective for organs that are easier to segment, such as kidneys. An example of this situation is the work of Zettler and Mastmeyer, (2021). In the study, 2d and 3d UNet models were compared. According to the comparison result, 3d UNet consumes more system memory than 2d UNet. UNet3d, in turn, requires 41 seconds more epoch time. UNet2d achieved about 1% higher success in liver segmentation and 2% higher success in kidney segmentation. The reason for this is the low number of axial slices.

A review of the literature shows that a LinkNet-based algorithm is not used in kidney segmentation. In this study, unlike the literature, the LinkNetB7 model was preferred. In the study using the KiTS19 dataset, the images were divided into 36 patches to avoid pixel loss. Contrast enhancement and normalization were applied to the KiTS19 dataset. In the second part of the study, the models and methods used are described in detail. The third section presents the obtained results compared to some studies. The fourth section summarizes the study and discusses what can be done in future studies.

## 2. Materials and Methods

A publicly available dataset with CT images from KiTS2019 was used for the study. During the training phase, the dataset was split into 80% training and 20% validation. The hyperparameters used are listed in Table 1. The results obtained with the 2d LinkNetB7 model used were combined and converted to a 3d form.

Table 1  
Hyper parameters

Parameter	Value
Learning Rate	0.0001
Optimizer	Adam
Output Function	Sigmoid
Loss Function	DLMSE
Epoch Number	50
Input Size	256x256x3

### 2.1. Dataset

It consists of kidney images CT from 300 patients between 2010 and 2018 in the KiTS19 dataset. These images are in NIFTI format and consist of a varying number of slices. In the study, the images in NIFTI format were converted to jpeg format and used for training. All slices were combined into a single folder without distinguishing between patients. Information about the KiTS19 dataset that was used can be found in Table 2.

Table 2  
KiTS19 Dataset

Parameter	Value
Slice thicknesses range	1mm to 5 mm
Number of files in NIFTI format	300 (210 for Training, 90 for Test)
Number of images in jpeg format	432000 (360000 for Training, 72000 for Test)
Licence information	Public CC BY-NC-SA

### 2.2. Pre-Processing Phase

First, normalization or contrast enhancement was performed with Clahe to distinguish the kidney from the abdominal cavity by increasing the contrast difference between the images. This process is shown in Fig 1.

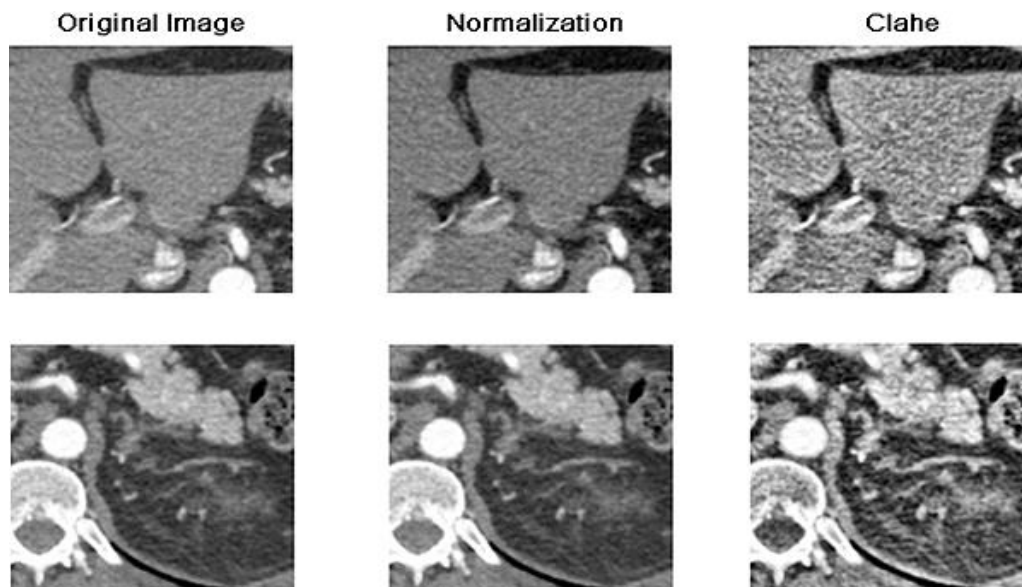


Figure 1. Image processing steps

In the next step, the images of the dataset are divided into 36 layers with a resolution of 256x256. With this method, there is no pixel loss for images up to 1536x1536 resolution, and pixel loss is reduced for higher resolutions. In addition, the images that could not contain kidneys in the training images of the study were not included in the system according to the mask value with the image processing technique. This process is shown in Fig 2.

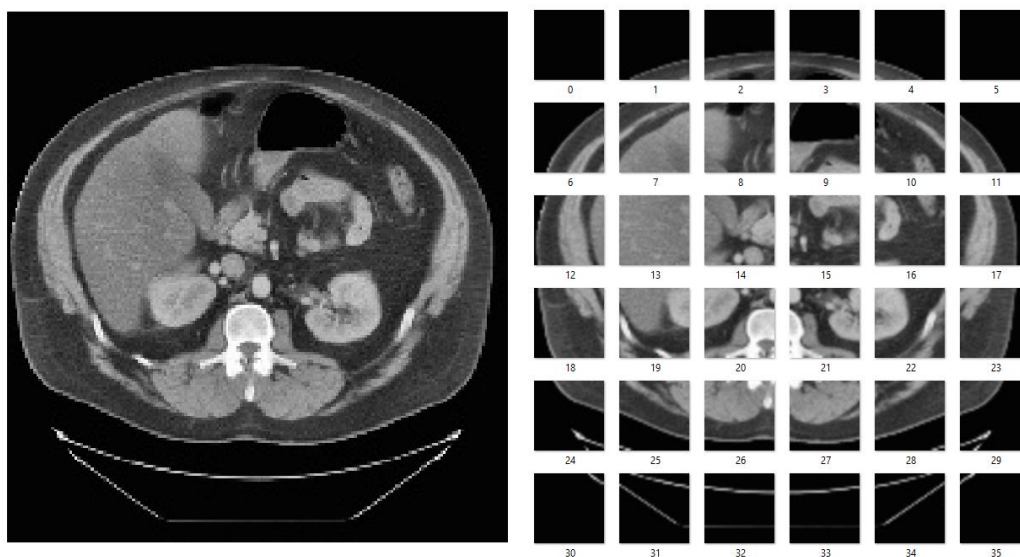


Figure 2. The process of dividing the image into patches

**2.3. LinkNet and LinkNetB7 Architecture**

Two features that distinguish LinkNet are its low training time and its success in medical image segmentation. This model was proposed in 2017. It consists of 4 coding blocks and 4 decoding blocks. In the coding blocks, Res-Net18 is preferred to reduce the epoch time. As with the UNet model, LinkNet can also achieve an increase in success by choosing different coding models (Chaurasia & Culurciello, 2017). The LinkNet architecture is shown in Fig 3.

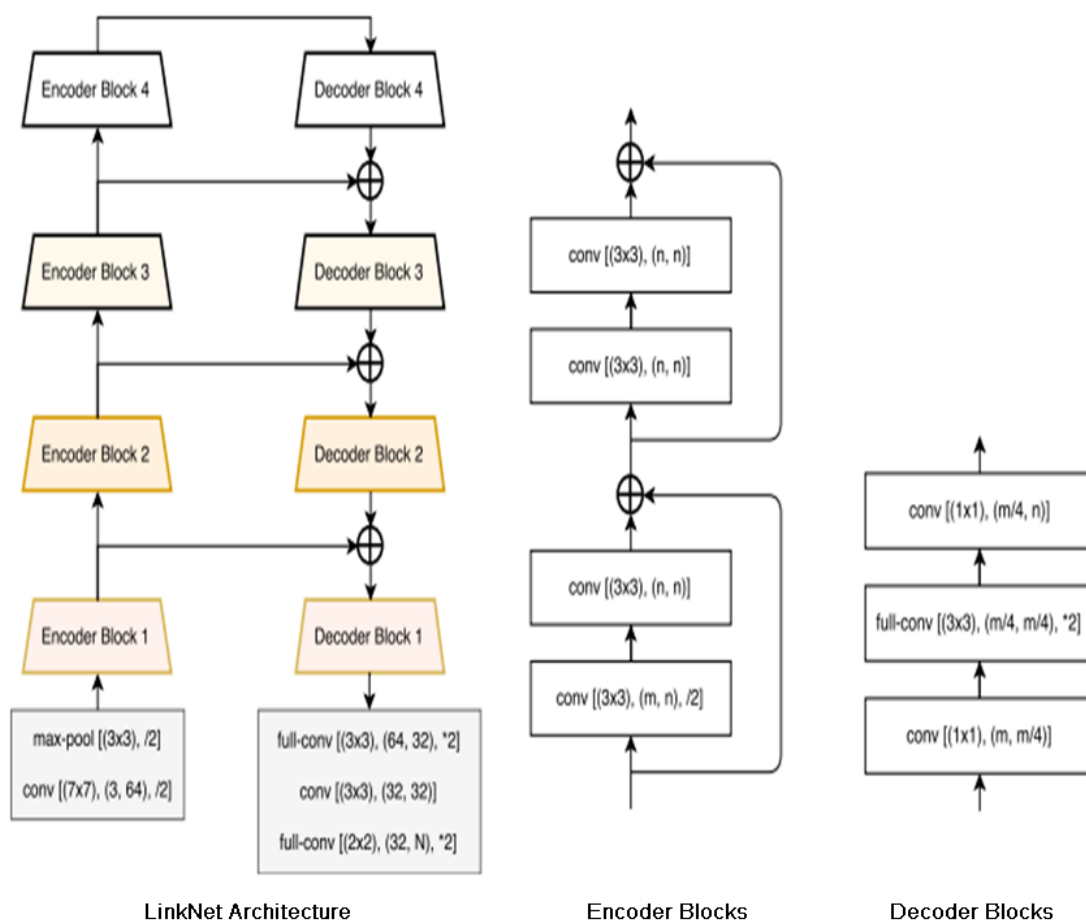


Figure 3. LinkNet architecture (Chaurasia & Culurciello, 2017)

The LinkNetB7 algorithm is a LinkNet-based model. In this model, EfficientNetB7 is preferred as the encoder. With the encoder blocks, the input image is reduced to half its size by pooling at each station. The attributes are extracted from the images in the encoder blocks. The number of attributes extracted with EfficientNetB7 has been increased. In terms of cost, the epoch time was higher than for the standard LinkNet.

A middle block was added to the architecture, which was not included in the original model. The middle block consists of a total of 3  $3 \times 3$  convolutional layers with 1024 cores. Feature extraction is also performed between the middle block and the encoder and decoder blocks. The image downsampled to  $8 \times 8$  resolution in the decoder blocks reaches 2x resolution with upsampling at each station. The activation function Relu is used.

Although the ResNet block added before the last layer increases the success by 0.1%, it was removed from the original LinkNetB7 architecture because it increases the epoch time and makes the algorithm cumbersome. Figure 4 shows the architecture of the algorithm. Encoder layers can be seen in Table 3.

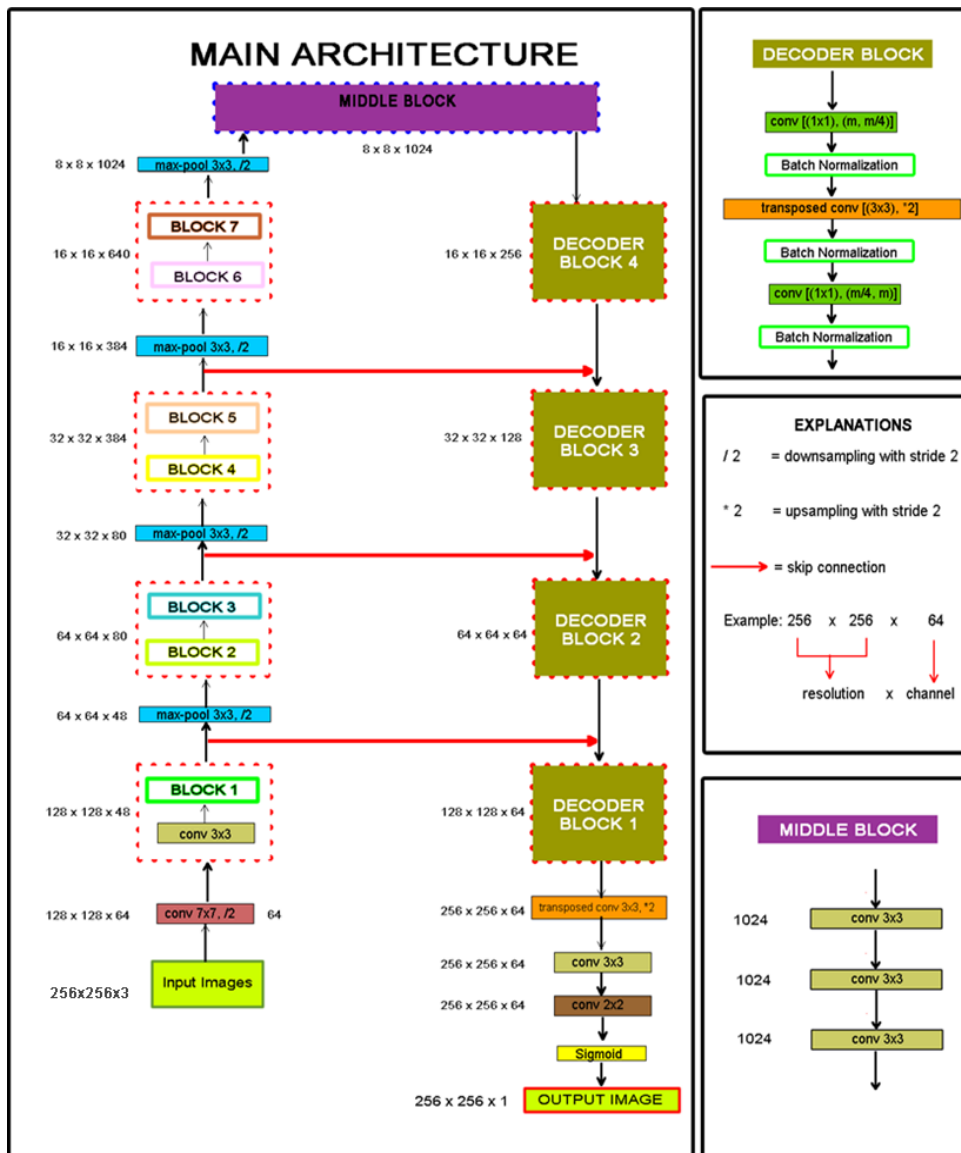


Figure 4. LinkNetB7 architecture (Akyel, & Arıcı, 2022)

Table 3  
Encoder Layers

Phase	Operator	Resolution	Channels	Layers
1	Conv 7x7, /2	128 x 128	64	1
2	Conv 3x3	128 x 128	64	1
3	Block 1 – MBconv1 3x3	128 x 128	32	3
4	Block 2 – MBconv6 3x3	64 x 64	48	7
5	Block 3 – Mbconv6 5x5	64 x 64	80	7
6	Block 4 – Mbconv6 3x3	32 x 32	80	10
7	Block 5 – Mbconv6 5x5	32 x 32	224	10
8	Block 6 – Mbconv6 5x5	16 x 16	384	13
9	Block 7 – Mbconv6 3x3	16 x 16	640	4

## 2.4. Metrics

### 2.4.1. Dice Coefficient

Dice coefficient calculates the match between the real (Y) and predicted (X) segmentation areas. The formula for dice coefficient is given in Equation 2.1 (Akyel, & Arıcı, 2022).

$$\text{Dice Coefficient} = (2 * |X \cap Y|) / (|X| + |Y|) \tag{2.1}$$

### 2.4.2. Loss Function

In this study, instead of using a single loss function, two different functions are combined and their advantages are combined. The loss functions used are dice loss (DL) and mean square error (MSE). The main advantage of die loss is that it is successful against oversegmentation errors. MSE, on the other hand, can increase success by reducing overall image details. As can be seen in Equation 2.2, the two functions are combined under the name DLMSE (Akyel, & Arıcı, 2022).

$$\text{DLMSE} = \text{MSE} + \text{DL} \quad (2.2)$$

### 2.4.3. Optimizer

In the study, adam was chosen as the optimizer. Adam is a stochastic gradient descent method (Akyel, & Arıcı, 2022). Adam can achieve high success from less epoch number.

### 2.4.4. Recall

Determines the accuracy rate of positively predicted data in the test dataset being actually positive (Akyel, & Arıcı, 2022).

$$\text{Recall} = \text{True Positive} / (\text{True Positive} + \text{False Negative}) \quad (2.3)$$

### 2.4.5. Precision

It is a measure of how positive predicted values in the test data set actually are. In Equation 2.4, the equation for calculating the estimation value is given (Akyel, & Arıcı, 2022).

$$\text{Precision} = \text{True Positive} / (\text{True Positive} + \text{False Positive}) \quad (2.4)$$

## 3. Results and Discussion

The model was run for 50 epochs with the parameters given in Table 1. Table 4 shows the results obtained in comparison with some other studies. And in Figure 5, training graphic can be seen. For the segmentation of images composed of layers, 3d models come to the fore because of their compatibility with this structure. 2d models, on the other hand, can be used for segmentation of CT images by considering all the sliced images as a single dataset. The biggest advantage of 2d models over 3d models is that they require less system resources. There are examples such as Zettler and Mastmeyer, (2021) where the 2d model is more successful than the 3d model in segmenting CT images of the liver. A look at Table 4 shows that the model used has a high degree of success. The main reason why the used model is more successful is that the blocks belonging to EfficientNetB7 were selected as encryption blocks.

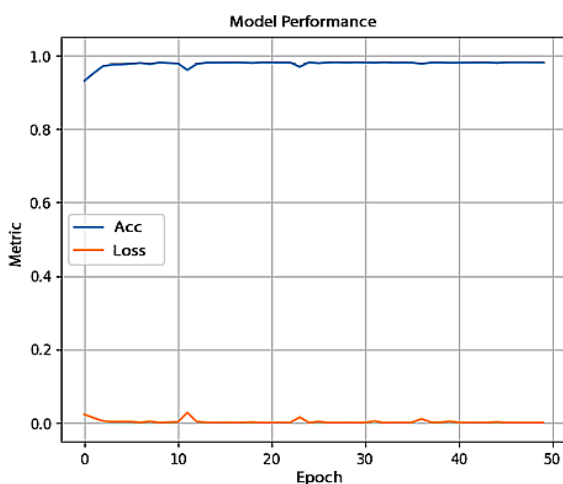


Figure 5. Training graphic

Table 4  
Comparison Results

Reference	Method	Dice Coefficient (%)	Precision (%)	Sensitivity (%)	Recall (%)	Dataset
Hsiao et al., 2022	EfficientNetB5	96.90	97.47	-	96.45	KiTS19
Da cruz et al., 2020	UNet2d	96.33	-	95.32	-	KiTS19
Zhao et al., 2020	UNet3d	96.90	97.10	-	96.80	KiTS19
Li et al., 2022	ResUnet	96.54	-	96.49	-	Own
Haghighi et al., 2018	UNet3d	87.50	92.7	-	-	DCE-MRI
UNet2d	UNet2d	96,50	96,55	95,90	96,20	KiTS19
UNet3d	UNet3d	96,80	96,85	96,10	96,25	KiTS19
Used Model	LinkNet	96.62	96.58	96.97	96.18	KiTS19
<b>Used Model</b>	<b>LinkNetB7</b>	<b>97.20</b>	<b>97.30</b>	<b>97</b>	<b>97</b>	<b>KiTS19</b>

### 3.1. Ablation Study

In this study, an ablation study was performed to investigate the effects of segmentation (ES), use of EfficientNetB7 as an encoder (EB7), contrast enhancement, and normalization methods (CN) on success. The results are shown in Table 5. Figure 6 shows examples of mask estimates.

Table 5  
Ablation Study

Structure	Dice Coefficient (%)
LinkNetB7	90
LinkNetB7 + ES	91.75
LinkNetB7 + EB7	94.05
LinkNetB7 + KN	91.80
LinkNetB7 + ES	92.04
LinkNetB7 + ES + EB7	95,35
<b>LinkNetB7 + ES + EB7 + CN</b>	<b>97.20</b>

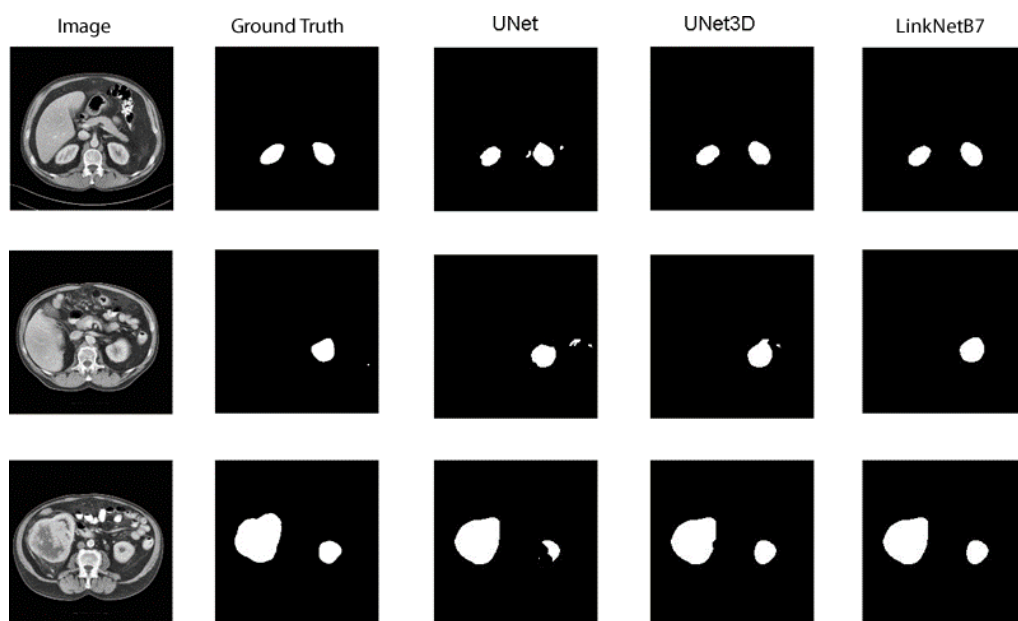


Figure 6. Sample segmentation results

#### 4. Conclusion

The results obtained in the study show that the LinkNetB7 model has a higher success than the other compared models. The success was 0.4% higher than that of the 3d-UNet model. The main reason is that segmentation is easier in kidney images and the number of layers is less. In addition, the success of the architecture in segmentation was also higher compared to UNet3d. There is no other study in the literature that uses LinkNetB7 for kidney segmentation. Therefore, this study found that the LinkNetB7 model was suitable for kidney segmentation. LinkNetB7 that is 2d model was preferred because of its accuracy in medical segmentation. Also 2d model requires fewer system memory than 3d models.

As can be seen in Table 6, the 2d LinkNetB7 model used requires less epoch time than 3d UNet + EfficientNetB7. Although the basic UNet model requires relatively less epoch time than LinkNet, the fact that LinkNet is more successful than UNet puts the LinkNet model forward. Also it was seen that the LinkNetB7 model has high success values in kidney segmentation.

Table 6  
Training times

Model	Epoch Time (min)
UNet3d	9.60
UNet3d + EfficientNetB7	13.10
LinkNet	8.70
UNet2d	8.55
LinkNetB7	11.10

As the resolution and number of images in the image datasets used in deep learning methods increase, the systems become insufficient. The slicing method can be used to solve this situation. In future studies, the system can be trained by using more epochs with higher input size in a system with better hardware. In future studies, different encoder models can be tried to consume less resources without decreasing the success rate.

#### Author Contributions

Cihan Akyel: prepared the data, created the model, analyzed the results and wrote the paper.

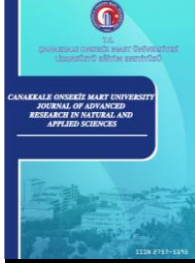
#### Conflicts of Interest

The authors declare no conflict of interest.

#### References

- Akyel C, & Arıcı N. (2022). LinkNet-B7: Noise Removal and Lesion Segmentation in Images of Skin Cancer. *Mathematics*, 10(5), 736-751. DOI: <https://doi.org/10.3390/math10050736>
- Budak, S., Sağlam, H. S., Köse, O., Kumsar, Ş., & Adsan, Ö. (2013). Böbrek Hücreli Karsinomada Radyolojik Tümör Boyutu ile Patolojik Boyutun İlişkisi, *Sakarya Medical Journal*, 3(4), 186-189, DOI: <https://doi.org/10.5505/sakaryamj.2013.92485>
- Chaurasia, A., & Culurciello, E. (2017). LinkNet: Exploiting The encoder Representations for Efficient Semantic Segmentation. *The IEEE Visual Communications and Image Processing (VCIP)*. St. Petersburg, FL, USA, Retrieved from: <https://arxiv.org/abs/1707.03718>
- Da Cruz, L. B., Araújo, J. D. L., Ferreira, J. L., Diniz, J. O. B., Silva, A. C., De Almeida, J. D. S., De Paiva, A. C., & Gattass, M. (2020). Kidney segmentation from computed tomography images using deep neural network, *Computers in Biology and Medicine*, 123, 1-12, DOI: <https://doi.org/10.1016/j.compbiomed.2020.103906>
- Demir, H., & Balçık, P. Y. (2022). Ödeyici Kurum Bakış Açısıyla İleri Evre Böbrek Kanserinde Kaynak Kullanımı: Eğitim and Araştırma Hastanesi Örneği, *Vizyoner Journal*, 13(34), 1-15. DOI: <https://doi.org/10.21076/vizyoner.991598>
- Devrim, T. (2019). Böbrek Tümörü Vakalarının Retrospektif Olarak Değerlendirilmesi, *Kırıkkale Üniversitesi Tıp Fakültesi Journal*, 21(2), 212-217, DOI: <https://doi.org/10.24938/kutfd.552211>

- Haghighi, M., Warfield, S. K., & Kurugol, S. (2018). Automatic renal segmentation in DCE-MRI using convolutional neural networks, *2018 IEEE 15th International Symposium on Biomedical Imaging (ISBI 2018)* (pp. 1-9). Washington, USA. Retrieved from: <https://ieeexplore.ieee.org/document/8363865>
- Hsiao, C., Lin, P., Chung, L., Lin, F. Y., Yang, F., Yang, S., Wu, C., Huang, Y., & Sun, T. (2022). A deep learning-based precision and automatic kidney segmentation system using efficient feature pyramid networks in computed tomography images, *Computer Methods and Programs in Biomedicine*, *221*, 1-17, DOI: <https://doi.org/10.1016/j.cmpb.2022.106854>
- Kallam, S., Kumar, M.S., Natarajan, V.A., & Patan, R. (2020). Segmentation of Nuclei in Histopathology images using Fully Convolutional Deep Neural Architecture. *The 2020 International Conference on Computing and Information Technology (ICCIT-1441)* (pp. 319-325). Tabuk, Saudi Arabia. Retrieved from: <https://ieeexplore.ieee.org/document/9213817>
- Kumar, S., Sathyadevi, G. & Sivanesh, S. (2011). "Decision Support System for Medical Diagnosis Using Data Mining," Retrieved from: <https://www.researchgate.net/publication/267934132>
- Körlükçü, E., Deresoy, F. A., Uluocak, N., Atılgan, D., Gümüşay, Ö., Beyhan, M., & Kılıç, Ş. (2019). Sarkomatoid renal hücreli karsinom: olgu sunumu and literatürün gözden geçirilmesi, *Anadolu Güncel Tıp Journal*, *1*(2), 42-46, DOI: <https://doi.org/10.38053/agtd.512103>
- Li, D., Xiao, C., Liu, Y., Chen, Z., Hassan, H., Su, L., Li, H., Xie, W., Zhong, W., & Huanglund, B. (2022). Deep Segmentation Networks for Segmenting Kidneys and Detecting Kidney Stones in Unenhanced Abdominal CT Images, *diagnostics*, *12*, 1-17, DOI: <https://doi.org/10.3390/diagnostics12081788>
- The KiTS19 Challenge Data: 300 Kidney Tumor Cases with Clinical Context, CT Semantic Segmentations, and Surgical Outcomes. Retrieved from: <https://arxiv.org/abs/1904.00445>
- Üyetürk, Ü., Üyetürk, U., & Metin, A. (2014). Böbrek Hücreli Kanser, *Gaziosmanpaşa Üniversitesi Tıp Fakültesi Journal*, *6*(1), 1-17. Retrieved from: <https://dergipark.org.tr/tr/pub/gutfd/issue/34239/378385>
- Zhao, W., Jiang, D., Queraltá, J. P., & Westerlund, T. (2020). MSS U-Net: 3d segmentation of kidneys and tumors from CT images with a multi-scale supervised U-Net, *Informatics in Medicine Unlocked*, *19*, 1-11, DOI: <https://doi.org/10.1016/j.imu.2020.100357>
- Zettler, N. & Mastmeyer, A. (2021). Comparison of 2d vs. 3d U-Net Organ Segmentation in abdominal 3d CT images. Retrieved from: [arxiv.org/abs/2107.04062](https://arxiv.org/abs/2107.04062)



## Investigation of Some Real Estate Valuation Problems in Turkey

Varol Koç<sup>1,\*</sup>

<sup>1</sup>Department of Civil Engineering , Faculty of Engineering, Ondokuz Mayıs University, Samsun, Turkey

### Article History

Received: 31.01.2023

Accepted: 24.06.2023

Published: 20.12.2023

### Research Article

**Abstract** – The urban population increases after the industrial revolution also increased the commercialization of real estate. In the future, this situation would require being able to determine the real estate values more than before. Today, real estate values are of much greater importance in terms of socioeconomic relations and activities in the world. Establishing a standardized real estate valuation system is among the important duties of public administrations. However, in general, the countries that could not catch up with the industrial revolution in the world and whose industrialization started very late and were not mature enough, could not reach the desired level in terms of real estate valuation. In other words, lagging in industrialization naturally leads to being late and behind in the real estate valuation branch, which is an output of industrialization. The problem created by this situation cannot remain local in today's socioeconomically globalized world. Therefore, the problem affects the whole world and developed countries. In this context, as an example, this study presents the contradictions related to the real estate legislation in Turkey and the application errors in valuation and offers suggestions for the elimination of all these.

**Keywords** – Real estate, valuation, development, public administration, regulations, cost analysis

## 1. Introduction

Economist M. Porter (1990) states that the competitiveness of a country depends on the development and innovation capability of its industry. The need for property, which has increased with industrialization, has also increased the importance of the correct valuation of properties. After the industrial revolution, the cadastralization of the lands with the licensing of the buildings and their taking them under the guarantee of the state was now an obvious necessity. In the following years, depending on the population concentration in the cities, lands and structures became subject to purchases, rents and guarantees, and immovables became more important elements of capital than ever before. At the end of the 20th century, determining the values of real estate became more significant than ever for the public and private sectors. In particular, the increase in population, the decrease in agricultural areas and the increase in urbanization were constantly increasing the values of immovables. Today, the fact that the real estate sector triggers the global economic crisis that has emerged especially in the recent period shows the importance of connecting real estate valuation activities to international standards. Because an established real estate valuation system produces fair and predictable results in practices such as the determination of public financial values, taxation, privatization, expropriation, and crediting. It guides in terms of insurance and capital market risks. For these, public administration valuation standardization should primarily be carried out with legal regulations and practices that will not cause conflicting results in public real estate.

Towards the 2000s, professions to determine the price of real estate for a fee began to be seen in many organizational structures all over the world (Morgan 1998; Ramsey 2004). The 2008 global financial crisis, which started due to the real estate markets, further demonstrated the importance of real estate valuation expertise

<sup>1</sup>  kvarol@omu.edu.tr

\*Corresponding Author

(Żróbek et al. 2013). Greater emphasis has been placed on the regulation of valuation services. There has been a lot of work in the literature on the concepts of real estate development and valuation, its applications, and its effects on urban transformation (d'Arcy et al 1997, Donaldson and Van der Merwe 1999, Palicki and Račka, 2016, Lai and Lorne 2019, Koç 2021a, b, c, Koç ve Çiçek 2021). By 2020, more than 60 countries now have valuation professional bodies that are members of the International Valuation Standards Council (IVSC 2020). Especially for today, it can be said that real estate trade is tightly regulated all over the world (RICS 2022). S. Bartke and R. Schwarze (2021) point out that in practice, nothing else is so strictly defined and controlled by laws as zoning laws. The inability to update the market values of properties over time according to the current selling price trend is an important reason for the global economic crisis that started in 2008 (Taylor 2009; Mooya 2011). Another reason is the inadequacy of the methodologies used to evaluate market values, which mainly require lengthy processes (D'Amato and Kauko 20017). Direct estimates may be affected by accepted approaches and lead to erroneous results (Bitner 2008; Downie and Robson 2008). As a result, the inadequacy of the valuation methods adopted by credit institutions created problems in the financial transmission of the housing price bubble in the USA. The static structures of valuations and the inability to understand complex socio-economic dynamics and their effects on the real estate market have led to the global economic crisis (Marco et al. 2020). The International Valuation Standards define a uniform and common guidelines among professionals to guarantee a unique code based on the same principles and rules and the public interest in valuation models (Gilbertson and Preston 2005). The need to control uncertainty aims to prevent or at least reduce the possibility of systemic financial and economic market crises, similar to those that occurred in the US subprime in 2007 (Marco et al. 2020).

The real estate sector and the determination of real estate values have become some of the most important elements of global economic relations, beyond being local. In this context, global organizations such as the United Nations, the World Bank and the European Union constantly emphasize the duties of the public administration in ensuring the transparency of the real estate market and establishing the real estate valuation system in their directives and statements (Eriksson et al. 2005; EC 2006; Peldschus 2010). Since the real estate sector is the trigger of the recent global economic crises, international scientific real estate valuations are being tried to be standardized (Cete and Yomralioglu 2013; EU 2004). Because real estate valuation; is also important in investment and stock market transactions, value and property records, and concepts such as cost, reconstruction and replacement (Açlar and Çağdaş 2002). The successful realization of the valuation directly depends on the determination of the properties of the real estate and the selection of the valuation criteria and method according to the market of the real estate based on this (Erkek et al., 2021). In the public and private sectors, it is very important to record the precedent values according to the properties of the immovable with a correct and proper system and to create a database. A standardized valuation system needs to be revised according to needs in line with the principles of continuous improvement. Thus, both fairness and transparency and healthy and sustainable real estate valuation are ensured (Erdem, 2020).

## 2. The Problems Investigated in This Study

In Turkey, especially in the valuation of public real estate, only the cost value is taken as the value of the real estate together with the land share. It is not correct to take the value of the real estate as equal to the cost spent in creating that real estate. Even determining with precedent values cannot be completely accurate. No real estate can be the same as other real estate. First, its point location is unique. For value, the property's unique social and natural environments must be considered. Based on the best usability of the property, the current value of the income that can be generated from the property over its future life should also be included (Bartke and Schwarze 2021). Van der Spek (2017)'s research has shown that real estate is perceived as a long-term income. So, this should be reflected in the valuation of the property. Thus, although the property can be valued using a variety of valuation methods, Vrbka et al. (2019) focused on the synthesis of valuation methods that determine the total amount of investment. Indeed, according to A. Sharkawy and W. Barnes (1992), there is no significant relationship between value-based underwriting criteria and default, and strict cost-based criteria are closely related to the probability of default. This shows that the valuation cannot be made with purely cost calculation, and the possible return on investment of the property must be considered. A market value estimate includes not only the continued use of the asset in its current state but also its full potential use. At the core of market value estimation is the concept of highest and best use (Appraisal Institute 2008). Valuation

is the activity of estimating the most probable selling price or 'market value' (D'Amato 2015). Taslan et al. (2013) state that the replacement value should be applied to appraise a house with social housing status. To determine the replacement value, operating expenses such as administration, maintenance, taxes, and insurance must be subtracted from the expected operating income such as rent and residual value. Because of the below-market rent, the replacement value of a social home will be lower than that of a private residence. This difference determines the market price discount range for development sites (Taslan et al. 2013). In any case, however, it is necessary to reflect the entrepreneur's earnings on the replacement value for social housing as well.

The fact that the expropriation and privatization and registration activities of the public are carried out by commissions formed in-house and composed of personnel who may not be very competent in valuation expertise, makes it difficult to determine the real values. This situation creates problems in public finance and the registration of public property values. It causes situations such as the possible reflections of public real estate values on the market to mislead the market, or especially expropriation activities are subject to objections and lawsuits. In practices in Turkey, the commissions that make the valuation of public immovables are generally composed of the employees of the public institution that owns the immovable. Most of these employees do not have competency in valuation expertise. The valuation of public buildings is usually made using the cost method as a customary method. As the value, the sum of the progress payments paid by the public institution to the contractor while having the building constructed is taken. The problem, however, is that entrepreneurial profit is not reflected in this value. As a result, the data files that will form the real estate valuation information system and the reflection of the values available in the market are adversely affected. Because, taking the value of the building equal to the price paid only for the construction of the building, that is, the cost, cannot be a correct approach in terms of market conditions and practices. In the cost value method, the profit of the entrepreneur, which is essentially different from the profit of the contractor, must also be reflected in the value. Keeping public buildings separate from this reality will result in the accounting of government properties not reflecting the real situation. This creates risks for the sustainable economy. In this study, this issue was emphasized by taking examples from the literature and applications. University campuses are often far from city centers and trading counterparts are difficult to find. For this reason, it is difficult to reflect the entrepreneur's profit to the cost value found from the progress payments also. For these reasons, especially the valuation of a college campus has been taken as an example, in terms of representing public immovables.

Moreover, in Turkey, two separate legal communiqués, one about the property tax and the other about the approximate unit cost of the structures, give different results, up to 25%, in the cost calculations for the same type of buildings. This situation causes contradictory data in the building information files, which are important for the real estate valuation system. In this study, this situation is also examined with legislative comparisons.

### **3. The Importance of Accounting for Public Immovables and the Situation in Turkey**

There are criticisms in the literature focusing on the role that accounting standards played in the 2008 global financial crisis (André et al. 2009; Bengtsson, 2011; Quagli & Ricciardi, 2010). Because accounting standards can affect resource allocation and a wide range of social actors (Farjaudon and Morales, 2013; Kothari et al. 2011; Llewellyn and Milne, 2007). For these reasons, it becomes important to include the public interest among the objectives of accounting regulators (Stuebs & Wilkinson, 2014). For these reasons again, both the European Union (EU) and the United Nations Inter-Agency Standing Committee (IASC) demand international harmonization of financial accounting standards. The institutional framework, historical background and current achievements of national accounting regulations are reviewed and compared by the EU and IASC. Therefore, national standard setters have important duties related to this process. Policies should be developed to ensure that national and international standard setters work in a mutually supportive manner rather than in a competitive manner (Thorell and Whittington 1994). However, problems in some national accounting standards could not be resolved in Europe. For example, the application of elements of the International Financial Reporting Standards based on the EU accounting Directive (2013/34/EU) to Czech accounting standards is still only partial (Jindrichovska and Kubickova 2017). Turkish accounting standards are also being tried to be regulated, but as discussed in this section, the desired successes have not been achieved yet. However, there are of course positive examples. For example, Sally Aisbitt (2002) notes that the first discussions of legal harmonization of financial reporting in Scandinavian countries were reported in the 1930s. Thus, financial reporting began early

in the Nordic countries, and legislation implemented in the 1970s was based on the proposal for a common Scandinavian Companies Act (Aisbitt 2002). The state, which is the highest level of social organization, must provide justice and security in society. These are the classical duties of the state. However, modern functions of the state such as economic development, fair income distribution, employment and stability have also emerged. To fulfil all its functions, the state becomes partners with the economic resources of the society through taxes, debts, purchases, and leases. It gives them back to society through utilities, purchases of goods and services, or transfer expenditure. These activities of the state cause various effects in terms of macroeconomics. These effects should be able to be measured and evaluated with government accounting. In addition to current assets such as income and expense items of the government, fixed assets that make up its assets are also included in the accounting. Because, in the public economy, what the state receives from the social segments and gives to them becomes clear only when the changes in the values of the state assets are taken into account in a period. These changes can be physical, such as wear and tear, or financial, such as profit and loss (Güngör, 1981).

In all societies, the state uses 25% or even more of the national income. Thus, the state is the largest institution that creates value movements in the economy. There is a special accounting system developed for the recording, tracking and auditing of these assets since the state is the largest resource collector and allocator in the economy. Thanks to this system, it is possible to monitor and control the values that the state receives from the national income (Aksoy, 1994). As a concept, property accounting refers to the acquisition of fixed assets of the state by purchasing or similar means, their use, evaluation, and disposal, keeping their records in a certain system and monitoring their physical and monetary changes (Bulutoğlu and Kurtuluş, 1988). Fixed assets are goods such as buildings, land, vehicles, movable properties, and fixtures. The values of fixed assets must be determined correctly. Because the benefit to be obtained from a good depends, first of all, on knowing the value of that good. However, in Turkey, although some accounts were included in the context of property accounting in the past in government accounting, which has been in practice for more than a century, these accounts were not operated due to various reasons, especially implementation difficulties (Kızılkaya, 2002). Until 2004, there was no "property accounting" in the government accounting system. The basis of government accounting system was based on the collection of revenues, payment of expenses, and advance, escrow, and dispatch transactions. The fixed assets that make up the state's assets were not seen in the accounts of the accountancy and were not included in the trial balance accounts (Altınok, 1973). In addition to these, there were also deficiencies in Turkey, such as the fact that government accounting was based on cash, lacked classification and coding, and hindered accountability because it was not suitable for financial reporting (Kerimoğlu, 2002). Based on these points, the legislator enacted the Public Financial Management and Control Law No. 5018, which includes reporting and financial control, aimed at creating public accountability and financial transparency to ensure more effective, economic, and efficient use of public resources.

The law introduced new reforms in public finance (Üçbaşı, 2004). A system is suitable for accounting and auditing by international standards is envisaged. (Aslan, 2004). Several innovations have been introduced in the context of accounting for fixed assets that constitute the state's assets, both with this law and with the regulations. For example, according to Article 58 of the Government Accounting Regulation, fixed assets include assets that are acquired for use for more than one year and are not expected to be converted into cash or consumed within one year.

Determining the value of the land is one of the responsibilities of the General Directorate of Land Registry and Cadastre (TKGM in Turkish) in Turkey (TKGM 2020). Although there are some academic studies investigating collective valuation with advanced statistical and machine learning techniques, there is no official definition of real estate value and annual property tax assessments representing market values (Güneş and Yıldız 2015, 2016). In this context, TKGM initiated some parcellation projects within the scope of the Land Registry and Cadastre Modernization Project (World Bank 2008). In 2018, TKGM Land Valuation Department was established to determine the value of immovables by collective valuation methods and to manage the valuation information centre (Official Gazette 2018). It is possible to evaluate vacant lands and similar low-income places with the market price method, buildings and similar fixed facilities with the cost method, and income lands and lands with the income capitalization method (Güngör 1981). Undoubtedly, a good government accounting system must include property accounts (fixed assets) as well as cash accounts (current assets). The

concept of efficiency, which was mostly expressed for public expenditures in Turkey until 2004, has now begun to be used for the fixed assets of the state, which are included in the state accounting system. Because Article 1 of the Law stipulates the effective, economic, and efficient use of public resources. Also, in the 4th article of the Law, movable and immovable properties are counted within the scope of public resources. As the quantity and quality of the fixed assets of the government will be included in the knowledge of public financial management, the management of these assets will become more effective. Otherwise, especially immovable properties, which are included in public resources, are not used in place and on time, they are left idle and thus the benefits to be obtained from them are deprived (Arslan 2004).

Accounting for the fixed assets of the state will also prevent the unbalanced distribution of goods between institutions. The fact that the fixed assets of the state are out of the accounting system results in an incomplete preparation of the state's balance sheet. However, good government accounting should not leave any transactions out of accounting and the accounts in question should be suitable for consolidation, in the context of providing information that can shed light on economic and fiscal policies. To achieve this, the State Accounting Regulation, which includes public institutions and organizations, has been put into effect (Bağbaşıoğlu, 2004). Because in Turkey, it has long been desired to bring public financial management to a modern financial control system by ensuring that public accounts are kept and reported by international standards and EU norms.

Based on developments in government accounting, international financial institutions such as OECD, IMF, World Bank and economic and political unions such as the EU need to create financial statistics and reports of other countries (Kerimoğlu, 2002). Because these institutions especially want the balance sheet of the country, they want to give loans. In this framework, government borrowing will be more rational, as property accounts will show the real state of the state's fixed assets (Akça, 1998). Since the expenses for the acquisition of fixed assets are capitalized and depreciated, government accounting will become solid and reliable data for public financial management.

#### **4. The Importance of Valuation of Public Immovables and the Operation in Turkey**

To use the immovables in public and private property by making cost-benefit analyses in line with the needs, their current values in the market should be determined. Real estate values: in addition to many transactions such as expropriation, insurance, privatization, and nationalization, it is also used for balance sheet accounts and transfer transactions in public administrations (Soto, 2017). Immovable values: it is necessary information to know on subjects such as buying-selling, investment and inheritance sharing. Public real estate also needs a valuation. For example, in Sweden; in the calculation of capital costs to produce services, in selling high-priced immovables and switching to cheaper immovables, in calculating the financial situation by including the value of the immovables to get a good rating from the government, in the transfer of public immovables in the local and regional administration of the central government, in the privatization of service buildings sold by the public or there were problems in pricing the immovables rented out and the value of public immovables was needed (Lundström & Lind, 1996).

The global real estate market consists of national public and private markets of local economies united across borders. Both public and private real estate play important roles in the value of real estate market offerings. The greater financial transparency of the European and North American economies has resulted in consistent patterns being established in both public and private real estate market cycles. But Asia's public real estate market cycles are volatile and there may be economic instability (Liow & Yeo, 2018). Asian markets are predominantly dominated by construction activities. Therefore, it is important for also global markets that real estate valuations are standard and scientific in these markets.

According to the annual report of the General Directorate of National Real Estate (MEGM), there are approximately 4,5 million Treasury properties in Turkey, which constitute approximately 37,6% of Turkey's surface area (MEGM, 2020). Owners of privately owned immovables have the right to dispose of their immovables as they wish, within the framework of legal rules (TMK, 2001). However, in areas where the benefit of the individual meets the benefit of the community, the benefit of the community is held superior (Constitutional Court of the Republic of Turkey, 1966). The public administrations of the central government within the scope of the general budget are represented by the legal entity "State", the immovables it acquires are registered under

the name of "Treasury" and are managed by the Ministry of Environment and Urbanization. The immovables belonging to other public administrations are registered in the land registry on behalf of their legal entities and each public institution manages it by itself. According to the Public Financial Management and Control Law No. 5018 (Public Property, 2003) and the Regulation on the Registration of Immovables Owned by Public Administrations (Public Record, 2006), the relevant institution is responsible for ensuring financial transparency regarding immovables and is monitored by the Ministry of Treasury and Finance. By the standards specified in the General Management Accounting Regulation, the accounting of immovables is ensured by making use of the Central Government Accounting Regulation. In administrative law, State and local administrations are defined as "public legal entities in the form of a group of persons". Public legal entities in the form of a collection of goods are also called 'public institutions' (Gözler, 2011). Examples of public institutions in Turkey are Universities, the General Directorate of Foundations, the General Directorate of Highways, the General Directorate of State Hydraulic Works, Capital Markets Board (Public Property, 2003).

State property in Turkey, on the other hand, is divided into two public goods and private property of the state. Public goods are derelict places, common goods and service goods. There are separate official norms such as Forest Law, Pasture Law and Coastal Law for some of the derelict places and common properties and they are traded within this scope. Service Goods are the goods registered in the land registry of other public legal entities other than the State Legal Entity. Private goods of the state are goods that are not public goods and contribute indirectly to the provision of public services with income. In other words, such goods are not allocated for public benefit or public use (Arslan 2017; MEGM 2019). The treasury lands and the facility of state-owned enterprises are the private property of the state within this scope. State property; while it is used socially in public services (such as government mansions, hospitals and schools) and for the general benefit of the public (such as roads, squares and pastures), it is also economically used for financial purposes (such as the sale or lease of treasury lands) (Söyler 2005a, 2005b). It is stated that there is a complexity about the places under the rule and disposal of the state, and it is still difficult to distinguish these goods from each other from past to present (Arslan 2017; Söyler 2007). The legal vacuum continues and there is a problem because "there is no clear distinction between private property owned by public legal entities and the status that public goods are subject to" (Kaplan 2004).

In the recording and accounting of public immovables as immovable value; records are kept on cost value, fair value, trace value and property tax value. The immovables under the title of "Immovables Registered in the Land Registry" are recorded over their cost value, and those whose cost value cannot be determined from these immovables are recorded over their current values (Public Record, 2006). The "cost value" is the sum of the current progress payment amounts paid for the manufacture of a building, the expropriation price or the purchase price, the expenses on the land title deed, the expenses made to make the real estate usable, or the sum of the values given. The current value corresponds to the normal trading value on the valuation day. However, in Central and General Management Accounting Regulations, the term "fair value" was accepted instead of "current value" (Public Record, 2006). In accounting, immovables acquired from tangible assets are considered at cost. However, for the building value, the profit of the entrepreneur should be reflected in the cost price.

The RICS EU (2008) on Sustainable Property Investment and Management highlighted an important issue when it stated: Even if professionals do not have a deep knowledge of the value of liquidity, there is a great deal of risk when they treat the property as an asset class with another degree of liquidity. Because Property assets are illiquid and have high transaction costs and are geographically related. In various previous studies, spatial relationships were discussed in real estate market analysis (Thibodeau et al., 1998; Bourassa. et al 2007; Des Rosiers et al., 2000). On January 17, 2020, the European Securities and Markets Authority initiated a consultation on draft guidelines on the completeness and consistency thresholds of securitization repository data. It aimed to set out the key elements of disclosure obligations for securitization transactions, as well as the operational standards of securitization. As a result, the stored data would improve information flows and data access, with the development of a centralized database built on environmental data for the financial sector (Richter 2020).

## **5. General Situation of University Real Estate in Turkey**

Places under the rule and disposal of the state, places in the common use of the public, places reserved for the performance of public services, immovables under the private ownership of the Treasury and State Properties under the administration and management of the State. Among these, the goods registered with the public legal entity and the use of which are in the public interest are public immovables (Cadastre 1987). Some of the immovables registered with the public legal entity are those belonging to universities. According to the historical development of universities in Turkey, campuses generally established outside the city consist of public immovables used by universities (Aydın, 2019). These immovables were mainly obtained as a result of the allocation of treasury or forest lands. Privately owned immovables were expropriated and registered in the name of the university. However, it is seen in the activity reports of the universities that there are immovable properties still waiting for expropriation.

For the immovables under the ownership and use of the university to be managed sustainably, good management should be ensured by incorporating their past and present features into a system. Universities should offer a livable campus life to future generations by better managing the immovables in their use. Establishing a parcel-based information system for this; is necessary to plan for protecting natural resources such as water, soil and living things in nature. In addition to an up-to-date, accurate and reliable cadastral map and title deed information such as property and value, zoning plans, topographic maps, geological maps, and other produced maps are also needed. In the real estate type of Universities in Turkey, the land is generally denser. Most of the universities have their legislation on real estate administration. The immovables managed by the universities may consist of piecemeal parcels on different campuses. The reason for this is in universities that are open to continuous development and technology, opening new departments, increasing student quotas. Universities are growing in parallel with the developments, and some land needs arise. In this context, valuation information should be obtained so that university immovables can be managed and planned very well.

State universities, by the State by law; foundation universities can be established by foundations subject to the supervision and control of the State (Constitution of the Republic of Turkey, 1982, Article 130). According to the statistical data for the year 2018-2019, there are 129 state universities and 74 foundation universities and 4 foundation vocational schools in Turkey (YÖK 2020). Higher Education Institution and Universities; it is classified as a special budget administration within the scope of the central government. The immovables registered in the name of the university in the land registry are service goods within the scope of public goods (Arslan, 2017). University immovables are permanently exempt from property tax, if they are not rented out. It is also exempt from fees and stamp tax (Tapu 2014).

## **6. As an Example, Valuation of a College Campus in Turkey**

Public immovables are public properties that are reserved for use in public services and that are identified in the name of legal entities in the land registry. University real estate is classified as public property. To inventory and account for these goods, their values should be calculated objectively (Ünel 2021). The establishment of a valuation infrastructure is essential to determine the classes of immovables and to manage them sustainably. In this section, as an example, immovable properties in a high school campus in Turkey are discussed. The factors that show the characteristics of the immovables and affect their value and their arrangement are exemplified. Common mistakes made in practice are shown and what should be done is explained. In other words, the path to be followed for the use of data in valuation analysis has been determined.

There are common practice errors in registering and accounting for immovable and movable properties of universities, which are public institutions. For example, in Turkish Universities, real estate valuation studies are generally carried out by collecting the amounts paid within the scope of progress payments for immovables whose tenders have been made and whose construction has been completed by the university. In the 2019 External Audit General Evaluation Report of the Turkish Republic Court of Accounts, published in September 2020, it is stated that one of the most common mistakes is not reflecting all aspects of the transactions of public institutions' real estate in the financial statements. The most common errors detected by the auditors of the court of accounts are that the immovables registered in the land registry in the name of the administration are not included in the institution's financial statements and the types of the immovables are not corrected.

The vocational school, which is the subject of the research, is located on the main real estate with a surface area of 44,000.00 m<sup>2</sup> and in the area marked as university in the zoning plan. There is an education block, a canteen building, an indoor parking lot, an energy block, a centre of the heat, a basketball court and guard-houses which were completed within the boundaries of the vocational school campus and used in education and training services. The prices paid to the contractor firm within the scope of the tender for the buildings used in the education and training services of the university were determined and used in the valuation with the cost method. With the completion of the construction of buildings or other structures, their temporary acceptance is made and a real estate valuation report is created. However, in public institutions, construction costs may change in final acceptance (Final Account) transactions after the tender period. For this reason, there may be changes in the expenditures of the building or other productions after the final acceptance. In this case, these changes are reported to the relevant unit based on the recorded immovable valuation report with their reasons, and a correction is requested.

Since public buildings are built for a specific purpose, they are structures that are not subject to purchase and sale. In the valuation of these structures, it is tried to determine their values by using the cost method. Cost method: instead of purchasing real estate, it considers the possibility that the same real estate or another real estate that will provide the same benefit can be built. This method aims to arrive at the cost value of the real estate on the valuation day. Cost approach: it is at the forefront in the valuation of properties that are not frequently traded in the market, in the valuation of buildings with private use, and when it is not an income generating property. In Turkey, especially the Real Estate Tax Law No. 1319 and the Expropriation Law No. 2942 envisage the valuation of built real estate using the cost method.

Since there are many buildings on the main immovable campus examined; the value of the main immovable will be determined by the peer comparison-market research method, as recommended in the Real Estate Tax Law, and the land value will be specified separately. Negotiations were held with local real estate companies to apply the peer comparison method in the district centre where the campus is located, and the average current price of the real estate was determined as 225 TL/m<sup>2</sup>. In this case, the value of the real estate, which is 44,000 m<sup>2</sup>, is 9,900,000 TL.

The construction was completed after the tender of the building immovables by the University in May 2014 and their provisional acceptance in December 2019. The total progress payments paid to the contractor by the administration while the buildings are completed and put into service are taken into the immovable records, and the immovable value is accepted as the construction cost. In the Regulation on the Registration of Immovables Owned by Public Administrations published in the Official Gazette dated October 2, 2006, and numbered 26307, productions are divided into classes according to the title deed. According to this regulation, outside the buildings, infrastructure, landscaping, etc. productions must also be recorded in the immovable records. However, there is one thing that should not be ignored. Movable materials within the scope of construction work are determined and a list is created. The costs of movable materials are reduced from the progress payments. Because these materials are within the scope of the tender and are in immovable buildings. Thus, the registration of both movable materials and immovable properties is determined and movable and immovable properties are recorded.

All buildings are on the same campus, within the same building construction site. Building styles are reinforced concrete carcasses. Building classes are determined as IV/A (university campuses) in the construction permits. The wall filling material of all of them is aerated concrete and the floor is a reinforced concrete plate beam system. The wastewater system of the buildings is sewerage, and the drinking water system is the city network. There is no wastewater or drinking water system in the energy building. There is no drinking water system in the parking garage building and the guard's hut. There is no communication system in the energy building and the parking garage building. There is no water tank in any of the buildings except the heating centre. The generator is only available in the education-administration building. Other information about the buildings is summarized together in Table 1. The building cost values shown in the last line of Table 1 are obtained from the sum of the progress payments paid to the contractor company for the buildings.

Table 1  
Building Features and Cost Values

	Eduction- admnst. building	Energy building	Cafeteria	Parking garage	Watch box	Guardhouse	Heating center
Floor area	3,000 m <sup>2</sup>	441 m <sup>2</sup>	475 m <sup>2</sup>	275 m <sup>2</sup>	2 x 7.3 m <sup>2</sup>	30 m <sup>2</sup>	475 m <sup>2</sup>
Number of floors	B+ G+ 4	B+ G	3	G+ 1	1	1	1
Height above the road	22.5 m	7.5 m	8.8 m	9 m	3 m	4 m	7.3 m
Total height	22.5 m	9.6 m	13.5 m	9 m	3 m	4 m	7.8 m
Construction year	2018	2018	2014	2014	2014	2014	2014
Heating system	central	none	central	none	O	O/ AC	none
heating fuel	NG	none	NG	none	E	E	none
Hot water supply	joint	none	joint	none	none	WH	HWB
Hot water fuel	none	none	none	none	none	E	NG
Lift	available	none	available	available	none	none	none
Disabled lift	available	none	available	available	none	none	none
Exterior	NS/A.	PP	NS/A	PP	A	A	PP
Fire escape	available	none	available	none	none	none	none
Canteen	none	none	available	none	none	none	none
Closed area	9,000 m <sup>2</sup>	800 m <sup>2</sup>	1,300 m <sup>2</sup>	2,250 m <sup>2</sup>	2x 10 m <sup>2</sup>	30 m <sup>2</sup>	500 m <sup>2</sup>
Cost (thousand TL)	10,000	700	2,750	1,300	98.5	150	1,500

\* B: basement , G: ground floor, O: oil radiator, AC: air conditioning, NG:natural gas, E: electric, WH: water heater, HWB: hot water boiler, NS: natural stone cladding, A: aluminum facade cladding, PP: plaster- paint.

Infrastructure and Landscape productions were made by the project within the scope of the tender, and the sum of the progress payments paid to the contractor company constitutes the infrastructure cost value. These values are 3,500,000 TL for infrastructure production and 3,750,000 TL for landscaping, and they are recorded in the real estate records as infrastructure and landscape values. Infrastructure, 950 m. Wastewater line, 270 m. retaining wall, 500 m. road construction, 650 m. rainwater line and 280 m. It consists of gallery production. There is landscaping covering a total building construction area of 44,000 m<sup>2</sup> within the landscape production. In addition, the basketball court and grass amphitheatre with an area of 17x30 m are also included in this production. According to these, the construction costs of the buildings, infrastructure and areas on the campus were calculated from the progress payments, and the construction costs shown in the 1st column of Table 2 were obtained. While calculating the payments of the structures according to the progress payments, the values including the Price Difference and Value Added Tax (VAT) should be taken as basis. Otherwise, the valuation to be made according to the cost method will not give the correct information. After the calculation of the Total Campus Construction Cost, the goods that are within the scope of the tender but will have the status of movable material should be listed and deducted from the progress payments paid on a building basis (Air conditioning, computers or devices that can be found in the electrical or mechanical room, etc.). These values are given in

the 2nd column of Table 2 . The movable material costs are specified in the 2nd column of Table 2; By deducting the building construction costs given in the 1st column, the basic construction costs of the building or other structures are obtained and shown in the 3rd column.

Table 2  
Campus building costs in separate units and in total

	Buildings construction costs	Movable materials costs	Buildings Costs
Education-administration building	10,000,000	400,000	9,600,000
Energy building	700,000	2,000	698,000
Cafeteria	2,750,000	10,000	2,740,000
Parking garage	1,300,000	-	1,300,000
Watch box- Guardhouse	250,000	1,500	248,500
Heating center	1,500,000	4,000	1,496,000
Infrastructure	3,500,000	-	3,500,000
Landscape	3,750,000	-	3,750,000
TOTAL	23,750,000	417,500	23,332,500

Thus, the campus construction and building construction costs of the District Vocational School Campus and buildings, which were built within the scope of the tender, were calculated. However, these values, which are obtained after deducting the values of the movable goods within the scope of the tender, are the progress payment values of the contractor company and include general expenses, price differences, VAT and contractor profit. Of course, the cost spent for the construction of the building is a value for use, namely the building service, to be obtained from that building, but the pure building value must be higher than this cost value. Otherwise, it would be to say that the state only needs to build buildings for compulsory public services. Although this seems to be true when it comes to the state, the same condition must also apply to other actors in the same market. In other words, private individuals and companies should have a structure built for only purposeful use. This claim means to say that individuals, public and private sector structures should not be subject to purchase and sale, apart from necessities, and it puts forward an attitude that is completely contrary to reality.

The contractor who undertakes the construction of the building has a profit expectation. Therefore, naturally, in the same way, even if they have the building built for use, the public or private institution or person or persons who has it built should hope to profit from these building activities. Because they spent the price, time and effort. To claim that the state should be exempt from this gain is to accept that a valuation has been made that does not comply with market conditions. This situation will inevitably be reflected in the market as price irregularity due to interaction in the same market. In terms of standardizing the valuation and generating data, this approach can have very problematic results. On the other hand, the commissions established by universities and public institutions in the valuation and registration processes of the buildings they own in Turkey generally determine the construction costs, which they obtain only from progress payments, as the construction value by deducting the costs of movable goods. This situation creates problems in the determination of the real value of the state's assets and the reliability of the data pool created from public-private value determinations.

The cost method calculates the value within the framework of the cost spent for the reconstruction of the building (Alptürk 2007). However, calculating within this framework does not mean that the value is only this price. Because the profit of the entrepreneur must be added to the cost of the reconstruction or repair-strengthening-restoration-rehabilitation applications of the building. The current absolute value of the building is obtained by deducting the financial equivalent of the depreciation of the building from the resulting value and adding the land value (Bakır 2009). These expressions can be expressed with a simple formula as follows (Ventolo & Williams 2001):

Building Value = [ Construction cost+Land value+Entrepreneur profit- Depreciation]

The value of the buildings is the sum of the construction cost and the sales profit of 20% of this and the purchase and sale price of the land, as stated in Article 19 of the Real Estate Taxes Regulation of the Republic of Turkey (TCRG 1972). The 20% sales profit expressed here can be called the profit of the entrepreneur and should not be confused with the profit of the contractor (Ramsett 1998; Karaca 2008; Özer 2010; Akkaynak 2014). Although it would be appropriate for the appraisers to determine the profit of the entrepreneur with market research, in Turkey conditions, at least based on the relevant regulation, a reasonable rate of 20% for public buildings can be accepted and used in public building valuations. In general, in Turkey, only the progress payment costs are taken in the valuation of public buildings according to the cost method, and only the approximate unit costs of the building are used in the cost analysis of the public and private buildings that are the subject of the lawsuit. This acceptance would be much more appropriate than just reflecting the progress payment values or calculating the value from the approximate unit costs of the building. Therefore, the total construction costs of the examined immovables, which are 23,332,500 TL in Table 2, are increased by 20% to include the profit of the entrepreneur, and the total value of the buildings is found as 27,999,000 TL. By adding 9,900,000 TL, which is the campus land value, to this value, the total value of the lands and structures of the district vocational school examined is 37,899,000 TL.

## **7. An Example of Contradiction in Real Estate Valuation Legislation in Turkey**

S. Gnat (2021) reports that in many developing countries real estate taxation reforms are underway or are planned. In these executions and plannings, the real estate value is accepted as a tax base. Because in countries with established market economies, real estate is usually taxed according to its value. Currently, the land taxation system has a major impact on land use and reallocation (Gnat 2021). The same can be said for housing taxation. According to the Real Estate tax law of the Republic of Turkey, the tax value for buildings is determined jointly by the Ministry of Treasury and Finance and the Ministry of Environment and Urbanization. According to the General Communiqué of the Property Tax Law, which is issued every year based on this law, the building cost classifications that are the basis for the property tax for the year 2021 are given in Table 3. Classification and unit cost values are presented in the same table for 2021, according to the communiqué on the approximate unit costs of buildings published by the Ministry of Environment and Urbanization every year. When these two separate legislative values are compared, it is seen that very different cost values can be taken for the same type of houses. Building approximate unit costs can be used in expert reports prepared for court cases, housing valuation reports prepared for banks' lending, and valuation of public buildings. However, there may be large differences between the building values obtained from approximate unit costs and the values based on taxation, supported by the inconsistency of the legislation. This situation causes the recorded building information to be contradictory in valuation.

Table 3

Comparison of house value charts in terms of real estate tax base and approximate unit costs of buildings in Turkey

	Costs based on property tax (TL/m <sup>2</sup> )			Building approximate unit costs (TL/m <sup>2</sup> )					
	Min.	Max.	Av.	3A	3B	4A	4B	4C	5A
Luxury	2,007	2,253	2,130	-	-	-	2,300	2,480	2,970
First class	1,268	1,393	1,330	-	-	1,920	-	-	-
Second class	812	964	888	-	1,800	-	-	-	-
Third class	573	685	629	1,360	-	-	-	-	-
Simple	292	412	352	1,360	-	-	-	-	-

In addition, in the table of approximate unit costs of the building, the buildings are divided into many classes and groups and gathered under a total of about 125 different titles. However, in this classification style, there is no clear classification of carrier system type and material, purpose of use and construction quality. In the table showing the unit cost prices for the tax base, the buildings were collected in approximately 880 different types. These different types are grouped distinctly based on the type and material of the carrier system (reinforced concrete carcass, masonry, etc.), the purpose of use (factory, hotel, cinema and theatre, etc.) and quality (luxury, 1st class, 2nd class, etc.). These two legislative charts do not use a common language in terms of classification of structures and this situation can easily lead to confusion.

## 8. Conclusion

In this study, 2 important situations that cause erroneous valuations in real estate valuation studies in Turkey are discussed. The first is the calculation of public real estate only with progress payment values. As a result, the entrepreneur's profit in public real estate is not reflected in the real estate value. However, the value of an immovable cannot be taken equal to the price spent only to create the immovable. The second issue is the difference between the construction cost classifications based on taxation and the approximate construction unit cost classifications in the legislation. This may cause the value taken as a basis for taxation to be smaller than the approximate cost of the building. However, the entrepreneur's profit should be added to the approximate cost of the building, which is normally calculated from the legislation charts, since it is subject to trading. In this case, the difference will be even greater. Because the value of the real estate subject to tax must already include the profit of the entrepreneur, representing the purchase and sale. However, when approximate valuations are made from the legislation tables, the tax value expected to include the profit of the entrepreneur is significantly smaller than the approximate cost of the structure that does not include the profit of the entrepreneur. Both the first and the second issue discussed in this study cause great inconsistencies in the recording and accounting of real estate values. Incorrect accounting and recording of building values negatively affect sustainable economic development due to the misleading valuations.

The conclusion information to be given as a summary on the first issue and what can be done to solve the problem can be expressed as follows: In practices in Turkey, the commissions that make the valuation of public immovables are generally composed of the employees of the public institution that owns the immovable. Most

of these employees do not have competency in valuation expertise. The valuation of public buildings is usually made using the cost method as a customary method. As the value, the sum of the progress payments paid by the public institution to the contractor while having the building constructed is taken. However, the problem is that the profit of the entrepreneur is not reflected in this value. As a result, the data files that will form the real estate valuation information system and the effects of the values found on the market are adversely affected. Because, taking the value of the building equal to the price paid only for the construction of the building, that is, the cost, cannot be a correct approach in terms of market conditions and practices. In the cost value method, the profit of the entrepreneur, which is essentially different from the profit of the contractor, must also be reflected in the value. Keeping public buildings separate from this reality will result in the accounting of government properties not reflecting the real situation. This creates risks for the sustainable economy. The value of the buildings is the sum of the construction cost and the sales profit of 20% of this and the purchase and sale price of the land, as stated in Article 19 of the Real Estate Taxes Regulation of the Republic of Turkey. The 20% sales profit expressed here can be called the profit of the entrepreneur and should not be confused with the profit of the contractor. Although it would be appropriate for the appraisers to determine the profit of the entrepreneur with market research, in Turkey conditions, at least based on the relevant regulation, a reasonable rate of 20% for public buildings can be accepted and used in public building valuations. This acceptance would be much more appropriate than just reflecting the progress payment values or calculating the value from the approximate unit costs of the building. In addition, personnel who will make valuations in public institutions should receive training on this subject. Specialist personnel trained to make valuation in public institutions can also be provided to serve in other public institutions in their own regions through inter-agency assignments.

The concluding information to be given as a summary about the second issue and what can be done to solve the problem can be also expressed as follows: The Ministry of Environment, Urbanization and Climate Change in Turkey publish approximate unit cost values according to building types every year. The published structure includes approximate unit costs, 15% contractor profit and 10% overheads. However, it does not include the land share price and the profit of the entrepreneur. In practice in Turkey, especially in expert reports requested by the courts, this table is used when determining the building values. However, the entrepreneur's profit is not added to the accounts when valuing the building based on approximate unit costs. This situation is problematic in terms of housing valuation on its own. For more qualified valuations, the court may request cost analysis from the experts more specifically according to the quantity calculations and unit price charts. However, in this case also, the building values are not found by adding the entrepreneur's profit. In addition, the housing values to be obtained from the approximate unit costs of the building, even without the entrepreneur's profit, are approximately 25% higher than the tax bases that are said to be based on taxation in the legislation. With the addition of entrepreneurial profits, the difference will become much larger. Therefore, it is essential to ensure coordination by reviewing legislation and management in Turkey. Same structure classification methodologies should be used in different calculation tables and should be corrected to give the same values. In court expertise and public or market valuations, not only costs, but also entrepreneurial profits supported by precedent values should be reflected in the building valuations.

### Author Contributions

This article is single authored.

### Conflicts of Interest

The authors declare no conflict of interest.

### References

- Açlar A, Çağdaş V. (2002) Real estate valuation for engineers, architects and experts, *TMMOB Chamber of Surveying and Cadastre Engineers*, 5-9.
- Aisbitt S. (2002) Harmonization of financial reporting before the european Company law Directives : the case of the Nordic Companies act , *Accounting and business Research*, 32:2 , 105-117. <https://doi.org/10.1080/00014788.2002.9728960>

- Akça, Y. (1998) Budget and Government Accounting, Istanbul University, Faculty of Economics Publication, No: 4047/555, Istanbul, p. 51.
- Akkaynak , B. (2014) Real Estate Valuation and an Application on Real Estate Valuation, Consultant: Yılgör , AG ., Mersin University . Social Science. Inst . Business USA, Mersin, 202 p.
- Aksoy S. (1994) Public Finance, Filiz Bookstore , Istanbul, 1994, p. 46.
- Alpturk , E. (2007). Real estate valuation guide, Publications of Finance and Law, Ankara, 411 p.
- Altınok T. (1973) Stock Accounting in Our Government Accounting System, *Journal of Finance*, Issue: 4, July-August, p. 6.
- Anayasa (1982). Constitution of the Republic of Turkey, Law Number: 2709, Date of Adoption: 18/10/1982 , Official Gazette Published; Date: 9/11/1982 Number: 17863 (Repeated), Code of Published; Edit: 5 Volumes: 22 Pages: 3.
- André , P., Cazavan - Jeny , A., Dick , W., Richard, C., & Walton, P. (2009). Fair value accounting and the banking crisis of 2008 – hitting the messenger. *Accounting in Europe* , 6 (1), 3 – 24. <https://doi.org/10.1080/17449480902896346>
- Appraisal Institute ( 2008) Appraisal of Real Estate , 13 edn , Appraisal Institute , Chicago, IL
- Arslan , A. (2004) Public Financial Management and Control Law No. 5018 and Regulations Made in the Expenditure System”, *Financial Guide Magazine*, Issue: 25, July-September, 88 p.
- Arslan , KO (2017). Determination of the Quality of Public Goods and Principles of Utilizing Public Goods, *TBB Journal*, 131, 57-86.
- Aydın, I. (2019). Academic Ethics, Ankara: Pegem Academy
- Bağbaşıoğlu , A. (2004) Boards to be Established and Regulations to be Made with the Public Financial Management and Control Law No. 5018, *Financial Guide Journal*, Issue: 24 (Free Supplement), April-June, p. 71.
- Bakır, H. (2009). Real estate valuation and finance mathematics , Detail Publishing, Ankara, 160s.
- Bartke , S. , & Schwarze , R. (2021). The economic role and emergence of professional valuers in real estate markets . *Land* , 10 (7), 683. <https://doi.org/10.3390/land10070683>
- Bengtsson , E. (2011). Repoliticizing accounting standard-setting—IASB, EU, and the global financial crisis. *Critical Perspectives in Accounting* , 22 (6), 567 – 580.
- Bitner , R. (2008). Confessions of a Subprime Lender : An Insider 's Story of Greed, Fraud, and Ignorance ; John Wiley & Sons : Hoboken , NJ, USA.
- Bourassa , SC, Cantoni , E. and Hoesli , M. (2007). Spatial dependency, housing submarkets and housing price prediction. *Journal of Real Estate Finance and Economics* , 35 (2): 143–160. <https://doi.org/10.1007/s11146-007-9036-8>
- Bulutoğlu , K. , Kurtuluş, E. (1988) Budget and Public Expenditures, Filiz Bookstore , Istanbul, p. 127.
- Cete , M. , Yomralioğlu , T. (2013) Re- engineering of Turkish land administration , *Survey Review* , vol . 45, iss . 330, p. 197-205.
- Cadastre (1987). Cadastre Law No. 3402, Official Gazette Published; Date: 9/7/1987 Issue: 19512, Published Code; Edit: 5 Volume: 26 Page: 229.
- Constitutional Court of the Republic of Turkey, (1966). Decisions of the Constitutional Court, Article No: 1966/3 Decision No: 1966/23 Date of Decision: 28/4/1966 , Official Gazette Date: 11/07/1966 Number: 12345
- D'Amato M. (2015) Income approach and property market cycle, *International Journal of Strategic property Management* 19:3 , p. 207-219. <https://doi.org/10.3846/1648715X.2015.1048762>
- D'Amato , M., Kauko , T. (2017) Valuation methods and the non-agency mortgage crisis. In *Advances of Automated Valuation Modeling* ; Springer : Cham , Switzerland, s. 23–32.
- d'Arcy, É., & Keogh, G. (1997). Towards a property market paradigm of urban change. *Environment and Planning A*, 29(4), 685-706. <https://doi.org/10.1068/a290685>
- des Rosiers , F., Theriaults , M., and Villeneuve , P. (2000) Decomposition of access and neighborhood factors in hedonic price modeling . *Journal of Real Estate Investment and Finance* , 18 (3): 291 – 315.
- Donaldson, S. E., & Van der Merwe, I. J. (1999). Urban transformation and social change in Pietersburg during transition. *Society in transition*, 30(1), 69-83. <https://doi.org/10.1080/10289852.1999.10520169>
- Downie , ML; Robson , G. (2008) Automatic valuation models: An international perspective. In the Proceedings of the RICS Automated Valuation Models Conference: AVMs today and Tomorrow ,

- London, UK, 4 November. <http://nrl.northumbria.ac.uk/id/eprint/1683>
- EC (European Council) (2006) Directive 2006/48/EC of the European Parliament and of the Council of 14 June 2006 relating to the taking up and pursuit of the business of credit institutions Official Journal of the European Union , L177: 1 – 200 .
- Eriksson , C. , Adair , A., McGreal , S., Webb , J. (2005) Harmonization of Investment Valuation Standards in Europe , *Journal of Real Estate Literature* , vol . 13, is. 1, p. 45-64. <https://doi.org/10.1080/10835547.2005.12090149>
- Erdem, N. (2019) Investigation of the Effectiveness of Turkey's Real Estate Valuation System , *Journal of Geomatik* , 4(1) p. 1-13
- Erdem, N (2020) The need for re - engineering in the real estate appraisal system in Turkey , *Survey Review* , vol . 52, it. 370, p. 84-86.
- Erkek B. , Erkek, E., Yalpir , S. (2021) The Most Effective and Most Efficient Use of Land Analysis: The Case of TKGM Oran Campus, *AKU J. Sci . Eng .* , 21, 015503, p. 147- 166.
- EU, (2004) European Union Land Policy Guidelines for Support to Land Policy design and Land Policy Reform Processes in Developing Countries , EU Tasks Force on Land Tenure .
- Farjaudon , AL, and Morales , J. (2013). Seeking consensus: The role of accounting in defining and reproducing prevailing interests . *Critical Perspectives in Accounting* , 24 (2), 154–171.
- Gilbertson , B ., Preston, D. (2005) A vision for valuation. *J Prop . val . Investment. Finance.* 23 , 123–140. <https://doi.org/10.1108/14635780510699998>
- Gnat , S. (2021). Property mass valuation on small markets, *Land* , 10 (4), 388. <https://doi.org/10.3390/land10040388>
- Gözler, K. (2011). On Misuse of Some Administrative and Legal Terms in Laws No. 5018 and 6085, *AUHFD*, 60(4), 837-919.
- Güneş, T. and Yıldız, Ü. , (2015) . Collective valuation techniques used in the land registry and cadastre modernization project of the Republic of Turkey. In: FIG workweek 2015 – from the wisdom of the ages to the challenges of the modern world . Sofia, Bulgaria. May 17-21.
- Güneş, T. and Yıldız, U., 2016 . Property valuation and taxation to improve local governance in Turkey . *Land use log* , 15 (2), 141 – 160.
- Güngör, A. , A. (1981) Turkish Government Accounting System as a Management Tool, *Ministry of Finance Inspection Board Publication*, No:231, Ankara, p. 8.
- IVSC (2020) International Valuation Standards Council annual Report 2019–20, London , United Kingdom .
- Jindrichovska I. & Kubickova D. (2017) The Role and current Status of IFRS in the Completion of National accounting Rules – Evidence from the czech Republic , *Accounting in Europe* , 14:1 -2, 56-66.
- Karaca H. (2008) Real Estate Valuation Methods and Comparison, Supervisor: Coşkun Z ., MS thesis, ITU Science and Technology. Inst . geode And Fotog . USA, Istanbul, 69 p.
- Kaplan, G. (2004). Transfer of Immovable Property and Judicial Control between Public Institutions and Legal Persons, *Journal of Maltepe University Faculty of Law*, Issue: 2004/1–2, 167–188.
- Kerimoğlu , B. (2002) Reform Studies in Government Accounting, *Financial Guide Journal*, Issue: 17, July-September, p. 97.
- Kızılkaya , E. (2002) Tangible Fixed Asset Accounts in Accrual Based Government Accounting, *Financial Guide Magazine*, Issue: 17, July-September, p. 105.
- Koç, V. (2021a) Taşınmaz Geliştirme Kavramının İrdelenmesi, V. Internartional Istanbul Scientific Research Congress, August 14- 15, Istanbul, pp. 294- 301.
- Koç, V. (2021b) Ayvalık İlçesi Özelinde Konut Değerleme Önerileri, Internartional Halich Congress on Multidisciplinary Scientific Research, August 15- 16, Istanbul, pp. 277- 285.
- Koç, V. (2021c) Taşınmaz Geliştirmede Risk Analizinin Yönetim Sistemleri Anlayışıyla İncelenmesi, Mühendislik Alanında Uluslar Arası Araştırmalar'da kitap bölümü, Ed. Aydemir, E., Eğitim Yayınevi, İstanbul, pp. 97- 121.
- Koç, V. ve Çiçek, E.N. (2021) Samsun İlinde Kentsel Dönüşüm ve Konut Değerleme ile İlgili bir Örnek, Internartional Halich Congress on Multidisciplinary Scientific Research, August 15- 16, Istanbul, pp. 286- 295.
- Kothari , SP, Ramanna , K., & Skinner , DJ (2011). What Should GAAP Look Like? A Survey and Economic Analysis, Working Paper No. 09-22, Harvard Business School, Boston, MA, 1-111.

<http://hdl.handle.net/1721.1/66935>

- Lai, L. W., & Lorne, F. T. (2019). Sustainable urban renewal and built heritage conservation in a global real estate revolution. *Sustainability*, 11(3), 850. <https://doi.org/10.3390/su11030850>
- Liow, KH & Yeo, S. (2018). Dynamic Relationships between price and Net Asset value for Asian Real Estate Stocks, *International Journal of Financial Studies*, 2018, 6, 28. <https://doi.org/10.3390/ijfs6010028>
- Llewellyn, S. and Milne, MJ (2007). Accounting as codified discourse. *Journal of Accounting, Auditing and Accountability*, 20 (6), 805 – 824. <https://doi.org/10.1108/09513570710830254>
- Lundström, S. & Lind, H. (1996). Valuation of public real estate : context and concept, *Journal of Property Valuation & Investment*, 14(4), 31-4. <https://doi.org/10.1108/14635789610153452>
- Marco L., Morano P., Tajani F., and di Liddo F. (2020) An Innovative GIS- Based Territorial Information tool for the Evaluation of Corporate Properties : An Application to the Italian Context " Sustainability 12, no. 14: 5836 <https://doi.org/10.3390/su12145836>
- MEGM, (2019). "State Property Legislation", [https://kurumsal.milliemlak.gov.tr/Yaynlarimiz/Devlet\\_Mallari\\_Mevzuati\\_Ekli.doc](https://kurumsal.milliemlak.gov.tr/Yaynlarimiz/Devlet_Mallari_Mevzuati_Ekli.doc) (7 April 2019).
- MEGM, (2020). Annual Report 2019. Ministry of Finance, General Directorate of National Real Estate (MEGM), Ankara.
- Mooya, M. (2011) Of Mice and Men: Automatic valuation models and the valuation profession. *Urban Stud.*, 48, 2265–2281.
- Morgan, JF (1998). the natural history of professionalisation and its effects on valuation theory and practice in the UK and germany, *Journal of Property Valuation and investment*.
- Official Gazette (2018). Presidential Amendment Decree on the organization of public institutions affiliated to the Ministry. Official Gazette of the Republic of Turkey, Number: 30479, Date: 15/07/2018.
- Özer, M. (2010) Financial and Quantitative Methods Used in Real Estate Valuation: An Application with TOPSIS and New Multiple Criteria Models, Supervisor: Baray, İ., MS Thesis, DEÜ Sos. know Inst. Economics USA, Izmir, 197 p.
- Palicki, S., & Račka, I. (2016). Influence of Urban Renewal on the Assessment of Housing Market in the Context of Sustainable Socioeconomic City Development. In Smart City 360°: First EAI International Summit, Smart City 360°, Bratislava, Slovakia and Toronto, Canada, October 13-16, 2015. Revised Selected Papers 1 (pp. 851-860). Springer International Publishing. [http://dx.doi.org/10.1007/978-3-319-33681-7\\_76](http://dx.doi.org/10.1007/978-3-319-33681-7_76)
- Peldschus, F. (2010) Economical analysis of projects management under consideration of multi - criteria decisions, *Ukio Technologinis ir Ekonominis Vystymas*, vol. 12, is. 3, p. 169-170. <https://doi.org/10.1080/13928619.2006.9637737>
- Porter, M. (1990). Competitive Advantage of Nations, *Harvard Business Review*, March -April: 73-91.
- Public Property (2003). Public Financial Management and Control Law No. 5018, Official Gazette Published Date: 24/12/2003 No: 25326, Code Published; Issue: 5 Volume: 42.
- Public Record (2006). Regulation on Registration of Immovables Owned by Public Administrations, Official Gazette Published; Date: 2/10/2006 Issue: 26307, Published Code; Issue: 5 Volume: 46.
- Ramsett ED (1998) The Cost Approach : An Alternative View, *The appraisal Journal*, New York, April, p.4.
- Ramsey, R. (2004). The urban land economics tradition : how heterodox economic theory survive in the real estate appraisal profession Of Wisconsin Government and business and the History of Heterodox Economics thought Emerald group Publishing limited. [https://doi.org/10.1016/S0743-4154\(03\)22058-7](https://doi.org/10.1016/S0743-4154(03)22058-7)
- Richter J. (2020) EU Regulatory development, law and financial Markets review, 14:1, 65-76.
- RICS (2022) Red Book Global Standards : <https://www.rics.org/en-za/upholding-professional-standards/sector-standards/valuation/red-book/red-book-global/> ( Accessed on 04.10.2022 ).
- RICS EU (2008) Advisory group on Sustainable Property Investment and Management, Sustainable property investment and management, key issues and major challenges, RICS Proceedings ( Available at [http://www.rics.org/Newsroom/Keyissues/Sustainability/SPIM\\_r\\_230908.html](http://www.rics.org/Newsroom/Keyissues/Sustainability/SPIM_r_230908.html), accessed February 10, 2023)
- Quagli, A. and Ricciardi, M. (2010). IAS 39 Amendment October 2008, as another earnings management opportunity: an analysis of the European banking industry, SSRN 1639925.
- Sharkawy, A., & Barnes, W. (1992). Cost, Value, and Hybrid - Based underwriting criteria, *Journal of Real*

- Estate Research* , 7 (2), 169-185. <https://doi.org/10.1080/10835547.1992.12090669>
- Soto , HD (2017). *The Secret of Capital*, Translated by M. Aygen, Liberte Publications, Ankara.
- Söyler, I. (2005a) Reflections of the Accounting of Fixed Assets of the State on Public Finance, *Accounting and Auditing Overview*, September, p. 105- 116.
- Söyler, I. (2005b). Evaluation of State Property in Terms of Public Finance, Ministry of Finance Research, Planning and Coordination Board, Publication No: 2005/368, Ankara
- Söyler, I. (2007). Places of Rule and Disposition of the State in Terms of Public Goods Theory, *Journal of the Court of Accounts*, 83, p. 57-68.
- Stuebs , M. and Wilkinson , B. (2014). Professionalizing the tax accounting profession: Fulfilling public interest reporting responsibilities . In S. Mintz (Ed.), *Public interest Accounting. Perspectives on Accountability, Professionalism and role in society* (pp. 27 – 50). springer . [https://link.springer.com/chapter/10.1007/978-94-007-7082-9\\_2](https://link.springer.com/chapter/10.1007/978-94-007-7082-9_2)
- Tapu (2014). Land Registry applications, General Directorate of Land Registry and Cadastre, *Department of Land Registry*, Ankara.
- Tasan K.T., Groetelaers DA, Haffner MEA, Van Der Heijden HM, & Altes WKK (2013) Providing Cheap Land for social Housing : Breaching the state aid Regulations of the single European Market?, *Regional Studies* , 47:4, 628-642. <https://doi.org/10.1080/00343404.2011.581654>
- Taylor, JB (2009) *Financial Crisis and Policy Responses: An Empirical Analysis of What Gone Wrong* ; 14631 Working Certificate No. National Bureau of Economic Research: Cambridge, MA, USA.
- TCRG (1972) Regulation on the Appraisal of the Tax Value to be Subject to Real Estate Tax, March 15, No: 14129, p. 1915-1927.
- Thibodeau , TG and Sabyasachi , B. (1998). Spatial autocorrelation in house prices analysis . *Journal of Real Estate Finance and Economics* , 17 (1): 61 – 85.
- Thorell P. & Whittington G. (1994) The harmonization of accounting within the EU, *European accounting review* , 3:2 , 215-240. <https://doi.org/10.1080/09638189400000019>
- TMK (2001). Turkish Civil Code No. 4721, Official Gazette Published; Date: 8/12/2001 Issue : 24607 Code of Published; Issue: 5 Volume: 41.
- TKGM (2020). Official website of TKGM , <https://www.tkgm.gov.tr/> Access date: 10.05.2020
- Üçbaş , A. (2004) What the Law No. 5018 Brought to Public Finance, *Fiscal Guide Magazine*, Issue: 25, July-September, p. 48.
- Ünel , FB ., Kuşak, L., Yakar, M. (2021) Preparation of Data for Sustainable Management by Examining Public Real Estate from a Legal Perspective: Mersin University, *Turkish Journal of Land Management*, 3(1), p. 08-24
- World Bank (2008). Project valuation document for 135.0 million euro loan proposed to the Republic of Turkey for the land registry and cadastral modernization project .Washington , DC: World Bank . <http://documents.worldbank.org/curated/en/608031468338987781/pdf/431740PAD0P106101official0use0only1.pdf>
- Van der Spek , M. (2017) Investin inf Real Estate Debt: Real Estate or Fixed Income? *Abacus-A J. Account. Finance. Bus. Stud.*, 53 , 349–370. <https://doi.org/10.1111/abac.12112>
- Ventolo , WL and Williams, MR (2001), *Fundamentals of real estate appraisal*, Dearborn estate Education , Chicago , 446s.
- Vrbka , J .; Junga , P.; Krulický , T. (2019) Methodology for determining the rental rate of return of built-up land. *Adalta J. Interdiscip . Res.*, 9 , 364–370.
- YÖK, (2020). Higher Education Information Management System, (28.11.2020) <https://istatistik.yok.gov.tr/>
- Żróbek , S. , Adamiczka , J., & Grover , R. (2013). Valuation for loan security purposes Of the Context Of A Property Market Crisis - The Case of the United Kingdom Andean Poland . *Real estate Management and Valuation* , 21 (4), 36-46. <https://doi.org/10.2478/remav-2013-0035>



## Seasonal changes in the fatty acid profile of *Cystoseira crinita* Duby, 1830, distributed on the Sinop Peninsula Coast of the Black Sea

Ali Karaçuha<sup>1\*</sup>, Gökhan Yıldız<sup>2</sup>, Melek Ersoy Karaçuha<sup>3</sup>

<sup>1,2</sup> Department of Basic Sciences, Faculty of Fisheries, Sinop University, Sinop, Türkiye

<sup>3</sup>Department of Occupational Health and Safety, Faculty of Health Sciences, Sinop University, Sinop, Türkiye

### Article History

Received: 18.02.2023

Accepted: 05.07.2023

Published: 20.12.2023

### Research Article

**Abstract** – This study aimed to determine the fatty acids profile and seasonal change in *Cystoseira crinita* Duby, 1830 from the Sinop Peninsula coasts. The fatty acids profile was analyzed by GC/MS and their seasonal variation was studied. Along the sampling, it was possible to identify 37 different fatty acids in *C. crinita*, from C4 to C22. It was determined that palmitic acid was the most abundant fatty acid in all seasons, and further, the season which provided the highest contents of SFA, PUFA, and MUFA was winter. As a matter of fact, in our study, it was determined that the highest PUFA values ranged from 40.63% in winter to 32.23% in summer. It has been determined that the MUFA value varies between 25.88% in winter and 30.79% in summer, and the SFA value varies between 33.50% in winter and 35.98% in summer. In this study, the PUFA/SFA ratio of *C. crinita* was determined to change between 1.01% - 1.21% from winter to summer. In addition, the total  $\omega$ -6/ $\omega$ -3 PUFA ratio was found to be greater than 1 and ranged from 1.61 (winter) to 2.07 (summer). The atherogenicity and thrombogenicity index and h/H ratio were calculated from the fatty acid profiles of *C. crinita*, and the AI index was determined to change from 0.71 (winter) to 0.74 (autumn), TI index was 0.44 (winter) to 0.58 (in summer). The h/H ratio of 1.71 (summer) to 2.00 (winter) was calculated. These results of our study showed that the seasons have a significant effect on the fatty acid profile and the fatty acids in *C. crinita* may have important contributions to human nutrition. For this reasons, it is thought that it is extremely important to reveal the nutritional content of different seaweed species that spread in the seas of Turkey and to observe the seasonal changes in their contents.

**Keywords** – Atherogenicity index, Black Sea, fatty acid, macroalgae, thrombogenicity index

## 1. Introduction

As marine primary producers, macroalgae are among the rich sources of lipids for the growth and reproduction of marine organisms (Ivanova, Stancheva, & Petrova, 2013; Schram, Kobelt, Dethier, & Galloway, 2018). Fatty acids (especially PUFA), which are transferred from macroalgae to fish and even humans through the food chain in marine ecosystems, are among the important nutrients (Sijtsma & de Swaaf, 2004; Filimonova, Goncalves, Marques, Trochc, & Goncalves, 2016; Caf, Özdemir, Yılmaz, Durucan, & Ak, 2019). However, it is stated that alternative sources may be needed as a source of PUFA due to the uncertainty in future fish stocks, and it is suggested that seaweeds can be used as a new source of PUFA (Dawczynski et al., 2007; Polat & Ozoguz, 2013; Vizetto-Duarte et al., 2015; Belattmania et al., 2018).

Macroalgae, particularly brown, are a part of the main diet of many countries (Dawczynski, Schubert, & Jahreis, 2007; Miyashita et al., 2012; Muradian, Vaiserman, Min, & Fraifeld, 2015), and different ratios of polysaccharides, antioxidants, vitamins, minerals, proteins, and lipids that contain (Schmid et al., 2018; Nunes, Valente, Ferraz, Barreto, & Carvalho, 2020; Al-Adilah et al., 2021). In addition, it has been suggested that brown seaweeds have great amounts of PUFA, which are not present in land plants (Kumari, Bijo, Mantri,

<sup>1</sup> ali\_karacuha@hotmail.com

<sup>2</sup> gokhanyildiz41@gmail.com

<sup>3</sup> melekeryoy57@hotmail.com

\*Corresponding Author

Reddy, & Jha, 2013; Polat & Ozogul, 2013; Schmid et al., 2018; Al-Adilah et al., 2021). Seaweeds have contained a significant amount of essential fatty acids, despite the low lipid concentration (Rocha et al., 2021), they can be used as an alternative to a marine lipid resource due to brown seaweeds abundance among coastal algae (Airanthi et al., 2011).

Although macroalgae are very diverse in their amount of nutrients (Dawczynski et al., 2007), it is reported that their contents are affected by geographical situation, sampling terms, environment, season, temperature, salinity, and light intensity (Nelson, Phleger, & Nichols, 2002; Polat & Ozoğuz, 2013; Silva, Pereira, Valentao, Andrade, & Sousa, 2013). Therefore, it is thought that it is important to determine the seasonal changes in the nutrient content in order to expand the use of brown seaweed as a total source of SFA (saturated fatty acid), MUFA (monounsaturated fatty acid) and PUFA (polyunsaturated fatty acid). On the other hand, there is little study about the substance of fatty acids of macroalgae in Turkey (Polat & Ozogul, 2008; Yazıcı et al., 2008; Caf, Yılmaz, Durucan, & Özdemir, 2015; Caf et al., 2019; Aras & Sayın, 2020). *Cystoseira crinita* from the order Fucales (Ochrophyta, Phaeophyceae) is one of the most common species of the Sinop coast (Karacuha & Ersoy-Karacuha, 2013), but no information with these species on seasonal variations in fatty acid content has been published.

The aim of this study that to define the seasonal changes in the fatty acid profile of *C. crinita*, which is widely distributed in the coastal waters of Sinop province.

## 2. Materials and Methods

Samples were collected seasonally in 2014 by scuba diving from various rocky substrates at 0 and 1 m depths of the Sinop Peninsula coast (Figure 1). The sample was then transferred to the laboratory, separated from foreign materials such as stone and sand, and dried on blotting paper after washing with distilled water. The dried samples were pounded into powder and stored at  $-20^{\circ}\text{C}$ . 0.5 grams of each sample were used for fatty acid analysis. For taxonomic classification of the species, [www.algaebase.org](http://www.algaebase.org) was consulted.

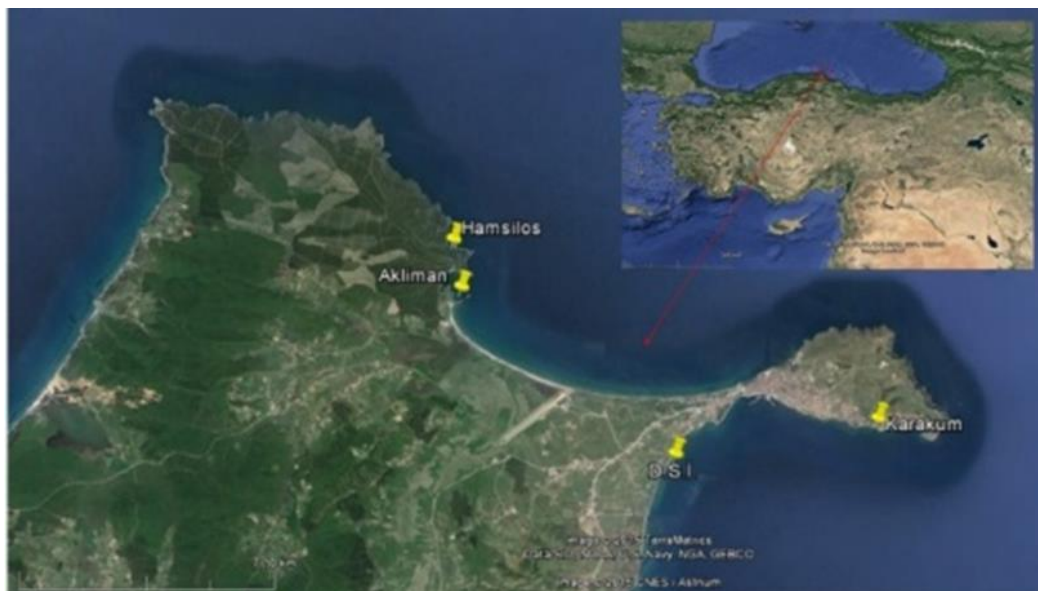


Figure 1. Sampling area (Google Maps).

### 2.1. Lipid extraction

Lipid extracts were prepared according to Bligh & Dyer (1959), using a mixture of chloroform and methanol. For this process, lipid samples were derivatized into methyl esters in a gas chromatography device (Thermo Scientific Trace 1310). In this process, 0.25 g of the extracted oil was dissolved by adding 4 ml heptane, after that 0.4 ml 2 N KOH was added. This mixture was then vortexed for 2 minutes followed by centrifugation at 5000 rpm for 5 minutes. After centrifugation, 1.5-2 ml of clear heptane phase was taken and transferred to glass tubes and GC/MS analysis was performed. Samples were injected into the device with the help of the autosampler (Autosampler AI 1310).

## 2.2. Fatty acid profile

The extracted algal lipid was then transesterified to fatty acid methyl esters (FAME) according to Ichihara et al. (1996). Samples were analyzed GC/MS gas chromatography-mass spectrometry (Thermo Scientific ISQ LT model). A 60 m long Trace Gold TG-WaxMS capillary column (Thermo Scientific code: 26088-1540) with an inner diameter of 0.25  $\mu\text{m}$  and a film thickness of 0.25  $\mu\text{m}$  was used for this analysis. The temperature of the injection block for the analysis was set to 240°C. In addition, the column temperature was programmed to remain constant at 100 °C for 3 minutes, and thereafter increase to 240 °C in increments of 4 °C/min. A separation ratio of 1:20 was applied using constant-flow (1 ml/min) helium gas as the carrier gas. Fatty acids were identified by comparing the standard FAME (fatty acid methyl ester) mixture of 37 components according to their arrival time. All analyses of fatty acids were performed in triplicate per biological sample during the sampling period. The results were given as mean $\pm$ standard deviation.

## 2.3. Lipid quality

Ulbricht & Southgate (1991) method to health lipid indices (AI and TI) to determine the nutritional and lipid quality of *C. crinita* was used.

The formula for calculating the Index of Atherogenicity (AI) is:

$$AI = \frac{C12:0 + (4 \times C14:0) + C16:0}{\sum(w-3 \text{ PUFA}) + \sum(w-6) \text{ PUFA} + \sum \text{MUFA}} \quad (2.1)$$

The formula for calculating the index of thrombogenicity (IT) is:

$$TI = \frac{C14:0 + C16:0 + C18:0}{(0.5 \times \sum \text{MUFA}) + (0.5 \times \sum w-6 \text{ PUFA}) + (3 \times \sum w-3 \text{ PUFA}) + (w-3/w-6)} \quad (2.2)$$

where PUFA and MUFA indicate monounsaturated and polyunsaturated FA.

The hypocholesterolemic/hypercholesterolemic (h/H) index is calculated to Santos-Silva, Bessa, & Santos-Silva (2002) method. The formula for calculating the Index of h/H is:

$$HH = \frac{(C18:1 + \sum \text{PUFA})}{(C14:0 + C16:0)} \quad (2.3)$$

## 2.4. Statistical analysis

Differences between seasonal average were evaluated using one-way ANOVA, followed by Tukey test ( $P < 0.05$ ). The contribution (percentage) of each fatty acid was taken into account during the calculations. Principal component analysis (PCA) was performed for sampling periods and fatty acid major classes (MUFA, SFA, and PUFA). All calculations were made with SPSS version 22.0.

## 3. Results and Discussion

In this study, the fatty acid profiles of *C. crinita* were analyzed by GC/MS, seasonally. It identified 37 different fatty acids from *C. crinita*, and are given in Table 1. It was determined that there were statistically significant differences in the fatty acid profile of *C. crinita* between seasons (Table 1). In this study, C16:0 (palmitic acid; from SFA) was determined to be the major fatty acid, followed by C18:1 $\omega$ 9c (elaidic acid; from MUFA), C20:4 $\omega$ 6 (arachidonic acid: ARA; from PUFA), C18:2 $\omega$ 6c (linoleic acid: LIN; from PUFA), C18:3 $\omega$ 3 ( $\alpha$ -linolenic acid: ALA; from PUFA), C20:5 $\omega$ 3c (eicosapentaenoic acid: EPA from PUFA), palmitoleic acid (C16:1; from MUFA), and oleic acid (C18:1 $\omega$ 9t; from MUFA), respectively. Palmitic acid was the dominant fatty acid during the study, with values ranging from 25.89 $\pm$ 0.99% total in summer to 24.32 $\pm$ 0.19% in winter. Similar to our finding, palmitic acid is reported to be the primary saturated fatty acid in several seaweeds (Kamenarska et al., 2002; Ivanova et al., 2013). Elaidic acid and oleic acid were the most abundant MUFAs in our study. Similarly, oleic acid is reported by Vizetto-Duarte et al. (2015) as one of the main fatty acids in brown seaweed, too. Besides, Kamenarska et al. (2002) reported that the main fatty acid for *C. crinita* from Eastern Mediterranean was palmitic acid, and then oleic and myristic acids. On the other hand, we determined that the total of PUFA was highest, followed by SFA and MUFA, respectively. (Table 1). PUFA was the most abundant component with 37.24% seasonal mean of total fatty acid. The seasonal mean of MUFA was 27.79%, and SFAs were 34.46%. Although this study results are concordant with the literatures

(Kumari et al., 2013), it has been found to differ from studies with *C. crinita*, which has the highest SFA values (Ivanova et al., 2013; Bouafif, Messaoud, Boussaid, & Langar, 2018) (Table 2).

Table 1

Seasonal change of fatty acid profile of *C. crinita* (percentage of the total FAME) with the significant differences between the seasons with one-way ANOVA and the Tukey test ( $p < 0.05$ ), and the result of indexes. (n=3).

Fatty acid (%)	SEASONS					F	Sig.
	Spring	Summer	Autumn	Winter			
C4:0	0.17±0.00 <sup>a</sup>	0.14±0.02 <sup>b</sup>	0.07±0.01 <sup>c</sup>	0.08±0.00 <sup>c</sup>	86.500	0.000	
C6:0	0.04±0.01 <sup>a</sup>	0.02±0.00 <sup>b</sup>	0.03±0.00 <sup>ab</sup>	0.02±0.01 <sup>b</sup>	9.833	0.005	
C8:0	0.05±0.00 <sup>a</sup>	0.02±0.01 <sup>b</sup>	0.04±0.01 <sup>a</sup>	0.01±0.01 <sup>b</sup>	35.000	0.000	
C10:0	0.02±0.01 <sup>a</sup>	0.01±0.01 <sup>a</sup>	0.02±0.01 <sup>a</sup>	0.01±0.00 <sup>a</sup>	1.222	0.363	
C11:0	0.02±0.00 <sup>b</sup>	0.01±0.01 <sup>c</sup>	0.04±0.00 <sup>a</sup>	0.01±0.01 <sup>c</sup>	44.667	0.000	
C12:0	0.03±0.00 <sup>ab</sup>	0.04±0.00 <sup>a</sup>	0.04±0.01 <sup>a</sup>	0.02±0.01 <sup>b</sup>	9.833	0.005	
C13:0	0.03±0.01 <sup>a</sup>	0.02±0.00 <sup>a</sup>	0.02±0.00 <sup>a</sup>	0.02±0.00 <sup>a</sup>	4.000	0.052	
C14:0	6.68±0.08 <sup>a</sup>	6.20±0.13 <sup>b</sup>	5.96±0.02 <sup>c</sup>	5.75±0.04 <sup>d</sup>	74.644	0.000	
C15:0	0.40±0.00 <sup>ab</sup>	0.39±0.01 <sup>b</sup>	0.40±0.01 <sup>ab</sup>	0.42±0.01 <sup>a</sup>	6.000	0.019	
C16:0	24.88±0.09 <sup>ab</sup>	25.89±0.99 <sup>a</sup>	24.64±0.07 <sup>ab</sup>	24.32±0.19 <sup>b</sup>	5.363	0.026	
C17:0	0.08±0.02 <sup>a</sup>	0.07±0.02 <sup>a</sup>	0.07±0.00 <sup>a</sup>	0.06±0.01 <sup>a</sup>	0.556	0.659	
C18:0	2.14±0.02 <sup>b</sup>	2.11±0.06 <sup>b</sup>	2.26±0.03 <sup>a</sup>	1.63±0.03 <sup>c</sup>	159.615	0.000	
C20:0	0.01±0.01 <sup>a</sup>	0.02±0.01 <sup>a</sup>	0.01±0.01 <sup>a</sup>	0.01±0.01 <sup>a</sup>	0.501	0.693	
C21:0	0.06±0.01 <sup>b</sup>	0.11±0.02 <sup>a</sup>	0.07±0.00 <sup>b</sup>	0.06±0.01 <sup>b</sup>	17.212	0.001	
C22:0	0.40±0.01 <sup>c</sup>	0.40±0.04 <sup>c</sup>	0.54±0.01 <sup>a</sup>	0.48±0.01 <sup>b</sup>	25.661	0.000	
C23:0	0.06±0.03 <sup>a</sup>	0.05±0.04 <sup>a</sup>	0.04±0.00 <sup>a</sup>	0.05±0.02 <sup>a</sup>	0.410	0.750	
C24:0	0.56±0.03 <sup>a</sup>	0.49±0.16 <sup>a</sup>	0.54±0.04 <sup>a</sup>	0.54±0.02 <sup>a</sup>	0.399	0.758	
<b>ΣSFA</b>	<b>35.61±0.11<sup>ab</sup></b>	<b>35.98±0.76<sup>a</sup></b>	<b>34.77±0.10<sup>b</sup></b>	<b>33.50±0.28<sup>c</sup></b>	<b>21.634</b>	<b>0.000</b>	
C14:1	0.34±0.01 <sup>a</sup>	0.33±0.02 <sup>a</sup>	0.22±0.00 <sup>b</sup>	0.17±0.00 <sup>c</sup>	188.385	0.000	
C15:1c	0.03±0.01 <sup>b</sup>	0.08±0.02 <sup>a</sup>	0.03±0.01 <sup>b</sup>	0.02±0.00 <sup>b</sup>	31.222	0.000	
C16:1	3.10±0.02 <sup>b</sup>	3.83±0.06 <sup>a</sup>	2.76±0.03 <sup>c</sup>	2.25±0.02 <sup>d</sup>	1033.804	0.000	
C17:1c	0.29±0.02 <sup>a</sup>	0.22±0.00 <sup>c</sup>	0.25±0.01 <sup>b</sup>	0.26±0.00 <sup>b</sup>	34.667	0.000	
C18:1ω9c	20.25±0.02 <sup>b</sup>	21.70±0.43 <sup>a</sup>	19.06±0.12 <sup>c</sup>	19.43±0.05 <sup>c</sup>	83.362	0.000	
C18:1ω9t	2.07±0.04 <sup>a</sup>	2.08±0.05 <sup>a</sup>	1.48±0.05 <sup>b</sup>	1.23±0.06 <sup>c</sup>	222.849	0.000	
C18:2ω6t	0.08±0.07 <sup>b</sup>	0.22±0.02 <sup>a</sup>	0.26±0.00 <sup>a</sup>	0.11±0.00 <sup>b</sup>	18.509	0.001	
C20:1c	0.13±0.01 <sup>c</sup>	0.32±0.03 <sup>a</sup>	0.19±0.02 <sup>b</sup>	0.12±0.02 <sup>c</sup>	89.213	0.000	
C22:1ω9	1.84±0.02 <sup>b</sup>	1.88±0.15 <sup>b</sup>	1.87±0.01 <sup>b</sup>	2.20±0.02 <sup>a</sup>	14.583	0.001	
C24:1	0.16±0.04 <sup>a</sup>	0.12±0.05 <sup>a</sup>	0.10±0.02 <sup>a</sup>	0.10±0.02 <sup>a</sup>	1.911	0.206	
<b>ΣMUFA</b>	<b>28.28±0.12<sup>b</sup></b>	<b>30.79±0.22<sup>a</sup></b>	<b>26.22±0.18<sup>c</sup></b>	<b>25.88±0.10<sup>c</sup></b>	<b>592.929</b>	<b>0.000</b>	
C18:2ω6c	7.95±0.02 <sup>b</sup>	7.36±0.19 <sup>c</sup>	8.94±0.06 <sup>a</sup>	7.90±0.02 <sup>b</sup>	132.422	0.000	
C18:3ω3	7.92±0.11 <sup>b</sup>	6.75±0.24 <sup>c</sup>	8.66±0.11 <sup>a</sup>	9.01±0.03 <sup>a</sup>	146.735	0.000	
C18:3ω6	0.16±0.03 <sup>c</sup>	0.57±0.03 <sup>a</sup>	0.26±0.01 <sup>b</sup>	0.14±0.01 <sup>c</sup>	275.033	0.000	
C20:2ω6c	0.48±0.03 <sup>b</sup>	0.64±0.08 <sup>a</sup>	0.48±0.00 <sup>b</sup>	0.50±0.02 <sup>b</sup>	11.441	0.003	
C20:3ω3c	0.01±0.01 <sup>a</sup>	-	-	0.02±0.01 <sup>a</sup>	0.250	0.643	
C20:3ω6c	1.39±0.02 <sup>c</sup>	1.44±0.15 <sup>c</sup>	2.26±0.05 <sup>a</sup>	2.01±0.01 <sup>b</sup>	89.229	0.000	
C20:4ω6	12.64±0.06 <sup>c</sup>	12.45±0.15 <sup>c</sup>	14.07±0.06 <sup>b</sup>	14.63±0.09 <sup>a</sup>	379.144	0.000	
C20:5ω3c	5.44±0.04 <sup>b</sup>	3.80±0.21 <sup>d</sup>	4.15±0.02 <sup>c</sup>	6.32±0.04 <sup>a</sup>	332.140	0.000	
C22:2c	0.06±0.03 <sup>a</sup>	0.11±0.05 <sup>a</sup>	0.06±0.02 <sup>a</sup>	0.05±0.02 <sup>a</sup>	2.700	0.116	
C22:6ω3c	0.05±0.01 <sup>b</sup>	0.11±0.05 <sup>ab</sup>	0.15±0.01 <sup>a</sup>	0.06±0.02 <sup>b</sup>	9.632	0.005	
<b>ΣPUFA</b>	<b>36.11±0.02<sup>c</sup></b>	<b>33.23±0.96<sup>d</sup></b>	<b>39.01±0.08<sup>b</sup></b>	<b>40.63±0.16<sup>a</sup></b>	<b>133.911</b>	<b>0.000</b>	
<b>ΣPUFAs/ΣSFAs</b>	<b>1.01±0.00<sup>c</sup></b>	<b>0.92±0.05<sup>d</sup></b>	<b>1.12±0.00<sup>b</sup></b>	<b>1.21±0.01<sup>a</sup></b>	<b>81.871</b>	<b>0.000</b>	
<b>ω-6</b>	<b>22.22±0.05<sup>c</sup></b>	<b>21.04±0.52<sup>d</sup></b>	<b>25.78±0.08<sup>a</sup></b>	<b>24.79±0.11<sup>b</sup></b>	<b>142.421</b>	<b>0.000</b>	
<b>ω-3</b>	<b>13.42±0.13<sup>b</sup></b>	<b>10.66±0.41<sup>c</sup></b>	<b>12.95±0.12<sup>b</sup></b>	<b>15.40±0.05<sup>a</sup></b>	<b>225.794</b>	<b>0.000</b>	
<b>ω-6/ω-3</b>	<b>1.65±0.02<sup>c</sup></b>	<b>2.07±0.03<sup>a</sup></b>	<b>1.99±0.03<sup>b</sup></b>	<b>1.61±0.01<sup>d</sup></b>	<b>337.026</b>	<b>0.000</b>	
<b>AI</b>	<b>0.80</b>	<b>0.79</b>	<b>0.74</b>	<b>0.71</b>	<b>81.871</b>	<b>0.000</b>	
<b>TI</b>	<b>0.51</b>	<b>0.58</b>	<b>0.50</b>	<b>0.44</b>	<b>142.421</b>	<b>0.000</b>	
<b>h/H</b>	<b>1.79</b>	<b>1.71</b>	<b>1.90</b>	<b>2.00</b>	<b>225.794</b>	<b>0.000</b>	

Different letters of inline are significantly different.

The PUFA/SFA proportion, which is widely used in determining the nutritional quality of foods, in this present study, was determined to change between 1.01%-1.21% winter to summer (Table 1). In addition, the total ω-6/ω-3 PUFAs ratio of *C. crinita* was found to be greater than 1 and ranged from 1.61 (winter) to 2.07 (summer) (Table 1). The ω6/ω3 PUFAs ratio also seemed to present seasonal variations. The amounts of the ω-3 PUFA ranged between 10.66±0.41% (in summer) and 15.40±0.05% (in winter), while the ω-6 PUFAs were verified, between 21.04±0.52% (in summer) and 24.79±0.11% (in winter) (Table 1, Figure 2). According to the WHO guideline, ω-6/ω-3 ratio must be lower than the 10 in the diet (Jayasinghe, Jinadasa, & Chinthaka, 2018). In our study, the ratios of the ω-6/ω-3 values of *C. crinita* are lower than the recommended level. Besides, it was

found that the ratio between PUFA/SFA was higher than one in all seasons except summer (0.92). In addition, *C. crinita* showed a PUFA/SFA ratio higher than 1 (Table 1). The PUFA/SFA ratio, which is the determinant of nutritive lipid quality in foods, was above 0.4 recommended by Wood (2004) in this study. Therefore, we can say that the PUFA/SFA ratio obtained from the studied samples are extremely important.

Table 2

The fatty acid, PUFA/SFA,  $\omega 6/\omega 3$ , AI, and TI index of *C. crinita* in comparison with the current study.

	Blacksea (Ivanova et al., 2013)	Mediterranean (Bouafif et al., 2018)	Present study
SFA	65.40	40.64	34.46
MUFA	11.88	27.71	27.79
PUFA	22.72	30.35	37.24
PUFA/SFA	0.35	0.75	1.07
$\omega 6/\omega 3$	1.01	4.79	1.82
IA	-	0.99	0.76
TI	-	0.94	0.51

In this study, the contents of PUFA were high (approximately 40.63 % in winter to 32.23% in summer). The contents of MUFA were low (25.88% in winter to 30.79% in summer), while SFA ranged from 33.50% in winter to 35.98 % in summer (Table 1, Figure 2). When the prominent fatty acids in the all- season were examined, it was determined that palmitic acid belonging to SFA was in the first place, followed by elaidic acid belonging to MUFA and arachidonic acid belonging to PUFA, respectively.

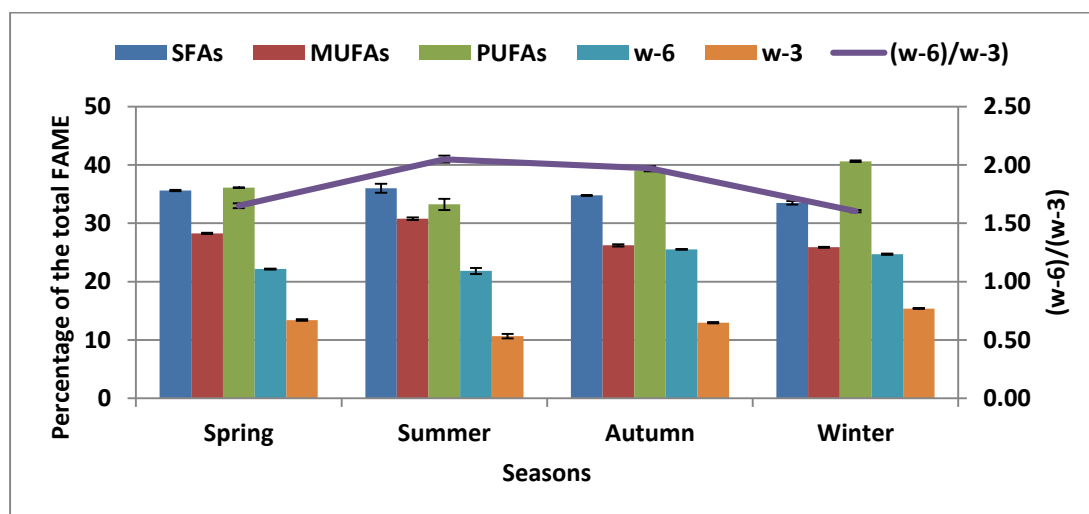


Figure 2. Comparison of the PUFA, SFA, MUFA,  $\omega$ -6,  $\omega$ -3, and (w-6)/w-3 ratio of *C. crinita*. (n = 3).

The fatty acid compositions changed from 33.50±0.28–35.98±0.76% saturated, to 25.88±0.10–30.79±0.22% monounsaturated and 32.23±0.96–40.63±0.16% polyunsaturated (PUFA) fatty acids (Figure 2). MUFA which predominates in this study was found to contain either 14 or 24 carbons (Table 1). Elaidic acid was the most potent MUFA with 21.70±0.43% of total FAME, especially in the summer. On the other hand, arachidonic acid (ARA) was the major PUFA (Table 1, Figure 3). Rajapakse and Kim (2011) reported that seaweeds are a good sources of PUFA that can be used for health, and Miyashita et al. (2012) declared that PUFA is obtained from especially brown seaweeds. In this study, the season with higher PUFA, SFA, and MUFA contents in *C. crinita* was winter. The results of our research showed lower SFA, but higher MUFA and PUFA, compared with findings from other studies with *C. crinita* (Ivanova et al., 2013; Bouafif et al., 2018) (Table 2). Similarly, Nelson, Phleger, & Nichols (2002) reported that the macroalgal total lipid ratio increased from winter to spring but decreased in summer. The different results in our study than the others may be because of the different environmental conditions of the habitats.

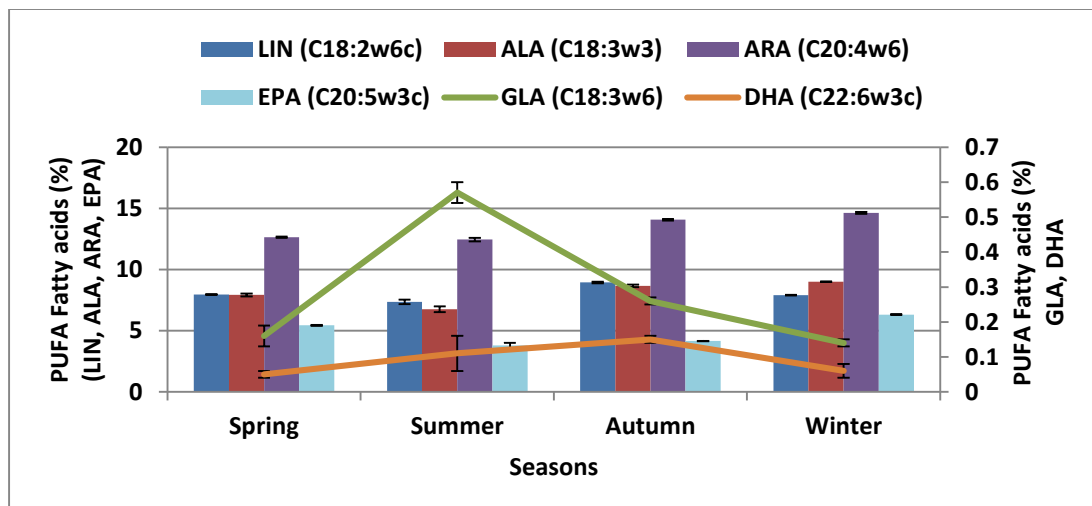


Figure 3. Comparison of the most abundant fatty acids of PUFA of *C. crinita*

The nutritional indexes of *C. crinita* were calculated from the fatty acid ingredients, and are given in Table 1 and Figure 4. It is stated that fatty acid found in macroalgae is extremely important in human nutrition,  $\omega 6/\omega 3$  PUFA ratio is important for health, and also AI and TI ratios should be less than one (Kumari. et al., 2013; Hamid et al., 2015; Schmid et al., 2018; Moreira et al., 2021). Studies have reported that high IA and IT values may worsen nutritional quality for human health (Ulbricht & Southgate, 1991; Bouafif et al., 2018). In this study, it was determined that the thrombogenic index (TI) values ranged from 0.44 (winter) to 0.58 (summer) and the values of the atherogenic index (AI) ranged between 0.71 (winter) and 0.74 (autumn) (Table 1, Figure 4). These values obtained in our study were found to be lower than the AI (0.99) and TI (80.94) values reported by Bouafif et al. (2018) (Table 2). In our study, *C. crinita* was determined to be a good source of  $\omega$ -6 and  $\omega$ -3, particularly arachidonic acid and  $\alpha$ -linolenic acid, respectively.

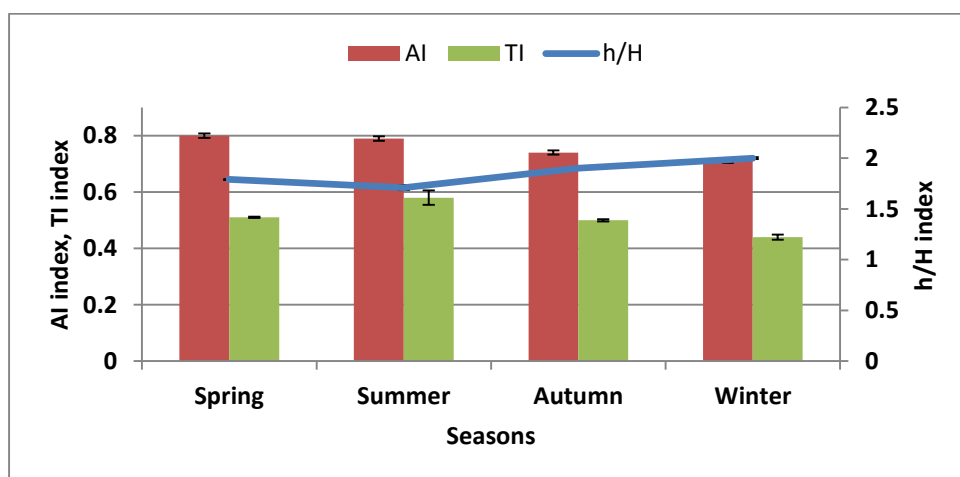


Figure 4. Results of Indexes according to the seasons.

In this study, PCA was calculated over the 7 fatty acids with the highest content to evaluate the relationship of fatty acids between seasons. Data were analyzed using direct oblimin rotation with Kaiser normalization for each component with eigenvalues greater than 1. The other fatty acids were removed from this analysis due to their low ratios, therefore promoting a more reliable the analysis. PCA explained 90.46% of the variables, PC1-77.83%; PC2-12.63% (Figure 5). The fact that total PUFA-LIN and total MUFA-SFA-EPA are in opposite positions on the plot indicate that they have opposite correlation.

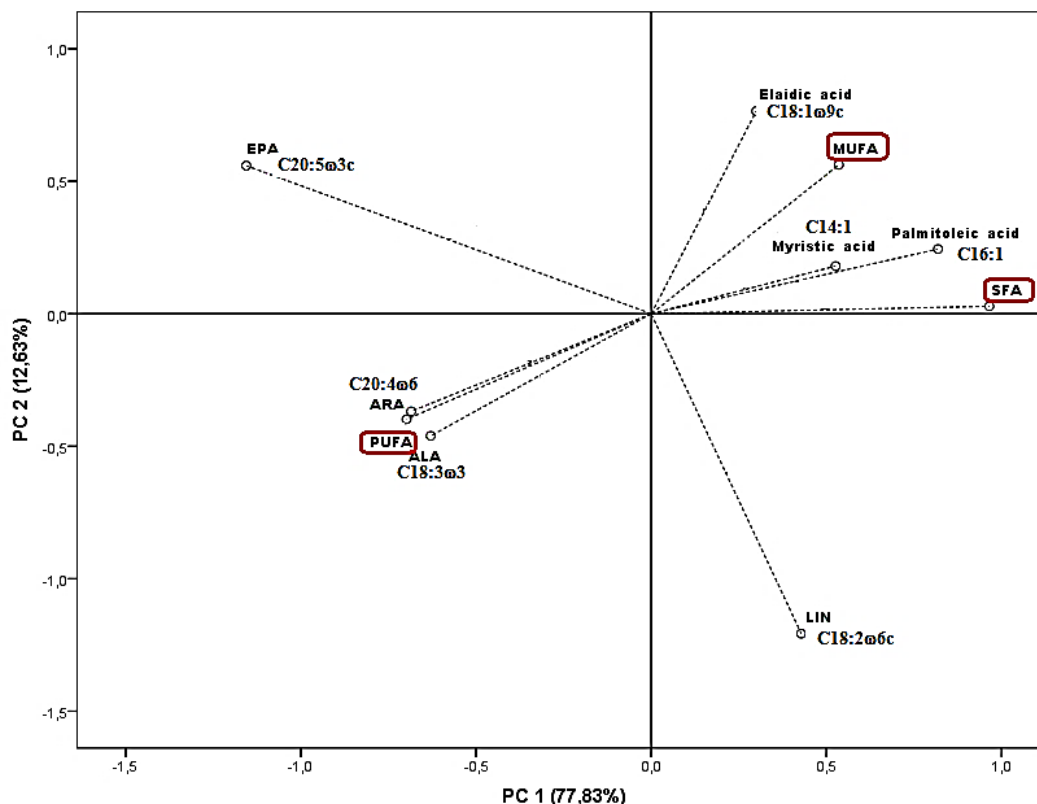


Figure 5. Results of loading plot of multivariate analysis (PCA).

#### 4. Conclusion

In conclusion, our findings showed that *C. crinata* has the highest PUFA content compared to SFA and MUFA. It was determined that among the fatty acids obtained in all seasons from this study, palmitic acid belonging to SFA was in the first place, followed by elaidic acid belonging to MUFA and arachidonic acid belonging to PUFA, respectively. The results of our research showed lower SFA, but higher MUFA and PUFA, compared with findings from other studies with *C. crinata*. Our research results also show that *C. crinata* can be a good source especially for arachidonic acid from  $\omega$ -6 and  $\alpha$ -linolenic acid from  $\omega$ -3. Moreover, in our study,  $\omega$ -6/ $\omega$ -3 PUFA ratio, which is important for health, was found at the recommended level (<10). In addition, PUFA/SFA ratio, which is the determinant of nutritional lipid quality in foods, and AI and TI ratios were again within the recommended values in *C. crinata*. These results suggest that the fatty acids in *C. crinata* may play an important role in human nutrition. In addition, our results demonstrated that the seasons have a significant effect on the fatty acid profile of the studied seaweed. As a matter of fact, in our study, it was determined that the highest PUFA values ranged from 40.63% in winter to 32.23% in summer. It has been determined that the MUFA value varies between 25.88% in winter and 30.79% in summer, and the SFA value varies between 33.50% in winter and 35.98% in summer. For this reasons, it is thought that it is extremely important to reveal the nutritional content of different seaweed species that spread in the seas of Turkey and to observe the seasonal changes in their contents.

#### Acknowledgment

Authors thank to Sinop University, Scientific and Technological Research Application and Research Center (SUBİTAM) for the analysis by gas chromatography-mass spectrometry (GC-MS).

#### Author Contributions

Ali Karaçuha: Collected data, planned the analysis and wrote the article

Gökhan Yıldız: Collected data, performed the analysis.

Melek Ersoy Karaçuha: Performed statistical analysis and wrote the article.

## Conflicts of Interest

The authors non declare conflict of interest.

## References

- Airanthi, M. K.W. A., Naoya, S., Sayaka, I., Nobuko, B., Masayuki, A., & Masashi, H. (2011). Effect of brown seaweed lipids on fatty acid composition and lipid hydroperoxide levels of Mouse Liver. *Journal of Agricultural and Food Chemistry*, 59(8), 4156-4163. DOI: <https://doi.org/10.1021/jf104643b>
- Al-Adilah, H., Al-Bader, D. A., Elktob, M., Kosma, I., Kumari, P., & Küpper, F. C. (2021). Trace element concentrations in seaweeds of the Arabian Gulf identified by morphology and DNA barcodes. *Botanica Marina*, 64(4), 327–338. DOI: <https://doi.org/10.1515/BOT-2021-0027>
- Aras, A., & Sayın, S. (2020). Determination of Potential of Some Marine Macroalgae for Future Functional Products. *Mediterranean Fisheries and Aquaculture Research*, 3(1), 22-35. Retrieved from: <https://dergipark.org.tr/tr/download/article-file/951086>
- Belattmania, Z., Engelen, A.H., Pereira, H., Serrão, E.A., Custódio, L., Varela, J. C., Zrid, R., Reani, A., & Sabour, B. (2018). Fatty acid composition and nutraceutical perspectives of brown seaweeds from the Atlantic coast of Morocco. *International Food Research Journal*, 25(4), 1520-1527. Retrieved from: [https://www.researchgate.net/publication/320347616\\_Fatty\\_acid\\_composition\\_and\\_nutraceutical\\_perspectives\\_of\\_brown\\_seaweeds\\_from\\_the\\_Atlantic\\_coast\\_of\\_Morocco](https://www.researchgate.net/publication/320347616_Fatty_acid_composition_and_nutraceutical_perspectives_of_brown_seaweeds_from_the_Atlantic_coast_of_Morocco)
- Bligh, E.G. & Dyer, W.J. (1959). A rapid method of total lipid extraction and purification. *Canadian Journal of Biochemistry and Physiolog*, 37, 911–917.
- Bouafif, C., Messaoud, C., Boussaid, M., & Langar, H. (2018). Fatty acid profile of *Cystoseira* C. Agardh (Phaeophyceae, Fucales) species from the Tunisian coast: Taxonomic and nutritional assessments. *Ciencias Marina*, 44(3), 169–183. DOI: <https://doi.org/10.7773/cm.v44i3.2798>
- Caf, F., Yılmaz, Ö., Durucan, F., & Özdemir, N. Ş. (2015). Biochemical components of three marine macroalgae (*Padina pavonica*, *Ulva lactuca* and *Taonia atomaria*) from the Levantine Sea coast of Antalya, Turkey. *Journal of Biodiversity and Environmental Sciences*, 6(4), 401-411. ISSN: 2220-6663 (Print) 2222-3045 (Online)
- Caf, F., Özdemir, N.Ş., Yılmaz, Ö., Durucan, F., & Ak, İ. (2019). Fatty acid and lipophilic vitamin composition of seaweeds from Antalya and Çanakkale (Turkey). *Grasas Aceites*, 70(3), e312. DOI: <https://doi.org/10.3989/gya.0704182>
- Dawczynski, C., Schubert, R., & Jahreis, G. (2007). Amino acids, fatty acids, and dietary fibre in edible seaweed products. *Food Chemistry*, 103(3), 891–899. DOI: <https://doi.org/10.1016/j.foodchem.2006.09.041>
- Filimonova, V., Goncalves, F., Marques, J. C., De Trochc, M., & Goncalves, A. M. M. (2016). Biochemical and toxicological effects of organic (herbicide Primextra® Gold TZ) and inorganic (copper) compounds on zooplankton and phytoplankton species. *Aquatic Toxicology*, 177, 33–43. DOI: <https://doi.org/10.1016/j.aquatox.2016.05.008>
- Hamid, N., Ma, Q., Boulom, S., Liu, T., Zheng, Z., Balbas, J., & Robertson, J. (2015). Seaweed minor constituents. In Tiwari, B. K. and Troy, D. J. (Eds.), *Seaweed Sustainability Food and Non-Food Applications*, (p. 193–242). London, Elsevier-Academic Press. DOI: <https://doi.org/10.1016/B978-0-12-418697-2.00008-8>
- Ichihara, K., Shibahara, A., Yamamoto, K. & Nakayama, T. (1996). An improved method for rapid analysis of the fatty acids of glycerolipids. *Lipids*, 31, 535–5.
- Ivanova, V., Stancheva, M., & Petrova, D. (2013). Fatty acid composition of Black Sea *Ulva rigida* and *Cystoseira crinita*. *Bulgarian Journal of Agricultural Science*, 19(S1), 42–47. Retrieved from: [https://www.researchgate.net/publication/259991334\\_Fatty\\_acid\\_composition\\_of\\_Black\\_Sea\\_Ulva\\_rigida\\_and\\_Cystoseira\\_crinita](https://www.researchgate.net/publication/259991334_Fatty_acid_composition_of_Black_Sea_Ulva_rigida_and_Cystoseira_crinita)
- Jayasinghe, G. D. T. M., Jinadasa, B. K. K. K., & Chinthaka, S. D. M. (2018). Study on lipid content and fatty acid profile of four marine macro algae (seaweeds) collected from south east coast of Sri Lanka. *Asian Journal of Chemistry and Pharmaceutical Sciences*, 3(1), 1-6. DOI: <https://doi.org/10.18311/ajcps/2018/22580>
- Kamenarska, Z., Yalcin, F., Ersöz, T., Calis, I., Stefanova, K., & Popov, S. (2002). Chemical composition of *Cystoseira crinita* Bory from the eastern mediterranean. *Zeitschrift für Naturforschung*, 57, 584–590. DOI: <https://doi.org/10.1515/znc-2002-7-806>

- Karacuha, A., & Ersoy-Karacuha, M. (2013). Changes of macroalgae biomass in Sinop peninsula coast of the Black Sea Turkey. *Turkish Journal of Fisheries and Aquatic Sciences*, 13, 725-736. DOI: [https://doi.org/10.4194/1303-2712-v13\\_4\\_18](https://doi.org/10.4194/1303-2712-v13_4_18)
- Kumari, P., Bijo, A., Mantri, V.A., Reddy, C., & Jha, B. 2013. Fatty acid profiling of tropical marine macroalgae: An analysis from chemotaxonomic and nutritional perspectives. *Phytochemistry*, 86, 44–56. DOI: <https://doi.org/10.1016/j.phytochem.2012.10.015>
- Miyashita, K., Bhaskar, N., Takayuki, T., Hiroyuki, K., Masayuki, A., & Masashi, H. (2012). Brown seaweed lipids as potential source of omega-3 PUFA in biological systems. In Kim, S.K. (Eds.), *Handbook of Marine Macroalgae: Biotechnology and Applied Phycology*, (p. 329–339). Chichester, Wiley-Blackwell. DOI: 10.1002/9781119977087.ch16
- Moreira, A. S., da Costa, E., Melo, T., Lopes, D., Pais, A., Santos, S. A., Pitarma, B., Mendes, M., Abreu, M. H., & Collén, P. N. (2021). Polar lipids of commercial *Ulva* spp. of different origins: Profiling and relevance for seaweed valorization. *Foods*, 10, 914. DOI: 10.3390/foods10050914
- Muradian, Kh., Vaiserman, A., Min, K. J., & Fraifeld, V. E. (2015). Fucoxanthin and lipid metabolism: A minireview. *Nutrition, Metabolism and Cardiovascular Diseases*, 25(10), 891–897. DOI: 10.1016/j.numecd.2015.05.010
- Nelson, M. M., Phleger, C. F., & Nichols, P. D. (2002). Seasonal lipid composition in macroalgae of the northeastern pacific ocean. *Botanica Marina*, 45, 58–65. DOI: 10.1515/BOT.2002.007
- Nunes, N., Valente, S., Ferraz, S., Barreto, M. C., & de Carvalho, M. A. P. (2020). Biochemical study of attached macroalgae from the Madeira Archipelago and beach-cast macroalgae from the Canary Islands: Multivariate analysis to determine bioresource potential. *Botanica Marina*, 63, 283–298. DOI: 10.1515/bot-2019-0022
- Polat, S., & Özoğul, Y. (2008). Biochemical composition of some red and brown macroalgae from the northeastern Mediterranean Sea. *International Journal of Food Science and Nutrition*, 59(7), 566-572. DOI: <https://doi.org/10.1080/09637480701446524>
- Polat, S., & Ozogul, Y. (2013). Seasonal proximate and fatty acid variations of some seaweeds from the northeastern Mediterranean coast. *Oceanologia*, 55, 375–391. DOI: <https://doi.org/10.5697/oc.55-2.375>
- Rajapakse, N., & Kim, S. K. (2011). Marine medicinal foods: implications and applications macro and microalgae. In Henry, J. (Eds.), *Advances in Food and Nutrition Research*, 64, (p.17–28). USA: Elsevier. Retrieved from: [https://books.google.com.bo/books?hl=tr&id=m0l\\_nPbhE-kC&q=Rajapakse#v=snippet&q=Rajapakse&f=false](https://books.google.com.bo/books?hl=tr&id=m0l_nPbhE-kC&q=Rajapakse#v=snippet&q=Rajapakse&f=false)
- Rocha, C. P., Pacheco, D., Cotas, J., Marques, J., Pereira, L., & Gonçalves, A. M. M. (2021). Seaweeds as valuable sources of essential fatty acids for human nutrition. *International Journal of Environmental Research and Public Health*, 18, 4968. DOI: <https://doi.org/10.3390/ijerph18094968>
- Santos-Silva, J., Bessa, R., & Santos-Silva, F. (2002). Effect of genotype, feeding system and slaughter weight on the quality of light lambs: II. Fatty acid composition of meat. *Livestock Production Science*, 77, 187–194. DOI: [https://doi.org/10.1016/S0301-6226\(02\)00059-3](https://doi.org/10.1016/S0301-6226(02)00059-3)
- Schmid, M., Kraft, L. G., van der Loos, L. M., Kraft, G. T., Virtue, P., Nichols, P. D., & Hurd, C. L. (2018). Southern Australian seaweeds: A promising resource for omega-3 fatty acids. *Food Chemistry*, 265, 70–77. DOI: <https://doi.org/10.1016/j.foodchem.2018.05.060>
- Schram, J. B., Kobelt, J. N., Dethier, M. N., & Galloway, A. W. E. (2018). Trophic transfer of macroalgal fatty acids in two urchin species: digestion, egestion, and tissue building. *Frontiers in Ecology and Evolution*, 6, 83. Retrieved from: <https://www.frontiersin.org/articles/10.3389/fevo.2018.00083/full>
- Sijtsma, L., & de Swaaf, M. E. (2004). Biotechnological production and applications of the w-3 polyunsaturated fatty acid docosahexaenoic acid. *Applied Microbiology and Biotechnology*, 64, 146–153. DOI: 10.1007/s00253-003-1525-y
- Silva, G., Pereira, R. B., Valentao, P., Andrade, P. B., & Sousa, C. (2013). Distinct fatty acid profile of ten brown macroalgae. *Revista Brasileira de Farmacognosia*, 23, 608-613. DOI: <https://doi.org/10.1590/S0102-695X2013005000048>
- Ulbricht, T., & Southgate, D. (1991). Coronary heart disease: Seven dietary factors. *The Lancet*. 338, 985-992. DOI: 10.1016/0140-6736(91)91846-m
- Vizetto-Duarte, C., Pereira, H., Bruno de Sousa, C., Pilar-Rauter, A., Albericio, F., Custódio, L., Barreira, L., & Varela, J. (2015). Fatty acid profile of different species of algae of the *Cystoseira* genus: a nutraceutical perspective. *Natural Product Research*, 29(13), 1264–1270. DOI: <https://doi.org/10.1080/14786419.2014.992343>

- Wood, J. D., Richardson, R. I., Nute, G. R., Fisher, A. V., Campo, M. M., Kasapidou, E., Sheard, P. R., & Enser, M. (2004). Effects of fatty acids on meat quality: a review. *Meat Science*, 66(1), 21–32. DOI: [https://doi.org/10.1016/S0309-1740\(03\)00022-6](https://doi.org/10.1016/S0309-1740(03)00022-6)
- Yazıcı, Z., Aysel, V., Öksüz, E., Köse, A., Cumali, S., & Güven, K. C. (2008). Fatty acid composition of marine macroalgae from the Black Sea and Dardanelles. *Toxicological & Environmental Chemistry*, 89(2), 371-379. DOI: <https://doi.org/10.1080/02772240601012366>



## Detection and Validation of A2 Milk Suitable for Consumers Having Milk Intolerance by ELISA Method

Mediha Esra Altuntop Yayla<sup>1,\*</sup>

<sup>1</sup>Department of Medical Biochemistry, Faculty of International Medicine, University of Health Sciences, İstanbul, Türkiye

### Article History

Received: 21.02.2023

Accepted: 20.06.2023

Published: 20.12.2023

### Research Article

**Abstract** – Casein proteins, which make up 80% of the total proteins in cow's milk, consist of mainly A1 and A2 genetic types which differ by a mutation that causes conversion from proline to histidine. Histidine-containing A1 protein undergoes proteolytic degradation in the gastrointestinal system, while this is not observed during the digestion of A2 protein. A1 milk consumption causes bloating, gas, discomfort and symptoms confused with lactose intolerance. Studies showed that A1 milk consumption may cause diabetes, coronary heart disease, arteriosclerosis, sudden infant death, and is associated with autism and schizophrenia. With an increasing trend in the world, A2A2 milk (milk without A1 protein) production is becoming widespread with consumer preferences; and, A2 milk takes its place on the market shelves. With the onset of this trend, the need for a new analysis on food safety became evident. It will be required by food control laboratories to test the absence of A1 protein in milk to be labeled as A2 milk. In this study, the quantitative analysis and validation of  $\beta$ -casein A1 and A2 proteins in cow's milk by Enzyme-Linked ImmunoSorbent Analysis (ELISA) method was investigated. The methods have detection limits of 1.8 and 0.8 ppm, and quantitation limits of 17 and 2.4 ppm for A1 and A2, respectively.

**Keywords** –  $\beta$ -casein A2 protein, cow milk, ELISA, food safety, method validation

## 1. Introduction

Casein proteins ( $\alpha_{S1}$ -,  $\alpha_{S2}$ -,  $\beta$ - and  $\kappa$ -casein) constitute approximately 80% of the total proteins in cow's milk (Bonfatti, Grigoletto, Cecchinato, Gallo, & Carnier, 2008); and,  $\beta$ -caseins constitute approximately 30% of these proteins. There are two main genetic types of  $\beta$ -caseins as A1 and A2. The distinguishing feature between these two forms of  $\beta$ -caseins is due to a mutation at position 67 of this 209 amino acid long protein. With this point mutation, A2 was thought to have undergone a point mutation that converts proline (Pro<sup>67</sup>) to a histidine (His<sup>67</sup>) in A1 in ancestors from European-type cows such as Holstein-Friesian, Ayrshire and Red (Kamiński, Cieslińska, & Kostyra, 2007). Therefore, although cow's milk produced in many countries is a mixture of A1 and A2  $\beta$ -casein variants, the His<sup>67</sup> mutation is not found in purebred Asian and African cows (Kamiński et al., 2007). Similarly, a histidine mutation at the equivalent position has not been found in other mammals, including humans, or a similar mutation has been observed very rarely (De Noni et al., 2009; Pal, Woodford, Kukuljan, & Ho, 2015).

Goat, sheep, camel, buffalo, yak and donkey milk consists of only A2 type milk, while most of the Holstein, Friesian, Ayrshire and British Storthorn cows produce either A1 or A1A2 milk, which are considered to be produced with higher yield (Boro, Naha, Saikia, & Prakash, 2016). Because of this feature, cow breeds with  $\beta$ -casein A1 mutation are thought to become widespread due to commercial concerns. Consumption of A1 milk creates a feeling of bloating, gas and discomfort. There are also studies showing that problems caused by A1 milk consumption are confused with lactose intolerance (Suchy et al., 2010). Studies have shown that A1 milk can cause type 1 diabetes, coronary heart disease, arteriosclerosis and sudden infant death (Sodhi,

<sup>1</sup>  medihaesra.yayla@sbu.edu.tr

\*Corresponding Author

Mukesh, Kataria, Mishra, & Joshii, 2012). In addition, A1 milk consumption is associated with diseases such as autism and schizophrenia (Woodford, 2006). All these studies bring along the increasing consumer demand for anti-A1 dairy. Many doctors recommend that consumers, especially those with celiac disease and stomach ulcers, and infants under one year old, should strictly avoid A1 milk.

A1 protein with His<sup>67</sup> mutation is quickly affected by proteolytic degradation, while A2 with Pro<sup>67</sup> is resistant. Therefore, A1 proteins cause the release of short  $\beta$ -casomorphin (BCM) opioid peptides during gastrointestinal digestion. Opioid is used to describe chemicals that have morphine-like effects in the body (Kamiński et al., 2007). Studies have shown that BCMs are released from  $\beta$ -casein A1 protein during gastrointestinal digestion, while BCM release after A2 protein digestion is minor (Boutrou et al., 2013; Kamiński et al., 2007). It has been proven that A1 slows down the opioid-induced gastrointestinal transit. Longer gastrointestinal transit times are thought to lead to increased effects of lactose fermentation and other dietary components such as FODMAPs, which, together with genetic predisposition, is hypothesized to be consistent with clinical and sub-clinical outcomes including digestive distress and pro-inflammatory effects (De Noni et al., 2009).

In recent years, A1-free (A2A2) cow's milk has been among the commercially sold milks in many countries such as Australia, England, the United States, New Zealand and the Netherlands, and these milks are advertised as suitable for the use of consumers with milk intolerance (Brooke-Taylor, Dwyer, Woodford, & Kost, 2017). Recently, Vietnam's largest dairy company, Vinamilk, has started A2A2 milk production by importing a type of cow that produces A1-free milk from New Zealand (Hang, 2018). In addition, baby foods produced with  $\beta$ -casein that do not contain A1 are sold in China and Australia, and there have been advertisements indicating that these foods are light and suitable for the baby's digestive system (Brooke-Taylor et al., 2017). A2 milk has been preferred among consumers at an increasing rate all over the world, and it is rapidly becoming widespread. Industry and governments have to regulate the food policies and make food safety and control laboratories perform food analysis that aims to characterize food products in terms of chemical composition, traceability, safety, quality, sensory perception and nutritional value (Jain & Gupta, 2005; Nestle, 2002; Silver & Bassett, 2008; Kudlejova & Risticovic, 2012; Tang, Vasas, Hatzakis, & Spyros, 2019). Therefore, the prevalence of A2 milk brings an obligation of a new test to be made by food safety and control laboratories in order to control the content of cow's milk so that the consumers are not misled. The products marketed as A2 dairy are required to be tested for the presence of A2  $\beta$ -casein protein and non-presence of A1  $\beta$ -casein protein by food control laboratories.

There are various methods in the literature that allow the detection of A1 and A2  $\beta$ -casein proteins in cow's milk. Capillary zone electrophoresis (De Noni, 2008), reverse-phase high-performance liquid chromatography (RP-HPLC) (Bonfatti et al., 2008), isoelectric focusing electrophoresis (Anna, Salvatore, Omar, & Eugenio, 2016), and urea-polyacrylamide gel electrophoresis (Duarte-Vázquez et al., 2018) are the main methods used to distinguish  $\beta$ -casein variants. More powerful methods such as liquid chromatography coupled mass spectrometry (LC-MS/MS) (Asledottir et al., 2017) or high resolution mass spectrometry (LC-HRMS) (Givens, Aikman, Gibson, & Brown, 2013) have also been successfully applied for the determination of protein types in milk and quantitative studies.

In this study, it was aimed to introduce and validate a new method to be used by food safety and control laboratories for the traceability and authenticity of A2 milk products. For the purpose of quantitative detection of  $\beta$ -casein A1 and A2 proteins in cow's milk, ELISA methodology was presented. Considering the method application by prevalent food control laboratories, ELISA is not only an easier assay to perform compared to aforementioned methods, but also accurate, sensitive and widely applicable. The applied method for quantitative detection of  $\beta$ -casein A1 and A2 proteins by ELISA had a limit of detection of 1.8 ppm and 0.8 ppm, and limit of the quantitation of 17 ppm and 2.4 ppm for A1 and A2 proteins, respectively.

## 2. Materials and Methods

### 2.1. Chemicals and Devices

The milk of genotypically tested cows of A1A1, A1A2 and A2A2 were obtained from Uluova Dairy Company (Çanakkale). "A1 ELISA Kit and A2 ELISA Kit" (GeneTel Laboratories LLC, USA) was used for the detection of A1 and A2 proteins by ELISA method. Kits contain ELISA microtiter strips coated with rabbit

anti- $\beta$ -casein polyclonal antibodies (pAbs), A1  $\beta$ -casein or A2  $\beta$ -casein protein standard solutions, chicken anti-A1 or anti-A2  $\beta$ -casein specific pAbs, rabbit anti-chicken IgY HRP conjugate, BSA for antibody dilution buffer, 10X Tris buffered saline (TBS) buffer, 50% solution of Tween-20 (Polyoxyethylene-Sorbitan Monolaurate) and 3, 3', 5, 5'-tetramethylbenzidine substrate (TMBS). Microcentrifuge tubes (Isolab, Turkey) and 50 mL sterile tubes (Falcon-Corning, USA) are also used for this analysis. The devices used in the analysis are micropipettes (Mettler Toledo Rainin Piper-Lite XLS, USA), vortex mixer (VWR International, USA), plate shaker/mixer (Bioer, China) and ELISA reader (Thermo Scientific Varioskan ® Flash, USA).

## 2.2. Sample Preparation

Solutions were prepared according to the manufacturer's instructions (GeneTel Laboratories LLC, A1 & A2 ELISA Kit Protocols). For the preparation of seven A1-containing standard solutions, seven 1.5 mL tubes are used. 10  $\mu$ L of 40  $\mu$ g/mL A1 standard and 990  $\mu$ L of antibody dilution buffer are added to the first tube to obtain 400 ng/mL A1 standard. 2X serial dilutions are made with antibody dilution buffer for the other standards, resulting in standard solution concentration of 400 ng/mL in the 1st tube, 200 ng/mL in the 2nd tube, 100 ng/mL in the 3rd tube, 50 ng/mL in the 4th tube, 25 ng/mL in the 5th tube, 12.5 ng/mL in the 6th tube and 6.25 ng/mL in the 7th tube.

Milk samples are prepared by diluting in the antibody dilution buffer. In general, casein proteins are not soluble at neutral pH and need a raise in pH. Therefore, in order to obtain soluble casein proteins, the first dilution is made with 0.5 M NaOH at a ratio of 1:100 (10  $\mu$ L milk + 990  $\mu$ L NaOH). Subsequent dilutions are made with the antibody dilution buffer. A1A1 or A2A2 milk should be diluted in the range of 1:10.000 – 1:100.000. A1/A2 milk should be diluted in the range of 1:10 – 1:1000. In a regular assay, for the samples which are expected to be negative for A1  $\beta$ -casein or A2  $\beta$ -casein, 1:100 dilution is used. However, since NaOH prevents the reaction, it is sufficient to dilute these milk samples only with the antibody dilution buffer.

## 2.3. ELISA

The protective tape on the microtiter strips is removed and the wells are washed 3 times with TBST. 100  $\mu$ L of standard solutions and diluted milk samples are added to the wells. The plate is mixed on a plate shaker at 400 rpm for 2 hours at room temperature. The wells are washed 3 times with TBST. A1 and A2 specific chicken IgY pAbs are prepared at 1:2000 and 1:300 dilutions, respectively in antibody dilution buffer, and 100  $\mu$ L of dilutions are added to each well and incubated while shaking for 2 hours at room temperature on a plate shaker. The wells are washed 3 times with TBST. Rabbit anti-chicken IgY HRP conjugate is prepared at a 1:1000 dilution in antibody dilution buffer and 100  $\mu$ L is added to each well and incubated while shaking for 1 hour at room temperature on a plate shaker. The wells are washed 5 times with TBST. 50  $\mu$ L of substrate (TMBS) is added to each well and incubated for 4-8 minutes for a color change (it is recommended to wait 8 minutes after the solution is added to the first well). The reaction is terminated with 50  $\mu$ L of 1 M HCl. An absorbance reading is taken at 450 nm immediately.

## 2.4. Evaluation of ELISA Results

For absorbance readings at 450 nm, Thermo Scientific Varioskan ® Flash device was used. For this purpose, the SkanIt RE for Varioskan Flash 2.4.3 software is used for the evaluation of the results. After defining the plate with respect to the positions of the standards and samples, as well as the concentrations of standards and dilutions of the samples, absorbance readings are taken at 450 nm. After the reading, the "Result" tab in the upper list is selected, and then, "Photometric 1" tab in the lower list is selected. From the calculation tools on the left side, "Quantitative CurveFit3" is clicked. On the page that opens, under the "Parameters" tab, as the "Fit Type", "Quadratic Polynomial" and as the "Transformation", "Conc. Logarithmic" and "Meas. Logarithmic" is selected. The software automatically lists the concentrations of the samples and draws the standard graphs. The analysis must be repeated, if any of the "blank" samples or the A2A2 milk sample in the A1 assay or the A1A1 milk sample in the A2 assay is calculated to be higher than the detection limit. Similarly, if the standard graph differs from the graph provided in the kit validation and quality assurance certificate, the analysis should be repeated. In addition, if the amount of protein calculated in the samples does not fall within the range determined in the standard graph, the analysis should be repeated by changing the dilution factor applied to the samples.

## 2.5. Method Validation

For the validation of ELISA, a) dynamic range, b) limit of detection (LOD), c) limit of quantification (LOQ), d) repeatability and e) measurement uncertainty parameters were considered (National Institute of Standards and Technology, 1995).

- a) In order to determine the dynamic range of the methods, 8 different standard concentrations were prepared by using A1 and A2 standards included in the kit content. The prepared standards were analyzed on 3 different days, re-prepared each time, and the dynamic range was determined.
- b) LOD was calculated for A1 assay by using milk with no  $\beta$ -casein A1, and for A2 assay by using milk with no  $\beta$ -casein A2. LOD was calculated as the mean of the sample + 3\*(standard deviation).
- c) LOQ was calculated as the mean of the sample without  $\beta$ -casein A2 (or A1) + 10\*(standard deviation).
- d) Repeatability study was performed by repeating the assay on 3 different days with standard samples. Within-assay repeatability was calculated by using standard curve plots and intra-assay repeatability was calculated by studies performed on two different days using A1A1 and A2A2 milk samples.
- e) Uncertainty of measurement was calculated by combining the uncertainty from automated pipettes, ELISA reader and repeatability. For each measurement, relative standard deviation (RSD) is calculated by dividing the standard deviation to the mean value. The combined standard deviation (RSD<sub>combined</sub>) was calculated by taking the square root of the sum of the squares of all RSD values.

## 3. Results and Discussion

Method validation is an essential part of the process that regulates the introduction of new products into the market (ISO/CASCO, 2018). When implementing the new method, the laboratory has to verify and validate that the method can be used for its intended purpose (FDA ORA, 2020). In this context, a study for method validation was conducted to detect  $\beta$ -casein A1 and A2 proteins in cow's milk by ELISA method. Within the scope of this method validation, a) dynamic range, b) limit of detection (LOD), c) limit of quantification (LOQ), d) repeatability and e) measurement uncertainty parameters were considered (National Institute of Standards and Technology, 1995).

In order to define the highest and lowest measurable concentrations, dynamic ranges of the ELISA methods were calculated. The dynamic range of the methods were determined (FDA ORA, 2020) by using 8 different concentrations of A1 and A2 standards included in the kit content (GeneTel Laboratories LLC, A1 & A2 ELISA Kit Protocols). The method provided a non-linear correlation in the form of quadratic polynomial between the measurement and the amount of the target (Plikaytis et al., 1994). The quadratic polynomial standard graph of the assays were plotted by using the concentration of standards (ppm) against the absorbance values obtained. The results are given in Figure 1. The equations of the standard graphs are given above the plots. The standard graphs were used to calculate the  $\beta$ -casein protein concentrations of the non-standard milk samples.

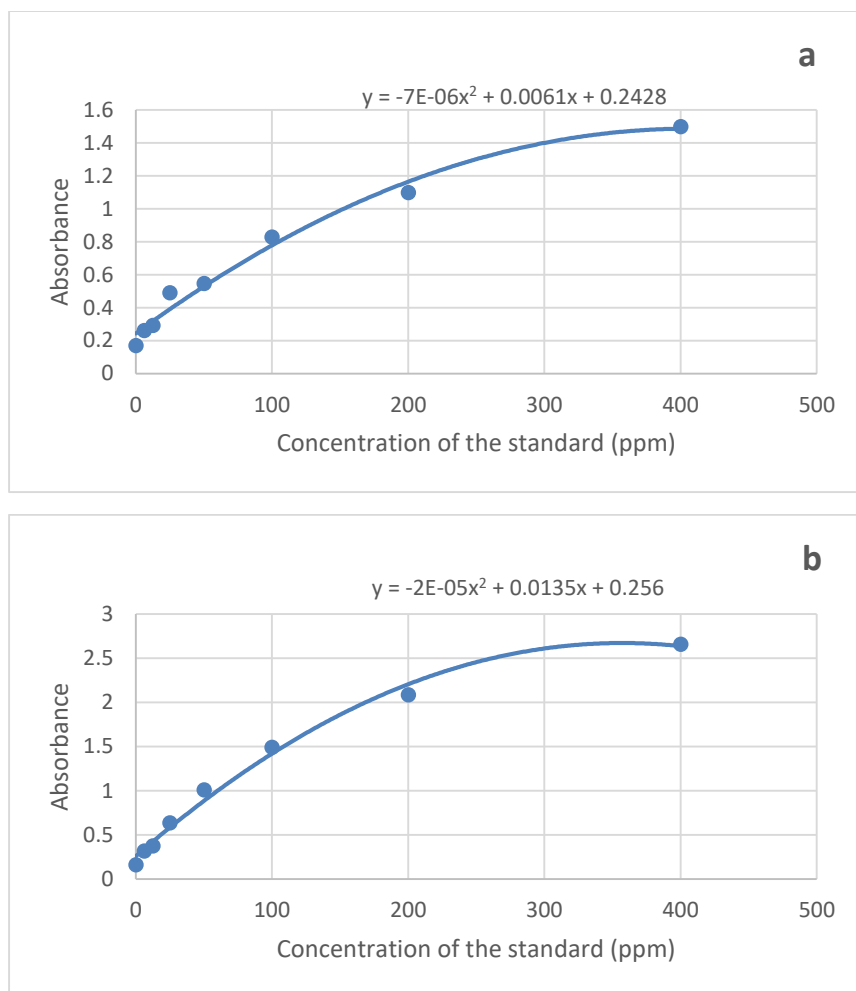


Figure 1. Standard graphs obtained for the ELISA methods of a)  $\beta$ -casein A1 and b)  $\beta$ -casein A2 for the dynamic range determination.

LOD was calculated based on the standard deviation of the blank sample which is the lowest concentration distinguishable (FDA ORA, 2020). LOD was calculated as the mean of the sample +  $3 \times$  (standard deviation). This calculation indicates the presence of the analyte, but does not allow for quantitative measurement. In order to show that there was no cross-reaction, as the sample without  $\beta$ -casein A1, A2A2 milk and as the sample without  $\beta$ -casein A2, A1A1 milk was used in 10 independent studies, and the mean and standard deviation of the measurements were calculated. The results are given in Table 1.

From the mean absorbance values measured, the LOD of the A1 test was calculated as  $0.147 + 3 \times 0.0172 = 0.198$ , the LOD of the A2 test was calculated as  $0.177 + 3 \times 0.024 = 0.250$ . By using the equations of the standard graphs, the corresponding concentration for an absorbance of 0.198 is 1.8 ppm, and an 0.250 is 0.8 ppm. Therefore, the detection limits of the methods were determined as 1.8 ppm for the A1 assay and 0.8 ppm for the A2 assay.

Table 1  
Determination of LOD

Sample no	Absorbances for A2A2 milk samples	Absorbances for A1A1 milk samples
1	0.123	0.152
2	0.138	0.159
3	0.158	0.169
4	0.172	0.155
5	0.148	0.148
6	0.162	0.196
7	0.124	0.207
8	0.153	0.215
9	0.130	0.194
10	0.160	0.173
mean	0.147	0.177
Standard deviation	0.0172	0.024

LOQ is the lowest concentration at which the analytical method operates with acceptable precision and repeatability (FDA ORA, 2020). According to the calculation made using the results shown in Table 1, the detection limit for the A1 assay was  $0.147 + 10 \times 0.0172 = 0.318$ , and the detection limit for the A2 assay was  $0.177 + 10 \times 0.024 = 0.421$ . From the equation of the standard graph, an absorbance of 0.318 corresponds to 2.3 ppm, and an absorbance of 0.421 corresponds to 4.0 ppm. Therefore, the LOQ of the methods were determined as 2.3 ppm for the A1 assay and 4.0 ppm for the A2 assay.

Due to the fact that the standard graphs of  $\beta$ -casein A1 and A2 ELISA tests are created with a quadratic rather than a linear slope, the absorbance values of standards with lower-concentration are very close to each other and may cause calculation errors (Plikaytis et al., 1994). For this reason, it was anticipated that inconveniences may be encountered in verifying the LOQ as calculated above; and therefore, instead of applying a routinely used LOQ calculation method, 4 different approaches were tested and verified for LOQ determination. The approaches used for LOQ determination were (Taverniers, De Loose, Van Bockstaele, 2004):

- Mean +  $10 \times$ (standard deviation)
- $3 \times$ LOD
- $10 \times$ LOD
- $1.5 \times$  the lowest calibration standard (150% of the target level for the analyte)

For each LOQ determination approach above, the calculated LOQ values for the A1 test were:

- 2.3 ppm
- 5.4 ppm
- 18 ppm
- 9.4 ppm

for the A2 test were:

- a. 4.0 ppm
- b. 2.4 ppm
- c. 8 ppm
- d. 9.4 ppm

The prepared four different LOQ samples were attempted to be detected with 4 parallel studies by A1 and A2 assays, and among the detectable LOQ values, the smallest value was accepted as the LOQ of the assay (Taverniers, De Loose, Van Bockstaele, 2004). The results are as shown in Table 2.

Among the different LOQ calculation approaches, 10\*LOD (18 ppm) and 3\*LOD (2.4 ppm) approaches for A1 and for A2 test, respectively were verified as the smallest values. The verification with 4 parallel studies was repeated by performing 10 parallel studies for the selected approach, and the verifiable LOQ value was found to be 17.10 ppm for the A1 test and 2.4 ppm for the A2 test. Therefore, the LOQ value of the methods were accepted as 17 ppm for the A1 test and 2.4 ppm for the A2 test.

Table 2

Results of LOQ verification with 4 different approaches. Each sample was run in 4 parallels. The concentrations were calculated from absorbance values by using the standard graph equation. The concentrations that cannot be calculated from the equation as a positive value are indicated as "< 6.25".

LOQ calculation method	A1 test			A2 test		
	Expected concentration	Observed absorbance (mean)	Observed concentration	Expected concentration	Observed Absorbance (mean)	Observed concentration
Mean + 10*SD	2.3 ppm	0.224	14.01 ppm	4.0 ppm	0.244	4.46 ppm
3*LOD	5.4 ppm	0.211	< 6.25ppm	2.4 ppm	0.193	2.38 ppm
10*LOD	18 ppm	0.229	17.01 ppm	8 ppm	0.276	6.20 ppm
1,5* the lowest calibration standard	9.4 ppm	0.216	< 6.25ppm	9.4 ppm	0.336	10.32 ppm

LOQ: Limit of Quantification

LOD: Limit of Detection

Repeatability of the assay defines the precision under the same operating conditions over a short period of time. The precision is described by statistical methods such as coefficient of variation or the confidence limits; and, it expresses within-laboratory variations, such as different days, different analysts, and different equipment (FDA ORA, 2020). In this study, for the calculation of repeatability parameter, 8 different concentration of standard samples were tested and the assay was repeated on 3 different days. The average of the coefficients of variation calculated for each standard value, given as percentage, was taken, and the mean variation value for the A1 test was calculated as 6.1%, and the variation value for the A2 test was calculated as 6.9%. Therefore, within-assay repeatability values calculated using standard curve plots were 6.1% for the A1 test and 6.9% for the A2 test. Intra-assay repeatability value was also calculated by studies performed on two different days using A1A1 and A2A2 milk samples. The results were given in Table 3.

The average of the coefficients of variation calculated for each milk sample, given as %, was taken, and the average variation values for the A1 and A2 tests were calculated as 10.3% and 2.9%, respectively. Therefore,

within-assay repeatability values calculated using milk samples were found to be 10.3% for the A1 test and 2.9% for the A2 test.

Table 3

Intra-assay reproducibility of  $\beta$ -casein A1 and A2 protein analyzes by ELISA method with milk samples. A1A1 milk samples were studied with A1 ELISA test, A2A2 milk samples were studied with A2 ELISA test.

	Concentration (mean, mg/mL)	Standard deviation	Variation (%)
A1A1 milk sample -1	65.5	3.1	4.8
A1A1 milk sample -2	47.2	7.5	15.9
A2A2 milk sample -1	1348.75	33.85	2.5
A2A2 milk sample -2	895.73	28.66	3.2

The objective of the validation of an analytical method is to ensure that every subsequent measurement made during routine analysis will be accurate enough to generate the desired robustness that the unknown true value can be approximated with minimum error for the sample's contents (Biswas & Saha, 2015; Ellison & Williams, 2007; EURACHEM/CITAC, 2001; ISO, 1995). This approximation is determined by the confidence level of the assays, which is calculated as uncertainty of measurement (FDA ORA, 2020). In order to calculate the uncertainty of measurement, ELISA method was primarily divided into two steps as "antigen-antibody reaction" and "HRP-substrate reaction" (Biswas & Saha, 2015) since both steps are time sensitive and small changes in volumes at  $\mu\text{L}$  levels thought to affect the result of the assay. For each step, the total uncertainty was calculated, consisting of the uncertainty from the automated pipettes (Table 4); and the combined RSD was calculated by combining these numbers with the uncertainty from the ELISA reader, and the uncertainty from repeatability. For each part, RSD was calculated separately, and  $\text{RSD}_{\text{combined}}$  was calculated by taking the square root of the sum of the squares of all RSD values (Biswas & Saha, 2015).

For the calculation of uncertainty coming from automated pipettes (Blues, Bayliss & Buckley, 2004), the pipettes that were used during the ELISA protocol were taken into account. Therefore, the standard uncertainties given in the calibration certificate of the 10  $\mu\text{L}$ , 100  $\mu\text{L}$  and 1000  $\mu\text{L}$  measuring automated pipettes were checked and noted (Table 4). Relative standard uncertainties were calculated by dividing standard uncertainty over the volume measured by the automated pipette. Then, RSDs for both "antigen-antibody reaction" and "HRP-substrate reaction" steps were calculated by taking the square root of the sum of the squares of relative standard uncertainties for each pipette used (equations 3.1 and 3.2)

Table 4  
Uncertainty of measurement from automated pipettes.

Automated pipettes	Standard uncertainty (from the certificate)	Relative standard uncertainty
10 $\mu\text{L}$	0.03	0.0030
100 $\mu\text{L}$	2.78	0.0278
1000 $\mu\text{L}$	2.78	0.0028

$$RSD_{(\text{antigen-antibody reaction})} = \sqrt{(0.003)^2 + (0.0278)^2 + (0.0278)^2} = 0.028 \quad (3.1)$$

$$RSD_{(\text{HRP-substrate reaction})} = \sqrt{(0.003)^2 + (0.0278)^2 + (0.0278)^2} = 0.028 \quad (3.2)$$

For the uncertainty calculation from the ELISA reader, as manufacturer's declaration, linearity was 0.02, repeatability was 0.05. Therefore, the uncertainty from the device during absorbance reading was calculated as the square root of the sum of the squares of each variable over the number of variables (equation 3.3)

$$RSD_{(\text{device})} = \frac{\sqrt{(0.02)^2 + (0.05)^2}}{\sqrt{2}} = 0.03808 \quad (3.3)$$

After the calculation of the uncertainty coming from “antigen-antibody reaction” step, “HRP-substrate reaction” step and the “device”, RSD for routine analytical uncertainty was calculated by only taking one-time performance of the assay into account (equation 3.4). Then, this number was also combined with the uncertainty coming from the performance of the assay on different days as the repeatability (equation 3.5). RSDs were calculated again by the square root of the sum of the squares of each variable.

$$RSD_{(\text{routine analytical uncertainty})} = \sqrt{RSD_{(\text{antigen-antibody reaction})}^2 + RSD_{(\text{HRP-substrate reaction})}^2 + RSD_{(\text{device})}^2}$$

$$= \sqrt{0.028^2 + 0.028^2 + 0.03808^2} = 0.055 \quad (3.4)$$

Until this stage, the calculations for both A1 and A2 tests were the same. Since the repeatability values of the A1 and A2 tests were different, the calculated value for the  $RSD_{\text{combined}}$  differed for each test.

$$RSD_{\text{combined}} = \sqrt{RSD_{(\text{repeatability})}^2 + RSD_{(\text{routine analytical uncertainty})}^2} \quad (3.5)$$

$$\text{For A1 test } RSD_{\text{combined}} = \sqrt{0.103^2 + 0.055^2} = 0.117 \quad (3.6a)$$

$$\text{For A2 test } \text{RSD}_{\text{combined}} = \sqrt{0.029^2 + 0.055^2} = 0.062 \quad (3.6b)$$

The total measurement uncertainty of the A1 test was found as 11.7% and that of the A2 test was found as 6.2%.

#### 4. Conclusion

There is an increasing consumer demand for A2 milk because of health issues or personal choices as A2 milk has also recently become widespread in many countries. With this demand, industry and governments become responsible for the control of the new product released into the market (Hawkes, 2007; Nestle, 2002; Silver and Bassett, 2008). Therefore, A2 milk and dairy products derived from A2 milk has to be checked for their authenticity. For this reason, food safety and control laboratories all around the world must follow and validate an acceptable assay preferentially in an accredited laboratory. This study will set an example for the quality control tests that should be applied for A2 milk and related dairy products in the market. By using the same test kits and following a similar validation and analysis system, many food control laboratories will be able to check the authenticity of the products declared to be from A2 milk in the market shelves; and therefore, consumers will be prevented from being deceived.

This study introduces a new test to be used for the determination of the authenticity of A2 milk, and the protocol to follow for its validation. The selection of ELISA methodology for this application was intended to make the assay easy to adapt to any food safety and control laboratories, since ELISA reader has been a widespread device and the methodology has been used extensively over the years. The immunological tests are simple, rapid, and requires only a small quantity of samples. Yet, there are substantial limitations to this study, which are mainly because of the discrimination of one amino acid difference between the two  $\beta$ -casein proteins. In the developed kits by the manufacturer, the antibodies used for the detection of A1 or A2  $\beta$ -casein were to detect and differentiate one amino acid difference between the two proteins, which might cause false positive results because of the high similarity between the two proteins. Therefore, the ELISA protocol followed had some drawbacks that were dealt during the validation process with the aforementioned implementations. The drawbacks were the lower-concentrated standards giving absorbance values very close to each other, blank samples giving non-zero absorbances; and hence, the routine LOQ calculation for ELISA did not let the verification of the calculated LOQ value. These drawbacks were overcome by plotting a non-linear standard graph and the LOQ determination approach mentioned above. With the validation study, the applicability of the method of quantitative determination of  $\beta$ -casein A1 and A2 proteins by ELISA method with real milk samples in an accredited food control laboratory has been demonstrated. The non-linearity of the standard graph of the ELISA kit used distinguishes this method from the ELISA methods that are routinely applied in food control laboratories; and, necessitated the standard curve generation in second-order polynomial form. Similarly, the approach applied in LOQ determination is different from routine ELISA validation protocols. Therefore, this validation study will set an example for many food control laboratories both for the analysis of A1-A2 ELISA tests and other new methods that would require a non-linear standard graph calculation and a discrete LOQ calculation approach.

Validated ELISA method was well suited for screening and quantification of  $\beta$ -casein A1 and A2 proteins in milk. The introduced methods can reliably detect  $\beta$ -casein A1 and A2 proteins quantitatively. Yet, for the authentication of A2 milk, the presence of A2  $\beta$ -casein and non-presence of A1  $\beta$ -casein are sufficient to test; therefore, qualitative interpretation of the assays are admissible. Nevertheless, it has been foreseen that similar to the problems experienced in determination of GMO contaminations for legal purposes, when A2 milk sector becomes more available, there will be A1-contamination problems that will lead laboratories to test for the amount of A1 protein present in the dairy product. Afterwards, the quantitative application of ELISA is expected to be applied more.

In summary, this validation study on an ELISA for the quantification of  $\beta$ -casein A1 and A2 proteins from milk samples revealed difficulties due to the high similarity between the two proteins to be differentiated. Even though an acceptable validation was achieved, for future studies, an inter-laboratory comparison test should

be arranged. Considering the increase in demand and supply in A2 milk sector all around world, for the authentication of A2 milk dairy in terms of food safety and regulations, food safety and control laboratories may reliably start to use the  $\beta$ -casein A1 and A2 detection assays validated by this study.

### Acknowledgement

The work on this study was carried out in TUBITAK Marmara Research Center, Food Institute, Food Molecular Biology Laboratory. The Laboratory staff Mr Serkan Savsar and Mr Fuat Arslan is thanked for their support and technical assistance. The author would also like to express her gratitude to Uluova Dairy Company, which provided the milk samples used in this study.

### Author Contributions

Mediha Esra Altuntop Yayla: The author of this study conceived and designed the analysis, collected data, performed statistical analysis and wrote the paper.

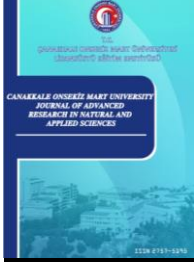
### Conflicts of Interest

The author declares no conflict of interest.

### References

- Anna, M., Salvatore, S., Omar, B., & Eugenio, M. (2016). Detecting-casein variation in bovine milk. *Molecules*, 21(141), 1-7.
- Asledottir, T., Le, T., Petrat-Melin, B., Devold, T., Larsen, L., & Vegarud, G. (2017). Identification of bioactive peptides and quantification of  $\beta$ -casomorphin-7 from bovine  $\beta$ -casein A1, A2 and I after ex vivo gastrointestinal digestion. *International Dairy Journal*, 71, 98-106.
- Biswas, S., & Saha, M.K. (2015). Uncertainty of Measurement for ELISA in a Serological Testing Laboratory. *Immunochemistry & Immunopathology: Open Access*, 1(2), 1-5. DOI: <http://dx.doi.org/10.4172/icoa.1000109>
- Blues, J., Bayliss, D., & Buckley, M. (2004). The calibration and use of piston pipettes. National Physical Laboratory Teddington, Middlesex, United Kingdom.
- Bonfatti, V., Grigoletto, L., Cecchinato, A., Gallo, L., & Carnier, P. (2008). Validation of a new reversed-phase high-performance liquid chromatography method for separation and quantification of bovine milk protein genetic variants. *Journal of Chromatography A*, 1195 (1), 101-106.
- Boro, P., Naha, B., Saikia, D., & Prakash, C. (2016). A1 and A2 Milk & Its Impact On Human Health. *International Journal of Science and Nutrition*, 7(1), 01-05.
- Boutrou, R., Gaudichon, C., Dupont, D., Jardin, J., Airinei, G., Marsset-Baglieri, A., Benamouzig, R., Tomé, D., & Leonil, J. (2013). Sequential release of milk protein-derived bioactive peptides in the jejunum in healthy humans. *American Journal of Clinical Nutrition*, 97, 1314–23.
- Brooke-Taylor, S., Dwyer, K., Woodford, K., & Kost, N. (2017). Systematic Review of the Gastrointestinal Effects of A1 Compared with A2  $\beta$ -Casein. *Advances in Nutrition*, 8(5), 739-748.
- De Noni, I. (2008). Release of beta-casomorphins 5 and 7 during simulated gastro-intestinal digestion of bovine beta-casein variants and milk-based infant formulas. *Food Chemistry*, 110 (4), 897-903.
- De Noni, R., FitzGerald, H., Korhonen, Y., Le Roux, C., Livesey, I., Thorsdottir, D., & Tomé, R. (2009). Scientific report of EFSA prepared by a DATEX working group on the potential health impact of  $\beta$ -casomorphins and related peptides. *EFSA Scientific Reports*, 231, 1–107.
- Duarte-Vázquez, M., García-Ugalde, C., Álvarez, B., Villegas, L., García-Almendárez, B., Rosado, J., & Regalado, C. (2018). Use of urea-polyacrylamide electrophoresis for discrimination of A1 and A2 beta casein variants in raw cow's milk. *Journal of Food Science and Technology*, 55(5), 1942-1947.
- Ellison, S.L.R., & Williams, A. (2007). EURACHEM/CITAC Guide: Use of uncertainty information in compliance assessment. 1st edn. Geneva, Switzerland.
- EURACHEM/CITAC. (2001). EURACHEM/CITAC Guide: Quantifying Uncertainty in Analytical Measurement. 3rd edn. Teddington, England.
- FDA ORA. (2020). Methods, Method Verification and Validation. ORA Laboratory Manual Volume II. Retrieved from <https://www.fda.gov/media/73920/download>.

- GeneTel Laboratories LLC (n.d.). A1 ELISA Kit Protocol. [Http://www.Genetel-Lab.com](http://www.Genetel-Lab.com). Retrieved March 15, 2021, from <http://www.genetel-lab.com/images/A1%20ELISA%20Kit%20Simple%20Test%20SOP.pdf>
- GeneTel Laboratories LLC (n.d.). A2 ELISA Kit Protocol. [Http://www.Genetel-Lab.com](http://www.Genetel-Lab.com). Retrieved March 15, 2021, from <http://www.genetel-lab.com/images/A2%20ELISA%20Kit%20Simple%20Test%20SOP.pdf>
- Givens, I., Aikman, P., Gibson, T., & Brown, R. (2013). Proportions of A1, A2, B and C  $\beta$ -casein protein variants in retail milk in the UK. *Food Chemistry*, 139(1), 549-552.
- Hang, T. (2018). Vinamilk tiên phong với sữa A2. Retrieved from <http://vietnamnet.vn/vn/kinh-doanh/vinamilk-tien-phong-voi-sua-a2-458398.html>
- Hawkes C. (2007). Regulating food marketing to young people worldwide: trends and policy drivers. *American Journal of Public Health*, 97(11), 1962–1973.
- ISO. (1995). Evaluation of measurement data — Guide to the expression of uncertainty in measurement. International Organization for Standardization (ISO), Geneva, Switzerland.
- ISO/CASCO, (2018). General requirements for the competence of testing and calibration laboratories (ISO/IEC 17025:2017). Retrieved from <https://www.iso.org/standard/66912.html>.
- Jain, V., & Gupta K. (2005). Food and Nutritional Analysis: Overview. *Encyclopedia of Analytical Science (Second Edition)*, 202-211.
- Kamiński, S., Cieslińska, A., & Kostyra, E. (2007). Polymorphism of bovine beta-casein and its potential effect on human health. *Journal of Applied Genetics*, 48, 189–98.
- Kudlejova, L., & Risticovic, S. (2012). 9 - Application of Solid-Phase Microextraction in Food and Fragrance Analysis. *Handbook of Solid Phase Microextraction*, 291-334.
- National Institute of Standards and Technology, (1995). Nomenclature in evaluation of analytical methods, including detection and quantification capabilities (IUPAC Recommendations 1995). *Pure and Applied Chemistry*, 67(10), 1699-1723.
- Nestle M. (2002). *Food Politics*. Berkeley and Los Angeles: University of California Press.
- Pal, S., Woodford, K., Kukuljan, S., & Ho, S. (2015). Milk intolerance, beta-casein and lactose. *Nutrients*, 7, 7285–7297.
- Plikaytis, B.D., Holder, P.F., Pais, L.B., Maslanka, S.E., Gheesling, L.L., & Carlone, G.M. (1994). Determination of parallelism and nonparallelism in bioassay dilution curves. *Journal of Clinical Microbiology*, 32(10), 2441-7. DOI: 10.1128/jcm.32.10.2441-2447.1994.
- Silver, L., & Bassett, M.T. (2008). Food safety for the 21st century. *Journal of the American Medical Association*, 300(8), 957–959.
- Sodhi, M., Mukesh, M., Kataria, R., Mishra, B., & Joshii, B. (2012). Milk proteins and human health: A1/A2 milk hypothesis. *Indian Journal of Endocrinology and Metabolism*, 16(5), 856.
- Suchy, F., Brannon, P., Carpenter, T., Fernandez, J., Gilsanz, V., Gould, J., Hall, K., Hui, S.L., Lupton, J., Mennella, J., Miller, N.J., Osganian, S.K., Sellmeyer, D.E., & Wolf, M.A. (2010). NIH consensus development conference statement: Lactose intolerance and health. *NIH Consensus State-of-the-Science Statements*, 27, 1-27.
- Tang, T., Vasas, M., Hatzakis, E., & Spyros, A. (2019). Chapter Five - Magnetic resonance applications in food analysis. *Annual Reports on NMR Spectroscopy*, 98, 239-306.
- Taverniers, I., De Loose, M., & Van Bockstaele, E. (2004). Trends in quality in the analytical laboratory. II. Analytical method validation and quality assurance. *Trends in Analytical Chemistry*, 23(8), 535-552.
- Woodford, K. (2006). A critique of Truswell's A2 milk review. *European Journal of Clinical Nutrition*, 60(3):437.



## Kent Parklarının Değerlendirilmesinde Biyofilik Tasarım Yaklaşımı: Ordu Örneği

Bağlan Özel Karaağaç<sup>1</sup>, Ömer Atabeyoğlu<sup>2\*</sup>

<sup>1,2</sup>Ordu Üniversitesi, Ziraat Fakültesi, Peyzaj Mimarlığı Bölümü, 52000, Ordu, Türkiye

### Makale Tarihiçesi

Gönderim: 24.03.2023

Kabul: 06.06.2023

Yayın: 20.12.2023

### Araştırma Makalesi

**Öz** – Kentler, insanların hayatlarının büyük kısmını geçirdikleri kompleks ve organik oluşumlardır. Ancak, insanların pek çok açıdan yoğun etkileşimde buldukları kentler ve içerdikleri fonksiyonlar zamanla son derece yapay bir karaktere bürünmüştür. Bu durum insanı ait olduğu doğadan uzaklaştırmış ve insanın fiziksel, ruhsal ve sosyal sorunlar yaşamasına yol açmıştır. Bu noktada yapılı çevre ve doğa uyumunu sağlama çabaları biyofilik tasarım girişimlerini doğurmuştur. Bu yaklaşım, yapılı çevre ve yaşam alanlarına doğal malzeme ve materyallerin getirilmesi ile insanın doğal çevreyle yeniden bağlantı kurmasına olanak tanır. Yapılı çevrelerde insan-doğa ilişkisinin güçlendirilmesi ve sürekliliğinin sağlanması önemlidir. Yapılı her çevre ve çevre parçasının doğa ile mevcut ilişkisinin çok yönlü olarak araştırılması eksiklerin belirlenmesi için önemlidir. Böylece çevre tasarımına doğru yaklaşımların optimum ölçüde dahil edilmesi sağlanabilir. Bu kapsamda çalışma, Ordu ili sahil parklarındaki fonksiyon alanlarının biyofilik tasarım ilkeleri doğrultusunda tam bir analizini sağlamaktadır. Çalışmanın amacı, kentlinin yoğun bir şekilde kullandığı kent parklarının kentliye ne düzeyde ve hangi özellikler ile doğa deneyimi sunduğunu belirlemektir. Böylece, kentlinin yapılaşmış ve yapaylaşmış kentsel ortam içerisinde aldığı hizmetin olumlu etkisini artırmaya yönelik geliştirme hedefleri de belirlenmiş olacaktır. Çalışma, 14 biyofilik tasarım kriteri doğrultusunda 4 sahil parkında ve 9 fonksiyon sınıfı özelinde yürütülmüştür. Buna göre; incelenen parklar biyofilik tasarım kriterlerini önemli ölçüde yerine getirmektedir. Çalışma sonucunda parkların geliştirilmesi ile ilgili öneriler de sunulmuştur.

**Anahtar Kelimeler** – Biyofili, biyofilik şehircilik, biyofilik tasarım, kent parkları, kentsel yeşil alanlar

## Biophilic Design Approach in Evaluation of Urban Parks: The Case of Ordu

<sup>1</sup>Department of Landscape Architecture, Faculty of Agriculture, Ordu University, 52000, Ordu, Türkiye

### Article History

Received: 24.03.2023

Accepted: 06.06.2023

Published: 20.12.2023

### Research Article

**Abstract** – Cities are complex and organic formations where people spend most of their lives. However, the cities and the functions they contain, in which people interact intensively in many respects, have taken on an extremely artificial character over time. This situation has distanced people from the nature to which they belong and has led to physical, mental and social problems. At this point, efforts to achieve harmony between the built environment and nature have led to biophilic design initiatives. It is important to investigate the existing relationship of each built environment and environmental part with nature in a multi-dimensional way to determine the deficiencies. Thus, optimum inclusion of the right approaches in environmental design can be ensured. In this context, the study provides a complete analysis of the functional areas in the coastal parks of Ordu province in line with the biophilic design principles. The aim of the study is to determine at what level and with what features the urban parks, which are used extensively by the citizens, offer nature experience. Thus, development targets will be determined to increase the positive effect of the service received by the citizens in the structured and artificial urban environment. The study was carried out in 4 coastal parks and 9 function classes in line with 14 biophilic design criteria. According to this; The investigated parks fulfill the biophilic design criteria to a great extent. As a result of the study, suggestions for the development of parks were also presented.

**Keywords** – Biophilia, biophilic design, biophilic urbanism, urban green spaces, urban parks

<sup>1</sup> baglanozel@hotmail.com

<sup>2</sup> omeratabeyoglu@odu.edu.tr

\*Sorumlu Yazar

## 1. Giriş

Sanayi Devrimi'nin öncesi ve sonrasında, insanların büyük çoğunluğu, hayatlarının çoğunu doğada geçirmişlerdir. Dolayısıyla, insan, doğa ile sürekli olarak etkileşim halinde olmuştur. Sosyal psikolog Erich Fromm, 1964 tarihli "The Heart of Man" adlı yayınında "biyofili" terimini ortaya atmıştır. Biyolog Edward O. Wilson daha sonra 1984'te ve 1993'te "Biyofili Hipotezi" ile kendi adını taşıyan bir başlıkla "biophilia" terimini popüler hale getirmiştir. Kellert ve Wilson'ın Biofili Hipotezini yayınlamasından bu yana geçen yirmi yılda, biyofiliyi destekleyen kanıtlar önemli ölçüde genişlemiştir (Ryan ve Browning, 2020). Biyofili, insanlığın doğayla doğuştan gelen biyolojik bağlantısıdır. Küresel kentleşmenin hızla artan sürecinde, insan ve doğa arasındaki bağın kopmaması adına, biyofilik tasarım kavramına ilginin arttığı görülmektedir. Biyofilik tasarım temeli, insanın yaşamını sürdürdüğü yapıyı çevreye ve yaşam alanlarına, doğal malzeme ve materyallerin getirilmesi, sürdürülmesi ve insan-doğa ilişkisinin güçlendirilmesi ilkesine dayanmaktadır (Yurtgün, 2020, Aykal & Özil, 2021). Biyofilik tasarım insan ve doğa arasındaki bağı tekrar kurmayı amaçlar. Bununla birlikte mesleki stres, bilişsel performans ve zihinsel sağlık gibi çağdaş kaygılar karşısında doğal nitelikleri değerlendirerek stresi azaltmak, yaratıcılığı ve net düşünmeyi teşvik etmek, fiziksel ve psikolojik sağlığı iyileştirmek ve iyileşmeyi hızlandırmak gibi faydaları vardır (Bolten ve Barbiero, 2020, Kellert 2005, Kellert ve Finnegan 2011, Browning vd., 2014). Biyofilik tasarım anlayışı, modern dünyada biyolojik bir organizma olarak insanlar için faydalı bir yaşama ortamı oluşturmayı hedefler (Kellert ve Calabrese, 2015).

Tarihi yapılardaki ve mekânlardaki doğal temalara, en eski insan yapılarında dahi rastlanmaktadır. Neolitik Göbekli Tepe'ye özgü stilize hayvanlar, Mısır Sfenksi, Yunan tapınaklarını süsleyen akantus yaprakları ve Rokoko tasarımının narin yapraklı tasarımı önemli örneklerdir. İspanya'da Elhamra Sarayı bahçesindeki avlular, Antik Çin'deki porselen balık kâseleri, Teotihuacan'daki (antik Mexico City) Kuşhane, Japon bonsai sanatı, Mısır soylularının evlerindeki papirüs havuzları, Ortaçağ Almanya'sındaki yazlık bahçeler ve Babil'in Asma Bahçeleri ise biyofilinın klasikleşmiş örneklerindendir (Ryan ve Browning, 2020).

Le Corbusier'in Radiant City'sinde, kent sakinleri için doğayla bağlantı sağlamaya çalışarak, çimenler ve ağaçlarla çevrili bir parka kuleler yerleştirmiştir. Manzarayı, çelik ve cam binalarla doldurmuş ve bu, özellikle binalar yükseldikçe zaman içinde insanları doğadan giderek daha fazla koparmıştır.

19. yüzyılda kentsel nüfus artışıyla birlikte doğal kaynakların tüketimi hızlanmıştır. Bu durum çevre üzerinde büyük bir baskı yaratmış ve kentlerdeki sağlık sorunları artış göstermiştir. Dolayısıyla insan sağlığını iyileştirmek, kentsel yaşamın stresini azaltmak ve yaşanabilir kentler için nitelikli kentsel yeşil alanlara ve kent parklarına olan ihtiyaç da artmıştır. Bu kapsamda bozulmuş kent dokusunun yenilenmesine ve gelişmesine büyük ölçüde katkılar ve fırsatlar sunan kent parkları, rekreasyonel, fizyolojik, sosyolojik, estetik ve fonksiyonel açılarından da kentsel nefes alma noktalarıdır. Dahası kent ve kentli ile güçlü bağlar kuran peyzaj alan kullanımlarıdır.

Son yıllarda insanlık doğayı keşfetmek, hissetmek ve doğaya dönmek için karşı koyulamaz bir arzuya kapılmıştır (Zhong, vd. 2021). 21. yüzyılın başında biyofili kavramı mimari alanda geliştirilip, uyarlanmış ve insanların bina ortamında doğal çevre ile etkileşim ihtiyaçlarının duygusal yönüne dikkat çekmiştir. Biyofilik şehircilik, kentsel açık yeşil alan planlamaları ile toplum sağlığını iyileştirici etkiye sahiptir (Littke, 2016).

Biyofilik tasarımın önemli bir dolaylı faydası, tasarım uygulamalarına rehberlik etmek ve sonrasında etkinliği değerlendirmek için nitel ve nicel bilim temelli ölçütlerin belirlenmesine yapılan vurgudur (Ryan ve Browning, 2020).

Kellert (2005)'e göre biyofilik tasarımın iki ana boyutu vardır. İlki, doğaya doğrudan, dolaylı veya sembolik olarak temastır. Bu yapıyı mekânın biçimlerinde ve işlevlerinde doğanın kalıplarının ve süreçlerinin kullanılmasıyla sağlanır. İkinci boyut ise, yer temellidir ve yapıyı çevre veya peyzaj ile belirli bir bölgenin kültürü arasındaki ilişkiyi tanımlar (Totaforti, 2020).

Kellert ve Calabrese (2015), biyofilik tasarımın etkili bir şekilde uygulanması için aşağıdakileri içeren temel koşulları belirlemiştir: Biyofilik tasarım,

- doğayla tekrar tekrar ve sürekli bir ilişki gerektirir.

- evrimsel süreç içerisinde, insanların zindeliğini, esenliğini ve de sağlığını, geliştiren doğal dünyaya ve insan adaptasyonlarına odaklanır.
- belirli alanlara ve ortamlara olan duygusal bağlılığı motive eder.
- insan ve doğa arasında, genişletilmiş sorumluluk ve ilişki duygusuyla, olumlu etkileşimleri teşvik eder.

Peyzaj Mimarlığı mesleği, diğer meslek disiplinleri içerisinde biyofilik tasarım yaklaşımını en fazla benimseyen tasarım anlayışına sahip olmasına rağmen, bu alanda yapılan çalışmalar oldukça sınırlıdır. Biyofilik tasarımın kentsel rekreasyon alanlarındaki uygulamalarını temel alan çalışma gözlemlenebilir ilkeler aracılığıyla mekan-doğa uyumunun tespit ve kontrol edilebilirliğine vurgu yapmayı öncelemektedir. Çalışma kapsamında, ‘Ordu kenti kıyı parklarının’ fonksiyonlarına göre sınıflandırılması ile her bir fonksiyon için; ‘Biyofilik Tasarım Kriterleri’ne uygunluğu araştırılmış; biyofilik tasarımın kentsel ortamlardaki faydalarını irdelemek ve geliştirmek amaçlanmıştır.

## 2. Materyal ve Yöntem

### 2.1. Materyal

Çalışma alanı olarak; Ordu kenti kıyı şeridi üzerinde konumlanan kıyı parkları seçilmiştir. Kent merkezi boyunca devam eden kıyı parkları dört bölümden oluşmaktadır. Bunlar batıdan doğuya doğru olmak üzere Rüşumat Parkı, Atatürk Parkı, Tayfun Gürsoy Parkı ile Akyazı Plajı ve Kıyı Parkı’dır (Şekil 1). Ordu kıyı parkları kent merkezinde olup, toplam uzunluğu 4970 m’dir. Çalışma alanı kapsamında bulunan Ordu kenti kıyı parkları, özgün ve modern bir tasarım anlayışına sahip olmasının yanı sıra içerisinde rekreasyonel aktiviteler, donatı elemanları ve kentsel yeşil alan kullanımları bakımından kent parkı niteliği taşımaktadır (Karaağaç, 2019). Ordu kent parkları, bölgenin diğer önemli cazibe merkezlerine yakın olması ve kent ile ilişkisinin rahatça kurulması nedeniyle bölge halkı tarafından sıklıkla tercih edilir. Rüşumat Parkı, Atatürk Parkı, Tayfun Gürsoy Parkı ve Akyazı Kıyı Parkı toplam alanı 196.876 m<sup>2</sup> olup, toplam uzunluğu ise 6471 m’dir.



Şekil 1. Çalışma alanı konumu.

Rüşumat Parkı: Kentin batı tarafında, Taşbaşı Mahallesi, Düz Mahalle ve Şarkiye Mahallesi boyunca Atatürk Parkı'na kadar uzanmaktadır. Kent parkının alanı 30.226 m<sup>2</sup> olup, 1255 m uzunluğundadır. Rüşumat Kent Parkı'nda, bisiklet yolu, yürüyüş yolları, kordon boyu gezi alanı, oturma alanları, sergi alanı, iskele ve çocuk oyun alanı gibi pek çok işlev bulunmaktadır.

Atatürk Parkı: Şarkiye Mahallesi'nde bulunmakta olup, 53000m<sup>2</sup> alana sahiptir. Bu alanın 12100m<sup>2</sup>'sini yeşil alanlar oluşturmaktadır. Park içerisinde oturma alanları, yöresel ürün satış alanları, skate park ve ters ev gibi

eğlence alanları, Atatürk Anıtı ve tören alanı, yürüyüş parkurları ve bisiklet yolları bulunmaktadır. Alanda ayrıca; 650 araçlık iki adet otopark, teleferik istasyonu ve kafeler de yer almaktadır.

Tayfun Gürsoy Parkı: Bahçelievler Mahallesi kıyı şeridi boyunca uzanmaktadır. Kent parkının toplam alanı 85000 m<sup>2</sup> ve uzunluğu 1290 m'dir. Parkta bisiklet yolu, koşu yolu, fitness alanları, çocuk oyun alanları, kafeler, otopark alanı, fuar alanı, spor sahaları, anıt alanları, plaj kullanımları ve benzeri fonksiyonlar yer almaktadır.

Akyazı Kıyı Plaj ve Park Alanı: Kentin doğu tarafında Akyazı Mahallesi boyunca kıyı şeridinde uzanmaktadır. Kent parkı, Tayfun Gürsoy Parkı'nın devamını oluşturmakta olup, Bahçelievler ve Akyazı Mahallelerini bağlayan Gazi Köprüsü'nden başlayarak, Durugöl Mahallesi'ne kadar devam eder. Kent parkının toplam alanı 28650 m<sup>2</sup> olup, 2475 m uzunluğundadır. Parkta; piknik alanları, yürüyüş parkurları, koşu ve bisiklet yolu, oturma alanları, su parkı ve survivor park gibi eğlence alanları, plaj, büfeler ve kafe gibi pek çok fonksiyon bulunmaktadır (Karaağaç, 2019).

## **2.2. Yöntem**

Çalışmada, Browning ve ark. (2014)'ının belirlemiş olduğu, 14 "Biyofilik Tasarım Kriteri" temel alınmıştır (Tablo 1). 14 kriter yerinde nitel olarak değerlendirilerek, gözlemlenmiştir. Biyofilik Tasarım Kriterleri yorum gerektirmeyen, somut olgular üzerine kurgulanmış olduğundan kriterin varlığının kanıtlarına mekanın sahip olması yeterli olmaktadır. Kriterlerin alandaki varlığına ilişkin tespitler alan ziyaretleri ve uzman gözlemleri ile gerçekleştirilmiştir.

Çalışma alanı, fonksiyonel alan kullanımları bakımından 9 sınıfa ayrılmış ve fonksiyon bazlı olarak parametreler incelenmiştir. Çalışma alanındaki fonksiyonel alan kullanımları; çocuk oyun alanları, oturma alanları, gezi alanları, açık yeşil alanlar, spor alanları, alışveriş alanları, eğlence alanları, ulaşım ve otoparklar, tören ve anıt alanlarıdır. Her bir fonksiyonel alan kullanımı çalışma alanını oluşturan dört rekreasyonel alan bazında ayrı ayrı değerlendirilmiştir. Çalışmayı oluşturan dört alan birbirinin devamı ve tamamlayıcısı olduklarından, çalışma bu dört alana değil fonksiyonlar üzerine kurgulanmıştır. Böylece, Ordu kenti tüm kıyı rekreasyon alanlarının 9 fonksiyon alanı özelindeki mevcut biyofilik potansiyeli ortaya koyulmuştur. Her bir parkta aynı fonksiyonlardan mevcut olup, bunlar birbirlerinin devamı ve tamamlayıcısı niteliktedir. Bu nedenle her bir park ve her bir parktaki her bir fonksiyonun birlikte oluşturdukları etki daha anlamlıdır.

Bu değerlendirme yapılırken; her bir fonksiyon alanı için biyofilik tasarım kriterlerinin varlığı değerlendirilmiştir. Objektif olmak bakımından kriterler; var, yok ve kısmen olmak üzere üç net kategoride değerlendirilmiştir. Bu kapsamda; bir kriterin mevcut olması durumunda 2 puan, kısmen var olması durumunda ise 1 puan verilmiştir. Kriterin bulunmaması durumunda ise puan verilmemiştir. Sadece "risk/tehlike" kriteri için ters bir ilişki mevcuttur. Bu kriter için 2 puan fonksiyon alanında risk/tehlike bulunmaması durumu için verilmiş, bulunması durumu için ise puan verilmemiştir. Kısmen risk/tehlike bulunması durumu için ise 1 puan verilmiştir. 14 kriterin toplam puanı o fonksiyon alanının kıyı rekreasyon alanları bütünündeki biyofilik şartlara uygunluğunu ortaya koymaktadır. Bu durumda tüm kriterlerin sağlanması durumunda alınabilecek en yüksek puan 28'dir. Eksik kriterler, hangi fonksiyon alanlarının hangi özellikçe geliştirilmesi gerektiğini gösterirken, puan durumu ise bu eksikliğin ne düzeyde olduğunu ortaya koymaktadır.

Tablo 1

## Biyofilik tasarım parametreleri

<b>Mekândaki Doğa</b>	1.Doğa ile görsel bağlantı	Doğanın unsurlarına, canlı sistemlere ve doğal süreçlere bir bakış
	2. Doğa ile görsel olmayan bağlantı	Doğaya, canlı sistemlere veya doğal süreçlere kasıtlı ve olumlu bir gönderme oluşturan işitsel, dokunsal, koku alma veya tat alma uyaranları
	3.Ritmik olmayan duyuusal uyaranlar	İstatistiksel olarak analiz edilebilen ancak kesin olarak tahmin edilemeyen doğa ile stokastik ve geçici bağlantılar
	4.Termal ve hava akışı değişkenliği	Doğal ortamları taklit eden hava sıcaklığı, bağıl nem, ciltteki hava akışı ve yüzey sıcaklıklarındaki küçük değişiklikler
	5.Su varlığı	Suyu görerek, duyararak veya dokunarak bir yerin deneyimini artıran bir durum
	6.Dinamik ve dağınmık ışık	Doğada meydana gelen koşulları yaratmak için zamanla değişen, değişen ışık ve gölge yoğunluklarından yararlanma
	7.Doğal sistemlerle bağlantı	Doğal süreçlerin, özellikle mevsimselliğin farkındalığı ve sağlıklı bir ekosistemin karakteristiği olan zamansal değişiklikler
<b>Doğal Analogiler</b>	8.Biyomorfik formlar ve desenler	Konturlu, desenli, dokuya sembolik göndermeler, doğada devam eden türemiş veya sayısal düzenlemeler
	9.Doğa ile maddi bağlantı	Belirgin bir yer duygusu yaratmak için minimum işlemle yerel ekolojiyi veya jeolojiyi yansıtan doğadan malzeme ve öğeler
	10.Karmaşıklık ve düzen	Doğada karşılaşılanlara benzer bir uzamsal hiyerarşiye uyan zengin duyuusal bilgi
<b>Mekânın Doğası</b>	11.Olasılık/Manzara	Gözetleme ve planlama için bir mesafeden engelsiz bir görüş
	12.Sığınak	Çevresel koşullardan veya ana faaliyet akışından, kişinin arkadan ve yukarıdan korunduğu bir sığınak yeri
	13.Gizem	Kişiyi çevrenin daha derinlerine gitmeye teşvik eden kısmen gizlenmiş görüşler veya diğer duyuusal araçlar yoluyla elde edilen daha fazla bilgi vaadi
	14.Risk/Tehlike	Güvenilir bir güvenlik önlemi ile birlikte tanımlanabilir bir tehdit

### 3. Bulgular

İncelenen kent parkları, içerdiği fonksiyon alanları ile rekreasyonel anlamda Ordu kentinde önemli görevler üstlenmiştir. Parklar, kent insanının doğayla buluşması ve bağ kurması açısından da büyük paya sahiptir. Ordu kenti kent parkları başlıca fonksiyonlar bazında kategorilere ayrılarak değerlendirmeye alınmıştır.

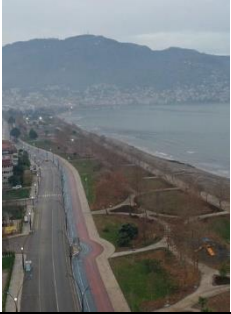
#### 3.1. Mekândaki Doğa

Bu kapsamda çalışma alanı değerlendirildiğinde, mekandaki doğa parametreleri bazında çok yüksek varlığa sahip olduğu görülmektedir. Zira çalışma alanının tamamı tüm fonksiyonları ile birlikte doğanın sunduklarından büyük ölçüde istifade etmektedir. Çalışma alanının kıyı boyunca uzanması nedeniyle deniz manzarasına doğrudan hakimdir. Bununla birlikte kentin bir bumerang andırır şekilde kavisli bir kıyı çizgisine yerleşmiş olması her nereden bakılırsa bakılırsın karşı kıyıların ve gerisindeki dağ ve tepelerin görüş alanına girmesini sağlamaktadır. Böylece doğal formlar ve barındırdıkları doğal öğeler, çalışma alanından hakim olunan görsel materyalin bir parçasına dönüşebilmektedir. Ayrıca, çalışma alanı içerisindeki yoğun plantasyon ve bu plantasyonda yaşayan hayvanlar doğa seyrini zenginleştirmektedir. Bununla birlikte çalışma alanı, doğa ile görsel olmayan bağlantılarca da zengindir. Yağışlı sürenin uzun olduğu kentte yağmur sonrası toprak kokusu, bir biri sıra açan çiçekli bitkilerin kokuları, yoğun plantasyon nedeniyle buralarda yaşayan kuşların sesleri, insanların ilgisine alışmış sokak canlılarının samimi iletişimi, dalga sesleri gibi pek çok olgu kentsel alan olmasına rağmen çalışma alanında yoğun şekilde istifade edilebilen duyuusal zenginliklerdir. Aynı zamanda yüksek nem, deniz ve kenti çevreleyen topoğrafya çalışma alanı üzerinde anlık veya uzun süreli hava akış yönü ve şiddeti ile termaller üzerinde etkilidir. Bu da çalışma alanını çevreleyen plantasyondan kaynaklı taze kokular ile çevreye hakim doğa seslerinin yönleri ve şiddeti üzerine etki etmekte, çeşitliliği ve zenginliği desteklemektedir. Çalışma alanı doğal kaynaklar bakımında zengin olmakla birlikte su varlığı bu çeşitlilikte öne çıkmaktadır. Çalışma alanına hakim olan deniz ile birlikte akarsular ve yapay su öğeleri görüntüleri, hissiyatları, yansıma ve ışıltılara etkileri ve temas ile gerek eğlence, gerek dinlenme, gerekse spor gibi aktivitelere doğanın dahlini mümkün kılmaktadır. Çalışma alanı doğrudan güneş ışığı alan şartlarda

bulunmakla birlikte, yer yer yoğun plantasyon etkisi doğal ışıkta efektler ve oyunlar da oluşturmaktadır. Ayrıca su ve deniz gibi yansıma yüzeyleri ışığın dağılımı ve alternatif etkilerde rol almaktadır. Alan içerisinde yapılan suni aydınlatma, geceleri doğrudan ve dolaylı yolla doğal öğelerin vurgulanması, görünür kılınması ve etkisinin güçlendirilmesini sağlayıcı tarzdadır. Özellikle plantasyon mevsimsel değişimlerin gözlemlenmesinde son derece etkilidir. Herdem yeşil ve yaprak döken, çiçekli, çiçeksiz ve meyveli bitkiler zamansal değişimleri fark edilir kılacak yoğunluk ve harmonidedir.

Tablo 2

Mekandaki doğa parametreleri

Mekândaki Doğa	1. Doğa ile görsel bağlantı 2. Doğa ile görsel olmayan bağlantı 3. Ritmik olmayan duyuşsal uyarılar 4. Termal ve hava akışı değişkenliği	5. Su varlığı 6. Dinamik ve dağınmık ışık 7. Doğal sistemlerle bağlantı		
				

### 3.2. Doğal Analojiler

Doğal analogiler, ister iç ister dış mekan mimarisinde olsun son derece etkili ve etkileyici yaşam alanları oluşturmada atlanmaması gerekenlerin başında gelir. Doğanın sıcaklığı, samimiyeti, zarafeti, duyarlılığı, hissettirdikleri ve duyumsanabilirliği yaşam alanını canlı odaklı, sağlıklı ve yaşanabilir kılmakta etkilidir. Doğa doğrudan ve dolaylı yollarla tasarıma ve yaşam alanına kazandırılırken; imgesel ve simgesel boyutunun etkisi de göz ardı edilmemelidir. Böylece materyalden forma, dokudan çağrışıma kadar pek çok şey hayal gücü ve teknik imkanlar doğrultusunda mekanın biyofilik tasarım karakterini güçlendirir.

Çalışma alanı doğal analogiler bakımından yüksek yeterliliğe sahip olmakla birlikte tam anlamıyla gereklilikleri yerine getirdiği söylenemez. Bununla birlikte; çalışma alanında dalgalara benzeyen oturma ve oyun birimleri, çeşitli canlıların kendileri ve ürettikleri materyallere benzetilerek kullanılmış oyun üniteleri, plastik objeler, bitki ve çiçek form ve desenlerine atıflar, doğal materyaller ve doğal dokulu kaplamalar ile doğayı taklit eden topoğrafik formlar çokça değerlendirilmiştir. Bu kullanımlar alana hem hareketlilik ve zenginlik katmış hem de kentin imajına vurgular yapmıştır. Böylece kent, kendi doğal ve kültürel zenginliklerini de gösterme fırsatı elde etmiştir. Ayrıca, bitkisel kullanımlar yer yer yetersizliklere sahip olsa da doğayı taklit etmeye çalışan tasarım doğanın izlenimleri ve zenginliklerini alana kazandırmakta etkilidir.

Tablo 3  
Doğal Analogiler parametreleri

Doğal Analogiler	8. Biyomorfik formlar ve desenler 9. Doğa ile maddi bağlantı 10. Karmaşıklık ve düzen
    	

### 3.3. Mekânın Doğası

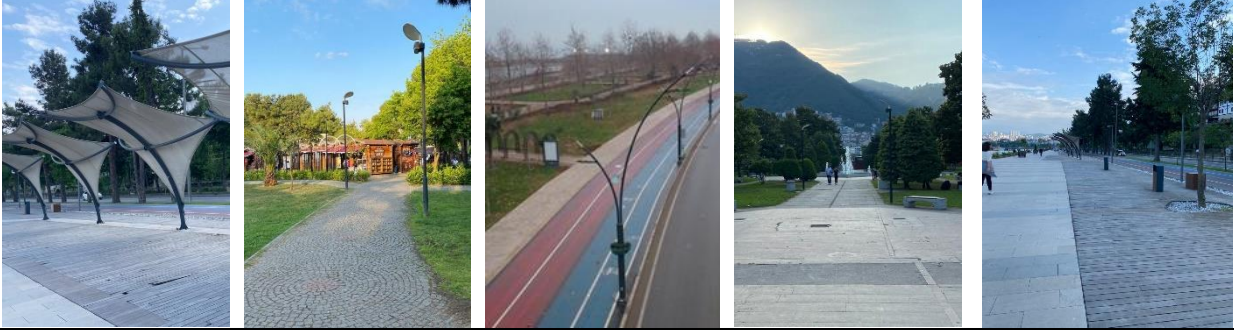
Doğa içinde bulunan canlılar için her sistemi ve içerdiği her niteliği ile eşsiz bir barınaktır. Böylece, doğa canlılara güvenli ve sağlıklı bir barınak sağlarken, barındırdığı canlılardan da sistemin işleyişine katkı elde eder. Bu nitelikli iş birliği insanların yaşam alanlarına kazandırıldığı ölçüde insan yapımı mekanlar işlev, anlam ve değerle yüklenir. İnsan, varlığı ve içgüdüleri gereği doğanın bir parçasıdır ve hiçbir şart altında doğadan kopmaz veya kopmayı tercih etmez. Dahası doğayı ve izlerini yaşam alanına çekmeyi, mekanı doğa ile zenginleştirmeyi, tamamlamayı ve bütünleştirmeyi arzu eder. Böylece kendisi de tamamlanır. Bu anlamda mekanın doğası kullanıcılara geniş perspektifler sunarken, mekan oluşturmaları, mekânsal zenginlikler oluşturmaları, güvenlik risklerini ise bertaraf etmelidir.

Çalışma alanı, deniz kıyısında olması ve kent parkı niteliğinde bulunması nedeniyle son derece geniş bir perspektifte ve uzun mesafeli görüş ve seyir alanına sahiptir. Böylece hem çevrenin hem de mekanın algılanabilirliği artırmakla birlikte, doğal etkilerin de alanda farkındalığı yükselmektedir. Bu genişlik ve ferah perspektif kente hakim doğal form ve dokuların çalışma alanının da parçasına dönüşmesini sağlamıştır, ki bu da biyofilik tasarım açısından istenilen bir durumdur. Bununla birlikte alanda pek çok yerde gerek yapısal üniteler, gerekse bitkisel doku ile korunaklı ve kullanıcıyı yapay çevresel etkenlerin olumsuzluklarından ayıran veya baskısını indirgeyen tasarım detayları mevcuttur. Bu, kullanıcının doğa hissiyatı ve mekanın doğası ile özdeşleşmesine fırsat oluşturur. Çalışma alanı kent içi kamusal bir rekreasyon alanı olduğundan güvenlik ve algılanabilirlik nedeniyle tam anlamı ile kapatıcılık, gizlilik, perdeleme gibi kullanım alanları ve tasarım detaylarına sahip değildir. Ancak yer yer topoğrafik değişimler, plantasyonda yer alan büyük ağaçlar ve çalı grupları, oturma alanları ve teraslardaki örtü elemanları, yarı kapalı oturma birimleri, diğer rekreatif nesnelere alandaki merak duygusunu artıran biyofilik öğelerdir. Alan içerisinde tahdit oluşturabilecek haller de söz konusudur. Alanın deniz kıyısı boyunca seyredir oluşu, denizden kaynaklı doğal tehditleri gündeme getirmektedir. Bunun dışında doğa temelli olmayan ancak, biyofilik özelliklerle bertaraf edilme imkanına sahip olmakla birlikte alana paralel ilerleyen araç yolu bir tehdit unsuru olarak değerlendirilebilir. Çalışma alanı içerisinde muhtelif yerlerde bulunan otoparklar, eğlence alanlarındaki oyun elemanları da zaman zaman ve belirli durumlar altında tehlike içermektedir.

Tablo 4

## Mekanın doğası parametreleri

<b>Mekânın</b>	<b>11. Olasılık/Manzara</b>
<b>Doğası</b>	<b>12. Sığınak</b>
	<b>13. Gizem</b>
	<b>14. Risk/Tehlike</b>



## 3.4. Fonksiyonel Değerlendirme

## 3.4.1. Çocuk Oyun Alanları

Çocuk oyun alanlarının çevresinde bulunan yoğun yeşil alan oluşumları nedeni ile kullanıcıların doğa ile görsel bağlantı kurmasına sebep olan çok sayıda doğal etken mevcuttur. Mevsimsel değişikliğiyle farklı manzaralar sunan bitkisel varlık, alanın hakim olduğu deniz ve tepe manzarası çocuk oyun alanlarında doğa ile görsel bağlantı kurulmasını sağlayan unsurlardır. Alanda, bireylerin doğayla görsel olmayan bağlantıyı kurmayı sağlayan duyuşsal uyaranlar da mevcuttur. Alanın yakınında yer alan denizdeki dalga sesleri, doğal dokular, kuş cıvıltıları, yaprak hışırtıları ve koku veren bitkisel uyaranlar ile doğa ile görsel olmayan bağlantı sağlanmaktadır. Çocuk oyun alanlarındaki kullanıcıların hareketi ve oyun alanındaki mekanik nesnelerin sesleri bir miktar baskılasa da; alanın çevresinde bulunan ağaç ve çalılar hafif bir esintiyle hareket etmesi ritmik olmayan duyuşsal uyaranların varlığını göstermektedir. Çocuk oyun alanlarının kıyı kesiminde denize yakın noktalarda kurgulanması ve etrafındaki farklı doku ve formdaki bitkilerin varlığı hava sıcaklığı, bağıl nem ve hava akışına etki ederek termal değişikliği sağlanmaktadır. Aynı zamanda oyun alanlarının denize çok yakın olması çocukların suyla görsel, duyuşsal ve dokunsal bağlantılarını sağlamaktadır. Çocuk oyun alanlarında doğal ışık ve gölge oyunlarının kullanılması ve doğal olguları ortaya çıkartıp destekleyecek aydınlatma koşulları bakımından eksiklikler tespit edilmiş olup, dinamik ve dağınık ışık ise yetersizdir. Kullanıcılar, çalışma alanı içerisinde mevsim değişimleri ve geçişlerini gözlemleme imkânı bulabilmekte ve dolayısı ile doğal sistemlerle bağlantı kurabilmektedir.

Çocuk oyun alanlarında doğadan esinlenerek tasarlanmış materyaller bulunmaktadır. Alan içerisinde deniz dalgasına benzetilen platform, kaydırak ve yapay tepe formları ile örümcek ağına benzetilen ipli tırmanma platformları, su parkında çiçek formu oyun elemanları gibi doğa ile uyumlu biyomorfik form ve desenlere rastlamak mümkündür. Alanların içerisinde kullanılan malzemelerin bir kısmı ahşap ve doğal zemin olmakla birlikte; geri kalanının kauçuk, polietilen, metal vb. materyaller olması nedeniyle doğayla maddi bağlantı kısmen sağlanabilmektedir. Çocuk oyun alanı içerisinde tüm mekanlar hiyerarşik bir düzende olup, karmaşıklık ve düzen ilkesi içinde tasarlanmıştır.

Çocuk oyun alanlarının konumlandırıldığı tüm noktalar, engelsiz görüş alanına sahip olup, olasılık/manzara değeri yüksek potansiyele sahiptir. Kent parkları içerisinde bulunan oyun alanları, bireylerin yoğun kullandığı alanlardır. Dolayısıyla sığınak ve korunma alanları içermemektedir. Çalışma alanı içerisinde farklı yükseklikteki ve biyofilik formdaki grup elemanları kullanıcılarda merak ve gizem uyandırmaktadır. Park içerisindeki çocuk oyun alanlarında risk/tehlike ilkesi kapsamında tehlike oluşturabilecek kullanımlar tespit edilmemiştir (Tablo 2).

Tablo 2  
Çocuk oyun alanlarında biyofilik tasarım parametreleri değerlendirmesi

Mekandaki doğa	Doğa ile görsel bağlantı	Doğa ile görsel olmayan bağlantı	Ritmik olmayan duyuşsal uyarılar	Termal ve hava akışı deęişkenlięi	Su varlıęı	Dinamik ve daęınık ışık	Doęal sistemlerle bağlantı
	**	**	**	**	**	*	**
Doęal analogiler	Biyomorfik formlar ve desenler		Doğa ile maddi bağlantı		Karmaşıklık ve düzen		
	**		**		**		
Mekanın doğası	Olasılık/Manzara		Sığınak	Gizem		Risk/Tehlike	
	**		*	**		**	

(\*\*): Sağlamakta, (\*): Kısmen sağlamakta)

### 3.5. Oturma Alanları

Ordu kent parkları oturma alanlarında, kullanıcıların doğayla görsel bağlantı kurmasını sağlayan çok sayıda öge mevcuttur. Mevsimsel olarak farklı manzaralar sunan bitkilerin varlığı ile oturur pozisyonda seyir imkanı sunan doğa ve deniz manzaraları alanlarda kullanıcıların doğa ile görsel bağlantı kurmasını sağlamaktadır. Doğayla görsel olmayan bağlantı bağlamında, çalışma alanına çok yakın olan denizin ve kıyıya vuran dalgaların sesi, oturma alanlarının etrafında gezinen ve uçan hayvanlar, mevcut ağaçların ve yaprakların sesleri gibi duyuşsal uyarılar doğayla görsel olmayan bağlantının kurulmasını sağlamaktadır. Ancak, alanın hemen yakınındaki araç yolundan kaynaklı trafik gürültüsü doğayla görsel olmayan bağlantıyı baskılayan ve zayıflatan bir etki oluşturmaktadır. Alanda bulunan ağaçlar, çiçekler, çalılar ve çimlerin esintiyle hareket etmesi ve denizdeki dalga hareketleri ritmik olmayan duyuşsal uyarıların varlığını göstermektedir. Benzer şekilde oturma alanlarındaki kullanıcı hareketleri, alanın yakınındaki bisiklet ve koşu yolunda hareket halinde bulunan bisiklet, elektrikli scooter, ginger vb. nesnelerin sesleri doğa ile duyuşsal uyarıları baskılamakta ya da etkisini zayıflatmaktadır. Çalışma alanında bulunan oturma alanlarının denize yakın noktalarda kurgulanması ve etrafındaki farklı doku ve formdaki bitkilerin varlığı ile hava sıcaklığı ve baęıl nemdeki deęişikler hava akışı deęişkenlięi sağlanmaktadır. Oturma alanlarının denize çok yakın mesafede olması seyir keyfinin yanı sıra duyuşsal uyarıları da harekete geçirmektedir. Oturma alanlarını çevreleyen çim alanların üzerindeki farklı ışık gölge yoğunlukları ile kullanıcılar ışığı doğrudan, ağaçların altındaki gölgelik ve açıklık alanlarda ise daęınık ve dinamik ışığı tecrübe etmekte olup, doğada meydana gelen aydınlatma koşulları taklit edilmiştir. Dolayısı ile oturma alanlarındaki dinamik ve daęınık ışıktan yeterince istifade edilmiştir. Kullanıcılar, çalışma alanında yer alan oturma alanlarındaki bitki türlerinin mevsimsel deęişimlerini ve geçişlerini gözlemlene imkânı bulabilmekte, deniz kıyısına inip deniz, kum ve doğa taşlarla temas halinde olabilmekte, doğa sistemlerle bağlantı kurabilmektedir.

Kent parklarındaki oturma alanlarında doğadan esinlenerek tasarlanmış oturma-dinlenme elemanları da bulunmaktadır. Alan içerisinde deniz dalgasına benzetilen ahşap banklar, taş formunda oturma birimleri, kıyı kenarında dinlenme ve seyir amaçlı şezlong görünümünde oturma-dinlenme birimleri gibi doğa ile uyumlu biyomorfik form ve desenlere rastlamak mümkündür. Buna rağmen, oturma alanlarında işlenmiş halde doğa taş ve ahşap malzemeler kullanılmış olsa da zeminlerinde uygulanan malzemeler doğallıktan uzaktır. Bu nedenle doğa ile maddi bağlantı kısmen sağlanabilmiştir. Oturma alanları içerisinde tüm mekanlar hiyerarşik bir düzende olup, karmaşıklık ve düzen ilkesi içinde tasarlanmıştır.

Kent Parklarındaki tüm oturma alanları ve bunların konumlandırıldığı tüm noktalar engelsiz görüş alanına sahip olup, olasılık/manzara değeri yüksek potansiyele sahiptir. Çalışma alanı içerisinde bulunan oturma alanları kullanıcıların yoğun kullandığı alanlar olup, alanda daha çok kullanıcıların dięer bireylerle birlikte zaman geçirebileceęi yarı kapalı ve üstü açık oturma birimleridir. Dolayısıyla sığınak ve korunma alanları içermemektedir. Çalışma alanı içerisinde farklı yükseklikteki donatı elemanları kullanıcılarda merak ve gizem uyandırmaktadır. Park içerisindeki oturma alanlarında risk/tehlike ilkesi kapsamında tehlike oluşturabilecek kullanımlar tespit edilmemiştir (Tablo 3).

Tablo 3  
Oturma alanlarında biyofilik tasarım parametreleri değerlendirmesi

Mekandaki doğa	Doğa ile görsel bağlantı	Doğa ile görsel olmayan bağlantı	Ritmik olmayan duyuşsal uyarılar	Termal ve hava akışı deęişkenlięi	Su varlıęı	Dinamik ve daęınık ışık	Doęal sistemlerle bağlantı
	**	**	**	**	**	**	**
Doęal analogiler	Biyomorfik formlar ve desenler		Doğa ile maddi bağlantı		Karmaşıklık ve düzen		
	*		*		**		
Mekanın doğası	Olasılık/Manzara		Sığınak		Gizem		Risk/Tehlike
	**		*		**		**

(\*\*): Sağlamakta, \*: Kısmen sağlamakta)

### 3.6. Gezi Alanları

Kullanıcıların gezi alanlarında seyir halindeyken bu alanlarının denize ve kıyıya paralel şekilde devam etmesi nedeniyle gezi alanlarında panoramik açılarından da hem deniz hem de doğa manzara seyir noktası çokça mevcuttur. Ayrıca gezi alanları boyunca farklı noktalarda resim ve kuş, balık, bitki figürlü heykeller gibi sanatsal objeler ile çeşitli bitki türlerinin varlığı da yine kullanıcıların doğa ile görsel bağlantı kurmasını sağlamaktadır. Gezi alanlarına paralel bir şekilde kıyı şeridi boyunca devam eden denizin ve kıyıya vuran dalgaların sesi doğayla görsel olmayan bağlantının kurulmasını sağlayan unsurlardır. Gezi alanlarında yer alan ağaçlar ve çalıkların yapraklarının rüzgar esintisiyle hareketi, denizdeki dalga hareketleri de yine ritmik olmayan duyuşsal uyarıların varlığını göstermektedir. Gezi alanlarındaki kullanıcıların hareketleri, bisiklet ve koşu yolunda hareket halinde bulunan bisiklet, elektrikli scooter, ginger, vb. mekanik nesnelerin çıkardığı sesler ile yakındaki araç yolundan kaynaklı trafik gürültüsü doğa ile olan bağlantıya zaman zaman zarar vermektedir. Gezi alanlarının denize paralel halde ve kıyı şeridi boyunca devam etmesi, farklı doku ve formdaki bitkilerin varlığı ile hava sıcaklığı ve baęıl nemdeki deęişikler termal sistem ve hava akışı deęişkenlięi sağlanmaktadır. Gezi alanlarının denize çok yakın mesafede ve kıyı boyunca devam etmesi gezinti yapanlar için hem manzara seyri hem de suyun varlığından kaynaklı duyuşsal uyarılar nedeniyle özeldir. Kullanıcılar, gezi alanlarında yer alan yeşil alanların ve sert zeminlerin üzerinde, ağaçların altındaki gölgelik ve açıklık alanlarda daęınık ve dinamik ışığı tecrübe etmektedir. Dolayısı ile gezi alanlarındaki dinamik ve daęınık ışık yeterli düzeyde deęerlendirilmiştir. Kullanıcılar, çalışma alanı içerisindeki gezi alanları boyunca bitki türlerinin mevsimsel ve zamansal deęişimlerini ve geçişlerini gözlemlene imkânı da bulabilmektedir. Ayrıca gezi alanlarının denize çok yakın konumda olmasından ötürü deniz, kum ve doğa taş ve malzemeler vasıtasıyla doğa sistemlerle bağlantı artmaktadır.

Kent parklarındaki gezi alanlarında doğadan esinlenerek tasarlanmış donatı elemanları bulunmaktadır. Alan içerisinde koçanlı fındık heykel ve figürleri, denizin içindeki balık ve hareketlerinden esinlenilmiş kentsel motif ve objeler, yine doğadan esinlenerek tasarlanmış salyangoz ve midye kabuğuna benzetilmiş kentsel objeler, fındık taşıyan sincap heykelleri gibi doğa ile uyumlu biyomorfik form, nesne ve desenlere rastlamak mümkündür. Gezi alanlarında işlenmiş halde doğa taş ve ahşap malzemeler kullanılmıştır. Doğal taşlardan imal edilmiş duvarlar ve zemin kaplamaları, gezinti alanlarının zeminlerinde kullanılan ahşap zemin kaplamaları ve doğadan esinlenerek tasarlanmış görüntü perdeleri ve objelerle gezi alanlarında doğa ile maddi bağlantı sağlanmıştır. Gezi alanları içerisindeki tüm mekanların hiyerarşik bir düzende olduğu söylenemez. Çünkü birçoğu daha sonradan gezi alanlarına eklenen materyaller ve donatı elemanlarıdır. Bu nedenle yapılan tasarımlar ile karmaşıklık ve düzen ilkesi kısmen sağlanmıştır.

Kent Parklarındaki bütün gezi alanları engelsiz görüş alanına sahip olup, olasılık/manzara deęeri yüksek potansiyele sahiptir. Çalışma alanı içerisinde bulunan gezi alanları kullanıcıların yoğun kullandığı alanlar olup, sığınak ve korunma alanları içermemektedir. Gezi alanları boyunca gözlemlenen farklı yükseklikteki ve biyofilik formdaki donatı elemanları kullanıcılarda merak ve gizem uyandırmaktadır. Çalışma alanındaki gezi alanları bir taraftan bisiklet yolu ve karayoluna, bir taraftan da denize paralel olarak kıyı şeridi boyunca devam etmektedir. Yeterli düzeyde güvenlik önlemleri alınmadığı için risk/tehlike ilkesi kapsamında tehlike oluşturabilecek durumlar olasılıklıdır (Tablo 4).

Tablo 4  
Gezi alanlarında biyofilik tasarım parametreleri değerlendirmesi

Mekandaki doğa	Doğa ile görsel bağlantı	Doğa ile görsel olmayan bağlantı	Ritmik olmayan duyuşsal uyarılar	Termal ve hava akışı deęişkenlięi	Su varlıęı	Dinamik ve daęınık ışık	Doęal sistemlerle bağlantı
	**	**	**	**	**	**	**
Doęal analogiler	Biyomorfik formlar ve desenler		Doğa ile maddi bağlantı		Karmaşıklık ve düzen		
	**		**		*		
Mekanın doğası	Olasılık/Manzara		Sığınak	Gizem	Risk/Tehlike		
	**		*	**	*		

(\*\* : Sağlamakta, \* : Kısmen sağlamakta)

### 3.7. Açık Yeşil Alanlar

Çalışma alanları denize çok yakın olup, hem deniz hem de doğa manzarasına hakimdir. Açık-yeşil alanlarda çeşitli tür ve formdaki zengin bitki varlığı ve bu bitkilerin görünümünün mevsimsel olarak farklılık göstermesi, buna ilaveten çeşitli rekreasyonel alan kullanımları ve bu kullanımlar arasında oluşturulan bitkisel geçişler de kullanıcıların doğa ile görsel bağlantı kurmasını sağlamaktadır. Ayrıca yeşil alanlar içerisinde sıklıkla rastlanan budanmış hayvan figürleri ve heykel formundaki sanatsal öğeler de doğa ile görsel bağlantı kurulmasını sağlayan unsurlardır. Çalışma alanı içerisinde kullanıcıların doğayla görsel olmayan bağlantının sağlanabilmesi için gerekli olan çok sayıda duyuşsal uyarılar mevcuttur. Açık-yeşil alanların denize oldukça yakın olması sebebiyle denizin ve kıyıya vuran dalgaların çıkardığı sesler, yeşil alanlarda gezinen hayvan sesleri, esinti nedeniyle hareket eden mevcut ağaçların ve yaprakların sesleri gibi duyuşsal uyarılar kullanıcıların doğayla görsel olmayan bağlantı kurmasını sağlayan unsurlardır. Yeşil alanlardaki mevcut bitkisel uygulamaların içerdiği ağaçlar ve çalıların yapraklarının esintiyle hareket etmesi ve denizdeki dalga hareketleri yine ritmik olmayan duyuşsal uyarıların varlığını göstermektedir. Ancak, açık-yeşil alanlarındaki kullanıcıların hareketleri, yeşil alanların çok yakınında bulunan bisiklet ve koşu yolunda hareket halinde bulunan bisiklet, elektrikli scooter, ginger, vb. mekanik nesnelerin çıkardığı sesler doğa ile bağı olumsuz etkilemektedir. Açık-yeşil alanlardaki hava akımları ve termal deęişkenlik sahil bandındaki yapılaşma ve kısmen yüksek katlı binalarca olumsuz etkilense de, yoğun yeşil doku ve farklı dokular oluşturan plantasyon ve yeşil açıklıklar tarafından olumlu etki kazanmaktadır. Ayrıca alan içerisinde bulunan açık-yeşil alanlarda doğa ve yapay su yüzeylerinin çevresi ve bitkilerle oluşturulan gölgelikli oturma alanları termal açıdan mikroklimatik ortam sağlamaktadır. Açık-yeşil alanlarda doğa ve yapay su öğeleri mevcuttur. Alanı kullanan bireyler suyun hem işitsel, hem görsel ve duyuşsal hem de dokunsal özelliğinden faydalanabilmektedir. Bu alanların tasarımlarında seçilen bitkisel materyaller de doğa alan algısı yaratmaktadır. Bu nedenle çalışma alanı suyun varlığı bakımından yeterlidir. Açık-yeşil alanlardaki dinamik ve daęınık ışık varlığı tasarımının başlangıcında düşünülmesi gereken bir konu olduğundan ışık faktörü sadece yetişmiş ağaçların oluşturduğu açıklık ve gölgelik alanlarda mevcuttur. Bu nedenle çalışma alanı ışık varlığı bakımından yetersizdir. Çalışma alanında doğa sistemlerle bağlantının kriteri olan doğa süreçlerin, özellikle sağlıklı bir ekosistemin özelliği olan mevsimsel ve zamansal deęişikliklerin ve geçişlerin farkındalığıyla seçilen uyumlu bitki türleriyle, ayrıca deniz kıyısına yakın konumda olduklarından deniz, kum, doğa taş gibi malzemelerle sağlanmıştır.

Ordu kent parklarındaki açık-yeşil alanlar, doğa analogiler bağlamında 3 kriter kapsamında değerlendirilmiş olup, bu kriterlerden ilki olan biyomorfik formlar ve desenler bakımından oldukça zengindir. Alan içerisinde doğadan esinlenerek tasarlanmış biyomorfik biçim ve dokulara rastlamak mümkündür. Bitkilerin budanmasıyla oluşturulan hayvan figürleri ve formları doğayla entegrasyonu sağlamaktadır. Açık-yeşil alanlarda doğayla malzeme bağlantısı sağlanmıştır. Açık-yeşil alanlarda özellikle bitkisel tasarımların çevresinde bulunan çit uygulamalarında kullanılan doğa ahşap malzemelerle yaratılan mekanlar öne çıkmaktadır. Ayrıca zemin kaplamalarında doğa veya doğala yakın malzemeler kullanılmış olması da doğa ile maddi bağlantının sağlandığını göstermektedir. Açık-yeşil alanlar içerisindeki tüm mekanların hiyerarşik bir düzende olduğu söylenemez. Çünkü birçoğu sonradan alanda uygulaması yapılmış farklı form ve dokudaki bitkisel materyaller ve donatı elemanlarıdır. Bu nedenle yapılan tasarımlar ile karmaşıklık ve düzen ilkesi kısmen sağlanmıştır.

Kent Parklarındaki açık-yeşil alanlar engelsiz görüş alanına sahip olup, olasılık/manzara değeri yüksek bir potansiyele sahiptir. Çalışma alanı içerisinde bulunan açık-yeşil alanlarda bitkisel uygulamalardaki geçişler ve çeşitlilik nedeniyle kullanıcılar açısından sığınak ve korunma alanları içermektedir. Açık-yeşil alanlarda sıkça gözlemlenen farklı yükseklikteki ve biyofilik formdaki bitkisel elemanlar kullanıcılarda merak ve gizem uyandırmaktadır. Çalışma alanındaki açık-yeşil alanlarda risk/tehlike ilkesi kapsamında tehlike oluşturabilecek unsurlar bulunmamaktadır (Tablo 5).

Tablo 5

Açık-yeşil alanlarda biyofilik tasarım parametreleri değerlendirmesi

Mekandaki doğa	Doğa ile görsel bağlantı	Doğa ile görsel olmayan bağlantı	Ritmik olmayan duyuşsal uyarılar	Termal ve hava akışı değışkenliđi	Su varlıđı	Dinamik ve dađınık ışık	Dođal sistemlerle bağlantı
	**	**	**	**	**	*	**
Dođal analogiler	Biyomorfik formlar ve desenler		Dođa ile maddi bağlantı		Karmaşıklık ve düzen		
	**		**		*		
Mekanın dođası	Olasılık/Manzara		Sığınak		Gizem		Risk/Tehlike
	**		**		**		**

(\*\*: Sağlamakta, \*: Kısmen sağlamakta)

### 3.8. Spor Alanları

Kent parklarında spor alanlarının kurgulandıđı alanların çevresinde bulunan yoğun yeşil alan oluşumları, dođa ve deniz manzaraları gibi dođal peyzaj görünümünün birlikte kullanımının sağlanması ile kullanıcıların dođa ile görsel bağlantı kurmasına sebep olan çok sayıda dođal alan algısı vardır. Mevsimsel değışikliđiyle farklı manzaralar sunan bitkilerin varlıđı, alanda hakim olan deniz ve Boztepe manzarası gibi unsurlar spor alanlarında dođa ile görsel bağlantı kurulmasını sağlayan unsurlardır. Alanda bireylerin dođayla görsel olmayan bağlantının kurulmasını sağlayan duyuşsal uyarılar çokçadır. Alanın yakınındaki dođal su ögesi olan denizin dalgalanması ile oluşun sesler, kokulu ve dokulu bitki varlıđı, kuş sesleri, yaprakların rüzgar ile çıkardığı sesler gibi uyarılar ile dođa ile görsel olmayan bağlantıyı sağlanmaktadır. Alanın çevresinde bulunan ağaç ve çalıların rüzgar esintiyile hareket etmesi ritmik olmayan duyuşsal uyarıların varlıđını göstermektedir. Ancak, spor alanlarındaki spor ve yürüyüş yapan kullanıcıların hareketi, spor alanındaki mekanik nesnelerin (bisiklet, elektrikli scooter ve ginger, v.b) sesleri zaman zaman dođal uyarıların önüne geçmektedir. Spor alanlarının denize yakın mesafede olması suyun varlıđını görsel, duyuşsal ve dokunsal olarak artırmaktadır. Alandaki ışık gölge oyunları ile dođada meydana gelen aydınlatma koşulları bakımından eksiklikler tespit edilmiş olup, dinamik ve dađınık ışık yetersizdir. Kullanıcılar çalışma alanı içerisinde hareket halindeyken mevsimsel değışimleri ve geçişleri gözleme imkânı bulabilmekte ve dolayısı ile dođal sistemlerle bağlantı kurabilmektedir.

Çalışma alanı içerisinde bulunan spor alanları dođadan esinlenerek tasarlanmış materyal ve yüzey desenleri bakımından yetersiz olup, biyofilik form ve desen bakımından da yetersizdir. Spor alanlarında yaratıcı ortamları geliştirmek adına renk seçimi yapılmış olsa da, zeminlerinde kullanılan malzemelerin bir kısmı kauçuk, bir kısmı ise renkli asfalt oluşu nedeni ile dođayla maddi bağlantı tam olarak sağlanamamıştır. Spor alanları hiyerarşik bir düzen içerisinde olup, mekanlar karmaşıklık ve düzen ilkesi içinde tasarlanmıştır.

Kent parkları içerisinde bulunan spor alanlarının bulunduğu tüm noktalar engelsiz görüş alanına sahip olup, olasılık/manzara değeri yüksek bir potansiyele sahiptir. Kent parkları içerisinde bulunan spor alanları, bireylerin yoğun olarak kullandıđı alanlardır. Bununla birlikte sığınak ve korunma alanları içermemektedir. Çalışma alanı, farklı yükseklikte ve biyofilik formda grup elemanları içermediğinden kullanıcılarda merak ve gizem uyandıran unsurlar oluşturmamaktadır. Park içerisindeki spor ve yürüyüş alanlarında özellikle yaya ve araç yoluna paralel ve yol boyunca devam eden bisiklet ve koşu yollarında yaya-arac çatışması oluşma riski yüksektir. Dolayısıyla risk/tehlike ilkesi kapsamında tehlike oluşturabilecek kullanımlar tespit edilmiştir (Tablo 6).

Tablo 6  
Spor alanlarında biyofilik tasarım parametreleri değerlendirmesi

Mekandaki doğa	Doğa ile görsel bağlantı	Doğa ile görsel olmayan bağlantı	Ritmik olmayan duyuşal uyarılar	Termal ve hava akışı deęişkenlięi	Su varlıęı	Dinamik ve daęımık ışık	Doęal sistemlerle bağlantı
	**	**	**	**	**	*	**
Doęal analogiler	Biyomorfik formlar ve desenler		Doęa ile maddi bağlantı		Karmaşıklik ve düzen		
	*		*		**		
Mekanın doğası	Olasılık/Manzara		Sığınak		Gizem		Risk/Tehlike
	**		*		*		*

(\*\*): Sağlamakta, (\*): Kısmen sağlamakta)

### 3.9. Alışveriş Alanları

Alışveriş ünitelerinin, çevresindeki oturma birimlerinin ve oturma basamaklarının mekan tasarımlarının deniz kıyısında olması deniz, tepe ve doğa manzaralarına hakim olmayı sağlamaktadır. Bu da kullanıcılara oturur pozisyonda iken manzara seyir imkanı sunmaktadır. Ayrıca mevsimsel olarak farklı manzaralar sunan bitkisel tasarımların varlığı ile kullanıcıların doğa ile görsel bağlantı kurması sağlanmaktadır. Doğayla görsel olmayan bağlantı bağlamında, çalışma alanına çok yakın olan denizin ve kıyıya vuran dalgaların sesi, denizin kokusu, alışveriş alanlarının etrafında gezinen hayvan sesleri, etraftaki mevcut ağaçların, çalılarının ve yaprakların sesleri gibi duyuşal uyarılar doğayla görsel olmayan bağlantının kurulmasını sağlamaktadır. Çalışma alanı içerisinde bulunan alışveriş alanlarındaki kullanıcı hareketleri, alışveriş alanlarına çok yakın ve paralelinde devam eden bisiklet ve koşu yolunda hareket halinde bulunan bisiklet, elektrikli scooter, ginger vb. nesnelerin sesleri, vapur ve gezinti teknelerinin çıkardığı sesler doğa ile iletişimde kopma sağlamaktadır. Ancak, alanın çevresinde bulunan ağaçlar, çiçekler, çalılar ve çimlerin esintiyle hareket etmesi, denizdeki dalga hareketleri doğaya dair ritmik olmayan duyuşal uyarılardır. Çalışma alanındaki alışveriş alanlarının denize yakın noktalarda kurgulanmış olması ve etrafındaki farklı doku ve formdaki bitkilerin varlığı ile hava sıcaklığı ve baęıl nemdeki deęişikler termal ve hava akışı deęişkenlięi sağlamaktadır. Alışveriş ünitelerinin kapalı mekanlar olması nedeniyle ancak açık durumda iken doğa hava akımı sağlanmaktadır. Ayrıca çalışma alanı içerisinde bulunan alışveriş alanlarındaki gölgelikli oturma birimleri ile açılır-kapanır üst örtü elemanları da mikroklimatik ortamlar oluşturmaktadır. Alışveriş alanlarının deniz kıyısında olması hem manzara seyri nedeni ile fazla tercih yaratmakta hem de suyun varlığının duyuşal etkisini artırmaktadır. Alışveriş alanlarını çevreleyen gezinti ve oturma alanlarının etrafında, ağaçların altındaki gölgelik ve açıklık alanlarda daęımık ve dinamik ışık tecrübe edilebilmekte olup, doğada meydana gelen aydınlatma koşulları taklit edilmiştir. Alışveriş alanlarındaki dinamik ve daęımık ışık ise yeterli düzeydedir. Kullanıcılar, çalışma alanı içerisindeki alışveriş alanlarındaki bitki türlerinin mevsimsel deęişimlerini ve geçişlerini gözlemleme imkânı bulabilmektedir. Ahşap ünitelerin çevresinde ortam oluşturmak için renkli ve ahşap basamaklı bir amfi tasarlanmıştır. Doğal malzeme seçimlerine dikkat edilerek, deniz, kum ve doğa taşlar ile kullanıcı temas imkanı bulabilmekte ve dolayısı ile doğa sistemlerle bağlantı kurabilmektedir.

Kent parklarındaki alışveriş alanlarının yakınlarında doğadan esinlenerek tasarlanmış oturma-dinlenme elemanları ve kent mobilyaları bulunmaktadır. Ayrıca ünitelerin yakınlarındaki bitkisel tasarımlarda doğa ile uyumlu biyomorfik form ve desenlere rastlamak mümkündür. Alışveriş alanlarında işlenmiş halde doğa taş ve ahşap malzemeler kullanılmış, zeminlerinde küp granit ve doğa taş deseni uygulamaları gibi doğa malzemeler veya doğa ile uyumlu malzemelere yer verilmiştir. Bu nedenle doğa ile maddi bağlantı sağlanmıştır. Alışveriş alanları içerisinde tüm mekanlar hiyerarşik bir düzende olup, karmaşıklik ve düzen ilkesi içinde tasarlanmıştır.

Kent Parklarındaki tüm alışveriş alanları ve de bunların konumlandırıldığı tüm noktalar engelsiz görüş alanına sahip olup, olasılık/manzara deęeri yüksek potansiyele sahiptir. Çalışma alanı içerisinde bulunan alışveriş alanları, kullanıcıların yoğun kullandığı alanlardır. Alanda daha çok kullanıcıların dięer bireylerle birlikte zaman geçirebileceęi yarı kapalı oturma ve üstü açık oturma birimleri mevcuttur. Yakınında tasarlanan bitkisel uygulamalardaki geçişler ve çeşitlilik nedeniyle kullanıcılar açısından kısmen sığınak ve korunma alanları içermektedir. Çalışma alanı içerisinde farklı yükseklikteki donatı elemanları kullanıcılarda merak ve gizem

uyandırmaktadır. Park içerisindeki oturma alanlarında risk/tehlike ilkesi kapsamında tehlike oluşturabilecek kullanımlar tespit edilmemiştir (Tablo 7).

Tablo 7

Alışveriş alanlarında biyofilik tasarım parametreleri değerlendirmesi

Mekandaki doğa	Doğa ile görsel bağlantı	Doğa ile görsel olmayan bağlantı	Ritmik olmayan duyuşsal uyarılar	Termal ve hava akışı değışkenliđi	Su varlıđı	Dinamik ve dađımık ışık	Dođal sistemlerle bağlantı
	**	**	**	**	**	**	**
Dođal analogiler	Biyomorfik formlar ve desenler		Dođa ile maddi bağlantı		Karmaşıklık ve düzen		
	**		**		**		
Mekannın dođası	Olasılık/Manzara		Sığınak	Gizem		Risk/Tehlike	
	**		**	**		**	

(\*\*): Sağlamakta, \*: Kısmen sağlamakta)

### 3.10. Eğlence Alanları

Kent parklarında bulunan eğlence alanlarının etrafında bulunan yoğun yeşil alan oluşumları nedeni ile kullanıcıların doğa ile görsel bağlantı kurmasına sebep olan çok sayıda doğa alan algısı vardır. Yeşil alanlar içerisinde ahşap çit ile çevrilmiş, granit platform üzerinde, zeminde dolamit taş üzerine kurgulanmış hayvan figürleri, çim alan içerisinde eşeđine ters binen masal kahramanı Nasrettin Hoca heykeli ve masal dinletisi, mevsim değışikliđiyle farklı manzaralar sunan bitkisel alan varlıđı, alanda hakim olan deniz, doğa ve boztepe manzaraları gibi unsurlar bireylerin doğa ile görsel bağlantı kurulmasını sağlayan unsurlardır. Eğlence alanlarının denize yakın olması nedeniyle deniz dalgalarının sesi, etraftaki kokulu ve dokulu bitki varlıđı, kuş ve serbest halde dolaşan hayvan sesleri gibi uyarılar doğa ile görsel olmayan bağlantıyı sağlamaktadır. Eğlence alanlarındaki bireylerin yoğunluđu ve hareketleriyle oluşun sesler, kaykay alanı ve su parkında çocukların ve mekanik aletlerin sesleri, ters evi ziyaret edenlerden ötürü kullanıcı hareketi ve yoğunluđu bađlı oluşun sesler doğa uyarılarını çođu zaman baskılamaktadır. Alanın çevresinde bulunan ađaç ve çalıların rüzgar etkisi ile hareketleri ritmik olmayan duyuşsal uyarılardır. Eğlence alanlarının kıyı kesiminde denize yakın noktalarda kurgulanması ve etrafındaki farklı doku ve formdaki bitkilerin varlıđı ile hava sıcaklıđı ve bađlı nemdeki değışikler termal ve hava akışı değışkenliđi sağlamaktadır. Eğlence alanlarının denize çok yakın olması nedeniyle su varlıđı görsel, duyuşsal ve dokunsal olarak sağlanmaktadır. Ayrıca alandaki su parkı, çocuklar için suyu çeşitli etkinlikler yaparak kullanma ve eğlenceli vakit geçirme imkanı sunmaktadır. Kullanıcılar, eğlence alanlarının etrafındaki yeşil alanlar ve sert zeminlerde ışık gölge oyunları ve ađaçların altındaki gölgelik ve açıklık alanlarda dađımık ve dinamik ışığı tecrübe etmektedir. Gezi alanlarındaki dinamik ve dađımık ışık yeterli düzeydedir. Kullanıcılar, çalışma alanı içerisindeki eğlence alanları ve çevresindeki bitki türlerinin mevsimler ve zamansal değışimlerini ve geçişlerini gözleme imkânı bulabilmekte; ayrıca deniz kıyısına yakın konumda olduklarından deniz ve doğayla, dolayısı ile doğa sistemlerle bağlantı kurabilmektedirler.

Eđlence alanlarında doğayı taklit ederek tasarlanmış materyaller bulunmaktadır. Alan içerisinde deniz dalgası formunda malzemeler, yunus balıđından esinlenerek tasarlanmış deniz bisikletleri, örümcek ađına benzetilen ipli tırmanma platformları ve alanların çevresindeki budanmış bitkisel form ve biçimler ile su parkındaki bitki formu oyun aletleri doğa ile uyumlu biyomorfik form ve desenlerdir. Su parkında materyal ve renk seçimleriyle biyomorfik dokuyu geliştirmek için ahşap ve doğa taş tercih edilmiştir. Eğlence alanlarında mekanlar hiyerarşik bir düzen içerisinde olup, tüm mekanlar karmaşıklık ve düzen ilkesi içinde tasarlanmıştır.

Eđlence alanlarının konumlandırıldığı tüm noktalar, engelsiz görüş alanına sahip olup, olasılık/manzara değeri yüksek potansiyele sahiptir. Kent parkları içerisinde bulunan eğlence alanları rekreasyonel açıdan bireylerin yoğun kullandığı alanlardır. Sığınak ve korunma alanları içermemektedir. Çalışma alanı içerisinde farklı yükseklikteki ve biyomorfik formdaki grup elemanları kullanıcılarda merak ve gizem uyandırmaktadır. Park içerisindeki eğlence alanlarında özellikle de kaykay, su parkı ve ip tırmanma gibi mekanlarda risk/tehlike ilkesi

kapsamında 3-6 yaş kullanıcılar açısından tehlike oluşturabilecek kullanımlar olduğu tespit edilmiştir (Tablo 8).

Tablo 8  
Eğlence alanlarında biyofilik tasarım parametreleri değerlendirmesi

Mekandaki doğa	Doğa ile görsel bağlantı	Doğa ile görsel olmayan bağlantı	Ritmik olmayan duyuşal uyarılar	Termal ve hava akışı deęişkenlięi	Su varlıęı	Dinamik ve daęınık ışık	Doęal sistemlerle bağlantı
	**	**	**	**	**	**	**
Doęal analogiler	Biyomorfik formlar ve desenler		Doęa ile maddi bağlantı		Karmaşıklik ve düzen		
	*		*		**		
Mekanın doęası	Olasılık/Manzara		Sığınak	Gizem		Risk/Tehlike	
	**		*	**		*	

(\*\*): Sağlamakta, (\*): Kısmen sağlamakta)

### 3.11. Ulaşım ve Otoparklar

Otopark alanlarının kıyı şeridinde ve denize çok yakın mesafede oluşu nedeniyle araç kullanırken ve park esnasında deniz ve doğa manzara seyir noktaları ile sıkça karşılaşılmaktadır. Ulaşım güzergahları ve otopark alanlarının bir tarafında karayolu diğer tarafında ise kıyı şeridi boyunca devam etmesi hem denizin ve kıyıya vuran dalgalarının sesi hem de araç yolundan kaynaklı trafik gürültüsü bu alanlarda doğayla görsel olmayan bağlantının kurulmasını etkileyen unsurlardır. Otopark ve ulaşım alanlarının denize paralel halde ve kıyı şeridi boyunca konumlandırılması, yakınındaki farklı doku ve formdaki bitkilerin varlığı ile hava sıcaklığı ve baęıl nemdeki deęişikler termal deęişkenlikler getirmektedir. Çalışma alanı içerisinde bulunan kapalı üniteler ve yakınlardaki sosyal tesisler de yine termal açıdan mikroklimatik ortamlardır. Alandaki dinamik ve daęınık ışık yeterli düzeydedir. Kullanıcılar, çalışma alanı içerisindeki gezi alanları boyunca bitki türlerinin mevsimsel ve zamansal deęişimlerini ve geçişlerini gözlemlene imkânı bulabilmekte, fakat doęal sistemlerle kısmen bağlantı kurabilmektedirler.

Kent parklarındaki ulaşım ve otopark alanlarında doğadan esinlenerek tasarlanmış veya doğa ile uyumlu biyomorfik form ve desenlere kısmen rastlanmaktadır. Çalışma alanlarında doęal malzemeler sınırlı sayıda olduğundan doğa ile maddi bağlantı kısmen sağlanmıştır. Otopark ve ulaşım alanları içerisindeki tüm mekanlar hiyerarşik bir düzen içerisindedir, dolayısıyla bu alanlar karmaşıklik ve düzen ilkesini sağlamaktadır.

Kent parkları içerisinde bulunan otopark ve ulaşım alanları engelsiz görüş alanına sahip olup, olasılık/manzara deęeri yüksek potansiyeldedir. Sığınak ve korunma alanları mevcut deęildir. Otopark ve ulaşım alanlarında kullanıcılarda merak ve gizem uyandıran mekanlara kısmen rastlandığı görülmüştür. Çalışma alanındaki ulaşım ve otopark alanları trafik ve araç yoğunluğunun fazla olduğu alanlar olduğundan risk/tehlike ilkesi kapsamında tehlike oluşturabilecek durumlara sıkça rastlanmaktadır (Tablo 9).

Tablo 9  
Ulaşım ve otoparklarda biyofilik tasarım parametreleri değerlendirmesi

Mekandaki doğa	Doğa ile görsel bağlantı	Doğa ile görsel olmayan bağlantı	Ritmik olmayan duyuşal uyarılar	Termal ve hava akışı deęişkenlięi	Su varlıęı	Dinamik ve daęınık ışık	Doęal sistemlerle bağlantı
	**	**	**	**	*	**	*
Doęal analogiler	Biyomorfik formlar ve desenler		Doęa ile maddi bağlantı		Karmaşıklik ve düzen		
	*		*		**		
Mekanın doęası	Olasılık/Manzara		Sığınak	Gizem		Risk/Tehlike	
	**		*	*		*	

(\*\*): Sağlamakta, (\*): Kısmen sağlamakta)

### 3.12. Tören ve Anıt Alanları

Mevsimsel değişimlerle farklı manzaralar sunan bitki varlığı, deniz ve boztepe manzarası gibi unsurlar, bireylerin doğa ile görsel bağlantı kurmasını sağlamaktadır. Alanda bireylerin doğayla görsel olmayan bağlantı kurmasını sağlayan duyuşsal uyaranlar da mevcuttur. Anıt ve tören alanlarının denize yakın olması ile denizin dalgalarının sesi, alandaki fiskiyeli süs havuzu, kuş cıvıltıları, diğer hayvan sesleri ve kokulu bitkiler, esinti nedeniyle hareket eden mevcut ağaçların ve yaprakların sesleri gibi duyuşsal uyaranlar kullanıcıların doğayla görsel olmayan bağlantı kurmasını sağlayan unsurlardır. Tören ve anıt alanlarının kent parklarının içinde konumlandırılmasından ötürü buradaki kullanıcı yoğunluğuyla oluşan sesler, Atatürk Parkı'nda bulunan teleferik istasyonu ve Tayfun Gürsoy Parkı'nda spor ve çocuk oyun alanlarına yakınlıktan kaynaklı kullanıcıların ve mekanik aletlerin çıkardığı sesler, alandaki fiskiyeli süs havuzu ritmik olmayan duyuşsal uyaranları etkilemektedir. Tören ve anıt alanlarına yakın mesafede olan deniz ve alandaki süs havuzu görsel, duyuşsal ve dokunsal olarak suya erişimi mümkün kılar. Alandaki dinamik ve dağınık ışık sadece yetişmiş ağaçların oluşturduğu açıklık-gölgelik alanlarda mevcuttur. Bu nedenle çalışma alanı, dinamik-dağınık ışık varlığı bakımından yetersizdir.

Anıt ve tören alanlarında zemin döşemesi olarak doğal taş tercih edilmiştir. Çalışma alanları içerisindeki tüm mekanlar hiyerarşik bir düzen içerisinde olup, mekanlar karmaşıklık ve düzen ilkesi içinde tasarlanmıştır.

Tören ve anıt alanlarının konumlandırıldığı tüm noktalar engelsiz görüş alanına sahip olup, olasılık/manzara değeri yüksektir. Bitkisel tasarım uygulamasındaki geçişler ve çeşitlilik kullanıcılar açısından korunma tesis eder. Park içerisindeki tören ve anıt alanlarında risk/tehlike ilkesi kapsamında tehlike oluşturabilecek kullanımlar tespit edilmemiştir (Tablo 10).

Tablo 10

Tören ve anıt alanlarında biyofilik tasarım parametreleri değerlendirmesi

Mekandaki doğa	Doğa ile görsel bağlantı	Doğa ile görsel olmayan bağlantı	Ritmik olmayan duyuşsal uyaranlar	Termal ve hava akışı değişkenliği	Su varlığı	Dinamik ve dağınık ışık	Doğal sistemlerle bağlantı
	**	**	**	**	**	*	**
Doğal analogiler	Biyomorfik formlar ve desenler		Doğa ile maddi bağlantı		Karmaşıklık ve düzen		
	*		**		**		
Mekanın doğası	Olasılık/Manzara		Sığınak		Gizem		Risk/Tehlike
	**		**		**		**

(\*\*): Sağlamakta, \*: Kısmen sağlamakta)

### 4. Sonuçlar

Çalışmanın yürütüldüğü dört sahil parkında yer alan 9 farklı fonksiyon 14 biyofilik tasarım parametresi bazında değerlendirilmiştir. Bu bulgular ışığında sahil parkları önemli ölçüde biyofilik tasarım parametrelerini sağlamaktadır. Bu sonuç kent merkezinde yer alan, yüksek kullanım yoğunluğuna sahip, kent baskısı altında, kentin dezavantajlarının yoğun şekilde yaşandığı lokasyonda, deniz kıyısında olması nedeniyle kentin en gözde alanı olan ve bu nedenle de artan kentli ihtiyaç ve beklentilerinin odağındaki parklar için oldukça önemlidir. Çalışma alanlarında yer alan fonksiyon grupları, biyofilik tasarımın ana parametreleri bakımından incelendiğinde “Alışveriş alanları”nın en yüksek toplam puanı aldığı görülmüştür. Bununla birlikte en düşük puanı “Ulaşım ve otoparklar” toplamıştır. Fonksiyon gruplarından alınan toplam puanlar bazında biyofilik tasarım ana parametreleri olan “Mekandaki doğa” 126 üzerinden 120 puanla en yüksek uyumu ortaya koymuştur. Bununla birlikte “Doğal analogiler” 54’de 45, “Mekanın doğası” ise 72’de 60 puan toplamıştır (Tablo 11).

Tablo 11

Fonksiyon alanlarının biyofilik tasarım ana parametrelerine göre puanları

Parametreler	Çocuk oyun alanları	Oturma alanları	Gezi alanları	Açık yeşil alanlar	Spor alanları	Alışveriş alanları	Eğlence alanları	Ulaşım ve otoparklar	Tören ve anıt alanları	TOPLAM	%
Mekândaki doğa (14p)	13	14	14	13	13	14	14	12	13	120/126	95
Doğal Analogiler (6p)	6	4	5	5	4	6	6	4	5	45/54	83
Mekânın doğası (8p)	7	7	6	8	5	8	6	5	8	60/72	83
Puan (28p)	26	25	25	26	22	28	26	21	26	225/252	89

Parklar, biyofilik tasarım alt parametrelerine göre değerlendirildiğinde ise; “Mekandaki doğa” ana parametresinin alt parametreleri olan “Doğa ile görsel bağlantı”, “Doğa ile görsel olmayan bağlantı”, “Ritmik olmayan duyuşal uyarılar” ve “Termal ve hava akışı değışkenliđi” tam puan olarak, şartları sağlamaktadır. Ayrıca, “Mekânın doğası” ana parametresinin alt parametresi olan “Olasılık/manzara” parametresi de tam puan almıştır. Bu kapsamda en düşük puanı ise “Sığınak” alt parametresi almıştır (Tablo 12).

Tablo 12

Kent parklarının biyofilik tasarım alt parametrelerine göre toplam puanları

Mekândaki doğa	Doğa ile görsel bağlantı	Doğa ile görsel olmayan bağlantı	Ritmik olmayan duyuşal uyarılar	Termal ve hava akışı değışkenliđi	Su varlığı	Dinamik ve dađınık ışık	Doğal sistemlerle bağlantı
Puan	18	18	18	18	17	14	17
Doğal analogiler	Biyomorfik formlar ve desenler		Doğa ile maddi bağlantı		Karmaşıklık ve düzen		
Puan	14		15		16		
Mekânın doğası	Olasılık/Manzara		Sığınak		Gizem		Risk/Tehlike
Puan	18		12		16		14

Sahil parkları biyofilik tasarım ilkeleri bakımından oldukça olumlu sonuçlar vermiş olsa da, zayıf veya eksik kalan ilkelerin sağlanması parkların oluşturduğu olumlu etkiyi artıracaktır. Her bakımdan doğa ve doğal özellikler ile desteklenmiş yaşam alanları birey ve toplum huzurunu temin ederek, kentli memnuniyetini artıracaktır. Bu kapsamda parklar, özellikle düşük puan alan “Risk/tehlike”, “Biyomorfik formlar ve desenler” ve “Sığınak” alt parametreleri açısından desteklenmeli ve eksiklerin giderilmesi sağlanmalıdır. Bununla birlikte; fonksiyon gruplarından “Ulaşım ve otoparklar” ile “Spor alanları” “Doğal analogiler” ve “Mekânın doğası” ana parametrelerince geliştirilmelidir.

Bununla birlikte bazı araçların kullanılması, kaynakların entegrasyonu ve yaklaşımların değerlendirilmesi mekanların bütüncül bir şekilde biyofilik dönüşümleri ve karakterlerinin oluşmasında etkili olacaktır;

- Donatılarda doğal materyallerin kullanımı artırılmalı
- Doğal form ve desenlerin kullanılmasına özen gösterilmeli
- Doğal ışık ve gölgelere olanak sağlanmalı
- Doğal hava hareketlerine müsaade edilmeli
- Bitki çeşitliliđi ve alanı artırılmalı
- Canlı çeşitliliđi ve hayvanların dahil olmasını sağlayıcı önlemler alınmalı
- Doğa ile görsel bağlantı artırılmalı, engel ve perdelemeler kaldırılmalı
- Doğa ile duyuşal (kokular, görüntüler, sesler, temas ve tadım) uyarılar geliştirilmeli

- Doğanın ruhu ve felsefesi temel alınmalı, yansıtılmalı
- Su varlığı, etkisi ve kullanımı desteklenmeli
- Kaynakların korunumu ve geri dönüşümü ilke edinilmeli
- Düzen ve sistem kurulurken doğa referans olmalı
- Doğanın mekan oluşturma, koruma ve güven verme özelliklerinden faydalanılmalı
- Gizemler barındırmalı
- Güvenli olmalı, riskleri azaltılmalı
- Mekan deneyimini artırmalı
- Biyobenzetim araçları değerlendirilmeli
- Doğal geometri, oran ve düzenler kullanılmalı

Böylelikle kentsel fonksiyonlardan en uzun süreli, en yoğun ve en çok katılımcıyla kullanılan otopark, ulaşım ve spor alanları daha geniş kitlelere, daha etkili bir şekilde hizmet verir duruma gelecektir. Ayrıca kentsel fonksiyonlar arasında estetik özelliği en düşük olan bu alanların estetik değerleri ve olumlu değerinin artması da bu yolla sağlanabilecektir. Yaşam alanlarının kalitesi, doğa ve doğanın çözümleri değerlendirilerek mümkün kılınır. Doğadan elde edilen kazanımlar birey ve kitlelerin yaşam kalitesi üzerine doğrudan etki eder. Böylece hem yaşam alanlarının toplam memnuniyeti yükselmiş hem memnuniyette süreklilik sağlanmış hem de geleceğe dönük olumlu gelişmeler için umut ve beklentilerin önü açılmış olacaktır.

#### Yazar Katkıları

Bağlan Özel Karaağaç: Çalışma fikri, alan çalışması, literatürün toplanması, yazım

Ömer Atabeyoğlu: Çalışma kurgusu, yöntemin uyarlanması, kontrol ve düzenleme, yazım

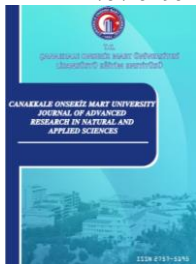
#### Çıkar Çatışması

Yazarlar çıkar çatışması bildirmemişlerdir.

#### Kaynaklar

- Bolten, B., & Barbiero, G. (2020). Biophilic Design: How to Enhance Physical and Psychological Health and Wellbeing in Our Built Environments. *Visions for Sustainability*, 13, 11-16. Erişim adresi: <https://www.ojs.unito.it/index.php/visions/article/view/3829>
- Browning, W., Ryan, C., & C lancy, J. (2014). 14 Patterns of Biophilic Design Improving Health & Well Being in The Built Environment, Terrapin Bright Green LLC. Erişim adresi: <https://www.terrapinbrightgreen.com/wp-content/uploads/2014/09/14-Patterns-of-Biophilic-Design-Terrapin-2014p.pdf>
- Fromm, E. (1964). *The Heart of Man: Its Genius for Good and Evil*. Harper and Row. Erişim adresi: <https://www.amazon.com/Heart-Man-Genius-Good-Evil/dp/1590561864>
- Karavaş, B. (2021). Botanik Bahçelerinin Biyofilik Tasarım Kriterleri Doğrultusunda Değerlendirilmesi: Nezahat Gökyiğit Botanik Bahçesi Örneği. *Kent Akademisi*, 14(3), 545-559. <https://doi.org/10.35674/kent.981889>
- Kellert, S.R., & Wilson, E.O. (1993). *The biophilia hypothesis*. Washington, DC: Island Press. Erişim adresi: <https://islandpress.org/books/biophilia-hypothesis>
- Kellert, S. R. (2005). *Building for Life: Designing and Understanding the Human-Nature Connection*. Island Press. Erişim adresi: <https://www.amazon.com/Building-Life-Understanding-Human-Nature-Connection/dp/1559637218>
- Kellert, S., & Finnegan, B. (2011). *Biophilic Design: The Architecture of Life*. Bullfrog Films.
- Kellert, S., & Calabrese, E. (2015). *The practice of biophilic design*. Terrapin Bright LLC. Erişim adresi: [https://biophilicdesign.umn.edu/sites/biophilic-net-positive.umn.edu/files/2021-09/2015\\_Kellert%20\\_The\\_Practice\\_of\\_Biophilic\\_Design.pdf](https://biophilicdesign.umn.edu/sites/biophilic-net-positive.umn.edu/files/2021-09/2015_Kellert%20_The_Practice_of_Biophilic_Design.pdf)

- Littke, H. (2016). Becoming biophilic: Challenges and opportunities for biophilic urbanism in urban planning policy. *Smart and Sustainable Built Environment*. Erişim adresi: <https://www.emerald.com/insight/content/doi/10.1108/SASBE-10-2015-0036/full/html>
- Özel Karaağaç, B. (2019). *Altınordu kent merkezinin açık-yeşil alanlarının mevcut durumunun değerlendirilmesi* (Yayınlanmamış yüksek lisans tezi). Ordu Üniversitesi, Ordu, Türkiye. Erişim adresi: <https://acikbilim.yok.gov.tr/handle/20.500.12812/102123>
- Özil, M. E., & Aykal, D. (2021). Biyofilik tasarımın Diyarbakır geleneksel konutlarında araştırılması. *Journal of Architectural Sciences and Applications*, 6(1), 45-58. <https://doi.org/10.30785/mbud.801022>
- Ryan, C. O., & Browning, W. D. (2020). Biophilic design. *Sustainable Built Environments*, 43-85. Erişim adresi: [https://link.springer.com/referenceworkentry/10.1007/978-1-0716-0684-1\\_1034](https://link.springer.com/referenceworkentry/10.1007/978-1-0716-0684-1_1034)
- Totaforti, S. (2020). Emerging biophilic urbanism: The value of the human–nature relationship in the urban space. *Sustainability*, 12(13), 5487. <https://doi.org/10.3390/su12135487>
- Yurtgün, Ö. (2020). Biyofilik tasarım kriterlerinin açık ofisler üzerinden değerlendirilmesi. *IDA: International Design and Art Journal* 2.2: 281-296. <https://doi.org/10.52460/issc.2021.050>
- Zhong, W., Schröder, T., & Bekkering, J. (2021). Biophilic design in architecture and its contributions to health, well-being, and sustainability: A critical review. *Frontiers of Architectural Research*. <https://doi.org/10.1016/j.foar.2021.07.006>



# Determination of Protein Amount in Nanosized Synthetic Liposomes by Surface Enhanced Raman Spectroscopy (SERS)

Şeyma Parlatan<sup>1\*</sup>

<sup>1</sup>Istinye University, Vocational School of Health Services, TR-34010, Zeytinburnu, Istanbul, Türkiye

## Article History

Received: 16.04.2023

Accepted: 18.08.2023

Published: 20.12.2023

## Research Article

**Abstract** – Accurate characterization of synthetic liposomes is essential since they give information about the vesicular structures in bodily fluids such as extracellular vesicles. The characterization tasks are generally the determination of the sizes of the liposomes and the profiling of the liposomes' content. Optical tweezers and Surface Enhanced Raman Spectroscopy (SERS) were used to profile the nanosized liposomes. The size distribution of the trapped liposomes (140 nm on average) was found by using Einstein's Brownian motion equation, consistent with the size distribution obtained from dynamic light scattering measurements. Besides, Gramicidin-encapsulated liposomes were measured using SERS, and statistically significant differentiation was found in Raman intensities between liposome populations with altering concentrations of proteins. This study uniquely measured size distributions of nano-sized liposomes with conventional optical tweezers (without plasmonics) and determined the chemical differences between empty and protein encapsulated liposomes with high accuracy using Raman spectroscopy.

**Keywords** – Liposome, optical trapping, surface enhanced Raman spectroscopy, Gramicidin, protein determination

## 1. Introduction

Liposomes are microscopic vesicles enclosing a liquid inner chamber in one or more lipid bilayer layers (lamella). These structures are biocompatible and biodegradable and do not produce an immune response (Laouini et al., 2012). Although it consists of amphiphilic phospholipid molecules, different biomolecules (functional group-linked phospholipid, cholesterol, cell membrane protein, etc.) are added to their structures, such as bioactive substance (drug, vaccine, gene) transport systems. They are widely used in various fields, including protein structure-function relationships and protein-lipid interactions (Laouini et al., 2012; Zhang, 2017). Efficiency and success in use areas depend on the liposome's structure and properties. The structure and properties of liposomes vary significantly according to their molecular contents, sizes, number of layers, charges, and the way they are formed (Alavi et al., 2017, Akbarzadeh et al., 2013). The diameters of liposomes range from 20 nm to a few  $\mu\text{m}$ . They can be classified in to different classes due to their number of layers, small-single-layer (20-100 nm), large-monolayer (>100 nm), very large-monolayer (>1000 nm), and multilayer (> 500 nm). Using monolayer liposomes allows the entrapped molecules to be uniformly stored in a single fluid compartment (Alavi et al., 2017). There are four different phospholipids commonly used in liposome construction. These are PC: Phosphocholine, DPPC: 1,2-dipalmitoyl-sn-glycero-3-phosphocholine, DMPC: 1,2-dimyristoyl-sn-glycero-3-phosphocholine, DLPC: 1,2-dilauroyl -sn-glycero-3-phosphocholine can be listed as DOPC 1,2-dioleoyl-sn-glycero-3-phosphocholine. After G. Gregoriadis (Gregoriadis & Ryman, 1971) proposed that liposomes for use as a drug delivery system, liposome studies advanced technological developments in various fields, especially in mathematics, theoretical physics, biophysics, chemistry, biochemistry, and biology disciplines. With the contribution of new methods and different fields,

<sup>1</sup>  seyma.parlatan@istinye.edu.tr

\*Corresponding Author

many developments such as remote drug loading, extrusion for homogeneous measurements, construction of long-circulation liposomes, and the development of liposomes containing nucleic acid polymers and liposomes containing drug combinations have emerged (Allen & Cullis, 2013) As they can also create model structures for exosomes, liposomes have proven to be very useful in processes that are difficult to understand.

The method used in this study to examine liposomes is optical tweezers. Optical tweezers is a method that was awarded the Nobel Prize in 2018 (Ashkin, 1997) and is based on the principle of momentum transfer to a micrometer or nanometer-sized particles by tightly focusing laser beams with the help of high numerical aperture lenses (Neuman & Block, 2004; Ashkin, 1997). Numerous applications of optical tweezers have been demonstrated over the years. In general, it has been found that this method enables a biological particle to remain undamaged in its environment for a long time, and position measurement allows measurement of optical forces. In one of these applications, studies were carried out using the escape force method utilizing particles with a diameter of 1  $\mu\text{m}$  via optical tweezers (Simon & Libchaber, 1992). In another study, direct observation by optical tweezers of the step movements of kinesin found kinesins to move in 8-nm steps (Svoboda et al., 1993). In addition, the optical tweezers system allowed the mechanical properties of polymers and biopolymers to be studied. The mechanical properties were observed to be consistent with the conventional muscle contraction model (Finer et al., 1994). Optical tweezers have been used to study living systems and biomolecules as well as model systems such as liposomes (cell membrane, exosome, etc.). One of the most interesting applications of these is the use of liposomes produced by the reversible phase evaporation method as a micro-chemistry laboratory with optical tweezers (Kulin et al., 2003). In this study, liposomes containing different types of optically trapped chemicals are combined systematically, and a chemical reaction is initiated with the mixture of their contents. Thus, it can be used as a micro-reactor. In another study, Foo et al. (Foo et al., 2003) showed that phosphatidylcholine liposomes are significantly deformed due to hydrodynamic forces. The mechanical properties of giant liposomes were demonstrated by using the dual optical tweezers method and the optical measurement of force constants by stretching the liposomes (Shitamichi et al., 2009). In two different studies conducted in 2011 and 2014, the chemical transport properties of liposomes, which have an important place in drug targeting, were examined in a controlled manner with the help of optical tweezers (Pinato et al., 2011; Shiomi et al., 2014).

Optical tweezers can also be combined with other analysis methods to examine various properties of trapped particles. Raman spectroscopy was utilized in this study since it is suitable for examining molecular properties of biological particles. In Raman spectroscopy, light scattering occurs by molecules when a monochromatic light from an illumination source interacts with the molecules in the structure of the illuminated sample and results in a fingerprint signal specific to the molecules inside the sample of interest. Many essential studies and applications have been made in biology and medicine with Raman spectroscopy. A study visualized the relationship of living cells with DNA with phosphate stretch vibration and proteins with amide I vibration (Cheng et al., 2002). Besides, water with OH stretch vibration (Dufresne et al., 2003) and lipidic reactions with CH stretch vibration have been observed (Nan et al., 2006). In addition to these studies, vibrational imaging of bilayer lipids has been achieved (Potma & Xie, 2003). Raman scattering has also created a powerful imaging method to study tissues in living organisms (Evans et al., 2005). Cherney and his team examined liposomes of 0.6  $\mu\text{m}$  (Cherney et al., 2003) and 3  $\mu\text{m}$  in diameter (Cherney et al., 2004) produced from different types of phospholipids (DMPC, DPPC, DLPC, DOPC) by Raman tweezers method in two studies conducted in 2003 and 2004. Following this study, extensive studies were conducted with particles 0.5  $\mu\text{m}$  in diameter and above with Raman tweezers (Hotani et al., 1999; Spyratou et al., 2015; Penders et al., 2018; Chan et al., 2005). Raman tweezers studies were also carried out by producing liposomes with diameters between 50 and 200 nm at submicron scale. In one of them, Kruglik trapped 50, 100, 200, and 400 nm liposomes to model the exosome behavior and studied Raman spectra (Kruglik et al., 2019). In this study, Kruglik determined the concentrations of these liposomes using the spectral ratios of CH<sub>2</sub> (1440) and H<sub>2</sub>O (1640) bond strengths.

Since spontaneous Raman is a method produces a weak signal, an amplification mechanism is necessary to extract information from the nanosized particles, which contains low volume of material, generally not sufficient to obtain observable spectra. We propose to apply Surface Enhanced Raman Spectroscopy (SERS), a special form of Raman spectroscopy to enhance molecular vibrations by matching the incident electromagnetic wave's frequency with the localized surface plasmons resonance frequency which occurs very

close to the metal surface (5-40 nm) (Stiles et al., 2008). Recently, it has been investigated how SERS efficiency increases with aptamer (Kim et al., 2010), gold nanostar (Lee et al., 2014), nanorod (Chaney et al., 2005), nanoshell (Jackson et al., 2003), nanoparticle (Kneipp et al., 2002) doped applications. Metal nanoshells are a class of nanoparticles with tunable optical resonances. In the article (Hirsch et al., 2003) an application of this technology to thermal ablative therapy for cancer is described. In another article, they carried out the first measurements of a solid-supported lipid bilayer on a SERS-active substrate and characterized the bilayer using SERS, atomic force microscopy, surface plasmon resonance spectroscopy, ellipsometry, and fluorescence recovery after photobleaching (Bruzas, 2019).

In this study, optical tweezers and SERS were applied to determine the size distributions of the vesicles and the amount of proteins inside PC liposomes. To our knowledge, this is the first application of SERS-tweezers on quantification of proteins in lipid nanovesicles. This study especially important for being a model for extracellular vesicle studies, which became quite impactful in the area of cancer research.

## 2. Materials and Methods

### 2.1. Generation of AuNP-free liposomes

A thin lipid film was formed to form AuNP-free liposomes (Kılıç, 2017). For this, 40  $\mu$ L of the phosphatidylcholine (PC, Figure 1A) stock solution (2.5 mg/mL) prepared in chloroform was poured into a round-bottomed flask (100 mL), and a thin film was formed by evaporating the chloroform under nitrogen gas by manually rotating it. Large, multilamellar liposomes (Large Multilamellar Vesicles, LMV) were then obtained by vigorously mixing the lipid layer by vortexing for 15 minutes in phosphate buffer (PBS; pH: 7.4 and 0.01 M).

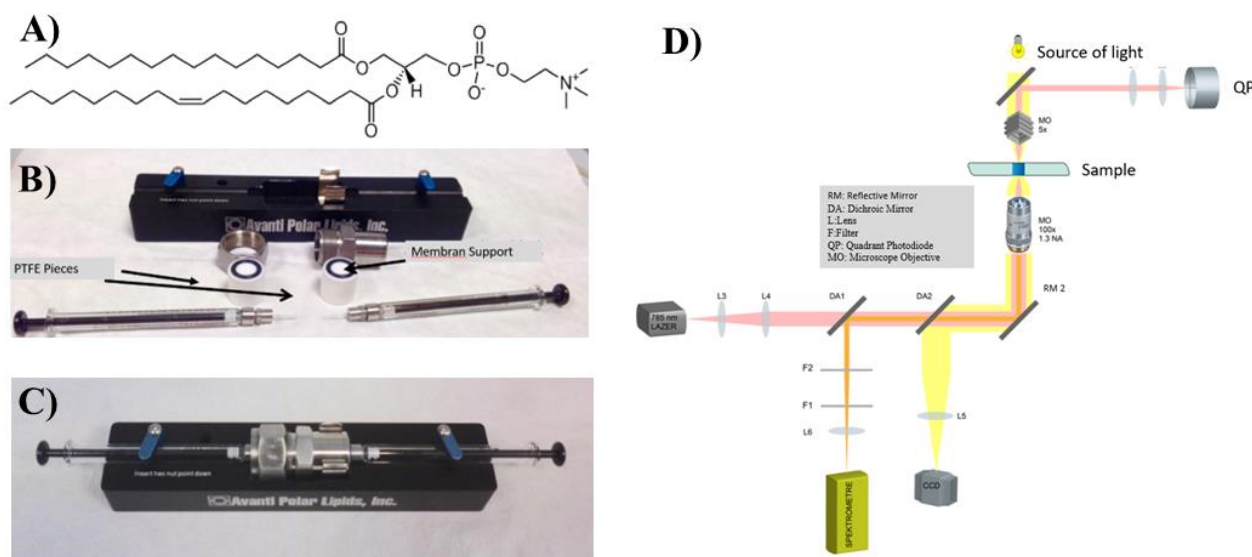


Figure 1. A) Structure of the phosphatidylcholine molecule. B) Mini extruder system components and C) combined view. D) Raman tweezers experimental setup.

The extrusion method was used to obtain a monolayer liposome (Small Unilamellar Vesicles, SUV) (Avanti Mini-Extruder, Figures 1-B and 1-C). For this, the LMV solution was passed through the polycarbonate membrane placed in the center of the extrusion system 21 times with syringes on both sides. Membranes with different pore sizes (50-1000 nm) were used to form liposomes of different sizes. The resulting LMV or SUV liposomes were stored in the falcon at +4 °C and used within 1-3 days after production (Kılıç & Kok, 2019).

### 2.2. Experimental setup

The Raman tweezers experimental setup, in which the liposomes are characterized, is given in Figure 1D and is basically built around a 785 nm, 500 mW single-mode diode laser, spectrometer, and microscope. In the

experimental setup, the 785 nm laser beam is directed to the microscope objective with the help of suitable lenses and reflective mirrors. The laser beam focused through the microscope objective (100x, 1.3 NA) reaches the sample. The rays passing through the sample reach the quadrant photodiode with the help of a reflective mirror (RM1) and lenses (L1, L2). The beams emitted from the white light source pass through the sample using lenses (L) and reach the CCD camera via the dichroic mirror (DA 2). Since the dichroic mirror (DA 2) has a long pass filter allowing beams with wavelengths larger than 650 nm, visible light below 650 nm is reflected. This beam is imaged on the camera as light with a wavelength greater than 650 nm passes through the mirror. The rays scattered from the sample are delivered to the spectrometer with the help of a reflective mirror (RM 2), dichroic mirror (DA 1), and filters (F1, F2). Since the dichroic mirror (DA1) has the property of transmitting wavelengths shorter than 805 nm, light above 805 nm wavelength is reflected and directed towards the spectrometer. Since the Raman scattering lights will have a wavelength above 785 nm, only Raman scattering beams reach the spectrometer.

### 2.3. Raman tweezers characterization of produced liposomes

The Raman spectra were acquired 14 times with a 30-second signal acquisition time for Raman, and the time average of the spectra was taken. The averaged spectra were normalized after baseline and background correction preprocessing and the statistical analysis was started. The signal collection time was planned to be 2 seconds in the SERS application.

## 3. Results and Discussion

### 3.1. Tweezers calibration with 5 $\mu\text{m}$ silicon beads

In optical tweezers experiments, calibration experiments are performed to qualitatively determine the magnitude of the optical force transferred to the laser tweezer particles. The calibration experiments find the size of the spring constant in the optical tweezers force, which conforms to Hooke's law. Thus, the change in optical force can be recorded by monitoring the center of mass changes. For silica beads with a diameter of 5  $\mu\text{m}$ , a linear variation of the spring constant versus laser power results from repeated calibration. The spring constant of the system depends on the laser power, where  $k = 0.16075 \cdot P + 3.7 \text{ pN}/\mu\text{m}$ .

Here the power values are the percentage values relative to the highest power reaching the sample plane. In the preliminary study, the system was gradually calibrated up to 100 nm, starting from test particles with a diameter of 5 micrometers, then readied for calibration of the forces acting on the nanometer-sized liposomes.

By adding Quadrant Photodetector (QPD) to the system, the Brownian motion of the particle in the sample plane was followed by voltage information based on the method known as back focal plane interferometry (back focal plane interferometry) in the literature. Since the commercial system allows the movement of the laser focus in a controlled manner, the voltage-position (V-X) relationship was found by moving a trapped particle linearly throughout the entire observation area (Figure 2A). When the linear region marked in blue in this graph is fit, the beta coefficient, which is directly related to the spring constant of the optical force, is obtained (Figure 2B).

### 3.2. Multilayer liposome measurements

The sample was prepared with liposomes called large multilamellar vesicles (LMV), and the Brownian motion of particles 1-3  $\mu\text{m}$  in diameter was measured. As a result of two different experiments, spring constants of 80-100 mW (Figure 2C) and then 40-70 mW (Figure 2D) were found. The size values of the measured liposomes were measured with the aid of a CCD camera using the device software. Experiments were continued by taking measurements from a region with no visible particles and observing that there was no voltage change. In addition, the Stokes-Einstein (1) diffusion equation given in equation 1 was used to determine the diameters of the trapped particles:

$$D = \frac{k_B T}{\gamma} \quad (3.1)$$

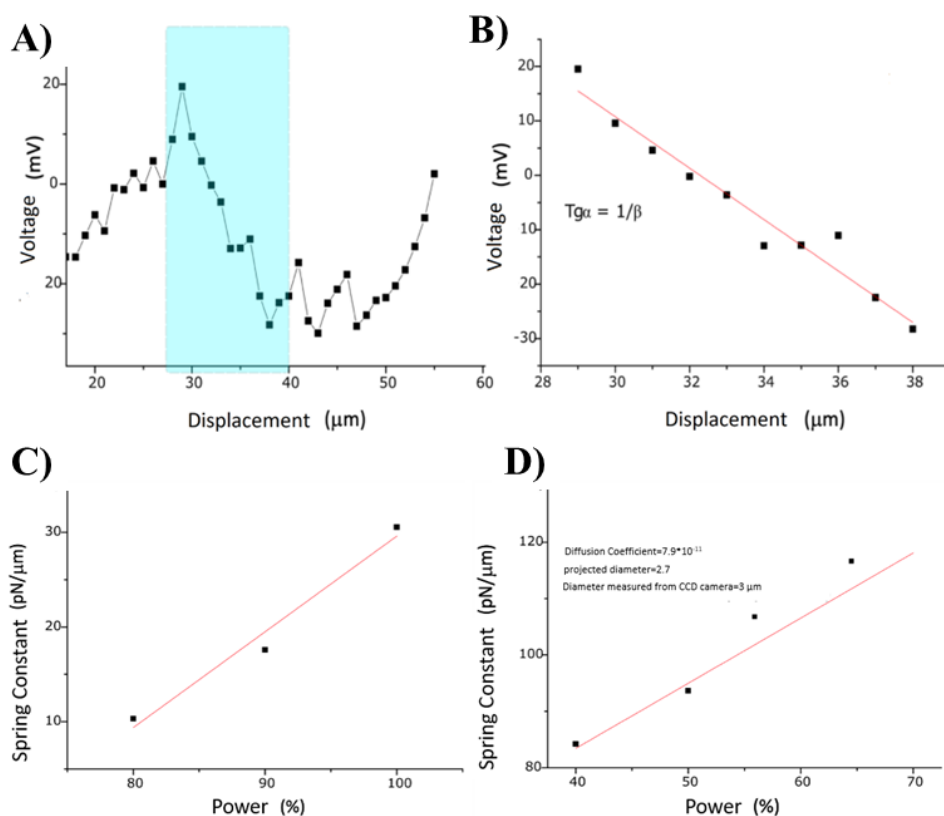


Figure 2. Calibration with QPD A) Voltage-displacement curve B) Linear fit on the selected region. Spring constant vs laser power calibration were measured for C) small unilamellar vesicles D) large multilamellar vesicles.

Here,  $k_B$ ,  $T$ , and  $\gamma$  are Boltzmann's constant ( $\text{m}^2 \cdot \text{kg} \cdot \text{s}^{-2} \cdot \text{K}^{-1}$ ), ambient temperature (K), and fluid friction coefficients, respectively. ( $\text{m} \cdot \text{Pa} \cdot \text{s}$ ). Since  $\gamma = 6\pi r\eta$ , the radius  $r$  value can be left alone and the fitted  $D$  value can be used. The open source optical tweezers power spectrum fit program named CPC package was used for the fit process (Hansen et al., 2006; Tolić-Nørrelykke et al., 2004).

### 3.3. Monolayer liposome measurements

Preliminary studies continued with experiments at SUVs with an average diameter of 100 nm. At this stage, since the particles cannot be seen with the naked eye under the microscope (due to the diffraction limit), voltage signals were followed, and the entry of the particles into the trap was indirectly investigated. Figure 3A and B shows the position signal distribution from QPD with and without particles in the trap. The variance decreases dramatically when the particle enters the trap. In the first case, the variance was  $2.1055e-16$ , with the particle in the trap was  $1.9936e-17$ .

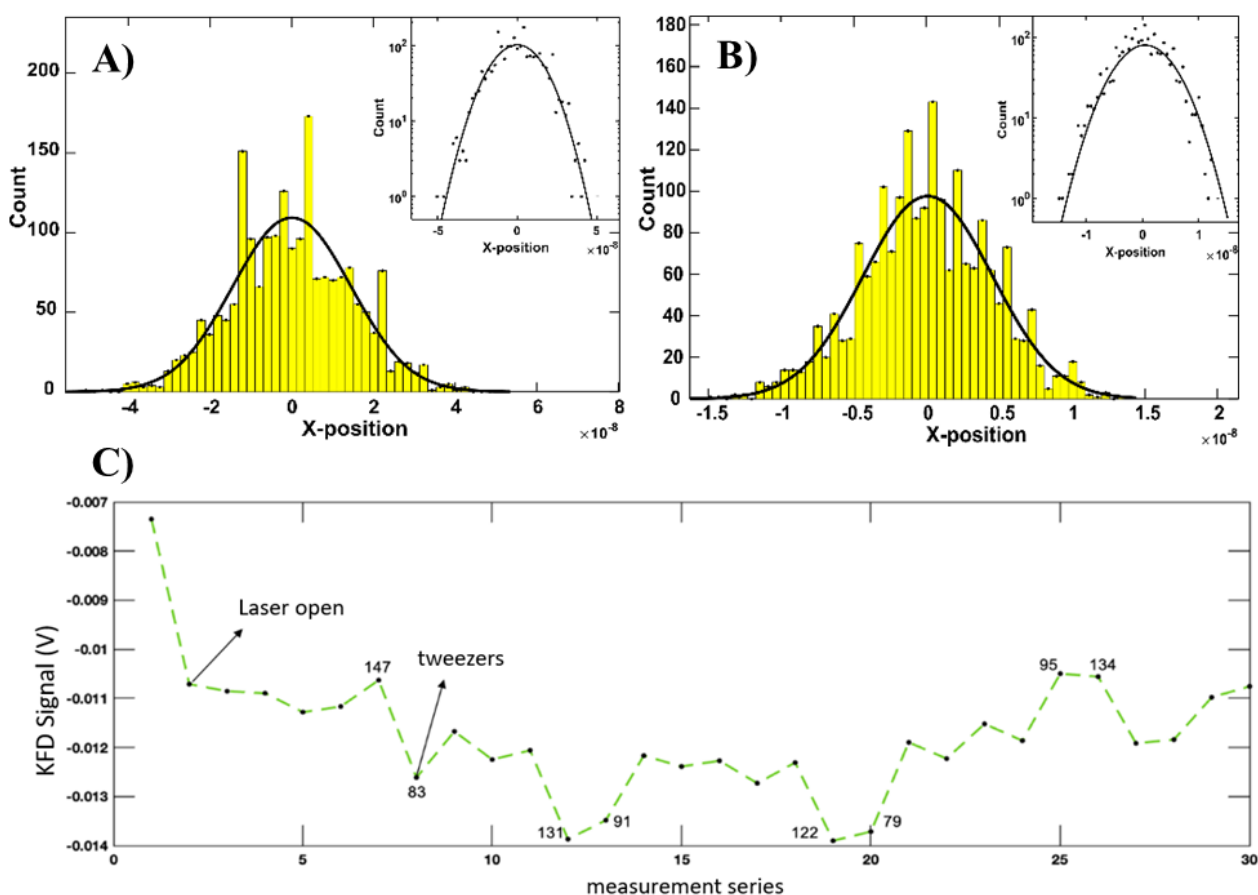


Figure 3. Position distribution with particle A) absent and B) present in the trap. C) Graph of calculated signal averages for understanding tweezers events.

150 consecutive oscilloscope recordings were made for each measurement. In the first recording, noise measurements were taken when the devices and laser trapping were turned off. In the second recording, the devices and laser were turned on with no trap. In the third measurement, the trapping events were recorded using the averages of five and the QPD voltage signal was compared with the measurement taken when the laser was turned on ( $t=0$ ). Figure 3C shows the average signal graph described.

By using corner frequencies and diffusion coefficients obtained as a result of Brownian motion tracking of liposomes, spring constant and estimated diameter values were obtained as in previous experiments. Estimated diameter values are given in nm around the data points on Figure 4. The spring constant value was found to be  $11.98 \pm 0.57 \text{ pN}/\mu\text{m}$  against 80% laser power. Figure 4 gives the diameter distributions obtained in optical tweezers studies of the liposomes produced with membranes with a pore diameter of 100 nm. Accordingly, the peak of the distribution obtained was around 140-150 nm, which is in agreement with the 140 nm result obtained previously as a result of the zeta-sizer measurement with the same type of membranes.

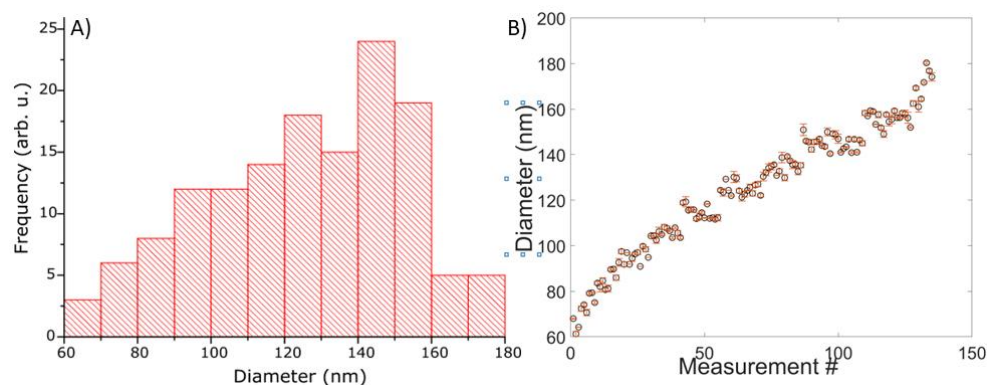


Figure 4. a) Histogram for diameter distributions of liposomes obtained with optical tweezers, 100 nm pore diameter membrane. b) Averages and standard errors of individual vesicle measurements.

SERS spectra of the liposomes produced in the study were also obtained. The surface plasmon resonance wavelength 785 nm obtained from Oceans was measured by drying 15  $\mu$ L liposome samples on gold surfaces and measured using Oceans QE Raman spectrometer in a similar setup as in Figure 1D, with collection times of 3 seconds. Since it is not possible to determine in which regions the liposomes bind on the surface with optical imaging (Liposome diameters are smaller than the diffraction limit of our microscope, which is 740 nm), a Raman map was obtained by scanning a 1.4 mm X 1.4 mm region on the surface. A model protein, Gramicidin, was used to test the potential of Raman microscopy to distinguish liposomes containing different biomolecules. The analyses performed by producing 1% and 10% Gramicidin-containing liposomes by volume determined that liposomes with and without Gramicidin showed different properties. Analysis results are given in Figure 5 B-D. Figure 5B and C shows that the classification accuracy is high, and the analysis showed 20 misclassified measurements among 3888 measurements taken from three different groups. Fig 5D also confirms that the principal components' distribution is well-clustered, with minor in-group variances and large between-group variances, which provided the accuracy we obtained from the analysis.

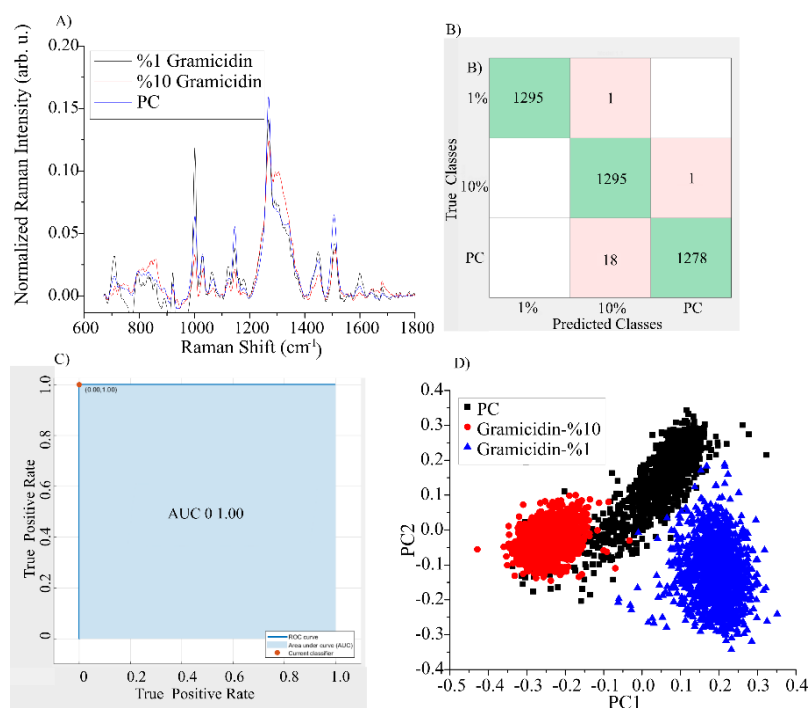


Figure 5. A) Comparison of Raman signals of averaged and L2 normalized PC liposome and liposomes containing 1% and 10% Gramicidin protein. B) Confusion table for test results after LDA analysis. C) ROC plot for LDA analysis. The area under the curve = 1.00. D) Principal component analysis (PCA) comparison of groups.

In this study, the size distribution of the vesicles was determined by optical tweezers using Einstein's diffusion coefficient equation utilizing the displacements of the individual particles inside the trap. This technique was demonstrated for the determination of trap stiffness (Gieseler et al., 2021, Viana et al., 2007, Singer et al., 2000) and the calculation of cell biomechanics (Serafetinides et al., 2013, Pesen et al., 2022, Zhang et al., 2019) before. To the author's knowledge, this is the first demonstration of the estimation of nanoliposomes' diameters by optical tweezers. Besides, the content of the vesicle was analyzed by surface-enhanced Raman spectroscopy. The author found that the signal from the lipid bilayer could be differentiated from the total liposome signal with protein with 1% and 10% concentration. As demonstrated before (Tukova et al., 2021), SERS analysis is sensitive in investigating liposome-protein systems. Here, the author presents a workflow to fully characterize nano-vesicles via SERS-tweezers, which paves the way towards label-free integrated extracellular vesicle analysis, which is important for cancer research.

#### 4. Conclusion

Characterization of nanosized vesicles smaller than 200 nm is challenging due to their small sizes, which is a limitation for optical methods due to the diffraction limit. Besides, the non-optical methods are generally low-throughput and generally do not give sensitive content information. Our Raman tweezers approach brought three advantages: i) The size distribution is sensitively measured using Brownian motion. ii) Content of the nanosized liposomes was measured using Raman spectroscopy. iii) With the help of machine learning methods, untrained protein concentrations can be potentially calculated. These synthetic vesicle measurements have the potential to simulate the extracellular vesicles, especially exosomes, present in the bodily fluids. Since the precise characterization of the exosomes are crucial for cancer diagnosis, a model experiment is highly important and our method shows that the controllable addition of cargo contents into syntenic liposomes and their Raman measurements may provide more accurate cancer diagnosis platforms.

#### Acknowledgement

The author thanks Boğazici University BUMILAB for their permission to perform the measurements in their facilities. The author thanks Şebnem Seherler for their help in the preparation of the liposomes.

#### Author Contributions

Şeyma Parlatan: Planning of the study, data collection and analysis, statistical analysis and article writing

#### Conflicts of Interest

The author declares no conflict of interest.

#### References

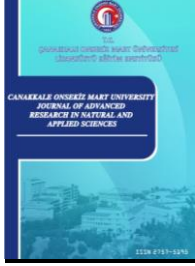
- Akbarzadeh, A., Sadabady, R.R., Davaran, S., Joo, S. W., Zarghami, N., Hanifehpour, Y., Samiei, M., Kouhi, M., Nejati-Koshk, K., (2013). Liposome: classification, preparation, and applications. *Nanoscale research letters*, 8(1), 1-9. Retrieved from: <https://doi.org/10.1186/1556-276X-8-102>
- Alavi, M., Karimi, N., Safaei, M., (2017). Application of various types of liposomes in drug delivery systems. *Advanced pharmaceutical bulletin*, 7(1), 3-9, Retrieved from: <https://doi.org/10.15171/apb.2017.002>
- Allen, T.M., Cullis, P.R., (2013). Liposomal drug delivery systems: from concept to clinical applications. *Advanced drug delivery reviews*, 65(1), 36-48. Retrieved from: <https://doi.org/10.1016/j.addr.2012.09.037>
- Ashkin, A., (1997). Optical trapping and manipulation of neutral particles using lasers. *Proceedings of the National Academy of Sciences*, 94(10), 4853-4860. Retrieved from: <https://doi.org/10.1073/pnas.94.10.4853>
- Bruzas, I., Brinson, B. E., Gorunmez, Z., Lum, W., Ringe, E., & Sagle, L. (2019). Surface-enhanced Raman spectroscopy of fluid-supported lipid bilayers. *ACS applied materials & interfaces*, 11(36), 33442-33451.

- Chan, J.W., Winhold, H., Lane, S.M., Huser, T., (2005). Optical trapping and coherent anti-Stokes Raman scattering (CARS) spectroscopy of submicron-size particles. *IEEE Journal of selected topics in quantum electronics*, 11(4), 858-863. Retrieved from: <https://doi.org/10.1109/JSTQE.2005.857381>
- Chaney, S.B., Shanmukh, S., Dluhy, R.A., Zhao, Y.P., (2005). Aligned silver nanorod arrays produce high sensitivity surface-enhanced Raman spectroscopy substrates. *Applied Physics Letters*, 87(3), 031908. Retrieved from: <https://doi.org/10.1063/1.1988980>
- Cheng, J.-X., Jia, Y.K., Zheng, G., Xie, X. S., (2002). Laser-scanning coherent anti-Stokes Raman scattering microscopy and applications to cell biology. *Biophysical journal*, 83(1), 502-509. Retrieved from: [https://doi.org/10.1016/S0006-3495\(02\)75186-2](https://doi.org/10.1016/S0006-3495(02)75186-2)
- Cherney, D.P., Conboy, J.C., Harris, J.M., (2003). Optical-trapping Raman microscopy detection of single unilamellar lipid vesicles. *Analytical chemistry*, 75(23),6621-6628. Retrieved from:<https://doi.org/10.1021/ac034838r>
- Cherney, D.P., Bridges, T.E., Harris, J.M., (2004). Optical trapping of unilamellar phospholipid vesicles: investigation of the effect of optical forces on the lipid membrane shape by confocal-Raman microscopy. *Analytical chemistry*, 76(17), 4920-4928. Retrieved from: <https://doi.org/10.1021/ac0492620>
- Dufresne, E.R., Corwin, E. I., Greenblatt, N. A., Ashmore, J., Wang, D. Y. , Dinsmore, A. D., Cheng, J. X., Xie, X. S., Hutchinson, J. W., Weitz, D. A.,(2003). Flow and fracture in drying nanoparticle suspensions. *Physical review letters*, 91(22), 224501. Retrieved from: <https://doi.org/10.1103/PhysRevLett.91.224501>
- Evans, C.L., Potma, E.O., Puoris'haag, M., Xie, X.S., (2005). Chemical imaging of tissue in vivo with video-rate coherent anti-Stokes Raman scattering microscopy. *Proceedings of the national academy of sciences*, 102(46),16807-16812. Retrieved from: <https://doi.org/10.1073/pnas.0508282102>
- Finer, J.T., Simmons, R.M., Spudich, J.A., (1994). Single myosin molecule mechanics: piconewton forces and nanometre steps. *Nature*, 368(6467), 113-119. Retrieved from: <https://doi.org/10.1038/368113a0>
- Foo, J.-J., Liu, K.-K., Chan, V., (2003). Thermal effect on a viscously deformed liposome in a laser trap. *Annals of biomedical engineering*, 31(3), 354-362. Retrieved from: <https://doi.org/10.1114/1.1555626>.
- Gieseler J., Gomez-Solano J. R., Magazzù A., Castillo I. P., Laura Pérez García, Marta Gironella-Torrent, Xavier Viader-Godoy, Felix Ritort, Giuseppe Pesce, Alejandro V. Arzola, Karen Volke-Sepúlveda, and Giovanni Volpe, "Optical tweezers — from calibration to applications: a tutorial," *Adv. Opt. Photon.* 13, 74-241 (2021)
- Gregoriadis, G., Ryman, B., (1971). Liposomes as carriers of enzymes or drugs: a new approach to the treatment of storage diseases. *Biochemical Journal*, 124(5),58P-58P. Retrieved from: <https://doi.org/10.1042/bj1240058p>
- Hansen,P.M., Tolić-Nørrelykke, I.M., Flyvbjerg, H., Berg-Sørensen, K., (2006). tweezercalib 2.0: Faster version of MatLab package for precise calibration of optical tweezers. *Computer physics communications*, 174(6), 518-520. Retrieved from: <https://doi.org/10.1016/j.cpc.2005.11.007>
- Hirsch, L.R., Stafford, R.J., Bankson, J.A., Sershen, S.R., Rivera, B., Price, R.E., Hazle, J.D., Halas, N.J., West, J.L., (2003) Nanoshell-mediated near-infrared thermal therapy of tumors under magnetic resonance guidance, 100 (23) 13549-13554, Retrieved from: <https://doi.org/10.1073/pnas.2232479100>
- Hotani, H., Nomura, F., Suzuki, Y., (1999). Giant liposomes: from membrane dynamics to cell morphogenesis. *Current opinion in colloid & interface science*, 4(5), 358-368. Retrieved from: [https://doi.org/10.1016/S1359-0294\(99\)90021-3](https://doi.org/10.1016/S1359-0294(99)90021-3)
- Jackson, J.B., Westcott, S.L., Hirsch, L.R., West, J.L., Halas,N.,J., (2003). Controlling the surface enhanced Raman effect via the nanoshell geometry. *Applied Physics Letters*, 82(2), 257-259. Retrieved from: <https://doi.org/10.1063/1.1534916>
- Kılıç A., Kok, F.N., (2019). Peptide-functionalized supported lipid bilayers to construct cell membrane mimicking interfaces. *Colloids and Surfaces B: Biointerfaces*, 176, 18-26. Retrieved from:

<https://doi.org/10.1016/j.colsurfb.2018.12.052>

- Kılıç, A., Jadidi, M.F., Özer, H. Ö., Kök, F.N., (2017). The effect of thiolated phospholipids on formation of supported lipid bilayers on gold substrates investigated by surface-sensitive methods. *Colloids and Surfaces B: Biointerfaces*, 160, 117-125. Retrieved from: <https://doi.org/10.1016/j.colsurfb.2017.09.016>
- Kim, N.H., Lee, S.J., Moskovits, M., (2010). Aptamer-mediated surface-enhanced Raman spectroscopy intensity amplification. *Nano letters*, 10(10), 4181-4185. Retrieved from: <https://doi.org/10.1021/nl102495j>
- Kneipp, K., et al., (2002). Surface-enhanced Raman spectroscopy in single living cells using gold nanoparticles. *Applied Spectroscopy*, 56(2),150-154.
- Kruglik, S.G., et al., (2019). Raman tweezers microspectroscopy of circa 100 nm extracellular vesicles. *Nanoscale*, 11(4), 1661-1679. Retrieved from: <https://doi.org/10.1039/C8NR04677H>
- Kulin, S., Kishore, R., Helmerson, K., Locascio, L., (2003). Optical manipulation and fusion of liposomes as microreactors. *Langmuir*, 19(20), 8206-8210. Retrieved from: <https://doi.org/10.1021/la0344433>
- Laouini, A., Jaafar-Maalej, C., Limayem-Blouza, I., Sfar, S., Charcosset, C., Fessi, H., (2012). Preparation, characterization and applications of liposomes: state of the art. *Journal of Colloid Science and Biotechnology*, 1(2), 147-168. Retrieved from: <https://doi.org/10.1166/jcsb.2012.1020>
- Lee, J., Hua, B., Park, S., Ha, M., Lee, Y., Fan, Z., Ko, H., (2014). Tailoring surface plasmons of high-density gold nanostar assemblies on metal films for surface-enhanced Raman spectroscopy. *Nanoscale*, 6(1), 616-623. Retrieved from: <https://doi.org/10.1039/C3NR04752K>
- Nan, X., Potma, E.O., Xie, X.S., (2006). Nonperturbative chemical imaging of organelle transport in living cells with coherent anti-stokes Raman scattering microscopy. *Biophysical journal*, 91(2), 728-735. Retrieved from: <https://doi.org/10.1529/biophysj.105.074534>
- Neuman, K.C., Block, S.M., (2004). Optical trapping. *Review of scientific instruments*, 75(9), 2787-2809. Retrieved from: <https://doi.org/10.1063/1.1785844>
- Pesen, T., Haydaroglu, M., Capar, S., Parlatan, U., & Unlu, M. B. (2022). Comparison of the human's and camel's erythrocyte deformability by optical tweezers and Raman spectroscopy. *bioRxiv*, 2022-08.
- Penders, J., Pence, I.J., Horgan, C.C., Bergholt, M.S., Wood, C.S., Najer, A., Kauscher, U., Nagelkerke, A. and Stevens, M.M., (2018). Single particle automated raman trapping analysis. *Nature communications*, 9(1), 1-11.
- Pinato, G., Raffaelli, T., D'Este, E., Tavano, F., & Cojoc, D. (2011). Optical delivery of liposome encapsulated chemical stimuli to neuronal cells. *Journal of biomedical optics*, 16(9), 095001-095001. Retrieved from: <https://doi.org/10.1117/1.3616133>
- Potma, E. O., Xie, X. S., (2003). Detection of single lipid bilayers with coherent anti-Stokes Raman scattering (CARS) microscopy. *Journal of Raman spectroscopy*, 34(9), 642-650. Retrieved from: <https://doi.org/10.1002/jrs.1045>
- Raman, C. V., Krishnan, K. S., (1928). A new type of secondary radiation. *Nature*, 121(3048), 501-502.
- Serafetinides, A. A., Makropoulou, M., & Spyratou, E. (2013, March). Optical tweezers and cell biomechanics in macro-and nano-scale. In 17th International School on Quantum Electronics: Laser Physics and Applications (Vol. 8770, pp. 309-321). SPIE.
- Shiomi, H., Tsuda, S., Suzuki, H., & Yomo, T. (2014). Liposome-based liquid handling platform featuring addition, mixing, and aliquoting of femtoliter volumes. *PLoS One*, 9(7), e101820. Retrieved from: <https://doi.org/10.1371/journal.pone.0101820>
- Shitamichi, Y., Ichikawa, M., & Kimura, Y., (2009). Mechanical properties of a giant liposome studied using optical tweezers. *Chemical Physics Letters*, 479(4-6), 274-278. Retrieved from: <https://doi.org/10.1016/j.cplett.2009.08.018>
- Simon, A., Libchaber, A. (1992). Escape and synchronization of a Brownian particle. *Physical review letters*, 68(23), 3375. Retrieved from: <https://doi.org/10.1103/PhysRevLett.68.3375>

- Singer, W., Bernet, S., Hecker, N., & Ritsch-Marte, M. (2000). Three-dimensional force calibration of optical tweezers. *Journal of Modern Optics*, 47(14-15), 2921-2931.
- Spyratou, E., Cunaj, E., Tsigaridas, G., Mourelatou, E. A., Demetzos, C., Serafetinides, A. A., Makropoulou, M. (2015). Measurements of liposome biomechanical properties by combining line optical tweezers and dielectrophoresis. *Journal of Liposome Research*, 25(3),202-210.
- Stiles, P. L., Dieringer, J. A., Shah, N. C., & Van Duyne, R. P., (2008). Surface-enhanced Raman spectroscopy. *Annu. Rev. Anal. Chem.*, 1, 601-626. Retrieved from: <https://doi.org/10.1146/annurev.anchem.1.031207.112814>
- Svoboda, K., Schmidt, C. F., Schnapp, B. J., & Block, S. M. (1993). Direct observation of kinesin stepping by optical trapping interferometry. *Nature*, 365(6448), 721-727.
- Tolić-Nørrelykke, I. M., Berg-Sørensen, K., & Flyvbjerg, H. (2004). MatLab program for precision calibration of optical tweezers. *Computer physics communications*, 159(3), 225-240. Retrieved from:<https://doi.org/10.1016/j.cpc.2004.02.012>
- Tukova, A., & Rodger, A. (2021). Spectroscopy of model-membrane liposome-protein systems: complementarity of linear dichroism, circular dichroism, fluorescence and SERS. *Emerging Topics in Life Sciences*, 5(1), 61-75.
- Viana, N. B., Rocha, M. S., Mesquita, O. N., Mazolli, A., Neto, P. M., & Nussenzeig, H. M. (2007). Towards absolute calibration of optical tweezers. *Physical Review E*, 75(2), 021914.
- Zhang, H. (2017). Thin-film hydration followed by extrusion method for liposome preparation. *Liposomes: Methods and protocols*, 17-22.
- Zhang, S., Gibson, L. J., Stilgoe, A. B., Nieminen, T. A., & Rubinsztein-Dunlop, H. (2019). Measuring local properties inside a cell-mimicking structure using rotating optical tweezers. *Journal of Biophotonics*, 12(7), e201900022.



# Investigation of Chlorophyll Mutations in Gamma Irradiated Naked Barley Genotypes

Namuk Ergün<sup>1,\*</sup>, Güray Akdoğan<sup>2</sup>, Saime Ünver İkincikarakaya<sup>3</sup>

<sup>1</sup>Department of Breeding and Genetics, Central Research Institute for Field Crops, Ankara, Türkiye

<sup>2,3</sup>Department of Field Crops, Faculty of Agriculture, Ankara University, Ankara, Türkiye

## Article History

Received: 24.04.2023

Accepted: 10.07.2023

Published: 20.12.2023

## Research Article

**Abstract** – The consumption of naked barley is significantly increasing as more people become aware of its beneficial role as a source of dietary fiber and  $\beta$ -glucan. As a result, breeding programs paid more attention to naked barley. Improvement of yield and quality of naked barley is hindered by the lack of available germplasm. Mutation breeding is an effective tool for generating variation for plant breeding. Chlorophyll mutations are often used as visual indicators in breeding research to determine the optimum mutagen dosage. The purpose of this study was to identify the types and frequency of chlorophyll mutations brought on by different gamma radiation doses in two genotypes of hullless barley and determine the effective dose ( $ED_{50}$ ) based on the mutation frequency. Seeds of naked barley line YAA7050-14 and cv. Yalin that have been irradiated with doses of 100, 150, 200, and 300 Gy gamma rays delivered by a Cobalt-60 source. Chlorophyll mutations were observed in 8-day-old  $M_2$  plants grown under greenhouse conditions. In the  $M_2$  plants of cv. Yalin, the highest mutagen frequency was observed at 250 and 300 Gy, while in line YAA7050-14, the highest mutation frequency was found at 300 Gy. The rate of chlorophyll mutation rose in both genotypes as the gamma ray doses increased. The *albino* type of chlorophyll mutation was found in the cv. Yalin at the greatest rate, whereas the *xantha* type was found in the line YAA7050-14. The most common chlorophyll mutation type was *albino*, while the least common type was *viridis* when both genotypes were considered together. Based on the mutation frequency, 250-300 Gy doses could be used to effectively in further research to create mutations in the naked barley genotypes.

**Keywords** – Chlorophyll mutations, gamma irradiation,  $M_2$  plants, naked barley

## 1. Introduction

Barley (*Hordeum vulgare* L.) is one of the oldest cultivated plants, which has been consumed as food for years (Badr et al., 2000, Lev-Yadun et al., 2000). Approximately, 3% of the barley produced worldwide is used as food in the world (Ullrich, 2011). Furthermore, the barley consumption is increasing day by day because functional foods are highly demandable by consumers. Barley is one of the functional ingredients since it is rich in dietary fibre and high beta-glucan (Bhatty, 1999). Naked (hullless) barley is preferred over hulled barley by food industry because (Newman & Newman, 2008) their hull and grain are easily separated from each other (Meints & Hayes, 2019) therefore grains are easily processed into food products. This technological characteristic plays the most important role in consuming naked barley as food (Meints et al., 2021).

The popularity of naked barley has encouraged breeders to increase their efforts to improve the yield and food quality of naked barley. Although it is possible to cross with naked barley in breeding studies, it is necessary to broaden the variation to obtain superior individuals in terms of yield and quality. One of the most effective

<sup>1</sup> namuk.ergun@tarimorman.gov.tr

<sup>2</sup> gakdogan@agri.ankara.edu.tr

<sup>3</sup> sunver@agri.ankara.edu.tr

\*Corresponding Author

ways of creating genetic variation required for naked barley breeding studies is mutation breeding (Chaudhary et al., 2019; Dyulgerova & Dyulgerov, 2022).

To achieve sufficient and effective variation in the plant species and cultivars in mutation breeding, it is important to determine the source of the mutagen to be used and the effective dose to be used in advance (Maluszynski et al., 2009) because the effective dose of mutagen depend on the plant species and cultivars (Nazarenko & Lykholat, 2020). In general, the rate of germinated or surviving plants (Ahumada-Flores et al., 2020), the rate of plant developmental retardation (Kodym et al., 2012) and the rate of chlorophyll mutations (Çiftçi & Şenay 2005) are used to determine effective doses and mutation frequencies. Chlorophyll mutations are successfully used as genetic markers in plant breeding programs to reveal the effects of mutagens and how the target genotype responds to the mutagen (Wani et al., 2011).

Chlorophylls are essential pigments used by the plant during photosynthesis (Yu et al., 2014). Due to the inhibition of photosynthesis, chlorophyll mutations are often lethal to plants (Wani et al., 2011). Hence, they are generally not useful for plant breeding. However, research on chlorophyll mutations could be useful to determine suitable mutagens and effective mutagen doses to increase genetic variability and agriculturally important mutations in plant species. Therefore, chlorophyll mutation scores are reliable indices for assessing the genetic effects of mutagenic treatments (Goyal et al., 2019). Depending on how the pigments of chlorophyll are affected by mutagens, the occurrence of chlorophyll mutations varies. Gustafsson (1940), classified the chlorophyll mutations obtained as *albino*, *xantha*, *alboviridis*, *viridis*, *tigrina*, *striata*, *maculata*, unidentified mutation, and plasma mutations into nine categories. Although some researchers have modified this classification, it is still the most common classifications in determining the mutation frequency in barley and other cereals.

This study aimed to determine how gamma radiation affects the frequency and range of chlorophyll mutations in the M<sub>2</sub> generation of two naked barley genotypes and the effective dose of gamma radiation that could be used in naked barley breeding.

## 2. Materials and Methods

Naked barley cultivar (cv.) Yalin and the naked barley line YAA7050-14 developed by the Central Research Institute for Field Crops (CRIFC) were used as plant material. Gamma-rays obtained from the 381 Gray/hour Cobalt 60 (60Co) source in the Ankara Nuclear Research and Training Centre (ANAEM) were used as the physical mutagen source. For and each dose and control, healthy and having nearly 12% moisture, seeds of naked barley cv. Yalin and line YAA7050-14 were prepared separately. The prepared seeds were irradiated with gamma rays at doses of 0 (Control), 100, 150, 200, 250, and 300 Gray (Gy). Seeds in the control group and irradiated at different doses were sown separately in the experimental field of the CRIFC to grow M<sub>1</sub> plants. After the required measurements were taken from the M<sub>1</sub> plants that reached harvest maturity, the main spikes were harvested by hand. The seeds of the main spikes of M<sub>1</sub> plants obtained by gamma irradiation at different doses were used to establish M<sub>2</sub> populations. For each dose in both genotypes, 1000 carefully hand-threshed and selected seeds were sown in containers under greenhouse conditions.

On the 8th day after sowing, germinated and emerged plants were counted and then chlorophyll mutations were observed. Chlorophyll mutations were grouped according to Gustafsson (1940 and 1946) as *albino* (white), *xantha* (yellow) and *viridis* (light green) and counted. The images of plants belonging to different chlorophyll mutations observed in the study are given in Figure 1. The frequencies of chlorophyll mutations was determined according to Gaul (1964) by the following formula (2.1). Additionally, linear regression analyses were performed to illustrate the relationship between gamma ray doses and mutation frequency (Freund et al., 2006).

$$\text{Mutation frequency (\%)} = \frac{\text{Number of mutant plants}}{\text{Total number of M}_2 \text{ plants}} \times 100 \quad (2.1)$$



Figure 1. Chlorophyll mutations in  $M_2$  plants (a: *Albino*, b: *Xantha*, c: *Viridis*, d: Control)

### 3. Results and Discussion

The chlorophyll mutations and frequencies observed in  $M_2$  plants of cv. Yalin are given in Table 1. The regression plot showing the relationship between different gamma-ray doses and chlorophyll mutation rates is given in Figure 2. As it is clearly seen in Table 1 and Figure 2, the incidence of chlorophyll mutations increased with increasing gamma ray doses. However, this increase in chlorophyll mutations was slow at first and then gradual. The total chlorophyll mutation rate was 0.74% at 100 Gy gamma dose. At 150 and 200 Gy gamma doses, a decrease was observed, and chlorophyll mutations were found at 0.35% and 0.24%, respectively. The rate of chlorophyll mutations started to increase again, especially at 250 and 300 Gy doses, and they were observed at a higher rate at these doses than at the others. The rate of *albino* plants was 0.39% and the rate of *xantha* plants was 0.77 % at the dose of 250 Gy in cv. Yalin. At 300 Gy dose, which is the dose with the highest rate of chlorophyll mutations, the rate of *albino* plants was 0.56 % and the rate of *xantha* plants was 0.97%.

Table 1

Chlorophyll mutations in  $M_2$  plants of cv. Yalin irradiated with different gamma ray doses

Doses (Gy)	Number of total plants	Chlorophyll mutations						Chlorophyll mutant plants	Mutation frequency (%)
		<i>Albino</i>	<i>Albino</i> (%)	<i>Xantha</i>	<i>Xantha</i> (%)	<i>Viridis</i>	<i>Viridis</i> (%)		
Control	950	0	0	0	0	0	0	0	0.00
100	811	2	0.25	2	0.25	2	0.25	6	0.74
150	846	2	0.24	0	0.00	1	0.12	3	0.35
200	832	2	0.24	0	0.00	0	0	2	0.24
250	778	3	0.39	6	0.77	0	0	9	1.16
300	720	4	0.56	7	0.97	0	0	11	1.53
Total	4937	13	1.66	15	1.99	3	0.36	31	4.02

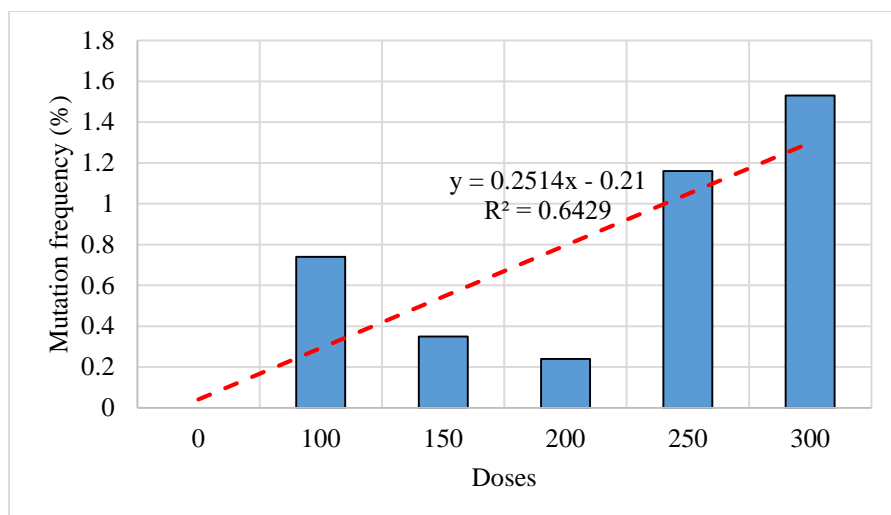


Figure 2. Regression graph between different gamma ray doses and chlorophyll mutation rate in  $M_2$  plants of cv. Yalin

The relative distribution of chlorophyll mutations in naked barley cv. Yalin was the same for all three types (33.3%) at a dose of 100 Gy. *Albino* mutations occurred in 66.7% and *viridis* mutations in 33.3% at the 150 Gy dose. At the 200 Gy dose, all chlorophyll mutations were *albino* type. The highest rate of chlorophyll mutations was 66.7% and 63.6% for the 250 and 300 Gy doses, respectively. When a general evaluation was made for cv. Yalin, it was observed that the highest chlorophyll mutation rate occurred in the *xantha* type with 48.4%. The *albino* type mutation rate was 41.9% and the *viridis* type mutation rate was 9.7% (Table 2).

Table 2

Relative spectrum of chlorophyll mutants  $M_2$  plants of cv Yalin

Doses (Gy)	<i>Albino</i> (%)	<i>Xantha</i> (%)	<i>Viridis</i> (%)
100	33.3	33.3	33.3
150	66.7	0	33.3
200	100.0	0	0
250	33.3	66.7	0
300	36.4	63.6	0
Total	41.9	48.4	9.7

The chlorophyll mutations detected in  $M_2$  plants of barley line YAA7050-14 grown under greenhouse conditions and their occurrence rates are given in Table 3. The regression graph of the relationship between different gamma doses and chlorophyll mutation rates is given in Figure 3. Similar to the cv. Yalin, the number and rates of chlorophyll mutations increased with the increase in gamma ray dose (Table 3, Figure 3). In the barley line YAA7050-14, the rate of chlorophyll mutation was determined as 0.96% at 100 Gy gamma ray dose, and similar to the cv. Yalin. A decrease in the rate of chlorophyll mutation was observed at 150 and 200 Gy gamma ray doses. At these doses, 0.21% and 0.25% chlorophyll mutations were detected, respectively. After the decrease, an increasing rate of chlorophyll mutations was observed at higher doses. Higher rates of chlorophyll mutation were observed at 250 and 300 Gy gamma doses (Figure 3).

In the barley line YAA7050-14, the rate of *albino* plants was 0.52% and the rate of *xantha* plants was 0.13% at 250 Gy dose. At the highest gamma ray dose (300 Gy) the rate of chlorophyll mutations observed was 1.62%. All the chlorophyll mutations in  $M_2$  plants at 300 Gy were *albino* (Table 3, Figure 3).

Table 3  
Chlorophyll mutations in M<sub>2</sub> plants of line YAA7050-14 irradiated with different gamma ray doses

Doses (Gy)	Number of total plants	Chlorophyll mutations						Chlorophyll mutant plants	Mutation frequency (%)
		<i>Albino</i>	<i>Albino</i> (%)	<i>Xantha</i>	<i>Xantha</i> (%)	<i>Viridis</i>	<i>Viridis</i> (%)		
Control	955	0	0	0	0	0	0	0	0
100	934	2	0.21	2	0.21	5	0.54	9	0.96
150	937	1	0.11	1	0.11	0	0	2	0.21
200	795	0	0	0	0	2	0.25	2	0.25
250	772	4	0.52	1	0.13	1	0.13	6	0.78
300	803	13	1.62	0	0.00	0	0	13	1.62
Total	5196	20	2.46	4	0.45	8	0.92	32	3.82

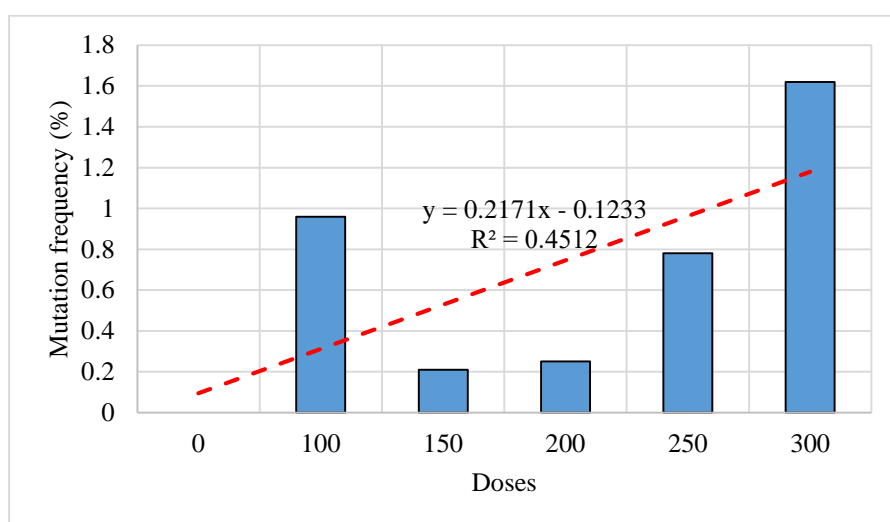


Figure 3. Regression graph between different gamma ray doses and chlorophyll mutation rate in M<sub>2</sub> plants of naked barley line YAA7050-14

In the naked barley line YAA7050-14, the highest chlorophyll mutation was seen in the *viridis* type with 55.6% at 100 Gy, while *albino* and *xantha* type mutations had the same rate with 22.2% at 100 Gy. *Albino* and *xantha* type mutations were found at equal rates (%50) at the 150 Gy dose. At 200 Gy dose, *viridis*-type chlorophyll mutation was observed in all mutant plants. The *albino* ratio was 66.7% and the *xantha* and *viridis* ratios were 16.6% at 250 Gy. At 300 Gy dose, *albino* type chlorophyll mutation was observed in all mutant plants. In the YAA7050-14 line, 62.5% of the total chlorophyll mutations were *albino* type, 25.0% were *viridis* type, and 12.5% were *xantha* type chlorophyll mutations (Table 4).

Table 4  
Relative spectrum of chlorophyll mutants M<sub>2</sub> plants of line YAA7050-14

Doses (Gy)	<i>Albino</i> (%)	<i>Xantha</i> (%)	<i>Viridis</i> (%)
100	22.2	22.2	55.6
150	50.0	50.0	0
200	0	0	100
250	66.7	16.7	17
300	100.0	0.0	0
Total	62.5	12.5	25.0

When the results of chlorophyll mutations in 8-day-old seedlings of M<sub>2</sub> plants of both barley genotypes are evaluated together, the highest rate of chlorophyll mutation occurred at 300 Gy gamma ray dose in both the cv. Yalin and line YAA7050-14. Chlorophyll mutation was observed in 1.53% of the plants that emerged at this dose in cv. Yalin and 1.62% in the line YAA7050-14. The most common chlorophyll mutation type in both genotypes was *albino*, followed by *xantha* type chlorophyll mutations in cv. Yalin and *viridis* type in naked barley line YAA7050-14. In similar studies, it was reported that the rate of chlorophyll mutations increased in parallel with the increase in mutagen doses (Arain, 1974; Sing et al., 1977; Sakin & Sencar, 2001, Çiftçi & Şenay, 2005). Moreover, Ünver (1989) reported that *albino* and *xantha* type mutations increased in M<sub>2</sub> plants as the dose of EMS (Ethyl methanesulfonate) increased in barley cv. Obruk 86. Gustafsson (1946) reported that *xantha* type mutations were six times less frequent than *albino* mutants and both types of chlorophyll mutations increased as the dose increased, but this increase was not linear.

While albinism in barley is determined by more than one gene region (Makowska & Oleszczuk, 2013), *xantha* mutations giving yellow color are usually governed by a single recessive gene (Motoyoshi, 1967; Liu et al., 2008). The combined use of physical and chemical mutagens in barley and wheat increases the frequency of chlorophyll mutation (Singh et al. 1977, Çiftçi and Şenay, 2005). The pigments involved in photosynthesis are called photosynthetic pigments and chlorophylls, the green pigments in plants, are the most active types among them. Chlorophylls are mostly found in chloroplasts in mesophyll cells in green leaves of plants and *chlorophyll-a*, and *chlorophyll-b* derivatives are found in higher plants (Kacar, 1996). Biochemical changes in these photosynthetic pigments (*chlorophyll-a*, *chlorophyll-b* and *xanthophyll*) and their deficiencies in plants are the main reasons for reduced viability at high mutagen doses (Marcu et al., 2013). While both green (chlorophyll) and yellow pigments are absent in *albino* mutants, only yellow pigments are present in *xantha* type mutants and green pigment is absent. In the *viridis* type, the proportions of yellow and green pigments are changed compared to normal plants (Gustafsson, 1946). Chlorophyll a and b deficiency causes the *chlorina*-type mutation that results in pale green leaf color, and there are different types defined by different gene regions (Simpson et al., 1985). In *albino*, *xantha*, and *chlorina* type mutations, plants mostly die 2-4 weeks after germination because they cannot photosynthesise, while in other types, the amount of chlorophyll approaches normal in time and they can continue their vitality until harvest maturity (Motoyoshi, 1967, Ahumada-Flores et al., 2021). Chlorophyll mutations, which are not of economic importance because they are generally lethal (Wani, 2017), are used as genetic, physiological, and biochemical markers and can be easily identified and examined in M<sub>2</sub> generation (Patial et al., 2017). Mutants deficient in chlorophyll could be easily detected as recessive alleles during germination (Ilhan, 2014). Chlorophyll mutations are one of the important parameters used to determine mutation frequency and mutation efficiency in M<sub>2</sub> generation (Sakin & Sencar, 2001, Çiftçi & Şenay, 2005). In mutation breeding studies, it is recommended to use the dose (effective dose) at which the highest chlorophyll mutation frequency is achieved (Çiftçi & Şenay, 2005). In our study, the highest chlorophyll mutation numbers were observed at 250 and 300 Gy doses in Yalin barley variety and at 300 Gy dose in YAA7050-14 barley line. Therefore, it can be said that the effective doses (ED<sub>50</sub>) in these genotypes are close to 250-300 Gy gamma-ray dose levels.

#### 4. Conclusion

The most common chlorophyll mutation in M<sub>2</sub> plants of cv. Yalin was *albino* type, while *xantha* type chlorophyll mutation was found in the line YAA7050-14. The highest chlorophyll mutations were found at 250 and 300 Gy gamma-ray doses in cv. Yalin and at 300 Gy gamma-ray dose in naked barley line YAA7050-14. Considering the chlorophyll mutations, it was determined that 250-300 Gy gamma-ray doses had the highest mutation frequency in naked barley genotypes. These doses could be utilized to generate mutant plants in naked barley breeding studies. Mutant plants have potential as gene sources for developing new naked barley varieties for human consumption.

#### Acknowledgement

The authors are grateful to Dr Ali Senay from the Ankara Nuclear Research and Training Centre for his help with gamma irradiation. We are also grateful to CRIFC for allowing us to use their greenhouse. This study

is based on Namuk ERGÜN's PhD thesis completed at Ankara University, Graduate Scholl of Natural and Applied Sciences under the supervision of Saime ÜNVER İKİNCİKARAKAYA.

### Author Contributions

Namuk Ergün: Conceptualization, running the experiments, collecting data, writing, and editing of original draft.

Güray Akdoğan: Investigation, writing-review and editing.

Saime Ünver İkincikarakaya: Conceptualization and supervision.

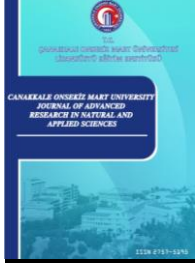
### Conflicts of Interest

The authors declare no conflict of interest.

### References

- Ahumada-Flores, S., Briceño-Zamora, M., García-Montoya, J., López-Cázar, C., Pereo-Galvez, A., Parra-Cota, F. & de los Santos-Villalobos, S. (2020). Gamma radiosensitivity study on wheat (*Triticum turgidum* ssp. *durum*). *Open Agriculture*, 5(1), 558-562. <https://doi.org/10.1515/opag-2020-0057>
- Ahumada-Flores, S., Pando, L. R. G., Cota, F. I. P., de la Cruz Torres, E., Sarsu, F., & de los Santos Villalobos, S. (2021). Gamma irradiation induces changes of phenotypic and agronomic traits in wheat (*Triticum turgidum* ssp. *durum*). *Applied Radiation and Isotopes*, 167, 109490. <https://doi.org/10.1016/j.apradiso.2020.109490>
- Arain, A. G. (1974). The effect of ethyl methanesulfonate treatment on floret sterility and chlorophyll mutation rate in barley. *Radiation Botany*, 14(4), 347-350. [https://doi.org/10.1016/S0033-7560\(74\)80027-X](https://doi.org/10.1016/S0033-7560(74)80027-X)
- Badr, A., Rabey, H. E., Effgen, S., Ibrahim, H. H., Pozzi, C., Rohde, W., & Salamini, F. (2000). On the origin and domestication history of barley (*Hordeum vulgare*). *Molecular biology and evolution*, 17(4), 499-510. <https://doi.org/10.1093/oxfordjournals.molbev.a026330>
- Bhatty, R. S. (1999). The potential of hull-less barley. *Cereal Chemistry*, 76(5), 589-599. <https://doi.org/10.1094/CCHEM.1999.76.5.589>
- Chaudhary, J., Deshmukh, R., & Sonah, H. (2019). Mutagenesis Approaches and Their Role in Crop Improvement. *Plants (Basel, Switzerland)*, 8(11), 467. <https://doi.org/10.3390/plants8110467>
- Çiftçi C.Y. & Şenay, A. (2005) Effect of separate and combined treatments of different doses of gamma rays and EMS on durum wheat (*Triticum durum* Desf.) in M1 generations. *Journal of Field Crops Central Research Institute* 14(1-2), 41-49. (in Turkish) [https://www.biotechstudies.org/uploads/pdf\\_329.pdf](https://www.biotechstudies.org/uploads/pdf_329.pdf)
- Dyulgerova, B., & Dyulgerov, N. (2022). Mutagenic effect of sodium azide on winter barley cultivars. *Agricultural Science and Technology*, 14(2), 27-33. <https://doi.org/10.15547/ast.2022.02.016>
- Gaul, H. (1964). Mutations in plant breeding. *Radiation Botany*, 4(3), 155-232. [https://doi.org/10.1016/s0033-7560\(64\)80069-7](https://doi.org/10.1016/s0033-7560(64)80069-7)
- Goyal, S., Wani, M.R. & Khan, S. (2019) Frequency and Spectrum of Chlorophyll Mutations Induced by Single and Combination Treatments of Gamma Rays and EMS in Urdbean. *Asian Journal of Biological Sciences*, 12, 156-163. <https://scialert.net/abstract/?doi=ajbs.2019.156.163>
- Gustafsson, Å. (1940). The Mutation system of the chlorophyll apparatus. *Acta Universitatis Lundensis*, 36(11), 1-40.
- Gustafsson, Å. (1946). The origin of albina and xantha mutations in barley. *Acta radiologica*, 27(3-4), 300-307. <https://doi.org/10.3109/00016924609135187>
- İlhan, D. (2014) Mutagenicity tests used in plants. *Kafkas University Institute of Natural and Applied Science Journal*, 7(1), 29-47. (in Turkish) <https://dergipark.org.tr/en/pub/kujs/issue/30901/334479>
- Kacar, B. (1996). Plant Physiology 4th Edition, Ankara University Faculty of Agriculture Publications, Publication No: 1447, 424, Ankara (in Turkish).
- Kodym A., Afza, R., Forster, B.P., Ukai, Y & Nakagawa, H. (2012) Methodology for physical and chemical mutagenic treatments. In: Shu Q.Y., Forster, B.F. & Nakagawa, H. (eds), *Plant mutation breeding and biotechnology*. CABI, FAO, Oxfordshire, UK pp. 169-180
- Lev-Yadun, S., Gopher, A., & Abbo, S. (2000). The cradle of agriculture. *Science*, 288(5471), 1602-1603. <https://doi.org/10.1126/science.288.5471.1602>

- Liu, Z. L., Yuan, S., Liu, W. J., Du, J. B., Tian, W. J., Luo, M. H., & Lin, H. H. (2008). Mutation mechanism of chlorophyll-less barley mutant NYB. *Photosynthetica*, 46, 73-78. <https://doi.org/10.1007/s11099-008-0013-0>
- Makowska, K. & Oleszczuk, S. (2013) Albinism in barley androgenesis. *Plant Cell Reports*, 33, 385-392. <https://doi.org/10.1007/s00299-013-1543-x>
- Maluszynski, M., Szarejko, I., Bhatia, R., Nichterlein, K. & Lagoda, P.J.L. (2009) Mutation techniques. In: Guimares, E., Ceccarelli, S., Weltzein, E. & Rajendran, P.G. (eds) *Plant breeding book*. FAO, Rome, pp 159-194.
- Marcu, D., Damian, G., Cosma, C., & Cristea, V. (2013). Gamma radiation effects on seed germination, growth and pigment content, and ESR study of induced free radicals in maize (*Zea mays*). *Journal of biological physics*, 39, 625-634. <https://doi.org/10.1007/s10867-013-9322-z>
- Meints, B., Vallejos, C., & Hayes, P. (2021). Multi-use naked barley: A new frontier. *Journal of Cereal Science*, 102, 103370. <https://doi.org/10.1016/j.jcs.2021.103370>
- Meints, B. & Hayes, P.M. (2019) Breeding naked barley for food, feed, and malt. In: Goldman, I. (ed) *Plant Breeding Reviews*, 43 (1). John Wiley & Sons, Inc., pp. 95-119.
- Motoyoshi, F. (1967). Chlorophyll formation in several chlorophyll mutants of sand oats and barley cultured on nutrient media. *The Japanese Journal of Genetics*, 42(5), 291-297. <https://doi.org/10.1266/jjg.42.291>
- Nazarenko, M. M., & Lykholat, T. Y. (2020). Variability at winter wheat varieties first generation which obtained mutagen action. *Ecology and Noospherology*, 31(2), 77-81. <https://doi.org/10.15421/032012>
- Newman, R.K. & Newman, C.W. (2008) Barley for food and health: Science, technology, and products. John Wiley & Sons, Inc., 243, New Jersey.
- Patil, M., Thakur, S. R., Singh, K. P., & Thakur, A. (2017). Frequency and spectrum of chlorophyll mutations and induced variability in ricebean (*Vigna umbellata* Thunb, Ohwi and Ohashi). *Legume Research-An International Journal*, 40(1), 39-46. <https://doi.org/10.18805/lr.v0i0F.10757>
- Sakin, M.A. & Sencar, Ö. (2001). Makarnalık buğday (*Triticum durum* Desf.) çeşitlerinin mutagenlere tepkileri. *Journal of Agricultural Faculty of Gaziosmanpaşa University*, 18(1), 89-93. <https://dergipark.org.tr/tr/pub/gopzfd/issue/7349/96160> (in Turkish)
- Simpson, D. J., Machold, O., Høyer-Hansen, G., & Von Wettstein, D. (1985). Chlorina mutants of barley (*Hordeum vulgare* L.). *Carlsberg Research Communications*, 50, 223-238. <https://doi.org/10.1007/BF02907148>
- Singh, R. M., Singh, J., & Srivastava, A. N. (1977). Mutagenic effects of gamma rays, EMS, and HA in barley. *Barley Genetics Newsletter*, 7, 60.
- Ullrich, S.E. (2011). Significance, adaptation, production, and trade of barley. In: Ullrich, S.E. (ed.). *Barley*, Blackwell Publishing Ltd., , Chichester, UK. pp. 3-13
- Ünver, S. (1989). The effect of different doses of EMS and the temperatures and periods of post washing applied on the some characters in M1 and M2 plants of barley (*Hordeum vulgare* L.) (in Turkish) (Unpublished PhD thesis). Ankara University, Ankara, Turkey.
- Wani, M. R., Khan, S., & Kozgar, M. I. (2011). Induced chlorophyll mutations. I. Mutagenic effectiveness and efficiency of EMS, HZ and SA in mungbean. *Frontiers of Agriculture in China*, 5, 514-518. <https://doi.org/10.1007/s11703-011-1126-y>
- Wani, M.R. 2017. Induced chlorophyll mutations, comparative mutagenic effectiveness and efficiency of chemical mutagens in lentils (*Lens culinaris* Medik). *Asian J. Plant Sci.*, 16: 221-226. <https://doi.org/10.3923/ajps.2017.221.226>
- Yu, K., Lenz-Wiedemann, V., Chen, X., & Bareth, G. (2014). Estimating leaf chlorophyll of barley at different growth stages using spectral indices to reduce soil background and canopy structure effects. *ISPRS Journal of Photogrammetry and Remote Sensing*, 97, 58-77. <https://doi.org/10.1016/j.isprsjprs.2014.08.005>



# Analysis of Acoustic Signals of Footsteps from the Piezoelectric Sensor

Bilge Çiğdem Çiftçi<sup>1</sup>, Gamze Kaya<sup>2\*</sup>, Mustafa Kurt<sup>3</sup>

<sup>1</sup>Department of Photonics, School of Graduate Studies, Erzurum Technical University, Erzurum, Türkiye

<sup>2</sup>Department of Electric and Energy, Çanakkale Vocational School of Technical Sciences, Çanakkale Onsekiz Mart University, Çanakkale, Türkiye

<sup>3</sup>Department of Electrical and Electronics Engineering, Faculty of Engineering, Çanakkale Onsekiz Mart University, Çanakkale, Türkiye

## Article History

Received: 05.06.2023

Accepted: 08.08.2023

Published: 20.12.2023

## Research Article

**Abstract** –Some materials can change their electrical polarization under the influence of a mechanical stress due to the piezoelectric effect. This stress-induced change in polarization produces a potential difference across the material. For this reason, the piezoelectric material generates an electrical signal when it is subjected to a pressure from acoustic energy. In this study, analysis of acoustic signals of footsteps from the piezoelectric sensor, especially for human footsteps, have been studied by considering the analytical relationship between the electrical signal generated from the sensor and the acoustic signal that provides the effect. We analyzed the acoustic signal data by assuming that the electrical output voltage of the piezoelectric sensor completely coincides with the frequency of the acoustic signals. The original signal was pre-processed using filtering systems and analyzed by the fast Fourier transform and power spectral density methods to extract descriptive spectral features of the signal. This preliminary study proposed a method as a sensor based piezoelectric security system to detect the acoustic signals that can indicate possible dangers to the safety of people or property. The source of the acoustic signal can be determined by matching it with the existing database using machine learning algorithms like face recognition systems for future goals.

**Keywords** – Acoustics, piezoelectric, sensors, signal processing, spectral analysis

## 1. Introduction

The Curie brothers discovered the piezoelectric phenomenon in 1880 by demonstrating the formation of surface charges on well-prepared crystals due to mechanical pressure. In piezoelectric systems, the conversion between mechanical energy and electrical energy has many applications in industry (Smith, 2005). Nowadays, piezoelectric elements find numerous applications in precise positioning systems (Li, Zhang, Jia, & Qian, 2009; Liu, Yan, & Özbay, 2018; Qiu, Wang, Zhang, & Han, 2013; Salvador, Plazas, Gimeno, & Carreres, 2012; Stefanski, Minorowicz, Persson, Plummer, & Bowen, 2017; Tian et al., 2019; Wang, Ho, & Jiang, 2021), hard disc drive systems (Khasawneh, Jaradat, Naji, & Al-Azzeh, 2018; Lim & Choi, 2007; Ohashi, Kajiwara, Iwadare, & Arisaka, 2005), vibration control (Chuaqui, Roque, & Ribeiro, 2018; Høgsberg, 2021; Pu, Zhou, & Meng, 2019), energy harnessing (Chelli et al., 2021; Guigon, Chaillout, Jager, & Despesse, 2008; Jacquelin, Adhikari, & Friswell, 2011; Kundu & Nemade, 2016; Moro & Benasciutti, 2010; Peigney & Siegert, 2013; van den Ende, van de Wiel, Groen, & van der Zwaag, 2011; Wu, Bao, & Wang, 2021; Xiang, Wang, Shi, & Zhang, 2013; Yatim, Ismail, S.J, hj.bakri, & Effendy, 2018) etc. Due to the interaction between the foot and the contact surface during walking, human footsteps produce vibrations and sound from a few Hertz to ultrasonic frequencies (A. Ekimov & J. Sabatier, 2006). The sound vibrations of different types of walking styles were measured on the outdoor floor surface with an ultrasonic ceramic sensor by Ekimov et.al. (A. Ekimov &

<sup>1</sup> bilgecigdmc@gmail.com

<sup>2</sup> gamzekaya@comu.edu.tr

<sup>3</sup> mkurt@comu.edu.tr

\*Corresponding author

J. Sabatier, 2006; A. Ekimov & J. M. Sabatier, 2006). Some test measurements were also conducted in air to see the difference the sound measurement on the ground where the vibration absorption is much higher. The results reveal that frictions of a footstep on the ground generate ultrasonic sound wave. It was shown that there is no remarkable dependence on the human footstep style for ultrasonic signals magnitude in air, unlike the seismic vibration signals (Ekimov & Sabatier, 2007). Recently, miniature seismometer networks have been used to protect areas requiring high security against unauthorized access. Against the disadvantages of existing seismometers such as high-power consumption and limited sensing range, Levy et. al. has developed a miniature seismometer with high resolution, low power consumption to detect intrusion in a protected area (Levy, Moras, & Pannetier, 2017).

In this study, we propose an approach to determine acoustic sound sources by considering the analytical relationship between the electrical signal generated from the sensor and the stimulating acoustic signal. We predict that the output signal spectrum obtained by Fast Fourier Transform (FFT) analysis of the step signals received in time-domain with sensor can be compatible with the frequencies of the applied acoustic signal. Thus, the signal can be interpreted by deriving the frequency values of the stimulating signal from the electrical signal generated by the piezoelectric sensor. Our preliminary study proposes a method to detect the acoustic signals that can indicate trespassing activities. In addition, the source of the acoustic signal can be determined by matching it with the existing database using machine learning algorithms like face recognition systems for future goals.

## 2. Materials and Methods

Polyvinylidene fluoride piezoelectric thin film sensors, also known as a low-cost vibration sensor, have become an attractive alternative to piezoelectric ceramics due to their properties such as flexibility, high chemical resistance, and thermal stability (Bregar, Starc, Čepon, & Boltežar, 2021). In general, piezoelectric ceramic materials are used in high frequency applications (200 Hz and above) while in low frequency applications, piezoelectric polymers are preferred. The acoustic pressure force acting on the piezoelectric sensor gives a certain voltage value at the exit of the strip. Since there is a direct relationship between the electrical signal obtained from the piezoelectric strip and the acoustic signal applied, the piezoelectric strip deforms in proportion to the frequency of the acoustic signals. High amplitude responses are obtained from low frequency signals. In this way, the low frequency acoustic signal generated by the human footstep can be perceived as a higher amplitude electrical signal. The acoustic signals detected by the piezoelectric strip are converted into digital signals at the piezoelectric sensor output. The flowchart of our algorithm for data processes is shown in Figure 1.

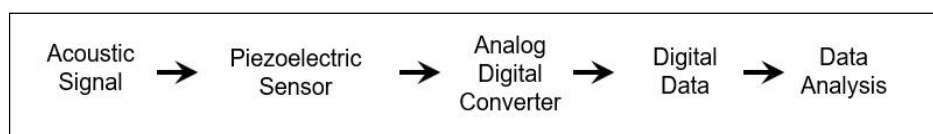


Figure 1. The schematic view of the system

In the process of listening to human footsteps on the computer, the sound data is read in the storage devices, transferred to the microprocessor, and transmitted to the Digital Signal Processor (DSP) on the sound card. The data decoded by the DSP is converted into analog audio signals by the sound card's digital-to-analog converter (DAC) and transmitted to the sound card's output and then to the speaker. After the digital audio signals in the computer are converted into analog form by the sound card and transmitted to the speakers, the vibrating speaker diaphragm converts the electrical signals into sound waves. Sound waves from the speaker are received by the piezoelectric structure. The piezoelectric strip structure deforms according to the acoustic signals of different frequencies. Acoustic signals coming to the piezoelectric material are taken from the output of the piezoelectric material and converted into digital signals via data acquisition system.

Signals detected in a system are usually measured as a function of time and then by using Fourier analysis they were transferred from time domain to frequency domain. Footsteps are complex sounds made up of many

different frequencies. Analysis of the frequency components of these harmonic sounds are done by the Fourier method and complex waves are decomposed in the form of simple harmonics. The analysis of the received signals is performed in MATLAB code for human step detection.

### 3. Results and Discussion

In Figure 2, we compare audio signals produced by a human walking on snow and hardwood floor in time and frequency domains. To investigate the spectral frequency details of the digitally recorded audio signals in Figure 2 (a) and (d), we applied the FFT algorithm as seen in Figure 2 (b) and (e), respectively. The signals in Figure 2 (b) and (e) have sampling rate at 48 kHz, FFT size of 854016 and time duration of about 18 seconds and sampling rate at 48 kHz, FFT size of 462863 and time duration of about 10 seconds, respectively. By using a median filter, we eliminated the noise without distorting the shape of the signals as seen in Figure 2 (c) and (f). We can clearly extract descriptive spectral features of the human footstep walking on snow and hardwood floor in frequency and filtered frequency domain as comparing Figure 2 (b) and (e) and Figure 2 (c) and (f), respectively.

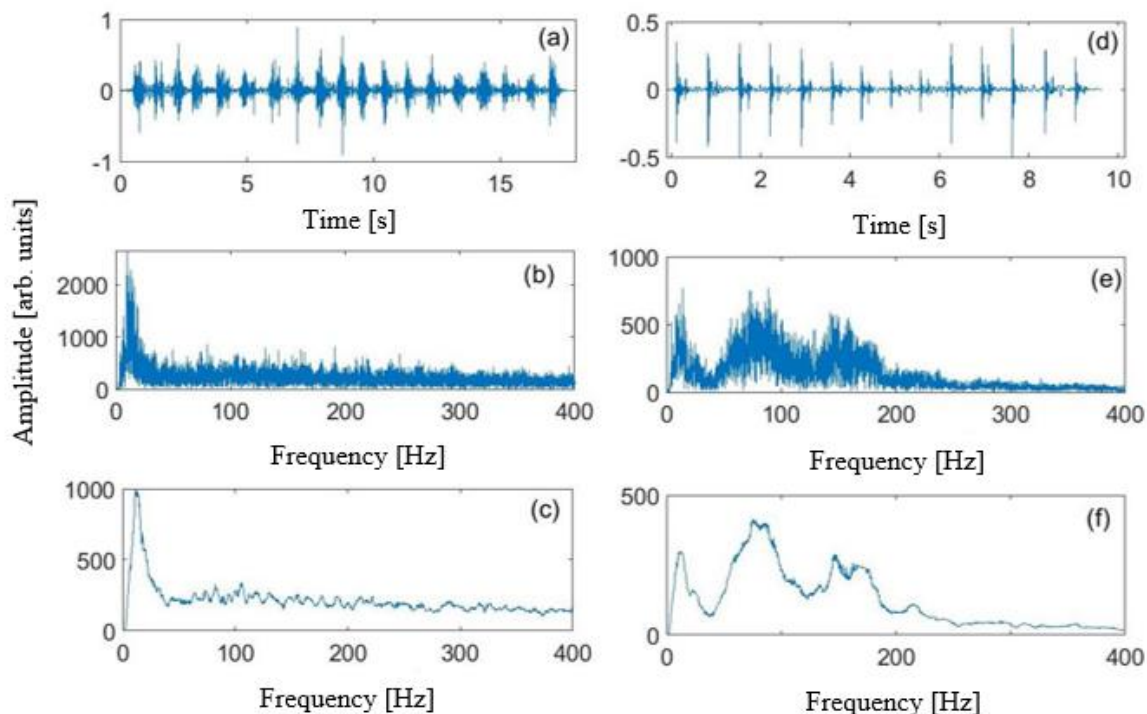


Figure 2. Human footstep walking on snow (a-c) and hardwood floor (d-f) in time domain, frequency domain, and filtered frequency.

A Power Spectral Density (PSD) is used to determine broadband random signals in the measure of signal power versus frequency. It is estimated by calculating the Fourier transform of the signal's autocorrelation function. In Figure 3, by the FFT and PSD we pre-processed original signals of a horse footsteps to extract descriptive spectral features of the signals. The signals of the footsteps are given in time domain, frequency domain and as frequency filtered. The sampling rate of the signal was measured at 44.1 kHz, FFT size 378726 and duration about 8 seconds. PSD estimates the power distribution of the signal in a specific frequency range. Figure 3 (d) which is PSD of the horse footsteps gives detailed on amplitude and locations of the peaks of the acoustic signal.

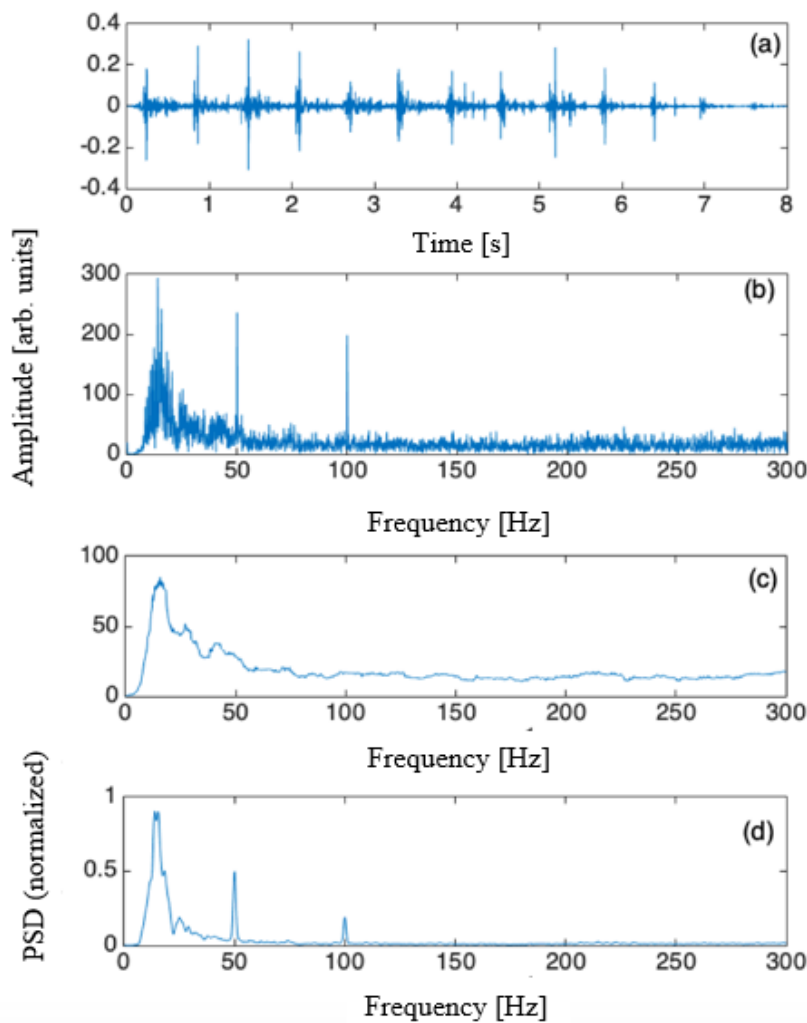


Figure 3. The horse footsteps (a) in time domain (b) in frequency domain (c) as filtered and (d) PSD frequency domain.

In Figure 4, we compare two different footsteps as labelled footsteps-1 and footsteps-2. The footsteps-1 and footsteps-2 were the footsteps of a person walking with shoes on hardwood floor and on rug over hardwood floor, respectively. Signals are compared using PSDs of signals. We can clearly observe that the extracted frequency information has the potential to discriminate between distinct acoustic sound sources. This study shows that our method can be used to detect and analyze acoustic signals.

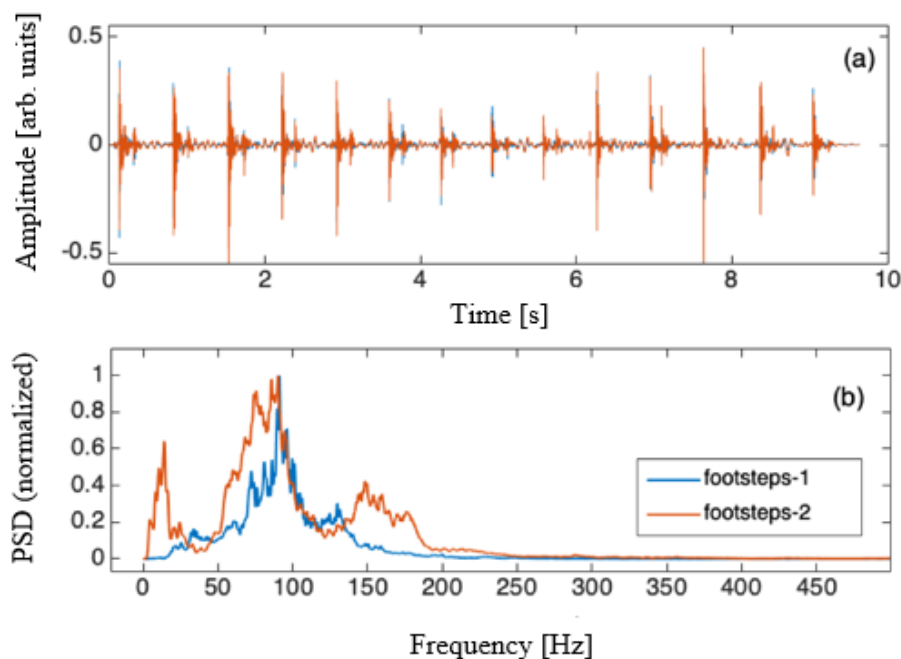


Figure 4. The signal of two different footsteps in (a) time domain and (b) frequency domain PSD.

#### 4. Conclusion

By assuming that the electrical output voltage of the piezoelectric sensor completely coincides with the frequency of the acoustic signals, we analyzed the acoustic signal data. The original signal was pre-processed using filtering systems and analyzed by the FFT and PSD methods to extract descriptive spectral features of the signal. We observed that meaning of the signal can be obtained by deriving the values of the stimulating acoustic frequency from the electrical signal generated by the piezoelectric sensor because of the acoustic signal. The equivalent of the interpreted signal from the library to be created can be easily determined with a promoted program. This preliminary study proposes a method as a sensor based piezoelectric security system to detect the acoustic signals that can indicate trespassing activities. The source of the acoustic signal can be determined by matching it with the existing database using machine learning algorithms like face recognition systems for future goals.

#### Acknowledgement

This work was supported by the Office of Scientific Research Projects Coordination at Çanakkale Onsekiz Mart University. Grant number: FYL-2019-2912.

#### Author Contributions

Bilge Çiğdem Çiftçi: Collected data and performed data analysis.

Gamze Kaya: Collected data, performed data analysis, and wrote the paper.

Mustafa Kurt: Conceived the concept, designed the analysis, and wrote the paper.

#### Conflicts of Interest

The authors declare no conflict of interest.

#### References

Bregar, T., Starc, B., Čepon, G., & Boltežar, M. (2021). On the Use of PVDF Sensors for Experimental Modal Analysis. *Topics in Modal Analysis & Testing*, 8, 279-281. doi: [https://doi.org/10.1007/978-3-030-47717-2\\_28](https://doi.org/10.1007/978-3-030-47717-2_28)

- Chelli, Z., Achour, H., Saidi, M., Laghrouche, M., Chaouchi, A., Rguiti, M., Courtois, C. (2021). Fabrication and characterization of PU/NKLNT/CFs based lead-free piezoelectric composite for energy harvesting application. *Polymer-Plastics Technology and Materials*, 1-13. doi: <https://doi.org/10.1080/25740881.2021.1888995>
- Chuaqui, T. R. C., Roque, C. M. C., & Ribeiro, P. (2018). Active vibration control of piezoelectric smart beams with radial basis function generated finite difference collocation method. *Journal of Intelligent Material Systems and Structures*, 29(13), 2728-2743. doi: <https://doi.org/10.1177/1045389X18778363>
- Ekimov, A., & Sabatier, J. (2006). Broad frequency acoustic response of ground/floor to human footsteps. *Defense and Security Symposium*, 6241, 62410L. doi: <https://doi.org/10.1117/12.663978>
- Ekimov, A., & Sabatier, J. M. (2006). Vibration and sound signatures of human footsteps in buildingsa). *The Journal of the Acoustical Society of America*, 120(2), 762-768. doi: <https://doi.org/10.1121/1.2217371>
- Ekimov, A., & Sabatier, J. M. (2007). Ultrasonic wave generation due to human footsteps on the ground. *The Journal of the Acoustical Society of America*, 121(3), EL114-EL119. doi: <https://doi.org/10.1121/1.2437847>
- Guigon, R., Chaillout, J.-J., Jager, T., & Despesse, G. (2008). Harvesting raindrop energy: experimental study. *Smart Materials and Structures*, 17(1), 015039. doi: <https://doi.org/10.1088/0964-1726/17/01/015039>
- Høgsberg, J. (2021). Vibration control by piezoelectric proof-mass absorber with resistive-inductive shunt. *Mechanics of Advanced Materials and Structures*, 28(2), 141-153. doi: <https://doi.org/10.1080/15376494.2018.1551587>
- Jacquelin, E., Adhikari, S., & Friswell, M. I. (2011). A piezoelectric device for impact energy harvesting. *Smart Materials and Structures*, 20(10), 105008. doi: <https://doi.org/10.1088/0964-1726/20/10/105008>
- Khasawneh, Q. A., Jaradat, M. A. K., Naji, M. I., & Al-Azzeh, M. Y. (2018). Enhancement of hard disk drive manipulator using piezoelectric actuator mechanisms. *Journal of the Brazilian Society of Mechanical Sciences and Engineering*, 40(11), 517. doi: <https://doi.org/10.1007/s40430-018-1432-x>
- Kundu, S., & Nemade, H. B. (2016). Modeling and Simulation of a Piezoelectric Vibration Energy Harvester. *Procedia Engineering*, 144, 568-575. doi: <https://doi.org/10.1016/j.proeng.2016.05.043>
- Levy, R., Moras, J., & Pannetier, B. (2017). Vibrating Beam MEMS Seismometer for Footstep and Vehicle Detection. *IEEE Sensors Journal*, 17(22), 7306-7310. doi: <https://doi.org/10.1109/JSEN.2017.2731858>
- Li, Y.-J., Zhang, J., Jia, Z.-Y., & Qian, M. (2009). A novel piezoelectric 6-component heavy force/moment sensor for huge heavy-load manipulator's gripper. *Mechanical Systems and Signal Processing*, 23(5), 1644-1651. doi: <https://doi.org/10.1016/j.ymsp.2009.02.004>
- Lim, S. C., & Choi, S. B. (2007). Vibration control of an HDD disk-spindle system utilizing piezoelectric bimorph shunt damping: I. Dynamic analysis and modeling of the shunted drive. *Smart Materials and Structures*, 16(3), 891-900. doi: <https://doi.org/10.1088/0964-1726/16/3/039>
- Liu, P., Yan, P., & Özbay, H. (2018). Design and trajectory tracking control of a piezoelectric nano-manipulator with actuator saturations. *Mechanical Systems and Signal Processing*, 111, 529-544. doi: <https://doi.org/10.1016/j.ymsp.2018.04.002>
- Moro, L., & Benasciutti, D. (2010). Harvested power and sensitivity analysis of vibrating shoe-mounted piezoelectric cantilevers. *Smart Materials and Structures*, 19(11), 115011. doi: <https://doi.org/10.1088/0964-1726/19/11/115011>
- Ohashi, F., Kajiwara, I., Iwadare, M., & Arisaka, T. (2005). Optimal design of smart carriage arm in magnetic disk drive for vibration suppression. *Microsystem Technologies*, 11(8), 711-717. doi: <https://doi.org/10.1007/s00542-005-0550-4>
- Peigney, M., & Siegert, D. (2013). Piezoelectric energy harvesting from traffic-induced bridge vibrations. *Smart Materials and Structures*, 22(9), 095019. doi: <https://doi.org/10.1088/0964-1726/22/9/095019>
- Pu, Y., Zhou, H., & Meng, Z. (2019). Multi-channel adaptive active vibration control of piezoelectric smart plate with online secondary path modelling using PZT patches. *Mechanical Systems and Signal Processing*, 120, 166-179. doi: <https://doi.org/10.1016/j.ymsp.2018.10.019>
- Qiu, Z.-c., Wang, B., Zhang, X.-m., & Han, J.-d. (2013). Direct adaptive fuzzy control of a translating piezoelectric flexible manipulator driven by a pneumatic rodless cylinder. *Mechanical Systems and Signal Processing*, 36(2), 290-316. doi: <https://doi.org/10.1016/j.ymsp.2012.10.008>
- Salvador, F. J., Plazas, A. H., Gimeno, J., & Carreres, M. (2012). Complete modelling of a piezo actuator last-generation injector for diesel injection systems. *International Journal of Engine Research*, 15(1), 3-19.

doi: <https://doi.org/10.1177/1468087412455373>

- Smith, R. C., Industrial, S. f., & Mathematics, A. (2005). Smart Material Systems: Model Developments: Society for Industrial and Applied Mathematics *Frontiers in applied mathematics Series Number 32*.
- Stefanski, F., Minorowicz, B., Persson, J., Plummer, A., & Bowen, C. (2017). Non-linear control of a hydraulic piezo-valve using a generalised Prandtl–Ishlinskii hysteresis model. *Mechanical Systems and Signal Processing*, 82, 412-431. doi: <https://doi.org/10.1016/j.ymsp.2016.05.032>
- Tian, Y., Cai, K., Zhang, D., Liu, X., Wang, F., & Shirinzadeh, B. (2019). Development of a XYZ scanner for home-made atomic force microscope based on FPAA control. *Mechanical Systems and Signal Processing*, 131, 222-242. doi: <https://doi.org/10.1016/j.ymsp.2019.05.057>
- van den Ende, D. A., van de Wiel, H. J., Groen, W. A., & van der Zwaag, S. (2011). Direct strain energy harvesting in automobile tires using piezoelectric PZT–polymer composites. *Smart Materials and Structures*, 21(1), 015011. doi: <https://doi.org/10.1088/0964-1726/21/1/015011>
- Wang, Y.-J., Ho, J.-L., & Jiang, Y.-B. (2021). A self-positioning linear actuator based on a piezoelectric slab with multiple pads. *Mechanical Systems and Signal Processing*, 150, 107245. doi: <https://doi.org/10.1016/j.ymsp.2020.107245>
- Wu, N., Bao, B., & Wang, Q. (2021). Review on engineering structural designs for efficient piezoelectric energy harvesting to obtain high power output. *Engineering Structures*, 235, 112068. doi: <https://doi.org/10.1016/j.engstruct.2021.112068>
- Xiang, H. J., Wang, J. J., Shi, Z. F., & Zhang, Z. W. (2013). Theoretical analysis of piezoelectric energy harvesting from traffic induced deformation of pavements. *Smart Materials and Structures*, 22(9), 095024. doi: <https://doi.org/10.1088/0964-1726/22/9/095024>
- Yatim, H., Ismail, F., S.J, F., hj.bakri, A., & Effendy, S. (2018). A Development of Piezoelectric Model as an Energy Harvester from Mechanical Vibration. *Chemical Engineering Transactions*, 63, 775-780. doi: <https://doi.org/10.3303/CET1863130>



## Anti-aging effect of TMQ on EPDM for Various Cure Systems

Şehriban Öncel<sup>1\*</sup>, Gürcan Gül<sup>2</sup>, Mahir Burak Efe<sup>3</sup>, Hakan Erdoğan<sup>4</sup>, Bağdagül Karağaç<sup>5</sup>

<sup>1</sup>Ford Otosan İhsaniye Vocational School of Automotive, İhsaniye Campus, Kocaeli University, Kocaeli, Türkiye

<sup>2,4</sup>Üntel Kabloları A.Ş., Demirciler OSB, Dilovası, Kocaeli, Türkiye

<sup>2,3,5</sup>Department of Polymer Science & Technology, Umuttepe Campus, Kocaeli University, Kocaeli, Türkiye

<sup>3</sup>Department of Chemical Engineering, Umuttepe Campus, Kocaeli University, Kocaeli, Türkiye

### Article History

Received: 24.04.2023

Accepted: 28.07.2023

Published: 20.12.2023

### Research Article

**Abstract** – Ethylene propylene diene rubber (EPDM) is a common raw material for weather resistant rubber products used in lots of areas such as cable, automotive, marine industry and aviation applications. Superior processing behaviour, electrical properties and moderate high temperature resistance also make EPDM an attractive raw material for a wide range of further industrial performance requirements. As well as the other general purpose rubbers, EPDM needs to be protected against thermo-oxidative aging. Short and long term aging behaviour of both sulfur and peroxide cured EPDM has been studied in literature. However, to the authors' best knowledge, there is not any study in literature systematically evaluating a common rubber antioxidant 2,2,4-trimethyl-1,2-dihydroquinoline (TMQ) for investigating theoretical life-time of EPDM based materials that were vulcanized with different crosslinking systems. In this study, effects of TMQ on the thermo-oxidative resistance of EPDM has been studied for conventional and efficient sulfur vulcanization systems as well as peroxide vulcanization system. Aging mechanism for different cases has been investigated by using structural, rheological and mechanical tests. Thermo-oxidative aging has been monitored by carbonyl index and activation energy. Arrhenius based life-time estimation methodology (ISO 11346) has also been employed to evaluate aging behaviour of the reference and TMQ containing (-T) compounds. TMQ was found to exhibit different levels of protection against thermo-oxidative aging for all the curing systems and at all aging conditions. As a result, higher aging activation energy for -T compounds has been attributed to extended service life of the material in the presence of TMQ.

**Keywords** – Arrhenius equation, curing systems, EPDM rubber, life-time estimation, thermo-oxidative aging

## 1. Introduction

Ethylene propylene diene rubber (EPDM) is a common raw material for rubber goods with superior resistance to heat, oxygen, ozone, humidity, ultraviolet radiation and electric discharge thanks to its structural properties, particularly its saturated backbone (Bouguedat et al. 2008; Tan et al. 2021). It is widely used in many applications such as cable insulation and sheathing, sealants, automotive goods, marine and aviation industries. Due to its good electrical properties, thermal aging resistance and relatively low density in their compounds, EPDM has an increasing demand particularly in cable industry and nuclear applications (Li et al. 2020). Terpolymer EPDM is synthesized by polymerization of ethylene and propylene in the presence of a diene monomer, which is commonly one of ethylidene norbornene (ENB), dicyclopentadiene (DCPD) and vinyl norbornene (VNB).

<sup>1</sup> sehriban.ancel@kocaeli.edu.tr

<sup>2</sup> gurcan.gul@untel.com.tr

<sup>3</sup> mahir.efe@untel.com.tr

<sup>4</sup> hakan.erdogan@untel.com.tr

<sup>5</sup> bkaraagac@kocaeli.edu.tr

\*Corresponding Author

Depending on the diene content, EPDM is able to vulcanize by sulfur as well as by peroxide and other crosslinking agents (Savran 2001; Simpson 2002). Besides, diene groups are not located on the main chain of EPDM, and this can provide exceptional resistance to weathering (Delor-Jestin et al. 2000; Sanches, Cassu, and De Cássia Lazzarini Dutra 2015). However, due to its low polarity, EPDM is not resilient to hydrocarbon based fuels and halogenated solvents. Promising heat, oxygen and ozone resistance of EPDM has been drawing attention to prepare rubber compounds for high-temperature applications by compounding EPDM with various anti-aging additives and/or various crosslinking systems. Despite the fact that it exhibits satisfactory resistance to thermo-oxidative aging, EPDM still needs to be protected against overall aging effects in order to exhibit superior performance during its long service life (Van Duin 2002). It is preferably compounded with stabilizing agents to improve its service temperature and useful service life. 2,2,4-trimethyl-1,2-dihydroquinoline (TMQ) is one of the most widely used stabilizer for EPDM. Vulcanization system has also significant impact on both service temperature and service life of EPDM based materials. Although various crosslinking agents can be used in EPDM compounds, sulfur vulcanization system is still one of the most preferred methods to produce EPDM vulcanizates. In sulfur vulcanization, accelerators and activators accompany with sulfur to shorten vulcanization time and to improve overall vulcanizate properties. The proposed reaction mechanism for sulfur vulcanization of EPDM is given in Figure 1 (Van Duin 2002). Here, diene group is ENB and vulcanization rate increases with ENB content of EPDM.

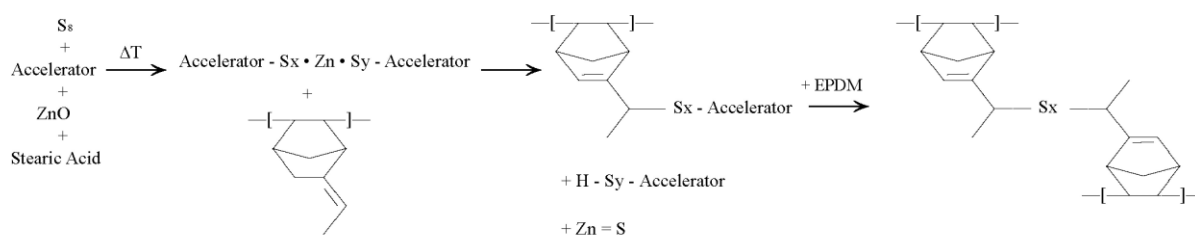


Figure 1. Proposed reaction mechanism for sulfur vulcanization of EPDM (Van Duin 2002)

Three different sulfur vulcanization systems can be designed to control crosslink types, which most likely occur. These are conventional (CV), semi-efficient (semi-EV) and efficient (EV) vulcanization systems (R. 2002). The amounts of sulfur and accelerators and the sulfur/accelerator ratio, which depend on the type of sulfur vulcanization system, have remarkable impact on the vulcanizate properties (Ciesielski 1999). The other popular vulcanization system for EPDM is peroxide crosslinking and the proposed reaction mechanism is depicted in Figure 2 (Van Duin 2002; Matador Rubber 2007). Both saturated and unsaturated rubbers are able to vulcanize by using organic peroxides. In peroxide vulcanization, radicals, which are formed on the polymer main chain by means of peroxides, combine to give C-C crosslinks. Optimum reaction temperature strongly depends on decomposition temperature of the peroxide; yet, peroxide vulcanization mainly occurs at 140-180°C. Peroxy-vulcanized rubber materials are able to be used at relatively high temperatures, they have good thermo-oxidative aging resistance and satisfactory dielectric properties. However, these vulcanizates exhibit lower flexibility, worse tensile and abrasion properties compared to the sulfur-vulcanized ones (Matador Rubber 2007).

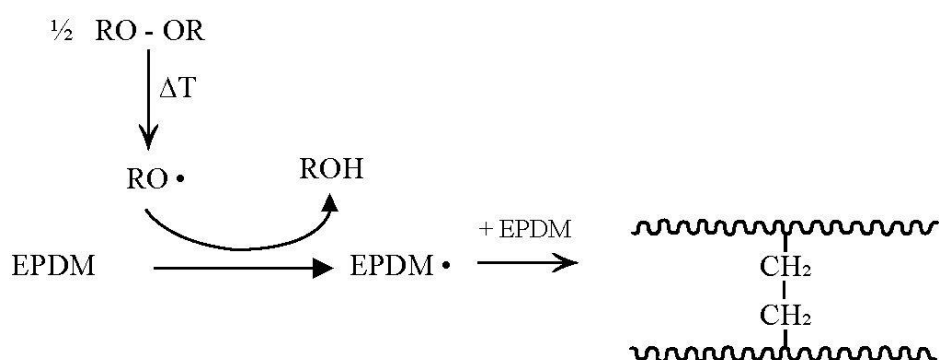


Figure 2. Proposed reaction mechanism for peroxide vulcanization of EPDM (Van Duin 2002; Matador Rubber 2007)

Along with the sulfur and peroxide vulcanization systems, resin vulcanization and high-energy ionizing radiation vulcanization are also among crosslinking methods for EPDM. Ionizing radiation and e-beam are preferred especially on cable sheathing applications (Matador Rubber 2007). Rubber materials tend to age due to radicalic reactions on the polymeric structures as for human body by time. The main approach to prevent and/or retard aging is to use various stabilizing agents such as antioxidants. These are the additives, which scavenge the free radicals so that they cannot affect the polymeric material. Chemical and/or physical changes in the polymer structure during thermo-oxidative aging depend strongly on the type polymer. Thermal aging takes place in rubber-based materials via two main mechanisms (Johlitz, Diercks, and Lion 2014; Polymer Properties Database n.d.). First mechanism is main chain scission. Common characteristics of the rubbers, which follows the first mechanism, is to have electron donor  $-\text{CH}_3$  group connected to the C atom on the double bond. This  $-\text{CH}_3$  group is vulnerable to oxidation. Second mechanism results with additional crosslinking. Rubbers following the second aging mechanism usually have highly electronegative groups such as halogens connected to the double bond and therefore they are highly stable (Mathew and De 1983; Nakajima 2000).

During the aging of polymers, the macromolecular structure is oxidized to form perhydrate and then these perhydrates turn into free radicals. Following that, other chain segments interact with the free radicals to form new perhydrates and then new free radicals. This consecutive process goes on over whole aging process. Antioxidants are able to inhibit/retard free radical attack onto polymer chains in order to break consecutive aging reactions. Besides, antioxidants can also decrease the concentration of hydroperoxides, which comes from thermo-oxidative degradation of the polymer (Li et al. 2020). Short and long term aging of both sulfur and peroxide cured EPDM has been studied in literature (Rojas Rodríguez, D'almeida, and Marinkovic 2021; R. Wang et al. 2020; Z.-N. Wang et al. 2020; Wang and Qu 2003; Zhang, X., Li, J., Chen, Z., Pang, C., He, S., Lin 2022). Many of the studies investigating aging mechanism of EPDM figure out crosslink density to increase during aging period. Aging behavior of EPDM due to UV exposure was studied and micro and macro surface cracks were correlated to oxidation reactions during aging by Tan et al. (Tan et al. 2021). In that study, aging of EPDM due to various external factors was explained with two main stages. In the first stage, chain scission reaction caused an increase in free volume and in gas permeability due to decreasing overall crosslink density. Accordingly, crosslink density was reported to increase in the second stage of aging process. In another study, thermo-oxidative aging of EPDM/carbon nanotube composites was investigated and increased overall crosslink density was reported (Zhang, X., Li, J., Chen, Z., Pang, C., He, S., Lin 2022).

Proposed heat and light-initiated photo-oxidation mechanism of EPDM is depicted in Figure 3. At the beginning of the reaction, peroxy radical ( $\text{ROO}\cdot$ ) is formed by means of external energy. Peroxy radical reacts with EPDM molecules to give alkyl radical ( $\text{R}\cdot$ ) and hydroperoxide ( $\text{ROOH}$ ), which then immediately turn into alkoxy ( $\text{RO}\cdot$ ) and hydroxy ( $\cdot\text{OH}$ ) radicals. Alkoxy and hydroxy radicals are able to react with EPDM molecule to give  $\text{H}_2\text{O}$  molecule and  $\text{R}\cdot$  radical.  $\text{R}\cdot$  radical is still very active to combine with air oxygen to yield  $\text{ROO}\cdot$  by means of a cyclic oxidation reaction. The most unstable radical among all is  $\text{RO}\cdot$  and various oxygen containing species such as esters, ethers and ketones may occur via  $\text{RO}\cdot$  reactions (Tan et al. 2021).

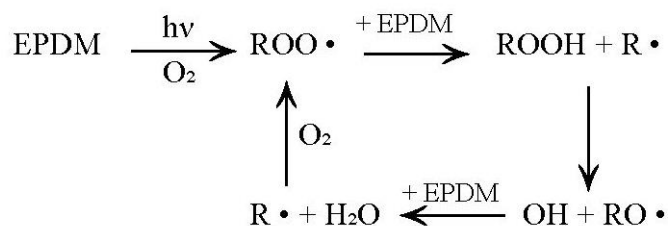


Figure 3. Proposed photo-oxidation mechanism of EPDM (Tan et al. 2021)

Anti-aging additives used in rubbers, which tend to degrade under the influence of oxygen, ozone and heat, are classified in ASTM D4676. These are basically defined as antioxidants and antiozonants and they are added into rubber compound in the amount of 1-4 phr (Ciesielski 1999; De and Jim R. White 2001). Antioxidants inhibit/retard the oxidation process by means of scavenging free radicals and hydroperoxides, which form during oxidation reaction (Li et al. 2020). The most widely used anti-aging additives in rubber industry are phenolic and amine based antioxidants (Khalaf, Helaly, and El-Sawy 2014). TMQ takes place among all with its competitive price and satisfactory anti-aging performance. It is effective for rubber materials at also relatively high service temperatures even used in 1-2 phr. Sequential configurations of TMQ during its anti-aging action is shown in Figure 4. Similar mechanisms have also been proposed in literature (Arvind Mafatlal Group and Nocil Limited 2010; Huntink and Datta 2003). TMQ follows subsequent reactions to give stable configurations in order to inhibit oxidation. Secondary amine group (=N-H) of TMQ turns into nitroso form (-NO) and this structure is very effective on anti-oxidation process. In general, amine based antioxidants are able to form nitroso radicals in the presence of ambient peroxy radicals, and thus they can trap alkyl radicals easily in order to terminate auto-oxidation process. This reaction cycle goes on until the nitroso radicals to decompose by uneven side reactions.

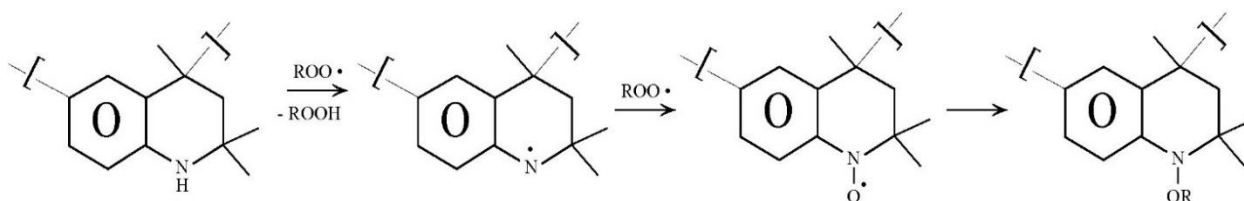


Figure 4. Sequential configurations of TMQ over its anti-aging action

Service life of the polymeric material as well as the degradation mechanisms are among the most important factors to take into account during material design. Polymers are affected by several external factors during their service life including mechanical, thermal, oxidative, chemical, biological, radiative and electrical factors. These deteriorative effects may cause further crosslinking, chain scission, chemical degradation and crystallization depending on the material type, rate and the amount of the deteriorative effect. The most common degradations result with fracture, change in color, swelling and dimensional changes in the material (Hulme and Cooper 2012).

Rubbers, due to their viscoelastic structure, exhibit time and temperature-dependent properties during deformation. For example, elastic modulus of a rubber material decreases when a constant load applied. This behavior is attributed to the molecules to change their arrangements by time in order to avoid local stress concentration. That is why the modulus value is measured as lower for short-term tests compared to long-term tests. Due to such time-dependent response, service life of the rubbers can only be measured for realistic test conditions and for a meaningful time period. However, such long tests are not practical of course; those properties reflecting the service life of the material need to be predicted by using well-defined models instead (Instruments n.d.). Service life or life-time prediction of the polymers are usually performed by employing

accelerated aging tests to let aging reactions occur in a shorter time period at higher temperatures (Celina, Gillen, and Assink 2005). In this method, test samples are exposed to gradually increasing temperatures and the related properties are monitored over time for all the test temperatures to figure out the degradation reaction (aging) kinetics (Hulme and Cooper 2012). Arrhenius method (ISO 11346, Rubber, vulcanized or thermoplastic – Estimation of life-time and maximum temperature of use), which is used in this study, is the most common and practical method to evaluate the relation between temperature and thermo-oxidative degradation reaction rate of the polymers (Huy and Evrard 1998). Very well-known Arrhenius equation is given in Equation 1.1, where  $K_T$  is the reaction rate constant at temperature  $T$ ,  $A$  is the frequency factor,  $E_a$  is the reaction activation energy and  $R$  is the universal gas constant (Woo and Park 2011).

$$K_T = A e^{\frac{-E_a}{RT}} \quad (1.1)$$

According to Arrhenius approach, rate of degradation reaction can be measured by following a specific property over time. In this approach, it is basically assumed that a specific level of change (due to degradation) in the related property at a relatively low temperature occurs in shorter time at higher degradation temperatures. Firstly, at least one specific property is selected to follow considering the expectations from the material on its service. Initial value of the property is recorded as the reference. Then the material test samples are subjected to thermal aging at three or more elevated temperatures, which the lowest one is at least 30°C higher than the expected service temperature of the material. Samples are tested over time with adequate intervals for each aging temperatures. For example, measurements should be performed more frequent for relatively high aging temperatures due to the fact that the service life will over earlier in this case. Threshold for service life or life-time of the material is usually defined as the time to loss half of the selected property, but the better is to consider the expectations from the material in more detail and then to define life-time threshold for individual cases. In Arrhenius model, all the test results for an aging temperature are evaluated to calculate the reaction rate constant for that temperature. Then, activation energy of the aging reaction is calculated with the rate constants obtained for different aging temperatures and used to extrapolate to time, that is called life-time of the material, to reach the same threshold at service temperature. Arrhenius method is also described in detail in ISO 11346.

In this study, thermal aging behavior of EPDM based samples, which were prepared by using various curing systems, with and without TMQ. Rheological, mechanical and structural properties were studied and life-time of these samples were calculated by using Arrhenius method.

## 2. Materials and Methods

### 2.1. Materials

EPDM rubber, Nordel 4770P with the Mooney viscosity (ML [1 + 4] @100°C) of 70±3 MU was purchased from Dow Chemicals. N550 type carbon black (CB, Omsk Carbon, Russia) was used as reinforcing filler. Kaolin (Polestar 200R, Imerys) was the other component of the filler system. Paraffinic oil (Petroyag, Turkey) was selected as process oil for dispersing the fillers in the compound matrix. The other components; zinc oxide, stearic acid, TMQ, sulfur, dicumyl peroxide, mercaptobenzotiazole disulfide (MBTS), tetramethyl thiuram disulfide (TMTD) and zinc dibutyldithiocarbamate (ZDBC) were obtained from various suppliers, which provide raw materials to tyre and rubber industries.

### 2.2. Methods

Rubber compounds were prepared by using various curing systems; compound formulations are given in Table 1. Compound codes were designed in order to define curing system and the presence of TMQ. Code “P” refers peroxide curing system, whereas code “SC” refers conventional sulfur curing system and code “SE” does efficient sulfur curing system. “T” in compound code means that the compound also contains 2 phr TMQ antioxidant. Compounds were prepared in a laboratory type Banbury mixer with 2 L of gross volume.

Homogenization and shaping the compounds were performed on a two-roll open mill, subsequently. Optimum curing time and rheological properties of the compounds were measured at 190°C by RADE MR-C3 moving die rheometer according to ASTM D2084. Compounds were moulded on a hydraulic hot press at the same temperature for their respective optimum cure times. Standard blades were used to cut the standard test samples from the vulcanized plaques prior to physical and mechanical characterization. Tensile properties were measured on a universal test machine (Testometric M350-10CT) according to ASTM D412. Tensile tests were also performed after thermal aging of the samples in an air-circulating oven operating at 50°C, 70°C, 100°C and 135°C for respective times to loss prescribed percentage (threshold) of their tensile properties. Tensile strength and 100% tensile modulus values were followed versus aging time at all the aging temperatures. According to the Arrhenius approach, life-time threshold of EPDM based rubber materials was assumed as 50% change in 100% tensile modulus after aging.

Unaged and aged sample surfaces were analyzed with Fourier Transform Infrared Spectroscopy (FTIR) equipped with Attenuated Total Reflection (ATR) configuration. FTIR (Perkin Elmer Spectrum 100 Optica FT-IR Spectrometer) spectrums were obtained for 650-4000  $\text{cm}^{-1}$  with the resolution of 4  $\text{cm}^{-1}$  according to ASTM D3677 and they were used for both qualitative and quantitative analysis. Periodical carbonyl index (CI) measurement was performed for following oxidative reactions. Absorption bands of carbonyl groups are between 1850-1650  $\text{cm}^{-1}$  and CI can be calculated by normalizing carbonyl peak to a selected reference peak in the spectrum. Here, in quantitative analysis, CI values of all the unaged and aged samples were calculated by using SAUB (Specified Area Under Band) methodology on ATR-FTIR (Almond et al. 2020).

Table 1  
Rubber compound formulations (in phr)

	EP	EP-T	EPSC	EPSC-T	EPSE	EPSE-T
EPDM (NORDEL 4770P)	100	100	100	100	100	100
Carbon black (FEF N550)	70	70	70	70	70	70
Calcinated kaolin	30	30	30	30	30	30
Paraffinic oil	20	20	20	20	20	20
Zinc oxide	5	5	5	5	5	5
Stearic acid	2	2	2	2	2	2
TMQ		2		2		2
DCP 40	5	5				
Sulfur 80			2.5	2.5	1	1
ZDBC			1	1	2	2
MBTS			1	1		
TMTD					2	2

### 3. Results and Discussion

#### 3.1. Rheological Properties

Rheological parameters such as minimum and maximum torque values (ML and MH respectively), scorch time ( $t_{s2}$ ) and optimum cure time ( $t_{90}$ ), which were obtained from the cure curves are given in Table 2. Cure extent (CE) that is related to amount of crosslinks occurred during vulcanization and cure rate index (CRI) values were calculated from the rheological data and they are also given in Table 2.

Table 2  
Rheological properties of the rubber compounds

	ML (dNm)	MH (dNm)	t <sub>s2</sub> (min)	t <sub>90</sub> (min)	CE (dNm)	CRI (min <sup>-1</sup> )
EP	5.49	18.63	0.16	1.00	13.14	119
EP-T	6.19	17.04	0.24	1.15	10.85	110
EPSC	5.88	18.78	0.26	1.25	12.90	101
EPSC-T	5.49	18.65	0.25	1.29	13.16	96
EPSE	5.90	19.70	0.23	1.19	13.80	104
EPSE-T	5.71	18.41	0.26	1.18	12.70	109

ML value is directly related to the viscosity of the rubber compound and therefore represents processability. From Table 2, it is seen that all the compounds have similar viscosity. It is expected to have lower cure extent in the case of an effective protection against thermo-oxidative aging since a powerful antioxidant can act as a radical scavenger. Indeed, a powerful radical scavenger also inhibits vulcanization reaction by blocking active crosslinking sites on the polymer chain. This phenomena is a well-known problem in rubber compounding and requires attention on selecting the appropriate type and amount of antioxidant for getting balanced cure extent and anti-aging effect (Li et al. 2020).

EP compound, which was prepared with peroxide and no TMQ, shows the highest cure rate and it starts to vulcanize earlier than the other compounds. Once TMQ is added into the compound (EP-T), both cure initiation time and optimum cure time increases. One other effect of TMQ on peroxide curing is that it significantly decreased cure extent. Cure extent, which is also defined as delta torque value, is proportional to crosslinking degree for a rubber compound (Li et al. 2020). In other words, in the presence of TMQ, less amount of crosslinks could occur over the same curing time. This could easily be attributed to TMQ to block the peroxy radicals that occur during peroxide vulcanization and therefore it adversely affects the crosslinking efficiency (Abdel-Aziz and Basfar 2000; Li et al. 2020). Due to that, EP-T compound showed 10% lower cure rate than EP compound. The same amount of decrease was also observed for EPSE-T compound, which was prepared with efficient sulfur curing system and with TMQ. However, there was no remarkable change in cure extent due to the addition of TMQ when curing system was selected as conventional sulfur (EPSC-T vs EPSC). This can be attributed to that excessive amount of curative species (sulfur based radicals) were already available in the reaction media.

### 3.2. Mechanical Properties

Tensile data of the vulcanizates were collected considering their expected retention for the respective aging temperatures. All tensile data was used in life-time estimation study. Aging periods were selected as 3 days, 1 week, 3 weeks, 10 weeks and 16 weeks for 50°C whereas the samples were subjected thermal aging for 2 days, 5 days, 1 week, 1.5 week and 2 weeks for 135°C. However, tensile strength values were compared in order to evaluate their tensile retentions for the same aging period (1 week), which was available for all of the vulcanizates. Tensile strength of the vulcanizates before (original) and after thermal aging for 1 week at various temperatures are given in Figure 5, Figure 6, and Figure 7. Aging conditions were selected as practical maximum service temperature of the material. When the original tensile strength values are evaluated, a slight decrease was observed and it was attributed to lower crosslinking level due to the presence of antioxidant. This finding shows a good correlation to the literature that some of the free radicals on peroxide vulcanization are terminated by antioxidant species resulting with deteriorated mechanical properties (Li et al. 2020). However, when the amount of decrease in tensile strength is compared within each vulcanization system, there could not be seen a linear trend. This finding can readily be attributed to different overall crosslink structures occurred during the selected vulcanization systems in this study. The highest original tensile strength values belong to

the EP samples and it was followed by EPSE samples. The lowest tensile strength values were measured for conventional sulfur vulcanization system unlikely that was given in literature for natural rubber and chloroprene rubber, which had basic isoprene structure (Yahya, Azura, and Ahmad 2011). For peroxide vulcanization, TMQ could significantly reduce retention in tensile strength of the vulcanizates, which were subjected to thermo-oxidative aging. This was more pronounced for relatively high aging temperatures. In contrast to the expectations, an equivalent protection could not be obtained for sulfur vulcanization.

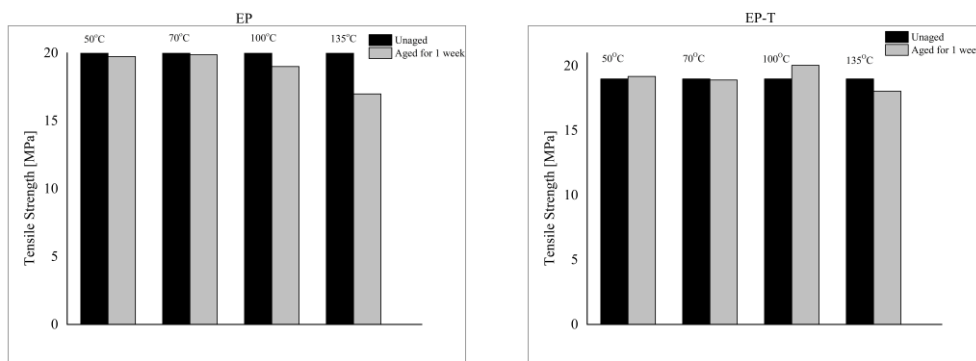


Figure 5. Tensile strength values of EP and EP-T vulcanizates before and after thermo-oxidative aging

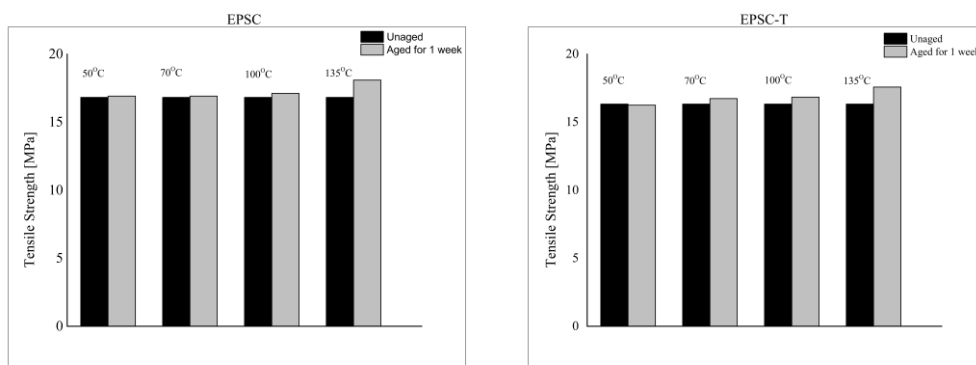


Figure 6. Tensile strength values of EPSC and EPSC-T vulcanizates before and after thermo-oxidative aging

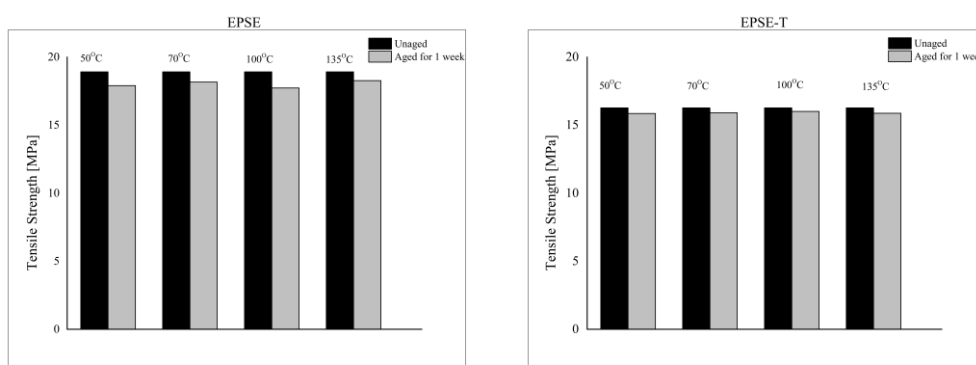


Figure 7. Tensile strength values of EPSE and EPSE-T vulcanizates before and after thermo-oxidative aging

### 3.3. Life-Time Estimation

To correlate long-term behaviour, theoretical life-time of the EPDM-based materials prepared with various vulcanization systems was estimated according to Arrhenius approach. For this purpose, 100% modulus values of the vulcanizates were monitored after aging for specified periods at  $T_1=150^\circ\text{C}$ ,  $T_2=135^\circ\text{C}$ ,  $T_3=100^\circ\text{C}$ , and  $T_4=70^\circ\text{C}$ . The time that corresponds to 50% change in the 100% tensile modulus of respective samples was considered as life-time threshold. Time data for all the aging temperatures was recorded as  $t_1$ ,  $t_2$ ,  $t_3$  and  $t_4$ , where  $t_i$  represents the time corresponding to the threshold modulus value at  $T_i$ . Although they were reported by

means of tensile retention in Figure 5, Figure 6 and Figure 7, aging at 50°C was not included in life-time estimation study due to extremely long aging time to reach the life-time threshold. Aging activation energy ( $E_a$ ) was calculated separately for all the aging temperatures according to the Arrhenius equation (Eq. 1.1). Then,  $E_a$  was placed into the equation 3.1 given below, which was obtained by processing Eq. (1.1) in order to yield the rate constant of the aging reaction at any temperature. Here, expected service temperature ( $T_s$ ) was selected as 25°C (298.15 K) and then the reaction rate constant ( $K_T$ ) was used to calculate estimated life-time ( $t_s$ ) of the sample at  $T_s$ . Activation energy values corresponding to thermo-oxidative aging reaction for all the vulcanizates are shown in Figure 8 and the calculated life-times are in Figure 9.

$$\ln(K_T) = B - \frac{E_a}{R T_s} \quad (3.1)$$

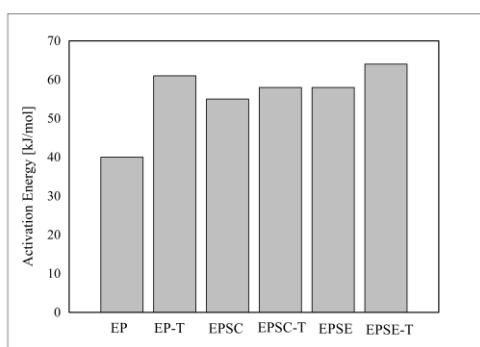


Figure 8. Activation energy for the aging reaction (kJ/mol)

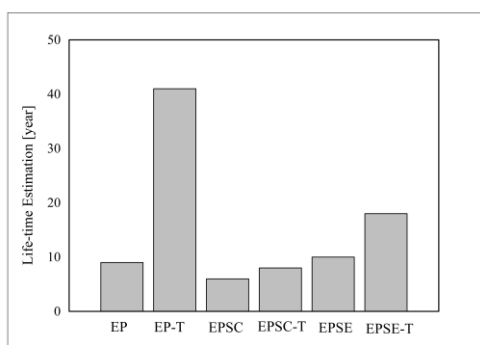


Figure 9. Estimated life time according to Arrhenius approach (in Years)

As it can be seen from the figures, the lowest activation energy was calculated for the case of peroxide vulcanization. Besides, TMQ was clearly found to improve estimated life-time of the peroxide-cured EPDM material about 4-folds by increasing aging activation energy. In spite of the fact that efficient sulfur vulcanization system could not yield good original mechanical strength compared to peroxide system, EPSE sample was found to have the longest life-time among all non-TMQ vulcanizates. Besides, addition of TMQ to that sample could almost double the life-time of the material (EPSE-T). It was concluded that, TMQ could increase aging activation energy for all of the vulcanization systems but it could improve less the conventional sulfur vulcanization system regarding life-time of the vulcanizates. As a result of the above evaluations, the main approach is to define a useful service life for the material rather than to find the time that corresponds to failure of the material. Therefore, the results can be used for comparing long-term behaviour of the materials, relatively. By using the same approach, it is available to predict life-time of rubber materials with different composition for another specified property and another threshold value.

### 3.4. FTIR Analysis

FTIR analysis is a practical method to investigate basic structural changes in rubber materials over aging in various conditions (Sanches et al. 2015). In this study, ATR-FTIR spectra of the vulcanizates over different

aging times at various temperatures was monitored to investigate anti-aging performance of TMQ for various curing systems as well as the aging mechanism. Spectral characterization was performed for the range of 1000–4000  $\text{cm}^{-1}$ . The relative FTIR spectra of all the vulcanizates were examined; one (EP) was shown in Figure 10 as an example. Changes in the oxygen containing functional groups -OH and C=O over thermo-oxidative aging were also shown in Figure 10. It is expected absorption band and the intensity of these species to increase over the aging period, which is initiated by oxygen attack to the polymer main chain (Almond et al. 2020; Ooi, Ismail, and Bakar 2013). A high intensity of the peak in the range of vibrations is explained with the eclipse for -OH and C=O groups.

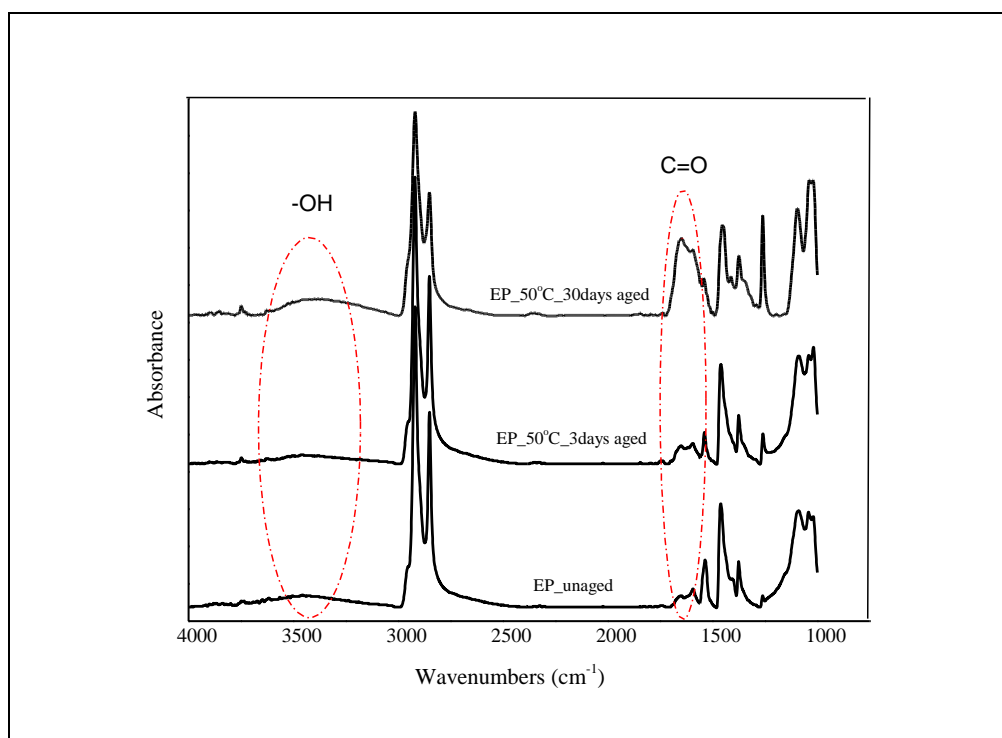


Figure 10. ATR-FTIR spectrum of EP over aging at 50°C

Figure 11 depicts structural changes in EP sample before and after aging for 3 and 30 days at 135°C. Characteristic peaks of EPDM are defined on the spectra given in the figure. 3355  $\text{cm}^{-1}$  peak in Figure 11 corresponds to the stretching vibration of -OH. The two peaks, which exhibit decreasing intensity, one at 2925  $\text{cm}^{-1}$  corresponds to the asymmetric stretching vibrations of methylene group whereas the other one at 2854  $\text{cm}^{-1}$  is related to the symmetric stretching vibrations of the same group on the saturated hydrocarbon backbone (Z.-N. Wang et al. 2020). Two new peaks at 1640  $\text{cm}^{-1}$  and 1595  $\text{cm}^{-1}$  were observed after aging. The one at 1640  $\text{cm}^{-1}$  corresponds to the stretching vibrations of the carbonyl group (C=O), and the other one at 1595  $\text{cm}^{-1}$  can be assigned to C=C stretching vibrations (Z.-N. Wang et al. 2020). The peaks at 1464  $\text{cm}^{-1}$  and 1377  $\text{cm}^{-1}$  are due to the bending vibration of  $\text{CH}_2$  groups and the symmetric C-H stretching vibration of methyl, respectively (Li et al. 2020). In Figure 11, it can clearly be seen the absorbance of the peaks at 3355  $\text{cm}^{-1}$ , 1640  $\text{cm}^{-1}$  and 1595  $\text{cm}^{-1}$  increase indicating the higher concentration of the corresponding functional groups during thermo-oxidative aging.

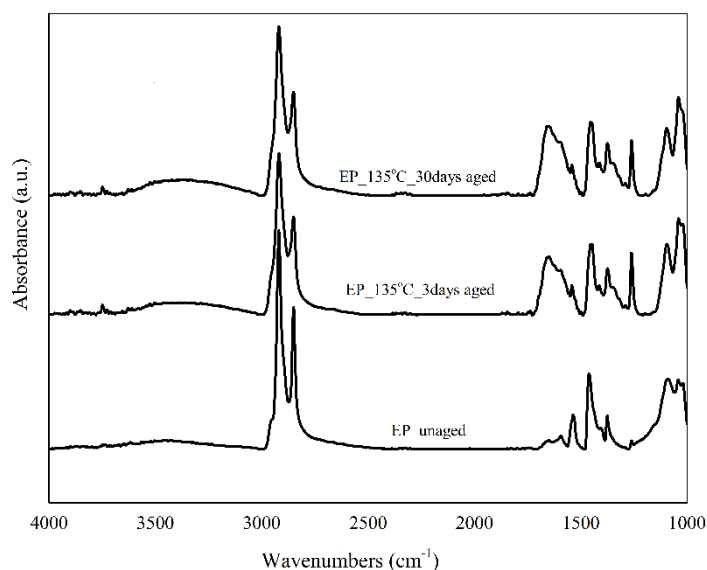


Figure 11. ATR-FTIR spectrum of EP over aging at 135°C

Since the carbonyl groups are known as the most indicative oxidation product, “carbonyl index (CI)” is a useful tool to determine extent of thermo-oxidative aging of EPDM based vulcanizates (Bouguedad et al. 2015). In this study, SAUB-CI (Specified Area Under Band-Carbonyl index) method has been used for quantitative analysis of the ATR-FTIR spectrum. CI was calculated by comparing the integration of 1850 to 1640  $\text{cm}^{-1}$  band absorbance (C=O) to that of -CH<sub>2</sub>- scissoring peak from 1500 to 1420  $\text{cm}^{-1}$ . The related expression for calculating CI is given in Equation (3.2) (Almond et al. 2020). Integration of the band absorbance, which is the area under the band, was calculated by using peak analysis tool of PerkinElmer Spectrum 10 Spectroscopy Software.

$$\text{Carbonyl index (CI)} = \frac{\text{Area under band}_{1850 \text{ cm}^{-1}-1640 \text{ cm}^{-1}}}{\text{Area under band}_{1500 \text{ cm}^{-1}-1420 \text{ cm}^{-1}}} \quad (3.2)$$

Carbonyl index values of all the vulcanizates were calculated over aging at 135°C and the results are given in Figure 12. A systematic increase in the concentration of C=O groups is clearly seen for all the samples as expected. However, TMQ showed a positive effect on protecting the vulcanizates against thermo-oxidative aging. This is more prominent for peroxide cured EPDM compound (EP-T), especially for long aging periods.

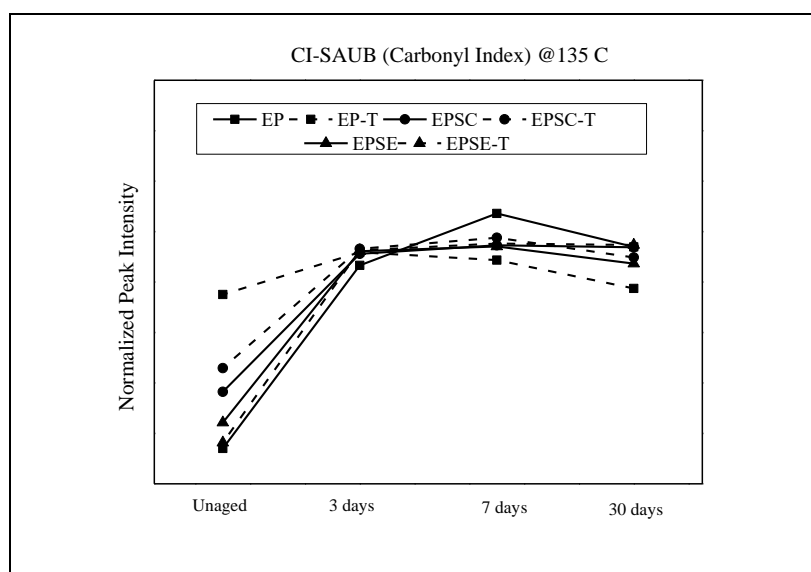


Figure 12. Calculated carbonyl index (CI) of the vulcanizates during aging at 135°C

#### 4. Conclusion

In this study, TMQ, which is a very common and commercially available antioxidant for industrial rubber applications, has been evaluated regarding its anti-aging effect on various curing systems. Arrhenius method (ISO 11346, Rubber, vulcanized or thermoplastic – Estimation of life-time and maximum temperature of use), which is widely used for characterizing industrial rubber goods, has also been used for predicting life-time of the compounds prepared with and without antioxidant. TMQ has found to be an effective agent for stabilizing EPDM based rubber compounds against thermo-oxidative aging, especially for long aging periods. Degree of stabilization depends strictly on the curing system. Due to the fact that different crosslink types occur in different amounts with peroxide and sulfur curing systems makes it harder to evaluate individual effect of TMQ on rheological and mechanical properties. However, it was concluded that TMQ could increase aging activation energy for all the vulcanization system studied and therefore longer useful life-time for the vulcanizates could be obtained. Significantly lower cure extent along with longer cure time for peroxide system in the presence of TMQ was attributed to radical scavenging activity that also indicated a powerful antioxidant.

#### Author Contributions

Şehriban Öncel: Organized the study plan, performed analysis, analyzed the data and wrote the article.

Gürcan Gül: Contributed to the experimental study and analyzed the data.

Mahir Burak Efe: Contributed to the experimental study.

Hakan Erdoğan: Performed analysis.

Bağdagül Karaağaç: Co-organized the study plan, analyzed the data and wrote the article.

#### Conflicts of Interest

The authors declare no conflict of interest.

#### References

- Abdel-Aziz, M. M., & Basfar, A. A. (2000). Aging of ethylene-propylene diene rubber (EPDM) vulcanized by  $\gamma$ -radiation. *Polymer testing*, 19(5), 591-602. [https://doi.org/10.1016/S0142-9418\(99\)00030-6](https://doi.org/10.1016/S0142-9418(99)00030-6)
- Almond, J., Sugumaar, P., Wenzel, M. N., Hill, G., & Wallis, C. (2020). Determination of the carbonyl index of polyethylene and polypropylene using specified area under band methodology with ATR-FTIR spectroscopy. *E-Polymers*, 20(1), 369-381. <https://doi.org/10.1515/epoly-2020-0041>
- Arvind Mafatlal Group, and Nocil Limited. 2010. Antioxidants & Antidegradants. Retrieved April 10, 2023. <https://www.nocil.com/Downloadfile/ETechnicalNote-Antioxidants-Dec2010.pdf>
- Bouguedad, D., Mekhaldi, A., Jbara, O., Rondot, S., Hadjadj, A., Douglade, J., & Dony, P. (2015). Physico-chemical study of thermally aged EPDM used in power cables insulation. *IEEE Transactions on Dielectrics and Electrical Insulation*, 22(6), 3207-3215. <https://doi.org/10.1109/TDEI.2015.005227>
- Bouguedad, D., Mekhaldi, A., Boubakeur, A., & Jbara, O. (2008). Thermal ageing effects on the properties of ethylene-propylene-diene monomer (EPDM). In *Annales de chimie (Paris. 1914)*, Vol. 33, No. 4, pp. 303-313. <http://dx.doi.org/10.3166/acsm.33.303-313>
- Celina, M., Gillen, K. T., & Assink, R. A. (2005). Accelerated aging and lifetime prediction: Review of non-Arrhenius behaviour due to two competing processes. *Polymer Degradation and stability*, 90(3), 395-404. <https://doi.org/10.1016/j.polymdegradstab.2005.05.004>
- Ciesielski, A. (1999). An introduction to rubber technology. iSmithers Rapra publishing.
- De, S. K., & White, J. R. (Eds.). (2001). Rubber technologist's handbook (Vol. 1). iSmithers Rapra Publishing.
- Delor-Jestin, F., Lacoste, J., Barrois-Oudin, N., Cardinet, C., & Lemaire, J. (2000). Photo-, thermal and natural ageing of ethylene-propylene-diene monomer (EPDM) rubber used in automotive

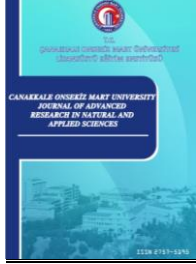
- applications. Influence of carbon black, crosslinking and stabilizing agents. *Polymer Degradation and Stability*, 67(3), 469-477. [https://doi.org/10.1016/S0141-3910\(99\)00147-0](https://doi.org/10.1016/S0141-3910(99)00147-0)
- Van Duin, M. (2002). Chemistry of EPDM cross-linking. *kautschuk gummi kunststoffe*, 55(4), 150-150.
- Hulme, A., & Cooper, J. (2012). Life prediction of polymers for industry. *Sealing Technology*, 2012(9), 8-12. [https://doi.org/10.1016/S1350-4789\(12\)70398-7](https://doi.org/10.1016/S1350-4789(12)70398-7)
- Huntink, N. M., Datta, R. N., & Noordermeer, J. W. M. (2004). Addressing durability of rubber compounds. *Rubber chemistry and technology*, 77(3), 476-511. <https://doi.org/10.5254/1.3547833>
- Le Huy, M., & Evrard, G. (1998). Methodologies for lifetime predictions of rubber using Arrhenius and WLF models. *Die Angewandte Makromolekulare Chemie*, 261(1), 135-142. [https://doi.org/10.1002/\(SICI\)1522-9505\(19981201\)261:262:1<135::AID-APMC135>3.0.CO;2-W](https://doi.org/10.1002/(SICI)1522-9505(19981201)261:262:1<135::AID-APMC135>3.0.CO;2-W)
- Instruments, T. A. (1999). Thermal analysis application brief. TA-125.
- Johlitz, M., Diercks, N., & Lion, A. (2014). Thermo-oxidative ageing of elastomers: A modelling approach based on a finite strain theory. *International Journal of Plasticity*, 63, 138-151. <https://doi.org/10.1016/j.ijplas.2014.01.012>
- Khalaf, A. I., Helaly, F. M., & El-Sawy, S. M. (2014). Effect of chitosan derivatives as rubber antioxidants for increasing durability. *Research on Chemical Intermediates*, 40, 1383-1401. <https://doi.org/10.1007/s11164-013-1046-y>
- Li, J., Zhou, C., Cao, D., & Liu, H. (2020). Synergistic Effects of Amine-Containing Antioxidants on the Aging Performances of Ethylene Propylene Diene Rubber. *Chemistry Select*, 5(16), 4961-4966. <https://doi.org/10.1002/slct.202001279>
- Rubber, M. (2007). *Rubber chemistry*. Education and culture.
- Mathew, N. M., & De, S. K. (1983). Thermo-oxidative ageing and its effect on the network structure and fracture mode of natural rubber vulcanizates. *Polymer*, 24(8), 1042-1054. [https://doi.org/10.1016/0032-3861\(83\)90158-1](https://doi.org/10.1016/0032-3861(83)90158-1)
- Nakajima, N. (2000). *Science and practice of rubber mixing*. iSmithers Rapra Publishing.
- Ooi, Z. X., Ismail, H., & Bakar, A. A. (2013). A comparative study of aging characteristics and thermal stability of oil palm ash, silica, and carbon black filled natural rubber vulcanizates. *Journal of Applied Polymer Science*, 130(6), 4474-4481. <https://doi.org/10.1002/app.39649>
- Polymer Properties Database. Thermal-Oxidative Degradation Of Rubber. Retrieved October 28, 2020. [http://polymerdatabase.com/polymer chemistry/Thermal Degradation Elastomers.html](http://polymerdatabase.com/polymer%20chemistry/Thermal%20Degradation%20Elastomers.html)
- Datta, R. N. (2002). Rubber curing systems (Vol. 12). iSmithers Rapra Publishing.
- Rojas Rodríguez, F. I., d'Almeida Moraes, J. R., & Marinkovic, B. A. (2021). Natural aging of ethylene-propylene-diene rubber under actual operation conditions of electrical submersible pump cables. *Materials*, 14(19), 5520. <https://doi.org/10.3390/ma14195520>
- Sanches, N. B., Cassu, S. N., & Dutra, R. D. C. L. (2015). TG/FT-IR characterization of additives typically employed in EPDM formulations. *Polímeros*, 25, 247-255. <https://doi.org/10.1590/0104-1428.1819>
- Savran, H. Ö. (2001). *Elastomer Teknolojisi - 1*. Rubber Society Publications. İstanbul, Türkiye.
- Simpson, R. B. (Ed.). (2002). *Rubber basics*. iSmithers Rapra Publishing.
- Tan, J. H., Chen, C. L., Wu, J. Y., He, R., & Liu, Y. W. (2021). The effect of UV radiation ageing on the structure, mechanical and gas permeability performances of ethylene-propylene-diene rubber. *Journal of Polymer Research*, 28, 1-10. <https://doi.org/10.1007/s10965-021-02447-8>
- Wang, R., He, Y., Wang, Z., Kang, H., Ma, J., & Jin, H. (2020, March). Effect of thermal aging on breakdown strength of EPDM rubber. In *IOP Conference Series: Materials Science and Engineering*, Vol. 768, No. 6, p. 062091. IOP Publishing. <https://doi.org/10.1088/1757-899X/768/6/062091>
- Wang, W., & Qu, B. (2003). Photo-and thermo-oxidative degradation of photocrosslinked ethylene-propylene-diene terpolymer. *Polymer degradation and stability*, 81(3), 531-537. [https://doi.org/10.1016/S0141-3910\(03\)00154-X](https://doi.org/10.1016/S0141-3910(03)00154-X)
- Wang, Z. N., Shen, S. L., Zhou, A. N., & Xu, Y. S. (2020). Experimental evaluation of aging characteristics of EPDM as a sealant for undersea shield tunnels. *Journal of Materials in Civil Engineering*, 32(7),

04020182. [https://doi.org/10.1061/\(ASCE\)MT.1943-5533.0003242](https://doi.org/10.1061/(ASCE)MT.1943-5533.0003242)

Woo, C. S., & Park, H. S. (2011). Useful lifetime prediction of rubber component. *Engineering Failure Analysis*, 18(7), 1645-1651. <https://doi.org/10.1016/j.engfailanal.2011.01.003>

Yahya, Y. R., Azura, A. R., & Ahmad, Z. (2011). Effect of curing systems on thermal degradation behaviour of natural rubber (SMR CV 60). *Journal of Physical Science*, 22(2), 1-14.

Zhang, X., Li, J., Chen, Z., Pang, C., He, S., & Lin, J. (2022). Study on thermal-oxidative aging properties of ethylene-propylene-diene monomer composites filled with silica and carbon nanotubes. *Polymers*, 14(6), 1205. <https://doi.org/10.3390/polym14061205>



## Gıda Sektöründe Çalışanların Salgın Hastalık Farkındalıkları: Çanakkale İli Örneği

Orkun Dalyan<sup>1\*</sup>, Mehmet Pişkin<sup>2</sup>, Erdal Canpolat<sup>3</sup>, Ömer Faruk Öztürk<sup>4</sup>

<sup>1</sup>İş Sağlığı ve Güvenliği Anabilim Dalı, Lisansüstü Eğitim Enstitüsü, Çanakkale Onsekiz Mart Üniversitesi, Çanakkale, Türkiye

<sup>2</sup>Gıda İşleme Bölümü, Çanakkale Teknik Bilimler Meslek Yüksek Okulu, Çanakkale Onsekiz Mart Üniversitesi, Çanakkale, Türkiye

<sup>3</sup>Fen Bilgisi Eğitimi Bölümü, Eğitim Fakültesi, Fırat Üniversitesi, Elazığ, Türkiye

<sup>4</sup>Kimya Bölümü, Fen Fakültesi, Çanakkale Onsekiz Mart Üniversitesi, Çanakkale, Türkiye

### Makale Tarihi

Gönderim: 03.02.2023

Kabul: 17.07.2023

Yayın: 20.12.2023

### Araştırma Makalesi

**Öz** – Dinamik ve sürekli büyüyen gıda sektörü personellerinin bireysel hijyen davranışları, gıda güvenliğinin yanı sıra bulaşıcı hastalıkların (özellikle de koronavirüs hastalığı) salgın boyutuna geçmesinde önemlidir. Bu çalışmada, salgın sırasında, gıda sektörü personellerinin sağlık ve gıda güvenliği hakkında bilgi ve tutumları ayrıca bu salgının farkındalığına etki eden hijyen kriterleri incelenmiştir. Çanakkale ilinde gıda sektörü çalışanları ile 01.11.2022–01.12.2022 tarihleri arasında 42 ifadeyi içeren anket çalışması gerçekleştirilmiştir. Olasılıksız örnekleme ile seçilen 124 personelin anket verileri, literatürde konuyla ilgili önceki çalışmalarla karşılaştırılmıştır. Katılımcıların %31,5'i 26-35 yaş aralığındadır. Katılımcıların %48,4'ü lise düzeyinde eğitim seviyesine sahiptir. Katılımcıların %56,5'i sigara kullanmamaktadır. Katılımcıların %73,4'ü hijyen eğitimi almamış, %72,6'sının ise çocuğu yoktur. Araştırma sonuçlarına göre, medeni durum, yaş, eğitim düzeyi, hijyen eğitimi alma ve çocuğu olma değişkenlerinin salgın hastalık farkındalığı ve bireysel hijyen davranışı üzerinde olumlu yönde etkisi olduğu belirlenmiştir. Sağlık ve gıda güvenliği eğitimi ile gıda sektörü personellerinin hijyen tutum ve davranışı için kendi beyanlarına dayalı uygulamalarını iyileştirmek, gıda sektörünün durumunu iyileştirebilir ve toplum sağlığı için bulaşıcı salgın hastalıkları en aza indirebilir. Bu nedenle, politika yapıcıların gıda sektörü işveren ve personelleri için sürekli gıda güvenliği ve bireysel hijyen eğitimi için çevrimiçi bir sistem tasarlamalarına acil bir ihtiyaç vardır.

**Anahtar Kelimeler** – COVID-19, Çanakkale, Gıda Sektörü, Hijyen Davranışları, Salgın Hastalık

## Epidemic Disease Awareness of Employees in the Food Sector: The Example of Çanakkale Province

<sup>1</sup>Department of Occupational Health and Safety, School of Graduate Studies, Çanakkale Onsekiz Mart University, Çanakkale, Türkiye

<sup>2</sup>Department of Food Quality Control and Analysis, Çanakkale Technical Sciences Vocational School, Çanakkale Onsekiz Mart University, Çanakkale, Türkiye

<sup>3</sup>Department of Science Education, Faculty of Education, Fırat University, Elazığ, Türkiye

<sup>4</sup>Department of Chemistry, Faculty of Science, Çanakkale Onsekiz Mart University, Çanakkale, Türkiye

### Article History

Received: 03.02.2023

Accepted: 17.07.2023

Published: 20.12.2023

### Research Article

**Abstract** – The personal hygiene behaviors of the dynamic and ever-growing food sector personnel are important for food safety, as well as for infectious diseases (especially coronavirus disease) to reach epidemic proportions. In this study, the knowledge, and attitudes of the food sector personnel about health and food safety during the epidemic, as well as the hygiene criteria that affect the awareness of this epidemic, were examined. A survey was conducted with food sector employees in Çanakkale between 01.11.2022 and 01.12.2022, including 42 statements. Survey data of 124 personnel selected by improbable sampling were compared with previous studies on the subject in the literature. 31.5% of the participants are between the ages of 26-35. 48.4% of the participants have a high school education level. 56.5% of the participants do not smoke. 73.4% of the participants did not receive hygiene training, and 72.6% did not have children. According to the results of the research, it was determined that the variables of marital status, age, education level, getting hygiene education and having a child had a positive effect on epidemic awareness and individual hygiene behaviour. Improving the health and food safety education and self-declared practices of food industry personnel for hygiene attitudes and behaviour can improve the situation of the food industry and minimize communicable epidemics for public health. Therefore, there is an urgent need for policy makers to design an online system for continuing food safety and personal hygiene education for food industry employers and staff.

**Keywords** – COVID-19, Çanakkale, Food Sector, Hygiene Behaviors, Epidemic Disease

<sup>1</sup> orkundalyan@outlook.com

<sup>2</sup> mehmetpiskin@comu.edu.tr

<sup>3</sup> eecanpolat@gmail.com

<sup>4</sup> ofozturk@comu.edu.tr

\*Sorumlu Yazar

## 1. Giriş

Birçok işletmede personellerinin yeme içme ihtiyacını karşılayan yemekhane bölümleri, çok dinamik ve sürekli aktif işyeri eklentileridir. Özellikle, koronavirus (COVID-19) salgını sırasında, gıda güvenliği bu işletmeler için en önemli öncelik olmalıdır (Angulo & Jones, 2006). COVID-19 salgını ile, bu birimler kendini organize etme mücadelesi vermekte ve hem gıda üreticilerinin hem de gıda tüketicilerinin sağlığını korumaya çalışmaktadır (WHO, 2020). COVID-19 gıda kaynaklı bir virüs değildir ve gıda da yaşayamaz veya gelişemez. Ancak, COVID-19 bulaşmış bir kişiyle temas eden biri, uygun hijyen ve önlemler olmadan yiyeceklerle uğraşırsa enfekte olabilir. Ayrıca 60°C'de en az 30 dakika ısıtma işlemi SARS gibi virüslerin öldürülmesinde etkilidir (Duda-Chodak vd., 2020). Gıda çalışanları öksürme, konuşma, nefes alma, hapşırma veya şarkı söyleme yoluyla virüsü yayabilir (Baier vd., 2020). Tüm bu faaliyetler, çevreleyen havaya yansıtılan patojenler içerdiğinde bulaşıcı bir aerosol oluşturabilir. Hem burundan hem de ağızdan dışarı verilen havanın, restoranlardaki müşteriler ve personel de dahil olmak üzere yakınlarda duran diğer kişilerin solunum bölgesinde hava ile karışabileceğinden şüphelenilmektedir (Tang vd., 2006). Virüs, enfekte bir kişinin vücut sıvılarıyla doğrudan temas yoluyla veya dolaylı olarak öksürme veya hapşırma parçacıklarıyla kirlenmiş yüzeylerle temas yoluyla bulaşır. Bu nedenle, gıda işleyicileri, el hijyeni ve maske takma başta olmak üzere hijyen maddelerine dikkatle uymalıdır (Kingdom GotU, 2020). Hijyen, genel olarak bireylerin sağlığına zarar verebilecek ortamlardan korunması için yapılan her türlü çalışma olarak tanımlanan eski bir kavramdır (Nurudeen & Toyin, 2020). Gıda işleme personelinin sağlığını yakından izlemek ve tüm enfekte kişileri, özellikle de hastalık belirtisi göstermediği halde virüsün taşıyıcılarını tespit etmek ve böylece yayılmasını önlemek de önemlidir (Feng, 2020). Herhangi bir düzeyde yanlış kullanım, COVID-19 salgınlarının ortaya çıkmasına veya yayılmasına katkıda bulunabilir. Gıda işleyicilerinin, gıda güvenliğini artırmak ve gıda endüstrisindeki uzun vadeli faydaları paylaşmak için uygun şekilde eğitilmesi çok önemlidir (Egan vd., 2007). Sürekli uygulamalı eğitimle, kirlenen gıdaları yemekten kaynaklanan risklerin yaygınlığı en aza indirilebilir (Soon, Baines & Seaman, 2012). Uygun sağlık ve gıda güvenliği eğitimi, COVID-19 salgınının oranını azaltmak için esastır (Olaimat vd., 2020). COVID-19 salgını eğitim sistemlerinde de farklılığa neden olmuştur (Dalyan vd., 2021). Teknolojik gelişmelerin de katkısıyla sağlık hizmetlerinin gelişmesi hastalıkların etkisini azaltmada etkili olmuştur. Ancak özellikle küresel boyuttaki salgınlara neden olan durumların kavranması hastalıkların engellenmesi konusunda en önemli adımdır (Türken & Köse, 2020). Yiyeceklerin tedarikçiden temin edilmesinden servis edilmesine kadar geçen süre içerisinde yemekhanenin genel hijyeni yanı sıra çalışan personellerin kişisel hijyenleri önem arz etmektedir (Yıldırım, 2014). Konu hakkında hijyen eğitimi alma zorunluluğu gibi kanuni yükümlülükler (Hijyen Eğitimi Yönetmeliği, 2013) getirilmiş olsa da özellikle gıda sektörü personellerinin hasta olduğu durumlarda enfeksiyonu yiyeceklere taşıyabilmekte ve bu durum sonucu toplu hastalıklar ortaya çıkabilmektedir (Yücel, 2000). Dünyanın küreselleşmesi neticesinde salgın hastalıkların ortaya çıkması ve yayılma hızının daha yüksek olması bilim insanları tarafından yayınlanan raporlarda belirtilmiştir (Özşahin & Arıbaş, 2021). Tedavisi bulunduğu ve salgının ortadan kalktığı düşünülen hastalıkların bile insan hayatını tehdit ettiği bir gerçektir. Yapılan araştırma ve çalışmalara rağmen salgın hastalıkların nerede, ne zaman ve hangi durumlarda ortaya çıkacağı henüz öngörülememektedir. Bu sebeple bireylerin salgın hastalıklar konusunda farkındalıklarının sürekli olarak yüksek tutulması gereklidir.

Literatürde öğrenciler üzerinde bireysel hijyen tutumları, hijyen davranışları araştırmaları (Bozeli, 2018; Taşkiran, Khorshid & Sarı, 2019) mevcut olmasının yanı sıra mutfak çalışanlarının da iş motivasyonu ve hijyen davranışlarının incelendiği araştırmalar mevcuttur (Şimşek & Şen, 2020). COVID-19 salgın sürecinde genel ve kişisel hijyen (Uğurlu-Kalkan vd., 2020; Çiçek, Şahin & Erkal, 2021), salgına karşı tutum (Özşahin & Arıbaş, 2021) ve gıda güvenliğinin incelendiği araştırmalar da mevcuttur (Tosun vd., 2022). Ancak işyerlerinde yemek üretiminin gerçekleştirildiği bölümlerde görevli personellerin hijyen davranışları ve COVID-19 gibi salgın hastalıklara karşı farkındalıklarının incelendiği araştırma mevcut değildir.

Bu çalışmada, Çanakkale ilinde gıda sektöründe görev alan personellerin salgın hastalık farkındalığı ve bireysel hijyen davranışlarını ölçmek amacıyla toplam 47 soru sorulmuştur. Çalışma verileri Sosyal Bilimler için İstatistik Programı (SPSS) 24.0 programı ile analiz edilmiştir. Araştırma sonuçları literatürde yer alan benzer araştırma sonuçları karşılaştırılmış ve gıda sektöründe görevli personellerin hijyen algılarını yükseltecek kriterler hakkında öneriler sunulmuştur.

Bu araştırma, 2022 Kasım-Aralık ayları içinde Çanakkale ilinde gıda sektöründe çalışan personellerin görüşleri ile sınırlıdır. Genelleme yapılırken evren-örneklem sınırlamasına dikkate alınmalıdır.

## **2. Materyal ve Yöntem**

### **2.1. Araştırmanın Amacı ve Modeli**

Bu çalışmanın amacı, gıda sektöründe görevli personellerin salgın hastalık farkındalığına etki eden bireysel hijyen davranışlarının tespit edilmesine yöneliktir. Bu amaç doğrultusunda gıda sektöründe görevli personeller ile anket yoluyla veri toplanmıştır. Kullanılan ankette yer alan ifadeler Büyükbeşe ve Dikbaş (2021) ile Gül ve Köse (2020) tarafından hazırlanmış olup, ölçekler kendi çalışmamıza uyarlanmıştır. Araştırmada kullanılan anket soruları Ek-1'de verilmiştir.

Çalışma için 31/10/2022 tarih ve E-84026528-050.01.04-2200252770 ile Çanakkale Onsekiz Mart Üniversitesi Lisansüstü Eğitim Enstitüsü Etik Kurulu tarafından onay alınmıştır.

Bu çalışmada aşağıda yer alan araştırma sorularına cevaplar aranmıştır:

- Gıda sektörü personellerinin bireysel hijyen davranış düzeyleri çalışanların demografik özellikleri bakımından farklılık göstermekte midir?
- Gıda sektörü personellerinin salgın hastalık farkındalık düzeyleri çalışanların demografik özellikleri bakımından farklılık göstermekte midir?
- Gıda sektörü personellerinin salgın hastalık farkındalık düzeylerini bireysel hijyen davranış düzeyleri etkilemekte midir?

### **2.2. Evren ve Örneklem Seçimi**

Araştırmanın evrenini, Çanakkale merkezinde gıda sektöründe görev yapan personellerin tamamı oluşturmaktadır. Örneklem büyüklüğü tespitinde ise madde analizi kullanılmıştır. Araştırma hedef yanıtlayıcı kitlesine yöneltilen anket ifadesi sayısı 47 olduğu için Kline (1994)' e göre katılımcı sayısı en az 94 (2 katı) en fazla 470 (10 katı) olmalıdır. Rastgele örneklem yönteminden seçkisiz örnekleme yöntemi kullanılarak 130 gıda sektörü personeline ulaşılmıştır (Yıldız, 2011). Hatalı ve eksik bilgileri bulunan 6 anket analiz sürecine dahil edilmemiştir. Sonuç olarak araştırmamızın örneklemini 124 birey oluşturmuştur.

### **2.3. Veri Toplama Araçları**

Bu çalışmada, katılımcıların salgın hastalık farkındalığı Büyükbeşe ve Dikbaş (2021) tarafından hazırlanan COVID-19 farkındalık geliştirme ölçeği (COVFÖ), bireysel hijyen davranışları ise Gül ve Köse (2020) tarafından hazırlanan hijyen davranışları belirleme ölçeği (HDÖ) baz alınarak örneklem ve araştırma mekanı gözetilerek kendi çalışmamıza uyarlanmıştır. Her iki ölçek içinde 5'li tip Likert ölçek kullanılmış olup cevaplar Kesinlikle Katılmıyorum (1) ile Kesinlikle Katılıyorum (5) arasında toplanmıştır. Katılımcıların bireysel özelliklerinin tespiti amacıyla ankette 8 adet soru yer almaktadır. Geliştirilen ölçek uzman görüşleri ile son halini almış ve çalışanlara yüz yüze uygulanmıştır. 20 personel ile yapılan pilot çalışma neticesinde ölçek güvenilirliğini düşüren madde olmaması nedeniyle revizyona ihtiyaç duyulmamıştır. 20 bireyin cevapladığı pilot verilerde araştırmaya eklenerek çalışma tamamlanmıştır. Araştırmanın verileri 01.11.2022–01.12.2022 tarihleri arasında edinilmiştir.

### **2.4. Verilerin İşlenmesi ve Analizi**

Araştırmada kullanılan ölçeklerin güvenilirliği için SPSS programı ile gerçekleştirilen analiz sonucunda 21 ifadeden oluşan COVFÖ güvenilirliği 0.893, Barlett's testi sonucu 0.000 ve Kaiser-Meyer-Olkin (KMO) ölçüm değeri 0.801 olarak bulunmuştur. Araştırmada kullanılan ölçeklerin geçerliliği için yapılan faktör analiz sonucunda COVFÖ anketinin 6 faktöre sahip olduğu ve toplam varyansın 73.53'ünü açıkladığı belirlenmiştir. 26 ifadeden oluşan HDÖ güvenilirliği 0.878, Barlett's testi sonucu 0.000 ve KMO ölçüm değeri 0.762 olarak bulunmuştur. Faktör analiz sonucunda HDÖ anketinin 8 faktöre sahip olduğu ve toplam varyansın 74.46'sını

açıkladığı belirlenmiştir. KMO değerlerinin 0.60'tan daha yüksek bulunması çalışma örnekleminin yeter büyüklükte olduğunu göstermektedir (Çokluk, Şekercioğlu & Büyüköztürk, 2012).

Normallik varsayımı sağlanan veriler ile katılımcıların kişisel özellikleri arasında anlamlı farklılıkların olup olmadığının tespiti için parametrik grupta yer alan analiz metotları kullanılmıştır (Eymen, 2007). Anlamlı farklılık bulunan değişkenler arasındaki ilişkinin düzeyinin belirlenmesinde ise Cohen (d) (Kayri, 2009) ve eta-kare ( $\eta^2$ ) etki büyüklüğü katsayıları hesaplanmıştır. Cohen d etki büyüklüğü; 0.2 ile 0.5 arasında küçük, 0.5 ile 0.8 arasında orta, 0.8 ile 1 arasında büyük ve 1'den büyükse çok büyük etki olarak yorumlanmıştır (Kılıç, 2014). Eta-kare etki büyüklüğü ise; 0.01'den küçükse çok küçük, 0.01 ile 0.06 arasında küçük, 0.06 ile 0.14 arasında orta ve 0.14'ten büyükse büyük etki olarak yorumlanmıştır (Büyüköztürk, Çokluk ve Köklü, 2006).

### 3. Bulgular ve Tartışma

Katılımcıların kişisel özelliklerinin frekans (f) ve yüzdeleri (%) Tablo 1'de verilmiştir.

Tablo 1  
Katılımcıların kişisel özelliklerinin frekans ve yüzdeleri

Demografik Özellikler		f	%
Cinsiyet	Kadın	55	44.4
	Erkek	69	55.6
Medeni Durum	Evli	70	56.5
	Bekâr	54	43.5
Yaş	18-25 yaş aralığı	21	16.9
	26-35 yaş aralığı	39	31.5
	36-45 yaş aralığı	31	25.0
	46-55 yaş aralığı	16	12.9
	56 yaş ve üzeri	17	13.7
Eğitim Düzeyi	İlköğretim	15	12.1
	Ortaöğretim	16	12.9
	Lise	60	48.4
	Ön Lisans	33	26.6
	Lisans	0	0.0
Görevi	Aşçı	3	2.4
	Aşçı Yardımcısı	6	4.8
	Servis Görevlisi	45	36.3
	Temizlik Görevlisi	70	56.5
Sigara Kullanma Durumu	Evet	54	43.5
	Hayır	70	56.5
Hijyen Eğitimi Alma Durumu	Evet	33	26.6
	Hayır	91	73.4
Çocuğu Olma Durumu	Var	34	27.4
	Yok	90	72.6

Tablo 1'e göre, Katılımcıların %55.6'sı erkek, %56.5'i evlidir. Katılımcıların %31.5'i 26-35 yaş aralığındadır. Katılımcıların %48.4'ü lise düzeyinde eğitim seviyesine sahiptir. Katılımcılardan 3'ü (%2.5) aşçı, 6'sı (%4.8) aşçı yardımcısı, 45'i (%36.3) servis görevlisi ve 70'i (%56.5) temizlik görevlisi olarak firmada görev almaktadır. Katılımcıların %56.5'i sigara kullanmazken %43.5'i sigara kullanmaktadır. Katılımcıların büyük çoğunluğu (%73.4) hijyen eğitimi almıştır. Katılımcıların %72.6'sının ise çocuğu vardır.

HDÖ ortalamasının medeni durum, hijyen eğitimi alma durumu ve çocuğu olma durumu değişkenlerine göre Bağımsız Değişken t-Testi sonuçları Tablo 2'de verilmiştir.

Tablo 2

HDÖ ortalamasının medeni durum, hijyen eğitimi alma durumu ve çocuğu olma durumu değişkenlerine göre Bağımsız Değişken t-Testi sonuçları

Değişken	Gruplar	N	$\bar{X}$	Sd	S.E.mean	t	p	d
Medeni Durum	Evli	70	3.88	0.30	0.03	7.557	0.000*	1.41
	Bekar	54	3.26	0.54	0.07			
Hijyen Eğitimi	Evet	33	4.00	0.26	0.04	7.451	0.000*	1.31
	Hayır	91	3.46	0.52	0.05			
Çocuğu Olma	Var	34	4.01	0.26	0.04	7.776	0.000*	1.38
	Yok	90	3.45	0.51	0.05			

Tablo 2'ye göre, evli personellerin HDÖ ortalaması  $\bar{X} = 3.88 \pm 0.03$ , bekar personellerin ise  $\bar{X} = 3.26 \pm 0.07$ 'dir. T testi sonuçlarına göre, HDÖ ortalaması ile medeni durum değişkeni arasında evli katılımcılardan yana bir farklılık vardır ( $t= 7.557$ ,  $p<0.05$ ). Cohen d ( $d = 1.41$ ) etki büyüklüğü katsayısına göre, evli olma durumu HDÖ ortalama değerine etkisi çok yüksek düzeydedir.

Hijyen eğitimi alan personellerin HDÖ ortalaması  $\bar{X} = 4.00 \pm 0.04$ , almayan personellerin ise  $\bar{X} = 3.46 \pm 0.05$ 'tir. T testi sonuçlarına göre, HDÖ ortalaması ile hijyen eğitimi alma durumu değişkeni arasında hijyen eğitimi alan katılımcılardan yana bir farklılık vardır ( $t= 7.451$ ,  $p<0.05$ ). Cohen d ( $d = 1.31$ ) etki büyüklüğü katsayısına göre, hijyen eğitimi alma durumu HDÖ ortalama değerine etkisi çok yüksek düzeydedir.

Çocuğu olan personellerin HDÖ ortalaması  $\bar{X} = 4.01 \pm 0.04$ , olmayan personellerin ise  $\bar{X} = 3.45 \pm 0.05$ 'tir. T testi sonuçlarına göre, HDÖ ortalaması ile çocuk olma durumu değişkeni arasında çocuğu olan katılımcılardan yana bir farklılık vardır ( $t= 7.776$ ,  $p<0.05$ ). Cohen d ( $d = 1.38$ ) etki büyüklüğü katsayısına göre, çocuk olma durumu HDÖ ortalama değerine etkisi çok yüksek düzeydedir.

HDÖ ortalamasının yaş ve eğitim düzeyi değişkenlerine göre Tek Yönlü Varyans analizi (ANOVA) sonuçları Tablo 3'te verilmiştir.

Tablo 3

HDÖ yaş ve eğitim düzeyi değişkenlerine göre ANOVA sonuçları

Değişken	Gruplar	N	$\bar{X}$	Sd	V.K.	K.T.	K.O.	F	p	$\eta^2$
Yaş	1	21	2.85	0.54	G. A.	18.040	4.510	33.711	0.000*	0.53
	2	39	3.55	0.35						
	3	31	3.77	0.31						
	4	16	3.97	0.27						
	5	17	4.03	0.25						
Eğitim Düzeyi	6	15	2.57	0.35	G. A.	26.123	8.708	133.344	0.000*	0.76
	7	16	3.21	0.12						
	8	60	3.73	0.12						
	9	33	4.05	0.38						
	10	0	0.00	0.00						

(1)= 18-25 yaş arası, (2)= 26-35 yaş arası, (3)= 36-45 yaş arası, (4)= 46-55 yaş arası, (5)= 56 yaş üzeri, (6)= İlköğretim, (7)= Ortaöğretim, (8)= Lise, (9)= Ön Lisans, (10)= Lisans

Tablo 3'e göre, HDÖ ortalaması ile yaş değişkeni arasında farklılık gözlenmiştir [ $F_{(4-119)}= 33.711, p<0.05$ ]. Anlamlı farkın yaş grupları arasında büyükten küçüğe doğru olduğu belirlenmiştir. Eta-kare ( $\eta^2= 0.53$ ) etki büyüklüğüne göre ise yaş değişkeninin HDÖ ortalamasına etkisi yüksek düzeydedir.

HDÖ ortalaması ile eğitim düzeyi değişkeni arasında farklılık gözlenmiştir [ $F_{(3-120)}= 133.344, p<0.05$ ]. Anlamlı farkın eğitim düzeyi artışına bağlı olarak arttığı belirlenmiştir. Eta-kare ( $\eta^2= 0.76$ ) etki büyüklüğüne göre ise eğitim düzeyi değişkeninin HDÖ ortalamasına etkisi yüksek düzeydedir.

COVFÖ ortalamasının medeni durum, hijyen eğitimi alma durumu ve çocuğu olma durumu değişkenlerine göre Bağımsız Değişken t-Testi sonuçları Tablo 4'te verilmiştir.

Tablo 4

COVFÖ ortalamasının medeni durum, hijyen eğitimi alma durumu ve çocuğu olma durumu değişkenlerine göre Bağımsız Değişken t-Testi sonuçları

Değişken	Gruplar	N	$\bar{X}$	Sd	S.E.mean	t	p	d
Medeni Durum	Evli	70	3.89	0.30	0.03	11.410	0.000*	2.12
	Bekar	54	3.04	0.48	0.06			
Hijyen Eğitimi	Evet	33	4.17	0.20	0.03	14.278	0.000*	2.43
	Hayır	91	3.29	0.47	0.05			
Çocuğu Olma	Var	34	4.15	0.20	0.03	14.082	0.000*	2.40
	Yok	90	3.28	0.47	0.05			

Tablo 4'e göre, evli personellerin COVFÖ ortalaması  $\bar{X} = 3.89 \pm 0.03$ , bekar personellerin ise  $\bar{X} = 3.04 \pm 0.06$ 'dır. T testi sonuçlarına göre, COVFÖ ortalaması ile medeni durum değişkeni arasında evli katılımcılardan yana bir farklılık vardır ( $t= 11.410, p<0.05$ ). Cohen d ( $d = 2.12$ ) etki büyüklüğü katsayısına göre, evli olma durumu COVFÖ ortalama değerine etkisi çok yüksek düzeydedir.

Hijyen eğitimi alan personellerin COVFÖ ortalaması  $\bar{X} = 4.17 \pm 0.03$ , almayan personellerin ise  $\bar{X} = 3.29 \pm 0.05$ 'tir. T testi sonuçlarına göre, COVFÖ ortalaması ile hijyen eğitimi alma durumu değişkeni arasında hijyen eğitimi alan katılımcılardan yana bir farklılık vardır ( $t= 14.278, p<0.05$ ). Cohen d ( $d = 2.43$ ) etki büyüklüğü katsayısına göre, hijyen eğitimi alma durumu COVFÖ ortalama değerine etkisi çok yüksek düzeydedir.

Çocuğu olan personellerin COVFÖ ortalaması  $\bar{X} = 4.15 \pm 0.03$ , olmayan personellerin ise  $\bar{X} = 3.28 \pm 0.05$ 'tir. T testi sonuçlarına göre, COVFÖ ortalaması ile çocuk olma durumu değişkeni arasında çocuğu olan katılımcılardan yana bir farklılık vardır ( $t= 14.082, p<0.05$ ). Cohen d ( $d = 2.40$ ) etki büyüklüğü katsayısına göre, çocuk olma durumu COVFÖ ortalama değerine etkisi çok yüksek düzeydedir.

COVFÖ ortalamasının yaş ve eğitim düzeyi değişkenlerine göre ANOVA sonuçları Tablo 5'te verilmiştir.

Tablo 5  
COVFÖ yaş ve eğitim düzeyi değişkenlerine göre ANOVA sonuçları

Değişken	Gruplar	N	$\bar{X}$	Sd	V.K.	K.T.	K.O.	F	p	$\eta^2$
Yaş	1	21	2.85	0.54	G. A.	34.927	8.732	181.949	0.000*	0.85
	2	39	3.55	0.35						
	3	31	3.77	0.31						
	4	16	3.97	0.27	G. İ.	5.711	0.048			
	5	17	4.03	0.25						
Eğitim Düzeyi	6	15	2.57	0.35	G. A.	24.062	8.021	58.063	0.000*	0.59
	7	16	3.21	0.12						
	8	60	3.73	0.12						
	9	33	4.05	0.38	G. İ.	16.576	0.138			
	10	0	0.00	0.00						

Tablo 5'e göre COVFÖ ortalaması ile yaş değişkeni arasında farklılık gözlenmiştir [ $F_{(4-119)}= 181.949$ ,  $p<0.05$ ]. Anlamlı farkın yaş grupları arasında büyükten küçüğe doğru olduğu belirlenmiştir. Eta-kare ( $\eta^2= 0.85$ ) etki büyüklüğüne göre ise yaş değişkeninin COVFÖ ortalamasına etkisi yüksek düzeydedir.

COVFÖ ortalaması ile eğitim düzeyi değişkeni arasında farklılık gözlenmiştir [ $F_{(3-120)}= 58.063$ ,  $p<0.05$ ]. Anlamlı farkın eğitim düzeyi artışına bağlı olarak arttığı belirlenmiştir. Eta-kare ( $\eta^2= 0.59$ ) etki büyüklüğüne göre ise eğitim düzeyi değişkeninin COVFÖ ortalamasına etkisi yüksek düzeydedir.

Katılımcıların kişisel özellikleri ile HDÖ ve COVFÖ ortalamalarının Pearson Korelasyon analizi sonuçları Tablo 6'da verilmiştir.

Tablo 6  
Pearson Korelasyon analizi sonuçları

	1	2	3	4	5	6	7
1- Hijyen Eğitimi	r 1 p -						
2- Çocuk	r 0.980 p 0.000**	1 -					
3- Medeni Durum	r 0.529 p 0.000**	0.540 0.000**	1 -				
4- Yaş	r -0.839 p 0.000**	-0.834 0.000**	-0.789 0.000**	1 -			
5- Eğitim Düzeyi	r -0.440 p 0.000**	-0.457 0.000**	-0.530 0.000**	0.640 0.000**	1 -		
6- HDÖ Ortalama	r 0.451 p 0.000**	-0.473 0.000**	-0.590 0.000**	0.657 0.000**	0.864 0.000**	1 -	
7- COVFÖ Ortalama	r 0.677 p 0.000**	-0.679 0.000**	-0.738 0.000**	0.898 0.000**	0.749 0.000**	0.806 0.000**	1 -

r=Pearson Korelasyon Katsayısı (2-yönlü), \*= $p<0.05$ , \*\*= $p<0.01$

Tablo 6 incelendiğinde, hijyen eğitimi alma durumu ( $\bar{X}= 1.73$ ,  $Sd= 0.44$ ) ile çocuğu olma durumu ( $\bar{X}= 1.72$ ,  $Sd= 0.44$ ) arasındaki ilişki Pearson Korelasyonu ile ölçülmüştür. Analiz sonucunda hijyen eğitimi alma durumu ile çocuğu olma durumu arasında büyük seviyede, olumlu etki eden anlamlı bir ilişki bulunmuştur [ $r_{(122)}= 0.980$ ,  $p<0.01$ ]. Hijyen eğitimi alma durumu ( $\bar{X}= 1.73$ ,  $Sd= 0.44$ ) ile yaş değişkeni ( $\bar{X}= 2.75$ ,  $Sd= 1.27$ ) arasında büyük seviyede, olumsuz etki eden anlamlı bir ilişki bulunmuştur [ $r_{(122)}= -0.839$ ,  $p<0.01$ ]. Hijyen eğitimi alma durumu ( $\bar{X}= 1.73$ ,  $Sd= 0.44$ ) ile eğitim düzeyi değişkeni ( $\bar{X}= 2.89$ ,  $Sd= 0.93$ ) arasında orta seviyede, olumsuz etki eden anlamlı bir ilişki bulunmuştur [ $r_{(122)}= -0.440$ ,  $p<0.01$ ]. Hijyen eğitimi alma durumu

( $\bar{X}$  = 1.73, Sd= 0.44) ile HDÖ ortalaması ( $\bar{X}$  = 3.61, Sd= 0.52) arasında orta seviyede, olumlu etki eden anlamlı bir ilişki bulunmuştur [ $r_{(122)}$  = 0.451,  $p < 0.01$ ]. Hijyen eğitimi alma durumu ( $\bar{X}$  = 1.73, Sd= 0.44) ile COVFÖ ortalaması ( $\bar{X}$  = 3.52, Sd= 0.57) arasında orta seviyede, olumlu etki eden anlamlı bir ilişki bulunmuştur [ $r_{(122)}$  = 0.677,  $p < 0.01$ ]. Eğitim düzeyi değişkeni ( $\bar{X}$  = 2.89, Sd= 0.93) ile HDÖ ortalaması ( $\bar{X}$  = 3.61, Sd= 0.52) arasında büyük seviyede, olumlu etki eden anlamlı bir ilişki bulunmuştur [ $r_{(122)}$  = 0.864,  $p < 0.01$ ]. Yaş değişkeni ( $\bar{X}$  = 2.75, Sd= 1.27) ile COVFÖ ortalaması ( $\bar{X}$  = 3.52, Sd= 0.57) arasında büyük seviyede, olumlu etki eden anlamlı bir ilişki bulunmuştur [ $r_{(122)}$  = 0.898,  $p < 0.01$ ].

Korelasyon analizi sonuçlarına göre; çocuğu olan ve yaşı genç olan personellerin hijyen eğitim almaya daha yatkın olduğu söylenebilir. Hijyen eğitiminin de HDÖ ve CVOFÖ algılarının pozitif yönde değişimine katkısı olduğu söylenebilir.

Üniversite öğrencilerinin bireysel hijyen tutumlarının incelendiği bir çalışmada, cinsiyet değişkeninde kız öğrenciler lehine anlamlı derece farklılık olduğu rapor edilmiştir (Taşkiran, Khorshid & Sarı, 2019). Türkiye genelinde COVID-19 salgın süresince kişisel ve genel hijyen tavırlarının araştırıldığı bir çalışmada, kadın katılımcıların hem bireysel hem de genel hijyen davranış ölçek ortalama değerlerinin erkek katılımcılara göre anlamlı şekilde daha yüksek bulunduğu rapor edilmiştir (Çiçek, Şahin & Erkal, 2021). Ülkemizin Trabzon ve Konya illerinde ikamet eden bireylerin COVID-19 salgınına yönelik tutum ve davranışlarının incelendiği bir çalışmada, kadınların erkeklere göre COVID-19'a yönelik hem tutumlarının hem de davranışlarının daha iyi düzeyde olduğu rapor edilmiştir (Özşahin & Arıbaş, 2021). Literatürdeki diğer çalışmaların aksine bu çalışmada, hijyen ve COVID-19 salgını farkındalıklarının cinsiyet değişkeni ile anlamlı bir farklılık bulunamamıştır. Bu durumun ortaya çıkmasında örneklem farklılıkları olduğu gibi cinsiyet değişkeni yanında etki eden diğer faktörlerin olabileceğini göstermektedir.

Türkiye genelinde COVID-19 döneminde hijyen tavırlarının araştırıldığı bir çalışmada, medeni durum değişkeni ile COVID-19 Hijyen ölçeği arasında anlamlı bir farklılık olmadığı rapor edilmiştir (Çiçek, Şahin & Erkal, 2021). Hong Kong'da yüz maskesinin takılmasını etkileyen faktörleri inceleyen bir çalışmada, evli bireylerin bekarlara göre daha çok maske kullanımına dikkat ettiği rapor edilmiştir (Tang & Wong, 2004). Türkiye'de COVID-19 salgını süresince bireylerin el yıkama tutumlarını inceleyen bir çalışmada, evli bireylerin bekar bireylere göre el yıkamaya ilişkin daha olumlu tutum içinde oldukları rapor edilmiştir (Uğurlu-Kalkan vd., 2020). Benzer şekilde bu çalışmada, HDÖ ve CVOFÖ farkındalıkları ile medeni durum değişkeni arasında evli personeller lehine anlamlı farklılık olduğu belirlenmiştir.

Mesleki ve Teknik Anadolu Lisesi öğrencilerinin hijyen davranışları ve tutumlarının incelendiği bir çalışmada, hijyen davranışları ölçeği puan ortalaması ile yaş değişkeni arasında anlamlı bir farklılık olmadığı rapor edilmiştir (Bozeli, 2018). COVID-19 salgını esnasında İran'da maske kullanımı hakkında gerçekleştirilen bir çalışmada, yüz maskesi kullanımının yaş artışı ile doğru orantılı olduğu raporlanmıştır. Özellikle 70 yaş üzerindeki katılımcıların neredeyse tamamı yüz maskesi kullanımını desteklediği rapor edilmiştir (Rahimi vd., 2021). Türkiye genelinde COVID-19 salgın süresince kişisel ve genel hijyen davranışlarının araştırıldığı bir çalışmada, yaş değişkeni ile el hijyeni konusunda anlamlı farklılık olduğu rapor edilmiştir. Özellikle 50 yaş ve üzeri olan bireylerin 34 yaş altı katılımcılara göre el hijyeni sağlamada daha aktif olduğu rapor edilmiştir (Çiçek, Şahin & Erkal, 2021). Benzer şekilde bu çalışmada, HDÖ ve CVOFÖ farkındalıkları ile yaş değişkeni arasında anlamlı farklılık olduğu belirlenmiştir. Ayrıca gerçekleştirilen korelasyon analizi sonuçlarına göre, katılımcıların yaş artışına bağlı olarak salgın hastalıklar konusundaki farkındalığının arttığı söylenebilir.

Ülkemizin Trabzon ve Konya illerinde ikamet eden bireylerin COVID-19 salgınına yönelik tutum ve davranışlarının incelendiği bir çalışmada, eğitim durumu değişkeni ile COVID-19'a yönelik tutum arasında anlamlı bir farklılık raporlanmamışken COVID-19'a yönelik davranışlarda anlamlı farklılık olduğu rapor edilmiştir. Anlamlı farklılığın eğitim düzeyi artışı ile doğru orantılı olduğu belirtilmiştir (Özşahin & Arıbaş, 2021). 60 yaş ve üzeri bireylerin COVID-19 farkındalığını etkileyen faktörlerin incelendiği bir çalışmada, lise mezunu olan bireylerin lisansüstü mezunu bireylere göre COVID-19 farkındalıklarının daha yüksek olduğu rapor edilmiştir (Tümer, Aygün & Tuna, 2022). Türkiye genelinde COVID-19 salgın hastalık döneminde kişisel ve genel hijyen davranışlarının araştırıldığı bir çalışmada, lise ve daha az eğitim düzeyine sahip katılımcıların COVID-19'a risk algısının yüksek olduğu rapor edilmiştir (Çiçek, Şahin & Erkal, 2021). Türkiye'de COVID-19 salgını süresince bireylerin el yıkama tutumlarını inceleyen bir çalışmada, eğitim

düzei lisans ve üzerinde olan katılımcıların el yıkamaya daha yatkın oldukları rapor edilmiştir (Uğurlu-Kalkan vd., 2020). Mutfak çalışanlarının iş motivasyonu ve hijyen davranışları arasındaki ilişkinin incelendiği bir çalışmada, eğitim düzei yüksek olan personellerin hijyen farkındalıklarının daha yüksek olduğu rapor edilmiştir (Şimşek & Şen, 2020). Benzer şekilde bu çalışmada, HDÖ ve CVOFÖ farkındalıkları ile eğitim düzei değişkeni arasında anlamlı farklılık olduğu belirlenmiştir. Ayrıca gerçekleştirilen korelasyon analizi sonuçlarına göre, katılımcıların eğitim düzei artışına bağlı olarak salgın hastalıklar konusundaki farkındalığının arttığı söylenebilir.

60 yaş ve üzeri bireylerin COVID-19 farkındalığını etkileyen faktörlerin belirlenmesi amacıyla gerçekleştirilen bir araştırma çalışmasında, eğitim durumu lise ve ön lisans olan katılımcıların Bulaşma Tedbiri Farkındalığı ve Hijyen Tedbiri Farkındalıklarının diğer katılımcılara göre daha yüksek olduğu rapor edilmiştir. Ayrıca sigara ve alkol kullanmayan katılımcıların Bulaşma Tedbiri Farkındalığı daha yüksek bulunduğu rapor edilmiştir (Tümer, Aygün & Tuna, 2022). Literatürdeki diğer çalışmaların aksine bu çalışmada, hijyen ve COVID-19 salgını farkındalıklarının sigara kullanma durumu değişkeni ile anlamlı bir farklılık bulunamamıştır. COVID-19 salgını sürecinde balık restoranlarının gıda güvenliğini inceleyen bir çalışmada, personellerin düzenli eğitimi neticesinde hijyen konusundaki olumsuz davranışlarının düzeleceği rapor edilmiştir (Tosun vd., 2022). COVID-19 salgını sırasında bir eğitim müdahalesinin sağlık ve gıda güvenliği üzerindeki etkisine ilişkin mevcut araştırma sonuçları, eğitim müdahalesinin bilgi düzeylerini arttırdığı, tutum düzeylerini olumluya çevirdiğini göstermiş ve sağlık ve gıda güvenliği eğitiminin önemli bir kapsam olduğunu ortaya koymuştur.

#### 4. Sonuçlar

COVID-19'un gıda kaynaklı bir hastalık olduğuna dair doğrudan ve güvenilir bir kanıt olmamasına rağmen, devam eden bir salgın bağlamında gıda ile temasın tamamen güvenli olduğu düşünülemez. Gıda sektörü personellerinin bireysel hijyen davranışlarının salgın hastalık farkındalık düzeylerine etkisinin incelendiği araştırma sonuçlarına göre, evli, 56 yaş üzeri, ön lisans mezunu, hijyen eğitimi alan ve çocuğu olan personellerin bireysel hijyen davranışları konusunda daha dikkatli olduğu söylenebilir. İşletmelerin hijyen eğitim programlarında bekar, genç, 56 yaş altı, eğitim düzei ön lisans altı olan personellere odaklanmaları önerilmektedir. Ayrıca herhangi bir demografik özelliğe bakılmaksızın tüm yemekhane personellerinin hijyen eğitimlerinin aldırılması gereklidir. COVID-19 ve benzeri salgın hastalıklar öncesi bireysel hijyen davranış kültürünün özellikle gıda sektöründe görev alan personellerde, hastalıkların salgın boyutunun kontrol altına alınması konusunda önemlidir. Araştırma sonuçlarında yer alan hijyen eğitimlerinin gıda sektöründe çalışan personellere belirli periyotlarda verilmesi bireysel hijyen davranışlarının kazandırılması açısından gereklidir. Bu sebeple işletmelerin kanuni zorunluluğu karşılamanın yanı sıra gıda sektörü personellerine rutin aralıklar ile hijyen eğitimlerini aldırması önerilmektedir. İlerleyen dönemlerde benzer konuda yapılacak çalışmalarda farklı örneklem ve farklı demografik özelliklerin uygulandığı çalışmaların yapılması araştırmacılara önerilmektedir.

Gıda sektöründe çalışanların sağlık ve gıda güvenliği eğitim müdahalelerinin iyileştirilmesi, COVID-19 ve diğer salgın hastalıkları en aza indirebilir ve gıda sektörünün durumunu iyileştirerek toplumun sağlığı için etkili bir adım olabilir. Araştırmacılar, gıda güvenliği iletişimcileri, sendikalar, medya ve diğer tüm ilgili sektörler, sağlık ve gıda güvenliği eğitimlerini ilerletmek için bu sektördeki çalışanları eğitmek için çaba sarfetmelidirler. Halk sağlığı yetkilileri, özellikle COVID-19 salgını sırasında, eğitim kursları için restoranlardaki gıda sektöründeki çalışanlara öncelik vermelidir. Ayrıca, politika yapıcıların bu çalışmanın sonuçlarını restoranlar için sağlık ve gıda güvenliği ve teftişine yönelik çevrimiçi bir sürekli eğitim sistemi tasarlamak için kullanmaları önerilir.

## Yazar Katkıları

Orkun Dalyan: Veri iyileştirme, Metodoloji, Kavramsallaştırma, Analiz, Yazma, orijinal taslak.

Mehmet Pişkin: Metodoloji, Yazılım, Yazım-orijinal taslak.

Erdal Canpolat: Veri iyileştirme, İnceleme, Görselleştirme, Yazma-orijinal taslak.

Ömer Faruk Öztürk: Yazma-inceleme ve düzenleme.

## Çıkar Çatışması

Yazarlar çıkar çatışması bildirmemişlerdir.

## Kaynaklar

- Angulo, F. J., & Jones, T. F. (2006). Eating in restaurants: A risk factor for foodborne disease? *Clinical Infectious Diseases*, 43(10), 1324–1328. DOI: <https://doi.org/10.1086/508540>
- Baier, C., Albrecht, U.-V., Ebadi, E., Vonberg, R.-P., & Schilke, R. (2020). Knowledge about hand hygiene in the Generation Z: A questionnaire-based survey among dental students, trainee nurses, and medical technical assistants in training. *American Journal of Infection Control*, 48(6), 708–712. DOI: <https://doi.org/10.1016/j.ajic.2020.02.002>
- Bozeli, E. (2018). *Sağlık meslek lisesinde okuyan öğrencilerin hijyen tutum ve davranışları* (Yüksek lisans tezi). Erişim adresi: <https://tez.yok.gov.tr/UlusalTezMerkezi>
- Büyükbeşe, T., & Dikbaş, T. (2021). Covid-19 farkındalık ölçeği (COVFÖ) geliştirme çalışması. *Abant Sosyal Bilimler Dergisi*, 21(2), 21-40. DOI: <https://doi.org/10.11616/basbed.vi.858037>
- Büyüköztürk, Ş., Çokluk, Ö., & Köklü, N. (2006). *Sosyal Bilimler için İstatistik*. Ankara: Pegem Akademi Yayıncılık. Erişim adresi: <https://www.nadirkitap.com/sosyal-bilimler-icin-istatistik-sener-buyukozturk-omay-cokluk-nilgun-kitap27859067.html>
- Çiçek, B., Şahin, H., & Erkal, S. (2021). Covid-19 Salgın Döneminde Bireylerin Kişisel ve Genel Hijyen Davranışlarının İncelenmesi. *Elektronik Sosyal Bilimler Dergisi*, 20(80), 2157-2173. DOI: <https://doi.org/10.17755/esosder.855150>
- Çokluk, Ö., Şekercioglu, G., & Büyüköztürk, Ş. (2012). *Sosyal Bilimler için çok Değişkenli İstatistik: SPSS ve Lisrel uygulamaları*. Ankara: Pegem Akademi Yayıncılık. Erişim adresi: <https://depo.pegem.net/9786055885670.pdf>
- Dalyan, H., Dalyan, O., Öztürk, Ö. F., & Pişkin, M. (2021). İş sağlığı ve güvenliğinde yüz yüze ve uzaktan eğitim sistemlerinin karşılaştırılması. *Karaelmas İş Sağlığı ve Güvenliği Dergisi*, 5(3), 219-228. DOI: <https://doi.org/10.33720/kisgd.1009459>
- Duda-Chodak, A., Lukasiewicz, M., Zięć, G., Florkiewicz, A., & Filipiak-Florkiewicz, A. (2020). Covid-19 pandemic and food: Present knowledge, risks, consumers fears, and safety. *Trends in Food Science & Technology*, 105, 145–160. DOI: <https://doi.org/10.1016/j.tifs.2020.08.020>
- Egan, M., Raats, M., Grubb, S., Eves, A., Lumbers, M., Dean, M., & Adams, MR (2007). A review of food safety and food hygiene training studies in the commercial sector. *Food Control*, 18(10), 1180–1190. DOI: <https://doi.org/10.1016/j.foodc.ont.2006.08.001>
- Eymen, E. (2007). *SPSS 15.0 Veri Analiz Yöntemleri*. Ankara: İstatistik Merkezi. Erişim adresi: [http://yunus.hacettepe.edu.tr/~tonta/courses/spring2009/bby606/SPSS\\_15.0\\_ile\\_Veri\\_Analizi.pdf](http://yunus.hacettepe.edu.tr/~tonta/courses/spring2009/bby606/SPSS_15.0_ile_Veri_Analizi.pdf)
- Feng, Y. (2020). *Keep Calm Handle Food Safely: COVID-19 Food Safety Implications for Extension Educators*. ABD: Purdue Extension. Erişim adresi: <https://www.extension.purdue.edu/extmedia/FS/FS-37-W.pdf>
- Gül, Ş., & Köse, E. Ö. (2020). Lise öğrencilerinin hijyen davranışlarını belirlemeye yönelik bir tutum ölçeği geliştirme çalışması. *Asya Öğretim Dergisi*, 8(1), 15-31. Erişim adresi: <https://dergipark.org.tr/tr/download/article-file/1153618>
- Hijyen Eğitimi Yönetmeliği. (2013, 05 07). Resmî Gazete (Sayı: 28698). Erişim adresi: <https://www.mevzuat.gov.tr/mevzuat?MevzuatNo=18552&MevzuatTur=7&MevzuatTertip=5>
- Kayri, M. (2009). Araştırmalarda gruplar arası farkın belirlenmesine yönelik çoklu karşılaştırma (Post-Hoc) teknikleri. *Fırat Üniversitesi Sosyal Bilimler Dergisi*, 19(1), 51-64. Erişim adresi:

- <https://dergipark.org.tr/tr/download/article-file/72000>
- Kılıç, S. (2014). Effect Size. *Journal of Mood Disorders*, 4(1), 44-46. DOI: <https://doi.org/10.5455/jmood.20140228012836>
- Kingdom GotU (2020). *Keeping workers and customers safe during COVID-19 in restaurants, pubs, bars, and takeaway services*. United Kingdom. Erişim adresi: <https://assets.publishing.service.gov.uk/media/5eb96e8e86650c278b077616/working-safely-during-covid-19-restaurants-pubs-takeaway-services-091120.pdf>
- Kline, P. (1994). *An Easy Guide to Factor Analysis*. New York: Routledge. Erişim adresi: <https://www.routledge.com/An-Easy-Guide-to-Factor-Analysis/Kline/p/book/9780415094900>
- Nurudeen, A., & Toyin, A. (2020). Knowledge of personal hygiene among undergraduates. *Journal of Health Education*, 5(2), 66-71. DOI: <https://doi.org/10.15294/jhe.v5i2.38383>
- Olaimat, A. N., Shahbaz, H. M., Fatima, N., Munir, S., & Holley, R. A. (2020). Food Safety during and after the era of the COVID-19 pandemic. *Frontiers in Microbiology*, 11, 1854. DOI: <https://doi.org/10.3389/fmicb.2020.01854>
- Özşahin, F., & Arıbaş, A. N. (2021). Covid-19'a yönelik tutum ve davranışların değerlendirilmesi ve bir uygulama. *Uluslararası Sağlık Yönetimi ve Stratejileri Araştırma Dergisi*, 7(2), 3911-401. Erişim adresi: <https://dergipark.org.tr/tr/download/article-file/1947834>
- Rahimi, Z., Shirali, GA, Araban, M., Mohammadi, MJ, & Cheraghian, B. (2021). Mask use among pedestrians during the Covid-19 pandemic in Southwest Iran: an observational study on 10,440 people. *BMC Public Health*, 21(1), 133. DOI: <https://doi.org/10.1186/s12889-020-10152-2>
- Soon, J. M., Baines, R., & Seaman, P. (2012). Meta-analysis of food safety training on hand hygiene knowledge and attitudes among food handlers. *Journal of Food Protection*, 75(4), 793–804. DOI: <https://doi.org/10.4315/0362-028X.JFP-11-502>
- Şimşek, M., & Şen, M. A. (2020). Mutfak Çalışanlarının İş Motivasyonu ve Hijyen Davranışı Üzerine Bir Çalışma. *Journal of Tourism and Gastronomy Studies*, 8(4), 3039-3051. DOI: <https://doi.org/10.21325/jotags.2020.750>
- Tang, C.S. and Wong, C.Y. (2004). Factors influencing the wearing of facemasks to prevent the severe acute respiratory syndrome among adult Chinese in Hong Kong. *Preventive Medicine*, 39(6), 1187-1193. DOI: <https://doi.org/10.1016/j.ypmed.2004.04.032>
- Tang, J., Li, Y., Eames, I., Chan, P., & Ridgway, G. (2006). Factors involved in the aerosol transmission of infection and control of ventilation in healthcare premises. *Journal of Hospital Infection*, 64(2), 100–114. DOI: <https://doi.org/10.1016/j.jhin.2006.05.022>
- Taşkıran, N., Khorshid, L., & Sarı, D. (2019). Üniversite Öğrencilerinin Hijyen Davranışlarının Karşılaştırılması. *Sağlık ve Toplum Dergisi*, 29(2), 65-78. Erişim adresi: <https://ssyv.org.tr/wp-content/uploads/2019/09/9-%C3%9Cniversite-%C3%96%C4%9Frencilerinin-Hijyen-Davran%C4%B1%C5%9Flar%C4%B1n%C4%B1n-Kar%C5%9F%C4%B1la%C5%9Ft%C4%B1r%C4%B1lmas%C4%B1.pdf>
- Tosun, Ş. Y., Doğruyol, H., Erkan, N., Köse Reis, İ., & Doğruyol Aladak, K. B. (2022). Kovid-19 Sürecinde Balık Restoranlarının Gıda Güvenliği Düzeyinin Değerlendirilmesi: Sarıyer/İstanbul Örneği. *Aydın Gastronomy*, 6(2), 137-153. DOI: [https://doi.org/10.17932/IAU.GASTRONOMY.2017.016/gastronomy\\_v06i1003](https://doi.org/10.17932/IAU.GASTRONOMY.2017.016/gastronomy_v06i1003)
- Tümer, A., Aygün, G., & Tuna, M. (2022). 60 Yaş ve üstü bireylerde koronavirüs (Covid-19) farkındalığı ve ilişkili faktörlerin incelenmesi. *İzmir Democracy University Health Sciences Journal*, 5(2), 304-316. DOI: <https://doi.org/10.52538/iduhs.1039571>
- Türken, M. ve Köse, Ş. (2020). Covid- 19 Bulaş yolları ve önleme, Tepecik Hastanesi örneği. *Tepecik Eğitim ve Araştırma Hastanesi Dergisi*, 30(Ek sayı), 36-42. DOI: <https://doi.org/10.5222/terh.2020.02693>
- Uğurlu-Kalkan, Y., Durgun, H., Nemutlu, E. ve Kurd, O. (2020). COVID 19 salgını sırasında bireylerin sosyal el yıkama bilgi ve tutumunun değerlendirilmesi: Türkiye örneği. *Journal of Contemporary Medicine*, 10(4),617-624. DOI: <https://doi.org/10.16899/jcm.745349>
- WHO. (2020). COVID-19 and Food Safety: Guidance for Food Businesses: interim guidance. Erişim adresi: <https://www.who.int/publications/i/item/covid-19-and-food-safety-guidance-for-food-businesses>
- Yıldırım, E. (2014). *Konaklama işletmelerinde mutfak ve servis personelinin iş tatmini ile kişisel hijyen bilgi ve uygulamaları* (Yüksek lisans tezi). Erişim adresi: <https://tez.yok.gov.tr/UlusalTezMerkezi>

- Yıldız, S. (2011). Sosyal bilimlerde örnekleme sorunu: Nicel ve nitel paradigmalardan örnekleme kuramına bütüncül bir bakış. *Kesit Akademi Dergisi*, 3(11), 421-442. DOI: <https://doi.org/10.18020/kesit.1279>
- Yücel, A. (2000). *İşletme Hijyeni* (Düzeltilmiş 4. bs.). Bursa: Uludağ Üniversitesi Basımevi. Erişim adresi: <https://www.nadirkitap.com/isletme-hijyeni-ahmet-yucel-kitap11233744.html>



## Çanakkale Kent Merkezi Kamusal Açık Alanlarının Kadın Kullanımı Açısından İrdelenmesi

Füsun Erduran Nemutlu<sup>1,\*</sup>, Sena Aksoy<sup>2</sup>, Nurana Nurullayeva<sup>3</sup>, Zeynep Pelin Morgül<sup>4</sup>

<sup>1</sup>Peyzaj Mimarlığı Bölümü, Mimarlık ve Tasarım Fakültesi, Çanakkale Onsekiz Mart Üniversitesi, Çanakkale, Türkiye  
<sup>2,3,4</sup>Kadın ve Aile Çalışmaları Anabilim Dalı, Yüksek Lisans Programı, Lisansüstü Eğitim Enstitüsü, Çanakkale Onsekiz Mart Üniversitesi, Çanakkale, Türkiye

### Makale Tarihi

Gönderim: 31.03.2023  
Kabul: 15.08.2023  
Yayın: 20.12.2023

### Araştırma Makalesi

**Öz** – Kentsel alanlar, farklı kamu hizmetlerinin bir arada yer aldığı, kozmopolit yaşam alanlarıdır. Kentsel açık alanlar ise doğal dengeyi korumalarının yanı sıra sosyo-kültürel paylaşımları da sağlayan önemli yerlerdir. Bu bağlamda kent yaşamının hızlı ve yorucu şartlarında birçok sorumluluğu üstlenen kadınların ihtiyaçları özel olarak incelenmeli ve disiplinler arası çalışmalarla ortaya konulmalıdır. Bu çalışmada Çanakkale kent merkezinin en yoğun kullanım alanları belirlenerek kadınların buralarda kent tasarımına bağlı yaşadıkları sorunların analiz edilmesi amaçlanmıştır. Çalışmanın yönteminde fiziki mekânların ve kullanılan kentsel elemanların, donatıların analiz edilebilmesi için 30 sorudan oluşan bir bilgi formu kullanılmıştır. Çalışma sonucunda kadınların kentsel alanların kullanımında güvenlik, konfor ve estetik açıdan sorun yaşadığı, kentsel donatıların yeterli olmadığı, kentsel açık ve yeşil alanların kadınlar ve dezavantajlı bireyler tarafından kullanımının zor olduğu, sosyal ve kültürel faaliyetlerin yetersiz olduğu belirlenmiştir. Her alanda ayrı ayrı belirlenen sorunların toplamının yüzdelik olarak sonucuna göre, kadınların kent merkezini kullanımında %66 oranında sorun yaşadıkları ortaya koyulmuştur. Çalışmada elde edilen veriler gelecekte yapılacak her türlü bilimsel çalışmalara örnek oluşturabilecek ve kent tasarım ve planlamasında kamu kurumlarına ve yerel yönetime katkı sağlayacaktır.

**Anahtar Kelimeler** – Dezavantajlı birey, evrensel tasarım, kadın dostu kent, kentsel açık alan, peyzaj tasarımı

## Examination of Public Open Spaces of Çanakkale City Center in Terms of Women's Use

<sup>1</sup>Department of Landscape Architecture, Faculty of Architecture and Design, Çanakkale Onsekiz Mart University, Çanakkale, Türkiye  
<sup>2,3,4</sup>Department of Women and Family Studies, Graduate Program, Graduate Education Institute, Çanakkale Onsekiz Mart University, Çanakkale, Türkiye

### Article History

Received: 31.03.2023  
Accepted: 15.08.2023  
Published: 20.12.2023

### Research Article

**Abstract** – Urban areas are cosmopolitan living spaces where different public services are located together. Urban open spaces are important places that provide socio-cultural sharing as well as protecting the natural balance. In this context, the needs of women, who take on many responsibilities in the fast and tiring conditions of urban life, should be specifically examined and revealed through interdisciplinary studies. In this study, it was aimed to determine the most intensive usage areas of Çanakkale city center and to analyze the problems that women experience in these areas due to urban design. In the method of the study, an information form consisting of 30 questions was used to analyze the physical spaces, urban elements and equipment used. As a result of the study, it has been determined that women have problems in terms of safety, comfort and aesthetics in the use of urban areas, urban facilities are not sufficient, urban open and green spaces are difficult to use by women and disadvantaged individuals, and social and cultural activities are insufficient. According to the result of the total of the problems determined separately in each area, as a percentage, it has been revealed that women experience problems at the rate of 66% in the use of the city center. The data obtained in the study will set an example for all kinds of scientific studies to be made in the future and will contribute to public institutions and local administration in urban design and planning.

**Keywords** – Disadvantaged individual, landscape design, universal design, urban open space, women friendly city

<sup>1</sup> fusunerduan@gmail.com

<sup>2</sup> senaksoy05@gmail.com

<sup>3</sup> nurananurullayeva6@gmail.com

<sup>4</sup> zeyneppepinsoydemir@gmail.com

\*Sorumlu Yazar

## 1. Giriş

Kentler, toplumu oluşturan bireylerin birlikte kurduğu, güvenli bir yaşam sürmeyi hedefledikleri, iletişim, eğitim, ticaret, aile kurma, sağlık, ulaşım, adalet, eğitim gibi yaşamsal ihtiyaçlarını sorunsuzca giderebilmeyi amaçladıkları yerleşimlerdir. Yılmaz ve Diktaş (2018)'in da belirttiği gibi sosyal, ekonomik ve kamusal bakımdan kentler, herkesin ihtiyaç duyacağı hizmet ve olanaklar ile bunlara kolayca erişilebilen, bir arada dayanışma ile yaşanabilen, yeterli alt yapı hizmetleri olan yerleşimlerdir.

Günümüzde Dünya nüfusunun büyük kısmının kentlerde yaşadığı düşünülmektedir (Mert, 2021). Türkiye İstatistik Kurumu'nun 2021 yılında yaptığı araştırmaya göre, Türkiye nüfusunun %93,2'sinin İl ve İlçe'lerde yaşadığı belirtilmiş olup, bu sayı gittikçe artmaktadır (Anonim, 2022). Bu durumda kentlerin tasarımı nüfus projeksiyonları dikkate alınarak ve sosyal yaşamın gerekleri doğrultusunda yeniden ele alınmalıdır. Çünkü kentsel alanın tüm kamusal mekânları (açık ve kapalı), kentleşme arttıkça tüm bireyler açısından konforlu ve yaşanabilir hale getirilmelilerdir.

Kentleşme süreci, sanayileşme ve ekonomik gelişmelerle ilerlerken, kentliyi olumsuz etkileyen birçok şeyi beraberinde getirmiştir (Çelik Çanga ve Çalışkan Mimarlar, 2022). Bunun en önemli nedeni, kent nüfusunun beklenmeyen bir şekilde artmasıdır. Bu nedenle konut ve yeşil alanların oranı yetersiz kalmakta, imar problemleri oluşmakta, trafik yoğunlaşmakta ve kentliye sunulması gereken hizmetlersınırlı kalmaktadır (Vural, 2020; Baltutar ve Artar, 2022). Ayrıca bireylerin toprağa dokunabileceği alanlar daralınca doğayla bağlantıları kesilerek beden ve ruh sağlığı da olumsuz etkilendiği göz önüne alınmalıdır (Çelik Çanga, 2021). Bu durum özellikle kentlerde yaşayan dezavantajlı bireyler açısından çok daha etkileyici olmaktadır. Kadınlar da toplumda daha fazla sorumluluk yüklenmeleri yanı sıra iş hayatındaki rolleri, annelik görevleri ile kentsel hizmetlerin yetersiz olduğu mekânlarda dezavantajlı durumdadır. Çünkü kadın kent sokaklarını erkeklerden daha farklı bir şekilde deneyimlemektedir.

Kadınlar tarihten bugüne toplumda baskı gören, birçok hususta dezavantajlı konumda olan kitleler arasında olmuşlar (Akçayır, 2021). Aslında sanayi devrimi kadının toplumsal yaşantısına şekil veren önemli bir süreç olmuştur. Sanayi devrimiyle birlikte aile hayatı ile çalışma hayatı birbirinden keskin çizgilerle ayrılmış, roller ve görevler belirlenmiştir. Bu noktada kadın ev içi görevleri üstlenerek sokağı deneyimlemekten uzak kalmıştır ve bu durumu zamanla kanıksamıştır. Türkiye İstatistik Kurumu'nun 2021 yılı verilerine bakıldığında, kadınların ev düzeni, ev işleri, çocuk bakımı ve alışveriş gibi daha çok içsel konularda karar vermeye yetkili oldukları, erkeklerin ise evde küçük tamirler, aylık faturaların ödenmesi, akraba ilişkileri, çocuklar ile ilgili konularda, tatil, eğlence gibi daha çok dışsal konularda karar organı oldukları ve sorumluluk aldıkları görülmektedir. Bu durum kadınların kentsel mekân kullanımlarında eşitlikli bir durum olduğunu göstermektedir (TÜİK, 2021). Bunun sonucu olarak kentsel tasarımda kadının özel ihtiyaçları ve sorunları göz ardı edilmiştir. Genelde üst yönetimlere ulaşamayan kadın, karar alma yetkisinde de geri kalmıştır.

Kentlerde kadının yaşadığı sorunların artmasına bağlı olarak, 1980'li yılların sonlarında kadının kentteki yeri üzerine tartışmalar ve çalışmalar yoğunlaşmıştır (Şenol, 2015). Bu sorunların en önemlilerinden biri, köyden kente göçün artmasıdır. Bu dönemde kentin sağladığı olanaklara kadınların daha kolay ulaşabilmesi ve kentin avantajlarından onların da rahatlıkla yararlanması gerekliliği çok belirgin olarak görülmüştür (Kaypak, 2019). Kentsel tasarımların ve kamusal tüm olanakların kadınlar için özgürleşme imkânları sunması, istihdam şansı yaratması ve tüm ihtiyaçlarına kolaylıkla ulaşabileceği hizmetler sunması beklenmektedir. Kadının kenti tercihinde bu özellikler ön plandadır. Ancak kentler kadınların çeşitli alanlarda sorunlar yaşadığı mekânlar haline gelmiştir (Acuner, 2016). Bu bağlamda kadın dostu kent programları geliştirilmiş ve ilkeleri oluşturulmuştur.

Kadın dostu bir kent, herkes için dost bir kentin anahtarı sayılır. Aslında kadın dostu kent tanımındaki nitelikler yerine getirildiğinde herkes için kentin kullanımı kolaylaşmış olacaktır. Bu kapsamda yapılacak çalışmalarda kadının tüm sürece dâhil edilmesi ve kullanıcıların katılımının sağlanması gereklidir. Çünkü kadınların kentlerde yaşadıkları sorunların ve ihtiyaçların yine kadınlar tarafından en iyi tanımlanacağı unutulmamalıdır. Bu kapsamda kadının kentsel açık mekânlarda ihtiyaçları, beklenti ve öncelikleri, alan çalışmaları ile belirlenmelidir. Bu çalışma bu gereklilikten yola çıkılarak yapılmıştır.

Çalışmada Çanakkale kent merkezinin en yoğun kullanım alanlarında kadınların kent tasarımına bağlı olarak yaşadıkları temel sorunların analiz edilmesi amaçlanmıştır.

### 1.1. Kentsel Tasarım ve Kadın Dostu Kent

Mekân “sosyal bir üretim” olarak algılandığında toplumsal cinsiyet ve mekân arasında bir ilişki olduğu farklı bilim insanları tarafından kabul edilmiştir. Bu ilişkide toplumsal cinsiyet, mekânsal tartışmalarda güçlü bir özne olarak ortaya çıkmaktadır. Bunun etkileri kent tasarımına yansır. Çünkü kentsel tasarımlar topluma bir ayna görevindedirler (Vanlıoğlu Yazıcı, 2020). Toplumun önemli ferdi olan kadınlar bu noktada önemlidir ve kent tasarımında ihtiyaçlarının dikkate alınması tüm sosyal hayatı kolaylaştıracaktır.

Kentlerde kadınlara yönelik, bir değişimin sağlanabilmesi için, kadınların konu hakkında söz sahibi olabilmeleri gerekmektedir. Erkeklerin daha önce hiç farkında olmadıkları konular, kadınların güvenliği veya kullanım kolaylığı için önem oluşturabilir. Mekânlar arası ulaşımın zorluğu, gece dışarı çıkamama gibi durumlar kadınlar için en önemli sorunların yalnızca bir kısmını oluşturmaktadır (Kiper, Korkut ve Üstün Topal, 2016). Bu bağlamda kentlerde kadının gidebildiği ve gidemediği bölgeler oluşmaktadır ve erkekler bunun farkında bile olmayabilirler.

Certeau, ve ark. (2010) çalışmalarında kent ve mekânlarından şöyle bahseder: Kadın-erkek, genç-yaşlı, herkes tarafından içinden geçilen bir kamusal uzamın pratiği olarak uygunluk açısından bakıldığında, cinsiyetler farkı şu ya da bu biçimde hesaba katılmalıdır. Ayrıca kentlerin bölgelere ayrıldığını ve belirli bölgelerin de cinsiyetlerden biri tarafından işaretlendiğini vurgulamaktadır (kahvehaneler gibi). Bunun ispatı olarak kadınların kamusal alanları belirli saatler dışında kullandıklarında yaşadıkları sorunlar veya erkeklerin çoğunluk olarak kullandıkları mekânlar ve sokaklardan geçerken kadınların tedirgin olmaları örnek verilebilir. Akşam saatleri ya da sabahın erken saatlerinde mekânların kadına güvensizleşmesi ile kullanılmaması gerektiği algısı ve alışveriş merkezleri gibi alanlarda boş zamanlarını değerlendirip sosyalleşmeye yönlendirilmeleri, aslında kadını kent açık mekânlarında sınırlandırmaktadır. Kentin tümünde her saat kadının yaşamının kolaylaştırılmasını sağlayacak tasarımlarla düzenlenmesi, kadın dostu kent anlayışını getirmiş ve ilkeler ortaya koyulmuştur.

Kadın dostu kent kavramında toplumun tüm bireyleri için güvenilir ve yaşanabilir bir kent oluşturmak hedeflenmektedir. Zaten imar planlarında kamu kullanımı için ayrılmış olan kentsel donatı alanları, bireylerin bir arada yaşamlarını sürdürdüğü, konaklama, ulaşım, eğitim, ibadet, sağlık, sosyo-kültürel ihtiyaçlarını karşıladıkları mekânlardır. Çelik Çanga ve Küçük (2022)'ün kent açık yeşil alan sistemleri ile ilgili çalışmalarında bu mekânlardan kentlilerin sorun yaşamadan faydalanmalarını sağlamaya yönelik planlama ve tasarımlar yapılması gereğini vurgulamış ve öneriler getirmiştir. Bu bağlamda kentlerde kadınların kamusal açık alanlarda dolaşımının kolaylaştırılması, ulaşım sıkıntısı çekmemesi, sokaklara güvenle çıkabilmesi, sokaklarda fiziksel zorluk yaşamamaları temel hedeftir ve mekânsal planlamalar modern kent anlayışında toplumsal cinsiyet eşitliği dikkate alınarak yapılır. Bunlar kentlerde kadın erkek eşitliğinin sağlanmasının ötesinde kadının ekonomik ve kültürel alanda güçlenmesini de sağlamaya yöneliktir (Baykan, 2015; Kiper vd. 2016). Türkiye’de toplumsal cinsiyet eşitliği çalışmalarını yerel yönetimlere taşıyan ilk proje olma özelliğini taşıyan kadın dostu kent projesi, 2006 yılında Sabancı Vakfı’nın desteği ile uygulanmaya başlanmıştır (Efe Güney ve Üstündağ, 2020). Bu projenin birinci aşaması 6 İl’de, ikinci aşamada ise 7 İl’de uygulanmıştır (Özsoy ve Sipahi, 2016; Çetintahra Ekşioğlu ve Efe Güney, 2019).

Kadın dostu kentler programının temel ilkeleri şöyle özetlenebilir (Efe Güney ve Üstündağ, 2020): Kamusal mekânlar iyi aydınlatılmalı; çıkmaz sokak, kıvrımlı yol ve sağır cepheler bulunmamalı; kamusal mekânlarda acil arama noktaları ve kent tanıtıcı levhaları bulunmalı; sığınma ve toplanma mekânları yapılmalı; otobüsler kentin en uzak noktalarına ulaşabilmeli; kadınlar geceleri otobüs durakları dışında da istediği yerde inebilmeli; belediye konutu veya resmi toplu konutlarda kadınlar için kota ayrılmalı; sokaklar etkinliklere olanak tanımalı; yol ve kaldırımlar kadın, çocuk, engelli, yaşlı vb. bireyler dikkate alınarak tasarlanmalı; kamusal açık ve yeşil alanların kadın kullanımı açısından güvenli, erişilebilir, estetik, etkili ve görünürlüğü yüksek olmalıdır.

Kadın dostu kent anlayışı yanı sıra fiziksel mekânların toplumun her kesimi açısından ulaşılabilir, yaşanabilir ve kullanılabilir olması, evrensel tasarım anlayışının temel hedefidir (Alptekin, 2022). Bu anlayışın temel ilkesi ihtiyaçlara ve tüm taleplere erişilebilirliğin sağlanmasıdır (Yılmaz ve Diktaş, 2018). Bunun için tasarımcı şu esaslara dikkat eder: Kenti herkes için tasarlar, evrensellik probleminin neler olduğunu belirler, evrensel

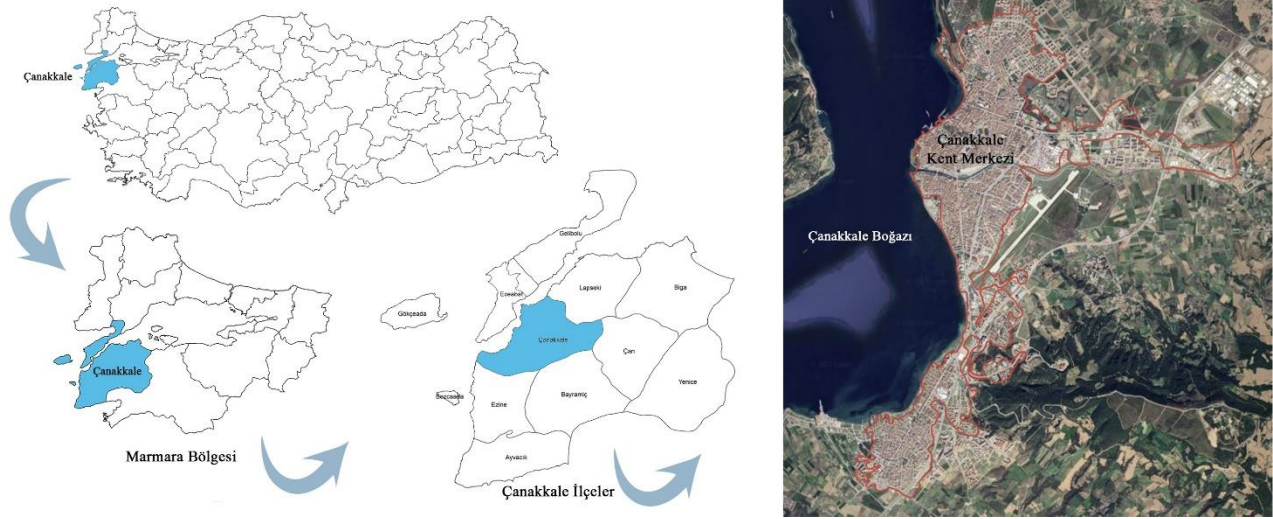
kullanımlar getirir, tasarımda tüm kenti hedefler ve her zaman kullanımı dikkate alır (Cavington ve Hannah, 1996; Aktaş, 2017; Hacıhasanoğlu, 2003). Bu ihtiyaçları karşılamaya yönelik, evrensel tasarım merkezi tarafından 1997 yılında, evrensel tasarım kavramının somutlaştırılması ve yaygınlaştırılması için şu ilkeler belirlenmiştir (Hacıhasanoğlu, 2003; Aktaş, 2017; Yılmaz ve Diktaş, 2018): Eşitlikçi kullanım, kullanımda esneklik (çeşitlilik), basit ve sezgisel kullanım, algılanabilir bilgilendirme ilkesi, tasarımda hata payı ilkesi, düşük fiziksel güç gereksinimi ilkesi, yaklaşım ve kullanım için uygun boyut ve mekân sağlanması ilkesi.

Evrensel tasarım engelli, engelsiz, kadın, genç, erkek, yaşlı gibi kişileri kategorize etmez. Amacı kişi ayırmadan çözüm üretmektir. Bu ilkeler yanı sıra kentsel dış mekânların yaşanabilir olması için, insan yaşamına huzur ve kolaylıklar sunan işlevsel ve estetik değeri olan peyzaj elemanları içermesini öngörür (Çelik, 2012). Bu bağlamda çalışmada alan analizleri için kullanılan bilgi formunun hazırlanmasında kadın dostu kent yaklaşımı yanı sıra bu ilkelere de dikkat edilmiştir.

## 2. Materyal ve Yöntem

Çanakkale, Güney Marmara Bölgesinde boğaza kıyısı olan, sahip olduğu tarihi ve doğal kaynakları ile ulusal ve uluslararası açıdan ilgi odağı bir İl'dir (Şekil 1). Bu nedenle kent, farklı illerden gelen ve yerleşen nüfus yanı sıra, özellikle turizm döneminde çok geniş kitlelerin kullanımına sahne olmaktadır.

Kent merkezi 9,737 km<sup>2</sup>'lik alana sahiptir. Kentin sosyal yaşamının en hareketli olduğu bölgeler: Aynalı çarşı, yürüyüş yolu ve çarşı çevresi, parklar, pazarlar, saat kulesi çevresi ve boğaz kıyısındaki kordon bölgesidir. Kentin tarihi yerleşim bölümü günümüzde kentsel sit alanı olarak koruma altında olup, dar sokaklara sahiptir. Bu alan kentlinin gün içinde ihtiyaçlarını karşılamak için en yoğun kullanımına sahiptir. Kordon ile birleşen çarşı yaya yolu olarak düzenlenmiştir. Kent çekirdeğini yeni gelişim alanına köprüler ile bağlayan Sarıçay çevresi de günümüzde cazibe merkezine dönüşmüştür.



Şekil 1. Çanakkale İli'nin ve kentin konumu (Goggle Earth 2023' den yararlanılarak hazırlanmıştır)

Çalışmada örnek alan olarak Çanakkale kent merkezinde nüfusun en yoğun olduğu ve tüm kentlinin kullanımı açısından kentsel sosyal hizmetlerin sunulduğu, kent çekirdeğindeki 5 bölge seçilmiştir. Seçilen örnek alanlar: 1- Eski kordon, 2- Halk Bahçesi bölgesi, 3- Hastane bölgesi, 4- Fevzipaşa Mahallesi, 5- Namık Kemal Mahallesi bölgeleridir ve 40° 8' 38.31" kuzey enlemi ve 26° 24' 4.86" doğu boylamı ile, 40° 8' 58.50" kuzey enlemi ve 26°24'7.34" doğu boylamı arasında yer alırlar. (Şekil 2). Çalışmada kullanılan yardımcı materyal ise kadınların bu alanları kullanımında yaşadıkları sorunların belirlenmesine yönelik hazırlanan bilgi formudur. Diğer yardımcı materyaller, kent haritası ve alanda yerinde çekilen fotoğraflardır.



Şekil 2. Çanakkale kent merkezi ve çalışma alanları: 1- Eski Kordon, 2- Halk Bahçesi bölgesi, 3- Hastane bölgesi 4- Fevzipaşa Mahallesi, 5- Namık Kemal Mahallesi (Goggle Earth 2023' den yararlanılarak)

Çalışma yönteminde Çanakkale kent merkezinde en yoğun kullanılan 5 bölge örnek alan olarak seçilmiştir. Bu alanlar yerinde mekânsal olarak incelenerek hazırlanan bilgi formu ile analizleri yapılmıştır. Bilgi formu çalışmanın farklı alanlara uygulanması ve karşılaştırılma olanağı sağlamaktadır.

Çalışmada kentsel tasarım ve kadın dostu kent ilkeleri ile ilgili gerekli literatür taramaları yapıldıktan sonra, kavramsal çerçeve oluşturulmuştur. Çalışmanın yönteminde Çanakkale kent merkezinde belirlenen alanlardaki fiziki mekânların ve kullanılan kentsel elemanların ve donatıların analiz edilebilmesi için 30 sorudan oluşan bilgi formu hazırlanmıştır. Formun hazırlanmasında kadın dostu kent anlayışı ile beraber evrensel tasarım ilkeleri göz önünde bulundurulmuştur. Toplam 30 maddeden oluşan bilgi formunda çalışma alanlarının irdelendiği konular: Güvenlik, aydınlatma, temizlik, erişilebilirlik, estetik görünüm, bilgilendirme, esneklik, donatı ihtiyaçları, algılanabilirlik ve konfordur. Her alan önce kendi içinde irdelenmiş, daha sonra tek bir tabloda bilgiler toplanarak karşılaştırma olanağı yaratılacak şekilde irdeleme yapılmıştır. Son aşamada her alanda belirlenen sorunların her biri bir puan olarak kabul edilerek, kentte kadınların sorun yaşama durumu, yaklaşık olarak, tablonun kendi içindeki verilere göre oranlama yapılarak yüzdeler orana dönüştürülmüştür. Çalışmada bir peyzaj mimarı mekânsal ve görsel değerlendirme yapmıştır. Çalışmada mekânsal incelemeler yanı sıra, mekan tasarımlarının kullanıcı üzerindeki etkileri ve kullanıcı ihtiyaçlarının sosyo-kültürel açıdan değerlendirilebilmesi için 2 psikolojik danışmanlık ve rehberlik uzmanı ile 1 sosyolog çalışmada görev almıştır. Çalışma ekibi belirlenen alanları birebir yerinde inceleyerek kullanıcıları gözlemlemiş ve hazırlanan bilgi formunu kendileri doldürmüştür. Kent kullanıcıları zaman zaman fikir bildirirse de çalışmada yöntem olarak kullanıcıların alanı kullanırken gözlemlenmesi ile fikir edinilmiştir.

Yöntemde çalışma alanları yerinde ayrıntılı olarak incelenirken kullanıcıların ihtiyaçlarının analiz edilmesini sağlayacak olan, ayrı ayrı tasarım ve kullanımların değerlendirilmesini sağlayan bilgi formu niteliğindeki çizelge ile bölgelerin kullanım durumları karşılaştırmalı olarak analiz edilmiştir. Değerlendirmelerde evrensel tasarım anlayışı ve kadın dostu kent kriterleri dikkate alınmıştır. Her alan için bu kullanımların bulunup bulunmama durumuna göre belirlenen sorunlar toplanmıştır. Bu toplamın 30 soruda bulunma durumu dikkate alınarak, yüzde ne kadar olduğu hesaplanmış ve alan değerlendirilmiştir.

### 3. Bulgular ve Tartışma

Belirlenen çalışma alanında öncelikle yollar, duraklar, kaldırımlar, yeşil alanlar, kentsel donatı elemanları ve diğer fiziki mekânlar, günlük ihtiyaçlar doğrultusunda incelenerek görseller ile belirlenmiştir. Alan araştırması yapılırken kent içi yaya sirkülasyonu, yolların yapısal özellikleri, ulaşım, sosyal mekânların kalitesi, güvenliği, estetik görünümüne, aydınlatma ve bilgilendirme olanaklarına önemle dikkat edilmiştir.

Kentin Çanakkale Boğazı kıyısını saran, Cevat Paşa Caddesi'nde yer alan Eski Kordon (1 nolu bölge) Çanakkale'nin önde gelen en hareketli bölgelerinden biridir. Bölge kentinin gece ve gündüz rekreasyonel etkinlikleri için çok yoğun kullandığı, özel günlerde yerel yönetim ve sivil kuruluşlar tarafından etkinliklerin

organize edildiği, sosyal ve kültürel paylaşım alanıdır. Ancak alanda kadınların kullanım sırasında yaşadığı birçok sorun vardır ve aydınlatma da yeterli değildir. Kordonun bir kısmında kafe ve pastanelerin kordonun kamuya ait yol kısmını işgal etmesi, özellikle dezavantajlı vatandaşlar ve kadınlar için kalabalık saatlerde geçişi engelleyerek sorun olmaktadır. Çocuklu kadınlar, bebek arabası veya engelli arabası sürenler için b durum daha da zorlaşmaktadır. Çocuklar çok hareketlidir ve hızla koşarak zor kontrol edilebilirler. Kaldırım kıyısını caddeden ayıran babalar vardır; ancak hem renkleri algılanamamakta, hem de keskin köşeleri yaralanmalara neden olmaktadır. Bisiklet yolu da kordonun bir bölümünden geçmektedir ve yürüyüş olanağı dar bir alana sıkışmıştır. Hatta motosikletler de bazen bu alanı kullanmaktadırlar. Görme engelli vatandaşlar için kullanılan iz yolubazen farklı malzemeler, bazen bisikletler vb. araçlar tarafından işgal edilmektedir. İz yolunun boyası da yer yer silinmiş olduğundan az gören vatandaş için dikkat çekici özelliği kaybolmuştur. En önemli tehlike, eski kordonun sahil kıyısında koruyucu bir bariyer bulunmamasıdır. Zaman zaman yapılan etkinliklerde alanın çok kalabalıklaşması yanı sıra, hızla bisikleti ile yanlış yola girenler ve top oynayan çocuklar için risk oluşturmaktadır. Deniz kıyısı tamamen kayalar ile kaplı olduğundan olası bir düşme durumunda yetişkinler ve özellikle çocuklar büyük risk altındadır (Şekil 3). Topuklu ayakkabı kullanan kadınlar için kıyıya yaklaşmak veya çocuğuna eşlik etmek oldukça zordur.



Şekil 3. Çanakkale Eski Kordonun deniz kıyısından görüntüleri (2022)

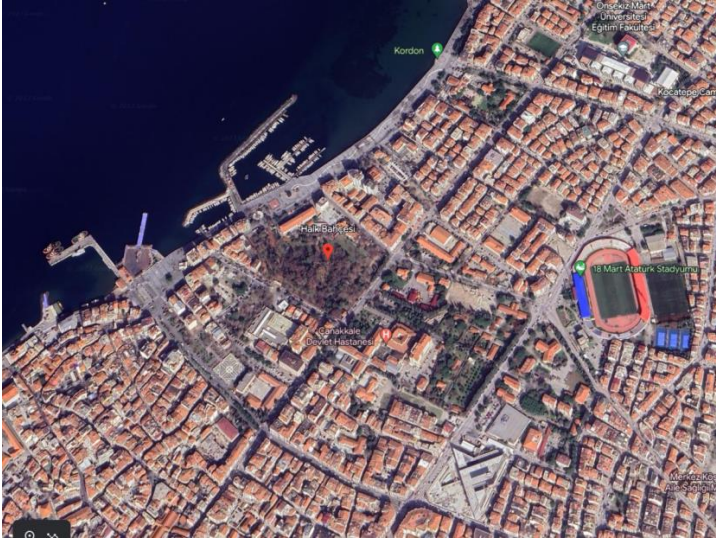
Kordon uzun bir alan olmasına karşın sadece aktif kullanılan bir çeşme bulunmaktadır ve yetersizdir. Anneler için en önemlisi çocukların ellerinin sürekli kirlenmesi ve hijyen sağlanmasıdır. Alanda heykel, tanıtımlar, donatılar, oyun ekipmanları, oturma üniteleri vardır ancak yeterli çöp kutusu yoktur. Kordonun zemin kaplamalarında takılıp düşmeye neden olabilecek bozuk bölümler vardır (Şekil 4). Kadınlar gün içinde bir çok sorumluluğu yerine getirmek durumunda kalabildiği için acele hareket edebiliyorlar. Özellikle ileri yaş dönemindeki tüm kişiler için takılıp düşmek çok risklidir. Bu durum yaşlı ebeveynine eşlik eden kadın ve anneler için daha da önemlidir.

Alanın başlangıcında bebek bakım ünitesi sadece bir tane olup, giriş kart ile kullanılmaktadır. Dışardan gelenler veya konuklar dikkate alınmamıştır.



Şekil 4. Kordondaki donatılardan bazı görüntüler (2022)

Çalışma alanı olarak seçilen ikinci bölge, kent merkezinde en büyük yeşil leke pozisyonundaki Halk Bahçesidir. Bu alan, kentli tarafından özellikle yaz aylarında sağladığı gölge ve serinliği ile tercih edilmektedir(Şekil 5). Sahilde dikkat çekici obje olan, temsili Truva Atı'nın ve Çanakkale Valiliği'nin arkasında, Kayserili Ahmet Paşa ve İnönü Caddesi'nin kesişim noktasında olup, 4 ana girişi bulunmaktadır.



Şekil 5. Kent merkezi, liman, Halk Bahçesi, Devlet Hastanesi ve Kordon (Goggle Earth, 2023).

Park kentin birçok mekânı arasında geçiş özelliği de göstermektedir. Ancak çevresinde yer alan duvarların yüksekliği acil bir durumda çıkışı zorlaştırmakta ve görünürlüğü kısıtlamaktadır. kalite kriterleri ve tasarım ilkelerine göre kadınların kendini güvende hissetmeleri açısından çıkılamayan alanlar olmamalıdır (Şekil 6a). Park alanının kadınlar tarafından en yoğun kullanılan bölümü çocuk oyun alanıdır. Ancak fiziki yapısında sorunlar vardır. Çevreden bir adımlık çukurda yapılmış olup zemindeki kod farkı nedeni ile hızlı hareket eden çocukların düşmesine neden olabilmektedir. Oyun ekipmanları küçük bir alana sıkıştırılmıştır ve yapılan teleferik bu kalabalık arasında risk oluşturmaktadır. Aileler küçük yaşta çocuklarına aletleri sürekli denetimli olarak kullanırmak durumunda kaldığından alan daha da kalabalık hale gelmektedir. Yaş gruplarına göre oyun alanları birbirinden ayrılmamıştır. Çocuk bahçesi duvarının kenarında çok yaşlı ve sert, uzun dikenli Yalancı Portakal (*Maklurapomifera*Schneid.) ağaçları çocuklar için çok tehlikeli olupaynı zammada kasvetli bir ortam oluşturmaktadır.

Günümüzde çocukların isteklerini karşılamaktan uzak oyun ekipmanları vardır. Zeminin kumdan oluşması çamura ve sokak hayvanlarının dışkılamasına da neden olmaktadır (Şekil 6b).



(a)

(b)

Şekil 6. Çanakkale Halk Bahçesi'nden genel görüntü (2022)

Park alanında bebek bakım ünitesi, tuvalet ve çeşme bulunmasına rağmen bunlara yeterli yönlendirme levhası yapılmamıştır. Parkın farklı girişini kullananlar bu mekânlara ulaşamamaktadırlar. Çocuklar suyla oynamayı sever ve çok hareketli olduklarından sürekli su içmek isterler. Anneler onlara yardımcı olurken çeşmeyi kullanımlar ergonomik olmalıdır. Ancak alanda yer alan çeşmenin tasarımından dolayı kullanıcıların üzerine atık suyu sıçratmaktadır. Aynı zamanda gideri olmadığı için atık sular çocuk oyun alanında birikerek çamur oluşturmakta ve sağlık açısından tehlike yaratmaktadır (Şekil 7a). Özel gereksinimi olan kadınlar için mekânlarda yeterli işaretleme de yer almamaktadır.

Sağlıklı yaşam için spor aletleri vardır. Bu aletlerin bilinçli kullanımı çok önemlidir ve alanda sakatlanmanın önlenmesi için bilgi panoları olmalıdır. Ancak bu alanda buna önem verilmediği gibi park içinden geçen bisikletliler alanda tedirginlik hissi yaratmaktadırlar (Şekil 7b,c).

Park alanında genel olarak süs bitkisi niteliği zayıf türler hâkim olup, mevcut olanlara yeterli bakım önlemi zamanında alınmamıştır. Böylece alanın rekreasyonel yönden mevcut bitkileri görsel açıdan ziyaretçileri mutlu etmekten uzaktır. Aynı zamanda alanda parkta yapılan incelemeler sonucu konfor ve imajının ortadan zayıfa doğru düşen değerde olduğu görülmüştür. Sosyallik yönünden orta, ulaşım yönünden iyi, farklı aktivitelerin bulunması yönünden ise zayıftır (Erduran ve Kabaş, 2010). Kadınların çocukları ile bu alanı uzun saatle kullandığı düşünülürse oturma ve dinlenme ünitelerinin daha fazla sayıda olması gerekir. Günümüzde park alanında bazı budamalar ve Ortanca (*Hydrangea macrophylla* Thunb.) gibi bitki dikimleri yapılsa da alanda çiçekleri ile etkili ve her mevsim ilgi uyandıran bitkilere yeterince yer verilmediğinden, kent parkı niteliği taşımaktan uzaktır.



(a)

(b)

(c)

Şekil 7. Çanakkale Halk bahçesinde yer alan bazı kullanımlar (2022)

Devlet hastanesi (3 nolu bölge) günümüzde şehir dışına taşınmış olup kent merkezinde bazı poliklinikler hizmet vermektedir. Onların da taşınması tartışma konusudur. Bu nedenle günümüzde çevresi bakımsız kalmış, yapısal olarak hasta bir kişinin yürümesi açısından, hem kaldırımları hem de yolları sorunludur. Bahçenin tasarımı hastaların kendilerini iyi hissetmeleri ve dinlenmeleri için farklı peyzaj bitkileri ile ve havuz



alandır (Şekil 10). Bu bölgede konumlanan Nalbantlar Caddesi ve Nalbantlar Sokak terkedilmiş harabe binalarıyla şehir güvenliği ve kadınların kullanımı açısından sağlıklı değildir.



Şekil 10. Sarıçay bölgesinden görünüm (2022)

İnönü köprüsü ve İnönü Caddesi üzerine yerleştirilen heykeller ve estetik unsurlarla, modern bir kent görünümü yaratılmaya çalışılsa da İnönü köprüsünden Fevzi Paşa Mahallesi'ne doğru olan bölüm uzun yıllar bakımsız kalmanın, kaderine terk edilmenin izlerini yansıtmaktadır (Şekil 11).



Şekil 11. İnönü köprüsünün iki tarafından görüntü (2022).

Çay Kenarı Sokağı, Dizdar Caddesi, Talimhane Sokak ve bunlara açılan sokaklara bir kadın yolunu kaybederek girebilir. Çünkü bölge tanımsızdır, çıkmaz sokaklar, dar vebirbirine açılan sokaklar vardır. Bu alan kent merkezi ile iç içe olmasına karşın izbe ürkütücü ve çöplerin kontrolsüzce döküldüğü mekânlara sahiptir. Sokak aralarında kalmış tarihi çeşme hem korunamamış hem de işlevsizdir. Fatih Camii'nin de yer aldığı Fatih Sokak içerisindeki çöplerle, terkedilmiş eski binalarla Tıflı Sokak, Nedime Hanım Sokak, Lale Sokak, Cami Sokak ve Zafer Meydanı ile Fevzi Paşa Mahallesi'nin iç sokakları, sağlıklaştırma ve kentsel dönüşüm çalışmaları yapılması gerektiği belirlenmiştir. Bu şekilde bakımsız kalan bölgeler her türlü tehlikeye açık yerlerdir. Medrese Sokak, Çimenlik Sokak gibi sınırlı alanlarda yapılan estetik çalışmalar ise Fevzi Paşa Mahallesi'nin tamamına bakıldığında oldukça yetersiz kalmaktadır (Şekil 12).



Şekil 12. Fevzipaşa Mahallesi'ne ait sokaklardan görünümler (2022).

Balıkxane Sokak ise Çimenlik Kalesi'nden paslı demir parmaklıklarla ayrılmaktadır. Gümrük Bölgesi olarak bilinen alanda sahil güvenliğinin kullandığı iskele, balıkçıların yoğun kullandığı bir alandır ve dört tarafında da korkuluk bulunmamaktadır. Güvenlik önlemlerinin iyi olmadığı bölgede ayrıca işletmeler kordonu da işgal etmektedir. Ayrıca bu bölgede kent mobilyalarının ve çöp kutularının eksikliği de dikkat çekmektedir (Şekil 13). Kadınların ücret ödemededen boğaz kıyısında dinlenebilecekleri oturma elemanları çok sınırlıdır.



Şekil 13. Çimenlik Kalesi'nin deniz kıyısı, Nusret Mayın Gemisi ve kafeler (2022)

Çanakkale kentinin kalabalık bölgelerinden biri olan Namık Kemal Mahallesi'nin Sarıçay boyu (5. bölge) olarak isimlendirilen alan, Atatürk Caddesi ve Setboyu Caddesi'nin kesişim alanından başlayarak Troya köprüsüne kadar uzanır (Şekil 14).



Şekil 14. Namık kemal Mahallesi (Goggle Earth 2023'den yararlanılarak)

İl'in farklı yerlerinden kullanıcıların ihtiyaçlarını karşıladığı Cuma pazarı(CUMPA) bu mahallededir ve kentin tarihine adını yazdırmıştır. Kadınların evin ekonomisi ve ihtiyaçlarını daha çok takip etmesi nedeni ile kentte farklı günlerde de pazar kurulmasına karşın, kadınlar Cuma günlerini ürün çeşitliliğinin daha fazla olması, köylerden ve farklı yerlerden satıcıların gelmesi nedenleri ile tercih etmektedirler ve çok kalabalıktır.

Kente çok yakın olan pazar yeri yürüme olarak iskele meydanına 30 dakika mesafededir. Ancak pazar yerinin kent tarafından girişinde bir çay bahçesi olmasına karşın bakımsız ve izbe görünümü nedeni ile kadınların kendini güvende hissederek dinlenebileceği alan olmaktan uzaktır. Oysa alışverişini yaptıktan sonra dinlenerek yoluna devam etmek ve diğer ihtiyaçlarını düşünmek için bir mekan ihtiyaç vardır. Bu bölgenin sağlıklılaştırılması ve Pazar girişinin daha modern, estetik bir görünüme kavuşturulması gereklidir (Şekil 15).

Pazar alanına yeterince hakim olmayan kadınlar ürün satış standlarının yerlerini kolaylıkla bulamaktadırlar. Pazar içinde herhangi bir yönlendirme veya levha, tanıtım yer almamaktadır. Ayrıca otopark alanı çok azdır ve çok katlı bir otopark yapılmalıdır. Çok katlı otopark yapılabilecek kadar geniş alanlar vardır. Araçların pazar kapılarının hemen yanında park etmesi ve geliş gidişlerin ortada dar, yüksek bir refüj ile ayrılması elinde ağır paket taşıyan kadınlar, özellikle çocukları ile gelenler ve yaşlılar için büyük sorun oluşturmaktadır.



Şekil 15. Çanakkale Cuma Pazarı'nın farklı girişlerinden görüntü (2022)

Pazar çevresinde marangoz ve demir atölyeleri, dükkanlar, eski belediye binası gibi farklı hizmetlerin sunulduğu yapılar yer almaktadır. Önlerinde yaya yürüme yeri olmayan bu yapılar eski, bakımsız ve kötü görüntüye sahipler.

Pazarın iç kısmı daha önce yenilenmiş, tezgahların kurulumu ve çatı sistemi ile modern görünüme kavuşturulmuştur. Ancak çevresindeki yol ve kaldırımların bozukluğu, izbe, bakımsız binalar, bozuk yollar ve düzensiz çöp kutuları tüm kentli için kötü görüntü oluşturmaktadır. Ancak kadınları daha fazla tedirgin eden bu görüntüler, kışın havanın erken kararması ile birlikte daha da korku yaratmaktadır. Ayrıca kaldırımların

işgali ve çevrenin karışık görünümü hem çocukları hem de kadınları psikolojik olarak yormakta ve rahatsız etmektedir (Şekil 16).



Şekil 16. Çanakkale Cuma Pazarı'nın çevresinden görüntüler (2022)

Bu bölgenin ana yollara yakınlığı ve yoğun kullanılan güzergâhta olması nedeni ile toplu taşıma olanağı iyidir. Pazar yeri ve Troya köprüsü alanında gidiş yönünde toplam 3, dönüş yönünde ise 4 durak bulunmaktadır. Ancak Setboyu Caddesinde ulaşım sınırlıdır. Bu caddeyi kentliler yaya olarak da kullanmakta, hatta Sarıçay çevresindeki yeşil alanda dinlenmektedirler. Bu park alanında spor aletleri, çocuk oyun parkı, basket sahası ve bisiklet yolu olsa da çeşme, oturma üniteleri, çöp kutusu, aydınlatma gibi donatı malzemeleri yoktur. Özellikle mesai çıkış saatlerinde bu durum sorun oluşturmaktadır. Ayrıca araçların durak alanlarını işgal etmesi denetim yetersizliğini göstermektedir. En önemli sorunlardan diğerleri; yeterli otopark olmaması, bisiklet yolunun olmaması ve yolların dar olmasıdır.

Çalışma alanları yerinde ayrıntılı olarak incelenmiş ve yukarıda görselleri ile sunulmuştur. Alan özelliklerinin değerlendirilebilmesi için hazırlanan bilgi formu ile bölgelerdeki kullanımların durumları karşılaştırmalı olarak analiz edilmiştir (Tablo 1). Değerlendirmelerde evrensel tasarım anlayışı ve kadın dostu kent kriterleri dikkate alınarak 30 madde belirlenmiş ve bunlar çerçevesinde alanların sorunları özetlenmiştir. Çalışmanın farklı alanlara uygulanabilmesi düşünülerek her alanda belirlenen sorunların toplam puanının yüzdeler olarak değerlendirilmesi yapılmıştır. Buna göre, Çanakkale kent merkezi kadın kullanımı açısından %66 oranında sorunlu bulunmuştur. Tüm çalışma alanlarının taşıma kapasitesinden daha kalabalık olması nedeni ile hizmetlerden eşit yararlanılamadığı görülmüştür. Ayrıca çalışma alanları peyzaj tasarımı açısından çok zayıf olup, bu durum en fazla kadınlar ve onların yetiştirdiği gelecek nesillere yaşanabilir sağlıklı kent ortamı sunulmasını engellemektedir. Çalışma alanlarından sadece Eski Kordon bölgesinin daha güvenli olduğu algısı vardır. Çünkü her saat sirkülasyonun devam etmesi ve yakında işyerleri olması görülebilirliği artırmakta olup, güven yaratmaktadır. Ancak hastane çevresinde bakımsız kalmış yeşil alanda budanmayan ağaçlar gizli ve denetimsiz bölgeler yaratmaktadır. Hastanenin içi kadar dışı da hijyenik ve bakımlı olmalıdır.

Tablo 1. Çalışma konusu olan bölgelerin karşılaştırılması.

Çanakkale kent merkezinin kadın kullanımı açısından analizi							
No	Analiz konuları	Halk Bahçesi	Hastane Bölgesi	Eski Kordon	Fevzi-paşa Mahal-	Namık Kemal Mah.	Sorum oranı
1	Kimlik olarak iyi algı yaratıyor mu? İmajı iyi mi?	Evet	Hayır	Hayır	Hayır	Hayır	4
2	Aydınlatma sayısı yeterli mi?	Evet	Evet	Hayır	Hayır	Hayır	3
3	Basit, kolay kullanımlı, konforlu mu?	Evet	Hayır	Evet	Hayır	Hayır	3
4	Oturulacak alan sayısı yeterli mi?	Hayır	Hayır	Evet	Hayır	Hayır	4
5	Çıkamaz sokak ve yol sorunu var mı?	Hayır	Evet	Hayır	Evet	Hayır	2
6	Çöp kutusu yeterli mi?	Evet	Evet	Hayır	Hayır	Hayır	3
7	Fiziksel saldırı ihtimali var mı?	Evet	Evet	Hayır	Evet	Evet	4
8	Irkçı saldırı ihtimali var mı?	Hayır	Hayır	Hayır	Evet	Evet	3
9	Soyulma ihtimali var mı?	Evet	Evet	Hayır	Evet	Evet	4
10	Yeterli sayıda yeşil alan var mı?	Evet	Evet	Evet	Hayır	Hayır	2
11	Toplu taşıma ulaşımı var mı?	Evet	Evet	Evet	Evet	Hayır	1
12	Ulaşım kolay mı ?	Evet	Evet	Evet	Hayır	Hayır	2
13	Yeterli sayıda durak var mı?	Evet	Evet	Evet	Hayır	Evet	1
14	Kalabalık sorunu var mı?	Evet	Evet	Evet	Evet	Evet	5
15	Ortam temiz mi?	Hayır	Evet	Hayır	Hayır	Hayır	4
16	Çeşme veya kaynak suyu var mı?	Evet	Hayır	Evet	Hayır	Hayır	3
17	Tuvalet var mı?	Evet	Hayır	Evet	Hayır	Hayır	3
18	Sakatlanma riski barındırıyor mu?	Evet	Hayır	Evet	Evet	Evet	1
19	Dezavantajlı bireyler için uygun şartlar var mı?	Hayır	Hayır	Hayır	Hayır	Hayır	5
20	Uygun yürüyüş alanları var mı?	Evet	Hayır	Evet	Hayır	Evet	2
21	Devam eden bisiklet yolu var mı?	Hayır	Hayır	Hayır	Evet	Hayır	4
22	Yaya kaldırımlarında sorun var mı?	Evet	Evet	Evet	Evet	Evet	5
23	Fiziksel aktivite yapılacak yerler var mı?	Evet	Hayır	Evet	Hayır	Evet	3
24	Peyzaj tasarımı yeterli mi?	Hayır	Hayır	Hayır	Hayır	Hayır	5
25	Görünürlük var mı?	Hayır	Hayır	Evet	Hayır	Evet	3
26	Zemin kaplamaları herkes için uygun mu?	Hayır	Hayır	Hayır	Hayır	Hayır	5
27	Estetik mi	Evet	Hayır	Evet	Hayır	Hayır	3
28	Bebek bakım odası yeterli ve uygun mu?	Hayır	Hayır	Hayır	Hayır	Hayır	5
29	Mekân tanımlayıcı ve bilgilendirici tabelalar var mı?	Hayır	Evet	Hayır	Hayır	Hayır	4
30	Sosyalleşme olanağına sahip mi?	Evet	Hayır	Evet	Hayır	Hayır	3

#### 4. Sonuç ve Öneriler

Çalışma alanı bölgeler halinde irdelenerek kadınların kentsel alan kullanımında yaşadığı en önemli sorunlar tüm alanlar genelinde düşünülerak çizelgeden elde edilmiş ve aşağıda özetlenmiştir. Bu sorunlar kentsel tasarım ilkeleri özelinde ana başlıklar şeklinde ele alınmıştır:

-Güvenlik: Çalışma alanlarının tümündeki mekanların her saat yeterli aydınlatmasının olmadığı, yeşil alanların bakımsız olduğu ve görünürlüğün yetersiz olduğu, izbe metruk alanların yer aldığı belirlenmiştir. Tanımsız çıkamaz sokaklar, yıkık, virane bölümler, kadınlar açısından tedirginlik yaratan ve dış

mekan kullanımını kısıtlayan en önemli unsurlardır ve sağlıklaştırma gereklidir. Kadınların güvenliğini sağlamak için belirli güvenli noktalar, acil alarmı ve bu noktalara yönlendirmeler de bulunmalıdır.

-Konfor: Kamusal açık alanlarda yeterli büyüklükte, ergonomik, estetik ve nitelik açısından uygun dinlenme alanı bulunmamaktadır. Kadınların alışveriş sırasında ve günlük yorucu tempolarında çocuklarının ve kendilerinin bakımı için temiz özel alanlara ihtiyaçları vardır. Çalışma alanlarında sadece kordonun son kısmında bebek bakım ünitesi ve tuvaletler vardır. Oysa sınırlı süreleri vardır ve en yakında olmalıdır. Kırık kaldırım taşları, kaygan zeminler, araç park edilen kaldırımlar, bisiklet ve motosikletlerin yaya yolunu kullanması gibi durumlar, çocukların, çocuklu kadınların, yaşlılar ve özel durumu olanların ulaşımını kısıtlamakta konforu azaltmaktadır.

-Algı: çalışma alanlarının tümünde sunulan kullanımlar ve hizmetler yeterince tanımlanmamış ve yönlendirme yapılmamıştır. Kente yeni gelenler, ziyaretçiler ve yaşlılar veya yoğun koşuturma içinde kafası karışan kadınların aradıkları her türlü şeye kolay ve hızlı ulaşabilmesi için tanıtım, yönlendirme, sokak, meydan, cadde isimlendirmeleri uygun standartlarda ve yeterli değildir. Tanımsız mekanlar vardır.

-Estetik: Kent estetiği, kadın kullanıcılar açısından çok önemli olup çalışma alanları bu yönden ele alınarak estetik tasarım çözümleri yaratılmalıdır. Kentsel alanlar estetik ve bakımlı görünüme sahip olduklarında güvenli ve konforlu oldukları algısı oluşmaktadır. Kadınlar için bu psikolojik etki açısından daha etkileyicidir. Çalışma alanlarında belirlenen tanımsız, estetik olmayan mekânlar, karışıklıklar, düzensiz tanıtım levaları, algılanması zor alanlar kadınların algısını zorlaştırmaktadır. Belirsizlik hissi yaratan alanlar kadınlar için yorucu, zaman kaybettirici ve endişe uyandırıcıdır.

- Donatı elamanı eksikliği: Çalışma alanlarında kadın kullanıcılar için yeterli dinlenme alanı, çöp kutusu gibi kent donatı elemanları bulunmamaktadır. Yaz aylarında sahil boyunca yeterli gölge mekanlar da yoktur. Özellikle engelliler ve dezavantajlı bireylerin kent açık mekânlarını kullanımı kolaylaştırılmamıştır. Oysa onların toplumla daha fazla bütünleştirilmeye ihtiyacı vardır ve onlarla ilgilenmek zorunda olan kadınlar da böylece açık alanlardan yeterince yararlanamamaktadırlar.

- Kullanımlar: Kadınların gün boyu ve iş çıkışlarında farklı mekânlardan ihtiyaçlarını karşılamaları gerektiği, hızlı hareket etme zorunlulukları, çocukları veya yaşlı ebeveynlerine bakmak durumunda olmaları dikkate alınarak çalışma alanında mevcut alan kullanımları yeniden ele alınmalı, estetik tasarımlar yapılmalı ve donatılar yenilenmelidir. Kentte görünürlüğün ve gözetimin de artırılması, kör noktaların bulunmaması önemlidir. Bu açılardan kent çekirdeğinin tarihi bölümünün dar sokak araları ve kaldırımları en dikkat çekici alanlardır.

Hayati önem taşıyan hastane, emniyet müdürlüğü, eczane gibi yerlerin kenti kullanan yabancılar için mutlaka tanıtılması, yönlendirmelerin olması gerekir. Bu yönden de çalışma alanları zayıftır. Kadınların en çok alışveriş yaptığı yer alan pazar alanının karşısındaki küçük sanayi işletmeleri kentin biraz daha dışına taşınmalıdır.

Kent parkları kentlilerin doğal bir alanda dinlenirken estetik görüntülerle ruhlarını dinlendirip kaliteli zaman geçirebilecekleri, farklı bitkileri tanıyabilecekleri ortamlar olmalıdır. Kadınlar açısından çocukları ile bunları paylaşmaları, günün yorgunluğunu atmaları ve sosyalleştikleri çok önemlidir. Yeşil alanlar hem kadınlar hem de çocukları için doğayı tanıma açısından açık hava laboratuvarıdır. Bu bağlamda kent yeşil alanları yetersizdir. Kadınların kültürel etkinliklere katılabileceği, farklı üretimler yaparak etkinlikler organize edebileceği açık yeşil alanlar düzenlenmelidir. Sahilde küçük birkaç tezgah bulunan Morabim Parkı artık yetersiz kalmaktadır. Ayrıca çocuklar için oyun alanları da çok yetersizdir. Halk Bahçesi içindeki zemin sorunlu olup günümüzde üretilen hijyenik ve riski düşük farklı yumuşak zeminler kullanılmalıdır.

Son yıllarda nüfusu hızla artan Çanakkale kozmopolit bir yapı kazanmıştır. Bu durum kamusal hizmetlerin artırılması ve çeşitlendirilmesi ihtiyacını kaçınılmaz kılmaktadır ve toplu taşıma sisteminde önemli sorunlar vardır. Çanakkale’de büyük alışveriş merkezi (Esas 17 Burda ), Üniversite Hastanesi ve Devlet Hastanesi aynı güzergâhta yer almakta olup, her yaş kentli tarafından çok sık kullanılmaktadır. Bu durumda kadınların durakta bekleme süreleri çok uzamaktadır. Özellikle akşam saatlerinde evlerine dönen kadınların sorun yaşamamaları için otobüs sayıları artırılmalı ve farklı hatlara ulaşım sağlanmalıdır.

Bu çalışmada Çanakkale’de kadınların en yoğun kullandıkları bölgeler seçilerek alan çalışması yapılmıştır. Elde edilen bilgiler kentsel alanda kadın kullanımı açısından nelere dikkat edilmesi hakkında yönlendirici

olacaktır. Çalışmada elde edilen veriler gelecekte yapılacak her türlü bilimsel çalışmaya örnek oluşturabilecek, kent tasarım ve planlamasında kamu kurumlarına ve yerel yönetime katkı sağlayabilecektir.

### Yazar Katkıları

Füsun ERDURAN NEMUTLU: Çalışma örnek alanı, kapsam ve yöntemini belirleyerek verileri sentezlemiş, değerlendirmeleri yapmış ve makaleyi yazmıştır.

Sena AKSOY: İş planı, organizasyon, literatür taraması, psikolojik, analiz ve tüm analizleri tabloda birleştirmiştir.

Nurana NURULLAYEVA: Literatür taraması, alan araştırması ve psikolojik ve sosyo kültürel analiz yapmıştır.

Zeynep Pelin MORGÜL: Literatür taraması, alan araştırması ve sosyo kültürel analiz yapmıştır.

### Çıkar Çatışması

Yazarlar çıkar çatışması bildirmemişlerdir

### Kaynaklar

- Acuner, D. (2016). Canavarlaş(tırıl)an kent sokakları: Kadının kent deneyimi üzerine bir değerlendirme. *Fe Dergi*, 8 (1), 1-14. Erişim adresi: <https://dergipark.org.tr/tr/pub/federgi/issue/51983/677655>
- Akçayır, G. (2021). T.C. *Belediyelerin toplumsal cinsiyet eşitliğini sağlamadaki rolü: kadın dostu kentler projesi kapsamında yer alan büyükşehir belediyeleri üzerine bir araştırma* (Yayımlanmamış Yüksek Lisans Tezi). T.C. Sakarya Üniversitesi, Sosyal Bilimler Enstitüsü Siyaset Bilimi ve Kamu Yönetimi Ana Bilim Dalı, Sakarya, Türkiye.
- Aktaş, G. (2017). Kadın açısından kente ilişkin mekan pratikleri. *Pamukkale Üniversitesi Sosyal Bilimler Enstitüsü Dergisi*, 27, 136-149. Erişim adresi: <https://dergipark.org.tr/tr/pub/pausbed/issue/34758/384469>
- Alptekin, E. (2022). *Evrensel tasarım kriterlerinin Aydın kentinde bir park örneğinde irdelenmesi* (Yayımlanmamış Yüksek Lisans Tezi). Aydın Adnan Menderes Üniversitesi, Fen Bilimleri Enstitüsü, Aydın, Türkiye. Erişim adresi: <http://adudspace.adu.edu.tr:8080/xmlui/handle/11607/4738>
- Anonim (2022). *İstatistiklerle kadın, 2021*. Türkiye İstatistik Kurumu Haber Bülteni. Sayı: 45635. Erişim adresi: <https://data.tuik.gov.tr/Bulten/Index?p=Istatistiklerle-Kadin-2021-45635>
- Baltutar, B. & Artar, M. (2022). Yaşanabilir bir kent mümkün mü? Bartın örneğinde araştırma, *Karadeniz 8. Uluslararası Sosyal Bilimler Kongresi* (pp.116-128). Bartın, Türkiye. Erişim adresi: [https://www.karadenizkongresi.org/\\_files/ugd/797a84\\_498b191c5c8c498d9690d012d8c60ac3.pdf](https://www.karadenizkongresi.org/_files/ugd/797a84_498b191c5c8c498d9690d012d8c60ac3.pdf)
- Baykan, D. D. (2015). *Yerel yönetimler için kadın dostu kent planlaması ve tasarım ilkeleri kitabı*. Uzerler Matbaacılık Sanayi Ltd. Şti., Ankara.
- Cavington, G. A. & Hannah, B. (1996). *Access by design*. Van Nostrand Reinhold, New York. ISBN: 978-0471287261, 240 p.
- Certeau, M., Giard, L. & Mayol, P. (2010). *İki arada. Gündelik hayatın keşfi-II. Konut, mutfak işleri* (Çeviren: Erkan Ataçay, Çağrı Eroğlu). Dost Kitabevi Yayınları, ISBN: 9789-752984059. Ankara.
- Çelik Çanga, A. & Çalışkan Mimarlar, H. (2022). Landscape reviews with user participation: Zeytinburnu medical and aromatic plants garden. Yazıcı K. (Yay. Haz.). *The Landscape and The City* içinde (s.79-84). Iksad Publications, ISBN: 978-625-6955-15-8.
- Çelik Çanga, A. (2021). Şifalı bahçeler için peyzaj planlama ilkeleri. Güngör S. (Yay. Haz.) *Mimarlık Planlama ve Tasarım Alanında Araştırma ve Değerlendirmeler- I* içinde (s. 81-100). Gece Kitaplığı, ISBN: 978-625-8075-40-3.
- Çelik Çanga, A. & Küçük, G.(2022). The place of historical spaces in urban open space systems: The example of Iznik. *International Journal of Landscape Architecture Research*, 6 (1), 56-71. Erişim adresi:<https://ijlar.org/index.php/ijlar/article/view/507>
- Çelik, A. (2012). The landscape of Kocaeli pedestrian walkway as an example of urban outdoor and user views. *Journal of Food, Agriculture & Environment*, 10 (2), 1262-1268. Erişim adresi: [https://www.researchgate.net/publication/294524203\\_The\\_landscape\\_of\\_Kocaeli\\_pedestrian\\_walkway\\_as\\_an\\_example\\_of\\_urban\\_outdoor\\_and\\_user\\_views](https://www.researchgate.net/publication/294524203_The_landscape_of_Kocaeli_pedestrian_walkway_as_an_example_of_urban_outdoor_and_user_views)

- Çetintahra Ekşioğlu, G. & Efe Güney, M. (2019). *Türkiye’de temsiliyet açısından kadın dostu kentler ve İzmir karşılaştırması, resent evaluations on humanities and social sciences*. Edit: Berrin Ceylan Ataman, Gülçin Taşkıran, 978-1-912503-72-8, IJOPEC. Publication Limited, London, 45-57.
- Efe Güney, M. & Üstündağ, B. (2020). Kadın dostu kent yaklaşımı kapsamında kentsel açık yeşil alanların değerlendirilmesi: Bornova örneği. *Süleyman Demirel Üniversitesi, Fen-Edebiyat Fakültesi, Sosyal Bilimler Dergisi*, 1 (36), 38-65. Erişim adresi: <https://dergipark.org.tr/tr/pub/sbe/issue/54000/686968>
- Erduran, F. & Kabaş, S. (2010). Parklarda ekolojik koşullarla dengeli, işlevsel ve estetik bitkilendirme ilkelerinin Çanakkale Halk Bahçesi örneğinde irdelenmesi. *Ekoloji*, 19 (74), Çevkor, 190-199. Erişim adresi: <https://search.trdizin.gov.tr/tr/yayin/detay/101966/>
- Goggle Earth (2023). *Çanakkale*. (Erişim: 10.03.2023). <https://earth.google.com/web/search/%C3%87anakkale/@40.12739055,26.42829299,42.58767787a,20805.08688811d,35y,0h,0t,0r/data>
- Hacıhasanoğlu, İ. (2003). Evrensel tasarım. *Tasarım + Kuram*, 2 (3), 93-101. Erişim adresi: <https://dergipark.org.tr/tr/download/article-file/209270>
- Kaypak, Ş. (2019). Kırsaldan kente göç ve toplumsal değişimde kadının yeri. *Çukurova Kadın Çalışmaları Kongresi (28-30 Kasım 2018), Disiplinlerarası Kadın Çalışmaları II*. Çukurova Üniversitesi, Adana.
- Kiper, T., Korkut, A. & Üstün Topal, T. (2016). Mekânsal planlamada kadın dostu kent yaklaşımı. *İdil*, 5 (26), 1777-1796. Erişim adresi: <https://www.idildergisi.com/makale/pdf/1476448733.pdf>
- Mert, M. K. (2021). Avrupa ve Türkiye’den örnekleriyle kadın dostu kentler. *EURO Politika*, 11, 122-129. Erişim adresi: <https://dergipark.org.tr/tr/pub/europ/issue/68222/1063378>
- Özsoy, B. & Sipahi, E. B. (2016). Türkiye’de kadın dostu olma iddiasında bir kent: Gaziantep. *Çağdaş Yerel Yönetimler*, 25 (3), 35-68. Erişim adresi: [https://www.researchgate.net/publication/321302916\\_](https://www.researchgate.net/publication/321302916_)
- Şenol, N. (2015). *Kadın dostu kentler Avrupa’dan örnekler*. VAKSA; Hacı Ömer Sabancı Vakfı. Birleşmiş Milletler Ortak Programı. Erişim adresi: <http://womenfriendlycities.com/content/docs/outputs/avrupadan-ornekler.pdf>
- Türkiye İstatistik Kurumu (TÜİK) (2021). *Toplumsal cinsiyet istatistikleri*. Erişim adresi: [https://www.tuik.gov.tr/media/announcements/toplumsal\\_cinsiyet\\_istatistikleri\\_2021.pdf](https://www.tuik.gov.tr/media/announcements/toplumsal_cinsiyet_istatistikleri_2021.pdf)
- Vanlıoğlu Yazıcı, N. (2020). Kadınların sesinden kamusal alanda toplumsal cinsiyet söylemi: Türkiye’de 8 Mart kutlamaları. *İdeal Kent*, 31 (11), 1657-1675. DOI:10.31198/idealkent.746277.
- Vural, H. (2020). Bingöl’ün yaşanabilir kent olma yolunda fiziki problemleri ve öncelikleri üzerine bir değerlendirme. *OPUS International Journal of Society Researches*, 15 (1), 5006-5031. Erişim adresi: <https://dergipark.org.tr/tr/pub/opus/issue/54352/672743>
- Yılmaz, N. & Diktaş, E. O. (2018). Eşitlikçi tasarımın kent merkezlerindeki kamusal alanlara yansımadaki temel esaslar. *Toplum ve Sosyal Hizmet*, 29 (1), 132-152. Erişim adresi: <https://dergipark.org.tr/tr/pub/tsh/issue/38635/448692>



## Atık Karbon Keçenin Pirol ile Polimerizasyonu ve Katot Olarak Kullanılabilirliği

Mesut Sezer<sup>1\*</sup>, Melike İşgören<sup>2</sup>, Sevil Veli<sup>3</sup>, Anatoli Dimoglo<sup>4</sup>

<sup>1,3</sup>Çevre Mühendisliği Bölümü, Mühendislik Fakültesi, Kocaeli Üniversitesi, Kocaeli, Türkiye

<sup>2</sup>Çevre Koruma ve Kontrol Bölümü, İzmit Meslek Yüksekokulu, Kocaeli Üniversitesi, Kocaeli, Türkiye

<sup>4</sup>Çevre Mühendisliği Bölümü, Mühendislik Fakültesi, Düzce Üniversitesi, Düzce, Türkiye

### Makale Tarihiçesi

Gönderim: 05.06.2023

Kabul: 26.08.2023

Yayım: 20.12.2023

### Araştırma Makalesi

**Öz** – Elektrokimyasal prosesler, atıksudaki karışık kirletici yükünü tek basamakta artabilmeleri ve kısa sürede yüksek giderim verimi sağlamaları nedeniyle yaygın olarak kullanılmaktadır. Son yıllarda bu arıtım yöntemleri ile ilgili en hızlı teknolojik gelişmeler yenilikçi elektrot üretimi alanında olup, birçok araştırmacı anot ve katot aktivitesini arttırmayı amaçlayan çalışmalar yapmaktadır. Bu çalışmaların bir diğer hedefi ise elektrot üretiminde en çok kullanılan ve yer kabuğundaki oranları her geçen gün azalan metallere alternatif olabilecek; elde edilmesi kolay, ucuz ve sürdürülebilir hammaddelerden elektrot eldesidir. Çalışmamızda kimyasal oksidatif polimerizasyon yöntemi kullanılarak atık karbon keçe (KK) üzerinde pirol monomerinin FeCl<sub>3</sub>.6H<sub>2</sub>O oksidantı ile polimerizasyonu yapılmıştır. Polimerizasyon sonucunda polipirol kaplı karbon keçe (KK/PPy) elde edilmiştir. KK/PPy ve KK'nın elektrot olarak etkinliği elektrooksidasyon prosesinde boya giderimi üzerinden araştırılmıştır. Ayrıca pirol konsantrasyonu (0.05-1 M), oksidant konsantrasyonu (0.05-0.5 M) ve sıcaklığın (5-60°C) katodun kütle artışı ve direnç azalışı üzerine etkisi incelenmiştir. En yüksek direnç azalışını sağlayan polimerizasyon koşulları 0.2 M pirol konsantrasyonu, 0.3 M FeCl<sub>3</sub>.6H<sub>2</sub>O konsantrasyonu ve sıcaklık 50°C olarak bulunmuştur. Optimum koşullarda üretilen KK/PPy ve işlem görmemiş KK elektrokimyasal prosesinde katot olarak kullanılarak aktiviteleri birbiri ile karşılaştırılmış ve boya gideriminde KK/PPy'nin daha etkili olduğu görülmüştür. Ayrıca tekstil atığı olarak ortaya çıkan atık karbon keçeden elektrot malzemesi üretilmesi sürdürülebilir bir yöntem olarak çevrenin ve doğal kaynakların korunması ilkesine hizmet eden yenilikçi bir yaklaşımdır.

**Anahtar Kelimeler** – Elektrooksidasyon, iletken polimerler, karbon keçe, kimyasal oksidatif polimerizasyon, polipirol

## Waste Carbon Felt Polymerization with Pyrrole and Usability as Cathode

<sup>1,3</sup>Department of Environmental Engineering, Faculty of Engineering, Kocaeli University, Kocaeli, Türkiye

<sup>2</sup>Department of Environmental Protection, İzmit Vocational School, Kocaeli University, Kocaeli, Türkiye

<sup>3</sup>Department of Environmental Engineering, Faculty of Engineering, Duzce University, Duzce, Turkey

### Article History

Received: 05.06.2023

Accepted: 26.08.2023

Published: 20.12.2023

### Research Article

**Abstract** – Electrochemical processes are widely used because they can remove the mixed pollutant load in wastewater in a single step and provide high removal efficiency in a short time. In recent years, the technological developments related to these treatment methods have been in the field of innovative electrode production. Researchers are striving to increase anode and cathode activity. Another goal of these studies is to produce electrodes from easy-to-obtain, cheap and sustainable raw materials that can be an alternative to metals that are most used in electrode production and whose ratios are decreasing day by day in the earth's crust. In this study, polypyrrole (PPy) coated carbon felt was obtained by polymerizing pyrrole monomer with FeCl<sub>3</sub>.6H<sub>2</sub>O oxidant on carbon felt (KK) using the chemical oxidative polymerization method (KK/PPy). The obtained KK/PPy and KK were investigated through dye removal in the electrooxidation process. The effects of pyrrole concentration (0.05-1 M), oxidant concentration (0.05-0.5 M), and temperature (5-60°C) on the mass increase and resistance decrease of the cathode were investigated. The best polymerization conditions were found to be 0.2 M pyrrole concentration, 0.3 M FeCl<sub>3</sub>.6H<sub>2</sub>O concentration, and temperature 50°C. KK/PPy produced under optimum conditions and untreated KK were used as cathodes in the electrooxidation process and their activities were compared. It was seen that KK/PPy was more effective in dye removal. In addition, the production of electrode material from waste, which is generated from textile is an innovative approach that serves the principle of protecting the natural resources as a sustainable method.

**Keywords** – Electrooxidation, conductive polymers, polypyrrole, carbon felt, chemical oxidative polymerization.

<sup>1</sup> mesut.sezer@kocaeli.edu.tr

<sup>2</sup> melike.isgoren@kocaeli.edu.tr

<sup>3</sup> sevilv@kocaeli.edu.tr

<sup>4</sup> anatolidimoglo@duzce.edu.tr

\*Sorumlu Yazar

## 1. Giriş

İçinde bulunduğumuz çağın küresel boyuttaki en önemli sorunlarından biri artan atıksu miktarı ve bileşiminin niteliksel değişimidir. Dolayısı ile atıksuların arıtımı her geçen yıl daha büyük bir önem kazanmaktadır (Vijayakumar, Saravanathamizhan ve Balasubramanian, 2016; Das, Sharma ve Purkait, 2022; Wagner ve Bauer, 2023). Atıksu arıtımında işletme kolaylığı ve kısa sürede arıtım sağlanması nedeniyle ayırma ve konsantre etmeye dayalı yöntemler daha çok tercih edilmektedir. Ancak bu proseslerde kirleticiler adsorpsiyon, membran filtrasyon veya koagülasyon gibi tekniklerle sıvı fazdan katı faza aktarılmakta ve böylelikle konsantre edilmektedir (Isgoren, Gengec ve Veli, 2017; Görücü vd., 2022). Diğer taraftan ileri oksidasyona dayalı sistemler kimyasal dönüşüm ile tehlikeli veya toksik atıksuları toksik olmayan son ürünlere dönüştürmektedir (Veli vd., 2019; Antony vd., 2020). Atıksu arıtımı için kullanılan elektrokimyasal teknolojiler kalıcı kirleticilerin hızlı ve tam bozulmalarını sağlayarak modern toplumların sürdürülebilir çevre hedefine ulaşmalarına önemli katkıda bulunmaktadır. Son yıllarda bu alanda yapılan araştırmalar sayesinde üretilen yeni malzemeler ve reaktör tipleri elektrokimyasal arıtımın verimliliğini artırmıştır (Martínez-Huitle vd., 2023). Elektrokimyasal oksidasyon prosesinde anodik oksidasyon, suda bulunan organik kirleticilerin bozunması için yaygın olarak kullanılan bir teknolojidir (Martínez-Huitle vd., 2015). Elektrokimya teknolojisi ile malzeme bilimindeki ilerlemeler elektrooksidasyon prosesinde kullanılan elektrotların hızla gelişmesine yol açmıştır (Filip vd., 2020). Son yıllarda yapılan çalışmalar ise katot malzemesinin üretimi ve modifikasyonu üzerine yoğunlaşmıştır. Bu alanda özellikle karbon malzemeli, flor, azot ve fosfor katkılı, karbon destekli metal-metal oksit, metal oksit katotlar çok çalışılmıştır (Du vd., 2021). Günümüzde maliyetinin düşük olması ve üretim kolaylığı sebebi ile katot malzemesi olarak karbon keçe kullanımı yaygınlaşmıştır. Bu malzemenin elektriksel iletkenlik özelliğinin geliştirilmesi için iletken/yarı iletken polimerler ile kaplanmaktadır (Gülümser, 2021).

Elektriksel olarak iletken polimerler, metallerin elektronik özellikleriyle, polimerlerin kimyasal ve mekanik özelliklerini birleştiren bir organik sınıftır (Kuhn, Child ve Kimbrell, 1995). İletken polimerler şarj olabilen pil üretimi, diyot, iletken kaplamalar, antistatik materyallerin eldesi, gaz sensörleri, bakteri ve toz tutmayan kıyafetlerin üretimi gibi çeşitli endüstrilerde kullanılmaktadır (Adamhasan, 2008; Oh, Hong ve Kim, 1999).

İletken polimerler arasında en fazla uygulama alanına sahip olanlar polianilin (PAni) ve polipirol'dür. Bu polimerlerin tercih edilmesinin başlıca sebepleri; iyi bir iletkenliğe sahip olmaları, dış koşullardan etkilenmemeleri, kolay ve ucuz bir şekilde sentezlenebilmeleri şeklinde sıralanabilir (MacDiarmid ve Epstein, 1994).

İletken polimerlerle kaplama işlemi kimyasal polimerizasyon, plazma polimerizasyonu, elektrokimyasal polimerizasyon ve aşılama polimerizasyonu gibi yöntemler kullanılarak yapılabilmektedir (Kutani vd., 2007).

Polianilin ve polipirol gibi iletken polimerlerin kullanılması kumaşların mekanik özelliklerini kaybetmeden iletken özellikte üretilmesine imkân sağlamaktadır (Cihaner, 2004). Bu sayede tekstil endüstrisinde elektriksel olarak iletken kumaş ve keçe üretiminde polimerler kullanılmaya başlanmıştır (Kang vd., 2005).

Kim ve arkadaşlarının yaptıkları çalışmada kimyasal ve elektrokimyasal polimerizasyon yöntemi kullanarak poliester (PET) dokuma kumaş üzerine polipirol kaplamışlardır. Kimyasal polimerizasyon yönteminde polimerizasyon sıcaklığı, oksitleyici ve monomer konsantrasyonu, oksitleyici türü gibi parametrelerin kumaşın elektriksel iletkenlik özelliği üzerine etkisini incelemiştir (Kim vd., 2002).

Kaynak ve arkadaşlarının yaptıkları çalışmada polipirol ile sürekli buhar polimerizasyon yöntemi kullanılarak iletken bir yapıya sahip yün, pamuk ve naylon iplikler üretilmiştir. Kullanılan  $FeCl_3$  çözeltisinin konsantrasyonu ve ipliklerin büküm miktarı değiştirilerek ipliklerin iletken özellikleriyle polipirolün kaplama derecesi incelenmiştir. Araştırma sonucunda polipirolün iplik içine olan penetrasyonu ve kaplamanın kalınlığı gibi özelliklerin ipliğin fiziksel parametreleri üzerine etkili olduğu bulunmuştur (Kaynak, Najar ve Foitzik, 2008).

Avloni ve arkadaşları poliester nonwoven ve poliester dimi kumaşlarını PPy ile kaplamışlardır. Kaplama işlemi sonucunda poliester dimi kumaşlarının yüzey direncini 40 ohm, poliester nonwoven kumaşının yüzey direncini ise 18 ohm olarak bulmuşlardır (Avloni vd., 2007).

Kincal ve arkadaşları antrakinin sulfonik asidi dopant olarak kullanarak in-situ polimerizasyon prosesi ile PET kumaşları PPy ile kaplamışlardır. Bunun sonucunda kumaşların yüzey direnç değerinin 20 ohm/kare olduğunu belirlemişlerdir (Kincal vd., 1998).

Hakansson ve arkadaşları kimyasal oksidatif polimerizasyon yöntemini kullanarak poliester-likra kumaşlarını PPy ile kaplamışlardır. Polimerizasyon süresinin ve dopant konsantrasyonunun yüzey direncine etkisini araştırmışlardır. Kaplama işlemi sonrasında kumaşların yüzey direnç değerlerinin 180-1300 ohm/kare aralığında olduğunu ifade etmişlerdir (Håkansson, Amiet ve Kaynak, 2006).

Bu çalışmada kimyasal oksidatif polimerizasyon yöntemi ile KK üzerine PPy kaplanacak ve bu malzemenin elektrooksidasyon prosesinde KK/PPy katot olarak kullanılabilirliği araştırılacaktır. Katodun kütleli artış ve direnç azalışı üzerine pirol konsantrasyonu, oksidant derişimi ve sıcaklık parametrelerinin etkisi incelenecek, en yüksek direnç azalışını sağlayan optimum kaplama koşulları belirlenecektir. Optimum koşullarda üretilen KK/PPy ve işlem görmemiş KK'nin elektrooksidasyon prosesinde katot olarak kullanılabilirliği boya giderimi üzerinden değerlendirilecektir.

## 2. Materyal ve Yöntem

Deneyisel çalışmalarda yerel bir tekstil fabrikasından temin edilen atık karbon keçeler 3x3 cm boyutlarında kesilerek kullanılmıştır.

Kimyasal oksidatif polimerizasyon yöntemi kullanılarak pirol monomerinin (C<sub>4</sub>H<sub>5</sub>N) demir (III) klorür heksahidrat (FeCl<sub>3</sub>.6H<sub>2</sub>O) oksidantı ile polimerizasyonu gerçekleştirilmiştir.

Karbon keçe üzerine pirol monomerinin in-situ polimerizasyonu için öncelikle belirli konsantrasyonda hazırlanan pirol monomeri distile su içerisinde çözülmüştür. Ardından bu çözelti içerisine 3x3 cm boyutundaki KK daldırılmış ve 30 dakika boyunca belirli bir sıcaklıkta çalkalayıcı içerisinde 120 rpm'de karıştırılmıştır. Başka bir beherde istenen konsantrasyonda hazırlanan FeCl<sub>3</sub>.6H<sub>2</sub>O distile su içerisinde çözülmüştür. Hazırlanan bu çözelti damla damla olacak şekilde karbon keçelerin içinde bulunduğu karışıma eklenmiştir. Belirli bir sıcaklıkta bu çözelti 150 dakika boyunca çalkalayıcı ile 120 rpm'de karıştırılmıştır. Karıştırma işlemi sonrasında karbon keçe örnekleri çözelti içerisinden çıkarılmıştır. Ardından distile su kullanılarak yıkanmış ve oda sıcaklığında kurutulmuştur (Lin vd., 2005).

Karbon keçelerin dirençleri iki nokta prob yöntemi kullanılarak ölçülmüştür. Prob yöntemi ile direnç ölçümü; multimetre (Wellhise-DT-830D) cihazının iki probunun karbon keçe üzerine yerleştirilerek direnç ölçümü yapılması esasına dayanmaktadır. Bu amaçla karbon keçe üzerinde 10 farklı noktadan direnç ölçülerek bunların aritmetik ortalaması alınmış ve ortalama direnç azalış değeri denklem 2.1 kullanılarak hesaplanmıştır.

$$\text{Direnç Azalışı (\%)} = \frac{R_1 - R_2}{R_1} \times 100 \quad (2.1)$$

Burada R<sub>1</sub> KK'nin direnci, R<sub>2</sub> ise polimerizasyondan sonraki KK/PPy'nin direncidir.

Karbon keçelerin kütleli artış değeri, kimyasal polimerizasyon yöntemi ile oluşan polipiroiden dolayı karbon keçenin kütleli artmasını ifade etmektedir ve kaplama işleminden önce ve sonra karbon keçelerin kuru ağırlıkları tespit edilerek denklem 2.2'de verilen formüle göre hesaplanmıştır.

$$\text{Kütle Artışı (\%)} = \frac{W_2 - W_1}{W_1} \times 100 \quad (2.2)$$

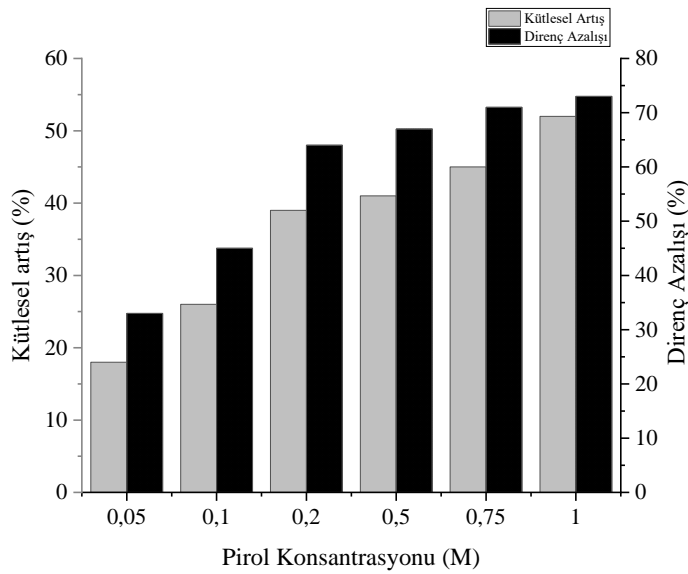
Burada  $W_1$  karbon keçe (KK)'nin kuru kütlesi,  $W_2$  ise KK/PPy'nin kuru kütlesidir.

### 3. Bulgular ve Tartışma

Bu çalışmada pirol konsantrasyonunun, oksidant derişiminin ve sıcaklığın, KK/PPy'ye ait kütle artışı ve direnç azalışı değerleri üzerine etkisi incelenmiştir.

#### 3.1. Pirol Konsantrasyonunun Etkisi

Pirol konsantrasyonunun kütle artışı ve direnç azalışı üzerine etkisinin araştırılması amacıyla 0.2 M  $FeCl_3.6H_2O$  ve 25°C sıcaklıkta, farklı pirol konsantrasyonları ile (0.05-1 M) KK/PPy üretimi gerçekleştirilmiştir. Elde edilen sonuçlar KK/PPy kütle artışı ve direnç azalışı üzerinden Şekil 1'de verilmiştir.



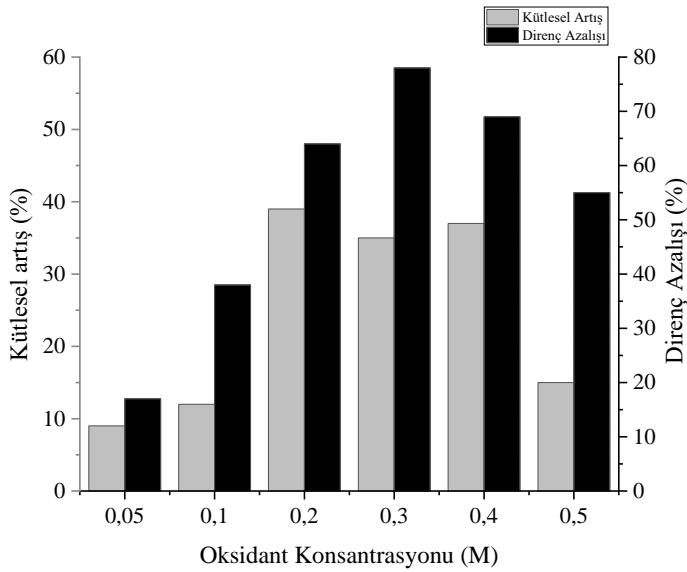
Şekil 1. Pirol konsantrasyonunun KK/PPy kütle artışı ve direnç azalışı üzerine etkisi

Şekil 1'deki sonuçlara göre en yüksek kütle artışı (%52) ve direnç azalışı (%73) pirol konsantrasyonunun 1 M olduğu durumda gözlenmiştir. Pirol konsantrasyonunun yükselmesine bağlı olarak KK/PPy kütle artışı ve direnç azalışında artma görülmüştür. Direnç azalışında meydana gelen artış, polimerizasyon esnasında kumaşın yapısında iletkenliği sağlayan kanalların meydana gelmesi ve bu kanalların sayısının artmasından kaynaklanmaktadır (Wang vd.,2012; Omastova, Pionteck ve Košina 1996; Rehan Abbasi vd., 2012).

Fakat 0,2 M pirol konsantrasyonundan daha yüksek değerlerde direnç azalışı bakımından anlamlı bir artış meydana gelmemiştir. Bu nedenle optimum pirol konsantrasyonu 0.2 M olarak seçilmiştir.

#### 3.2. Oksidant Konsantrasyonunun Etkisi

Kütle artışı ve direnç azalışı üzerine oksidant konsantrasyonunun etkisinin incelenmesi için optimum olarak belirlenen 0.2 M pirol ve 25°C sıcaklıkta, farklı oksidant ( $FeCl_3.6H_2O$ ) konsantrasyonları ile (0.05-0.5 M) KK/PPy üretimi yapılmıştır. Sonuçlar Şekil 2'de verilmiştir.



Şekil 2. Oksidant konsantrasyonunun KK/PPy kütle artışı ve direnç azalışı üzerine etkisi

Şekil 2'den görüldüğü üzere en yüksek %39'luk kütle artışı 0.2 M'lık  $\text{FeCl}_3 \cdot 6\text{H}_2\text{O}$  konsantrasyonunda ulaşılırken, %78'lik en yüksek direnç azalışına ise 0.3 M  $\text{FeCl}_3 \cdot 6\text{H}_2\text{O}$  konsantrasyonunda ulaşılmıştır. Elektrooksidasyon prosesinde iletkenlik artışı önemli bir parametre olduğundan optimum oksidant konsantrasyonu 0.3 M  $\text{FeCl}_3 \cdot 6\text{H}_2\text{O}$  olarak belirlenmiştir.

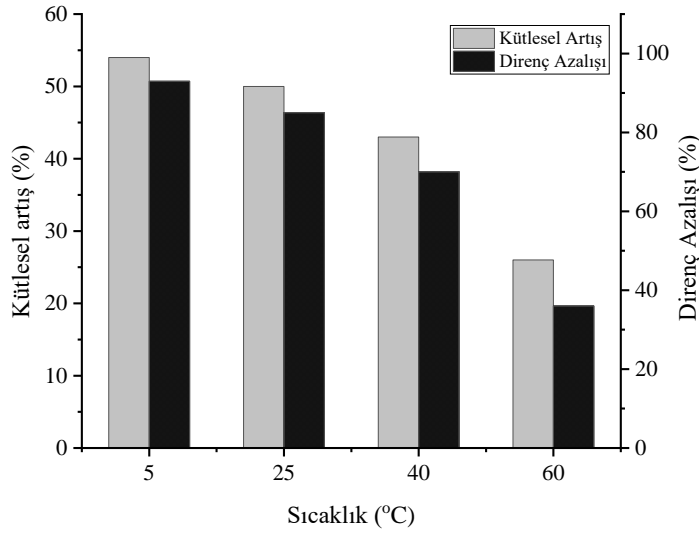
0.05-0.3 M oksidant konsantrasyonlarında direnç azalışında artış gözlemlenmiştir. Artan oksidant derişimine bağlı olarak kütle artışı ve iletkenlikte meydana gelen artışın sebebi polimer gövdesi üzerindeki dopant iyonunun artışından kaynaklanmaktadır. (Saravanan, Shekhar ve Palaniappan, 2006). Ayrıca düşük oksidant derişimlerinde çözeltideki oksidant miktarı az olduğu için polimerizasyon başlangıçta hızlı olmaktadır. Polimerizasyonun hızlı gerçekleşmesi kısa zincirlerin oluşmasını sağlamaktadır. Buna bağlı olarak konjugasyon da kısa olmakta ve iletkenlik düşük kalmaktadır (Lei, Cai ve Martin, 1992).

0.3-0.5 M aralığında oksidant konsantrasyonunda artış devam ederken direnç azalışında azalma meydana gelmektedir. Bunun nedeni, PPy'nin kimyasal polimerizasyonunda yükseltgen olarak kullanılan demir tuzlarının konsantrasyonundaki aşırı artışın, polipirolün iletkenliğinin düşmesine sebep olmasıdır. Bu durumun ikincil veya yan ürünün kopolimerizasyonundan kaynaklandığı düşünülmektedir (Sayar, 2008).

Literatürde bu çalışmaya benzer sonuçların elde edildiği bir yayında PPy/Polipropilen (PPy/PP) kompozitinin hazırlanmasında  $\text{FeCl}_3$  yükseltgen olarak seçilmiştir.  $\text{FeCl}_3$  konsantrasyonunun artışıyla iletkenlik de yükselmiştir. 0.05 M'dan daha yüksek  $\text{FeCl}_3$  konsantrasyonlarında iletkenlik  $10^{-1}$  S/cm'nin üstüne çıkarken 0.5 M'dan daha yüksek konsantrasyonlarda ise kompozitin iletkenliği en fazla 2 S/cm'ye kadar çıkmıştır. Daha yüksek konsantrasyonlarda ise iletkenlikte anlamlı bir artış gözlenmemiştir. (Yang vd., 1996). Aramid/PPy kompozitinin iletkenliğine  $\text{FeCl}_3$  konsantrasyonunun etkilerinin incelendiği bir çalışmada  $0^\circ\text{C}$  ve  $20^\circ\text{C}$ 'de yapılan deneylerde  $\text{FeCl}_3$  konsantrasyonunun artışıyla birlikte her iki sıcaklıkta da iletkenlikte artış meydana gelmiştir.  $\text{FeCl}_3$  derişimi %15'e ulaştıktan sonra iletkenlikte anlamlı bir artış olmamıştır (Cho ve Jung, 1997).

### 3.3. Sıcaklığın Etkisi

Sıcaklığın kütle artışı ve direnç azalışı üzerine etkisini inceleyebilmek amacıyla optimum olarak belirlenen 0.2 M pirol ve 0.3 M  $\text{FeCl}_3 \cdot 6\text{H}_2\text{O}$  konsantrasyonunda 5, 25, 40 ve  $60^\circ\text{C}$ 'lik ortamda polimerizasyon yapılmıştır (Şekil 3).



Şekil 3. Sıcaklığın KK/PPy kütleli artış ve direnç azalışı üzerine etkisi

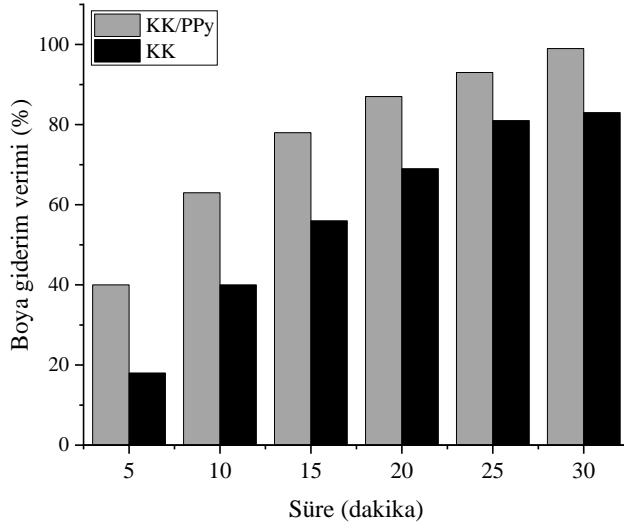
Şekil 3 incelendiğinde en yüksek kütleli artış (%54) ve direnç azalışı (%93) 5°C’de ve en düşük kütleli artış (%26) ve direnç azalışı (%36) 60°C’de meydana gelmiştir. Sıcaklığın azalmasıyla kütleli artış ve direnç azalışı yüzdelerinde artış gözlemlenmiştir. Bu sebeple optimum polimerizasyon sıcaklığı 5°C olarak belirlenmiştir.

Polipirolün düşük sıcaklık değerlerinde iletkenliğin daha yüksek olduğu yapılan çalışmalarda da ortaya konmuştur. Örneğin 0-5°C gibi düşük sıcaklıklarda demir tuzları sulu çözeltide en yüksek iletkenliği elde edebilmek amacıyla kullanılmıştır (Myers, 1986).

Sıcaklık artışına bağlı olarak PPy veriminde meydana gelen azalmanın sebebi PPy polimerizasyonunun ekzotermik oluşu ile açıklanabilir. (Lu, Pich ve Adler, 2004). Sıcaklık artışıyla birlikte düşük molekül ağırlıklı çözünebilir ürünlerin meydana gelmesi mümkün olmaktadır. Düşük molekül ağırlıklı polimerlerde çeşitli sebeplerden dolayı iletim yolunda kesilmeler olmakta ve bu nedenle iletkenlikte azalmalar meydana gelmektedir (Duran vd., 2009). Ayrıca sıcaklığın artışıyla birlikte iletkenliğin azalmasının bir sebebi polimer gövdesindeki dopant anyonlarının kaybı olarak gösterilebilir (Saravanan, Shekhar ve Palaniappan, 2006).

### 3.4. KK ve KK/PPy’nin EO Prosesindeki Verimliliğinin İncelenmesi

KK ve optimum koşullarda üretilen KK/PPy katotlarının elektrooksidasyon prosesi ile boya (Isolan Bordeaux 2S-B) giderim verimi üzerinden etkinlikleri incelenmiştir. Bu amaçla elektrooksidasyon prosesinin koşulları; çalışma hacmi 250 ml, paslanmaz çelik anot, başlangıç boya konsantrasyonu 25 mg/L, elektrolit konsantrasyonu 0.5 g/L NaCl, akım yoğunluğu 2 mA/cm<sup>2</sup> ve reaksiyon süresi 30 dakika olarak seçilmiştir. Zamana bağlı çizilen boya giderim verimlerine ait grafik Şekil 4’te verilmiştir.



Şekil 4. KK ve KK/PPy'ye ait boya giderim verimleri

Şekil 4'e göre işlem görmemiş karbon keçe katot olarak kullanıldığında, 30 dakikalık elektrooksidasyon sonucunda %83'lük boya giderimi sağlamıştır. Karbon keçe üzerine polipirol kaplanması ile elde edilen malzemenin kullanılması halinde ise verim %99'a yükselmiştir. Kaplama işlemi ile meydana gelen iletkenlik artışı aynı zamanda katodun elektro-katalitik aktivitesini artırarak boya giderim veriminin yükselmesine sebep olmuştur.

#### 4. Sonuçlar

Elektrooksidasyon prosesinde giderim verimini etkileyen en önemli unsurlardan biri elektrodun tipidir. Son yıllarda yapılan çalışmalar anodun geliştirilmesinin yanı sıra katot etkinliğinin artırılması üzerine yoğunlaşmıştır. Bu çalışmada karbon keçe polipirol ile kaplanarak iletkenliği artırılmış ve elektrooksidasyon prosesi ile boya gideriminde katot olarak kullanılmıştır. Yapılan deneyler artan pirol konsantrasyonunun ile kütsel artışın ve direnç azalışının arttığını göstermiştir. PPy'nin karbon keçeye kaplanmasında oksidant olarak kullanılan  $FeCl_3 \cdot 6H_2O$ 'in optimum konsantrasyonu 0.3 M olarak bulunmuştur. Ayrıca reaksiyon sıcaklığı azaldıkça KK/PPy'in direnci azalmıştır. İşlem görmemiş karbon keçe ve KK/PPy'nin elektrooksidasyon sonrası boya giderim verimleri sırasıyla %83 ve %99 olarak bulunmuştur. Bu çalışma sonucunda iletken polimerlerin atık karbon keçeye kaplanarak katot olarak kullanılmasının sürdürülebilir bir yaklaşım olduğu, kaplama prosesinin kolaylığı ve elektrot işlevselliği açısından gelecek çalışmalara ışık tutabileceği görülmüştür. Ayrıca ileriki çalışmalarda farklı iletken polimerler ile kaplama yapılarak çeşitli atıksularda da katot olarak kullanılabilirliği incelenebilir.

#### Yazar Katkıları

Mesut Sezer: Veri toplamış ve analizini yapmıştır, makaleyi yazmıştır.

Melike İşgören: Veri toplamış ve analizini yapmıştır, makaleyi yazmıştır.

Sevil Veli: Analizi planlamış ve tasarlamıştır.

Anatoli Dimoglo: Analizi planlamış ve tasarlamıştır.

#### Çıkar Çatışması

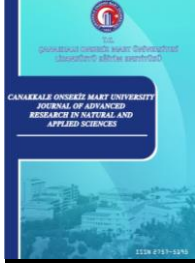
Yazarlar çıkar çatışması bildirmemişlerdir.

**Kaynaklar**

- Adamhasan, A.S. (2008). *Poliester polianilin, pamuk polianilin kompozit kumaşlarının hazırlanması ve elektriksel özelliklerinin incelenmesi* (Yüksek lisans tezi). Erişim adresi: <https://tez.yok.gov.tr/UlusalTezMerkezi>
- Antony, J., Niveditha, S. V., Gandhimathi, R., Ramesh, S.T. ve Nidheesh, P. V. (2020). Stabilized landfill leachate treatment by zero valent aluminium-acid system combined with hydrogen peroxide and persulfate based advanced oxidation process, *Waste Management*, (106), 1–11. <https://doi.org/10.1016/j.wasman.2020.03.005>
- Avloni, J., Ouyang, M., Florio, L., Henn, A.R. ve Sparavigna, A. (2007). Shielding effectiveness evaluation of metallized ve polypyrrole-coated fabrics. *Journal of Thermoplastic Composite Materials*, 20(3), 241–254. <https://doi.org/10.1177/0892705707076718>
- Cho, J.W. ve Jung, H. (1997). Electrically conducting high-strength aramid composite fibres prepared by vapour-phase polymerization of pyrrole. *Journal of Materials Science*, 32(20), 5371–5376. <https://doi.org/10.1023/A:1018627113857>
- Cihaner, A. (2004). *Electrochemical synthesis of crowned conducting polymers: Nature of radical cations in polymerization and mechanism of conductivity* (Doktora tezi). Erişim adresi: <https://tez.yok.gov.tr/UlusalTezMerkezi>
- Das, P.P., Sharma, M. ve Purkait, M.K. (2022). Recent progress on electrocoagulation process for wastewater treatment: A review. *Separation and Purification Technology*, (292), 121058. <https://doi.org/10.1016/j.seppur.2022.121058>
- Du, X., Oturan, M.A., Zhou, M., Belkessa, N., Su, P., Cai, J., Trellu, C. ve Mousset, E. (2021). Nanostructured electrodes for electrocatalytic advanced oxidation processes: From materials preparation to mechanisms understanding and wastewater treatment applications. *Applied Catalysis B: Environmental* (296), 120332. <https://doi.org/10.1016/j.apcatb.2021.120332>
- Duran, N.G., Karakişla, M., Aksu, L. ve Saçak, M. (2009). Conducting polyaniline/kaolinite composite: Synthesis, characterization and temperature sensing properties. *Materials Chemistry and Physics* 118(1), 93–98. <https://doi.org/10.1016/j.matchemphys.2009.07.009>
- Filip, J., Cajthaml, T., Najmanova, P., Cernik, M. ve Zboril, R. (2020). *Advanced Nano-Bio Technologies for Water and Soil Treatment*. Springer. [https://doi.org/10.1007/978-3-030-29840-1\\_22](https://doi.org/10.1007/978-3-030-29840-1_22)
- Görücü, S., Gülümser, Ç., Sezer, M. ve Veli, S. (2022). Azo dye removal from aqueous solution by powder graphite: Investigation of parameter effects and optimization by Box-Behnken design. *Journal of Advanced Research in Natural and Applied Sciences*, (9), 56-64. <https://doi.org/10.28979/jarnas.1110677>
- Gülümser, Ç. (2021). *İleri oksidasyon yöntemleriyle boyar madde içeren sulu çözeltilerin yeni fotokatalitik elektrotlar ile arıtılabilirliğinin incelenmesi* (Doktora tezi). Erişim adresi: <https://tez.yok.gov.tr/UlusalTezMerkezi>
- Håkansson, E., Amiet, A. ve Kaynak, A. (2006). Electromagnetic shielding properties of polypyrrole/polyester composites in the 1-18 GHz frequency range. *Synthetic Metals*, 156(14–15), 917–925. <https://doi.org/10.1016/j.synthmet.2006.05.010>
- Isgoren, M., Gengec, E. ve Veli, S. (2017). Evaluation of wet air oxidation variables for removal of organophosphorus pesticide malathion using Box-Behnken design. *Water Science and Technology*. 75(3), 619-628. <https://doi.org/10.2166/wst.2016.479>
- Kang, T.S., Lee, S.W., Joo, J. ve Lee, J.Y. (2005). Electrically conducting polypyrrole fibers spun by electrospinning. *Synthetic Metals*, 153(1–3), 61–64. <https://doi.org/10.1016/j.synthmet.2005.07.135>
- Kaynak, A., Najar, S.S. ve Foitzik, R.C. (2008). Conducting nylon, cotton and wool yarns by continuous vapor polymerization of pyrrole. *Synthetic Metals*, 158(1–2), 1–5. <https://doi.org/10.1016/j.synthmet.2007.10.016>
- Kim, M.S., Kim, H.K., Byun, S.W., Jeong, S.H., Hong, Y.K., Joo, J.S., Song, K.T., Kim, J.K., Lee, C.J. ve Lee, J.Y. (2002). PET fabric/polypyrrole composite with high electrical conductivity for EMI shielding. *Synthetic Metals*, 126(2–3), 233–239. [https://doi.org/10.1016/S0379-6779\(01\)00562-8](https://doi.org/10.1016/S0379-6779(01)00562-8)
- Kincal, D., Kumar, A., Child, A.D. ve Reynolds, J.R. (1998). Conductivity switching in polypyrrole-coated textile fabrics as gas sensors. *Synthetic Metals*, 92(1), 53–56. <https://doi.org/10.1016/s0379->

6779(98)80022-2

- Kuhn, H.H., Child, A.D. ve Kimbrell, W.C. (1995). Toward real applications of conductive polymers. *Synthetic Metals*, 71(1–3), 2139–2142. [https://doi.org/10.1016/0379-6779\(94\)03198-F](https://doi.org/10.1016/0379-6779(94)03198-F)
- Kutanis, S., Karakişla, M., Akbulut, U. ve Saçak, M. (2007). The conductive polyaniline/poly(ethylene terephthalate) composite fabrics. *Composites Part A: Applied Science and Manufacturing*, 38(2), 609–614. <https://doi.org/10.1016/j.compositesa.2006.02.008>
- Lei, J., Cai, Z. ve Martin, C.R. (1992). Effect of reagent concentrations used to synthesize polypyrrole on the chemical characteristics and optical and electronic properties of the resulting polymer. *Synthetic Metals*, 46, 53–69. <https://doi.org/10.1016/j.reactfunctpolym.2013.06.008>
- Lin, T., Wang, L., Wang, X. ve Kaynak, A. (2005). Polymerising pyrrole on polyester textiles and controlling the conductivity through coating thickness. *Thin Solid Films*, 479(1–2), 77–82. <https://doi.org/10.1016/j.tsf.2004.11.146>
- Lu, Y., Pich, A. ve Adler, H.J.P. (2004). Synthesis and characterization of polypyrrole dispersions prepared with different dopants. *Macromolecular Symposia*, 210, 411–417. <https://doi.org/10.1002/masy.200450646>
- MacDiarmid, A.G. ve Epstein, A.J. (1994). The concept of secondary doping as applied to polyaniline. *Synthetic Metals*, 65(2–3), 103–116. [https://doi.org/10.1016/0379-6779\(94\)90171-6](https://doi.org/10.1016/0379-6779(94)90171-6)
- Martínez-Huitle, C.A., Rodrigo, M.A., Sirés, I. ve Scialdone, O. (2015). Single and coupled electrochemical processes and reactors for the abatement of organic water pollutants: A critical review. *Chemical Reviews*, 115(24), 13362–13407. <https://doi.org/10.1021/acs.chemrev.5b00361>
- Martínez-Huitle, C.A., Rodrigo, M.A., Sirés, I. ve Scialdone, O. (2023). A critical review on latest innovations and future challenges of electrochemical technology for the abatement of organics in water. *Applied Catalysis B: Environmental*, 328(July 2022). <https://doi.org/10.1016/j.apcatb.2023.122430>
- Myers, R.E. (1986). Chemical oxidative polymerization as a synthetic route to electrically conducting polypyrroles. *Journal of Electronic Materials*, 15(2), 61–69. <https://doi.org/10.1007/BF02649904>
- Oh, K.W., Hong, K.H. ve Kim, S.H. (1999). Electrically conductive textiles by in situ polymerization of aniline. *Journal of Applied Polymer Science*, 74(8), 2094–2101. [https://doi.org/10.1002/\(SICI\)1097-4628\(19991121\)](https://doi.org/10.1002/(SICI)1097-4628(19991121)74<2094::AID-POLA10974628(19991121)>3.0.CO;2-9)
- Omastova, M., Pionteck, J. ve Košina, S. (1996). Preparation and characterization of electrically conductive polypropylene/polypyrrole composites. *European Polymer Journal*, 32(6), 681–689. [https://doi.org/10.1016/0014-3057\(95\)00206-5](https://doi.org/10.1016/0014-3057(95)00206-5)
- Rehan Abbasi, A.M., Mangat, M.M., Baheti, V. ve Militky, J. (2012). Thermal properties of cotton fabric coated with polypyrrole. *Journal of Fiber Bioengineering and Informatics*, 5(2), 163–168. <https://doi.org/10.3993/jfbi06201205>
- Saravanan, C., Shekhar, R.C. ve Palaniappan, S. (2006). Synthesis of polypyrrole using benzoyl peroxide as a novel oxidizing agent. *Macromolecular Chemistry and Physics*, 207(3), 342–348. <https://doi.org/10.1002/macp.200500376>
- Sayar, N. (2008). *PEM yakıt hücrelerinde platiniz metal nanokompozit katalizörler* (Yüksek lisans tezi). Erişim adresi: <https://tez.yok.gov.tr/UlusalTezMerkezi>
- Veli, S., Arslan, A., Gülümser, C., Topkaya, E., Kurtkulak, H., Zeybek, S., Dimoglo, A, Işgören, M. (2019). Advanced treatment of pre-treated commercial laundry wastewater by adsorption process: Experimental design and cost evaluation. *Journal of Ecological Engineering*, 20(10), 165-171. <https://doi.org/10.12911/22998993/113136>
- Vijayakumar, V., Saravanathamizhan, R. ve Balasubramanian, N. (2016). Electro oxidation of dye effluent in a tubular electrochemical reactor using TiO<sub>2</sub>/RuO<sub>2</sub> anode. *Journal of Water Process Engineering*, (9), 155–160. <https://doi.org/10.1016/j.jwpe.2015.12.006>
- Wagner, M. and Bauer, S. (2023). Industrial and municipal wastewater treatment with a focus on water-reuse. Basel, Switzerland. Erişim adresi: <https://doi.org/10.3390/books978-3-0365-6255-1>
- Wang, jikui, Cai, G., Zhu, X. ve Zhou, X. (2012). Oxidative chemical polymerization of 3, 4-ethylenedioxythiophene and its applications in antistatic coatings. *Journal of Applied Polymer Science*, (124), 109–115. <https://doi.org/10.1002/app.35045>.



# The Effect of the Increasing Doses of Vermicompost Applications to Soil on Some Nutrient Concentrations in Olive (*Olea europaea* L.) Leaves

Ayşe Nur Coşkun<sup>1</sup>, Ali Sümer<sup>2\*</sup>

<sup>1,2</sup>Department of Soil Science and Plant Nutrition, Faculty of Agriculture, Çanakkale Onsekiz Mart University, Çanakkale, Türkiye

## Article History

Received: 07.07.2023

Accepted: 18.09.2023

Published: 20.12.2023

## Research Article

**Abstract** – This research was conducted on young olive (*Olea europaea* L.) trees in a private cultivation land located in Bozkoy closed to Geyikli District of Çanakkale Province, Türkiye in the year 2018. The study aimed to investigate the effects of different doses of vermicompost [(control) 0, 2, 4, 6 kg tree<sup>-1</sup>] on macro and micro nutrient elements of olive trees. Randomized complete block design was established applying four doses with 5 replications. Vermicompost was applied to the soil in a depth of 15-20cm under the crown projection area. During the fruit maturity stage, the leaf samples were collected from annual shoot tip leaves. Macro nutrient element concentrations namely nitrogen (N), phosphorus (P), potassium (K), calcium (Ca), and magnesium (Mg) stayed inside the limit values upon applications of increasing doses of vermicompost. While the changes were statistically non-significant. Even though, this research was an annual study comprised on a single year, where N was in an increasing trend and 2 kg tree<sup>-1</sup> was found to be the most effective dose of vermicompost on N values (17.13 g kg<sup>-1</sup>). Among the leaf micro nutrient elements, statistically significant increases were obtained by 2 kg tree<sup>-1</sup> on copper (Cu) (31.32 mg kg<sup>-1</sup>), on manganese (Mn) (50.77 mg kg<sup>-1</sup>), and 6 kg tree<sup>-1</sup>, on zinc (Zn) (21 mg kg<sup>-1</sup>); while a decrease was observed on iron (Fe) concentration by 6 kg tree<sup>-1</sup> (100.88 mg kg<sup>-1</sup>). Micro nutrient elements remained under the limit of toxic effect upon all the applications. The dose 2 kg tree<sup>-1</sup> was determined to be the most suitable one in terms of both macro and micro element concentrations under such trial circumstances.

**Keywords** – Leaf element concentration, olive tree, organic fertilization, plant nutrient, vermicompost

## 1. Introduction

Natural needs of human beings such as feeding, sheltering, healthy life, dressing and heating have been increased in parallel with the increasing world's population and ecological conditions. Agriculture, which is crucial for the nutrient supply to maintain human life also forms the basis of economy. While the unconscious use of chemical fertilizers and pesticides threaten the human and environmental health, improper agricultural practices may contaminate the soil, cause environmental problems as well as the consumption of natural sources.

Since enlarging the agricultural lands in Türkiye is not possible, preservation of the current agricultural land is crucial. "Organic and sustainable" terms evolved in the process for the search of appropriate and modern practices to preserve the natural balance (Acikgoz, 2009). The main element in the sustainable soil efficiency is the soil organic matter. Addition of organic matters to meet the low organic matter in the soil of Türkiye is obligatory. Animal manure, plant residues, mulching, farmyard manures and compost are among the leading practices to enhance the number of soil organic matters. Along with the above-mentioned practices, the organic matter can also be increased by the conscious and trained farmers who comprehend the situation by which the organic matter content is low in 79% of the soils in Türkiye (Eyüpoğlu, Kurucu, & Talaz, 1999). Organic matter loss due to some reasons is still higher than the addition of them to the soils. Therefore, educating the farmers about the different methods of soil cultivation and not performing scouting, and leading them to good

<sup>1</sup>  aysenurcoskun.94@icloud.com

<sup>2</sup>  sumer@comu.edu.tr

\*Corresponding Author

agricultural practices will help the conservation and then preservation of the current soil organic matter and the efforts to increase them.

There is a delicate balance on earth so that every single living organism has a vital role and benefit to the nature. Use of organic fertilizers and microorganisms in agriculture is on the table according to the researches. As a result, vermicompost which is known for its positive effects among the organic materials has become important. Vermicompost is the process of conversion of natural wastes to fertilizer by decomposing by earthworms. These fertilizers are called “vermicompost” or “vermicast”. Manure of the earthworms (vermicompost) which are called as “ecosystem engineers” include live nitrogen fixing fungi (Demir, Sönmez, & Polat, 2010). Beneficial microorganisms, plant nutrient elements, rhizobium bacteria, coelom liquid and enzymes enhance the structure of soil. Earthworms affect the soil fertility and plant production, and can also enhance the balance of soil, increase soil permeability and porosity as well as mix organic matter (OM), lime and fertilizers with soil. Different studies revealed that the vermicompost enhanced plant height, fresh weight and root development (Sönmez, Çıtak, Koçak, & Yaşın, 2011). The reason why vermicompost is important for agriculture and soil is that besides containing soluble and available forms of macro and micro nutrients. It also includes organic compounds and microorganisms that enhance plant growth. Nutrients in the organic wastes passing through the worms’ gut can be easily uptake by the plants without any loss since they are thrown out after naturally chelated and are in colloidal form. Earthworms are known to inhibit the soil erosions with the help of the galleries they open via which they decrease the surface water in inclined lands and inhibit the water flow (Edwards & Arancon 2022).

In this study, olive (*Olea europaea* L.) trees, which are one of the most important crop in Mediterranean countries and also an important source of income of the farmers in Geyikli District of Çanakkale Türkiye, were selected as research material. Olive trees were about 14-15 years old and Ayvalık oil type. Vermicompost was produced from farmyard manure and organic wastes. The aim of this research is to investigate the effect of increasing rates of vermicompost applications on olive tree leaf nutrient concentrations.

## 2. Materials and Methods

The study to investigate the effect of different doses of vermicompost on the nutrients of olive trees was conducted on Ayvalık oil type olive (*Olea europaea* L.) trees of 14-15 years old situated in a private production land located in Ezine/Geyikli District of Çanakkale Province located on 39° 50' 12" N, 26° 12' 4" E. The vermicompost used in the study was produced as a result of composting fermented farmyard manure and organic wastes produced by the earthworms reared in Çanakkale Onsekiz Mart University, Faculty of Agriculture in the years 2017 and 2018. An amount of vermicompost was obtained and dried in the incubator for 48 hours at 60-80 °C of temperature (Kacar & İnal, 2010). After the drying process, the vermicompost was grinded with a stain knifed grinder. Macro and micro nutrients were determined with ICP-OES after proper extraction (Müftüoğlu, Türkmen, & Çıkkılı, 2014). The results of fertilizer analysis are given in Table 1.

Table 1.

Nutrient content of the applied vermicompost (VC)

	pH	EC (dS m <sup>-1</sup> )	Or- ganic-C (%)	C/N	OM (%)	N (g kg <sup>-1</sup> )	P (g kg <sup>-1</sup> )	K (g kg <sup>-1</sup> )	Ca (g kg <sup>-1</sup> )	Mg (g kg <sup>-1</sup> )	Fe (ppm)	Mn (ppm)	Cu (ppm)	Zn (ppm)
VC	6.10	2.38	30.12	13.51	51.93	22.25	9.43	16.92	20.75	5.58	2455.2	160.9	38.1	87

The experiment was conducted on 20 trees according to randomized complete block design with five replications and four different doses. Soils have been sampled in February from the crown projection area (0-30 cm) of the trees in research plots. Results are given in Table 2. Basic fertilization is arranged (Irget, Anaç, Kılıç, Tepecik, & Özer, 2010). Each plot received 10 kg da<sup>-1</sup> K<sub>2</sub>SO<sub>4</sub>, 10 kg da<sup>-1</sup> MAP in November and 20 kg da<sup>-1</sup> (NH<sub>4</sub>)<sub>2</sub>SO<sub>4</sub> in April. The vermicompost doses were determined as 0 (control), 2, 4 and 6 kg tree<sup>-1</sup> upon the dry weight, except the control treatment. The determined amount of vermicompost was applied as burying to 15-20 cm depth to the tree crown projection area on the date of 18.02.2018. Additionally, each tree received 100 liters of water after vermicompost application.

Table 2.

Properties and nutrient contents of the soil of the study area

Fundamental Analyses		Macro Nutrients		Micro Nutrients	
pH (Richards, 1954)	7.51	Total N (%) (Bremner & Mulvaney 1982)	0.03	Available Fe (ppm) (Lindsay & Norvell, 1978)	7.12
EC (%) (U.S. Salinity Lab. Staff, 1954)	0.06	Available P (ppm) (Olsen & Sommers, 1982)	5.62	Available Mn (ppm) (Lindsay & Norvell, 1978)	8.49
Organic Matter (%) (Nelson & Sommers, 1996)	0.69	Available K (ppm) (Jackson, 1985)	180.71	Available Cu (ppm) (Lindsay & Norvell, 1978)	1.35
Soil Texture (Bouyoucos, 1951)	Loam	Available Ca (ppm) (Jackson, 1985)	3637.54	Available Zn (ppm) (Lindsay & Norvell, 1978)	0.12
CaCO <sub>3</sub> (%) (Loeppert & Suarez, 1996)	8.05	Available Mg (ppm) (Jackson, 1985)	59.87		
		Available Na (ppm) (Jackson, 1985)	13.01		

Usanmaz, Canözer, & Özahçı (1988) reported that the olive trees grew well on the range of pH between 6.0-8.0, and the soil was appropriate for olive cultivation. According to the results, the soil was mildly alkaline without any saltiness risk. Llamas (1984) indicated that the olive soils should have organic matter of  $\geq 1\%$ . The soil in this study was determined to be very poor in terms of organic matter. The lime in the loamy soil was found to be high. Uyanık & Ekinçi (2017) and Kacar & Katkat (2022) indicated that the loamy soil was appropriate for olive cultivation as long as homogeneity was maintained. Among the macro elements, the soil N was very low, P and K was deficient. Genç, Moltay, Soyergin, Fidan, & Sütçü (1991) indicated that the soil in Marmara region olive soils should have Mg amount of 66-930 mg kg<sup>-1</sup>. The concentrations of Ca, and Na in the soil of this study were sufficient. The Zn concentration, among the micro nutrients, was deficient while Cu, Fe, and Mn concentrations were sufficient.

The fruit ripening time when the proper leaf sampling time for olive trees started (30.11.2018 for this study) Bozkaya, 2009; Kutlu & Şen, 2011), the couple of leaves on the middle of the tip of annual shoot were taken for the purpose of sampling. Around 180 leaves were obtained from each tree and got ready for analysis in the laboratory. All samples were washed to remove any adhering soil particles and rinsed with distilled water. The plant samples were dried at 65-70 °C for 48 h and then grinded and made ready for analysis. Leaf samples were used for total nitrogen determination with Kjeldahl method which is a wet decomposition method (Nelson & Sommers, 1980). Plant extracts were obtained with dry decomposition to determine the macro and micro nutrient elements except N, using ICP-OES (Perkin Elmer OPTIMA-5300 DV) device.

Analysis of variance of the data was carried out with *F* test, multiple comparison of the means were done with Duncan Multiple Comparison ( $\alpha < 0.05$ ).

### 3. Results and Discussion

#### 3.1. Effect of Vermicompost on N Concentration of Leaf

The results of the N concentration in olive leaves upon applications of increasing rates of vermicompost (0, 2, 4 and 6 kg tree<sup>-1</sup>) are given in Figure 1.

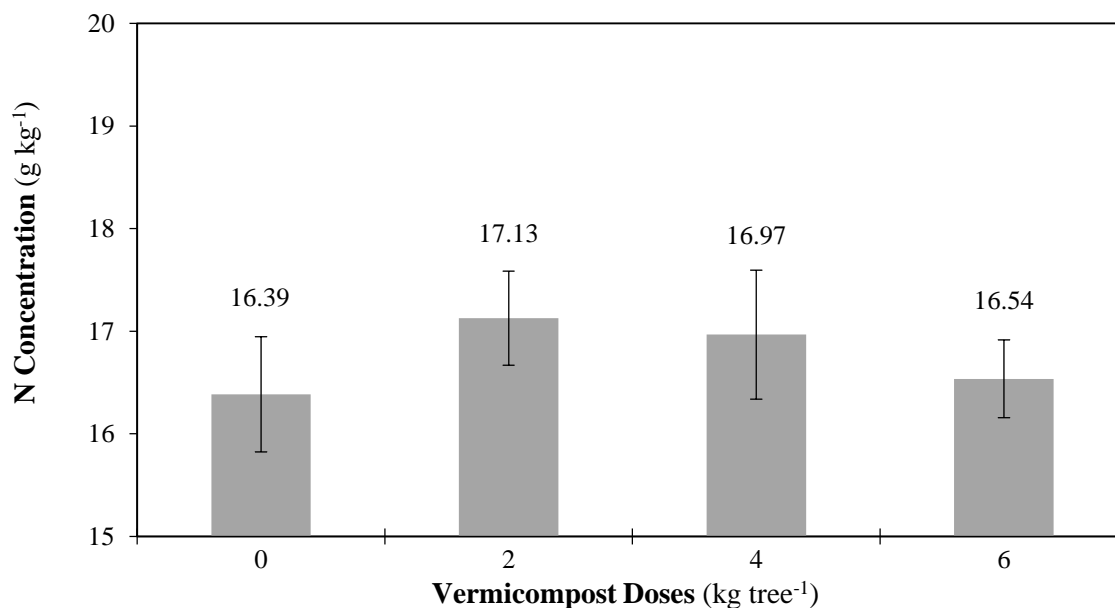


Figure 1. The effect of vermicompost applied to soil at increasing rates on olive tree leaf total N concentration

Compared to (16.39 g kg<sup>-1</sup>), the N concentration of olive leaves were found to be 17.13, 16.97 and 16.54 g kg<sup>-1</sup> upon increasing rates of vermicompost (2, 4 and 6 kg tree<sup>-1</sup>) shown in Figure 1. The N concentrations increased by 4.51%, 3.53% and 0.91% upon 2, 4 and 6 kg tree<sup>-1</sup>, respectively as compared to the control treatment. Although, there are increases in N concentrations and they were non-significant statistically. The highest N concentration was obtained by the application of 2 kg tree<sup>-1</sup> vermicompost (Figure 1).

The N concentrations of olive tree was inside the limit values in all applications including the control treatment (Jones, Wolf, & Mills, 1991; Haspolat, 2006) and the levels were sufficient. Zincirlioğlu (2010) conducted research with Ayvalık oil type olives in Ayvalık region and reported that the N concentrations in the leaves were recorded between 0.74-1.33% in traditional gardens, while they were observed between 0.90-1.48% in organic gardens. The N concentrations in all the applications including the control, were 1.67% in average and sufficient according to Reuter & Robinson (1986). Şahin (2013) determined that the organic fertilizer application of different doses (0-0.5-1 and 1.5 kg tree<sup>-1</sup>) did not affect the leaf N content significantly on his study of two years. These results were compatible with those of our study. The results of the same study showed that the N content of the leaves in the first year were noted as 1.12% upon 0.5 kg tree<sup>-1</sup>, 1.07% upon 1 kg tree<sup>-1</sup>, and 1.24% upon 1.5 kg tree<sup>-1</sup> applications, while they were 0.91% upon 0.5 kg tree<sup>-1</sup>, 0.90% upon 1 kg tree<sup>-1</sup> and 0.95% upon 1.5 kg tree<sup>-1</sup> applications in the second year of the study where the N contents were lower than that of the first year of the study.

### 3.2. Effect of Vermicompost on P Concentration of Leaf

The results of the P concentration in olive leaves upon applications of increasing rates of vermicompost (0, 2, 4 and 6 kg tree<sup>-1</sup>) are given in Figure 2.

Compared to control (0.97 g kg<sup>-1</sup>) the P concentrations in olive plant were 0.90, 1.00 and 0.91 g kg<sup>-1</sup> with increasing rates of vermicompost (2, 4, and 6 kg tree<sup>-1</sup>) shown in Figure 2. 2 and 6 kg tree<sup>-1</sup> vermicompost applications decreased the P concentration of the tree while 4 kg tree<sup>-1</sup> increased it compared to the control treatment. Although, there were increases and decreases, and they were non-significant statistically (Figure 2).

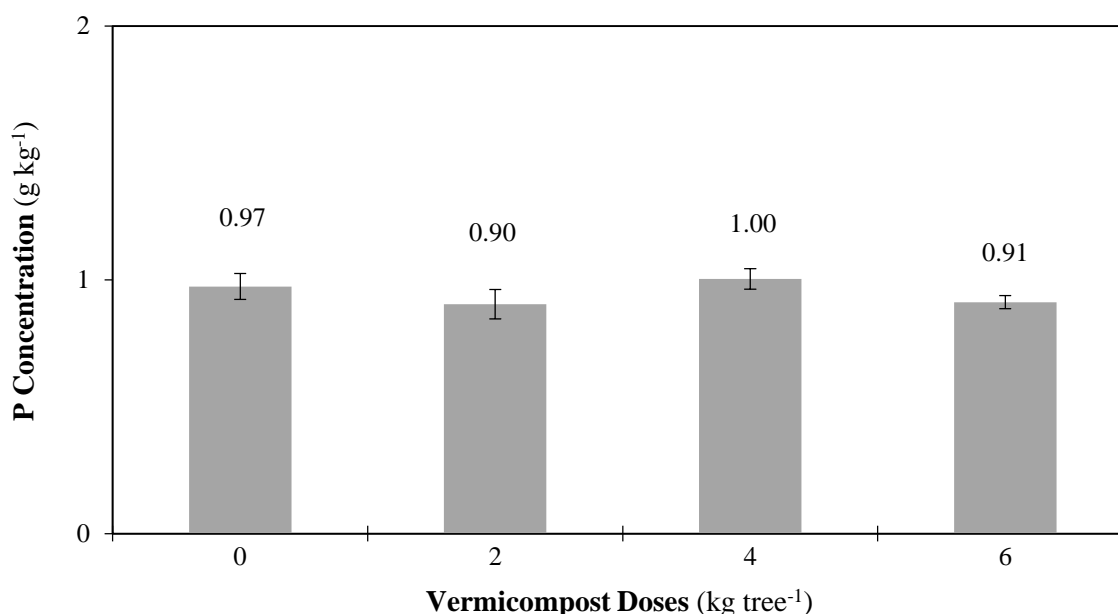


Figure 2. The effect of vermicompost applied to soil at increasing rates on olive tree leaf P concentration

The P concentrations of olive leaves were on the lowest value ( $>1.0 \text{ g kg}^{-1}$ ) of the limit values described by Jones et al. (1991). Llamas (1984) reported  $\text{P}_2\text{O}_5$  should be  $\geq 50 \text{ mg kg}^{-1}$  for olive cultivation. Frantzeskakis, Vassouglou, & Androulakis (1977) reported that the available phosphorus should be  $\geq 20 \text{ mg kg}^{-1}$  and that the response of olive to phosphorus to be low (Zincirlioğlu, 2010). In our study, the vermicompost applications were not effective on P concentrations in olive leaves can be explained by lower mineralization rate in soil although vermicompost contains higher P than that of the farmyard manure (Çıtak, 2011).

### 3.3. Effect of Vermicompost on K Concentration of Leaf

The results of K concentration in olive leaves upon applications of increasing rates of vermicompost (0, 2, 4 and 6  $\text{kg tree}^{-1}$ ) are given in Figure 3.

As compared to control treatment ( $11.95 \text{ g kg}^{-1}$ ), the K concentrations of olive leaves were recorded as 11.04, 11.31 and  $11.65 \text{ g kg}^{-1}$  upon increasing rate of vermicompost (2, 4 and 6  $\text{kg tree}^{-1}$ ) applications shown in Figure 3. The decreases according to control with 2, 4, and 6  $\text{kg tree}^{-1}$  applications were observed as 7.62%, 5.36% and 2.51%, respectively. Variations in K concentrations were statistically non-significant. The reason for the non-significant change in leaf K can be available K in soil being in sufficient amount.

Zincirlioğlu (2010) reported that the K concentration in olive is between 0.9-1.4% in the first year of study, 0.5-1.2% in the second year in traditional gardening, while it was noted as between 0.6-1.2% in the first year and between the 0.5-1.1% in the second year in organic gardening.

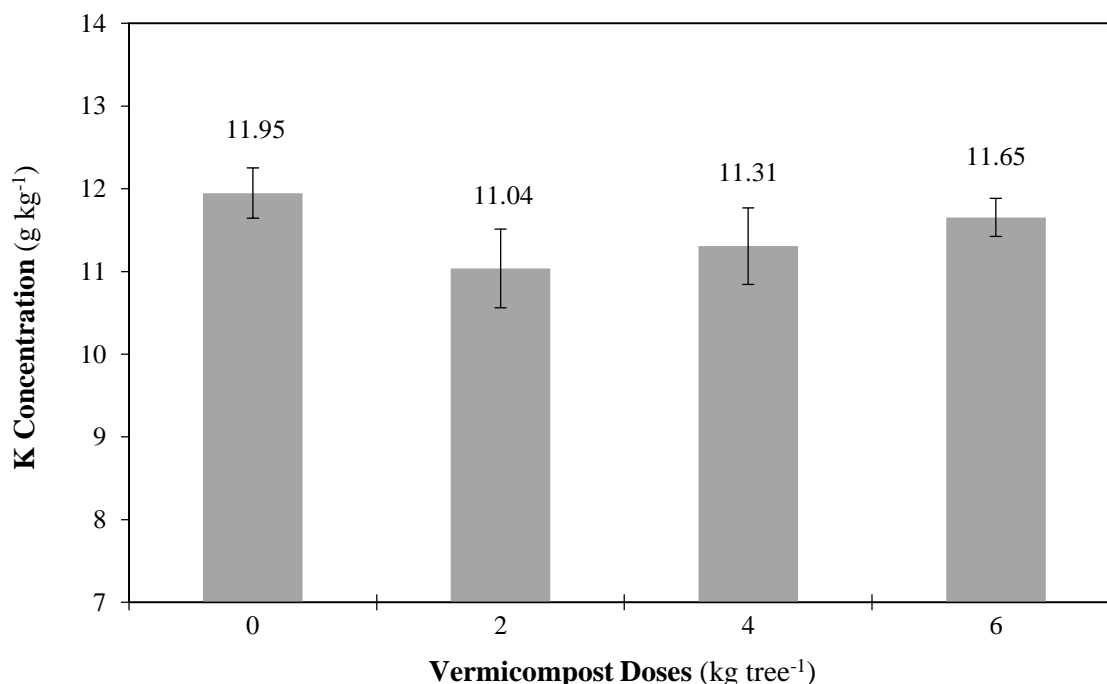


Figure 3. The effect of vermicompost applied to soil at increasing rates on olive tree leaf K concentration

Şahin (2013) determined in two-year study that the vermicompost did not have significant effect on olive leaf K concentrations, however, the interaction of year x dose was significant. K values (0.09-0.13%) were insufficient in both years according to Reuter & Robinson (1986).

K concentrations were found into the limit values (Haspolat, 2006; Reuter & Robinson, 1986) and in sufficient limits different doses of vermicompost application. The available K in soil was sufficient (Table 2) and this might be the reason why there were no significant change in olive leaves in terms of K concentrations.

### 3.4. Effect of Vermicompost on Ca Concentration of Leaf

The results of Ca concentration in olive leaves upon applications of increasing rates of vermicompost (0, 2, 4 and 6 kg tree<sup>-1</sup>) are given in Figure 4.

As compared to control treatment (16.18 g kg<sup>-1</sup>), Ca concentrations of olive tree upon increasing vermicompost applications (2, 4, and 6 kg tree<sup>-1</sup>) were recorded as 16.78%, 15.78% and 16.57%, respectively shown in Figure 4. While 2 and 6 kg tree<sup>-1</sup> increased Ca concentration of olive, 4 kg tree<sup>-1</sup> decreased when that compared with the control treatment. Although there are increases and decreases as compared to control treatment, are not found to be statistically significant (Figure 4).

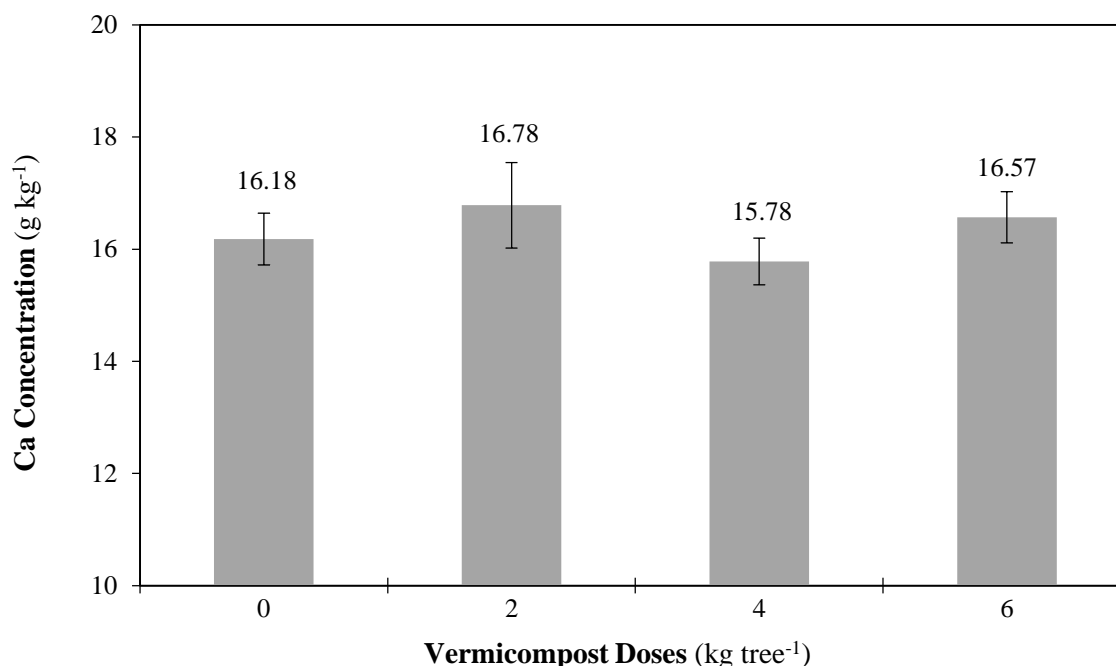


Figure 4. The effect of vermicompost applied to soil at increasing rates on olive tree leaf Ca concentration

Reuter & Robinson (1986) indicated that the available Ca should be between 1.4-2.4% for the good development for olive cultivation. The effect of vermicompost on olive Ca was between 1.5-1.6% in our study, and it was compatible with the previous study literatures. Ca concentrations of olive leaves upon different doses of vermicompost were found into the limit values (Jones et al., 1991; Haspolat, 2006), and they were all sufficient. Eryüce (1980) reported that the Ca in leaves of Ayvalık type trees as recorded as 0.88-2.14%. Our results are similar to the previous study literatures. Şahin (2013) reported that the Ca concentrations in olive leaves were the highest upon vermicompost application (0.136%) in the first year of study where the doses were applied between 0- 0.5- 1 and 1.5 kg tree<sup>-1</sup>. In the second year of study, there was an increase upon vermicompost application, however, the concentration was not sufficient according to Reuter & Robinson (1986). Macro plant nutritional elements (N, P, K, Ca and Mg) were found to be different in Tepecik et al., (2022).

### 3.5. Effect of Vermicompost on Mg Concentration of Leaf

The results of Mg concentration in olive leaves upon applications of increasing rates of vermicompost (0, 2, 4 and 6 kg tree<sup>-1</sup>) are given in Figure 5.

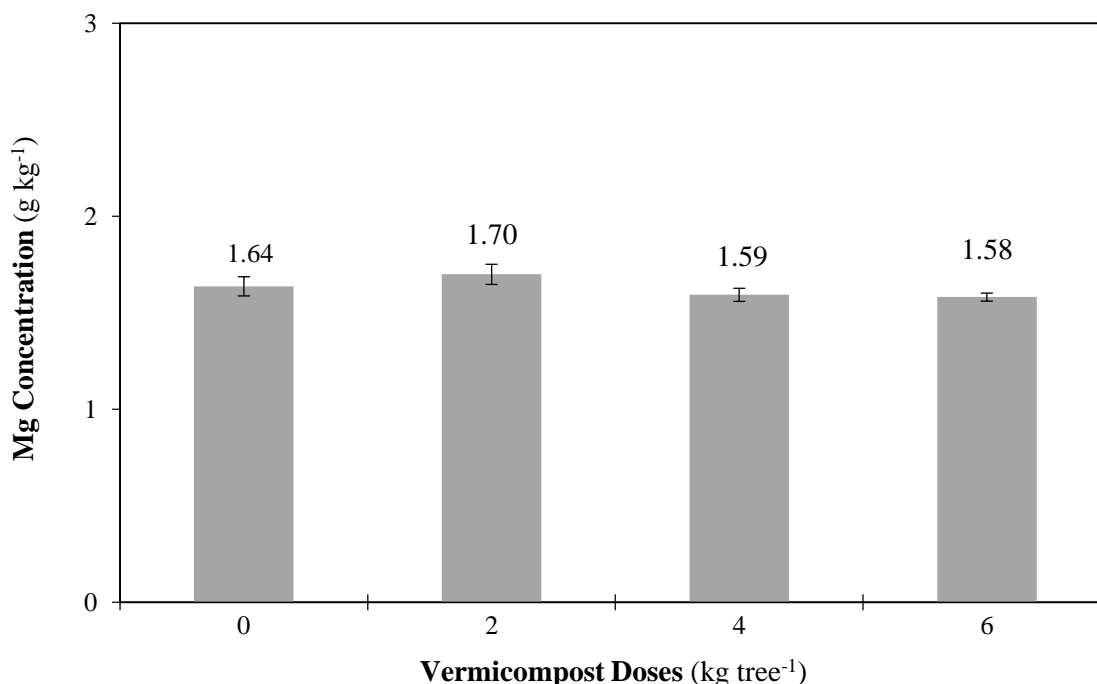


Figure 5. The effect of vermicompost applied to soil at increasing rates on olive tree leaf Mg concentration

As compared to the control treatment (1.64 g kg<sup>-1</sup>), the Mg concentrations with increasing rates of vermicompost applications (2, 4, and 6 kg tree<sup>-1</sup>) were found to be 1.70, 1.59 and 1.58 g kg<sup>-1</sup> shown in Figure 5. There was an increase in Mg concentration of olive upon 2 kg tree<sup>-1</sup> vermicompost dose as compared to control treatment, but there were decreases with 4 and 6 kg tree<sup>-1</sup> vermicompost doses. Although, there are increases and decreases, and were not statistically significant (Figure 5).

Eryüksel (2016) observed the changes on onion, garlic, parsley and purslane by vermicompost application in 2 kg pots. The results of the study were similar to ours as there was increase up to 2 kg tree<sup>-1</sup> dose and later there were decreases. Mg concentrations were low in all applications including control treatment according to Jones et al. (1991). In our research, none of the applications significantly affected plant Mg concentration. As described in Table 2, the deficiency of soil for Mg can be the reason of Mg concentrations being below the limit values. Eryüce (1980) revealed the Mg levels in Ayvalık type as recorded as 0.12-0.37%, while Seferoğlu (1996) observed it as 0.15-0.31%. The results of our study were similar to the above-mentioned ones.

### 3.6. Effect of Vermicompost on Fe Concentration of Leaf

Results regarding the Fe concentration in olive leaves upon applications of increasing rates of vermicompost (0, 2, 4 and 6 kg tree<sup>-1</sup>) are given in Figure 6 and they are significantly importance at  $p < 0.05$  level. When compared to the control treatment (127.62 mg kg<sup>-1</sup>), increasing rates of vermicompost (2, 4, and 6 kg tree<sup>-1</sup>) the Fe concentrations in olive leaves were found to be 117.63, 121.95 and 100.88 mg kg<sup>-1</sup>, respectively given in Figure 6. There were decreases in Fe concentrations upon 2, 4, and 6 kg tree<sup>-1</sup> vermicompost applications when compared with the control treatment, and such decreases were as 7.83%, 4.44% and 20.95%. Variation in Fe concentration in leaves were found non-significant in control treatment, 2 and 4 kg tree<sup>-1</sup> doses, but the decrease upon 6 kg tree<sup>-1</sup> application was found significantly importance (Figure 6).

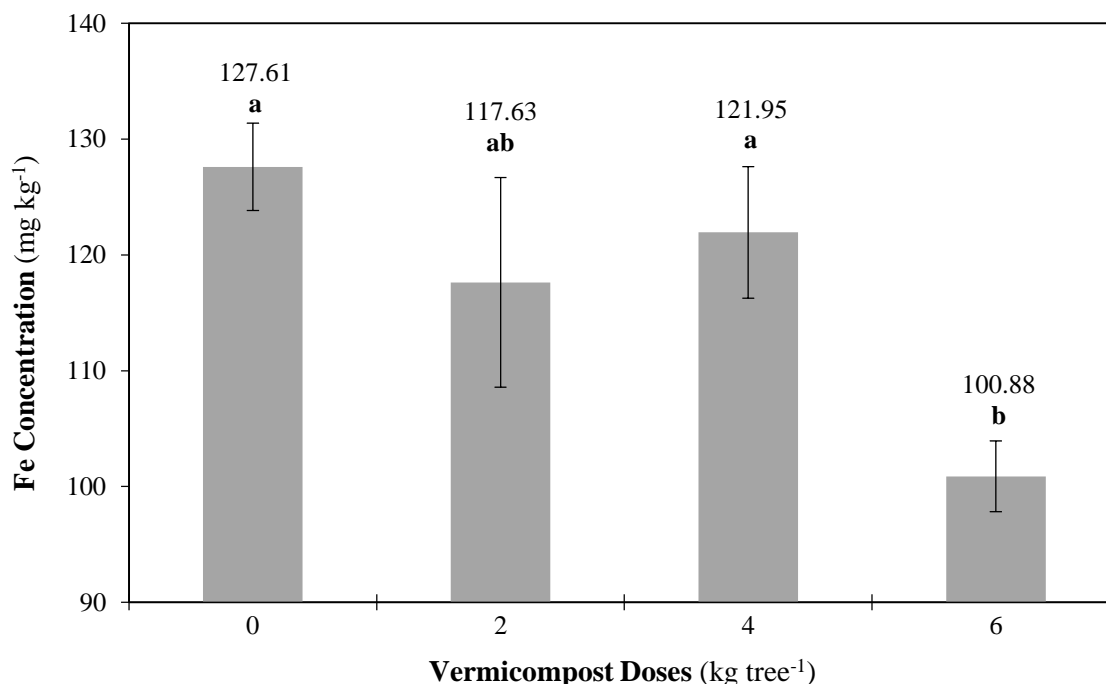


Figure 6. The effect of vermicompost applied to soil at increasing rates on olive tree leaf Fe concentration

Adiloğlu, Eryılmaz, Adiloğlu & Solmaz (2016) described that the vermicompost applications (200, 400 and 800 kg da<sup>-1</sup>) decreased the Fe concentrations as compared to control treatment, and the rates changed between 18.81 and 49.82 mg kg<sup>-1</sup> in case of sunflower. When we evaluated the Fe concentrations of olive as 100.88-127.62 mg kg<sup>-1</sup> upon different vermicompost doses, and then they are very high in all of the applications according to Haspolat (2006). The Fe concentrations in control treatment and all other vermicompost applications were lower than the toxic effect limit (>460 ppm). Eryüksel (2016) conducted a pot experiment in 2kg of pots contained onion, garlic, parsley and purslane where different doses of vermicompost (0.5%, 25%, 50%, 75% and 100%) were applied. Fe was observed to increase with the increasing rate of vermicompost in garlic and purslane. In our study, there was a significant decrease upon the highest vermicompost application shown in Figure 6. Alpaslan & Taban (1996) reported that Fe decreased Zn uptake in plants, and Zn negatively affected the uptake of Fe, when Fe x Zn interaction was analyzed. As seen in Figure 9, the highest Zn concentration was observed in 6 kg tree<sup>-1</sup> dose. Increased Zn might have decreased the Fe concentration based on the above-mentioned interaction. Güneş, Alpaslan, & İnal (2002) obtained different results and reported that the fertilizer application increased the Fe concentration of plant as compared to control treatment.

### 3.7. Effect of Vermicompost on Mn Concentration of Leaf

Results regarding to the concentration of Mn presence in the leaves of olive upon applications of increasing rates of vermicompost (0, 2, 4 and 6 kg tree<sup>-1</sup>) are given in Figure 7, and they are significantly importance at  $p < 0.05$ . As compared with the control treatment (42.87 mg kg<sup>-1</sup>), the Mn concentrations in olive tree with increasing vermicompost doses (2, 4, and 6 kg tree<sup>-1</sup>) were determined as 50.77, 39.69 and 47.96 mg kg<sup>-1</sup>, respectively shown in Figure 7. A significant increase (18.43%) in Mn concentration upon 2 kg tree<sup>-1</sup> vermicompost was observed as compared to the control treatment. There was non-significant difference in applications of 4 and 6 kg tree<sup>-1</sup> vermicompost. 2 kg tree<sup>-1</sup> vermicompost application was determined to be the application with the highest concentration of Mn recorded as 50.77 mg kg<sup>-1</sup> (Figure 7).

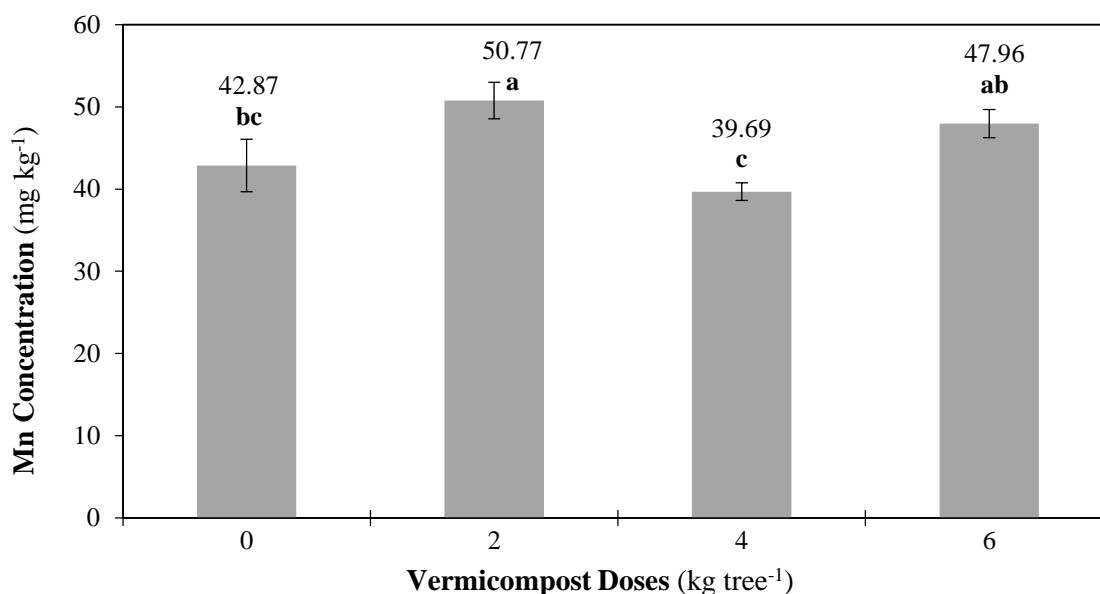


Figure 7. The effect of vermicompost applied to soil at increasing rates on olive tree leaf Mn concentration

When different doses of vermicompost were applied to olive tree, the concentrations of Mn were found to be into the limit values (Jones et al., 1991; Haspolat, 2006) and the values of Mn were all sufficient including the control treatment. The concentration of Mn in leaves were lower than the toxic effect level (>164 ppm) in all of the applications including the control treatment (Figure 7). Şahin (2013) reported that the concentrations of Mn in leaves were recorded as 50.37-57.75 and 52.37 ppm upon applications of 0.5-1 and 1.5 kg tree<sup>-1</sup>, respectively, in the first year of study, while they were 41.00-60.12 and 68.87 ppm in the second year. The results of the above-mentioned study are compatible with those of our study.

### 3.8. Effect of Vermicompost on Cu Concentration of Leaf

Results regarding to Cu concentration in olive leaves upon applications of increasing rates of vermicompost (0, 2, 4 and 6 kg tree<sup>-1</sup>) are given in Figure 8, and they found significantly important at  $p < 0.001$ . The Cu contents of olive were found to be 31.32, 14.72, and 22.37 mg kg<sup>-1</sup> with increasing rates of vermicompost (2, 4, and 6 tree<sup>-1</sup>) when compared to control treatment (24.79 mg kg<sup>-1</sup>) shown in Figure 8. The results showed that when compared to control treatment, the Cu content in olive significantly increased 26.34% with 2 kg tree<sup>-1</sup> vermicompost ( $p < 0.001$ ) while a significant decrease upon 4 kg tree<sup>-1</sup>, and no significant change with 6 kg tree<sup>-1</sup>. The highest ratio of Cu in olive tree was observed by 2 kg tree<sup>-1</sup> vermicompost application (Figure 8).

According to Haspolat (2006), the Cu concentration on 4 kg tree<sup>-1</sup> was sufficient, high upon 6 kg tree<sup>-1</sup> and in control treatment, and very high upon 6 kg tree<sup>-1</sup> application. The concentration of Cu in control treatment and the other vermicompost applications were all lower than the toxic effect level (>78 ppm) given in Figure 8. Şahin (2013) conducted a study for two years with organic fertilizer application using different doses (0-0.5-1, and 1.5 kg tree<sup>-1</sup>) and showed that they significantly affected the Cu contents. In the first year of study, the lowest concentration was obtained from cattle manure and the highest in case of vermicompost. While in the second year of study, there was a decrease in all applications of fertilizer, except the control treatment. The Cu content increased with increasing fertilizer application in the first year of study. The Cu content was found to be 47.500 ppm upon 1.5 kg tree<sup>-1</sup>. In our study, the highest Cu concentration was found as 31.32 mg kg<sup>-1</sup> with 2 kg tree<sup>-1</sup> vermicompost application (Figure 8).

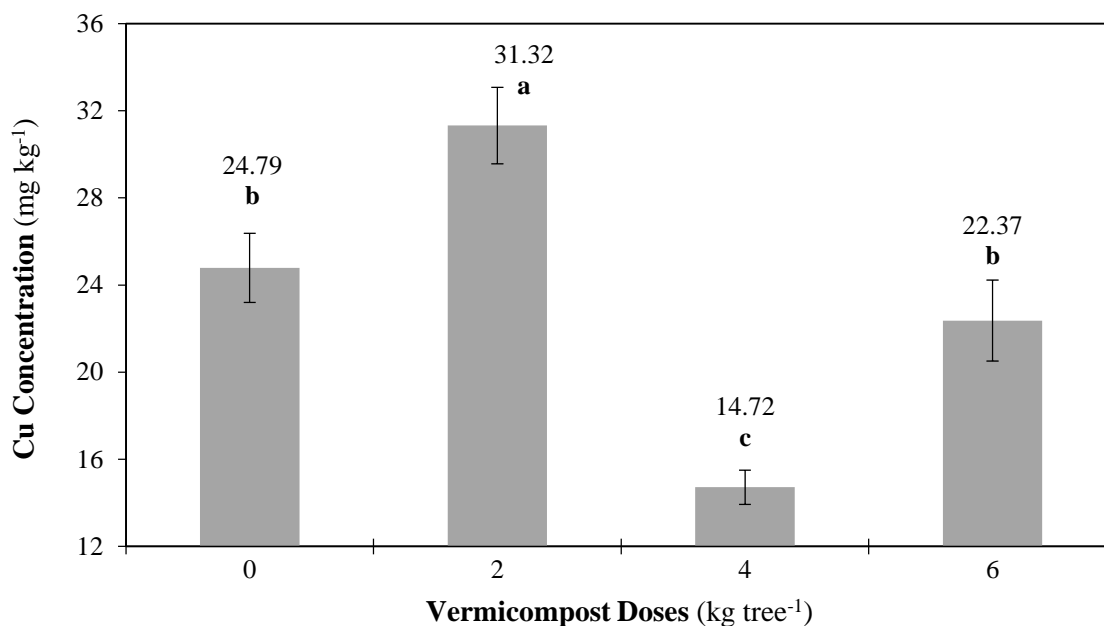


Figure 8. The effect of vermicompost applied to soil at increasing rates on olive tree leaf Cu concentration

### 3.9. Effect of Vermicompost on Zn Concentration of Leaf

The effect of increasing rates of vermicompost applications (0, 2, 4 and 6 kg tree<sup>-1</sup>) on Zn concentration of olive tree are significantly importance at  $p < 0.05$  as shown in Figure 9.

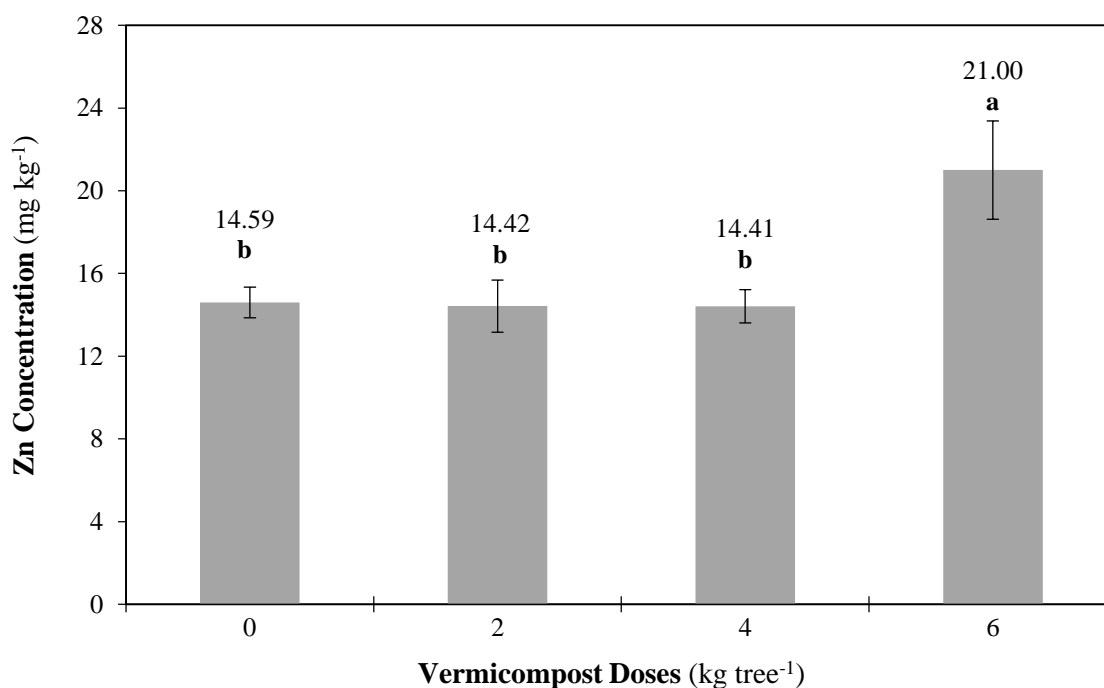


Figure 9. The effect of vermicompost applied to soil at increasing rates on olive tree leaf Zn concentration

As compared with control treatment (14.59 mg kg<sup>-1</sup>), the concentrations of Zn in olive upon increasing rates of vermicompost (2, 4 and 6 kg tree<sup>-1</sup>) were determined as 14.42, 14.41 and 21.00 mg kg<sup>-1</sup>, respectively (Figure 9). There was non-significant variation upon 2 and 4 kg tree<sup>-1</sup> vermicompost applications when compared to control treatment, but there was a significant increase upon 6 kg tree<sup>-1</sup> application at  $p < 0.05$  (Figure 9). Zn concentration results were low in control treatment, 2 and 4 tree<sup>-1</sup> but increased sufficiently upon 6 kg tree<sup>-1</sup>

application (Haspolat, 2006). Eryüksel (2016) observed the changes in onion, garlic, parsley and purslane using different doses of vermicompost (0.5%, 25%, 50%, 75% and 100%) in 2kg pots. The results showed that the Zn element increased as vermicompost dose increased in all the plants. According to Sharma & Deb (1988), soil organic matter increased the diffusion rate of Zn as well as the uptake of plants. The Zn occurring as a result of microbial activity and forming chelate is uptake more by plants. Srivastava & Sethi (1981) reported that organic fertilizer given to the alkaline soil poor in organic matter increase the solubility and availability of Zn. The highest Zn concentration of leaf upon the highest vermicompost (6 kg tree<sup>-1</sup>) can be explained by the mentioned study.

#### 4. Conclusion

Organic fertilizers have been applied together with a dense application of fertilizers in Türkiye similar to developed countries. Vermicompost is one of the frequently used organic fertilizers. Besides the ameliorating effects on the physical and biological structure of soil, clean content without negative effects on human beings and environmental health are the positive aspects of vermicompost. Another importance of vermicompost for soil and agriculture is the macro and micro nutrient elements being dissolved and available for plants. According to Bellitürk (2018), research regarding to economic analyses on single use of vermicompost or its combination with chemical fertilizers are limited. Principally, this study planned by considering the need to carry out studies on olive, which is important for the agriculture sector of Türkiye. And it is thought to assist other research in the future.

This study carried out on olive trees of Ayvalık oil type (age of 14-15) under field conditions in Geyikli district of Çanakkale Province. The effects of different doses of vermicompost [0 (control), 2, 4 and 6 kg tree<sup>-1</sup>] on macro and micro nutrient element uptake by olive leaves were investigated.

The concentrations of macro nutrients upon different doses of vermicompost applications remained to the limit values in all treatments including the control and there was non-significant difference between different doses. The values of N started to increase even though it was a single year study, and the dose of 2 kg tree<sup>-1</sup> was observed to increase the concentration of N which was the highest. No change in concentrations of leaf P, Ca, K and Mg was observed. The low concentration of leaf Mg can be related to the deficiency of soil for Mg, therefore, fertilization containing Mg besides vermicompost is suggested for this region. The satisfactory results for Cu and Mn in olive leaves were observed upon 2 kg tree<sup>-1</sup> and best result for Zn was observed upon 6 kg tree<sup>-1</sup> dose. The values of all the micro nutrients were below the toxic effect limit values. The dose of 2 kg tree<sup>-1</sup> was seen to the suggested dose of vermicompost for olive trees. Besides the vermicompost, Zn and Fe can be suggested to be applied to soil in chelated form or as leaf fertilization. Addition of organic matters are crucial for the soil due to the nonsufficient organic matter in the soil of Türkiye. Since olive is a perennial tree, a study of at least 3 years, including 2 existence years, is suggested and more satisfactory results are projected to be obtained upon different methods of application, applied doses, and variations during the application processes.

#### Author Contributions

Ali Sümer: Conducted the research and wrote the article.

Ayşe Nur Coşkun: Made soil and plant analysis and statistical analysis.

This article is based on a master's thesis from "Ayşe Nur Coşkun"

#### Conflicts of Interest

The authors declare no conflict of interest.

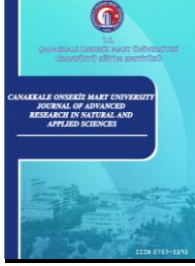
#### References

- Acikgoz, E.F. (2009). Effect of Chemical and Organic Fertilizer Applications on Lettuce (*Lactuca sativa* L. var. *crispa*) Nitrate Accumulation. *Asian Journal of Chemistry*, 21(7), 5427-5430. [https://asianjournalofchemistry.co.in/user/journal/viewarticle.aspx?ArticleID=21\\_7\\_65](https://asianjournalofchemistry.co.in/user/journal/viewarticle.aspx?ArticleID=21_7_65)
- Adiloğlu, A., Eryılmaz, A. F., Adiloğlu, S., & Solmaz, Y. (2016). Artan Miktarlarda Akvakültür Atığı Uygulamasının Salata (*Lactuca sativa* L. var. *crispa*) Bitkisinin Bazı Makro ve Mikro Bitki Besin Elementi

- İçerikleri Üzerine Etkisi. *Journal of Tekirdag Agricultural Faculty*, 13(2), 96-101. <https://dergipark.org.tr/tr/download/article-file/178658>
- Alpaslan, M., & Taban, S. (1996). Çeltikte (*Oryza Sativa* L.) Çinko-Demir İlişkisi. *Journal of Agricultural Sciences*, 2, 45-49. [https://doi.org/10.1501/Tarimbil\\_0000000361](https://doi.org/10.1501/Tarimbil_0000000361)
- Bellitürk, K. (2018). Vermicomposting in Turkey: Challenges and Opportunities in Future. *Eurasian Journal of Forest Science*, 6 (4), 32-41. <https://doi.org/10.31195/ejejfs.476504>
- Bouyoucos, G.H. (1951). A Recalibration of the Hydrometer Methods for Making Mechanical Analysis of Soil. *Agronomy Journal*, 43, 434-438. <https://doi.org/10.2134/agronj1951.00021962004300090005x>
- Bozkaya, F. (2009). *Dolu Yılında Zeytin (Olea Europaea L.) Bitkisinde Mineral Bitki Besin Maddelerinin Mevsimsel Değişiminin İncelenmesi*. (Unpublished master's thesis). Adnan Menderes University, Aydın, Türkiye. <http://hdl.handle.net/11607/861>
- Bremner, J.M., & Mulvaney, C.S. (1982). *Nitrogen-Total*. In: Methods of soil analysis. Part 2. Chemical and microbiological properties, Page, A.L., Miller, R.H. and Keeney, D.R. Eds., American Society of Agronomy, Soil Science Society of America, Madison, Wisconsin, 595-624. <https://doi.org/10.2134/agronmonogr9.2.2ed.c31>
- Çıtak, M. (2011). *Boş Yılında Zeytin (Olea europaea L.) Bitkisinde Mineral Bitki Besin Maddelerinin Mevsimsel Değişiminin İncelenmesi*. (Unpublished master's thesis). Adnan Menderes University, Aydın, Türkiye. <http://hdl.handle.net/11607/948>
- Demir, H., Sönmez, İ., & Polat, E. (2010). *Ülkemiz İçin Yeni Bir Organik Gübre: Solucan Gübresi*. International Conference on Organic Agriculture in Scope of Environmental Problems (pp.15). Famagusta, Cyprus (KKTC). <https://avesis.akdeniz.edu.tr/yayin/3c5a502b-fc6d-4179-8245-9d50e522e4f3/ulkemiz-icin-yeni-bir-organik-gubre-solucan-gubresi>
- Edwards, C.A. & Arancon, N.Q. (2022). *The Influence of Environmental Factors on Earthworms*. Biology and Ecology of Earthworms, Fourth Edition, Springer, pp. 191–232. [https://doi.org/10.1007/978-0-387-74943-3\\_7](https://doi.org/10.1007/978-0-387-74943-3_7)
- Eryüce, N. (1980). Ayvalık Bölgesi Yağlık Zeytin Çeşidi Yapraklarında Bazı Besin Elementlerinde Bir Vegetasyon Periyodu İçindeki Değişimler. *Ege Journal of Agricultural Research*, 17(2), 209-221. [https://scholar.google.com/scholar?hl=tr&as\\_sdt=0%2C5&q=N+Eryuce++Ziraat+Fakultesi+dergisi-Ege+Universitesi%2C+1980&btnG=](https://scholar.google.com/scholar?hl=tr&as_sdt=0%2C5&q=N+Eryuce++Ziraat+Fakultesi+dergisi-Ege+Universitesi%2C+1980&btnG=)
- Eryüksel, S. (2016). *Farklı Oranlarda Vermikompost Uygulamasının Bazı Sebzelerin Besin Elementi İçerikleri Üzerine Olan Etkileri*. (Unpublished master's thesis). Namık Kemal University, Tekirdağ, Türkiye. <https://acikerisim.nku.edu.tr/xmlui/bitstream/handle/20.500.11776/1175/0050507.pdf?sequence=1>
- Eyüpoğlu, F., Kurucu, N., & Talaz, S. (1999). Nutritional status of cereals grown in Central Anatolian Plateau. *International conference on Orta Anadolu'da hububat tarımının sorunları ve çözüm yolları*, 8-11 Haziran 1999. (pp. 275–279). Konya, Türkiye. <https://www.cabdirect.org/cabdirect/abstract/20000712315>
- Frantzeskakis, J., Vassoglou, N., & Androulakis, J. (1977). An Investigation of the Potassium Status in Some Olive Orchards in Western Crete. *Hort. Abst.*, 47(12), 995-1934. [https://scholar.google.com/scholar?hl=tr&as\\_sdt=0%2C5&q=+Investigation+of+the+Potassium+status+in+some+olive+Orchards+in+western+crete&btnG=](https://scholar.google.com/scholar?hl=tr&as_sdt=0%2C5&q=+Investigation+of+the+Potassium+status+in+some+olive+Orchards+in+western+crete&btnG=)
- Genç, Ç., Moltay, G., Soyergin, S., Fidan, A.E., & Sütçü, A.R. (1991). Marmara Bölgesi Sofralık Zeytinlerinin Beslenme Durumu. Atatürk Bahçe Kültürleri Araştırma Enstitüsü. Yalova, Türkiye. <https://kutuphane.tarimorman.gov.tr/vufind/Record/10906>
- Güneş, A., Alpaslan, M., & İnal, A. (2002). *Bitki Besleme ve Gübreleme*. Ankara Üniversitesi Ziraat Fakültesi, Yayın No.1526, Ankara. <http://hdl.handle.net/20.500.12575/12643>
- Haspolat, G., 2006. *Gemlik Zeytin Çeşidinde Biyolojik Olarak Şelatize Edilmiş KNO<sub>3</sub>, ZnSO<sub>4</sub> ve MgSO<sub>4</sub>'ün Yapraktan Uygulanmasının ve Plastik Malç Uygulamasının Vegetatif Gelişmeye ve Meyve Verimine Etkisi*. (Unpublished master's thesis). Çukurova University, Adana, Türkiye. <https://tez.yok.gov.tr/UlusalTezMerkezi/tezDetay.jsp?id=yQFpiiR5QuTyMBkShM43gA&no=Kxc1ElUK-SywfjXrqdTA>
- İrget, M.E., Anaç, D., Kılıç, C.C., Tepecik, M., & Özer, K. (2010). Determination of Nitrogen Rates in Olive (*Olea europaea* cv Memecik). *Asian Journal of Chemistry*, 22 (2); 1435-1444 [https://www.researchgate.net/profile/Mehmet-Irget/publication/281766799\\_Determination\\_of\\_Nitrogen\\_Rates\\_in\\_Olive\\_Olea\\_europaea\\_cv\\_Memecik/links/5715e5f108ae8ab56695bb52/Determination-of-Nitrogen-Rates-in-Olive-Olea-europaea-cv-Memecik.pdf](https://www.researchgate.net/profile/Mehmet-Irget/publication/281766799_Determination_of_Nitrogen_Rates_in_Olive_Olea_europaea_cv_Memecik/links/5715e5f108ae8ab56695bb52/Determination-of-Nitrogen-Rates-in-Olive-Olea-europaea-cv-Memecik.pdf)

- Jackson, M.L. (1985). *Soil Chemical Analysis: Advanced Course*. 2nd Edition, Parallel Press, University of Wisconsin-Madison Libraries, USA. [https://books.google.com.tr/books/about/Soil\\_Chemical\\_Analysis.html?id=VcEOK9QCkVEC&redir\\_esc=y](https://books.google.com.tr/books/about/Soil_Chemical_Analysis.html?id=VcEOK9QCkVEC&redir_esc=y)
- Jones, J. B. Jr., Wolf, B., & Mills, H.A. (1991). *Plants Analysis Handbook A practical sampling, preparation, analysis, and interpretation guide*. Micro- Macro Publishing, Inc., Georgia 30607, USA. <https://www.cabdirect.org/cabdirect/abstract/19921969819>
- Kacar, B., & İnal, A. (2010). *Bitki Analizleri*. Nobel Yayınevi, Türkiye. [https://www.nobelyayin.com/kitap\\_2734.html](https://www.nobelyayin.com/kitap_2734.html)
- Kacar, B., & Katkat, A.V. (2022). *Gübreler ve Gübreleme Tekniği*. Nobel AkademikYayıncılık, Türkiye. <https://www.nobelyayin.com/gubreler-ve-gubreleme-teknigi-2599.html>
- Kutlu, E., & Şen, F. (2011). Farklı Hasat Zamanlarının Gemlik Zeytin (*Olea europea* L.) Çeşidinde Meyve ve Zeytinyağı Kalitesine Etkileri. *Ege Journal of Agricultural Research*, 48(2), 85-93. <https://dergipark.org.tr/tr/download/article-file/59373>
- Lindsay, W.L., & Norvell, W.L. (1978). Development of a DTPA Soil Test Zinc, Iron, Manganese and Copper. *Soil Sci. Soc. Am. Journal*, 42, 421-428. <https://doi.org/10.2136/sssaj1978.03615995004200030009x>
- Llamas, J.F. (1984). *Basis of Fertilization in Olive Cultivation and the Olive Tree's Vegetative Cycle and Nutritional Needs*. International Course on the Fertilization and Intensive Cultivation of the Olive Cultivation. UNDP-FAO, Cordoba-Spain. [https://scholar.google.com/scholar?hl=tr&as\\_sdt=0%2C5&q=Basis+of+Fertilization+in+Olive+Cultivation+and+the+Olive+Tree%E2%80%99s+Vegetative+Cycle+and+Nutritional+Needs&btnG=](https://scholar.google.com/scholar?hl=tr&as_sdt=0%2C5&q=Basis+of+Fertilization+in+Olive+Cultivation+and+the+Olive+Tree%E2%80%99s+Vegetative+Cycle+and+Nutritional+Needs&btnG=)
- Loeppert, R.H., & Suarez, D.L. (1996). *Carbonate and Gypsum*. In: Sparks D.L. (Ed), *Methods of Soil Analysis*. Part 3-Chemical Methods. SSSA Book Series: 5, Madison, pp. 437-474. <https://doi.org/10.2136/sssabookser5.3.c15>
- Müftüoğlu, N.M., Türkmen C., & Çıkılı Y. (2014). *Toprak ve Bitkide Verimlilik Analizleri* (2. Basım). Nobel Yayın Dağıtım, Ankara. pp.218. <https://avesis.comu.edu.tr/yayin/f33a4875-2cd9-4319-915b-62d7b6e201d0/toprak-ve-bitkide-verimlilik-analizleri-2-baski>
- Nelson, D.W., & Sommers, L.E. (1980). Total Nitrogen Analysis of Soil and Plant Tissues. *Journal of Association of Official Analytical Chemists*, 63(4), 770-778. <https://doi.org/10.1093/jaoac/63.4.770>
- Nelson, D.W. & Sommers, L.E. (1996). *Total Carbon, Organic Carbon and Organic Matter*. In: Sparks D.L. (Ed), *Methods of Soil Analysis*. Part 3-Chemical Methods. SSSA Book Series: 5, Madison, Wisconsin, pp. 961-1010. <https://doi.org/10.2134/agronmonogr9.2.2ed.c29>
- Olsen, S.R., & Sommers, L.E. (1982). *Phosphorus*. *Methods of Soil Analysis: Part 2 Chemical and Microbiological Properties*, Second Edition, Agronomy Monographs, Madison WI, pp 403-430. <https://doi.org/10.2134/agronmonogr9.2.2ed.c24>
- Reuter, D.J., & Robinson, J.B. (1986). *Plant Analysis An Interpretation Manual*, Second Edition, Inkata. Australia. <https://books.google.com.tr/books?id=MhG9BAAQBAJ&printsec=frontcover&hl=tr#v=onepage&q&f=false>
- Richards, L.A. (1954). *Diagnosis and Improvement of Saline and Alkali Soils*. United States Department of Agriculture Handbook, 60. [https://www.ars.usda.gov/ARSUserFiles/20360500/hb60\\_pdf/hb60complete.pdf](https://www.ars.usda.gov/ARSUserFiles/20360500/hb60_pdf/hb60complete.pdf)
- Seferoğlu, S. (1996). *Ayvalık ve Edremit Yöresinde Yetiştirilen Ayvalık Zeytin Çeşidinin Beslenme Statüsü ile Kimi Öğeleri Arasındaki İlişkiler*. (Unpublished doctoral dissertation). Ege University, İzmir, Türkiye. <https://tez.yok.gov.tr/UlusalTezMerkezi/tezDetay.jsp?id=0eBF-W2-aJfLQKGk3fwFsQ&no=0eBF-W2-aJfLQKGk3fwFsQ>
- Sharma, K.N., & Deb, D.L. (1988). Effect of Organic Manuring on Zinc Diffusion in Soils of Varying Texture. *J. Indian Soc. Soil Sci.*, 36, 219-224. [https://scholar.google.com/scholar?hl=tr&as\\_sdt=0%2C5&q=Effect+of+organic+manuring+on+zinc+diffusion+in+soils+of+varying+texture&btnG=](https://scholar.google.com/scholar?hl=tr&as_sdt=0%2C5&q=Effect+of+organic+manuring+on+zinc+diffusion+in+soils+of+varying+texture&btnG=)
- Sönmez, S., Çıtak, S., Koçak, F., & Yaşın, S. (2011). Effects of vermicompost and farmyard manure applications on spinach (*Spinacia oleracea* var. L.) growth and soil fertility, *Horticultural Studies*, 28(1), 56-69. <https://www.acarindex.com/horticultural-studies/vermikompost-ve-ahir-gubresi-uygulamalarinin-ispacak-spinacia-oleracea-var-l-bitkisinin-gelisimi-ve-toprak-verimliliği-uzerine-etkileri-893067>
- Srivastava, O.P., & Sethi, B.C. (1981). Contribution of farm yard manure on the build up of available zinc in an aridisol. *Communications in Soil Science and Plant Analysis*, 12(4), 355- 361. *Communications in Soil Science and Plant Analysis*. <https://doi.org/10.1080/00103628109367156>

- Şahin, G. (2013). *Organik Zeytin Yetiştiriciliğinde Farklı Gübre Dozlarının Toprak Özellikleri, Yaprak Besin Elementi İçeriği ve Yağ Kalitesi Üzerine Etkileri*. (Unpublished master's thesis). Adnan Menderes University, Aydın, Türkiye. <http://adudspace.adu.edu.tr:8080/xmlui/handle/11607/40>
- Tepecik, M., Esetlili, B.Ç., & Bilge, B. (2022). Effect of Foliar Magnesium Fertilizer Application on Plant Nutrient and Chlorophyll Olive (*Olea Europaea* L.) Plant. *Agro International Conference on Agriculture Azerbaijan State Agrar University June 04-06*, pp 20-26. <https://umoti-uzhnu.university/agro-international-conference-on-agriculture/>
- Usanmaz, D., Canözer, Ö., & Özahçı, E. (1988). Zeytinlerde Soğuk Zararı ve Alınacak Önlemler. *Zeytincilik Araştırma Enstitüsü Yayınları No:41*, İzmir, Türkiye. <https://kutuphane.tarimorman.gov.tr/vufind/Search/Results?look-for=%22Zeytincilik+Ara%C5%9Ft.Enst.Md.Yay%C4%B1n+No%3A%22&type=Series>
- U.S. Salinity Lab. Staff. (1954). *Diagnosis and Improvement of Saline and Alkali Soils*. United States Department of Agriculture Handbook, 60. U.S.A. [https://www.ars.usda.gov/ARSUserFiles/20360500/hb60\\_pdf/hb60complete.pdf](https://www.ars.usda.gov/ARSUserFiles/20360500/hb60_pdf/hb60complete.pdf)
- Uyanık, S., & Ekinci, H. (2017). Geyikli Yöresi (Çanakkale) Topraklarının Bazı Fizikokimyasal Özellikleri, Sınıflandırılması ve Verimlilik Durumunun İncelenmesi. *Comu Journal Agric. Fac.*, 5(2), 87-96. <https://dergipark.org.tr/tr/download/article-file/391511>
- Zincirlioğlu, N. (2010). *Organik ve Geleneksel Zeytin Yetiştiriciliğinde Bitki Beslenme Durumunun Meyve, Yaprak ve Zeytinyağında Önemli Kalite Ölçütleri Üzerindeki Etkilerinin Belirlenmesi*. (Unpublished doctoral dissertation). Ege University, İzmir, Türkiye. <https://tez.yok.gov.tr/UlusalTezMerkezi/tezDetay.jsp?id=5x5N4osUXpx8yZKy3HtXdg&no=DcEq7gsZz6KdFBDljV52A>



# Position Control Using Trajectory Tracking and State Estimation of a Quad-rotor

Muharrem Mercimek<sup>1\*</sup>, Onur Sarıpınar<sup>2</sup>

<sup>1</sup>Department of Control and Automation Engineering, Faculty of Electrical and Electronics Engineering, Yıldız Technical University, İstanbul, Türkiye

<sup>2</sup>Department of Control and Automation Engineering, Faculty of Electrical and Electronics Engineering, Yıldız Technical University, İstanbul, Türkiye

## Article History

Received: 23.06.2023

Accepted: 04.09.2023

Published: 20.12.2023

## Research Article

**Abstract** – Quad-rotor aircrafts are unmanned aerial vehicles that have gained significant popularity in recent years and have been developed for use in many areas. Such vehicles are capable of vertical take-off and landing and are used in various applications. To operate a quad-rotor aircraft efficiently and safely, fundamental issues such as mathematical modeling, control, and state estimation need to be studied. Mathematical modeling involves creating a holistic model of the various subsystems of the aircraft including aerodynamic, kinematic, dynamic and control systems. The control system is a mechanism used for the aircraft to perform the desired movements. State estimation techniques are used to obtain and predict information about the state of the aircraft. This study includes position control using a trajectory generation algorithm. Attitude estimation of the quad-rotor is improved with the Explicit Complementary Filter (ECF) and the state estimations is improved with the Extended Kalman Filter (EKF). Different from other studies, the results are obtained by feeding the model with a state estimation filter. The performances of the filters used for state estimation are compared.

**Keywords** – Quad-rotor, position control, trajectory tracking, state estimation

## 1. Introduction

Recently, unmanned aerial vehicles (UAVs) have been ever more attracting the attention of researchers and different kinds of industries due to their versatility, flexibility, low research and development costs (Pines & Bohorquez, 2012; Yoon & Doh, 2022).

Navigating a mobile platform from its initial point to a desired destination is a complex challenge in the field of robotics. A technique to produce time-optimal trajectories with the help of parametric functions was presented in (Bouktir, Haddad & Chettibi, 2008). The vehicle's movement along a path was governed by a continuously increasing function. Their numerical approach was designed to work in cases involving minimum time transfers problems. To move a quad-rotor as quickly as feasible from an initial to a final position, (Cham-seddine, Li, Zhang, Rabbath & Theilliol, 2012) suggested a flatness-based trajectory planner. They used a Sliding Mode Controller (SMC) and a Linear Quadratic Regulator (LQR). Implementing the controller using the linearized model of the vehicle resulted in effectively constraining the roll and pitch angles, demonstrating the success of this approach.

The researchers in (Hoffmann, Waslander & Tomlin, 2008) developed a tracking controller that linked waypoints using line segments at a designated speed. A trajectory tracking system built on model predictive control was presented in (Castillo, Moreno & Valavanis, 2007). Their controller was tested on a miniature helicopter to track the waypoints. To decrease the computational cost the control was tested on a simplified vehicle model.

<sup>1</sup>  [mercimek@yildiz.edu.tr](mailto:mercimek@yildiz.edu.tr)

<sup>2</sup>  [onur.saripinar@std.yildiz.edu.tr](mailto:onur.saripinar@std.yildiz.edu.tr)

\*Corresponding Author

The proportional-integral-derivative (PID) position and velocity tracking controllers and the predictive controller were compared in their research. An optimization-based framework of excavation trajectory generation was developed in (Yang, Long, Song, Pan & Zhang, 2021), various optimizing criteria for different terrains shapes were studied.

One of the traditional problems in quad-rotor is dealing with state estimation. There are literature surveys on filtering techniques to estimate the parameters involved in state estimation. The Kalman filter and the Complementary filter are frequently employed methods in linear systems due to their frequency filtering characteristics (Mahony, Hamel & Ptlimlin, 2008). The Kalman filter is the subject of numerous studies (Hetenyi, Gatzky & Blazovics, 2016; Beck et al., 2016; Sebesta & Boizot, 2014; Hall, Knoebel & McLain, 2008) in the field of flight control. The standard Kalman filter is adapted to calculate the attitude of the air vehicle in (Hall et al., 2008). The estimated values are obtained through the utilization of an enhanced Kalman multiplicative filter. The estimation process incorporates data from accelerometers, gyroscopes, and GPS to gather information. An Unscented Kalman Filter (UKF) was suggested in (De Marina, Pereda, Giron-Sierra & Espinosa, 2012) three-axis attitude determination method as the observer was utilized. It was reported that the method functioned well, but the computational cost was high.

In this study, position control using the state estimation and trajectory tracking of a quad-rotor is implemented. Different from other studies, the results are obtained by feeding the model with a state estimation filter. The performances of the filters used for state estimation are compared.

In Section 2, the mathematical model of the quad-rotor, along with its kinematics, dynamics, and control, is introduced. Section 3 discusses the filter methods developed for state estimation. The experimental results and a comparison of the designed filters are presented in Section 4. Finally, in Section 5, the study concludes by highlighting the accomplishments and discussing potential future work.

## 2. Quad-rotor Mathematical Model

The mathematical model characterizes the motion and behavior of the system based on the input parameters of the model and external factors affecting the system. It relates inputs to outputs. By utilizing the mathematical model, it becomes feasible to anticipate the position as well as the state of the quad-rotor by knowing the propellers' four angular velocities.

The quad-rotor aircraft is capable of maneuvering in three-dimensional space by harnessing the forces generated by its four engines. To maintain the angular momentum, rotors 2 and 4 rotate counterclockwise, while rotors 1 and 3 rotate clockwise. Figure 1 depicts the impact of these rotor forces.

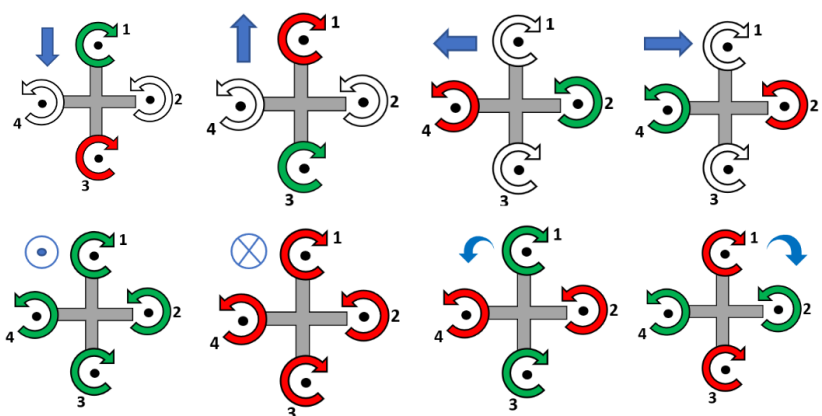


Figure 1. Four rotor movements according to lifting forces (green rings; fast rotation and red rings, slow rotation)

### 2.1. Quad-rotor Coordinate frames

For the mathematical model, it is crucial to establish two coordinate frames (Benic, Piljek & Kotarski, 2016);

- Earth Fixed Frame:  $F^E$  is an inertial right-hand coordinate frame, where the positive direction of the  $Z_E$  axis is from the earth. The quad-rotor attitude  $\eta$  and position  $\xi$  are defined within this coordinate frame (Figure 2).
- Body Fixed Frame:  $F^B$  is a coordinate frame fixed to the quad-rotor's body axis. The origin of  $F^B$  coincides with the quad-rotor's center of gravity. Linear velocities  $v_b$ , angular velocities  $w_b$ , forces  $f_b$ , and torques  $T_b$  are defined within this coordinate frame.

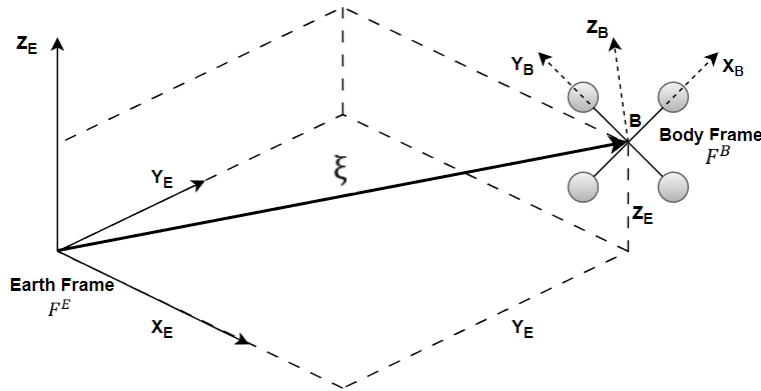


Figure 2. Earth and Body Frames

The quad-rotor's position is determined by the vector  $\xi$ , which represents the displacement between the origin of the Earth Fixed Frame and the Body Fixed Frame;

$$\xi = [x \quad y \quad z]^T. \tag{2.1}$$

The quad-rotor's attitude, denoted by  $\eta$ , is determined by the orientation of the Body Fixed Frame with respect to the Earth Fixed Frame. The orientation is described by three successive rotations around the coordinate axes of the Earth Fixed Frame. The quad-rotor's rotation around the y-axis is governed by the pitch angle  $\theta$ . The rotation around the x-axis is determined by the roll angle  $\varphi$ , and the rotation around the z-axis is determined by the yaw angle  $\psi$ ;

$$\eta = [\varphi \quad \theta \quad \psi]^T. \tag{2.2}$$

### 2.2. Quad-rotor Kinematic Model

The kinematics of a rigid body with 6 degrees of freedom are given by (Benic et al., 2016);

$$\dot{\varepsilon} = Jv \tag{2.3}$$

where  $\dot{\varepsilon}$  is comprised of a vector linear and angular velocity relative to the  $F^B$ . The generalized velocity vector  $v$  is expressed in  $F^B$  and  $J$  represents the generalized transformation matrix.  $\varepsilon$  includes the position  $\xi$  and attitude  $\eta$  as follows;

$$\varepsilon = [\xi \quad \eta]^T = [x \quad y \quad z \quad \varphi \quad \theta \quad \psi]^T. \tag{2.4}$$

Generalized velocity vector  $v$  within  $F^B$  is defined in a similar manner;

$$v = [v^b \quad \omega^b]^T = [u \quad v \quad w \quad p \quad q \quad r]^T. \tag{2.5}$$

The generalized rotation and transformation matrix facilitate the transfer of velocities from the Body Fixed Frame to the Earth Fixed Frame, providing a more intuitive representation of quad-rotor motion. This matrix comprises four submatrices;

$$J = \begin{bmatrix} R & 0_{3 \times 3} \\ 0_{3 \times 3} & T \end{bmatrix} \tag{2.6}$$

where R is the rotation matrix;

$$R = \begin{bmatrix} \cos \psi \cos \theta & \cos \psi \sin \theta \sin \varphi - \sin \psi \cos \varphi & \cos \psi \sin \theta \cos \varphi + \sin \psi \sin \varphi \\ \sin \psi \cos \theta & \sin \psi \sin \theta \sin \varphi + \cos \psi \cos \varphi & \sin \psi \sin \theta \cos \varphi - \cos \psi \sin \varphi \\ -\sin \theta & \cos \theta \sin \varphi & \cos \theta \cos \varphi \end{bmatrix}. \tag{2.7}$$

To address the requirement of converting measured values between different coordinate frames, a rotation matrix is employed. This matrix enables the transfer of the linear velocity vector from one coordinate frame to another through matrix multiplication. The matrix R is used for this purpose and it is an orthonormal matrix.

Angles as well as angular velocities are acquired within the Earth Fixed Frame. To transfer angular velocities from the Body Fixed Frame to the Earth Fixed Frame, a transformation matrix T is utilized;

$$T = \begin{bmatrix} 1 & \sin \varphi \tan \theta & \cos \varphi \tan \theta \\ 0 & \cos \varphi & -\sin \varphi \\ 0 & \frac{\sin \varphi}{\cos \theta} & \frac{\cos \varphi}{\cos \theta} \end{bmatrix}. \tag{2.8}$$

To transfer angular velocities from the Earth Fixed Frame to the Body Fixed Frame, the angular velocity vector in  $F^E$  needs to be multiplied by  $T^{-1}$ .

### 2.3. Quad-rotor Dynamics

The dynamics of a quad-rotor are described using differential equations derived from the Newton-Euler method. These equations incorporate the mass ( $m$ ) and inertia ( $I$ ) of the body, accounting for the dynamics of a rigid body with six degrees of freedom.

Quad-rotor has a symmetrical structure in which the four rotors in the quad-rotor are aligned with the  $X_B$  and  $Y_B$  axes. By assuming that the principal inertial axes align with the coordinate axes of  $F^B$ , the inertial matrix is simplified to a diagonal matrix with  $I_{xx} = I_{yy}$ .

$$I = \begin{bmatrix} I_{xx} & 0 & 0 \\ 0 & I_{yy} & 0 \\ 0 & 0 & I_{zz} \end{bmatrix} \tag{2.9}$$

The dynamics of the quad-rotor are defined as follows;

$$\begin{bmatrix} m I_{3 \times 3} & 0_{3 \times 3} \\ 0_{3 \times 3} & I \end{bmatrix} \begin{bmatrix} \dot{v}^b \\ \dot{\omega}^b \end{bmatrix} + \begin{bmatrix} \omega^b \times (m \omega^b) \\ \omega^b \times (I \omega^b) \end{bmatrix} = \begin{bmatrix} f^B \\ \tau^B \end{bmatrix} \tag{2.10}$$

where  $I_{3 \times 3}$  is the identity matrix. The term  $\dot{v}^b$  refers to the linear acceleration vector,  $\dot{\omega}^b$  represents the angular acceleration vector,  $f^B$  denotes the force vector acting on quad-rotor and  $\tau^B$  represents the torque vector that is exerted on the quad-rotor.

If the generalized force vector is defined as  $\Upsilon$ ;

$$\Upsilon = [f^B \ \tau^B]^T = [F_x \ F_y \ F_z \ \tau_x \ \tau_y \ \tau_z]^T. \tag{2.11}$$

Equation (2.11) can be written in the following form;

$$I_B \dot{v} + C_B(v)v = \Upsilon \tag{2.12}$$

where  $\dot{v}$  represents the generalized acceleration vector,  $I_B$  represents inertia matrix of the system,  $C_B(v)$  represents the Coriolis-centripetal matrix. Parameters of the quad-rotor are given in Table 1.

Table 1  
The parameters of quad-rotor model

Parameter	Value	Unit
$m$	0.95	$kg$
$m_w$	0.01	$kg$
$l$	0.23	$m$
$g$	9.81	$kg\ m/s^2$
$I_w$	0.000065	$kg\ m^2$
$J_x$	0.0075	$kg\ m^2$
$J_y$	0.0075	$kg\ m^2$
$J_z$	0.0013	$kg\ m^2$

2.4. Controller Structure of the Quad-rotor

PID is a common control scheme used in industrial applications. It is widely used for the control of quad-rotors as well. The PID controller receives the feedback signal and compares it with a setpoint or reference signal, resulting in an error signal. Its objective is to minimize the difference between the plant/process variable and the setpoint or reference signal. The controller's behavior is determined by the combination of three control actions: proportional, integral, and derivative. The outputs of these actions are combined and provided as input to the plant/process as follows;

$$u(t) = K_p e(t) + K_i \int_0^t e(t) dt + K_d \frac{de(t)}{dt} \tag{2.13}$$

where,  $K_p$  is the proportion coefficient, the output of the error multiplied by a certain gain value and calculates the current error,  $K_i$  is the integral coefficient, the integral effect means the sum of errors the system has made in the past and  $K_d$  is the derivative coefficient, it has a proportional effect on the output of the system according to the variation of the error. That is, it calculates the estimation of the future error. A conventional PID structure can be depicted using blocks, as shown in Figure 3a. In this study, the position controller, linear velocity controller, attitude controller, and angular velocity controller were designed using PID (Figure 3b) and the values of the PID coefficients were optimized using the MATLAB optimization toolbox. The PID coefficients of controllers are given in Table 2.

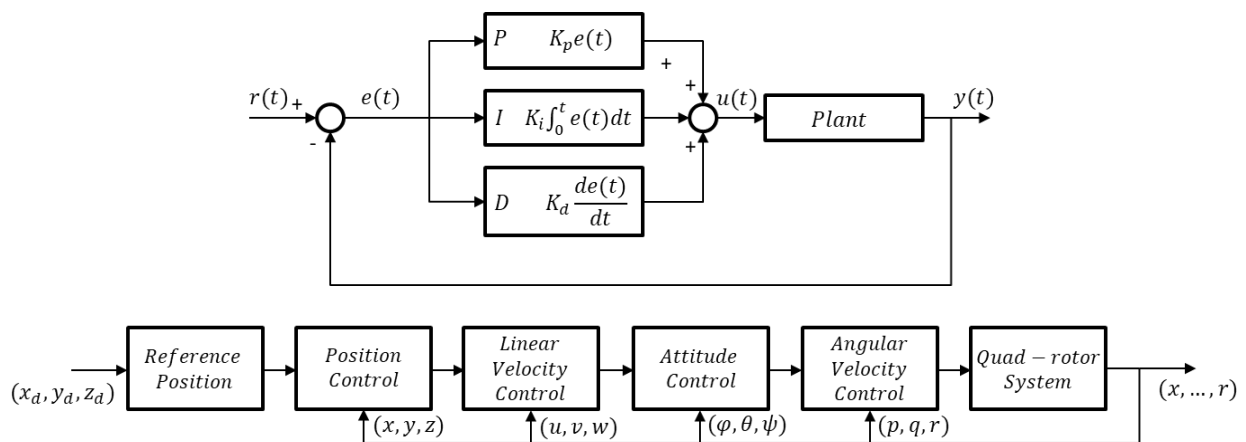


Figure 3. a) General PID controller schematic, b) The overall control blocks for the quad-rotor in this study

Table 2  
PID coefficients of controllers.

Control Terms	Position	Linear Velocity	Attitude	Angular Velocity
$K_p$	6.05	3.1	1.2	0.8
$K_i$	8.15	1.5	0.8	0.69
$K_d$	3.2	0.05	0.03	0.017

The designed controller outputs are shown in Figure 4 and Figure 5. In Figure 4 the reference signal the one that the system should follow when the position information from the trajectory generation algorithm is presented to the quad-rotor system. The signal labeled as 'sensor measurements' contains data obtained from sensor models, where white noise is added to the original sensor data values. Additionally, another signal displays the data as the designed controller outputs. P, Q, R signals shown in Figure 4 correspond to the angular velocity parameters. The North, East Down values indicate the quad-rotor's position along the NED axes The U, V signals presented in Figure 5 are the velocity of the quad-rotor on the NED axes. One can notice that  $\psi$  and W signals are not included in the graphs, since  $\psi$  and W are not controlled indeed in the system designed for the quad-rotor.  $\phi$  and  $\theta$  are the angle between the body axis of the quad-rotor and the NED axes respectively, and they provide essential information about the quad-rotor's attitude. Instead of employing lowercase notation like  $(p, q, r)$ , it becomes evident that the use of uppercase letters like P, Q, R serves to signify these signals within the simulations.

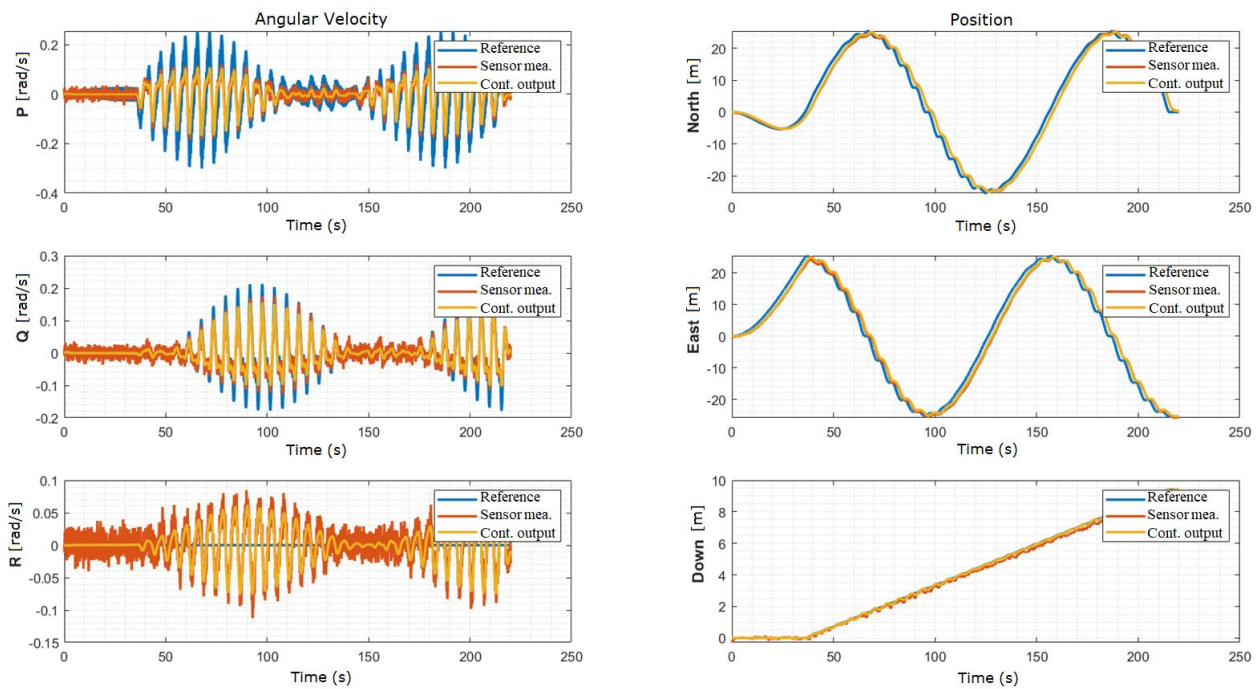


Figure 4. Angular velocity control and position control

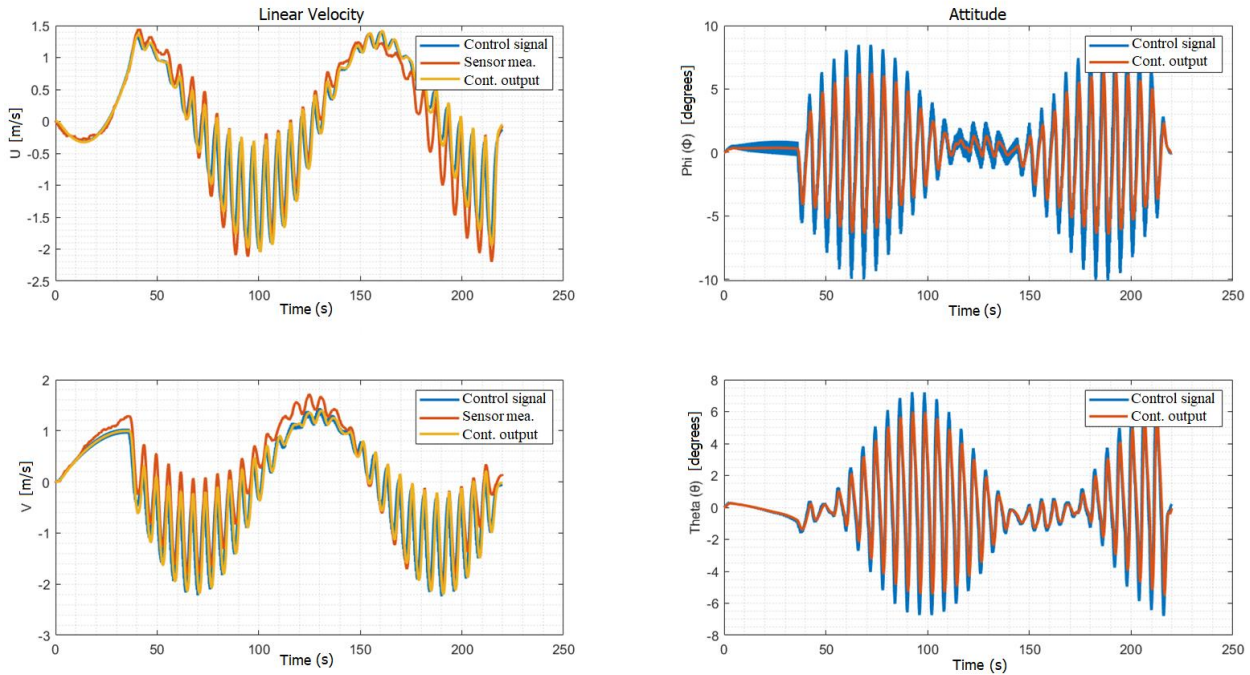


Figure 5. Linear velocity control and attitude control

### 2.5. Trajectory Tracking Algorithm

To initiate the trajectory tracking algorithm, the initial step involves generating a trajectory for subsequent tracking. The waypoints represent the planned path that the dynamic system should follow to efficiently achieve the tracking. The trajectory generation algorithm populates waypoints at a specified sampling rate and trajectory model. This trajectory then serves as the source for providing reference values for yaw angle, altitude, and linear velocity. The control system operates on these trajectories.

In the trajectory generation algorithm, the desired positions, i.e. waypoints, are determined on the (x, y, z) axes and the desired speed is determined at these waypoints. A system of linear equations will be created and generated with the help of the matrix.

The position of the quad-rotor equation can be expressed as follows;

$$\begin{aligned}
 x(t) &= a_0 + a_1t + a_2t^2 + a_3t^3 \\
 y(t) &= b_0 + b_1t + b_2t^2 + b_3t^3 \\
 z(t) &= c_0 + c_1t + c_2t^2 + c_3t^3
 \end{aligned}
 \tag{2.14}$$

where  $t$  is time, and each one is a cubic function with real coefficients. The velocity of the quad-rotor equation can be expressed as follows;

$$\begin{aligned}
 v_x(t) = \dot{x}(t) &= a_1 + 2a_2t + 3a_3t^2 \\
 v_y(t) = \dot{y}(t) &= b_1 + 2b_2t + 3b_3t^2 \\
 v_z(t) = \dot{z}(t) &= c_1 + 2c_2t + 3c_3t^2
 \end{aligned}
 \tag{2.15}$$

2.16 is obtained by solving 2.14 and 2.15 by specifying the first condition with an index value of 0 and the last condition with an index value  $f$ ;

$$G = \begin{bmatrix} 1 & t_0 & t_0^2 & t_0^3 \\ 1 & t_f & t_f^2 & t_f^3 \\ 0 & 1 & 2t_0 & 3t_0^2 \\ 0 & 1 & 2t_f & 3t_f^2 \end{bmatrix}, \begin{bmatrix} x_0 \\ x_f \\ v_{x0} \\ v_{xf} \\ y_0 \\ y_f \\ v_{y0} \\ v_{yf} \\ z_0 \\ z_f \\ v_{z0} \\ v_{zf} \end{bmatrix} = \begin{bmatrix} G & 0_{4 \times 4} & 0_{4 \times 4} \\ 0_{4 \times 4} & G & 0_{4 \times 4} \\ 0_{4 \times 4} & 0_{4 \times 4} & G \end{bmatrix} \begin{bmatrix} a_0 \\ a_1 \\ a_2 \\ a_3 \\ b_0 \\ b_1 \\ b_2 \\ b_3 \\ c_0 \\ c_1 \\ c_2 \\ c_3 \end{bmatrix} \tag{2.16}$$

The following expressions represent the linear matrix equations;

$$A\kappa = \mathcal{B} \tag{2.17}$$

$$\kappa = A^{-1}\mathcal{B} \tag{2.18}$$

and there is a very concise way of writing a system of linear equations, where  $A$  is a matrix,  $\kappa$  and  $\mathcal{B}$  are vectors (usually of different sizes). As a result of the solution of the expression given in 2.16, the above linear equation results in a cubic polynomial that generates a trajectory according to the desired velocity dynamics between the start and end waypoints. Controlling the velocity dynamics as a result of generating the third-degree polynomial is important in terms of control. To control the applied force, a higher-order polynomial proposition can be made that can be reduced to the derivative of the acceleration.

Each range of waypoints is expressed by a different equation as a result of applying the trajectory generation algorithm to each one separately. The trajectory generation algorithm was given to the quad-rotor as a position reference. Thus, the quadcopter successfully followed the specified trajectory. The simulation results of trajectory tracking created according to the equations 2.14-2.18 are shown in Figure 6.

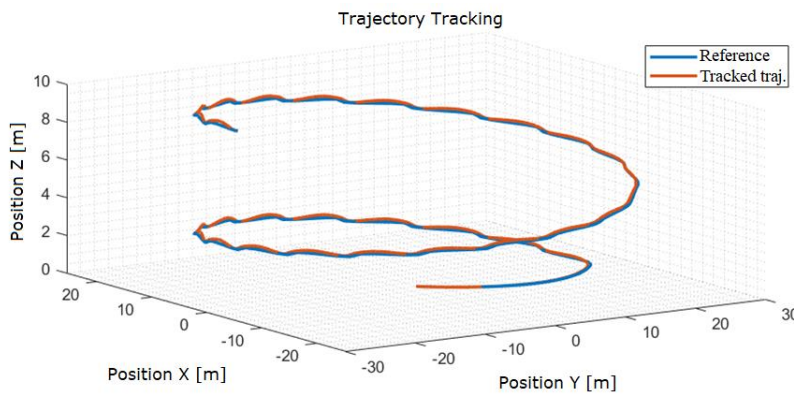


Figure 6. Trajectory tracking

### 3. Quad-rotor Attitude Estimation

Accurate and reliable attitude estimation is required for quad-rotor aircraft to fly successfully and perform their tasks. Attitude estimation is the process of estimating the current state of the aircraft, i.e., its position, speed, attitude, and angular velocity. A quad-rotor aircraft is usually equipped with various sensors such as accelerometers, gyroscopes, magnetometers, and barometers. These sensors measure the speed, acceleration, altitude, and orientation of the aircraft. However, the accuracy and precision of the sensors can be limited and may give inaccurate measurements due to external factors. Therefore, filtering and estimation algorithms are used in state estimation. Widely utilized algorithms, such as the Complementary Filter and Kalman Filter, analyze sensor data and rectify errors to estimate the aircraft's state. By leveraging sensor data and taking into

account the physical model, these filtering algorithms make use of estimation techniques to determine the current state.

### 3.1. Explicit Complementary Filter use for Attitude Estimation

The attitude estimation complementary filter employs low-pass filtering to refine a low-frequency attitude estimate. The attitude estimate is derived by applying high-pass filtering to biased high-frequency accelerometer data and integrating the output of the gyroscope. These estimates are then combined to obtain a comprehensive estimate of attitude. If the pitch angle and roll angle of a quad-rotor are treated as decoupled processes, it is possible to design a Single Input Single Output filter for each signal, (Buskey, Roberts, Corke, Ridley & Wyeth, 2004). Figure 7 depicts the Explicit Complementary Filter (ECF) implementation.

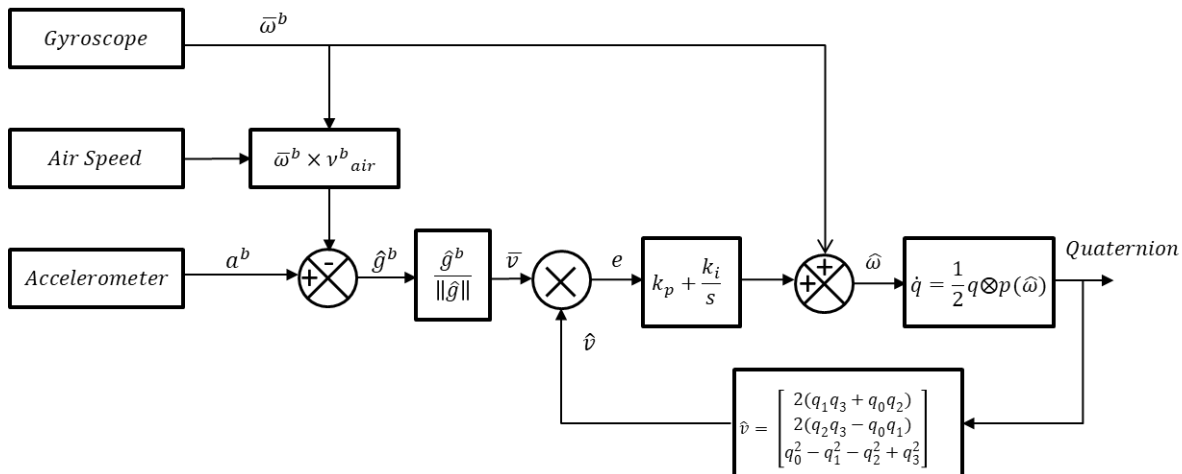


Figure 7. Acceleration compensated Explicit Complementary Filter scheme (edited from (Euston, Coote, Mahony, Kim & Hamel, 2008)

In addition to the measured angular velocities  $\bar{\omega}^b$ , the ECF also captures the inertial direction, indicated as  $\bar{v}$ ;

$$\bar{v} = \frac{\hat{g}^b}{|\hat{g}^b|} \tag{3.1}$$

where the estimation of the gravitational direction  $\hat{g}^b$  obtained from the system is used to derive the inertial direction  $\bar{v}$ .

The ECF can be represented as a quaternion as follows (Euston et al., 2008);

$$\dot{\hat{q}} = \frac{1}{2} \hat{q} \otimes p(\hat{\omega} + \delta) \tag{3.2}$$

$$\delta = k_p e + k_i \frac{e}{s} \tag{3.3}$$

$$e = \bar{v} \times \hat{v} \tag{3.4}$$

where  $\hat{q}$  represents an estimate of the system attitude in a quaternion form. The innovation term  $\delta$  here is generated by a PI block and the error  $e$  represents the relative rotation between the measured inertial direction  $\bar{v}$  and the predicted inertial direction  $\hat{v}$ . The proportional gain is denoted as  $k_p$ , while  $k_i$  represents the integral gain.

The estimated gravitational direction  $\hat{v}$  aligns with the z-axis of the inertial frame;

$$\hat{v} = \begin{bmatrix} 2(q_1q_3 + q_0q_2) \\ 2(q_2q_3 - q_0q_1) \\ q_0^2 - q_1^2 - q_2^2 + q_3^2 \end{bmatrix}. \quad (3.5)$$

The most common approach for compensation with the ECF involves the use of proportional or proportional-integral (PI) control. The proportional component is used to make the frequency transition between the gyro estimates obtained by the quaternion update and the attitude estimates based on accelerometers. Gyro bias is adjusted for the use of the integral term in the PI correction.

### 3.2. Extended Kalman Filter use for State Estimation

The Extended Kalman Filter (EKF) utilizes both the system and observation expressions to perform state estimation in nonlinear systems. The algorithm uses the final prediction state and the associated error covariance matrix to perform state estimation.

The EKF filter linearizes the system equations using the Taylor series or by taking the Jacobian. It then computes the prediction state using the linearized system equations. (Crasidis & Junkis, 2011). The observation equations are similarly linearized and provide feedback to ensure agreement between the forecast state and actual observations. This process updates the system state and covariance matrix, reducing errors and providing a more accurate estimate (Wang, Yang, Hatch & Zhang, 2004);

$$\begin{aligned} x_k &= f(x_{k-1}, u_k) + w_k \\ z_k &= h(x_k) + v_k \end{aligned} \quad (3.6)$$

where  $w_k$  represents the normal random process with zero mean and covariance matrix  $Q_k$ .  $v_k$  represents the white Gaussian noise in the measurements also with zero mean and covariance matrix  $R_k$ .  $u$  denotes the control vector, while  $z_k$  represents the output of sensors measuring the state vector component  $x_k$  of the state vector at time step  $k$ . Considering 2.4 and 2.5, the state vector can be expressed in the form as follows;

$$x_k = [x \ y \ z \ u \ v \ w \ \varphi \ \theta \ \psi]^T. \quad (3.7)$$

Expressions in 3.6 are nonlinear; therefore, we use the EKF where the model is linearized in a certain neighborhood of the considered point  $(\hat{x}^k, u_k)$  via an expansion into a Taylor series (Crasidis & Junkins, 2011);

$$\begin{aligned} x^{k+1} &\approx f(\hat{x}^k, u_k) + F_k(x - \hat{x}^k) + w_k \\ z_k &\approx h(\hat{x}^k) + H(x_k - \hat{x}^k) + v_k \end{aligned} \quad (3.8)$$

where

$$F_k = \left( \frac{\partial f}{\partial x} \Big|_{x = \hat{x}^k} \right), H_k = \left( \frac{\partial h}{\partial x} \Big|_{x = \hat{x}^k} \right) \quad (3.9)$$

The expressions for extrapolation and correction of the EKF follow;

$$\hat{x}^k = f(\hat{x}^{k-1}, \hat{u}^{k-1}) \quad (3.10)$$

$$P_k = F_k P_{k-1} F_k^T + Q_k \quad (3.11)$$

$$K_k = \frac{P_k H_k^T}{H_k P_k H_k^T + R_k} \quad (3.12)$$

$$P_k = (I - K_k H_k) P_k \quad (3.13)$$

### 4. Experimental Results

In this section, the position control using trajectory generation and state estimation of the quad-rotor implemented in MATLAB ®2022a Simulink environment are presented. The model runs by feeding the estimation results to the controller.

The North, East, and Down (NED) position of the quad-rotor and the result of the EKF filter are shown in Figure 8. The North, East, and Down (NED) velocity of the quad-rotor and the result of the EKF filter are shown in Figure 9. Quad-rotor attitude is estimated with ECF and EKF and the results are shown in Figure 10. The data represented with the legend sensor measurements is the position/velocity/direction information obtained from the GNSS sensor model of the system.

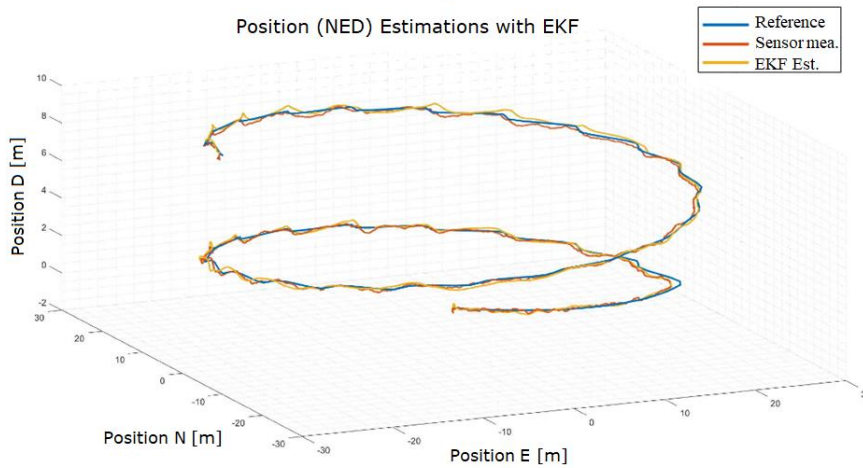


Figure 8. North, East, and Down (NED) position of the quad-rotor

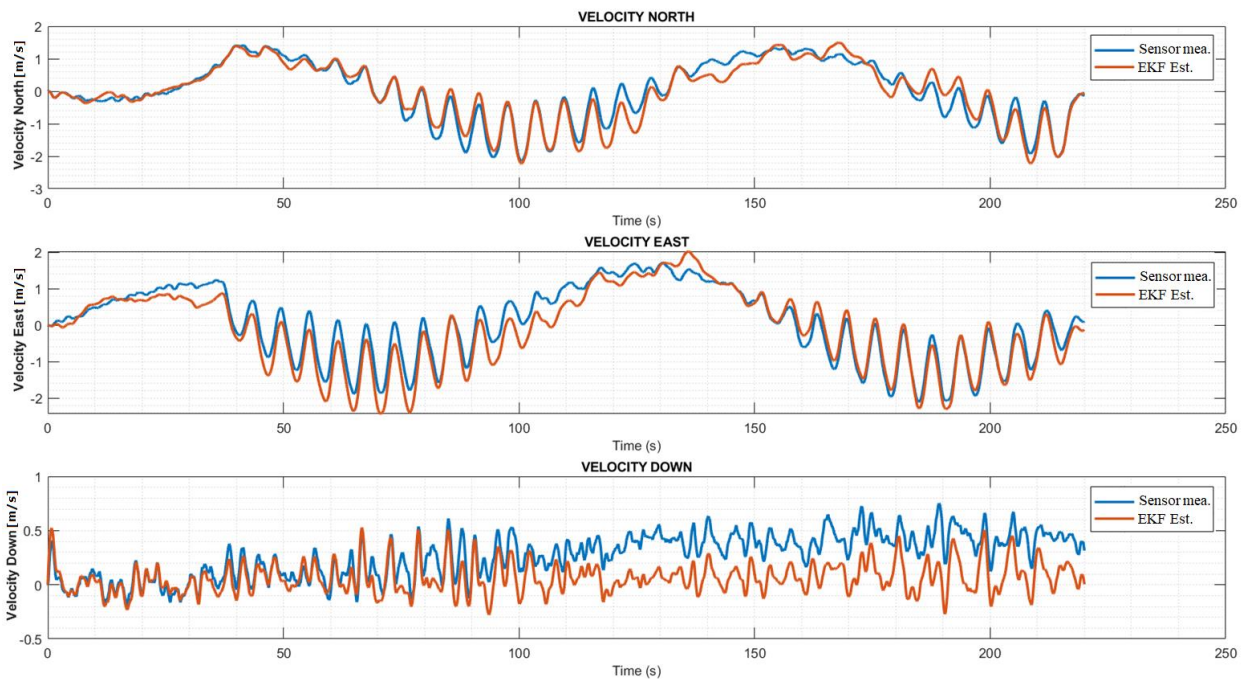


Figure 9. North, East, and Down (NED) velocity of the quad-rotor

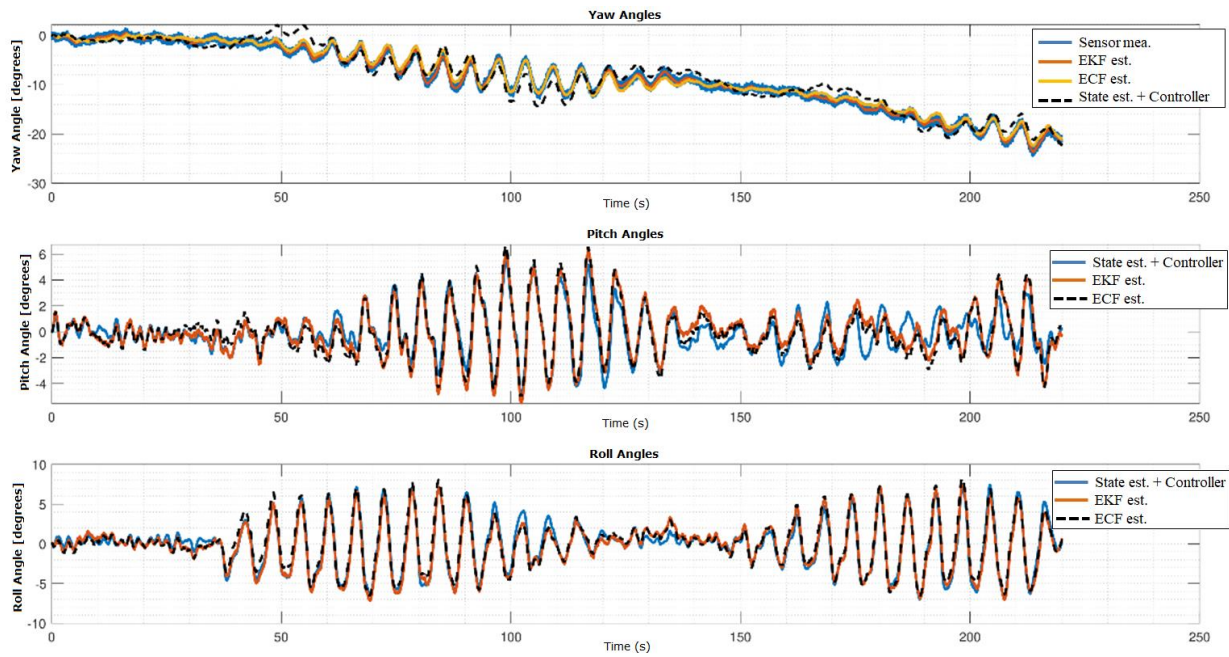


Figure 10. The attitude angles of the quad-rotor

The Root Mean Square Error (RMSE) values of the estimated states with EKF filter are given in the Table 3, since the error difference is difficult to notice on the figures. The values shown in this table vary depending on the process noise matrix and the Gaussian measurement noise matrix which are normally utilized with zero mean and covariance matrix. These matrices are formed considering parameters of the utilized sensor models and their regular working conditions. Upon examining the outcomes, it is evident that the EKF filter exhibits minimal prediction errors. Table 4 illustrates the RMSE values of the attitude estimation errors for EKF and ECF filters. The RMSE values given in this table were created by taking the attitude signal difference between filter estimations and the reference signals computed from the trajectory. The attitude estimation accuracy of the ECF filter is worse than that of the EKF filter, regarding the RMSE values of the filters' attitude estimates. This is because the ECF method is a fixed gain filter and cannot track the dynamic properties of the quad-rotor adaptively. The EKF and ECF filter estimation errors are computed for both the noisy and noise free data.

Table 3

The RMSE of the EKF state estimation

State	RMSE
Position [NED]	0.449 m
Velocity [NED]	0.25 m/s
Yaw ( $\psi$ )	0.26 °
Pitch ( $\theta$ )	0.22 °
Roll ( $\varphi$ )	0.22 °

Table 4  
Attitude estimation of filters comparison table

RMS	Yaw ( $\psi$ )	Pitch ( $\theta$ )	Roll ( $\varphi$ )	Simulated Data Behaviour
ECF Error	1,62°	0,89°	0,76°	Noisy
EKF Error	0,62°	0,8°	0,61°	Noisy
EKF-ECF Error	1,55°	0,4°	0,64°	Noisy
ECF Error	0,97°	0,59°	0,51°	Noise Free
EKF Error	0,42°	0,54°	0,59°	Noise Free
EKF-ECF Error	1,18°	0,32°	0,58°	Noise Free

## 5. Conclusions

In this study, the state estimation, and position control using trajectory generation of a quad-rotor aircraft are implemented. The performances of the filters used for state estimation are compared.

Position control was executed on the quad-rotor by planning an optimal path as waypoints within the trajectory tracking algorithm. These waypoints were populated and used to create a trajectory through the trajectory generation algorithm at a specified sampling rate.

Dynamic modeling of the system was conducted, and sensor models were developed for state estimation. Explicit Complementary Filter and Extended Kalman Filter are designed for attitude estimation and state estimation respectively. Differing from other studies, we integrated the output of the designed filter into the controller while the quad-rotor tracked the trajectory. Our analysis revealed that the filters introduced minimal errors during quad-rotor trajectory tracking.

In our upcoming research, we will focus on path planning and trajectory optimization for the quad-rotor. We will also explore state estimation techniques, including the Unscented Kalman Filter (UKF), Adaptive Gain Complementary Filter (AGCF), and Particle Filters (PF), and compare their state estimates.

## Author Contributions

Muharrem Mercimek: All design activities, experimental studies, measurements, and theoretical calculations were made under the supervision of Muharrem Mercimek. The manuscript was formulated, edited, and revised by the same author.

Onur Sarıpinar: The system model for the quad-rotor was created; the position controller, the trajectory tracking algorithm, and the design of the attitude estimation filters were implemented by Onur Sarıpinar. The analysis of the filters that perform state estimation was also carried out by the same author.

## Conflicts of Interest

The authors declare no conflict of interest.

## References

- Baldi, T.L., Farina, F., Garulli, A., Giannitrapani, A., and Prattichizzo, D. (2019). Upper Body Pose Estimation Using Wearable Inertial Sensors and Multiplicative Kalman Filter. *IEEE Sens. J.*, 20, 492–500. DOI: <https://doi.org/10.1109/JSEN.2019.2940612>
- Beck, H. Lesueur, J., Charland-Arcand, G., Akhrif, O., Gagne, S., Gagnon F., and Couillard, D. (2016). Autonomous takeoff and landing of a quadcopter. *International Conference on Unmanned Aircraft Systems (ICUAS)*, 475-484. DOI: <https://doi.org/10.1109/ICUAS.2016.7502614>
- Benic, Z, Piljek, P., and Kotarski, D. (2016). Mathematical modelling of unmanned aerial vehicle with four

- rotors. *Interdisciplinary Description of Complex Systems*, 14(1), 88-100.  
DOI: <http://dx.doi.org/10.7906/indecs.14.1.9>
- Bouktir, Y. Haddad, M., and Chettibi, T.(2008).Trajectory planning for a quad-rotor helicopter. *16th Mediterranean Conference on Control and Automation*, 1258–1263.  
DOI: <https://doi.org/10.1109/MED.2008.4602025>
- Buskey, G., Roberts, J., Corke, P., Ridley, P., and Wyeth, G. (2004) Sensing and control for a small-size helicopter. *Experimental Robotics VIII: Springer Tracts in Advanced Robotics*, 5.  
DOI: [https://doi.org/10.1007/3-540-36268-1\\_43](https://doi.org/10.1007/3-540-36268-1_43)
- Castillo, C. L., Moreno, W., and Valavanis, K. P., (2007). Unmanned helicopter waypoint trajectory tracking using model predictive control. *Mediterranean Conference on Control and Automation*.  
DOI: <https://doi.org/10.1109/MED.2007.4433726>
- Chamseddine, A., Li, T., Zhang, Y., Rabbath, C.-A. and Theilliol, D. (2012). Flatness-based trajectory planning for a quad-rotor unmanned aerial vehicle test-bed considering actuator and system constraints. *American Control Conference (ACC)*, 920–925.  
DOI: <https://doi.org/10.1109/ACC.2012.6315362>
- Crasidis, J. L., Junkis, J. L. (2011) *Optimal Estimation of Dynamic Systems Second Edition* –CRC.
- De Marina, H. G., Pereda, F. J., Giron-Sierra, J. M. and Espinosa, F. (2012). UAV attitude estimation using unscented Kalman filter and triad. *IEEE Transactions on Industrial Electronics*, 59(11), 4465-4474.  
DOI: <https://doi.org/10.1109/TIE.2011.2163913>
- Euston, M., Coote, P., Mahony, R., Kim J., and Hamel, T. (2008). A complementary filter for attitude estimation of a fixed-wing UAV. *2008 IEEE/RSJ International Conference on Intelligent Robots and Systems*, Nice, France, 340-345. DOI: <https://doi.org/10.1109/IROS.2008.4650766>
- Hall, J. K., Knoebel, N. B., and McLain, T. W. (2008). Quaternion attitude estimation for miniature air vehicles using a multiplicative extended Kalman filter. *IEEE Position, Location and Navigation Symposium*, 1230- 1237. DOI: <https://doi.org/10.1109/PLANS.2008.4570043>
- Hetenyi, D., Gatzky, M. and Blazovics, L. (2016). Sensor fusion with enhanced Kalman Filter for altitude control of quad-rotors. *IEEE 11th International Symposium on Applied Computational intelligence and Informatics (SACI)*, 413-418. DOI: <https://doi.org/10.1109/SACI.2016.7507412>
- Hoffmann, G., Waslander, S., and Tomlin, C. (2008). Quad-rotor helicopter trajectory tracking control. *AIAA Guidance, Navigation and Control Conference and Exhibit*, 1–14.  
DOI: <https://doi.org/10.2514/6.2008-7410>
- Markley, F.L., Crassidis, J.L. (2014). *Fundamentals of Spacecraft Attitude Determination and Control*. Space Technology Library, 33. Springer, New York, NY. DOI: <https://doi.org/10.1007/978-1-4939-0802-8>
- Mahony, R., Hamel T., and Pflimlin, J.-M. (2008). Nonlinear complementary filters on the special orthogonal group. *IEEE Trans. on Automatic Control*, 53(5), 1203-1218.  
DOI: <https://doi.org/10.1109/TAC.2008.923738>
- Pines D. J., Bohorquez F. (2012). Challenges Facing Future Micro-Air-Vehicle Development, *Journal of Aircraft*, 43(2):290-305. DOI: <https://doi.org/10.2514/1.4922>
- Sebesta, K.-D., Boizot, N. (2014). A real-time adaptive high-gain EKF, Applied to a quadcopter inertial navigation system. *IEEE Trans. on Industrial Electronics*, 61(1), 495-503.  
DOI: <https://doi.org/10.1109/TIE.2013.2253063>
- Shen, C., Zhang, Y., Guo, X., Chen, X., Cao, H., Tang, J., Li, J., Liu, J. (2020). Seamless GPS/inertial navigation system based on self-learning square-root cubature Kalman filter. *IEEE Transactions on Industrial Electronics*, 68(1), 499–508. DOI: <https://doi.org/10.1109/TIE.2020.2967671>
- Suh, Y.S. (2020). Attitude Estimation Using Inertial and Magnetic Sensors Based on Hybrid Four-Parameter Complementary Filter. *IEEE Trans. Instrum. Meas.*, 69, 5149–5156.  
DOI: <https://doi.org/10.1109/TIM.2019.2950826>
- Usman, M. (2020) *Quad-rotor Modelling and Control with MATLAB/Simulink Implementation*, Thesis (B.S.), LAB University of Applied Sciences.
- Vik, B., Fossen, T. I. (2001). A nonlinear observer for GPS and INS integration. *40th IEEE Conference on Decision and Control*, 2001. DOI: <https://doi.org/10.1109/CDC.2001.980726>
- Wang, M., Yang, Y., Hatch, R.R., and Zhang, Y. (2004). Adaptive filter for a miniature mems-based attitude and heading reference system. *Position Location and Navigation Symposium*, 193–200, 26-29 April,

2004. DOI: <https://doi.org/10.1109/plans.2004.1308993>

Yang, Y., Long, P., Song, X., Pan, J., and Zhang, L. (2021). Optimization-Based Framework for Excavation Trajectory Generation. *IEEE Robotics and Automation Letters*, 6(2), April, 2021.

DOI: <https://doi.org/10.1109/LRA.2021.3058071>

Yoon, J., Doh, J. (2022). Optimal PID control for hovering stabilization of quadcopter using long short term memory. *Advanced Engineering Informatics*, 53, 101679.

DOI: <https://doi.org/10.1016/j.aei.2022.101679>

Zheng, L., Zhan, X., Zhang, X. (2020). Nonlinear Complementary Filter for Attitude Estimation by Fusing Inertial Sensors and a Camera. *Sensors*, 20, 6752. DOI: <https://doi.org/10.3390/s20236752>

Zuo, Z. (2010). Trajectory tracking control design with command-filtered compensation for a quad-rotor, *IET Control Theory Appl.*, 4, (11), 2343–2355. DOI: <https://doi.org/10.1049/iet-cta.2009.0336>



## Yapı Bilgi Modellemesi ve Coğrafi Bilgi Sistemleri Entegrasyonu için IFC'den CityGML ve CityJSON Veri Formatlarına Dönüşümün İncelenmesi

Özlem Korkmaz<sup>1,\*</sup>, Melih Başaraner<sup>2</sup>

<sup>1,2</sup> Harita Mühendisliği Bölümü, İnşaat Fakültesi, Yıldız Teknik Üniversitesi, İstanbul, Türkiye

### Makale Tarihçesi

Gönderim: 23.08.2023  
Kabul: 20.09.2023  
Yayın: 20.12.2023

### Araştırma Makalesi

**Öz** – Yapı bilgi modellemesi (YBM) ve coğrafi bilgi sistemleri (CBS) entegrasyonu; yapı ve tesis planlama ve yönetimi, akıllı şehirler ve mekânsal dijital ikiz gibi uygulamalar için kritik öneme sahiptir. YBM, yapı yaşam döngüsü boyunca zengin geometrik ve semantik bilgilere sahipken, CBS; mekânsal modelleme, analiz ve görselleştirme yetenekleri sağlar. Bu nedenle, YBM ve CBS iç ve dış mekân bağlamında birbirini tamamlayan temel sistemlerdir. Öte yandan, uygulama odakları, mekânsal kapsamlar, koordinat sistemleri, semantik ve geometrik temsiller ve ayrıntı düzeyleri açısından farklılıklara sahip olmaları, bu iki sistemin entegrasyonunda zorluklar meydana getirmektedir. Entegrasyon için veri düzeyinde geometrik dönüşüm ve semantik aktarım yapılmalıdır. YBM verileri için genel olarak endüstri temel sınıfları (IFC), CBS verileri için ise CityGML, CityJSON veya shape dosyası formatı kullanılmaktadır. Entegrasyon için bazı teknikler ve teknolojiler mevcut olsa da halen çözülmemiş sorunlar mevcuttur. Bu nedenle, YBM ve CBS entegrasyonu ve veri değişim formatları aktif araştırma konusu olmaya devam etmektedir. CityJSON'ın kent modellerini 3B temsil etmek için kullanılan yeni bir veri standardı olması nedeniyle veri değişimi için uygulanmasına yönelik çok fazla çalışma bulunmamaktadır. Ayrıca, CityGML'in hafif versiyonu olarak oluşturulan CityJSON'ın uygulamalarda CityGML'den farkı merak konusudur. Bu çalışmada, IFC formatındaki üç farklı yapıya ait YBM veri seti, semantik aktarım ve geometrik dönüşüm ile Safe FME Workbench yazılımı kullanılarak CityGML ve CityJSON formatlarına dönüştürülmüştür. Bu bağlamda, YBM'den CBS'ye dönüşüm incelenmiş ve CityGML ile CityJSON veri değişim formatları ile elde edilen bulgular değerlendirilmiştir.

**Anahtar Kelimeler** – Yapı bilgi modellemesi, coğrafi bilgi sistemleri, veri entegrasyonu, semantik aktarım, geometrik dönüşüm

## An Investigation of Conversion from IFC to CityGML and CityJSON Data Formats for Building Information Modeling and Geographic Information Systems Integration

<sup>1,2</sup> Department of Geomatic Engineering, Faculty of Civil Engineering, Yıldız Technical University, İstanbul, Türkiye

### Article History

Received: 23.08.2023  
Accepted: 20.09.2023  
Published: 20.12.2023

### Research Article

**Abstract** – The integration of building information modeling (BIM) and geographic information systems (GIS) is critical for applications such as construction and facility planning and management, smart cities and spatial digital twin. While BIM has rich geometric and semantic information throughout the building lifecycle, GIS provides spatial modeling, analysis, and visualization capabilities. Therefore, BIM and GIS are fundamental systems that complement each other in the context of indoor and outdoor spaces. On the other hand, the differences in application focus, spatial scopes, coordinate systems, semantic and geometric representations and levels of detail create challenges in the integration of these two systems. Industry foundation classes (IFC) are generally used for BIM data, and CityGML, CityJSON or shape file formats are used for GIS data. For BIM data, IFC are generally used, while for GIS data, CityGML, CityJSON, or shapefile formats are employed. Moreover, the distinction between CityJSON, developed as a light version of CityGML, and its implementation in applications compared to CityGML is a subject of interest. In this study, BIM datasets of three different structures in IFC format are converted into CityGML and CityJSON formats through semantic transfer and geometric transformation with FME Workbench software. In this context, the conversion from BIM to GIS is investigated, and obtained findings are evaluated by comparing the CityGML and CityJSON data exchange formats.

**Keywords** – Building information modeling, geographic information systems, data integration, semantic transfer, geometric transformation

<sup>1</sup> okorkmaz@yildiz.edu.tr

<sup>2</sup> mbasaran@yildiz.edu.tr

\*Sorumlu Yazar

## 1. Giriş

Son yıllarda yapı bilgi modellemesi (YBM), coğrafi bilgi sistemleri (CBS), sanal/artırılmış gerçeklik (VR/AR) ve nesnelerin interneti (IOT) gibi bilgi ve iletişim teknolojilerinde yaşanan gelişmelerle birlikte, akıllı şehirler, dijital ikiz ve yapıların yaşam döngülerinin yönetimi gibi uygulamalar üzerine çalışmalar yoğunlaşmıştır (Sulaiman, Liu, Binalhaj, Al-Kasasbeh, ve Abudayyeh, 2021). Bu uygulamalar için YBM ve CBS, temel sistemler olarak kullanılmaktadır. YBM ve CBS entegrasyonu, YBM'deki bina modellerinin görselleştirme ve analiz için bir CBS ortamına entegre edilmesini gerektiren akıllı şehir ve mekânsal dijital ikiz için temel bir tekniktir (Xia, Liu, Efremochkina, Liu, ve Lin, 2022; Zhu ve Wu, 2021a). Bu amaçla, YBM verilerinin CBS tarafından erişilen bir biçime/formata dönüştürülmesi gerekir (Zhu vd., 2021a). YBM ve CBS entegrasyonu, bina yaşam döngüsü yönetiminin her aşamasında çevrenin binaya ve binanın çevreye etkilerinin anlaşılmasına katkı sağlar. Böylelikle, bina yaşam döngüsünde bulunan fizibilite, planlama, inşaat, operasyon ve bakım aşamalarında sürdürülebilir kararların alınması, uygulama takviminin geliştirilmesi, belirli bir konumdaki inşaat maliyetinin belirlenmesi ve bina performans analizleri daha kolay hale gelmektedir (Bansal, 2021). Bina yaşam döngüsünde; tadilat, güçlendirme ve yenileme tesis yönetiminin önemli bileşenleridir (Wong, Ge, ve He, 2018). YBM teknolojisi, paydaşlar arasındaki iletişimi geliştirmek için binalar ile ilgili bilgileri içeren üç boyutlu (3B) bir bina modeli sağlarken; CBS, bina çevresiyle ilgili bilgilerin analizi ile mekânsal verilerden yararlanarak tesis yönetimindeki çalışmaları kolaylaştırır (Sulaiman vd., 2021). YBM ve CBS entegrasyonu, acil durum yönetimi gibi iç mekân uygulamaları (örneğin, bir yangın durumunda yönlendirme ve tahliye yollarını bulma) (Isikdag, Underwood, Aouad, ve Troud, 2007; Chen, Wu, Shen, ve Chou, 2014) etkin enerji (Niu, Pan, ve Zhao, 2015) ve çevre yönetimi (Zhao, Liu, ve Mbachu, 2019; Wang, Deng, Won, ve Cheng, 2019), kesintisiz navigasyon (Teo ve Cho, 2016) gibi iç ve dış mekân bağlantısı gerektiren servisler (Kang, 2018) gibi pek çok uygulamada kullanılabilir.

YBM, 3B nesne tabanlı bir modellemedir. Nesnelere parametrelerle (örneğin, yükseklik ve derinlik) ve kuralarla (örneğin, bir duvar yüksekliği azaltılırsa, çatı konumunun otomatik olarak değişmesi) temsil ederek özelliklerle birlikte geometri oluşturmaya olanak sağlar (Bolpagni, 2022). CBS, yeryüzündeki veya yakınındaki mekânsal olarak tanımlanabilen nesnelerin ve olayların modellenmesi, analizi ve sunumu için bilgisayar tabanlı bir araçtır. CBS teknolojisi, sorgu ve istatistiksel analiz gibi yaygın veri tabanı işlemlerini haritaların sunduğu benzersiz mekânsal görselleştirme ve analiz avantajlarıyla bütünleştirir (Longley, 2008; Longley, Goodchild, Maguire, ve Rhind, 2015). YBM, yapıyı çevreleyen mekândan bağımsız lokal bir koordinat sistemi kullanırken; CBS, doğrudan ya da dolaylı olarak bir coğrafi koordinat sisteminde tanımlı olup yapının çevresiyle bağlantı sağlayan bir köprü niteliğindedir (Bansal, 2021). Öte yandan, YBM ve CBS'de farklı kavramsal veri modelleri ve formatları kullanıldığı için veri alışverişinde problemler meydana gelmektedir (Zhu vd., 2021a). YBM ve CBS entegrasyonu, iki metodoloji arasındaki ayrıntı düzeyleri, geometrik temsil yöntemleri, arşivleme yöntemleri ve semantik içerik açısından farklılıklar nedeniyle karmaşıktır (Vacca ve Quaquero, 2020). Bu amaca yönelik olarak literatürde birçok çalışma mevcuttur. Genellikle YBM'den CBS'ye veri dönüşümü yapılsa da CBS'den YBM'ye, YBM ve CBS'nin üçüncü bir sisteme aktarılması biçiminde üç farklı entegrasyon yapılabilmektedir (Ma ve Ren, 2017; Zhu ve Wu, 2022).

YBM/CBS veri dönüşümü yapılırken YBM verileri için endüstri temel sınıfları (industry foundation classes - IFC), 3B CBS verileri için ise CityGML, CityJSON (Ohuri, Ledoux, ve Peters, 2022a) ve shape dosyası formatı kullanılmaktadır (Zhu vd., 2022). IFC; buildingSMART tarafından mimarlık, mühendislik ve inşaat (AEC) uygulama alanı içinde bilgi alışverişi için oluşturulan birincil açık veri şemasıdır (Herle, Becker, Wollenberg, ve Blankenbach, 2020). CityGML ise OGC tarafından genişletilebilir işaretleme dili (XML) formatında tanımlanan coğrafya işaretleme dili (GML)'ne dayalı olarak şehirlerin ve çevresinin 3B modellerini depolama kapasitesine sahip açık standartlı bir veri modeli ve değişim formatıdır (Sani ve Rahman, 2018). YBM, geometrik ve semantik verilerden oluşmaktadır. Geometri; nesnelerin şekli, büyüklüğü ve konumu hakkında veri sağlarken, semantik ise sınıf türü, materyal ve işlevler gibi özellikler hakkında veri sağlar. Bu nedenle YBM ve CBS arasındaki dönüşüm, geometrik dönüşümün yanında semantik aktarımı da içermelidir (Zhu vd., 2021a). İki sistem arasındaki geometrik dönüşüm, örneğin FME (Adouane, Stouffs, Janssen, ve Domer, 2020), BIMServer ve FME üzerine kurulu ArcGIS'in bir uzantısı olan Data Interoperability (DI) gibi bazı ticari yazılım paketleri kullanılarak gerçekleştirilebilir. Fakat bu araçların hiçbiri hem geometrik hem semantik verileri bütünüyle başarılı bir biçimde dönüştüremez (Sani vd., 2018). Bu nedenle yeni yöntemlere ihtiyaç vardır. Son dönemde, YBM ve CBS entegrasyonu için semantik web teknolojileri ve kaynak tanımlama çerçevesini (resource description framework - RDF) esas alan entegre mekânsal bilgi modeli (IGIM) yaklaşımı kullanılmıştır (Hor, Jadidi, ve Sohn, 2016). Ayrıca araştırmacılar, YBM ve CBS'nin birlikte çalışabilirliğini desteklemek

için çeşitli veri alışverişi formatları geliştirmiştir. IFG (IFC for GIS) veri modeli ve buildingSMART veri sözlüğü (bSDD), YBM'nin CBS gibi diğer mühendislik uygulama alanlarıyla entegrasyonuna yönelik çalışmalarına örnektir. IFG'nin amacı, tek bir veri türünü içe veya dışa aktararak bina ve CBS verilerinin alışverişini sağlamaktır. Fakat, bina ve coğrafi bilgilerin temsili için birçok heterojen sınıf vardır. Bu nedenle, hem bina hem de CBS sınıfları için farklı bir birlikte çalışabilirlik formatı uygulamak daha mantıklıdır (Karan, Irizarry, ve Haymaker, 2015). bSDD, bir veri sözlüğü olmanın yanı sıra, sınıflandırmaları ve onların özelliklerini, izin verilen değerleri, birimleri ve çevirileri barındıran çevrimiçi bir servistir. bSDD, veri kalitesini ve bilgi tutarlılığını garanti etmek için standartlaştırılmış bir iş akışı sağlayarak veri tabanı içindeki tüm içerik arasında bağlantı kurulmasına olanak tanır (Costin, Ouellette, ve Beetz, 2023).

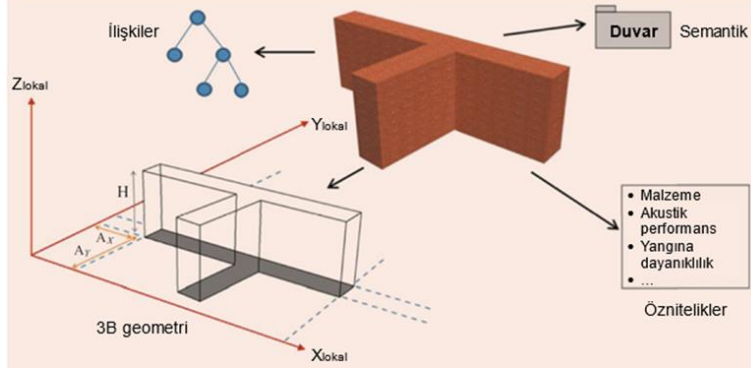
Yukarıda belirtildiği üzere, YBM ve CBS entegrasyonunun eksiksiz biçimde gerçekleştirilmesinin önünde halen çeşitli zorluklar bulunmaktadır. Bu amaçla, IFC'den CityGML'e dönüşüm için bazı yazılımlar kullanılsa da özellikle 3B kent modellemeye yönelik görece yeni bir format olan CityJSON ile ilgili yeterli bir değerlendirme mevcut değildir. Buradan hareketle, bu makalede mevcut teknolojiler ile IFC'den gerek CityGML'e gerekse CityJSON'a geometrik dönüşüm ve semantik aktarımı üç farklı bina örneğinde gerçekleştirilmekte ve elde edilen bulgular irdelenmektedir. Böylece, YBM ve CBS entegrasyonuna yönelik yaygın ve yeni formatlara dayalı karşılaştırmalı bir performans değerlendirmesi ortaya konarak gelecek çalışmalara ışık tutulması amaçlanmaktadır.

### 1.1. Yapı Bilgi Modellemesi (YBM) ve Coğrafi Bilgi Sistemleri (CBS)

Bilgisayar destekli tasarım (CAD) tabanlı, genellikle 2B klasik yaklaşımın yerini, semantik açıdan zengin, 3B nesne yönelimli YBM almıştır. YBM'nin modelleme paradigması, CAD yaklaşımından farklı olarak, nesne yönelimli bir yöntem ve semantik veri modellemesine dayanmaktadır. YBM; veri depolamanın, veri alışverişinin ve süreçlerin aşamalı olarak sayısallaştırılmasını içerir. YBM; semantik, (fiziksel, işlevsel, teknik ve betimleyici) öznitelikler, 3B geometri ve diğer yapı elemanlarıyla ilişkiler gibi çeşitli özelliklere sahip bina nesnesi veya bina bileşenlerini (örneğin, duvar, kiriş ve kolon) içerir (Şekil 1). Zaman, maliyet planları veya belgeler gibi diğer veriler de bileşenlerde saklanabilir. Böylece, bileşen odaklı modellere dayalı olarak, malzeme listelerinin oluşturulması, maliyet planlaması veya kütle/hacim hesaplamaları gibi çeşitli analizler ve simülasyonlar mümkün hale gelir (Blankenbach ve Becker, 2022).

YBM; binalardaki duvarlar, döşemeler, merdivenler, borular, kablolar, elektrik fişleri vb. sayısal tanımları olan (Casini, 2022) bir dizi nesnenin kombinasyonundan oluşan ayrıntılı nesne modeline sahip bina modellerine odaklanmaktadır. Her nesne, genellikle fiziksel görünümü tanımlayan 3B geometri, malzeme türleri, tahmin edilen kullanım ömrü, modeldeki diğer bileşenlerle ilişkileri, boyutları ve üreticinin verileri gibi bilgileri raporlayarak tanımlayan ve sınıflandıran verilere sahiptir. Bu nedenle duvar, kolon, pencere veya kapı gibi nesnelerin YBM'de bir anlamı vardır (Kolbe ve Donaubauer, 2021). YBM, tüm geometrik ve işlevsel öznitelikler de dahil olmak üzere semantik olarak zengin bilgileri akıllı nesnelere koleksiyonunda bütünleştirir (Bansal, 2021). Böylece, bir kez tanımlanan nesnenin birden çok modele yerleştirilmesi mümkün olur. Ayrıca nesnelere değiştirilmesiyle, her bir model otomatik olarak güncellenmektedir. Otomatik olarak modelin güncellenmesi hataları azaltmaktadır. Manuel müdahalelere ek olarak, parametre olarak bilinen bir dizi önceden programlanmış kural veya algoritma da mevcuttur. Örneğin, duvarların zemin seviyesinden başlayıp tavana ulaşmasını sağlamak için bir kural oluşturulabilir, bu durumda tavan yüksekliği (zeminden tavana olan yükseklik) değiştirildiğinde duvarlar otomatik olarak buna göre ayarlanacaktır (Casini, 2022). YBM, bina bilgilerini dinamik olarak alan, sunan ve ilişkisel veri tabanı kullanan bir yazılım aracıdır (Lawrence, Darwich, ve Means, 2018).

CBS, bir bilgi sisteminin tüm özelliklerine sahip bir mekânsal karar destek sistemidir. Planlama, yönetim, depolama ve problem çözümü için geometrik ve semantik verilerin elde edilmesini, modellenmesini, düzenlenmesini, analizini, sunumunu ve yönetimini sağlamaktadır. CBS ile diğer bilgi sistemleri arasındaki en büyük fark, CBS verilerinin coğrafi referanslı olmasıdır. CBS'nin temel ögesi; konum bilgisi ve bu konumla ilgili diğer tüm öznitelikleri içeren mekânsal bilgilerdir (Löwner, Gröger, Benner, Biljecki, ve Nagel, 2016). Mekânsal bilgiler, kavramsal model aracılığıyla gerçekliği temsil eder ve normal olarak koordinatları, mekânsal ilişkileri, öznitelikleri ve daha geniş kapsamda zaman ve metaveri bileşenlerini içerir (Liu vd., 2017).



Şekil 1. YBM için semantik veri modelleme (Blankenbach vd., 2022)

## 1.2. YBM ve CBS Farklılıkları

YBM ve CBS, sırasıyla mimari ve coğrafi mekâna ilişkin sayısal temsilleri sağlasa da odak noktaları farklı olan iki sistemdir. YBM, binalara odaklanırken, CBS binaların çevresindeki mekânsal bilgilere odaklanmaktadır. YBM, inşaat projelerine ve nispeten mikro düzeyde veri oluşturan bina iç bileşenlerine önem verirken, CBS, topografik harita örneğinde olduğu gibi daha çok makro düzeyde bilgiler üretmek için kullanılır (Wang, Pan, ve Luo, 2019). YBM'nin mekânsal kapsamı nispeten küçüktür (Longley, 2008). Bu nedenle, nesnelere genellikle bağıl olarak konumlandırılarak (Zhu vd., 2022) lokal düzlemsel (kartezyen) koordinat sisteminde aşamalı biçimde oluşturulmaktadır (Longley, 2008; Zhu vd., 2022). Aksine, CBS genellikle bölgesel, ulusal veya global olarak coğrafi mekândaki doğal ve yapay varlıkları (olguları), 2B veya 3B olarak modeller. Bu nedenle, dünyanın elipsoidal şekli dikkate alınarak (Longley, 2008) her bir nesne, coğrafi (örn. WGS84) ya da projeksiyon (harita) koordinat sisteminde (örn. GK (TM) Orta Meridyen 30°/TUREF) mutlak olarak konumlandırılır (Adouane vd., 2020).

YBM, hiyerarşik bir veri modelini esas alırken (Karan vd., 2015; Noardo vd., 2021); CBS, ilişkisel ya da nesne-ilişkisel veri tabanına dayalıdır (Karan vd., 2015). 3B katı modellerde nesnelere temsilleri, sınır temsili (boundary representation - B-rep), süpürerek katı model oluşturma (sweep solid - SS) ya da yapıcı katı geometri (constructive solid geometry - CSG) teknikleriyle oluşturulabilir. YBM, bu üç tekniği de destekleyen IFC formatında olsa da genellikle CSG ve SS temsillerini kullanmaktadır (Zhu vd., 2022). CBS ise B-rep ve yüzey modellerini kullanır (Ma vd., 2017). Kısaca; uygulama odakları, kullanıcılar, gelişim aşamaları, mekânsal ölçekler ve kapsam, koordinat sistemleri, semantik ve geometrik temsiller, ayrıntı düzeyleri, bilgi depolama ve erişim yöntemleri açısından farklılıklar olduğu için iki sistem arasında uyumsuzluklar meydana gelmektedir (Liu vd., 2017). Uyumsuzluklarına rağmen bu iki sistem birbirlerine veri sağlayarak birbirlerini tamamladıkları için entegre edilmeleri önemlidir (Demir Altıntaş ve İlal, 2022).

## 1.3. Veri Değişim Formatları

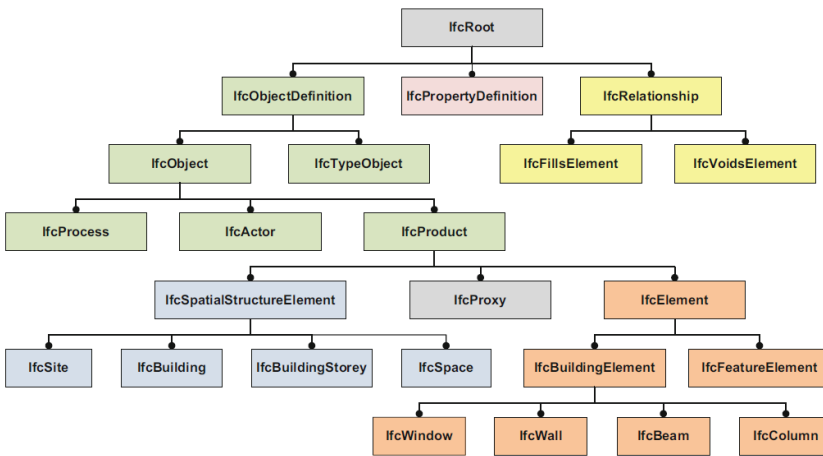
YBM ve CBS entegrasyonu için bazı veri değişim formatları mevcuttur. Bu değişim formatları; açık, tarafsız bir değişim formatı olan IFC (Zhu, Wang, Wang, Wu, ve Kim, 2019) ve semantik 3B kent modellerinin depolanması ve değişimi için temel açık veri modeli ve formatı olan CityGML'dir (Biljecki, Kumar, ve Nagel, 2018). YBM için genel veri formatı; AEC uygulama alanındaki yapı ve inşaat faaliyetlerini tanımlayan ve bilgi alışverişini sağlayan, açık, tarafsız ve nesne tabanlı bir veri formatı olan IFC'dir. Uluslararası Standardizasyon Örgütü (ISO 16739:2013) tarafından tescil edilmiş resmi uluslararası standarttır. CBS'de, CityGML, JSON türevi CityJSON ve shape dosyası olmak üzere veri formatları mevcuttur. CityGML ağırlıklı olarak teorik çalışmalarda yer almakla birlikte, shape dosyası daha çok uygulamaya yönelik çalışmalarda kullanılmaktadır (Zhu vd., 2019). Shape dosyası, YBM ve CBS entegrasyonunda en sık kullanılan CBS platformu ArcGIS'in yerel bir formatıdır, topluma açıktır ve QGIS gibi birçok açık kaynaklı yazılım tarafından desteklenir (Zhu vd., 2021a).

### 1.3.1. IFC

IFC, binanın yaşam döngüsü boyunca karmaşık iletişim ve bilgi paylaşım süreçlerini yönetmek için bina projelerinde kullanılan standartlaştırılmış bir açık veri modelidir. IFC, genellikle daha küçük çaplı bina ve

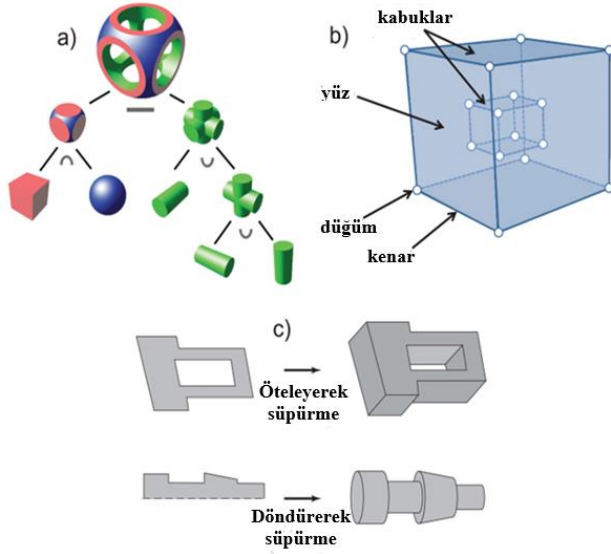
altyapı bileşenlerinin (mekanik, elektrik ve sıhhi tesisat bileşenleri) ve bu bileşenlere ilişkin ağ verilerinin yüksek geometrik ve semantik ayrıntıyla modellenmesine yönelik olarak tasarlanmıştır (Donkers, Ledoux, Zhao, ve Stoter, 2016). IFC, çeşitli disiplinler için ilgili yapıları, inşaat alanıyla ilgili kullanımları ve süreçleri, tipik yapı elemanlarının semantik tanımını, geometrik temsilini ve ilişkilerini içermektedir (Noardo vd., 2021).

IFC, buildingSMART tarafından geliştirilen EXPRESS tabanlı bir veri standardıdır. AEC uygulama alanları içinde açık ve tarafsız bir değişim formatıdır (Zhu vd., 2019). IFC; kaynak katmanı, çekirdek katmanı, birlikte çalışabilirlik katmanı ve uygulama alanı katmanı olmak üzere dört temel kavramsal katman içerir. Her IFC katmanı birkaç alt şema içermektedir (Rajabifard, Atazadeh, ve Kalantari, 2019). IFC dosyasında semantik; varlıkların, özneliklerin ve ilişkilerin bir karışımı olarak depolanır. Varlıkların (sınıfların) bir kısmı IfcBuildingElement'in alt varlıkları (IfcColumn, IfcBeam vb.) olarak tutulmaktadır. Bu varlıklar, bir binanın sahip olabileceği birçok farklı işlevi temsil etmek için kullanılabilir. Ancak bu bilgiyi sağlamayan, yaygın olarak genel işlev için kullanılan IfcBuildingElementProxy sınıfı da mevcuttur. Dağıtım elemanları (ör. ısıtma, soğutma, havalandırma ve sıhhi tesisat) gibi standardın diğer bölümlerinde de benzer alt sınıflar mevcuttur. IFC modelinde yer almayan nesnelerin temsilleri için IfcProduct'ın alt sınıfı olan IfcProxy ögesi mevcuttur. Bu tür genel sınıfların olması, özelleştirilmiş nesnelerin modellere eklenmesini desteklemek için kullanışlı olsa da nesnelerin yorumlanmasını zorlaştırmaktadır. Ayrıca, aynı türden bir nesneyi birkaç varlık aracılığıyla depolamak çoğu zaman mümkündür. IfcProduct ise üst soyu olan IfcObject, IfcObjectDefinition ve çekirdek katmanındaki en üst varlık olan IfcRoot'u içermektedir (Rajabifard vd., 2019; Ohori, Ledoux, ve Peters, 2022b) (Şekil 2).



Şekil 2. IFC sınıf hiyerarşisinin IfcBuildingElement içeren bir kısmı (Borrmann, Beetz, Koch, Liebich ve Murnic, 2018)

IFC'de, 3B katı modellerde nesnelerin temsil edilebilmesi için, B-rep, SS ya da CSG teknikleri kullanılmaktadır (Donkers vd., 2016; Zhu vd., 2019; Zhu vd., 2022). B-rep, sınırlayıcı yüzeyleri kullanan bir 3B nesneyi temsil eder (Şekil 3a). Genellikle pencereler ve kapılar gibi karmaşık nesneler için kullanılır. CSG, 3B nesneleri temsil etmek için ilkel nesnelere ilişkin bir dizi mantıksal (boolean) işlemin (fark, birleşim ve kesişim) sonucunu kullanır. İlkel nesneler; küreler, koniler, piramitler veya silindireler olabilir (Şekil 3b). SS, süpürme yolu ile bağlantılı olarak bir 3B geometriyi tanımlamak için bir 2B profil (daire, dikdörtgen ve çokgen) kullanır (Şekil 3c) (Donkers vd., 2016; Zhu vd., 2019). Bu temsiller bağımsız olarak kullanılabilir veya bir hiyerarşide birbirleriyle birleştirilebilir. Çıkarma ilişkileri, boşluk mekanizması yoluyla açıklıkları temsil eden IfcOpenings ve IfcSpaces önemlidir. IfcOpening, bir geometriden (örneğin, IfcWall'daki bir pencere için veya IfcSlab'daki bir merdiven için bir boşluk oluşturulması) çıkarılan 3B nesneleri tanımlar (Ohori vd., 2022b).



Şekil 3. IFC’de kullanılan katı model örnekleri: (a) İlk nesnelere mantıksal işlemler sonucu oluşturulan CSG, (b) yüzeyler kullanılarak oluşturulan B-rep ve (c) 2B profillerin süpürme işlemleri sonucu oluşan SS (Rajabifard vd., 2019)

YBM’deki LOD (Level Of Development) (Bkz. Bölüm 2.2.3.), hem gerekli olan geometrik ayrıntıyı hem de gerekli semantik bilgileri sağlayarak, bilgilerin kapsamını tanımlar (Casini, 2022). Bu iki kavram birlikte geliştirildikleri için genellikle uyumlu hale gelirler (Alhusban, 2021). Genel olarak; LOD100, binanın şeklini temsil eden tek bir bloktan oluşabilir. Ayrıca LOD100, yalnızca alan ve hacim gibi temel ölçümler için uygundur. LOD200, girişlerin gerçek boyutlarını doğru biçimde temsil eder. LOD300’de nesnelere daha ayrıntılı ve doğrudur. LOD400, nesnelere küçük ayrıntıların eklenmesiyle onların en doğru temsillerini sağlar (Ingram, 2020). LOD500 ise sahada mevcut olan durumu yansıtmaktadır (Casini, 2022) (Şekil 4).

LOD 100	LOD 200	LOD 300	LOD 400	LOD 500
Kavramsal	Yaklaşık geometri	Hassas geometri	İmalat	Gerçekleşen proje

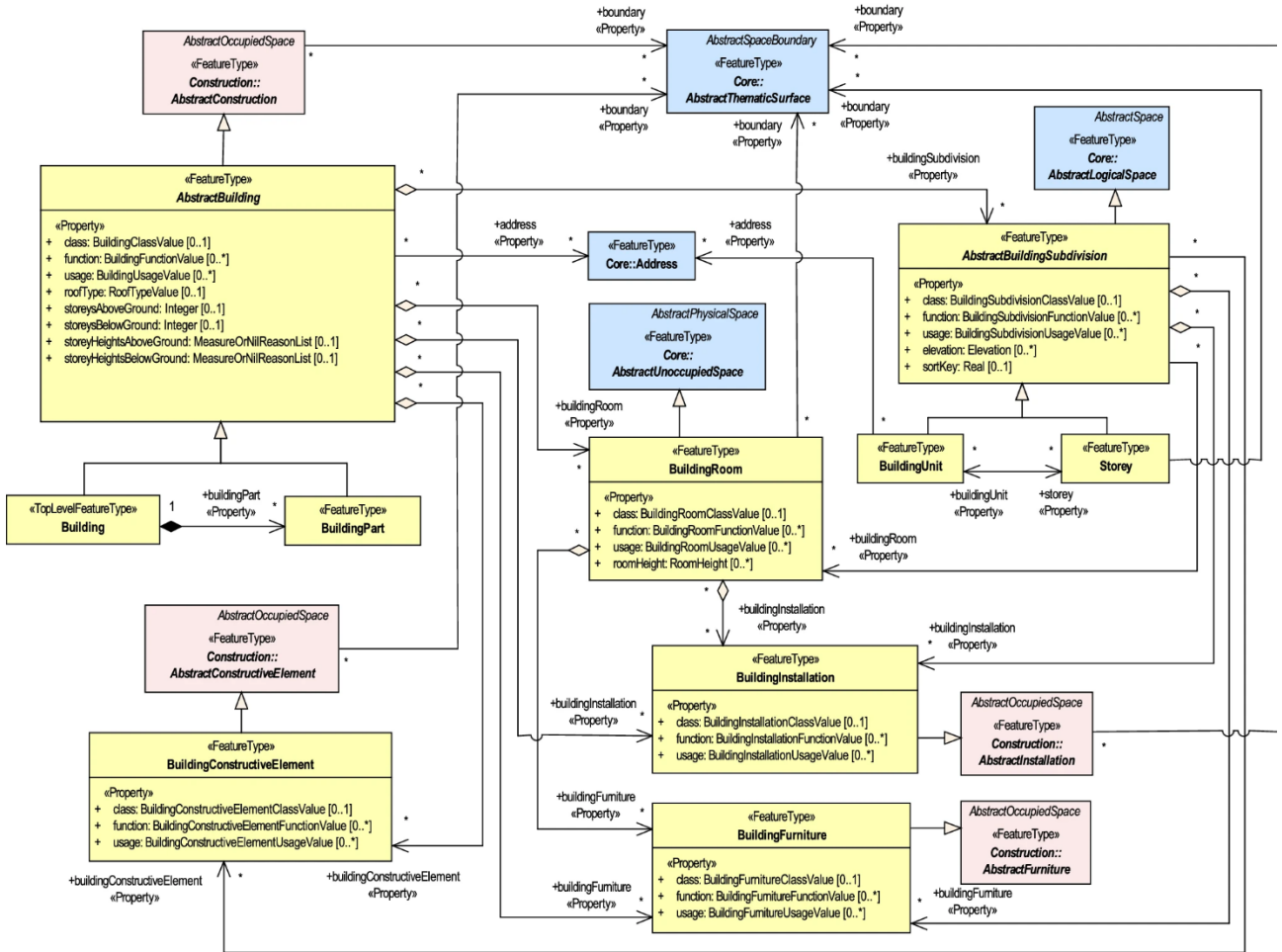
Şekil 4. Aynı varlığın LOD100-500 arası gelişim düzeyi değişimi (Blankenbach vd., 2022)

### 1.3.2. CityGML

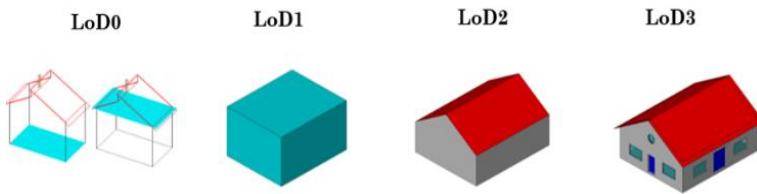
CityGML, OGC tarafından XML formatında tanımlanan GML’ye dayalı olarak kentlerin ve çevresinin 3B modellerini depolayabilen açık standart bir veri modeli ve değişim formatıdır (Sani vd., 2018). CityGML; binalar, yollar, demiryolları, tüneller, köprüler, su kütleleri, bitki örtüsü ve arazi gibi kentsel alandaki varlıklar için kavramsal bir şema tanımlar (Yao vd., 2018). CityGML’nin avantajı, elektrik dağıtımı veya tüketimi, trafik, gürültü ve kirliliğin yayılması gibi çeşitli olguları simüle etmek için bir şehri modelleyebilmesidir (Kolbe vd., 2021). CityGML’de semantik ve geometrik/topolojik özniteliklerle modelleme desteklenir (Al Kalbani ve Rahman, 2022). Semantik düzeyde; binalar, duvarlar, pencereler veya odalar gibi nesnelere ile temsil edilir. Tanımlamalar aynı zamanda nesnelere ilişkin öznitelikleri ve nesnelere arasındaki ilişkileri ve birleştirme (parça-bütün) hiyerarşilerini de içerir (Şekil 5). Geometrik düzeyde; geometri, mekânsal konumu ve kapsamı temsil eden tematik nesnelere atanır. Karmaşık geometriler, temel geometrilerden birleştirme hiyerarşisiyle oluşturulabilir (Kolbe vd., 2021). CityGML, 3B nesnelere geometrisini temsil etmek için iki kısıtlamayla ISO19107’nin bir alt kümesini kullanır: GM\_Curves yalnızca doğrusal olabilir (bu nedenle yalnızca

LineStrings ve LinearRings kullanılmış) ve GM\_Surfaces yalnızca düzlemsel olabilir (bu nedenle Polygons kullanılır) (Ohori vd., 2022a).

CityGML 3.0 veri formatında, mekânsal nesnelerin geometrik ayrıntılarının tanımlanmasına göre düşükten yükseğe dört farklı LoD (Level of Detail) (Bkz. Bölüm 2.2.3.) mevcuttur. LoD0, düzlemsel (2B) temsilleri; LoD1, prizmatik blok model temsilleri; LoD2, genelleştirilmiş geometrik temsilleri ve LoD3, en yüksek geometrik karmaşıklıkta temsilleri kapsar. LoD0'dan LoD3'e kadar olan tanımlar, ilkesel olarak önceki CityGML sürümleriyle aynıdır, ancak tüm nesne türlerini kapsayacak biçimde genişletilmiştir. Dış ve iç mekân nesneleri ve tüm öznitelikler, LoD0'dan LoD3'e kadar temsil edilebilir hale getirilmiştir. Bu nedenle önceki CityGML versiyonlarında bulunan ve iç mekâna ait nesnelere kapsayan LoD4 kavramından vazgeçilmiştir (Löwner vd., 2016). CityGML 3.0 veri formatına göre hacimsel gerçek dünya nesnelere, LoD0'da tek noktalar, LoD0/2/3'te çoklu yüzeyler, LoD1/2/3'te katılar, LoD2/3'te çoklu eğriler/çizgiler ile temsil edilebilir (OGC, 2021) (Şekil 6).



Şekil 5. CityGML 3.0 Bina Modülü (Kutzner, Chaturvedi, ve Kolbe, 2020)



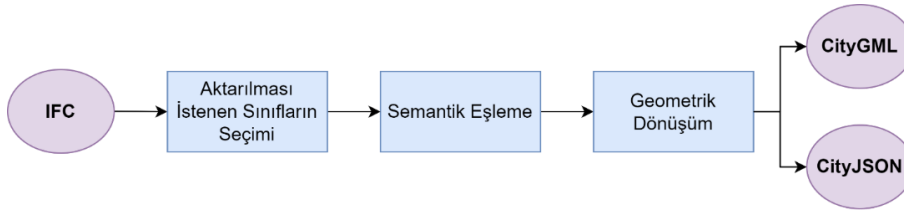
Şekil 6. Aynı binanın LoD0-3 arası ayrıntı düzeyi değişimi (OGC, 2021)

### 1.3.3. CityJSON

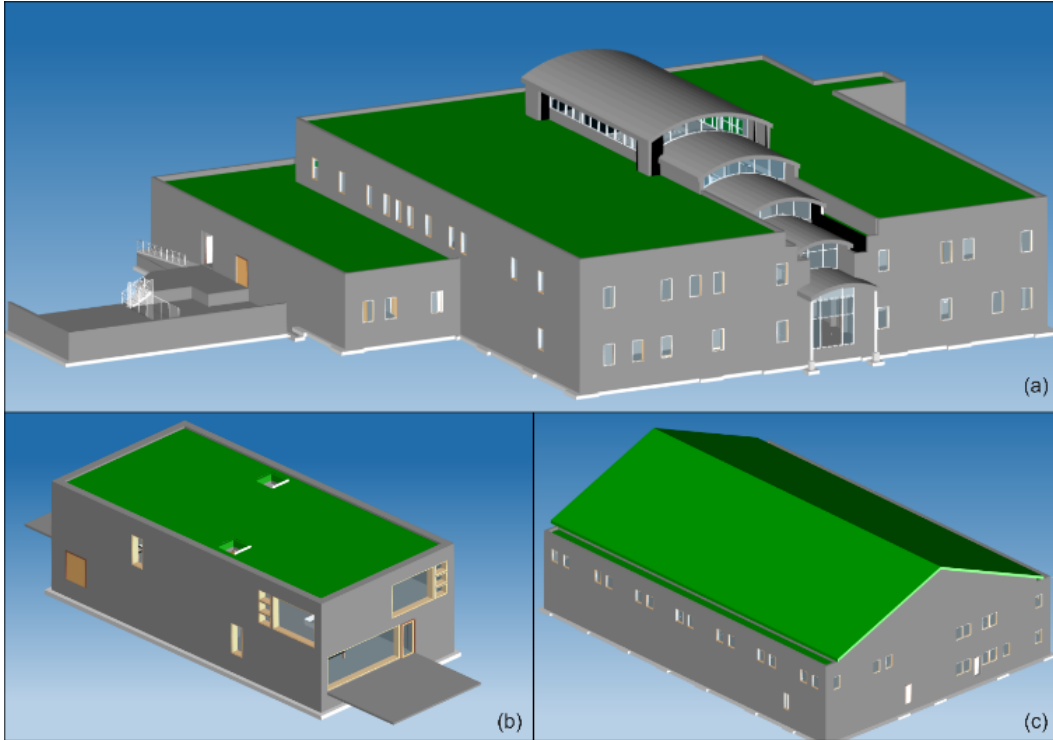
CityJSON, CityGML veri modelinin (sürüm 3.0) bir alt kümesi için insanlar tarafından okunabilen, bilgisayarların ayrıştırması ve kullanması kolay bir veri değişim formatı olarak tasarlanan JSON (JavaScript Object Notation) (Nurseitov, Paulson, Reynolds ve Izurieta, 2009) tabanlı bir kodlamadır. Kentlerin ve peyzajların/arazilerin sayısal 3B modellerinin nasıl saklanacağını tanımlar. CityJSON'un amacı, CityGML'in okunması ve işlenmesi için ayrıntılı ve karmaşık olabilen GML kodlamasına bir alternatif sunmaktır. CityJSON'un, hem veri setlerini okumak hem de bunları oluşturmak için kolay kullanıma sahip olması amaçlanmaktadır (Ohori vd., 2022a). CityJSON veri formatında bulunan "Building" sınıfında, çatı yüzeyi "RoofSurface", zemin ve döşemeler "GroundSurface", duvarlar "WallSurface", kapanış yüzeyleri "ClosureSurface", dış tavan yüzeyi "OuterCeilingSurface", dış zemin yüzeyi "OuterFloorSurface", pencere "Window" ve kapı "Door" sınıflarına öznitelik olarak sahip olabilmektedir (Ledoux ve Dukai, 2022).

## 2. Materyal ve Yöntem

YBM ve CBS veri entegrasyonu için IFC 2x3 formatında bulunan farklı geometrik ve semantik verilere sahip bir medikal klinik, bir ofis ve iki katlı bir apartmana ait statik, mimari ve tesisat projelerini içeren üç adet YBM (Şekil 8) (<https://www.wbdg.org/bim/cobie/common-bim-files>) geometrik dönüşüm ve semantik aktarım ile Safe FME Workbench yazılımı kullanılarak CityGML 2.0 ve CityJSON 1.0.1 veri formatlarına dönüştürülmüştür (Şekil 7).



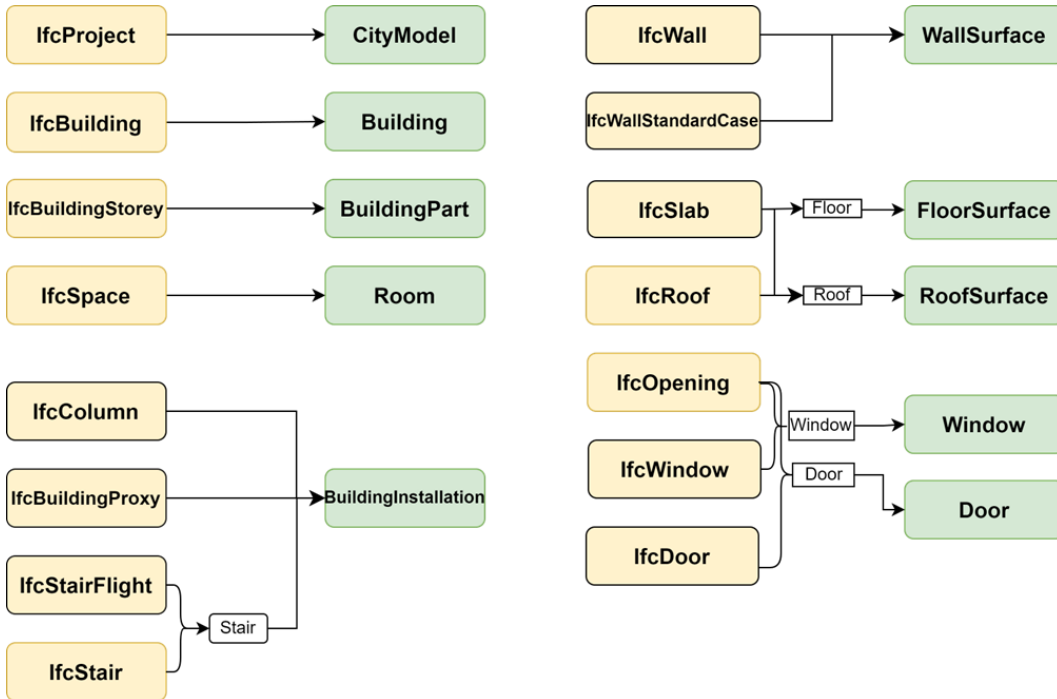
Şekil 7. IFC'den CityGML ve CityJSON dönüşüm adımları



Şekil 8. (a) Medikal klinik, (b) iki katlı apartman ve (c) ofise ait statik ve mimari projelerin birleşimini içeren YBM'ler

## 2.1. Semantik Aktarım

YBM bütünlüğü için semantik ve geometrik bilgiler önemlidir. En yüksek verimlilikle birlikte çalışabilirlik, veri entegrasyonunun semantik yönüyle garanti edilir. Semantik birlikte çalışabilirliğin kilit noktası, veri dönüştürme sırasında bilgi yönetim sistemleri arasındaki özniteliklerin ve ilişkilerin korunmasını sağlamaktır (Malinverni vd., 2022). Geometri, semantik bilginin eklenebileceği çerçeveyi oluşturmaktadır ve yapı modellerini ek bilgilerle zenginleştiren semantiktir. Bu nedenle, geometrik verilerin yanında semantik veriler de doğru şekilde aktarılmalıdır. YBM'deki semantik veriler, bileşen türü ve kullanılan malzemeler gibi yapı bileşenlerinin öznitelikleri, özellikleri ve bu bileşenler arasındaki ilişkileri ifade eder (Zhu vd., 2022). Semantik aktarım, semantik eşleme yaklaşımıyla gerçekleştirilmiştir. Semantik eşleme, aktarılan semantiğin doğruluğunu sağlamak için IFC ve CityGML'deki sınıflar arasında bağlantıların kurulmasını ifade eder. Yapı elemanlarının eşlenmesi, özniteliklerin ve ilişkilerin eşlenmesini içerir (Zhu, Wright, Wang, ve Wang., 2018). Semantik eşleme, iki sınıf arasında bir bağlantı kurar, böylece kaynak sınıftan gelen bilgiler hedef sınıfa eşlenebilir (Zhu vd., 2022). Ancak, IFC'de sınıf sayısının fazla olması ve her verinin aktarılmasının gerekli olmaması nedeniyle çeşitli veri sınıfları seçilmiştir. CityGML'deki bir bina hem katı model hem de bu katı modelin yüzeyleri için semantik özelliklere sahip olabilir. IFC, semantiği depolamak için farklı bir yapıya sahiptir ve nesnelere ilişkiler ağı aracılığıyla birbirine bağlıdır. CityGML semantiğinin bir IFC nesnesinden çıkarılması için çoğu durumda IFC sınıfı ve nesnenin türü yeterlidir. Bununla birlikte, en uygun semantik eşleme için ilişkilerin anlaşılması da önemlidir (Donkers vd., 2016). IFC'nin hiyerarşik yapısının CityGML'den karmaşık olması (örneğin, IFC'de kapılar duvarlara ait açıklıklara, CityGML'de ise kapılar doğrudan duvarlara aittir.) ya da IFC'deki bazı yapı elemanı parçalarının farklı sınıflarda bulunması gibi (örneğin, pencerelerin ve merdivenlerin parçaları IfcMember sınıfında yer alır. Ancak, CityGML'e dönüştürülürken bu parçalar üst sınıfları olan pencere ya da merdivenlerde bulunmalıdır.) problemlerin çözülmesi için IFC'deki nesnelere alt soy ve üst soylarının bulunmasını gerektirir. IFC ve CityGML'in semantik eşlenmesinde Donkers vd. (2016) ve Cecchini (2019) (Şekil 9) esas alınarak ve eklemeler yapılarak eşleme yapılacak sınıflar belirlenmiştir. CityJSON'da ise "Building" sınıfı altında çeşitli semantik yüzeyler ile IFC varlıkları eşleştirilmiştir (Tablo 1).



Şekil 9. IFC ve CityGML sınıflarının semantik eşlenmesi (Sarı renk IFC sınıflarını ve yeşil renk CityGML sınıflarını göstermektedir. Siyah dış çizgisi olmayan kutucuklarda yer alan sınıflar geometrik bilgi taşımazlar) (Cecchini, 2019)

Tablo 1

## IFC sınıfları ve eşlendikleri CityGML ve CityJSON sınıfları

Sınıf	IFC Sınıfı	CityGML Sınıfı	CityJSON Sınıfı/ Semantik Yüzeyi
Proje	IfcProject	CityModel	Building
Bina	IfcBuilding	Building	Building
Oda	IfcSpace	Room	Building
Kolon	IfcColumn	BuildingInstallation	Building/ClosureSurface
Kiriş	IfcBeam	BuildingInstallation	Building/ClosureSurface
Döşeme	IfcSlab	FloorSurface	Building/GroundSurface
Temel	IfcFooting	BuildingPart	Building
Kapı	IfcDoor	Door	Building/Door
Pencere	IfcWindow	Window	Building/Window
Çatı	IfcRoof	RoofSurface	Building/RoofSurface
Duvar	IfcWall IfcWallStandardCase	WallSurface	Building/WallSurface
Cam Perde Duvar/ Giydirme Cephe Vitriini	IfcCurtainWall	Window	Building/Window
Cam	IfcPlate	Window	Building/Window
Dikme	IfcMember	Window	Building/Window
Merdiven	IfcStair	BuildingInstallation	Building
Merdiven Kolu	IfcStairFlight	BuildingInstallation	Building
Sahanlık	IfcSlab	BuildingInstallation	Building
Korkuluk ve Küpeşte	IfcRailing	BuildingInstallation	Building
Yanak (Kiriş profil)	IfcMember	BuildingInstallation	Building
Mobilya/ Eşya	IfcFurnishingElement	BuildingFurniture	Building
Tesisat	IfcFlowTerminal	IntBuildingInstallation	Building

## 2.2. Geometrik Dönüşüm

Geometrik dönüşüm, bina modellerinin geometrisinin CBS’de kullanılabilir biçimde dönüştürülmesidir. YBM ve CBS, farklı modelleme paradigmaları kullandığı için geometrik dönüşüm gereklidir. Bu durumda ele alınması gereken üç ana sorun; referans sistemi, 3B geometri ve ayrıntı düzeyi farklılıklarıdır (Zhu vd., 2018). Bu nedenle geometrik dönüşüm; koordinat sistemi dönüştürme, coğrafi referanslama ve temsil dönüştürme gibi bir dizi alt görevden oluşur (Zhu vd., 2022).

### 2.2.1 Temsil Dönüştürme

Modelleme paradigmasındaki farklılıklardan biri 3B modellerin açık veya örtük olabilmesinden kaynaklanmaktadır (Zhu vd., 2022). Temsil dönüştürme, örtük modellerin açık modellere dönüştürülmesini ifade eder. Örtük modeller, parametrik modelleme yöntemleriyle (CSG ve SS) oluşturulur ve bir dizi parametre ile temsil edilirken, açık modeller B-rep gibi açık noktalarla temsil edilirler. YBM, hem örtük modelleri hem de açık modelleri kullanabilir (Malinverni vd., 2020), yani IFC; CSG, B-rep ve SS’den birini veya bunların kombinasyonunu kullanabilmektedir (Ma vd., 2017). Parametrik modellerin şekil, boyut ve konumu kolayca ayarlanabildiği için, başka bir ifadeyle geometri düzenlemede daha esnek olmaları nedeniyle IFC, genellikle SS ve CSG’yi kullanır. IFC, parametrik olmayan B-Rep’i yalnızca gerektiğinde kullanır. CBS ise parametrik modellemede yetersiz olduğundan açık modelleri (katı modeller veya yüzey modelleri) kullanır. CSG ve SS’nin B-Rep’e dönüştürülmesi, bu modellerin CBS’de kullanılmasına olanak tanır (Zhu vd., 2022).

### 2.2.2. Coğrafi Referanslama

Coğrafi referanslama, orijinal olarak bir harita veya raster görüntüyü coğrafi mekânda karşılık geldiği konumla ilişkilendirme sürecini ifade eden bir terimdir. Bina modelleri, yol ağı gibi CBS ortamındaki diğer mekânsal veriler ile entegre edilecekse, coğrafi referanslama gereklidir (Zhu vd., 2021a). Bir nesneyi coğrafi referanslamak, nesnenin doğru coğrafi konuma yerleştirilmesi için koordinatlarının dönüştürülmesini kapsar

(Diakite ve Zlatanova, 2020). Coğrafi referanslama yöntemleri, CBS’de mevcuttur. Bu nedenle bu entegrasyondaki problemler, IFC standartlarından kaynaklanmaktadır (Zhu vd., 2022). Coğrafi referanslı YBM, CBS’deki diğer mekânsal veri setleriyle entegre edilebilir (Ingram, 2020). IFC4’ten önceki IFC sürümleri, mekânsal referans bilgilerinin tanımlanması için açıkça belirtilmiş bir varlığa sahip değildir ve coğrafi referanslama için yeterli olmadıkları düşünülmektedir. YBM ve CBS farklı koordinat sistemlerini farklı biçimlerde kullanır (Ma vd., 2017). YBM, nesnelerin lokal düzlemsel koordinat sisteminde (3B kartezyen koordinat sistemi) tanımlandığı lokal konumlandırma sistemini benimser. Bir nesnenin lokal konumlandırma sistemi, başka bir nesneyle ilişkilidir. Örneğin, bir pencerenin lokal konumlandırma sistemi, bir duvarın lokal konumlandırma sistemiyle ilişkili olabilir. Bu mekanizma, model değişikliğini kolaylaştırmaktadır (Zhu vd., 2018). CBS ise genellikle bölgeleri, ülkeleri ve hatta tüm dünyayı kapsayan uygulamalara odaklandığı için bir coğrafi koordinat sistemi kullanır; içindeki her nesne, enlem, boylam ve yükseklik şeklinde mutlak koordinatlara sahiptir (Deng, Cheng, ve Anumba, 2016; Zhu vd., 2022). CBS lokal düzlemsel koordinat sistemi de kullanılabilir, ancak çoğu durumda coğrafi koordinat sistemi kullanmaktadır (Zhu vd., 2018). Bu nedenle, geometrik dönüşüm esnasında koordinat sistemi dönüşümü yapılmalıdır (Zhu vd., 2022). Referans sistemi dönüşümü için 2.1 ve 2.2 denklemlerinin kullanımı önerilmektedir. Lokal koordinat sistemindeki nesnelerin köşelerinin koordinatlarını hesaplamak için matris denklemi 2.1’de gösterildiği gibidir. Burada D, süpürme mesafesi ve  $(V_x, V_y, V_z)$ , süpürmenin yön vektörüdür (Wu ve Hsieh, 2007). Koordinatları lokal sistemden gerçek dünya sistemine dönüştürmek için matris denklemi 2.2’de bulunan  $(\theta_x, \theta_y, \theta_z)$  X, Y, Z koordinat sisteminin eksenlerini X', Y', Z' eksenlerine paralel yapmak için sırasıyla X' eksenini, Y' eksenini ve Z' eksenini etrafındaki dönüş açılarıdır.  $(\Delta x, \Delta y, \Delta z)$  ise yerel koordinat sisteminin orijininin gerçek dünya koordinat sistemine öteleme vektörüdür (Sani vd., 2018; Wu vd., 2007).

$$\begin{bmatrix} x' \\ y' \\ z' \end{bmatrix} = D \cdot \begin{bmatrix} V_x \\ V_y \\ V_z \end{bmatrix} + \begin{bmatrix} x \\ y \\ z \end{bmatrix} \quad (2.1)$$

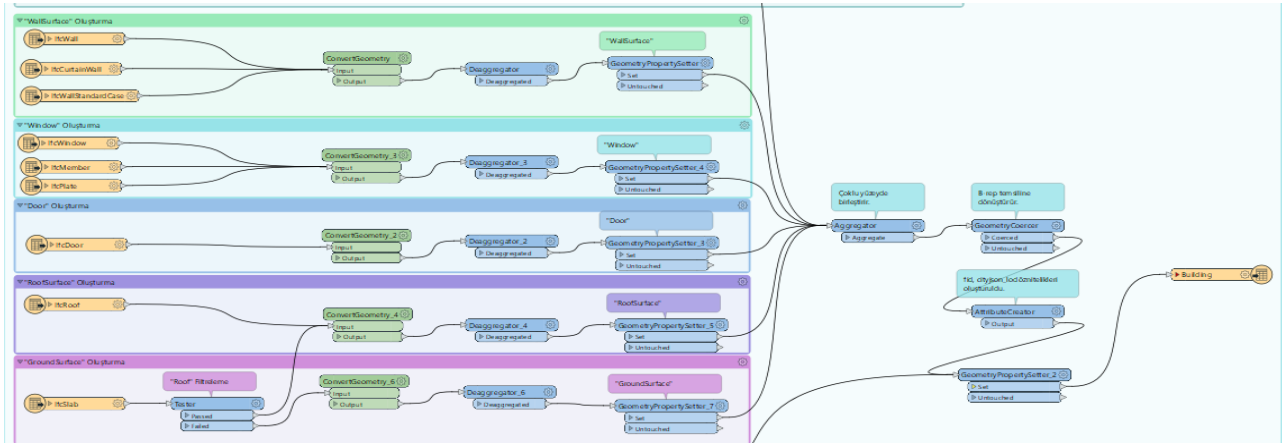
$$\begin{bmatrix} x_2 \\ y_2 \\ z_2 \end{bmatrix} = \begin{bmatrix} 1 & 0 & 0 \\ 0 & \cos \theta_x & \sin \theta_x \\ 0 & -\sin \theta_x & \cos \theta_x \end{bmatrix} \begin{bmatrix} \cos \theta_y & 0 & -\sin \theta_y \\ 0 & 1 & 0 \\ \sin \theta_y & 0 & \cos \theta_y \end{bmatrix} \begin{bmatrix} \cos \theta_z & \sin \theta_z & 0 \\ -\sin \theta_z & \cos \theta_z & 0 \\ 0 & 0 & 1 \end{bmatrix} \begin{bmatrix} x_1 \\ y_1 \\ z_1 \end{bmatrix} + \begin{bmatrix} \Delta x \\ \Delta y \\ \Delta z \end{bmatrix} \quad (2.2)$$

### 2.2.3 Ayrıntı Düzeyi Dönüşümü

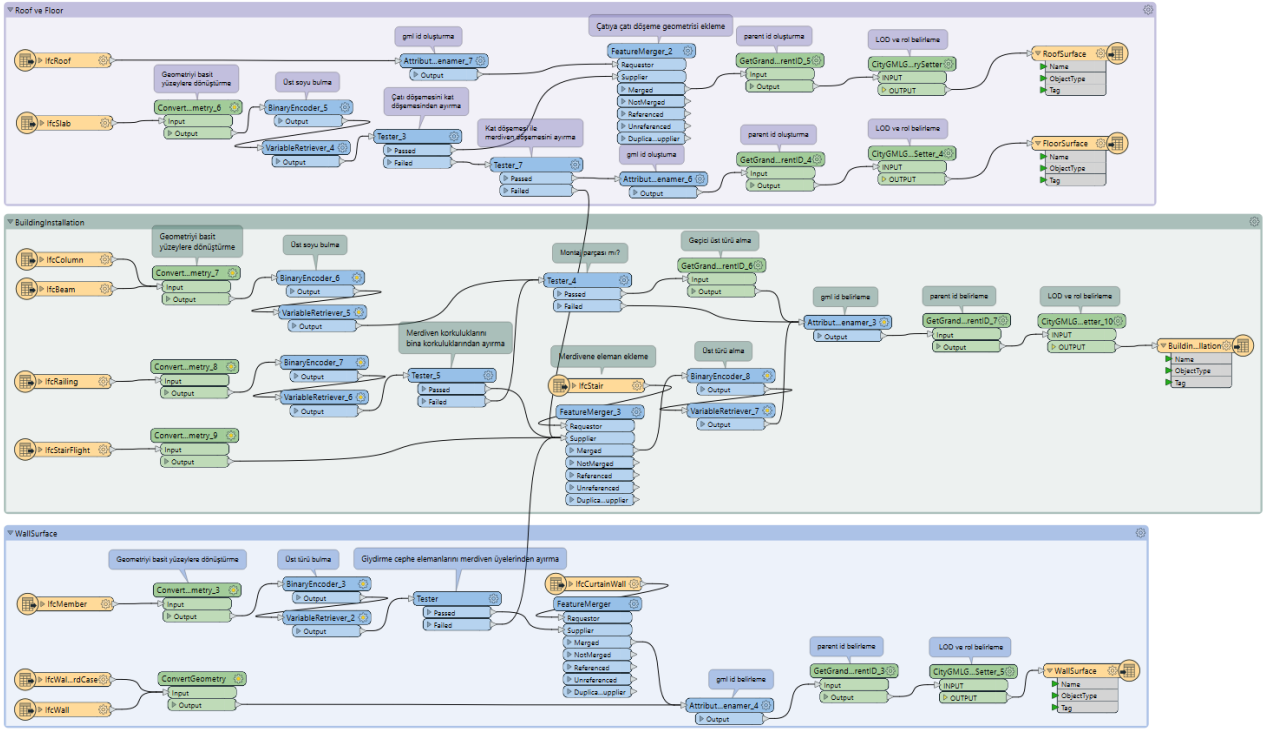
Hem YBM hem de CBS, bina modellerinde bulunan bilgi miktarını gösteren bir terime sahiptir (Zhu vd., 2022). Yapıların tasarımı ve planlaması, ön tasarım ve kavramsal planlama ile başlayıp uygulama planlaması ile bitecek biçimde adım adım gerçekleştirilir. Bu, inşaat mühendisliği ve bina inşaatında CBS ve YBM tabanlı planlama için eşit derecede geçerlidir. Bunun için sayısal modeller ve dolayısıyla bileşenler başlangıçta yalnızca kaba ayrıntılandırma gerektirir. Rafine planlama ile (planlama uygulaması veya planlama onayı için belgelerin sunulması, kütlelerin veya miktarların belirlenmesi, maliyet tahmini vb.), hem geometrik hem de semantik bilgi için ayrıntılandırma talepleri artar. Planlamada model nesnelerinin ayrıntılandırılmasıyla farklı gereksinimleri karşılamak için, LOD kavramı geliştirilmiştir. LOD kavramı, doğruluk düzeyiyle (level of accuracy - LOA) karıştırılmamalıdır. LOA, bir bileşenin mevcut durumunun ölçümündeki geometrik doğruluğu veya daha sonra ölçme verilerinden türetilen modelin geometrik doğruluğunu tanımlar (Blankenbach ve Becker, 2022). CityGML, modellerde yer alan bilgi miktarını belirtmek için LOD’den kısmen farklı olarak LoD kavramını kullanmaktadır (Zhu ve Wu, 2022; Alhusban, 2021). LOD, YBM’deki çeşitli planlama aşamaları sırasında kademeli olarak daha ayrıntılı hale geldiğinden, çeşitli planlama aşamalarına uyacak biçimde oluşturulmuştur. Öte yandan CBS, zaten var olan gerçek dünyayı temsil ettiği için sisteme aktarılması gereken gerçek dünya nesnelerinin belirlenmesi gerekmektedir. LoD kavramı, genelleştirme ilkesini takip etmektedir. Düşük LoD’de, küçük veya daha az önemli yapı parçalarının veya elemanlarının modellenmediği veya basitleştirildiği anlamına gelir (Blankenbach vd., 2022). LoD, bütün bina modeline odaklanarak bina modelinin içermesi gerekenleri belirtmektedir. LOD ise binanın bileşenlerine ve bina bileşenlerinde nelerin olması gerektiğine odaklanmaktadır. Bu nedenle geometrik dönüşüm sırasında bulunması gereken yapı elemanlarını belirlemek önemlidir (Zhu ve Wu, 2021b).

### 3. Bulgular ve Tartışma

IFC'den CityGML'e ve CityJSON'a dönüşüm için medikal klinik, ofis binası ve iki katlı apartman olmak üzere üç farklı binada FME Workbench yazılımı ile geometrik dönüşüm ve semantik aktarım gerçekleştirilmiştir. YBM'deki binalara ait nesnelere LOD400 ayrıntı düzeyine sahiptirler. IFC 2x3'ten CityJSON 1.0.1'e dönüşüm için geometrik dönüşüm ve semantik aktarım gerçekleştirilmiştir. Geometrik dönüşüm için IFC'deki karmaşık katı model, FME Workbench'teki dönüştürücüler yardımıyla basit bileşik yüzeylere dönüştürülmüştür. Bu yüzeylerin CityJSON'daki semantik yüzeylerle eşleştirilebilmesi ve her bir yüzeyin ayrı olarak tanımlanabilmesi için yüzeyler ayrıştırılmıştır. Bu ayrıştırılan yüzeyler Tablo 1'de de belirtilen CityJSON'daki semantik yüzey isimlerine uygun olacak biçimde eşleştirilmiştir. Semantik olarak eşleştirilen bu yüzeyler B-rep geometrisi oluşturacak biçimde birleştirilmiştir. LoD ve kimlik verileri belirlenerek "Building" sınıfına aktarılmıştır (Şekil 10). IFC 2x3'ten CityGML 2.0'ye dönüşüm için geometrik dönüşüm ve semantik aktarım gerçekleştirilmiştir. Geometrik dönüşüm için IFC'deki karmaşık katı model FME Workbench'teki dönüştürücüler yardımıyla basit yüzeylere dönüştürülmüştür. Semantik aktarım için ise IFC sınıfları Tablo 1'de de belirtilen CityGML sınıflarıyla eşleştirilmiştir. Ancak, sınıfların eşleştirilmesinde çeşitli sorunlarla karşılaşmıştır. IFC'de nesneye ait parçaların farklı sınıflarda bulunması ya da farklı türdeki nesnelerin aynı sınıfta bulunması gibi karmaşıklıklar mevcuttur. Ayrıca, CityGML'de bina elemanlarının bulunduğu sınıfların az olması ve hiyerarşik yapısının farklı olması nedeniyle IFC'deki nesnelerin üst soylarına uygun olacak biçimde sınıflar oluşturulmuştur. Bu nedenle, öncelikle IFC sınıflarındaki varlıklara ait üst soy/alt soy bilgisi elde edilmiştir. Ardından, varlıklara ait soy bilgisi ve özellikler esas alınarak sorgulamalar yapılmıştır. CityGML'e aktarılabilecek varlıklara ait kimlik verileri, LoD'si ve yapıdaki rolleri belirlenerek CityGML'deki sınıflarla eşleştirilmiştir (Şekil 11). CityGML ve CityJSON'da LoD3 düzeyinde sonuçlar elde edilmiştir. Coğrafi referanslama ise IFC 2x3 versiyonunda binalara ait koordinat sistemleri, başlangıç koordinatları ve bunlar ile ilgili bilgi bulunmaması nedeniyle tam olarak gerçekleştirilememiş de FME Workbench ile ya da veri formatlarının dönüşümü sonucu CBS ortamına aktarılmasıyla gerçekleştirilmiştir. Ancak, CityJSON'ın CBS ortamında açılmasındaki problemlerden dolayı CityGML'in coğrafi referanslanması daha kolay gerçekleştirilmiştir. Bina bağlamındaki bulgular makalenin devamında incelenmiştir.

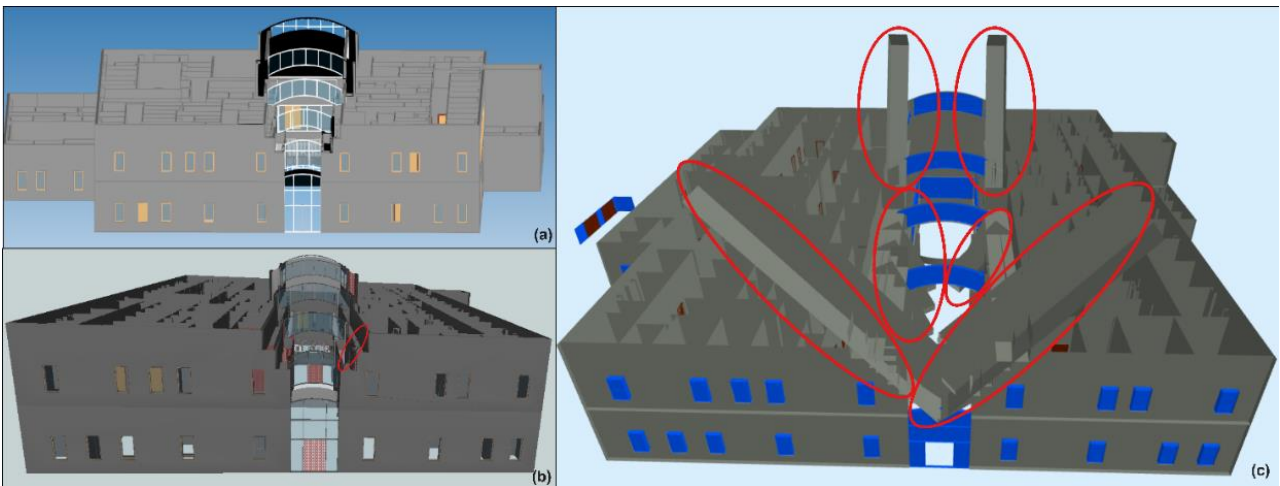


Şekil 10. FME Workbench ile IFC'den CityJSON'a dönüşüm örneği

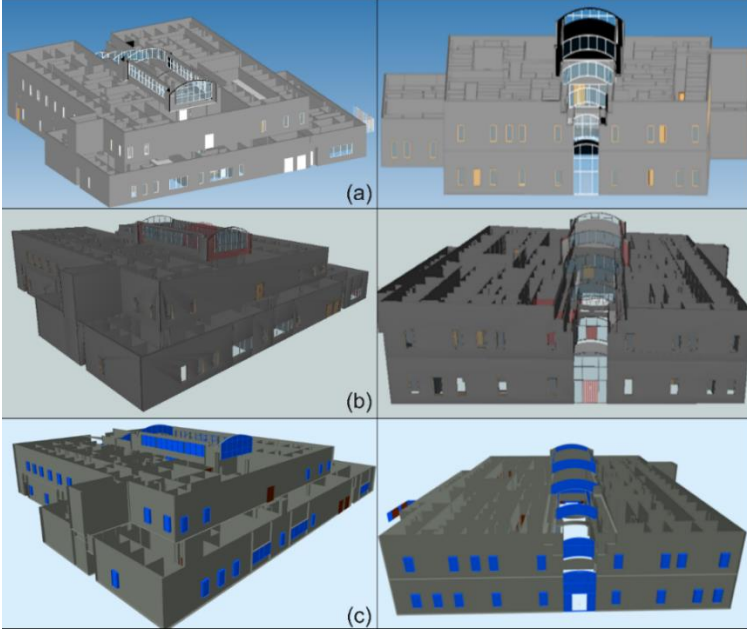


Şekil 11. FME Workbench ile IFC'den CityGML'e dönüşüm örneği

Medikal kliniğe ait mimari projenin IFC'den CityJSON'a dönüştürülmesinde semantik aktarımda problem yaşanmamıştır. Ancak, geometrik dönüşümde dış duvarların zikzaklı (girintili - çıkıntılı) olması nedeniyle binanın geometrik bütünlüğünü bozacak biçimde çıkıntılı dikdörtgen prizmalar oluşmuştur (Şekil 12). Binanın genel yapısının bozulmaması için sorgulamalar ile dikdörtgen prizmaların binadan çıkarılması sağlanmıştır. Ancak, yine de şekillerdeki bozukluklar tamamen giderilememiştir (Şekil 13). Aynı zamanda, bina dokusunun korunması için "IfcCurtainWall" olarak bulunan cam içeren giydirme cephe vitrinlerinin "wall" yerine "window" olarak aktarılması tercih edilmiştir. IFC'den CityGML'e dönüşümde ise semantik aktarımda problem yaşanmamıştır. Geometrik dönüşümde ise zikzaklı yapıda ince bir dikdörtgen prizma meydana gelse de (Şekil 12) bina bütünlüğü bozulmamaktadır (Şekil 13).

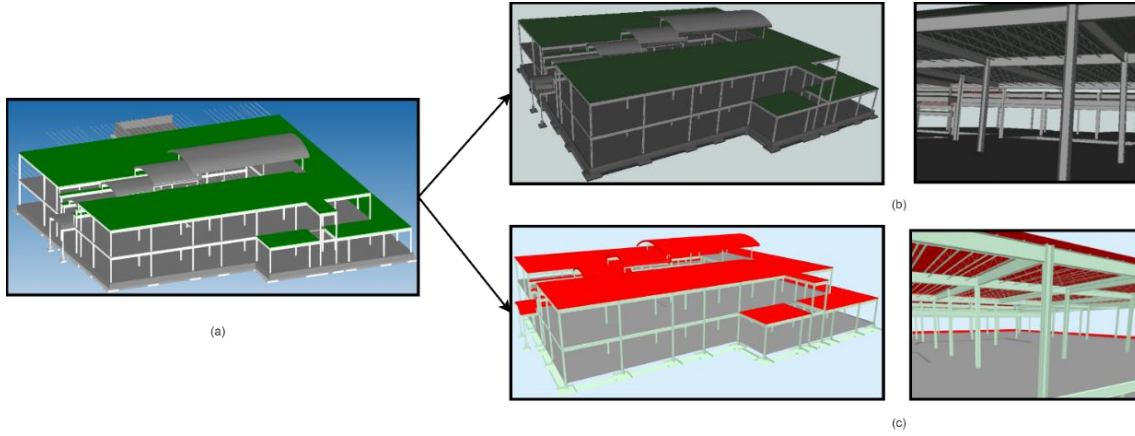


Şekil 12. Medikal klinik mimarisi: (a) IFC, (b) CityGML ve (c) CityJSON formatı



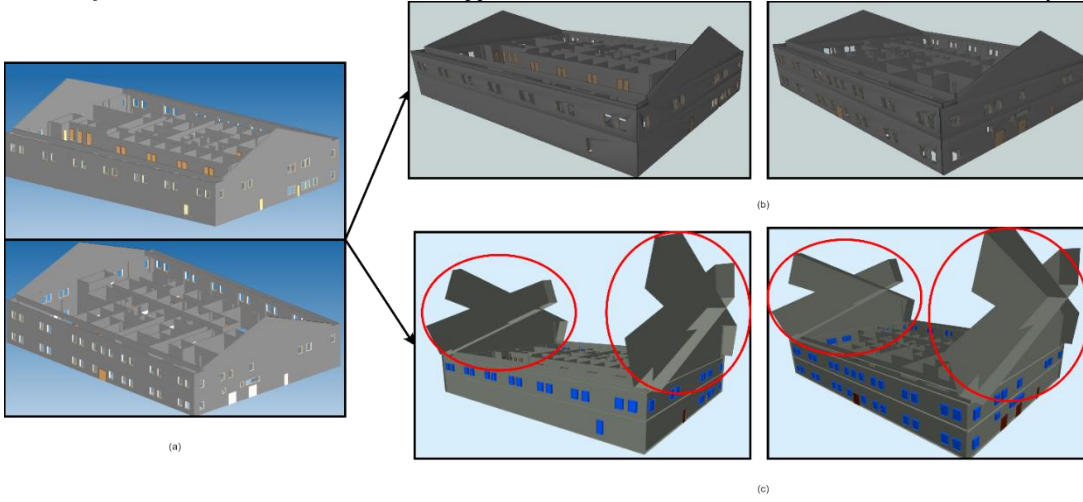
Şekil 13. Medikal kliniğine ait mimari projenin (a) IFC'den (b) CityGML ve (c) CityJSON formatına dönüşümü

Medikal kliniğe ait statik projenin IFC'den CityJSON'a dönüştürülmesinde geometrik dönüşüm ve semantik aktarımda problem yaşanmamıştır. IFC'den CityGML'e dönüşümde ise semantik aktarımda IfcRoof ve IfcSlab'ın üst soy/alt soy karmaşası nedeniyle metal çatı nesnelere geometrik olarak aktarılamamıştır. Bu problem çatı olarak aktarılan semantik nesne sınıfının "roofsurface" yerine "floorsurface" olarak aktarılması ile çözülmüştür. Bu sayede geometrik dönüşümde de sorun kalmamıştır (Şekil 14).

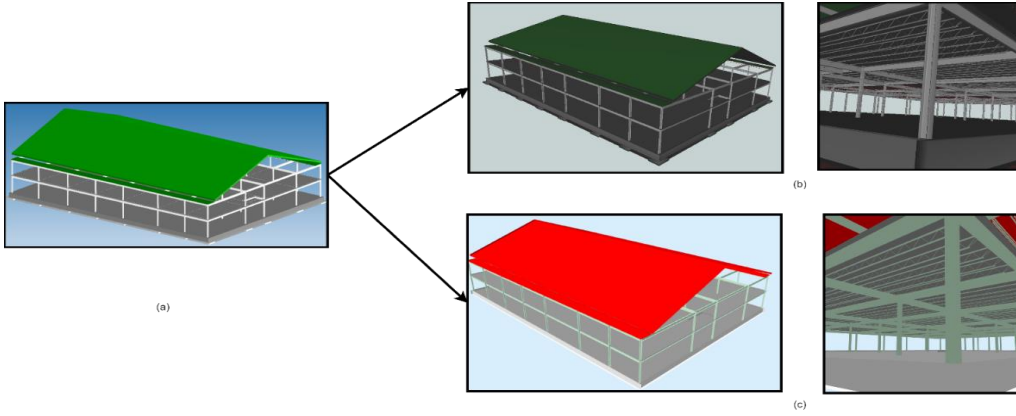


Şekil 14. Medikal kliniğine ait statik projenin (a) IFC'den (b) CityGML ve (c) CityJSON formatına dönüşümü

İnceleme yapılan diğer bir bina ise ofis binasıdır. Ofis binasına ait mimari projenin IFC'den CityJSON'a dönüştürülmesinde semantik aktarımda problem yaşanmamıştır. Ancak, geometrik dönüşümde dış duvarların üçgen biçiminde olması nedeniyle binanın geometrik bütünlüğünü bozacak biçimde çıkıntılı dikdörtgen prizmalar oluşmuştur. IFC'den CityGML'e dönüşümde ise geometrik dönüşüm ve semantik aktarımda problem yaşanmamıştır (Şekil 15). Ofis binasına ait statik projenin IFC'den CityJSON'a dönüştürülmesinde geometrik ve semantik olarak problem yaşanmamıştır. IFC'den CityGML'e dönüşümde ise semantik aktarımda IfcRoof ve IfcSlab'ın üst soy/alt soy karmaşası nedeniyle metal çatı nesnelere geometrik olarak aktarılamamıştır. Bu problem, çatı olarak aktarılan semantik nesne sınıfının "roofsurface" yerine "floorsurface" olarak aktarılması ile çözülmüştür. Bu sayede, geometrik dönüşümde de sorun kalmamıştır (Şekil 16).

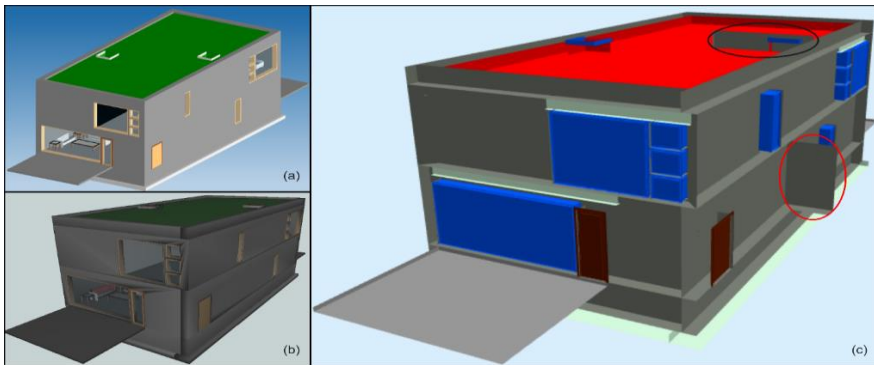


Şekil 15. Ofis binasına ait mimari projenin (a) IFC'den (b) CityGML ve (c) CityJSON formatına dönüşümü



Şekil 16. Ofis binasına ait statik projenin (a) IFC'den (b) CityGML ve (c) CityJSON formatına dönüşümü

İnceleme yapılan son bina ise iki katlı apartmandır. İki katlı apartmana ait projenin IFC'den CityJSON'a dönüştürülmesinde semantik aktarımda problem yaşanmamıştır. Ancak, geometrik dönüşümde bitişik duvarlarda ve çatıya ait bir duvarda bina dışına uzanan duvarlar oluşmuştur. IFC'den CityGML'e dönüşümlerde geometrik ve semantik aktarımda problem yaşanmamıştır (Şekil 17).



Şekil 17. İki katlı apartmana ait projenin (a) IFC'den (b) CityGML ve (c) CityJSON formatına dönüşümü

Farklı binaların IFC'den CityGML'e dönüşümler incelendiğinde geometrik dönüşümlerde zikzak biçiminde olan geometriler hariç sorun yaşanmamıştır. Semantik aktarımda ise karmaşık hiyerarşik yapılar nedeniyle genellikle çatı aktarımında problemler meydana gelmiştir. IFC'den CityJSON'a dönüşümler incelendiğinde ise zikzaklı, üçgen ya da birbirine bitişik geometrilerin çeşitli sorunlara neden olduğu gözlemlenmiştir. Semantik aktarımda ise tüm nesnelere "Building" sınıfında yer alırken, semantik yüzeylerin öznitelik olarak bulunması semantik aktarımı kolaylaştırmıştır. Ancak, semantik yüzey sayısının az olması nesnelere buldukları sınıfların anlaşılabilirliğini azaltmıştır. Ayrıca, CityGML'e göre yeni bir format olan CityJSON'ın okunabildiği programlarda bile hata vermesi gibi bazı zorluklarla karşılaşmıştır. CityJSON formatı, henüz geniş kullanıcı kitlesine sahip olmadığından, mevcut coğrafi veri işleme araçlarıyla tam uyumluluk sağlayamayabilir, doğrudan desteklenmeyebilir veya sınırlı destek sunabilir. Bu nedenle, gelecekte CityJSON'ın geniş kitlelere ulaşmasıyla birlikte uyumluluk sorunlarının azalacağı düşünülmektedir.

#### 4. Sonuçlar

Bu makalede, YBM ve CBS entegrasyonu, başlıca açık formatlar kullanılarak geometrik dönüşüm ve semantik aktarım adımlarıyla uygulamalı olarak ele alınmıştır. Bu bağlamda, bir medikal klinik, bir ofis binası ve iki katlı bir apartmanın statik ve mimari projelerine ilişkin YBM'ler, FME Workbench yazılımı ile IFC formatından, semantik 3B kent modeli veri değişim formatları olan CityGML ve CityJSON'a LoD3 ayrıntı düzeyinde dönüştürülmüştür. Bu dönüşümler incelendiğinde, CityGML ve CityJSON veri formatlarıyla basit ve ayrık geometrilerin dönüşümünde oldukça iyi sonuçlar elde edilmiştir. Ancak, CityGML veri formatı karmaşık ve bitişik geometrilere sahip binalarda CityJSON'a göre daha iyi sonuçlar vermiştir. Semantik aktarımda ise, IFC'den CityGML'e farklı sınıfların oluşturulması, CityJSON'daki semantik yüzeylerin öznitelik olarak aktarılmasından daha karmaşıktır ve uygulanmasını zorlaştırmaktadır. CityJSON, şu aşamada geometrik ve semantik açıdan karmaşıklığı az olan uygulamalar için uygun bir çözüm yolu sunmaktadır. CityJSON'ın okunabildiği programların artması ile coğrafi referanslama ve analizlerin kolaylaşması beklenmektedir. Ayrıca, CityGML'e kıyasla türetildiği veri formatı (XML'e karşın JSON) dikkate alındığında web ortamında daha avantajlı olması da gelecekteki çalışmalar için tercih edilirliliğini arttırabilir. Ek olarak, CitySON'da semantik aktarım için yeni semantik yüzeyler tanımlanarak eşleme işleminin kolaylaştırılabileceği düşünülmektedir.

#### Yazar Katkıları

Özlem Korkmaz: Literatür araştırması, yöntem geliştirme, veri edinimi, uygulama ve makale yazımı

Melih Başaraner: Çalışmanın kurgulanması, literatür araştırması, yöntem geliştirme ve makalenin gözden geçirilerek iyileştirilmesi

#### Çıkar Çatışması

Yazarlar çıkar çatışması bildirmemişlerdir.

#### Kaynakça

- Adouane, K., Stouffs, R., Janssen, P., ve Domer, B. (2020). A model-based approach to convert a building BIM-IFC data set model into CityGML. *Journal of Spatial Science*, 65(2), 257-280. <https://doi.org/10.1080/14498596.2019.1658650>
- Al Kalbani, K., ve Rahman, A. A. (2022). 3D city model for monitoring flash flood risks in Salalah, Oman. *International Journal of Engineering and Geosciences*, 7(1), 17-23. <https://doi.org/10.26833/ijeg.857971>
- Alhusban, M. (2021). Understanding BIM information management processes through international BIM standards. Hosseini, R. M., Khosrowshahi, F., Aibinu, A. A., ve Abrishami, S. (ed.). *BIM teaching and learning handbook - implementation for students and educators*. Oxon, Routledge, 169-183.
- Demir Altıntaş, Y., ve İlal, M. E. (2022). Integrating building and context information for automated zoning code checking: A review. *ITcon*, 27, 548-570. <https://doi.org/10.36680/j.itcon.2022.027>
- Bansal, V. K. (2021). Integrated framework of BIM and GIS applications to support building lifecycle: a move toward nD modeling. *Journal of Architectural Engineering*, 27(4), 05021009.

- Biljecki, F., Kumar, K., ve Nagel, C. (2018). CityGML Application Domain Extension (ADE): overview of developments. *Open Geospatial Data, Software and Standards*, 3(1), 1-17. <https://doi.org/10.1186/s40965-018-0055-6>
- Blankenbach, J., ve Becker, R. (2022). Building information modeling. Kresse, W., & Danko, D. (ed.) *Springer handbook of geographic information*, 2. baskı. Springer, Berlin, 613-628. <https://doi.org/10.1007/978-3-030-53125-6>
- Bolpagni, M., (2022). Building information modelling and information management. Bolpagni, M., Gavina, R., ve Ribeiro, D. (ed.). *Industry 4.0 for the built environment: Methodologies, technologies and skills*. Structural Integrity 20. cilt, Springer, Cham, 29-39. <https://doi.org/10.1007/978-3-030-82430-3>.
- Borrmann, A., Beetz, J., Koch, C., Liebich, T., ve Munic, S. (2018). Industry foundation classes: A standardized data model for the vendor-neutral exchange of digital building models. Borrmann, A., König, M., Koch, C., ve Beetz, J. (ed). *Building information modeling: Technology foundations and industry practice*. Springer Nature, 81-126. <https://doi.org/10.1007/978-3-319-92862-3>
- Casini, M. (2022). Building information modeling. Casini, M. (ed.) *Construction 4.0: Advanced technology, tools and materials for the digital transformation of the construction industry*. Woodhead Publishing, Kidlington, 189-219.
- Cecchini, C. (2019). From data to 3D digital archive: A GIS-BIM spatial database for the historical centre of Pavia (Italy). *Journal of Information Technology in Construction*, 24(Nov), 459-471. Erişim adresi: <https://www.itcon.org/2019/24>
- Chen, L. C., Wu, C. H., Shen, T. S., ve Chou, C. C. (2014). The application of geometric network models and building information models in geospatial environments for fire-fighting simulations. *Computers, Environment and Urban Systems*, 45, 1-12. <https://doi.org/10.1016/j.compenvurbsys.2014.01.003>
- Costin, A., Ouellette, J. W., ve Beetz, J. (2023). Building product models, terminologies and object type libraries. Pauwels, P., ve McGlenn, K. (ed.) *Buildings and semantics*. CRC Press/Balkema, Leiden, 4-24.
- Deng, Y., Cheng, J. C. P., ve Anumba, C. (2016). Mapping between BIM and 3D GIS in different levels of detail using schema mediation and instance comparison. *Automation in Construction*, 67, 1-21. <https://doi.org/10.1016/j.autcon.2016.03.006>
- Donkers, S., Ledoux, H., Zhao, J., ve Stoter, J. (2016). Automatic conversion of IFC datasets to geometrically and semantically correct CityGML LOD3 buildings. *Transactions in GIS*, 20(4), 547-569. <https://doi.org/10.1111/tgis.12162>
- Kang, T. (2018). Development of a conceptual mapping standard to link building and geospatial information. *ISPRS International Journal of Geo-Information*, 7(5), 162. <https://doi.org/10.3390/ijgi7050162>
- Herle, S., Becker, R., Wollenberg, R., ve Blankenbach, J. (2020). GIM and BIM: How to obtain interoperability between geospatial and building information modelling? *PFG - Journal of Photogrammetry, Remote Sensing and Geoinformation Science*, 88(1), 33-42. <https://doi.org/10.1007/s41064-020-00090-4>
- Hor, A. H., Jadidi, A., ve Sohn, G. (2016). BIM-GIS integrated geospatial information model using semantic web and RDF graphs. *ISPRS Annals of the Photogrammetry, Remote Sensing and Spatial Information Sciences III-4*, 73-79. <https://doi.org/10.5194/isprs-annals-III-4-73-2016>
- Niu, S., Pan, W., ve Zhao, Y. (2015). A BIM-GIS integrated web-based visualization system for low energy building design. *Procedia Engineering*, 121, 2184-2192. <https://doi.org/10.1016/j.proeng.2015.09.091>
- Isikdag, U., Underwood, J., Aouad, G., ve Trodd, N. (2007). Investigating the role of building information models as a part of an integrated data layer: a fire response management case. *Architectural Engineering and Design Management*, 3(2), 124-142. <https://doi.org/10.1080/17452007.2007.9684636>
- Ingram, J. (2020). *Understanding BIM: The past, present and future*. Routledge, Abingdon, Oxon.
- Karan, E. P., Irizarry, J., ve Haymaker, J. (2015). BIM and GIS integration and interoperability based on semantic web technology. *Journal of Computing in Civil Engineering*, 30(3), 04015043. [https://doi.org/10.1061/\(ASCE\)CP.1943-5487.0000519](https://doi.org/10.1061/(ASCE)CP.1943-5487.0000519)
- Kolbe, T. H., ve Donaubaue, A. (2021). Semantic 3D city modeling and BIM. Shi, W., Goodchild, M. F., Batty, M., Kwan, M., ve Zhang, A. (ed.). *Urban informatics*. Springer, Singapore, 609-636. [https://doi.org/10.1007/978-981-15-8983-6\\_34](https://doi.org/10.1007/978-981-15-8983-6_34)
- Kutzner, T., Chaturvedi, K., ve Kolbe, T. H. (2020). CityGML 3.0: New functions open up new applications. *PFG - Journal of Photogrammetry, Remote Sensing and Geoinformation Science*, 88(1), 43-61.

- <https://doi.org/10.1007/s41064-020-00095-z>
- Lawrence, T., Darwich, A. K., ve Means, J. K. (2018). Project strategies and early design. Lawrence, T., Darwich, A. K., ve Means, J. K. (ed.). *ASHRAE green guide design, construction, and operation of sustainable buildings*, 5. baskı, ASHRAE, Atlanta, 41-71.
- Ledoux, H. ve Dukai, B. (2022). *CityJSON Specifications 1.1.3*. Erişim adresi: <https://www.cityjson.org/specs/1.1.3/>
- Ledoux, H., Ohori, K. A., Kumar, K., Dukai, B., Labetski, A., ve Vitalis, S. (2019). CityJSON: A compact and easy-to-use encoding of the CityGML data model. *Open Geospatial Data, Software and Standards*, 4(1), 1-12. <https://doi.org/10.1186/s40965-019-0064-0>
- Liu, X., Wang, X., Wright, G., Cheng, J. C. P., Li, X., ve Liu, R. (2017). A state-of-the-art review on the integration of building information modeling (BIM) and geographic information system (GIS). *ISPRS International Journal of Geo-Information*, 6(2), 53. <https://doi.org/10.3390/ijgi6020053>
- Longley, P. A., Goodchild, M. F., Maguire, D. J., ve Rhind, D. W. (2015). *Geographic information science and systems*, 4. baskı. John Wiley & Sons, Hoboken, NJ, 1-32.
- Longley, P. A. (2008). Geographic information systems (GIS). Kemp K (ed.). *Encyclopedia of geographic information science*. SAGE Publications, Thousand Oaks, California, 190-194.
- Ma, Z., ve Ren, Y. (2017). Integrated application of BIM and GIS: An overview. *Procedia Engineering*, 196, 1072-1079. <https://doi.org/10.1016/j.proeng.2017.08.064>
- Malinverni, E. S., Naticchia, B., Lerma Garcia, J. L., Gorreja, A., Lopez Uriarte, J., ve di Stefano, F. (2022). A semantic graph database for the interoperability of 3D GIS data. *Applied Geomatics*, 14, 53-66. <https://doi.org/10.1007/s12518-020-00334-3>
- Nurseitov, N., Paulson, M., Reynolds, R., ve Izurieta, C. (2009). Comparison of JSON and XML data interchange formats: A case study. *Caine*, 9, 157-162. <https://citeseerx.ist.psu.edu/document?repid=rep1&type=pdf&doi=84321e662b24363e032d680901627aa1bfd6088f>
- OGC (2021). *OGC City Geography Markup Language (CityGML) Part 1: Conceptual Model Standard*, Erişim adresi: <https://docs.ogc.org/is/20-010/20-010.html>
- Ohori, K. A., Ledoux, H., ve Peters, R. (2022a). Chapter 10: Semantic 3D city models. *3D modeling of the built environment v.08* (Yayımlanmamış kitap), 91-105. Erişim adresi: <https://github.com/tudelft3d/3dbook/releases>
- Ohori, K. A., Ledoux, H. ve Peters, R. (2022b). Chapter 11: Building information models. *3D modeling of the built environment v.08* (Yayımlanmamış kitap). 107-116. Erişim adresi: <https://github.com/tudelft3d/3dbook/releases>
- Rajabifard, A., Atazadeh, B., ve Kalantari, M. (2019). Chapter 3: Fundamentals of the BIM environment - opportunities for land administration. *BIM and urban land administration*. CRC Press, Boca Raton, 81-120.
- Sani, M. J., ve Rahman, A. A. (2018). GIS and BIM integration at data level: A review. *Int. Arch. Photogramm. Remote Sens. Spatial Inf. Sci., XLII-4/W9*, 299-306. <https://doi.org/10.5194/isprs-archives-XLII-4-W9-299-2018>
- Sulaiman, M., Liu, H., Binalhaj, M., Al-Kasasbeh, M., ve Abudayyeh, O. (2021). ICT-based integrated framework for smart facility management: An industry perspective. *Journal of Facilities Management*, 19(5), 652-680. <https://doi.org/10.1108/JFM-11-2020-0084>
- Teo, T. A., ve Cho, K. H. (2016). BIM-oriented indoor network model for indoor and outdoor combined route planning. *Advanced Engineering Informatics*, 30(3), 268-282. <https://doi.org/10.1016/j.aei.2016.04.007>
- Vacca, G., ve Quaquero, E. (2020). BIM-3D GIS: an integrated system for the knowledge process of the buildings. *Journal of Spatial Science*, 65(2), 193-208. <https://doi.org/10.1080/14498596.2019.1601600>
- Wang, H., Pan, Y., ve Luo, X. (2019). Integration of BIM and GIS in sustainable built environment: a review and bibliometric analysis. *Automation in Construction*, 103, 41-52. <https://doi.org/10.1016/j.autcon.2019.03.005>
- Wang, M., Deng, Y., Won, J., ve Cheng, J. C. (2019). An integrated underground utility management and decision support based on BIM and GIS. *Automation in Construction*, 107, 102931. <https://doi.org/10.1016/j.autcon.2019.102931>
- Wong, J. K. W., Ge, J., ve He, S. X. (2018). Digitisation in facilities management: A literature review and

- future research directions. *Automation in Construction*, 92, 312-326. <https://doi.org/10.1016/j.autcon.2018.04.006>
- Wu, I. C., Hsieh, S. H. (2007). Transformation from IFC data model to GML data model: methodology and tool development. *Journal of the Chinese Institute of Engineers*, 30(6), 1085–1090. <https://doi.org/10.1080/02533839.2007.9671335>
- Xia, H., Liu, Z., Efremochkina, M., Liu, X., ve Lin, C. (2022). Study on city digital twin technologies for sustainable smart city design: A review and bibliometric analysis of geographic information system and building information modeling integration. *Sustainable Cities and Society*, 84, 104009. <https://doi.org/10.1016/j.scs.2022.104009>
- Zhao, L., Liu, Z., ve Mbachu, J. (2019). An integrated BIM–GIS method for planning of water distribution system. *ISPRS International Journal of Geo-Information*, 8(8), 331. <https://doi.org/10.3390/ijgi8080331>
- Zhu, J., Wang, X., Wang, P., Wu, Z., ve Kim, M. J. (2019). Integration of BIM and GIS: geometry from IFC to shapefile using open-source technology. *Automation in Construction*, 102, 105-119. <https://doi.org/10.1016/j.autcon.2019.02.014>
- Zhu, J., Wright, G., Wang, J., ve Wang, X. (2018). A critical review of the integration of geographic information system and building information modelling at the data level. *ISPRS International Journal of Geo-Information*, 7(2), 66. <https://doi.org/10.3390/ijgi7020066>
- Zhu, J., ve Wu, P. (2021a). Towards effective BIM/GIS data integration for smart city by integrating computer graphics technique. *Remote Sensing*, 13(10), 1889. <https://doi.org/10.3390/rs13101889>
- Zhu, J., ve Wu, P. (2021b). A common approach to geo-referencing building models in industry foundation classes for BIM/GIS integration. *ISPRS International Journal of Geo-Information*, 10(6), 362. <https://doi.org/10.3390/ijgi10060362>
- Zhu, J., ve Wu, P. (2022). BIM/GIS data integration from the perspective of information flow. *Automation in Construction*, 136, 104166. <https://doi.org/10.1016/j.autcon.2022.104166>